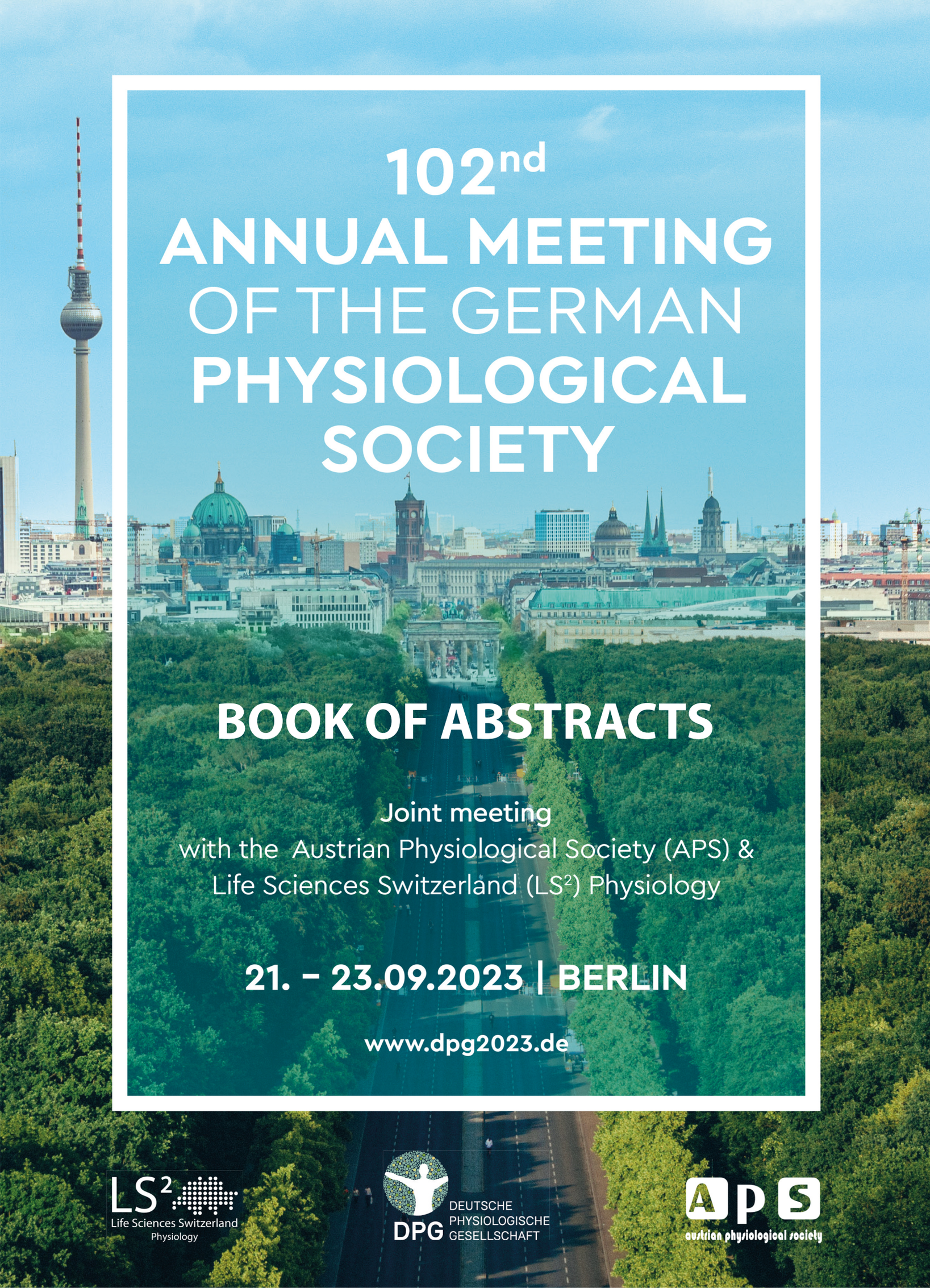

102nd ANNUAL MEETING OF THE GERMAN PHYSIOLOGICAL SOCIETY

BOOK OF ABSTRACTS

Joint meeting
with the Austrian Physiological Society (APS) &
Life Sciences Switzerland (LS²) Physiology

21. – 23.09.2023 | BERLIN

www.dpg2023.de

LS² Life Sciences Switzerland Physiology

DPG DEUTSCHE PHYSIOLOGISCHE GESELLSCHAFT

APS austrian physiological society

TABLE OF CONTENT

PLENARY LECTURES

PL 01
Development and evolution of the human neocortex – neural stem cells, human-specific genes, and human-specific protein variants

Wieland B. Huttner

Max Planck Institute of Molecular Cell Biology and Genetics, Dresden, Germany

Two major classes of neural stem and progenitor cells (NPCs) in the developing neocortex can be distinguished. First, NPCs that reside in the ventricular zone (VZ), i.e. neuroepithelial cells, apical (or ventricular) radial glia (aRG), and apical intermediate progenitors, collectively referred to as apical progenitors (APs). Second, NPCs that reside in the subventricular zone (SVZ), i.e. basal (or outer) radial glia (bRG) and basal intermediate progenitors, collectively referred to as basal progenitors (BPs). Neocortex expansion is thought to be linked to an increased abundance and proliferative capacity of BPs.

In my lecture, I will report the following (after an introduction into the topic):

- The human-specific gene *ARHGAP11B* amplifies basal progenitors.
- This ability of *ARHGAP11B* depends on a single C-to-G base substitution.
- ARHGAP11B protein is imported into mitochondria and promotes glutaminolysis.
- *ARHGAP11B* can expand the primate neocortex.
- *ARHGAP11B*-mediated neocortex expansion increases cognitive performance.
- Neandertal apical progenitors (APs) exhibit a shorter metaphase than modern humans.
- Neandertal APs make more chromosome segregation errors than modern humans.
- Modern human vs. Neandertal transketolase-like 1 (TKTL1) differs by only 1 amino acid.
- Modern human, but not Neandertal, TKTL1 increases basal radial glia and neurons.
- In fetal modern human neocortex, *TKTL1* is most highly expressed in the frontal lobe.

PL 02
The roles of glia and pericytes in early Alzheimer's disease

Tania Quintela Lopez, Francesca Puletti, Nils Korte, Ross Nortley, Pablo Izquierdo, Chanawee Hirunpattarasilp, **David Attwell**

UCL, Neuroscience, Physiology & Pharmacology, London, UK

It is common when studying Alzheimer's disease (AD) to focus mainly on generation of amyloid beta (Aβ) and hyperphosphorylated tau, and the changes of synaptic function and loss of cognitive power that they eventually produce. In this lecture I will emphasise Aβ-driven factors that probably contribute early in the disease to later cognitive decline: a decrease of cerebral blood flow generated in part by microglia and a change in the properties of myelinated axons.

We previously showed that, in vivo in human AD and in a mouse model (APP^{NL-G-F}) of AD, capillaries (but not arterioles or venules) become constricted as a result of pericytes contracting [1]. This was predicted to roughly halve cerebral blood flow. Human and mouse brain slice experiments suggested that the capillary constriction reflects oligomeric Aβ evoking, in microglia and pericytes, generation of reactive oxygen species that then trigger the release of endothelin-1 (ET, possibly from endothelial cells or astrocytes) which evokes pericyte contraction. We have also shown that contraction of pericytes is amplified by a mechanism in which ET-evoked Ca^{2+} release from intracellular stores activates the TMEM16A chloride channel, generating a depolarization that opens voltage-gated calcium channels [2]. We now report that giving to AD mice the voltage-gated calcium channel (CaV) blocker nimodipine in their drinking water from early in AD increased capillary diameter at

pericytes, reduced leukocyte stalling at pericyte somata, improved CBF and attenuated brain hypoxia. Aβ-evoked pericyte contraction in human cortical tissue was also greatly reduced by CaV block. Thus, awareness of the possibility of glia- and pericyte-mediated capillary constriction reveals new therapeutic targets to increase blood flow in AD, and possibly other neurological pathologies.
We previously showed that the conduction speed of myelinated axons can be tuned, not only by altering the number of wraps of myelin, but also by altering the dimensions of the node of Ranvier [3]. Furthermore, damage to the white matter has been suggested to be associated with AD. We now report that oligomeric Aβ rapidly induces a lengthening of the node of Ranvier, which is expected to alter the conduction speed of the myelinated axon and thus disrupt neural circuit function. Understanding the mechanism of this elongation may open up new therapeutic targets for early AD.

Supported by the ERC and Wellcome Trust.

References
[1] Nortley R, Korte N, Izquierdo P, Hirunpattarasilp C, Mishra A, Jaunmuktane Z, Kyrargyri V, Pfeiffer T, Khennouf L, Madry C, Gong H, Richard-Loendt A, Huang W, Saito T, Saido TC, Brandner S, Sethi H, Attwell D. (2019) Amyloid β oligomers constrict human capillaries in Alzheimer's disease via signaling to pericytes. Science 365, eaav9518.
[2] Korte, N., Ilkan, Z., Pearson, C.L., Pfeiffer, T., Singhal, P., Rock, J.R., Sethi, H., Gill, D., Attwell, D., Tammaro, P. (2022) The Ca^{2+}-gated channel TMEM16A amplifies capillary pericyte contraction and reduces cerebral blood flow after ischemia. J. Clin. Invest. 132, e154118.
[3] Arancibia-Carcamo, I.L., Ford, M.C., Cossell, L., Ishida, K., Tohyama, K. & Attwell, D. (2017) Node of Ranvier length as a potential regulator of myelinated axon conduction speed. eLife 6, e23329.

PL 03
The physiology of Lysosomal Ion Channels

Dejian Ren

University of Pennsylvania, Philadelphia, USA

Question

Lysosomes play fundamental physiological roles ranging from material digestion and recycling to metabolism, cellular clearance and gene expression regulation. The clearance function is particular important for long-lived neurons, and lysosome malfunction is thought to be a major cause of neurodegenerative diseases. Compared to those of plasma membranes, the biophysical properties of lysosomes are poorly defined.

Methods

We have used patch clamp electrophysiological recording to systematically reveal lysosomal ion conductances. We also used mouse and human genetics to reveal their physiological functions.

Results

We have detected lysosomal ion channels permeable to K+, Na+ and Cl-. These channels are regulated by extracellular nutrients and growth factors via unique mechanisms involving the mTOR and AKT kinases. The channels regulate lysosomal physiology such as pH homeostasis and organelle fusion. High prevalence genetic variations in the TMEM175 channel alter channel properties and bidirectionally influence the susceptibility to neurodegenerative diseases such as Parkinson’s disease.

Conclusions

Lysosomes have multiple ion channels. They regulate lysosomal physiology and malfunctions are associated with human diseases.

The work has been supported, in part, by grants from the National Institute of General Medical Sciences and the National Institutes of Health National Heart, Lung, and Blood Institute.

References
[1] Cang, C., Bekele, B., and Ren, D. (2014). The voltage-gated sodium channel TPC1 confers endolysosomal excitability. Nat Chem Biol *10*, 463-469.
[2] Cang, C., Zhou, Y., Navarro, B., Seo, Y.-J., Aranda, K., Shi, L., Battaglia-Hsu, S., Nissim, I., Clapham, D.E., and Ren, D. (2013). mTOR regulates lysosomal ATP-sensitive two-pore Na+ channels to adapt to metabolic state. Cell *152*, 778-790.
[3] Cang, C., Aranda, K., Seo, Y.J., Gasnier, B., and Ren, D. (2015). TMEM175 Is an Organelle K(+) Channel Regulating Lysosomal Function. Cell *162*, 1101-1112. 10.1016/j.cell.2015.08.002.
[4] Wie, J., Liu, Z., Song, H., Tropea, T.F., Yang, L., Wang, H., Liang, Y., Cang, C., Aranda, K., Lohmann, J., et al. (2021). A growth-factor-activated lysosomal K(+) channel regulates Parkinson's pathology. Nature *591*, 431-437.

[5] Riederer, E., Cang, C., and Ren, D. (2022). Lysosomal Ion Channels: What Are They Good For and Are They Druggable Targets? Annual review of pharmacology and toxicology. 10.1146/annurev-pharmtox-051921-013755

PL 04
Vascular aging and dementia: from molecular changes to physiological alterations

Milagros Romay, M. Luisa Iruela-Arispe

Northwestern University, Cell & Developmental Biology Department, Feinberg School of Medicine, Chicago, USA

The author has objected to a publication of the abstract.

TEACHING LECTURE

TL01
Respiratory Physiology in the times of COVID

Wolfgang Kübler

Charité, Institute of Physiology, Berlin, Germany

The emergence of the COVID-19 pandemic in early 2020 not only triggered unprecedented scientific discovery in virology, immunology and vaccination, but also drove exceptional research efforts to understand the impact of SARS-CoV-2 infection on virtually all aspects of respiratory physiology. In this teaching lecture, we will revisit basic principles of respiratory physiology in health and disease, using COVID-19 as prime example. Discussions will comprise principles of lung mechanics and lung fluid homeostasis, gas exchange and ventilation-perfusion matching, oxygen transport, and control of breathing.

SYMPOSIA

S 01 | Plasticity of the Cardiac Dyad: From Single Contractions to Remodeling in Disease

S 01-01
The cardiac dyad as a central signalling structure in myocyte calcium handling

Christian Soeller

University of Bern, Physiology, Bern, Switzerland

The cardiac dyad, a structure formed between opposing sarcolemmal and sarcoplasmic reticulum membranes in ventricular myocytes, is the tightly confined space where many critical events of cardiac Ca^{2+} handling are orchestrated. Its important role is mostly a consequence of the restricted space in which a number of key proteins come into close proximity and any influx of calcium is effectively "amplified" as compared to an otherwise equivalent space in the bulk cytosol. Most recent quantitative data on dyadic protein distribution and dyad structure stems from 3D electron microscopy as well as fluorescence super-resolution microscopy, two approaches that provide important complementary information. Recently, we and others have correlated the distribution of proteins and dyad structures with dynamic calcium signals which support the importance of the dyad as the place where Ca^{2+} release events such as Ca^{2+} sparks originate. A particular emphasis is placed on the dyadic distribution of the cardiac type 2 ryanodine receptor (RyR2). I will present new data from applying 3D MINFLUX fluorescence super-resolution microscopy to investigate RyR2 arrangements in mouse ventricular myocytes. We present the first purely optical data of RyR2 distribution with sub-molecular resolution and determine the location of individual RyR2 subunits with high precision (~3 nm) in all directions. This allows estimating not only the location but also the 3D orientation of RyR2s in intact cells. Due to the true molecular resolution of MINFLUX microscopy we were able to measure labelling efficiency in-situ using a novel procedure. Our new data suggests a resolution to apparent discrepancies between previous data from electron microscopy and super-resolution data that may be at least partially explained by effects of labeling efficiency. We will discuss how this new molecular resolution imaging approach may enable a more critical assessment of the concept of RyR clusters as functional Ca^{2+} release units and refine our understanding of the cardiac dyad as the central signalling structure in cardiac Ca^{2+} handling.

S 01-02
Plasticity of dyadic structure and function

William E. Louch

University of Oslo, Institute for Experimental Medical Research, Oslo, Norway

Question

Contraction of the heart is reliant on the shortening of individual cardiomyocytes, elicited by Ca^{2+} release at sub-cellular structures called dyads. Despite the fundamental role of dyads in triggering the heartbeat, their precise functional arrangement remains unclear, both in health and disease.

Methods

Emerging microscopy techniques, including live-cell super-resolution (PALM) imaging, were employed to link the nanoscale arrangement of key dyadic proteins and membranes to function.

Results

PALM imaging in living cardiomyocytes linked fundamental Ca^{2+} release events called "sparks" to their Ryanodine Receptor (RyR) clusters of origin. This analysis showed that distinct channel clusters can collaborate to generate "travelling" sparks [1]. However, RyR arrangements and function are highly malleable, as prolonged β-adrenergic stimulation leads to dispersal of RyR clusters, and slowed Ca^{2+} spark kinetics. This phenomenon is particularly relevant during diseases like heart failure with reduced ejection fraction (HFrEF), where β-adrenergic tone is elevated, and dispersed RyR arrangements contribute to dyssynchrony and slowing of the overall Ca^{2+} transient [2]. We have also observed

great plasticity of t-tubule structure. We found that t-tubules are carefully assembled in the developing heart by the concerted actions of three proteins: Bridging integrator-1 (BIN1), Myotubularin-1, and Dynamin-2 [3]. This process is dependent on augmenting cardiac workload during development [4]. However, excessively high workload, as occurs in HFrEF, is linked to degradation of t-tubule structure and a reversion to an immature phenotype [5]. In combination, derangements on both sides of the dyad (t-tubule disruption and RyR dispersion) critically impair Ca^{2+} release and contractility in HFrEF.

Conclusions

Nanoscale changes in dyadic structure promote fine-tuning of Ca^{2+} release in health, but deranged Ca^{2+} homeostasis in HFrEF. Our data suggest that newfound regulators of dyadic structure and function may serve as novel therapeutic targets in this disease.

I am grateful to the postdoctoral fellows and PhD students in my group, who have acquired the presented data: Michael Frisk, Xin Shen, Yufeng Hou, Harmonie Perdreau-Dahl, Terje Kolstad, and David Lipsett. I also thank the European Research Council and the Norwegian Research Council for generous financial support.

References

[1] Hou Y, Laasmaa M, Li Jia, Shen X, Manfra O, Norden ES, Le C, Zhang L, Sjaastad I, Jones PP, Soeller C, and Louch WE. Live-cell photo-activated localization microscopy correlates nanoscale ryanodine receptor configuration to calcium sparks in cardiomyocytes (2023) *Nat Cardiovasc Res*, 2:251–267.

[2] Shen X, van den Brink J, Bergan-Dahl A, Kolstad TR, Norden ES, Hou Y, Laasmaa M, Aguilar-Sanchez Y, Quick AP, Espe EKS, Sjaastad I, Wehrens XHT, Edwards AG, Soeller C, and Louch WE. Prolonged β-Adrenergic Stimulation Disperses Ryanodine Receptor 2 Clusters in Cardiomyocytes (2022) *eLife*, 11:e77725.

[3] Perdreau-Dahl H, Lipsett DB, Frisk M, Kermani F, Carlson CR, Brech A, Shen X, Bergan-Dahl A, Hou Y, Tuomainen T, Tavi P, Jones PP, Lunde M, Wasserstrom JA, Laporte J, Ullrich ND, Christensen G, Morth JP, and Louch WE. BIN1, myotubularin, and dynamin-2 coordinate t-tubule growth in cardiomyocytes (2023) *Circ Res* 26, 132:e188-e205.

[4] Manfra O, S Louey, Jonker SS, Perdreau-Dahl H, Frisk M, Giraud GD, Thornburg KL, and Louch WE. Augmenting Workload Drives T-tubule Assembly in Developing Cardiomyocytes (2023) *J Physiol*, doi: 10.1113/JP284538.

[5] Frisk M, Le C, Shen X, Røe AT, Hou Y, Manfra O, Silva G, van Hout I, Norden E, Aronsen JM, Laasmaa M, Espe EK, Zouein F, Lamberts R, Dahl CP, Sjaastad I, Lunde IG, Coffey S, Cataliotti A, Gullestad L, Tønnessen T, Jones PP, Altara R, and Louch WE. Etiology-dependent Diastolic Myocardial Calcium Homeostasis in Patients with Heart Failure and Preserved Ejection Fraction (2021) *J Am Coll Cardiol*, 77:405-419.

S 01-03
Ultrastructural reconstruction of the dyad during cardiomyocyte contraction

Joachim Greiner, David Kaltenbacher, Thomas Kok, Peter Kohl, Eva Rog-Zielinska

University Heart Centre Freiburg and Faculty of Medicine, University of Freiburg, Institute for Experimental Cardiovascular Medicine (IEKM), Freiburg, Germany

The structure and function are tightly interlinked in cardiomyocytes. However, the ultrastructural dynamics during the cardiac action potential, including mechanical organelle deformation, are poorly understood. Dynamics of contracting cardiomyocytes are conventionally resolved using light microscopy, a modality with orders of magnitudes lower spatial resolution compared to electron-based imaging.

Here, we use action potential-synchronised high pressure freezing to assess the ultrastructural dynamics during cardiac contraction with electron tomography, resulting in a spatial resolution of $(1.2\ nm)^3$ and millisecond temporal resolution. In brief, cardiomyocytes were isolated from left-ventricular rabbit tissue slices, high pressure-frozen, freeze-substituted, heavy metal-stained, resin-embedded, and cut into 200–300 nm sections. Then, the cardiomyocytes were imaged using electron tomography on a 300 kV transmission electron microscope. The resulting images were reconstructed and segmented utilising fully convolutional neural networks into 3D organelle models. When necessary, reconstructions were refined within a custom-developed software. This workflow allowed for the time-efficient segmentation of sarcoplasmic reticulum, the transverse-axial tubular system, caveolae, microtubule, and mitochondria. To generate a deeper comprehension of the complex intracellular structure and organisation, we developed a portable, interactive in-browser visualization.

Using this workflow, we generated and visualised 353 3D reconstructions of cardiomyocyte organelles, including the sarcoplasmic reticulum and the transverse-axial tubular system (Figure 1). We analysed dyad dimensions, coupling distances, and deformation of the t-tubular geometry. Our proof-of-principle study resolves the structural dynamics of cardiomyocytes in a nanoscopic, three-dimensional, and millisecond-accurate manner. Precisely understanding the ultrastructure and its mechanical modulation thereof, ultimately in human cardiomyocytes under

both physiological and pathophysiological conditions, is key in advancing our current state-of-the-art treatment and diagnosis of cardiac diseases.

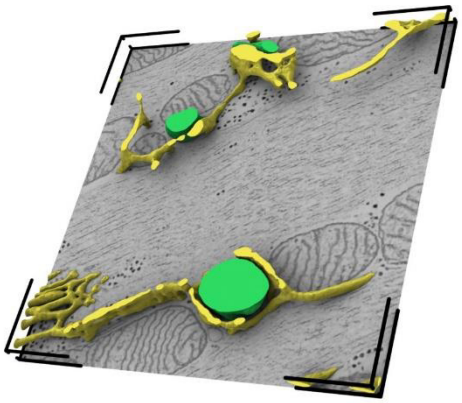

Time-resolved 3D organelle model.
Time-resolved 3D organelle model of the sarcoplasmic reticulum (yellow) and transverse-axial tubular system (green). Cardiomyocytes in this reconstruction were high-pressure-frozen in a relaxed state (0 ms offset to the action potential initiation). The reconstruction has a dimension of 3.14 µm x 3.14 µm x 180 nm and a voxel size of $(1.2\ nm)^3$.

S 01-04
The ultrastructure of elementary calcium signals as revealed by realtime nanoscopy

Qinghai Tian[1], Marcel Lauterbach[2], Wayne Chen[3], **Peter Lipp**[1]

[1] Saarland University, Medical Faculty; PZMS; Molecular Cell Biology, Homburg, Germany
[2] Saarland University, Medical Faculty; CIPMM, Physiology, Homburg, Germany
[3] University of Calgary, Cumming School of Medicine; Department of Physiology & Pharmacology, Calgary, Canada
[4] Saarland University; PZMS, Molecular Cell Biology, Homburg, Germany

The author has objected to a publication of the abstract.

S 01-05
Mechanisms and Pathways of Cardiomyocyte T-Tubule Loss

Thomas Seidel

Friedrich-Alexander-Universität Erlangen-Nürnberg, Institut für Zelluläre und Mollekulare Physiologie, Erlangen, Germany

A reduction in t-tubular density and remodeling of t-tubular shape and organization are common features of heart failure (HF) with reduced ejection fraction and ischemic heart disease, as demonstrated by numerous studies in animal models or cardiac tissue samples obtained from HF patients. T-tubule loss contributes to contractile dysfunction and HF progression by slowing the kinetics and amplitude of intracellular Ca^{2+} signals and may prevent cardiac recovery. T-tubule loss also affects cardiomyocyte electrophysiology and has been suggested to promote cardiac arrhythmias. The pathophysiological consequences of t-tubule loss are the subject of intense research, and new studies continue to reveal new details on this topic. However, the pathomechanisms underlying t-tubule loss and remodeling remain more elusive, not at least because of the intrinsic interrelationship between HF and t-tubule remodeling and the high complexity of HF-induced changes in cardiomyocyte gene expression. Although several proteins linked to the cardiac dyad have been suggested to be involved in t-tubule development, maintenance and degradation, for example JPH2, BIN1, nexilin or dysferlin, their respective roles have not been clarified completely and it remains widely unclear what cellular mechanisms and signaling pathways drive t-tubule loss in vivo and in vitro.
This presentation provides an overview of what is known about cellular mechanisms and pathways of t-tubule loss and then focusses on protein kinase C and related downstream inflammatory and hypertrophic signals that may contribute to loss or remodeling of the transverse tubular system in animal and human cardiac myocytes.

S 01-06
Dysferlin stabilizes the cardiac dyad and mediates hypertrophic remodeling in left-ventricular pressure overload

Nora J. Paulke[1], Carolin Fleischhacker[1], Yannik Zühlke[1], Nina Zaremba[1], Mufassra Mushtaq[1], Tobias Kohl[1], Daniel Kownatzki-Danger[1], Gerd Hasenfuß[1], Julia Preobraschenski[2], Eva Rog-Zielinska[3], Stephan E. Lehnart[1], Sören Brandenburg[1]

[1] University Medical Centre Göttingen, Clinic of Cardiology and Pneumology, Heart Research Centre, Göttingen, Germany
[2] University Medical Centre Göttingen, Institute for Auditory Neuroscience, Göttingen, Germany
[3] University Medical Centre and Faculty of Medicine, Institute for Experimental Cardiovascular Medicine, UHZ, Freiburg, Germany

Introduction

Ferlins are transmembrane proteins with 7 Ca^{2+}-sensitive C2 domains that mediate membrane fusion and repair events in striated muscle cells. Ventricular myocytes (VMs) predominantly express Dysferlin, whose deficiency has been associated with cardiac dysfunction. Here, we propose that Dysferlin plays a critical role in maintaining the integrity of the tubular endomembrane system *and* the cardiac dyad, and that Dysferlin is required for the proliferation of tubular membranes as a prerequisite for hypertrophic remodeling in left ventricular (LV) pressure overload.

Results

Multi-colorSTimulated Emission Depletion (STED) nanoscopy of immunolabeled mouse and human atrial and VMs localized punctate Dysferlin signals accumulating at specific domains of the T-tubular system. Precisely, co-immunolabeling identified Dysferlin clusters at junctional membrane contact sites of the tubular system with the sarcoplasmic reticulum (SR) in nanometric proximity to RyR2 Ca^{2+}-release units. Complexome profiling based on Blue Native PAGE prior to mass spectrometry analysis (LC-MS/MS) showed protein interactions of Dysferlin with RyR2 and the SR membrane tether protein Junctophilin-2 (JP2) in high molecular weight complexes. Dysferlin pull-down and co-immunoprecipitation experiments confirmed RyR2, JP2 and Caveolin-3 as Dysferlin-interacting proteins. Furthermore, in a transgenic mouse model of cardiac JP2 overexpression, polyadic tubule-SR junctions promoted the locally increased expression of Dysferlin clusters. Importantly, Dysferlin protein expression is also upregulated in LV hypertrophy induced by transverse aortic constriction (TAC) (192% in left ventricles post-TAC as compared to sham). Electron tomography demonstrated the proliferation and dilatation of axial tubules 4 weeks post-TAC (difference of means TAC vs. sham +0.95 ± 0.45 AT/10 μm^2, n = 17/17 left VMs, $p<0.01$), and STED nanoscopy visualized Dysferlin clusters highly decorating newly shaped axial tubule membranes in isolated WT VMs post-TAC. In contrast, Dysferlin knockout (KO) VMs failed to develop new axial tubules as analysed by live-cell membrane imaging. Meanwhile, mortality 4 weeks post TAC was not increased in KO mice. Interestingly, echocardiography revealed that Dysferlin KO prevented from LV hypertrophy, further confirmed by single cell measurements.

Conclusions

Nanoscale imaging and biochemical approaches identified Dysferlin as an interaction partner of cardiac dyad proteins, thereby stabilizing tubule-SR junctions for functional excitation-contraction coupling. In addition, we show that pressure overload-induced tubular system reorganization critically depends on Dysferlin to promote hypertrophic remodeling, specifically by facilitating the proliferation of axial tubule membranes and tubule-SR junctions. Hence, Dysferlin emerges as a novel therapeutic target to control the stability of cardiac dyads, and to regulate tubular system proliferation necessary for LV hypertrophy.

S 02 | Novel GPCR-based optical tools to investigate organ function and behaviour

S 02-01
A new family of genetically-encoded catecholamines indicators

Tommaso Patriarchi

University of Zurich, Zurich, Switzerland

Genetically-encoded sensors are a key emerging technology that is much needed to visualize the extracellular dynamics of neuromodulators such as catecholamines. In particular these tools allow us to monitor behaviorally-relevant and task-specific catecholamine fluctuations, the

kinetics of their release and uptake, as well as the spatial organization of the release events in the brain. Our laboratory is currently focused on the development of highly-sensitive and multicolor genetically-encoded optical probes for catecholamines. In this talk I will introduce our recent progress in this direction.

S 02-02
Illuminating the brain - genetically encoded sensors to explore neuronal circuitries

Olivia A. Masseck

Universität Bremen, Synthetische Biologie, Bremen, Germany

Understanding how neuronal networks generate complex behavior is one of the major goals of Neuroscience. Neurotransmitter and Neuromodulators are crucial for information flow between neurons and understanding their dynamics is the key to unravel their role in behavior. We recently developed a new family of genetically encoded serotonin (5-HT) sensors (*sDarken*) on the basis of the native 5-HT_{1A} receptor and circularly permuted GFP. *sDarken* 5-HT sensors are bright in the unbound state and diminish their fluorescence upon binding of 5-HT. Sensor variants with different affinities for serotonin were engineered to increase the versatility in imaging of serotonin dynamics. Experiments *in vitro* and *in vivo* showed the feasibility of imaging serotonin dynamics with high temporal and spatial resolution. As demonstrated here, the designed sensors show excellent membrane expression, have high specificity and a superior signal-to-noise ratio, detect the endogenous release of serotonin and are suitable for *in vivo* imaging. In addition, we will present a new red-shifted genetically encoded calcium indicator (PinkyCaMP) that will further expand the existing toolbox to image neuronal activity.

We would like to espcially thank all of our collaborators: Martin Fuhrmann, Andreas Reiner, and Simon Wiegert.
We thank Dr. Andy Tinker (UCL London, UK) who kindly provided HEK cells stably expressing GIRK1 and GIRK2 subunits. pAAV.CAG.SF-iGluSnFR.A184V was a gift from L. Looger (Addgene plasmid #106199). We also thank Reinhard Seifert (Core Facility for Genetic Engineering, Research Center Caesar, Bonn) who kindly provided CNG channels. cpGFP from: pN1-GCamp6m XC (Addgene number #111543, Depositor: Xiaodong Liu). pAAV.Syn.NES.jRCaMP1a.WPRE.SV40 was a gift from Douglas Kim & GENIE Project (Addgene plasmid # 100848). pAAV-Syn-ChrimsonR-tdT was a gift from Edward Boyden (Addgene plasmid # 5917). A.R. was supported by funding from the NRW-Rückkehrprogramm and the Deutsche Forschungsgemeinschaft (DFG RE 3101/3-1). O.A.M was funded by the Deutsche Forschungsgemeinschaft (DFG MA 4692/6-1 and - Projektnummer 122679504 - SFB 874). J.S.W. received funding for this project by the DFG (SPP 1926, WI4485-3/2, FOR2419, WI4485-2/2, and SFB935, B8). M.F. was supported by funding from the European Research Council (ERC-CoG MicroSynCom 865618).

References

[1] Kubitschke, M., Müller, M., Wallhorn, L., Pulin, M., Mittag, M., Pollok, S., Ziebarth, T., Bremshey, S., Gerdey, J., Claussen, K. C., Renken, K., Groß, J., Gneiße, P., Meyer, N., Wiegert, J. S., Reiner, A., Fuhrmann, M., & Masseck, O. A. (2022). Next generation genetically encoded fluorescent sensors for serotonin. *Nature communications*, *13*(1), 7525. https://doi.org/10.1038/s41467-022-35200-w

S 02-03
Synchronization of neuronal networks and modulation of synaptic plasticity by non-visual opsin variants.

Stefan Herlitze

Ruhr-Universität Bochum, Department of Zoology and Neurobiology, Bochum, Germany

G protein-coupled receptors (GPCRs) in neuronal circuits modulate intracellular signaling cascades and are involved in regulating action potential (AP) firing, synaptic transmission and plasticity. GPCR signal duration, specificity and adaptation depend on the precise trafficking and localization of the GPCR within its subcellular signaling domain. However, precise control and visualizing traffic-dependent GPCR signals in neurons is difficult, but important to understand the contribution of GPCRs to synaptic plasticity and to elucidate how this is altered during neurodegenerative and neuropsychiatric diseases. In general, GPCRs couple to the four main G protein families $G_{i/o}$, G_s, $G_{q/11}$ and $G_{12/13}$. Synaptic plasticity is in particular controlled by the $G_{i/o}$ and $G_{q/11}$ pathway. We have established various optogenetic tools to control and visualize

these two signaling pathways using different vertebrate opsins including rod/cone opsins (Li et al., 2005; Masseck et al., 2014) and parapinopsin (Eickelbeck et al., 2019) for controlling the $G_{i/o}$ pathway, and melanopsin for controlling the $G_{q/11}$ pathway.
Here we will present our newest results regarding the control of synaptic plasticity in the cerebellar cortex specifically in mGluR1 receptor domains (Surdin et al., 2023). In addition, we characterized a "reverse" light-activated GPCR from zebrafish (Opn7b), which allows to constitutively control $G_{i/o}$ coupled GPCR pathways in the mouse brain (Karapinar et al., 2021).

S 02-04
Optogenetic stimulation of G_s signaling to investigate cardiac arrhythmia mechanisms

Vanessa Dusend, Philipp Sasse

University Bonn, Physiology I, Bonn, Germany

β-adrenergic G_s signaling regulates heart rate and cardiac output during physical activity, but in pathologic conditions can also promote calcium leak from the sarcoplasmic reticulum during diastole in ventricular cardiomyocytes, leading to premature ventricular contractions (PVC). This mechanism can trigger lethal ventricular tachycardia (VT) in patients with hereditary arrhythmia, such as catecholaminergic polymorphic ventricular tachycardia (CPVT), after myocardial infarction or during heart failure. Theoretically, β-adrenergic stimulation of the sinus node may be protective by increasing the heart rate and shortening the diastolic interval.
To investigate differential effects of regional G_s signaling, we established optogenetic G_s stimulation by generating a mouse line expressing Jellyfish opsin (JellyOp), a light-activated G_s coupled GPCR, in cardiomyocytes [1]. This line was crossed with a calsequestrin (Casq2) knock-out mouse as a model for CPVT (JellyOp x Casq2-/-). Regional illumination of the sinus node, the atrio-ventricular node and the ventricles showed differential effects on heart rhythm and arrhythmogenesis. The transmural arrhythmogenic potential of the left ventricle was investigated by comparing the effect of endocardial illumination with an intracardiac light catheter to epicardial illumination with identical intensity and area. Endocardial illumination induced PVC in ventricular-paced JellyOp x Casq2-/- hearts with more than 10-fold higher light sensitivity than epicardial illumination (N=5). Accordingly, endocardial ablation using Lugol solution significantly reduced light-induced PVCs.
Importantly, increasing heart rate from 200 bpm to 400 bpm prevented PVC generation (N=5). These findings indicate an increased propensity for PVC, particularly in the endocardium, upon selective G_s activation in the ventricle, facilitated by low heart rate. Inhibition of phosphodiesterases did not abolish the endo- to epicardial difference. Regional specific analysis of the phosphorylation status revealed a higher phospholamban phosphorylation increase upon G_s activation in the endocardium.
In addition to PVC, the influence of G_s activation on the stability and complexity of reentry VT was investigated. Illumination increased VT vulnerability and duration upon S1S2 electrical stimulation (N=3). In some hearts with long-running monomorphic VT JellyOp stimulation converted VT into polymorphic morphology with higher complexity. Voltage mapping of the anterior ventricular epicardium revealed a light-induced switch from a stable rotor to an unstable, meandering rotor in the right ventricle with a higher dominant frequency.
In conclusion, optogenetic methods allow regional discrimination of G_s signaling effects on ventricular arrhythmia. G_s activation promotes PVC generation in the endocardium and enhances the vulnerability and stability of reentry VT and the risk of degradation into high-frequency ventricular fibrillation. (N = individual hearts)

References
[1] Makowka P, Bruegmann T, Dusend V, Malan D, Beiert T, Hesse M, et al. Optogenetic stimulation of Gs-signaling in the heart with high spatio-temporal precision. Nature Communications. 2019 Mar 20;10(1):1281.

S 02-05
Finding new OptoGPCRs in nature: broadening the wavelength spectra and dynamic ranges

Alina Pushkarev[1], Camille Brouillon[1], Marjorie Lienard[4], David Buhrke[1], Johannes Vierock[1], Megan Porter[3], Sonja Kleinlogel[2], Peter Hegemann[1]

[1] Humboldt-Universität zu Berlin, Institute of Biology Experimental biophysics, Berlin, Germany
[2] University of Bern, Institute of Physiology, Bern, Switzerland
[3] University of Hawai'i, School of life Sciences, Mānoa, USA
[4] Lund University, Functional Zoology, Lund, Sweden

Question

Although crustaceans have intrigued the scientific world for a long time. In order to prove that animals such as the mantis shrimp indeed see beyond the visible spectrum, absorbance measurements were made directly on the eyes complemented with behavioral studies.

Crustacean rhodopsins are especially interesting since they can detect wavelengths beyond the visual spectrum. Humans call the visual spectrum this way since it is our limitation as a species. In reality, different insects, marine animals, and fungi can detect light waves beyond this range.

Rhodopsins that absorb at the far end of the visible spectrum are important for use in the field of optogenetics for controlling neuronal activity by expressing light-activated proteins in otherwise blind neurons. Infrared-absorbing rhodopsins are useful since the red wavelengths penetrate the tissue and scatter more in the neuronal tissue. Far-red-absorbing rhodopsins are scarce in nature, and one of their bearers are stomatopod crustaceans (a famous member is the peacock mantis shrimp), which can detect wavelengths ranging from UV (310 nm wavelength) to infrared (over 700 nm) by using different rhodopsins.

Methods

Crustacean rhodopsins were chosen through phylogeny and known phenotypes and expressed both in human and yeast cells. The well-expressing rhodopsins were studied biochemically to determine their usefulness for optogenetic application.

Results

In this work, I will present the opsins we were able to express and characterize from crustaceans, many of which are bistable.

Conclusions

Crustaceans are a good source of new bistable rhodopsins for optogenetic applications

S 03 | Novel approaches in understanding mechanisms of deep brain stimulation in movement disorders (Symposium of CRC 1270 ELAINE Electrically active Implants)

S 03-01
Synaptic dynamics underlying deep brain stimulation - translating rat to human single cell recordings

Leon Amadeus Steiner

Charité - Universitätsmedizin, Berlin, Germany

Parkinson's disease (PD) is a common movement disorder that has been associated with excessive oscillatory and neuronal synchronization of basal ganglia circuits. Deep brain stimulation (DBS) of the subthalamic nucleus (STN) disrupts this pathological synchronization, but synaptic underpinnings of this intervention are of ongoing debate. Scrutinizing synaptic dynamics underlying DBS in both rat and human single cell recordings, we have employed a translational approach to investigate the synaptic mechanism of action of subthalamic DBS.

In the rat, utilizing multi-neuron patch clamp recordings, we have shown that the input of inhibitory projections to STN is sustained at high stimulation frequencies (HFS) in contrast to rapidly depressed excitatory input (Steiner et al., 2019 J Neuroscience). Capitalizing on the unique opportunities of intraoperative microelectrode and human single-neuron recordings, we replicated the persistency of synaptic inhibition at HFS in the human STN, establishing that synaptic inhibition at DBS targets is frequency- and projection-source specific (Steiner et al., 2022 Brain Stimulation). Thus, these translational efforts have helped identify the synaptic mechanism by which DBS masks neuronal burst firing that encodes for excessive oscillatory synchronization, a hallmark of PD pathophysiology (Steiner et al., 2017, Movement Disorders; Scherer, Steiner et al., 2022, Proc Natl Acad Sci U S A).

References
[1] **Steiner LA**, Barreda Tomás FJ, Planert H, Alle H, Vida I, Geiger JRP. Connectivity and Dynamics Underlying Synaptic Control of the Subthalamic Nucleus. *J Neurosci*. 2019.

[2] **Steiner LA**, Kühn AA, Geiger JR, Alle H, Popovic MR, Kalia SK, Hodaie M, Lozano AM, Hutchison WD, Milosevic L. Persistent synaptic inhibition of the subthalamic nucleus by high frequency stimulation. ***Brain Stimul.*** 2022.

[3] **Steiner LA**, Neumann WJ, Staub-Bartelt F, Herz DM, Tan H, Pogosyan A, Kuhn AA, Brown P. Subthalamic beta dynamics mirror Parkinsonian bradykinesia months after neurostimulator implantation. ***Mov Disord***. 2017.

[4] Scherer M, **Steiner LA**, Kalia SK, Hodaie M, Kühn AA, Lozano AM, Hutchison WD, Milosevic L. Single-neuron bursts encode pathological oscillations in subcortical nuclei of patients with Parkinson's disease and essential tremor. ***Proc Natl Acad Sci U S A***. 2022.

S 03-02
Electrophysiological Investigations on the mechanisms of DBS in a dystonia model

Denise Franz[1], Marco Heerdegen[1], Fabiana S. Kragelund[1], Anika Lüttig[2], Franz V. Plocksties[3], Angelika Richter[2], Rüdiger Köhling[3]

[1] University Medical Center Rostock, Oscar Langendorff Institute of Physiology, Rostock, Germany
[2] University of Leipzig, Institute of Pharmacology, Pharmacy and Toxicology, Veterinary Faculty, Leipzig, Germany
[3] University of Rostock, Institute of Applied Microelectronics and Computer Engineering, Rostock, Germany

Question

Pallidal deep brain stimulation (DBS) is an effective treatment for generalised or cervical dystonia, which improves dystonia severity by up to 60 %. Despite increasing clinical trials, the pathophysiology of dystonia and the mechanisms of DBS are still unclear. With our experiments, we are investigating how deep brain stimulation influences synaptic transmission and network activities within the cortico-basal ganglia-thalamo-cortical as well as the cerebello-thalamo-cortical pathways.

Methods

We implanted bipolar stimulation electrodes bilaterally to the dt^{sz} mutant hamster's globus pallidus internus under deep isoflurane anaesthesia [1] [2]. We connected these to STELLA, a software-driven implantable modular stimulation device [3] for continuously long-term DBS (130 Hz, 50 µA) over 11 days. We defined two experimental groups: a) the DBS group, with activation of DBS 3-4 days after surgery, and b) the sham group, where the DBS remained turned off over the total period. The electrophysiological activities of striatal, thalamic, cortical, and cerebellar neurons were analysed using patch clamp and microelectrode array recordings in acute parahorizontal (appr. 30 ° off-horizontal) brain slices.

Results

For ventral motor thalamic (VMT) neurons, we detected a significantly higher frequency of mixed spontaneous synaptic (excitatory and inhibitory) activity in the DBS group, 7.0±2.0 Hz (n = 11), compared to the sham group, 3.0±1.0 Hz (n = 11). Isolating spontaneous inhibitory postsynaptic currents (sIPSCs) by inhibition of glutamatergic synaptic transmission with D-AP5 (50 µM) and CNQX (10 µM) revealed no difference in the frequency between the sham group (2.0±0.5 Hz) and the DBS group (1.9±0.6 Hz). Rather, the DBS group indicated a significantly shorter interspike interval (ISI) of mixed synaptic currents [4].

In striatal medium spiny neurons, we directly recorded spontaneous currents (sEPSC) by blocking IPSC with gabazine. In contrast to the VMT, DBS led to a distinct decrease in sEPSC frequency.

Conclusions

Our results indicated that the inhibitory activity did not differ between the sham and DBS groups. That may reveal that the DBS of the pallidum, which directly sends inhibitory projections to VMT neurons, does not affect the frequency of sIPSC in these neurons but alters the activity pattern by affecting the ISI. The upregulation of the excitatory tone in VMT neurons of the DBS group and downregulation within the striatum pointed out that DBS has complex network-wide effects.

This study is supported by the German Research Foundation (DFG) within the Collaborative Research Centre (SFB 1270/1,2 ELAINE 299150580). We are also grateful to Tina Sellmann for the implantation surgeries.

References

[1] StartFragmentHeerdegen, M., Zwar, M., Franz, D., Hörnschemeyer, J., Neubert, V., Plocksties, F., Niemann, C., Timmermann, D., Bahls, C., van Rienen, U., et al. (2021). Mechanisms of pallidal deep brain stimulation: Alteration of cortico-striatal synaptic communication in a dystonia animal model. Neurobiol. Dis. *154*, 105341.EndFragment

[2] StartFragmentPaap, M., Perl, S., Lüttig, A., Plocksties, F., Niemann, C., Timmermann, D., Bahls, C., van Rienen, U., Franz, D., Zwar, M., et al. (2020). Deep brain stimulation by optimized stimulators in a phenotypic model of dystonia: Effects of different frequencies. Neurobiol. Dis. *147*, 105163.EndFragment
[3] StartFragmentPlocksties, F., Kober, M., Niemann, C., Heller, J., Fauser, M., Nüssel, M., Uster, F., Franz, D., Zwar, M., Lüttig, A., et al. (2021). The software defined implantable modular platform (STELLA) for preclinical deep brain stimulation research in rodents. J. Neural Eng. *18*, 056032.EndFragment
[4] StartFragmentFranz, D., Heerdegen, M., Santana Kragelund, F., Lüttig, A., Perl, S., Richter, A., and Köhling, R. (2023). P-68 Deep brain stimulation alters synaptic tone on ventroanterior-ventrolateral thalamic neurons in dystonic dtsz mutant hamsters. Clin. Neurophysiol. *148*, e39–e40.EndFragment

S 03-03
Human neural cell models of dystonia

Philipp Capetian, Enes F. Aydin, Robert Blum, Nina Königl, Jens Volkmann

Universitätsklinikum Würzburg, Neurologische Klinik und Poliklinik, Würzburg, Germany

Dystonias are brain disorders characterized by involuntary muscle contractions, devoid of any neurodegenerative processes. These disorders are predominantly regarded as network dysfunctions, as they often lack evident structural abnormalities or explicit neurodegeneration. Consequently, creating accurate experimental models for these disorders presents specific challenges.

The advent of reprogramming techniques, enabling the conversion of somatic cells into stem cells, has revolutionized the availability of human neural cells for in vitro analyses, a feat that was previously considered virtually impossible. Nevertheless, establishing functional networks of human neurons differentiated from stem cells in a laboratory setting remains a formidable task.

In this presentation, we introduce our methodology for deriving induced neural stem cells from fibroblast cultures of dystonia patients through plasmid transfection, followed by their subsequent differentiation into neurons in vitro. We delve into various techniques employed for the formation of neural networks and explore their impact on the development of neural connections. We also examine neural activity through calcium imaging, showcasing its visualization and quantification. Our findings indicate that achieving fully mature and widespread spontaneous activity, capable of modulation by glutamatergic and GABAergic compounds, continues to pose a significant challenge.

S 03-04
Neurophysiological biomarkers to optimize deep brain stimulation in movement disorders

Karlo Lizarraga

University of Rochester, Motor Physiology and Neuromodulation Program, Department of Neurology, Rochester, USA

Currently available deep brain stimulation (DBS) systems concomitantly modulate pathological and non-pathological activity by continuously delivering electrical pulses of pre-defined amplitude, frequency and duration. Modulation of pathological activity translates into motor symptom control but modulation of non-pathological activity may result in unwanted and often subtle side effects [1]. DBS therapy can be optimized by specifically targeting pathological activity while minimizing unintended stimulation of non-pathological activity. A team-based, interdisciplinary, patient-centered process should be in place to offer DBS to patients with favorable risk/benefit profiles. Neurophysiological information could offer additional diagnostic and prognostic information in selected patients at this stage. Subsequently, accurate surgical implantation of DBS leads is vital to deliver therapy within key sensorimotor regions. Several pre-operative and intra-operative imaging modalities provide increasingly precise anatomical guidance. Neurophysiological information obtained by intraoperative microelectrode recordings, intraoperative stimulation, and other techniques, could further increase surgical accuracy and guide selection of the DBS lead to be implanted [2,3]. Post-operatively, DBS therapy can be anatomically optimized by directional stimulation and physiologically optimized by targeting pathophysiological signals [2]. Directional stimulation using segmented DBS leads could improve the anatomical efficiency of stimulation by targeting regions associated with clinical benefit while avoiding regions associated with side effects. Directional stimulation cannot compensate for inaccurately placed leads but it could optimize outcomes and energy consumption in patients with well-placed or slightly misplaced leads. A commercially available DBS system allows for post-operative measurement of local field potentials (LFPs) using inactive contacts of the DBS leads, while delivering stimulation through active contacts. This system has the potential to reduce the time it takes to

optimize DBS by targeting pathological LFPs. In Parkinson's disease, akinetic-rigid symptoms correlate with LFPs abnormally synchronized in the beta band (13-35Hz). DBS-associated symptom improvement correlates with suppression of abnormal low beta synchronization (13–20Hz) and facilitation of high frequency gamma synchronization (35–250Hz). In dystonia, LFPs abnormally synchronize in the theta/alpha (4-13Hz), beta and gamma (60-90Hz) bands. Phasic dystonic symptoms and their gradual response to DBS correlate with changes in theta/alpha synchronization. Neurophysiological techniques could also help identify subtle DBS side effects [4]. Adaptive DBS systems will use individualized pathological characteristics of neurophysiological signals to automatically deliver therapeutic electrical pulses of specific spatial and temporal parameters.

The preliminary work presented in this lecture was supported by the Schmitt Program in Integrative Neuroscience (SPIN) Pilot Project Program 2022, through the Del Monte Institute for Neuroscience at the University of Rochester. The author would like to thank his collaborators at the University of Rochester: Eleni Patelaki, Ph.D., Angela Hewitt, M.D., Ph.D., Hannah Mesmer, B.Sc., Andrew Wensel, M.D., Edward G. Freedman, Ph.D., and John J. Foxe, Ph.D. The author would like to thank all members of the Motor Physiology and Neuromodulation Program at the Department of Neurology at the University of Rochester in Rochester, NY, USA, including all members of the DBS team, Carol Zimmerman, R.N., and Michael Williams.

References

[1] Lizarraga KJ, Gnanamanogaran B, Al-Ozzi TM, et al. 2022. Lateralized Subthalamic Stimulation for Axial Dysfunction in Parkinson's Disease: A Randomized Trial. Movement Disorders 37(5):1079-1087.
[2] Sirica D, Hewitt AL, Tarolli CG, et al. 2021. Neurophysiological biomarkers to optimize deep brain stimulation in movement disorders. Neurodegenerative Disease Management 11(4):315-328.
[3] Scherer M, Steiner LA, Kalia SK, et al. 2022. Single-neuron bursts encode pathological oscillations in subcortical nuclei of patients with Parkinson's disease and essential tremor. Proceedings of the National Academy of Science USA 119(35):e2205881119
[4] Lizarraga KJ, Patelaki E, Mesmer H, et al. 2023. Mobile brain-body imaging markers of treatment-related responses in a man with Parkinson's disease. Clinical Neurophysiology (In Press).

S 03-05
Mathematical Modelling of Deep Brain Stimulation

Jens Starke[1], **Konstantinos Spiliotis**[1], Rüdiger Köhling[2]

[1] *University of Rostock, Institute of Mathematics, Rostock, Germany*
[2] *Universitätsmedizin Rostock, Oscar-Langendorff-Institut für Physiologie, Rostock, Germany*

Over the past years, mathematical models have contributed to explain brain functionality in healthy and pathological cases. Detailed investigations for different model parameters are almost impossible in neural experiments, but the analysis and simulations of mathematical models can uncover such details and allow to understand parameter-dependent critical transitions in brain activities. In this direction, we developed a large-scale computational model for movement disorders. The model of the basal ganglia network consists of the following parts: subthalamic nucleus (STN), globus pallidus (external GPe and internal GPi), extended with the regions of striatum, thalamus and motor cortex (MC). The connectivity of the model is based on multimodal imaging data. Parkinsonian conditions are simulated by assuming reduced dopaminergic input and corresponding pronounced inhibitory or disinhibited projections to GPe and GPi. Macroscopic variables are derived from the network as mathematical quantities, which correlate closely to thalamic responses. Simulating deep brain stimulation (DBS) of the STN affects the dynamical behavior of the entire network, increasing the thalamic activity to levels close to healthy. Analyzing the network structure and the dynamics under healthy, Parkinsonian and DBS conditions, intending to improve DBS treatment, we propose (a) optimal DBS frequency ranges above 130Hz, (b) an optimal target position of the electrode (sweet spot) for improved motor symptoms, (c) a synaptic desensitization of the pallidothalamic connectivity as one possible mechanism of DBS treatment.

Funded by the Deutsche Forschungsgemeinschaft (DFG, German Research Foundation) – SFB 1270/2 - 299150580.

References

[1] Siettos, C. and Starke, J.: Multiscale modeling of brain dynamics: from single neurons and networks to mathematical tools. Wiley Interdisciplinary Reviews: Systems Biology and Medicine 8, 438–45 (2016).
[2] Spiliotis, K., Starke, J., Franz, D., Richter, A. and Köhling, R.: Deep brain stimulation for movement disorder treatment: exploring frequency-dependent efficacy in a computational network model. Biological Cybernetics 116, 93-116 (2021).

[3] Spiliotis, K., Butenko, K., van Rienen, U., Starke, J. and Köhling, R.: Complex network measures reveal optimal targets for deep brain stimulation and identify clusters of collective brain dynamics. Frontiers in Physics 10 (2022).

S 04 | Ion channels in pulmonary physiology and disease

S 04-01
Ion channels in pulmonary physiology and disease

Andrea Olschewski

Medical University of Graz, Experimental Anesthesiology, Department of Anesthesiology and Intensive Care Medicine, Graz, Austria

The author has objected to a publication of the abstract.

S 04-02
In-depth characterization of CFTR variants for personalized medicine approaches in cystic fibrosis

Valeria Capurro[1], Emanuela Pesce[1], Valeria Tomati[1], Federico Cresta[2], Cristina Pastorino[1], Mariateresa Lena[3], Carlo Castellani[2], Renata Bocciardi[1,3], **Nicoletta Pedemonte**[1]

[1] IRCCS Istituto Giannina Giannina, UOC Genetica Medica, Genoa, Italy
[2] IRCCS Istituto Giannina Giannina, UOSD Centro Fibrosi Cistica, IRCCS Istituto Giannina Gaslini, Genova, Italy, Genoa, Italy
[3] University of Genoa, Department of Neurosciences, Rehabilitation, Ophthalmology, Genetics, Maternal and Child Health (DINOGMI), Genoa, Italy

Question
In Italy, 30% of patients with cystic fibrosis (CF) carry CFTR variants not included among those for which modulators have been approved and are thus defined as “orphan mutations”. Most of them have unknown mechanism of action and sensitivity to CFTR modulators. Our study aims at providing each CF patient with the best therapeutic option available by assessing its responsiveness to the different treatments, thus defining its “theratype”. The project, relying on the use of patients’ nasal epithelial cells is focusing on: 1. understanding the molecular mechanism by which orphan mutations cause CFTR loss of function; 2. defining their responsiveness to CFTR modulators.
Methods
Epithelial cells, obtained by nasal brushing, are cultured using a well-established protocol. Approved drugs or compounds under development are tested on nasal epithelia by means of electrophysiological techniques. Molecular analysis of CFTR transcripts is performed by standardized molecular biology procedures; functional and biochemical characterizations are also realized both in native and heterologous systems.
Results
To date, we have recruited >350 donors. We have characterized patients carrying complex alleles: in some cases, the presence of additional variants was unknown. The molecular characterization of CFTR transcripts we performed was crucial to identify the presence of such additional variants impacting the response to CFTR modulators. Interestingly, our study also confirms the importance of the cell background in the evaluation of CFTR modulator effects, as in the case of the mutant G1244E protein, whose processing and function as well as its pharmacological sensitivity, are markedly dependent on the cell context.

Effective modulators have been identified for more than 50% of the patients. CFTR rescue varies from 5% to 80% compared to that measured in non-CF nasal cells.
Conclusions
So far, our study has demonstrated that a significant fraction of Italian patients carries mutations that can be rescued by modulators, and thus they might benefit from treatment with these drugs. The study also highlights the existence of poorly responsive mutations that will require novel therapeutic approaches based on optimized modulators or, in other cases, molecular-based strategies.

Finally, our results draw attention to the need for the development of novel potentiators having different mechanisms with respect to ivacaftor to improve channel activity for mutants with severe gating defect.

This work was supported by the Italian Cystic Fibrosis Foundation grant (FFC #10/2021), by the Cystic Fibrosis Foundation grant (PEDEMO20G0), by the Italian Ministry of Health (GR-2018-12367126).

The authors thank the people with CF for their participation in this study and their continuous support of their work.

S 04-03
CFTR and lung endothelial barrier regulation in respiratory infections

Lasti Erfinanda[1,2], Lin Zou[1,11], Birgitt Gutbier[3], Laura Kneller[3], Sarah Weidenfeld[1], Laura Michalick[1], Disi Lei[1,11], Katrin Reppe[3], Luiz Gustavo Teixeira Alves[3], Bill Schneider[3], Qi Zhang[1], Caihong Li[1], Diana Fatykhova[3], Paul Schneider[4], Wolfgang Liedtke[5], Eisei Sohara[6], Timothy J. Mitchell[7], Achim D. Gruber[8], Andreas Hocke[2,3], Stefan Hippenstiel[3,2], Norbert Suttorp[2,3], Andrea Olschewski[9], Marcus A. Mall[10,2], Martin Witzenrath[3,2], Wolfgang M. Kübler[1,2]

[1] *Charité-Universitätsmedizin Berlin, Institute of Physiology, Charité-Universitätsmedizin Berlin, Berlin, Germany*
[2] *German Center for Lung Research (DZL), associated partner site, Berlin, Germany*
[3] *Charité - Universitätsmedizin Berlin, corporate member of Freie Universität Berlin, Humboldt-Universität zu Berlin, and Berlin Institute of Health, Department of Infectious Diseases and Pulmonary Medicine, Berlin, Germany*
[4] *DRK Clinics, Department for General and Thoracic Surgery, Berlin, Germany*
[5] *Duke University Medical Center, Departments of Neurology, Neurobiology and Clinics for Pain and Palliative Care, Durham, USA*
[6] *Graduate School of Medical and Dental Sciences, Tokyo Medical and Dental University, Department of Nephrology, Tokio, Japan*
[7] *University of Birmingham, Institute of Microbiology and Infection, Birmingham, UK*
[8] *Freie Universität Berlin, Institute of Veterinary Pathology, Berlin, Germany*
[9] *Medical University of Graz, Experimental Anaesthesiology, Department of Anaesthesiology and Intensive Care Medicine, Graz, Austria*
[10] *Universitätsmedizin Berlin, Department of Pediatric Pulmonology, Immunology and Intensive Care Medicine, Charité, Berlin, Germany*
[11] *German Heart Center Berlin, Berlin, Germany*

Pneumonia is the most common cause of the acute respiratory distress syndrome (ARDS), a potentially fatal lung disease characterized by hyperinflammation and endothelial barrier failure. Infectious and inflammatory stimuli can cause rapid downregulation of cystic fibrosis transmembrane conductance regulator (CFTR), and inhibition of CFTR was found to increase lung microvascular endothelial permeability *in vitro*. Here, we identify loss of lung microvascular endothelial CFTR as important pathomechanism in lung endothelial barrier failure in pneumonia-induced ARDS, delineate the molecular signaling pathway underlying this effect and identify CFTR potentiation as novel therapeutic strategy in ARDS.

CFTR was downregulated following *Streptococcus pneumoniae* (*S.pn.*) infection in human and murine lung tissue. CFTR downregulation was also observed in human pulmonary microvascular endothelial cells (HPMECs) following infection with *Pseudomonas aeruginosa* or stimulation with pneumolysin (PLY), a virulence factor of *S.pn.*, or by plasma from COVID-19 patients. Isolated perfused lungs revealed that CFTR inhibition increased endothelial permeability in parallel with intracellular Cl^- and Ca^{2+} concentrations ($[Cl^-]_i$, $[Ca^{2+}]_i$). Inhibition of the Cl^- sensitive with-no-lysine kinase 1 (WNK1) replicated the effect of CFTR inhibition on endothelial permeability and endothelial $[Ca^{2+}]_i$ while WNK1 activation attenuated it. Lungs of heterozygous Wnk1-deficient mice (*Wnk1*$^{+/-}$) showed spontaneous leak. Endothelial $[Ca^{2+}]_i$ transients and permeability in response to inhibition of either CFTR or WNK1 were prevented by inhibition of the cation channel transient receptor potential vanilloid 4 (TRPV4). Mice deficient in *Trpv4* (*Trpv4*$^{-/-}$) developed less lung edema and protein leak than their wild-type littermates following infection with *S. pn.* The CFTR potentiator ivacaftor prevented CFTR loss and reduced endothelial leak in response to PLY or plasma from COVID-19 patients *in vitro*, and prevented lung edema and protein leak after *S. pn.* infection *in vivo*.

Lung infection causes rapid loss of CFTR that promotes lung edema formation through intracellular Cl^- accumulation, inhibition of WNK1 and subsequent disinhibition of TRPV4, resulting in endothelial Ca^{2+} influx and vascular barrier failure. Ivacaftor prevents CFTR loss and may thus present a promising therapeutic strategy in ARDS due to severe pneumonia including COVID-19.

Supported by the German Research Foundation (CRC-TR84, C09).

S 04-04
K_{Ca}3.1 channels in non-small cell lung cancer progression

Albrecht Schwab, Luca M. Todesca, Emma Bulk

Universität Münster, Institut für Physiologie II, Münster, Germany

K_{Ca}3.1 channels play an important pathophysiological role in non-small cell lung cancer (NSCLC). Their overexpression and/or the hypomethylation of their promoter predict a poor prognosis of NSCLC patients. Since cancer patients usually die of the sequelae of cancer metastasis we reasoned that K_{Ca}3.1 channels must contribute to steps of the metastatic cascade. Using a combination of patch clamp, live-cell imaging and atomic force microscopy, we could show that K_{Ca}3.1 channels promote NSCLC cell aggressiveness by modulating processes such as migration, proliferation and tumor cell extravasation. Recent data show that K_{Ca}3.1 channels are not only expressed in the plasma membrane, but that they are also found in the inner membrane of mitochondria. MitoK_{Ca}3.1 channels regulate the potential of the inner mitochondrial membrane and thereby modulate ROS production. We will discuss which functional properties of NSCLC cells are regulated by this mechanism. Taken together, our findings lend support to viewing K_{Ca}3.1 channels as potential therapeutic target in NSCLC.

This work was supported by the Deutschen Forschungsgemeinschaft (Research Training Group GRK 2515, Chemical Biology of Ion Channels).

S 04-05
Endolysosomal ion channels in lung physiology and pathophysiology

Christian Grimm

LMU University of Munich, Pharmacology, Munich, Germany

Intracellular ion channels in lysosomal and endosomal organelles are gaining more and more traction in academia and industry. Research on members of the TRP (transient receptor potential) family of non-selective cation channels has been awarded with the Nobel Prize in Medicine/Physiology in 2021. The TRPML channels or mucolipins are members of the TRP channel family but in contrast to most other TRP channels they reside in endosomal and lysosomal membranes. Mutations in TRPML1 in humans are causative for the neurodegenerative lysosomal storage disorder mucolipidosis type IV while mutations in TRPML3 in mice cause deafness and circling behaviour. Recently (Spix et al., 2022) it could be shown that knockout of the Trpml3 gene in mice exacerbates the emphysema/COPD phenotype in elastase treated mice and that TRPML3 is critically involved in the endocytosis/reuptake of MMP12 from broncho-alveolar fluid. MMP12 has long been known as critical factor in emphysema/COPD development and MMP12 polymorphisms in humans are associated with emphysema/COPD. Here we present recently published and unpublished data on the role of endolysosomal cation channels in lung physiology and pathophysiology. We postulate clinical relevance of TRPMLs in lung pathophysiology and suggest these channels as novel pharmacological targets for lung disease therapy

Spix, B., Butz, E.S., Chen, C.-C., Scotto Rosato, A., Tang, R., Jeridi, A., Kudrina, V., Plesch, E., Wartenberg, P., Arlt, E., Briukhovetska, D., Ansari, M., Güñes Güñsel, G., Conlon, T.M., Wyatt, A., Wetzel, S., Teupser, D., Holdt, L.M., Ectors, F., Boekhoff, I., Boehm, U., García Añoveros, J., Saftig, P., Giera, M., Kobold, S., Schiller, H.B., Zierler, S., Gudermann, T., Wahl-Schott, C., Bracher, F., Yildirim, A.Ö., Biel, M., Grimm, C. # (2022) Lung emphysema and impaired macrophage elastase clearance in mucolipin 3 deficient mice. Nature Commun. 13:318.

Grimm, C., Cuajungco, M.P., van Aken, A.F.J., Schnee, M., Jörs, S., Kros, C.J., Ricci, A.J., Heller, S. (2007) A helix-breaking mutation in TRPML3 leads to constitutive activity underlying deafness in the varitint-waddler mouse. PNAS 104:19583-19588.

Chen, C.-C.,Keller, M., Hess, M., Schiffmann, R., Urban, N., Wolfgardt, A., Schaefer, M., Bracher, F., Biel, M., Wahl-Schott, C., Grimm, C.# (2014) A small molecule restores function to TRPML1 mutant isoforms responsible for mucolipidosis type IV. Nature Commun. 5:4681.

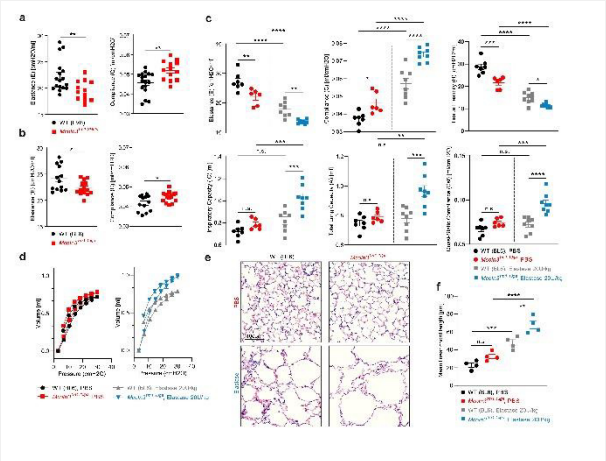

Lung phenotype in TRPML3 knockout mice

S 05 | Decoding the fine control of interneurons in behavior

S 05-01
The role of dentate gyrus interneuron types in pattern separation

Marlene Bartos

University of Freiburg, Physiology I, Freiburg, Germany

The hippocampus is the brain's center for episodic memories about our life. Its subregions, the dentate gyrus (DG), CA3, 2, and 1, are differentially involved in the encoding and recall of episodic memories. While hippocampal principal cells represent episodic features like movement, space, and context, much less is known about the role of GABAergic interneurons (IN) in regulating information processing. We use two-photon calcium imaging of parvalbumin (PV)- and somatostatin (SOM)-expressing INs in the DG, CA3/2, and 1 of head-fixed mice during foraging in virtual environments. Throughout hippocampal subfields, both IN-types show moderate spatial tuning. PV-INs increase their activity with running-speed and reduce it in novel environments. SOM-INs displayed a dichotomy: CA1-3 SOM-INs behaved similar to PV-INs, but in the DG, their activity increase during immobility and in novel environments. Congruently, inhibition of DG SOM-INs with h4MDi designer receptors (DREADDs) caused increased activation in novel environments and decreased context selectivity of DG granule cells (GC), while suppression of DG PV-INs had opposite effects, particularly in familiar environments. Our data indicate a new form of novelty-dependent, dynamic routing of information through hippocampal subfields tailored to cognitive demands and controlled by distinct inhibitory circuits.

S 05-02
Long-term stable and context specific spatial representation in somatostatin interneurons and granule cells of the dentate gyrus

Antje Kilias, Marlene Bartos

University of Freiburg, Institute for Physiology I, Freiburg, Germany

Memories associating personal experiences and places can be recalled even after extended periods of life time. The identity of their long-term storage sites is, however, controversially discussed. Despite the current prevailing theory that episodic memories are fully reallocated to cortical areas after an initial encoding phase within the hippocampus, lesion studies suggest that memories might be partially retained within the hippocampus. Recordings of hippocampal activity have ruled out CA1-3 as potential storage sites. We therefore hypothesized that sparsely active and spatially tuned DG granule cells (GCs) efficiently store and retrieve episodic memories over extended live spans. Furthermore, somatostatin-positive interneurons (SOM-IN) control the dendritic inputs from EC to GCs and might therefore play a crucial role in stabilizing long-term memories.

We employed two-photon *in vivo* calcium imaging of GCs and SOM-INs in mice navigating through virtual environments to investigate the formation, discrimination and recall of spatial memories. We show that formation and stabilization of spatial maps representing novel environments emerge in GCs over the course of 4-5 subsequent days. After map formation, representations remain remarkably stable, with individual GCs even maintaining their place field characteristics for up to 90 days. Artificial increase in GCs excitability using depolarizing DREADDs created novel place cells but their reactivation on subsequent days did not result in the stabilization of their place fields or substantial enlargement of map representations, suggesting a tight inhibitory control of place field formation.
In agreement with this we found that SOM-IN form context specific spatial maps although with lower spatial resolution and stability. The observed map stability in both DG populations was substantially higher than of place maps formed by CA1 pyramidal cells. CA1 maps emerge on the first day of exposure but become progressively dissimilar over days.
Thus, we propose that GCs and SOM-IN in the DG interact in forming long-lasting, highly stable and context-specific ensembles and that this is an important requirement for long-term storage of spatial and contextual memories.

S 05-03
Cortical Vasoactive Intestinal Polypeptide (VIP)-expressing Interneurons and the Broadcasting of Salience

Francesco Ferraguti, Enrica Paradiso, Arnau Ramos-Prats

Medical University of Innsbruck, Pharmacology, Innsbruck, Austria

Adaptive behavior critically depends on the detection and attribution of salience. The anterior insular cortex (aIC) has long been proposed as a key player in the detection of behaviorally relevant stimuli, as part of the brain system known as the “salience network”. However, to date, little is known about the contribution of aIC interneurons to the processing of salient stimuli. Based on a multidisciplinary approach including whole-brain connectivity tracing, imaging of neural calcium dynamics and optogenetic modulation in freely moving mice across different experimental paradigms, we propose a role for vasoactive intestinal polypeptide-expressing (VIP+) interneurons in the aIC in mediating adaptive behaviors in response to salient events of both aversive and positive nature. Our findings enlighten novel cellular mechanisms underlying salience processing in the aIC and show that VIP+ interneurons are centrally positioned within the salience network to participate to the broadcasting of salience.

This work was supported by the Austrian Science Fund grants F44-17-B23 and W012060.

S 05-04
Bi-directional communication between oligodendrocyte precursors and interneurons defines interneuron activity and cognition

Xianshu Bai

University of Saarland, Molecular Physiology, Homburg, Germany

Question
Cortical neural circuits are complex but very precise networks of balanced excitation and inhibition (E/I). Yet, the molecular and cellular mechanisms that form the E/I balance are just beginning to emerge. Cortical inhibition is mainly achieved by GABAergic interneurons. Emerging body of evidence suggests that oligodendrocyte precursor cells (OPCs) modulate interneuron activity. However, whether and how $GABA_BRs$ of OPCs are involved in this process is yet unknown.
Methods
NG2-$CreER^{T2}$ x $GABA_{B1}^{fl/fl}$ mice were used to conditionally knock out (cKO) $GABA_B$ receptors specifically from OPCs. Interneuron density and myelination were analysed by immunostaining for parvalbumin (PV), SMI 312 and myelin oligodendrocyte glycoprotein (MOG) in the medial prefrontal cortex (mPFC). Interneuronal activity was assessed by electrophysiological recording combined with immunostaining for vesicular GABA transporter (vGAT) or cFos. To assess the impact of circuit dysregulation in the mutant mice, we performed electroencephalography (EEG) recording and social cognitive behaviour tests.

Results

In the mPFC of cKO mice, OPC differentiation and myelination were reduced. By performing triple immunostaining for PV, SMI312 and MOG, we found that hypomyelination occurred mainly in PV^+ interneurons. This change was due to suppressed interneuron activity already at 2w, as shown by vGAT, cFos immunostaining and electrophysiological analysis in the cKO mPFC. Consequently, OPCs received less GABAergic input and committed less differentiation. In addition, we found that interneuron hypoactivity was associated with their supernumerary population. This was due to reduced TWEAK (TNF-like weak inducer of apoptosis, also known as Apo3l) release from cKO OPCs during development. Since TWEAK-releasing OPCs specifically induced interneuron apoptosis, the E/I balance in the cKO mPFC was disturbed. These physiological and morphological changes were accompanied by a severe deficit in the social cognitive behaviour of the mutant mice.

Conclusions

Our findings uncover a bidirectional communication between interneuron and OPC. During development, OPCs sense GABA via $GABA_BR$ and release TWEAK to optimize interneuron population and function, which is pivotal for interneuron myelination and network function in mPFC.

Deutsche Forschungsgemeinschaft (SPP 1757 and SFB 894 to F.K.; FOR2289 to F.K. and A.S.; SPP1757 Young Investigator grant to X.B.), the BMBF (EraNet-Neuron, JTC2014: BrIE to F.K.), the European Commission (H2020-MSCA-ITN-2016 EU-GliaPhD to F.K.), the Romanian UEFISCDI (PCE 227 to F.K.) and University of Saarland (HOMFORexzellent2017 and NanoBioMed Young Investigator grant 2021 to X.B.).

S 06 | Artificial Intelligence in Physiology… Status, Challenges, Perspectives

S 06-01
AI in Clinical Brain Research

Moritz Seiler

Berlin, Germany

In my talk "AI in Brain Research", I will show how machine and deep learning methods can be used to diagnose neurological and psychiatric diseases based on brain MRI data in combination with other data, and will discuss current challenges including robustness, explainability, and confounding variables.

S 06-02
Photonic Data Science: Linking vibrational spectral data to (bio-)medial information using machine learning and chemometrics

Thomas Bocklitz[1]

[1] University Bayreuth, Artificial Intelligence in Spectroscopy and Microscopy / Institute of Computer Science, Bayreuth, Germany
[2] Leibniz Institute of Photonic Technology, Photonic Data Science, Jena, Germany
[3] Friedrich Schiller University, Photonic Data Science / Institute of Physical Chemistry (IPC) and Abbe Center of Photonics (ACP), Jena, Germany

Question

Optical measurement techniques are applied in various disciplines like life science and medicine. This rise of applications of photonic technologies is based on an improvement of the measurement methods and setups, leading to larger datasets, but also to the development of data science methods leading to the possibility to analyze these larger datasets. Finally, the extraction of high-level (bio-medical) information from subtle differences in the (bio-medical) photonic data can be performed using these data science methods. Thereby, the extracted high-level information depends on the task and the sample, e.g., tissue types, disease states and/or other properties of the samples are examples of high-level information in the bio-medical domain.

Methods

Photonic measurement techniques which are often used for biomedical samples are vibrational spectroscopic techniques like Raman spectroscopy and multi-contrast microscopy. These measurement methods feature several advantages because vibrational fingerprints are measured in a non-destructive manner. To extract the maximal amount of information from these vibrational fingerprints, the whole data life cycle of the spectroscopic data including data generation, data modelling and data archiving need to be studied in a holistic way. Especially, the experimental design, the sample size planning, the data pre-treatment, the data pre-processing, chemometric and machine learning based data modelling, model transfer methods and transfer learning are relevant, and must be combined in a data pipeline, which standardizes the vibrational data and extracts reliable high-level information.

Results

In this contribution we will present our studies to construct a standardized data analysis pipeline for bio-medical Raman spectra [1] including artificial intelligence (AI) based data models to allow the extraction of diagnostic relevant information. Besides this, we will present studies to generate artificial staining using non-linear multi-contrast microscopy and deep learning techniques [2].

Conclusions

With the use of photonic data science, optical measurements can be used to extract bio-medical information in a reliable and robust manner. This information can be used afterward for diagnostics and prognostics.

This work is supported by the BMBF, funding program Photonics Research Germany (FKZ: 13N15466, 13N15706, 13N15710) and is integrated into the Leibniz Center for Photonics in Infection Research (LPI). The LPI initiated by Leibniz-IPHT, Leibniz-HKI, UKJ and FSU Jena is part of the BMBF national roadmap for research infrastructures.

References

[1] S. Guo, J. Popp, and T. Bocklitz, "Chemometric Analysis in Raman Spectroscopy: from Experimental Design to Machine Learning based Modelling," Nature protocols, vol. 16, no. 12, pp. 5426–5459, 2021, doi: 10.1038/s41596-021-00620-3.

[2] P. Pradhan, et al., Thomas Bocklitz, "Computational tissue staining of non-linear multimodal imaging using supervised and unsupervised deep learning," Biomedical Optics Express, vol. 12, no. 4, pp. 2280–2298, 2021, doi: 10.1364/BOE.415962.

S 06-03
Explainable AI and its application to molecular data

Grégoire Montavon[1]

[1] *Freie Universität Berlin, Mathematics and Computer Science, Berlin, Germany*
[2] *BIFOLD - Berlin Institute for the Foundations of Learning and Data, Berlin, Germany*

Explainable AI is a recent development in machine learning that brings transparency into complex ML black-boxes. Such transparency enables us, among others, to verify the inner-workings of an ML model and to verify that it relies on decision strategies that the user would consider meaningful. Explainable AI has a further use: Applied in combination with well-trained ML models, it provides a novel tool for data analysis, allowing for the uncovering of complex nonlinear relations between the multiple variables of a dataset.

In the first part of the talk, I will present an Explainable AI technique called Layer-wise Relevance Propagation (LRP) that can efficiently and robustly identify input features of an ML model that are relevant for its predictions. I will then present an application of LRP to molecular data, where our aim is to extract complex relations between molecular features. Unlike simple correlation approaches, our approach based on LRP enables us to extract relations at an instance-level or a subgroup level, thereby allowing for the production of organ-specific insights from a multi-organ dataset.

In the second part of this talk, I will present recent technical developments of Explainable AI that broaden its practical usefulness by generating more sophisticated and more informative explanations for a broader range of ML models. Specifically, I will present extensions of Explainable AI beyond classification models, higher-order Explainable AI, and a recent approach to disentangle explanations into multiple components.

S 06-04
In the Scientific Method we Trust: A Hypothesis-centric Approach to Artificial Intelligence in Biomedicine

Axel Mosig[1], Florian Boge[2]

[1] *Ruhr University Bochum, Center for Protein Diagnostics, Bochum, Germany*
[2] *TU Dortmund, Institute for Philosophy and Political Science, Dortmund, Germany*

Question

Explainability has been discussed as an important cornerstone of transparent and trustworthy AI [1] especially in high-stakes fields like medicine. In this connection, it is striking and has been criticized [2] that currently dominant practices of explanation in the field of eXplainable Artificial Intelligence (XAI) are expert-centric: Many explainability methods are post-hoc and associate an interpretable representation to a given Machine Learning (ML) output that must then be assessed by a human expert. But in science more generally, we do not rely on expert judgement as the ultimate arbiter for the quality of an explanation: Proposed explanations have to face the tribunal of experience in order to count as scientific and credible [3]. In other words, they need to have testable consequences.

Methods

In recent work [4], one of us has introduced the framework of Falsifiable eXplanations for Artificial Intelligence (FXAI), wherein explanations are required to correspond to falsifiable hypotheses in the sense of empirical science. FXAI thus addresses the missing link between data-centric machine learning and the deductive aspects of the scientific method.

We here elaborate on central aspects of FXAI, with a focus on medical applications, and address their implications for the trustworthiness of ML-systems. In particular, we argue that some core problems of XAI arise from how ML and its outcomes relate -- or fail to relate -- to evidence about physical reality. As such, the predominant problems are not exclusively computational but of a fundamental, philosophical nature.

Results and Conclusions.

We present two applications of FXAI in the identification of patterns of disease related to colorectal carcinoma subtypes and Alzheimer's disease. Finally, we consider the impact of experimental testability of explanations on trustworthiness.

References

[1] Ghassemi M, Oakden-Rayner L, Beam AL 2021, The false hope of current approaches to explainable artificial intelligence in health care. The Lancet Digital Health, 3(11):e745–e750

[2] Kundu S 2021, AI in medicine must be explainable. Nature medicine, 27(8):1328–1328

[3] Douglas HE 2009, Reintroducing prediction to explanation. Philosophy of Science, 76(4):444–463

[4] Schuhmacher D et al 2022, A framework for falsifiable explanations of machine learning models with an application in computational pathology. Medical Image Analysis, 82:102594

S 06-05
The ethics of AI in medicine: From a local to a global context, and back

Tijs Vandemeulebroucke

University of Bonn, Bonn Sustainable AI Lab, Institut für Wissenschaft und Ethik, Bonn, Germany

The use of artificial intelligence (AI) has gained tremendous attention in society due to publicly available systems such as ChatGPT, LaMDa etc. Before this public attention, AI was already being introduced into different medical and healthcare settings in the form of medical imaging, recommender systems, robotics, support in administration, etc. When one takes into account all the different suggested medical and healthcare settings in which AI could be implemented, it seems that the possibilities are limitless.

In this presentation I will argue that that this perceived limitlessness of AI should be questioned on grounds of its impact on natural environments all over the world and as such, indirectly, its impact on the health of people all over the world. In this presentation I will first introduce some applications of AI in medical and healthcare settings and present some of the ethical tensions these applications can cause.

After, I will present one bioethical approach, a principlist approach, that could guide us through these tensions. Finally, I will argue that our current view on the ethical tensions caused by the application of AI in medical and healthcare settings and the described principlist approach are too locally oriented and as such miss important ethical tensions that play out on a global level. Hence, a global bioethics approach to AI in medical and healthcare settings will be presented, an approach which takes into account the pressure AI puts on global natural environments and the people dependent on these environments. In the end, this presentation will make clear that the question we need to be able to answer is "Who is the patient when we are speaking about implementing and using AI in medicine and healthcare?"

S 07 | Cellular Communications: When inflammation meets thrombosis

S 07-01
Signaling mechanisms of the hemostatic system

Wolfram Ruf

Johannes-Gutenberg-University Medical Center, Center for Thrombosis and Hemostasis, Mainz, Germany

The hemostatic system has essential roles in anti-microbial host defense and tissue repair after injury. Coagulation activation in response to endogenous and exogenous danger signals paves the way for fibrin deposition and platelet activation that engage in multiple interactions with cells of the innate immune system leading to thrombo-inflammation. In this context, signaling of coagulation protease through the G protein-coupled protease activated receptors (PARs) emerged as crucial regulators of toll-like receptor dependent macrophage and dendritic cell differentiation and polarization. In addition to liver synthesized coagulation factors circulating in the blood, our recent studies have uncovered new regulatory roles for immune cell-expressed coagulation proteases in autocrine PAR signaling involved in tissue-specific inflammation and autoimmunity. This presentation will focus on interactions of innate immune and coagulation signaling in inflammation, viral infection and autoimmune disease and discuss therapeutic implications of specific targeting of coagulation receptors.

S 07-02
Inflammation and thrombosis, translational perspective

Thomas Renné

University Medical Center-Hamburg (UKE), Institute of Clinical Chemistry and Laboratory Medicine (O26), Hamburg, Germany

Combinations of proinflammatory and procoagulant reactions are the unifying principle for a variety of disorders affecting the cardiovascular system. The plasma contact system is a plasma protease cascade initiated by factor XII (FXII) that activates the proinflammatory kallikrein-kinin system and the procoagulant intrinsic coagulation pathway. Anionic surfaces induce FXII zymogen activation to form proteolytically active FXIIa. Bacterial surfaces also have the ability to activate contact system proteins, indicating an important role on host defense using the cooperation of the inflammatory and coagulation pathways. Recent research has shown that the inorganic polymer polyphosphate exposed by procoagulant platelets activates FXII *in vivo* and can induce coagulation in pathological thrombus formation. Experimental and clinical studies have shown that interference with FXII and polyphosphate provides thromboprotection without a therapy-associated increase in bleeding renewing interest in the FXIIa-driven intrinsic pathway of coagulation as a therapeutic target. A key aspect of the presentation will be analysis of common principles, interactions and cross-talk between coagulation and inflammation, to identify novel therapeutic targets. Elucidating the polyphosphate initiated FXII-driven contact system offers the exciting opportunity to develop strategies for safe interference with both thrombotic and inflammatory diseases.

S 07-03
Inflammation-induced leukocyte extravasation occurs at specific hotspot at the vascular wall.

Jaap van Buul

Amsterdam UMC, Medical Biochemistry, Amsterdam, Netherlands

Leukocytes leave the vessel wall to clear local infections. They efficiently cross the endothelial inner layer of the vessel wall without disrupting vascular homeostasis. Moreover, when leukocytes cross the endothelial lining, they give the impression that this occurs at predefined places in the endothelial lining. Some locations even favor the migration of multiple leukocytes that breech the endothelium in rapid succession. We and others have identified such exit sites as transendothelial migration (TEM) hotspots. These hotspots occur in *in vivo* as well as *in vitro* and suggest that this is regulated in a strict local manner. Indeed, we have identified some of the important players in this process, however, the exact rules of how this is orchestrated are not completely understood. In this presentation, I will focus on these specific transmigration routes of leukocytes and how they determine where to leave the vasculature. These findings may have a great clinical impact as it may be possible to steer specific exiting of the leukocytes to regions of infections more efficiently.

S 07-04
New insights into the role of hemostatic proteases in lung diseases - translational approach

Malgorzata Wygrecka

Justus-Liebig University, Center for Infection and Genomics of the Lung, Giessen, Germany

Accumulating evidence suggests that activation of the alveolar coagulation cascade may play a role in the pathogenesis of lung diseases. Hypercoagulability observed under these conditions arises from the imbalance between locally produced pro- and anti-coagulant factors, in combination with leakage of plasma proteins into the alveolar space. Increased levels and activity of proteins belonging to the extrinsic blood coagulation pathway such as tissue factor, factor VII, or factor X, in combination with suppressed activity of urokinase, due to high expression of plasminogen activator inhibitor-1, are major factors that are responsible for the interstitial and intraalveolar accumulation of fibrin. Although fibrin is required for reparative processes and normal wound healing, persistent and excessive deposition of extravascular fibrin is thought to contribute to the pathomechanism of lung diseases, in several ways. For instance, fibrin may serve as a reservoir of profibrotic growth factors and as a provisional matrix on which (myo)fibroblasts migrate, proliferate and produce collagen. In addition, fibrin can incorporate and thus impair function of pulmonary surfactants leading to atelectasis and loss of lung function. Despite these profibrotic activities of fibrin, numerous gain-of-function and loss-of-function approaches revealed no benefit of the fibrin formation blockage in lung injury models suggesting that cellular rather than pro-/anti-coagulant effects of hemostatic proteins might contribute to the development of lung diseases. In line with this contention, numerous studies demonstrated that hemostatic factors promote cell proliferation and differentiation, extracellular matrix production, and cytokine release. A potential role of cellular activities of hemostatic proteins in the pathogenesis of lung diseases is further underscored by the results showing that direct inhibition of their receptors confers protection in animal models of acute and chronic lung injury. Although the majority of preclinical studies highlighted extrinsic blood coagulation factors and their receptors as potential therapeutic targets, recent studies reported that factors belonging to the intrinsic blood coagulation pathway may also serves as promising drug targets in lung disease scenarios. Here, factor XII (FXII) gained particular attention. FXII stands at the crossroads of coagulation and inflammation, and, in addition, it regulates a number of cellular activities. Its potential clinical use is further highlighted but the findings demonstrating a dispensable role of FXII in physiologic hemostasis. The talk will focuses on non-classical, intriguing functions of coagulation proteases in lung diseases and will highlight their path forward to the clinical development.

S 07-05
TGF-beta driven thromboinflammation and fibrosis: importance for Chronic Thromboembolic Pulmonary Hypertension

Katrin Schäfer

University Medical Center Mainz, Department of Cardiology, Cardiology I, Mainz, Germany

Endothelial cells line the inner layer of all blood vessel and participate in many physiological functions. In the quiescent state, endothelial cells express factors to prevent leucocyte adhesion, platelet activation or blood clot formation. Haemodynamic, hypoxic or metabolic stressors impact on endothelial cells and affect their gene expression and state of differentiation. Endothelial dysfunction is a major driver of vascular inflammation and atherosclerosis. The imbalance of pro- and anti-thrombotic factors expressed on activated endothelial cells favours thrombus formation, both in the arterial and the venous system, but also plays a role in thrombus resolution and remodelling. Notably, endothelial cell-poor, fibrotic thrombi obstruct the pulmonary artery lumen in patients with Chronic Thromboembolic Pulmonary Hypertension (CTEPH), a rare and progressive pulmonary vascular disease leading to (right) heart failure and death if left untreated. In two translational studies, we could show the importance of antiangiogenic growth factors, that are transforming growth factor beta (TGFβ) and angiopoietin-2, during venous thrombus resolution in mice and in patients with CTEPH. Microarray analysis of endothelial cells outgrown from pulmonary endarterectomy specimens confirmed misregulated genes in pathways involved in extracellular matrix organisation and degradation or genes involved in collagen formation, including factors downstream of TGFβ. Spatial laser microdissection followed by nCounter gene expression analysis and immunohistochemistry of tissue microarrays localised the potential disease candidate to vessel-rich regions. Importantly, plasma levels of misregulated endothelial factors were elevated in CTEPH patients and decreased after surgical removal of the thrombofibrotic material. Proof-of-concept studes using lentiviral overexpression in human pulmonary artery endothelial cells phenocopied the gene expression patterns seen in patient endothelial cells. Taken together, our findings in cultivated cells, patient material and transgenic mice with cell-specific deletion of antiangiogenic or profibrotic factors support the central role of endothelial cells as mediators of thrombus revascularisation and resolution.

S 08 | Synaptic mechanisms of autoimmune encephalitis

S 08-01
Anti-NMDAR autoantibodies disrupt hippocampal structural plasticity and place cell dynamics

Sabine Liebscher[1,2]

[1] *University hospital Munich, Ludwig-Maximilians University Munich, Institute of Clinical Neuroimmunology, Martinsried, Germany*
[2] *University hospital Cologne, Dept. of Neurology, Cologne, Germany*

Anti-NMDA receptor (NMDAR) autoimmune encephalitis is a severe immunological condition, caused by autoantibodies (abs) targeting subunits of the NMDA receptor. The disease is characterized by a plethora of psychiatric and neurological deficits, most prominently including schizophrenia-like symptoms and memory/ cognitive dysfunction. The neural and circuit mechanisms giving rise to the complex symptoms typical of NMDAR autoimmune encephalitis, remain poorly understood. To address this aspect, we chronically assessed structure and function of neuronal subtypes in the CA1 region of the hippocampus, a region that displays the most intense auto-antibody binding in the brain, in mice icv infused with anti-NMDAR. Exposure to NMDAR autoantibodies rendered dendritic spines, the structural of postsynapses, more instable, as indicated by an increased turnover rate of these synaptic structures. To probe the impact of neuronal function, we subjected mice to a spatial learning task in a virtual reality. NMDAR abs infused mice displayed clear memory deficits in the VR task. Surprisingly, at the neuronal level this memory deficit was accompanied by compromised place cell dynamics, rendering them more rigid.
We thus believe that disrupted dynamics of spatial representations could amongst others represent a neural correlate of memory and cognitive deficits typical of anti-NMDAR autoimmune encephalitis.

S 08-02
Blocking human N-methyl-D-aspartate receptors within seconds with a monoclonal autoantibody

Manfred Heckmann

Julius-Maximilians-University Würzburg, Department of Neurophysiology, Würzburg, Germany

Autoantibodies against ionotropic N-methyl-D-aspartate receptors (NMDARs) from patients with autoimmune encephalitis are pathogenic and induce typical disease signs upon passive-transfer. Receptor internalization is a critical long-term antibody effect in this disease. Here we focus on direct and acute effects of a specific patient autoantibody on NMDAR function. Acute effects are relevant since receptors could be directly blocked, modulated or even activated by binding an antibody. We performed cell-attached single channel recordings in human embryonic kidney cells transfected with the GluN1 and GluN2A subunit of the NMDAR and investigated direct effects of a specific and well-characterized monoclonal patient autoantibody (immunoglobulin G #003-102) against the amino-terminal domain of the glycine-binding GluN1 subunit of the receptors. Antibodies were applied via recording electrodes and subsequent receptor activity was monitored for 300 seconds. Immunoglobulin G #003-102 reduced simultaneous receptor openings significantly compared to the control immunoglobulin G (P = 0.038) at low concentrations of glutamate and glycine (median 2 versus 3 in 23 measurements with immunoglobulin G #003-102 and 30 controls, respectively). Similarly, at high concentrations of glutamate and glycine, simultaneous receptor openings were highly significantly reduced with patient-derived compared to control antibodies (P = 0.003). However, antigen-binding fragments of immunoglobulin G #003-102 did not reduce the duration of individual receptor openings. In conclusion acute binding of monoclonal immunoglobulin G #003-102 rapidly blocks NMDARs and thus is functionally relevant prior to receptor internalization. Complete immunoglobulin G is necessary for this acute blocking effect and we propose the design of engineered monovalent immunoglobulin G as a new strategy to shield pathogenic epitopes on NMDARs.

S 08-03
Pathogenic effects of $GABA_B$ receptor autoantibodies on neuronal signaling and memory consolidation

Josefine Sell[1], Eleonora A. Loi[1], Vahid Rahmati[1], Hans-Christian Kornau[2,3], Dietmar Schmitz[2,3], Christian Geis[1]

[1] *Jena University Hospital, Section Translational Neuroimmunology, Jena, Germany*
[2] *Charité - Universitätsmedizin Berlin, Neuroscience Research Center, Berlin, Germany*
[3] *German Center for Neurodegenerative Diseases (DZNE), Berlin, Germany*

Question

$GABA_B$ receptor ($GABA_BR$) encephalitis is an autoimmune disorder with immunoglobulin G (IgG) antibodies targeting pre- and postsynaptic $GABA_BRs$. Patients suffer from severe memory dysfunction and epileptic seizures. $GABA_BRs$ are G-protein coupled receptors and mediate complex synaptic signaling in glutamatergic as well as GABAergic neurons by regulating presynaptic neurotransmitter release and postsynaptic excitability. Here we aimed to investigate the pathophysiological effect of human serum antibodies on neuronal synaptic transmission, structural changes at the synapse and memory.

Methods

Purified patient-derived immunoglobulin G antibodies (Control- and anti-$GABA_BR$-IgG) were used in a mouse model of continuous 14-day cerebroventricular infusion via osmotic pumps. To investigate $GABA_BR$ mediated regulation of synaptic transmission, somatic patch-clamp recordings of CA1 pyramidal neurons were performed and special stimulation protocols were applied on afferent fibers. To reveal IgG-effects on $GABA_BR$ function, either the $GABA_BR$ agonist baclofen or the antagonist CGP55845 was applied by bath perfusion. Memory and cognition was examined via novel object recognition (NOR) and novel object location (NOL) test.

Results

$GABA_BR$ antibodies affected excitatory synaptic transmission and short-term plasticity of heteroreceptors, as they reduced eEPSC amplitudes and the agonist effect of baclofen onto paired pulse ratios. Furthermore, they block presynaptic autoreceptors on inhibitory synapses, leading to less depression during repetitive IPSC stimulation. In contrast, postsynaptic $GABA_BR$-activated K^+-currents and action potential firing is not influenced by patient's IgGs. Evaluation of cognitive function trough behavioral paradigm suggests an influence of the anti-$GABA_BR$-IgG on the consolidation and maintenance of contextually precise memory, but not for the initial encoding of the memory.

Conclusions

Our results provide evidence that $GABA_BR$ antibodies antagonize the receptor preferably on presynaptic auto- and heteroreceptors, but have less direct pathogenic effect on postsynaptic $GABA_BR$-downstream signaling. These changes may contribute to severe neuronal dysfunction as the basis of memory dysfunction and increased seizure susceptibility.

References

[1] Geis, C, Planaguma, J, Careno, M et al., 2019, 'Autoimmune seizures and epilepsy', *J Clin Invest*; 129(3):926-940.

[2] Lancaster, E, Lai, M, Peng, X et al., 2010, 'Antibodies to the GABAB receptor in limbic encephalitis with seizures: case series and characterisation of the antigen', *Lancet Neurol*; 9(1):67-76.

[3] Gerrard, LB, Tantirigama, MLS, Bekkers, JM, 2018, 'Pre- and Postsynaptic Activation of $GABA_B$ Receptors Modulates Principal Cell Excitation in the Piriform Cortex', *Front Cell Neurosci*, 12:28.

S 08-04
Glycine receptor autoantibodies and their pathological effects on glycinergic neurotransmission

Carmen Villmann

University Hospital, Institute for Clinical Neurobiology, Würzburg, Germany

Stiff Person Syndrome (SPS) and progressive encephalomyelitis with rigidity and myoclonus (PERM) are rare neurological disorders of the central nervous system. 20% of SPS patients harbour autoantibodies (aAb) against the glycine receptor (GlyR) while in PERM the number is about 50% of patients. In the adult organism, GlyRs are formed by α and β subunits with GlyRβ being essential for the synaptic localization of the inhibitory ion channels. Binding of GlyR aAbs to its target has so far been shown exclusively to GlyRα subunits. As pathological mechanisms of the GlyR aAbs, receptor crosslinking followed by internalisation and most likely degradation, complement activation, and direct blocking effects at the functional level have been described. Moreover, our group could demonstrate a significant disturbance in the escape behavior of zebrafish larvae following injection with purified patient IgG. The generated impaired escape response in the animal model is compatible with stiffness and immobility in humans.

In the GlyRα1 subunit, a common N-terminal binding epitope for the aAbs was identified which is localized at the surface of the protein and thus easily accessible by the aAbs. The extracellular N-terminal domain of the GlyRα1 subunit shares a high degree of sequence homology with GlyRβ making it not unlikely that GlyRβ-specific autoantibodies exist and contribute to the disease pathology. We investigated serum from 58 patients for aAbs with specificity to the GlyRβ subunit. Various cellular approaches were used to define specificity. Most strikingly, aAbs that bind exclusively to GlyRα1 differ in functional consequences for the ion channel from autoantibodies targeting GlyRβ. Altogether, physiological measurements exhibited that GlyRβ aAbs antagonize inhibitory neurotransmission by affecting receptor function rather than localization.

This work is supported by the Germany Research Foundation, SYNABS FOR3004 (VI586).

S 08-05
Human monoclonal LGI1 autoantibodies increase neuronal excitability

Dietmar Schmitz

Charité, Neuroscience Center, Berlin, Germany

The author has objected to a publication of the abstract.

S 08-06
Effects of anti-LGI1 human monoclonal antibodies on mouse behavior, ultrastructure,and ion channel distribution at synapses and axon initial segments

Ryuichi Shigemoto

Institute of Science and Technology Austria (ISTA), Klosterneuburg, Austria

Question
Leucine-rich glioma-inactivated 1 (LGI1) protein, a soluble secreted protein, links pre-synaptic and post-synaptic ADAM22/23 proteins across the synaptic cleft, and is also expressed abundantly at the axon initial segment in the hippocampus. Anti-LGI1 autoantibodies have been found in serum and CSF of acquired epilepsy patients with limbic encephalitis (LGI1 autoimmune encephalitis). Our question is how the LGI1 autoantibodies cause hyperexcitability in these patients.
Methods
Monoclonal LGI1 autoantibodies prepared from LGI1 autoimmune encephalitis patients were injected into the mouse hippocampus. The behavior of these animals was monitored for 48 hours, the ultrastructure of mossy fiber boutons was analyzed with electron microscopy, and the distribution of voltage-gated potassium and calcium channels on the axonal membrane was examined by freeze-fracture replica labeling.
Results
Mice injected with the LGI1 autoantibodies but not normal control human IgG showed epilepsy 1-2 days after the injection, mimicking the patient's symptoms. We found a significant decrease of synaptic vesicles in the dentate gyrus mossy fiber terminals after epileptic episodes, indicating hyperactivity of the dentate granule cells. Such epileptic episodes may be triggered by disturbances in voltage-gated ion channels at axon terminals or initial segments since human autoantibodies to LGI1 were recently shown to co-immunoprecipitate voltage-gated potassium and calcium channel subunits from rodent brain tissues. Different voltage-gated ion channels are important for maintaining homeostasis of hippocampal neuronal activities. Thus, we examine the number and density of Kv1 potassium channel subunits and Cav2.1 calcium channel subunits at synapses and axon initial segments. In the mossy fiber active zone, the density of Cav2.1 tended to decrease in the LGI1 autoantibody-injected animals, suggesting that the hyperactivity of the mossy fibers was not due to facilitated vesicular release caused by the increase of Cav2.1. The density of Kv1 subunits was very low at the active zone in both groups of animals. Immunolabeling for Ankyrin G on the replica materials clearly identified the axon initial segments. The quantification of ion channels there is ongoing.
Conclusions
Alteration of the density of ion channels may trigger hyper-excitability of neurons and could be involved in the etiology of epilepsy in the LGI1 autoimmune encephalitis. Injection of the patient's anti-LGI1 antibodies causing epilepsy in mice induced a significant reduction of synaptic vesicles in mossy fiber boutons, providing a good model for examining changes in ion channel densities at synapses and axon initial segments in the hippocampus.

This work was supported by Austrian Science Fund (FWF, I4638).

S 09 | The Tight Junction: Barrier, Channel, and More

S 09-01
How to seal tricellular corners

Mikio Furuse

National Institute for Physiological Sciences, Division of Cell Structure, Okazaki, Japan

Tight junctions (TJs), one mode of cell-cell junctions in vertebrates, play essential roles in the epithelial barrier function by regulating the passage of solutes via the paracellular pathway. In addition to TJs between adjacent cells, epithelial cells have to obliterate the extracellular space at tricellular contacts, where the corners of three cells meet, to establish full barrier function. Tricellular contacts contain specialized TJs designated tricellular TJs (tTJs), where three closely-attached vertical TJs, called central sealing elements, squeeze the extracellular space. Two types of integral membrane proteins, tricellulin and angulin family proteins, including angulin-1/LSR, angulin-2/ILDR1, and angulin-3/ILDR2, are known as molecular components of tTJs. Although the impact of tTJs in epithelial barrier function appears to be much less than bicellular TJs considering their percentage in the total paracellular pathway, human genetics and knockout mice studies have reported that the impairment of tTJ proteins causes various pathological conditions: hearing loss, renal concentrating defects, cholestasis, etc. However,

the molecular mechanism behind tTJ formation had remained largely unsolved except that angulin recruits tricellulin to tricellular contacts. Recent studies in a renal epithelial cell line MDCK using the genome editing-mediated gene disruption have clarified how angulin and tricellulin are involved in tTJ formation. Angulin plays a central role in the tricellular plasma membrane contacts independent of tricellulin. Angulin binds to ZO-1, a scaffolding protein of TJs, and recruits claudin to tricellular contacts to form central sealing elements. Meanwhile, tricellulin is required for the connection of short TJs to the central sealing elements to generate intact tTJs. In this presentation, I will report on the molecular organization of tTJs based on recent findings in cell biological studies.

References
[1] Masuda S, Oda Y, Sasaki H, Ikenouchi J, Higashi T, Akashi M, Nishi E, Furuse M. 2011. LSR defines cell corners for tricellular tight junction formation in epithelial cells. *J Cell Sci* 124:548-55.
[2] Higashi T, Tokuda S, Kitajiri S, Masuda S, Nakamura H, Oda Y, Furuse M. 2013. Analysis of the 'angulin' proteins LSR, ILDR1 and ILDR2--tricellulin recruitment, epithelial barrier function and implication in deafness pathogenesis. *J Cell Sci* 126:966-77.
[3] Oda Y, Sugawara T, Fukata Y, Izumi Y, Otani T, Higashi T, Fukata M, Furuse M. 2020. The extracellular domain of angulin-1 and palmitoylation of its cytoplasmic region are required for angulin-1 assembly at tricellular contacts. *J Biol Chem* 295:4289-4302.
[4] Sugawara T, Furuse K, Otani T, Wakayama T, Furuse M. 2021. Angulin-1 seals tricellular contacts independently of tricellulin and claudins. *J Cell Biol* 220:e202005062.

S 09-02
New molecular and functional insight into the invertebrate septate junctions

Sima Jonusaite[1,4], Nathalie Oulhen[2], Yasushi Izumi[3], Mikio Furuse[3], Gary Wessel[2], Andreas Heyland[4]

[1] *University of Kiel, Institute of Physiology, Kiel, Germany*
[2] *Brown University, Department of Molecular Biology, Cell Biology and Biochemistry, Providence, USA*
[3] *National Institute for Physiological Sciences, Division of Cell Structure, Okazaki, Japan*
[4] *University of Guelph, Department of Integrative Physiology, Guelph, Canada*

Question

Epithelia are essential for separating physiologically distinct body compartments and require effective paracellular barriers provided by the tight junctions (TJs) in vertebrates and septate junctions (SJs) in invertebrates. Unlike TJs, multiple morphological variants of SJs exist specific to different epithelia and/or phyla but the evolutionary significance of varied SJ morphology is unclear because of the paucity of information on SJ associated proteins and their functions in diverse invertebrate representatives. A number of SJ components have been identified and tested in the epithelia of insects, primarily the fruit fly *Drosophila melanogaster*, which possesses two types of SJs with complex molecular architecture. Here we explored the diversity, expression characteristics, and function of candidate SJ proteins in the epithelia of a deuterostome invertebrate, the sea urchin *Strongylocentrotus purpuratus*.

Methods

S. purpuratus v5 genome was searched for *Drosophila* SJ-associated protein orthologs and expression of key annotated genes analyzed by in situ RNA hybridization and single cell RNA sequencing analysis. Candidate SJ protein expression and subcellular localization were determined using immunohistochemistry and western blotting. SJ protein function was tested using CRISRP/Cas9 mutagenesis and vivo-morpholino (vMO)-mediated knockdown, and cell-impermeable 3-5 kDa FITC-dextran flux assay.

Results

By use of in situ RNA hybridization and scRNA-seq we found that the expression of genes encoding candidate SJ-associated transmembrane and cytoplasmic scaffold molecules was dynamically regulated during early sea urchin life stages with developmentally distinct epithelia expressing different cohorts of SJ genes. Amongst the gut-enriched genes was the expression of *S. purpuratus* homolog of *Drosophila* smooth-type SJ integral protein Mesh, required for SJ formation and macromolecule permeability in the fly's intestinal and renal systems. In the sea urchin larva, Mesh was also localized to intestinal SJs within the midgut and hindgut. Functional perturbation of SpMesh by both CRISPR/Cas9 mutagenesis and vMO-mediated knockdown revealed a breakdown in the gut-paracellular barrier in the early larvae as quantitated by increased permeability to FITC-dextran.

Conclusions

This study provides first insight into the molecular SJ complex of echinoderm epithelia and uncovers a shared function of Mesh-homologous proteins in forming intestinal barrier in invertebrates. In light of the notion that the paracellular diffusion barrier is a fundamental cellular aspect

in metazoans and that echinoderms are the deuterostome sister group of TJ-bearing vertebrates, further investigation of SJ proteins in this taxon is of great interest not only in terms of the physiology of occluding junctions, but also their evolution.

Funding from Natural Sciences and Engineering
Research Council of Canada, the National Institutes of Health (USA), the National Science
Foundation (USA), Grant-in-Aid for Scientific
Research (C) from the Japan Society for the Promotion of Science, and a Funding Program for Next Generation,
World Leading Researchers (NEXT Program) from the Japan
Society for the Promotion of Science initiated by the Council for Science
and Technology Policy.

S 09-03
Functionality of claudin-3 in proximal and distal kidney tubules

Susanne Milatz

Kiel University, Institute of Physiology, Kiel, Germany

Claudin-3 is a ubiquitously expressed component of the tight junction. In cell culture models, it has been characterized as a sealing claudin, increasing the transepithelial electrical resistance and impeding the paracellular passage of ions and other solutes. In the renal tubule, claudin-3 is expressed from the proximal straight tubule to the medullary collecting duct.
In order to unravel the function of claudin-3 in different nephron segments, where it is co-expressed with diverse other claudins, claudin-3-deficient mice and control littermates were analyzed by means of single tubule perfusion, diffusion potential measurements, urine analysis, qPCR, Western blotting and confocal microscopy.
In contrast to findings in cell culture models, absence of claudin-3 from cortical thick ascending limbs did not alter the transepithelial electrical resistance but led to a change in paracellular preferences for Ca^{2+}, Mg^{2+}, Na^{+} and Cl^{-}. Similar effects were observed in the proximal straight tubule.
In conclusion, claudin-3 might act as a modulator of paracellular ion permeability at the two main sites of paracellular Na^{+}, Ca^{2+} and Mg^{2+} reabsorption in the kidney: the proximal tubule and the cortical thick ascending limb. It increases the preference for Na^{+} and Ca^{2+} to the detriment of Cl^{-} and Mg^{2+} permeabilities.

S 09-04
Na^{+} transport is impaired via claudin-8 and ENaC dysregulation in *Campylobacter* infection.

Roland Bücker

Charité - Universitätsmedizin Berlin, Clinical Physiology / Nutritional Medicine, Medical Department of Gastroenterology, Infectious Diseases, Rheumatology, Berlin, Germany

Background
Campylobacter jejuni and *Campylobacter concisus* are bacterial human pathogens of the gut, inducing diarrhea by epithelial barrier dysfunction. However, the relation of epithelial leakage and sodium transport function during the *Campylobacter* infection is underestimated. The objective of our studies was to delineate the effects of *Campylobacter* spp. on Na^{+} transport through the epithelial Na^{+} channel (ENaC) in a colonocyte model or in colon biopsies, while characterizing in parallel the epithelial barrier by tight junction (TJ) protein analysis.
Methods
To determine ENaC activity in vitro, we used human intestinal epithelial cells HT-29/B6-GR/MR, in which glucocorticoid (GR) and mineralocorticoid receptors (MR) had been transfected. GR/MR activation is crucial for ENaC activity. In Ussing chambers, aldosterone in combination with butyrate and dexamethasone induced an amiloride-blockable short-circuit current (ΔIsc), which serves as a measure of ENaC-mediated Na^{+} absorption. ΔIsc was recorded from *C. concisus*-infected HT-29/B6-GR/MR cell monolayers. In another study, colon

biopsies were taken during endoscopy of patients acutely infected with *C. jejuni*. Again, ENaC activity was measured by the drop in ΔIsc after blockage with amiloride during aldosterone stimulation. In both studies, the TJ protein expression and localization was assessed by Western blotting and confocal laser-scanning microscopy.

Results

In HT-29/B6-GR/MR cell monolayers, *C. concisus* infection inhibited ENaC-dependent Na^+ absorption, which was reflected by a reduction in ΔIsc by 58%. In parallel, we observed that *C. concisus* induced changes of the TJ protein claudin-8 in HT-29/B6-GR/MR cell monolayers, leading to impaired retention of Na^+. In *C. jejuni*-infected colon tissues, the Na^+ malabsorption was affected to a greater extend, and parallel the changes of TJ expression were broader as claudin-2, -3, -4 and -8 were affected. Cytokine signaling responsible for changes in ENaC subunit expression were identified.

Conclusions

Impaired ENaC-mediated Na^+ absorption as cause of malabsorptive *Campylobacter* diarrhea was detected. In addition to the leak-flux type of watery diarrhea due to TJ disruption, this represents a further diarrheal pathomechanism. Our results indicate that *C. concisus* and *C. jejuni* downregulate ENaC-mediated Na^+ transport by inhibiting β- and γ- ENaC subunits via ERK signaling and mucosal cytokine induction. Remarkably, the function of the TJ protein claudin-8 is to prevent back-leakage of absorbed Na^+ from the tissue into the lumen under physiological conditions. However, under the infection with *Campylobacter*, this barrier function is weakened by downregulation and redistribution of claudin-8 off the TJ domain, which exacerbates the Na^+ loss and causes water flow into the intestinal lumen (leak-flux), adding to the malabsorptive diarrhea. Thus in *Campylobacter* infection, Na^+ retention and absorption is inhibited by claudin-8 and ENaC dysregulation.

S 09-05
Angulins and tricellulin: critical players for molecular passage in intestinal epithelia

Susanne M. Krug

Charité - Universitätsmedizin Berlin, Clinical Physiology / Nutritional Medicine, Berlin, Germany

The intestinal epithelium forms a crucial barrier that selectively allows for absorption of nutrients while preventing the passage of harmful substances. The tight junction (TJ) is an essential component of that barrier regulating paracellular permeability. While the passage of ions and small molecules is mainly regulated by proteins of the bicellular TJ, the tricellular TJ, which is formed at the contact points of three cells, appears to be critical for paracellular passage of larger molecules. Tricellulin and the angulins are the main components of tricellular TJ and have barrier-forming and stabilizing functions.

The macromolecule barrier is known to be disturbed in inflammatory bowel diseases (IBD) which are distinguished into two main forms, ulcerative colitis (UC) and Crohn's disease (CD). In UC, we found that tricellulin expression was downregulated, leading to an impaired tricellular barrier. This change in expression was regulated by a main cytokine of UC, interleukin-13, via one of its receptors, IL13Ra2 [Krug et al. 2018, Mucosal Immunol.]. In CD however, tricellulin expression was unaltered but its localization was shifted away from crypt regions towards surface epithelium [Krug et al. 2018, Mucosal Immunol.]. This redistribution of tricellulin we hypothesized to be linked to a disturbed expression of angulins. We found that angulin-1, which is known to regulate tricellulin's proper tricellular localization and in intestinal tissue is normally distributed in the lower crypts [Higashi et al. 2013, J. Cell Sci.], was indeed downregulated in CD and that this change in expression was controlled by the adipokine leptin, which is released by 'creeping fat', a characteristic of CD [Hu JCE et al. 2020, Int. J. Mol. Sci.]. This downregulation could allow the shift of tricellulin localization within the crypt as another angulin, angulin-2, that also interacts with tricellulin is located all over the crypt [Higashi et al. 2013, J. Cell Sci.] and was unaffected in IBD [Hu JCE et al. 2020, Int. J. Mol. Sci.; Hu JCE et al. 2021, BMC Gastroent.].

In conclusion, angulins and tricellulin play critical roles in regulating macromolecular passage across the intestinal epithelium, and dysregulation of these proteins can disrupt barrier function, contributing to the development of gastrointestinal disorders via enhanced luminal antigen uptake.

S 10 | Advances in the study of physiological and pathophysiological aspects of organic cation transporters

S 10-Intro
Welcome address

Giuliano Ciarimboli

Universitätsklinikum Münster, Med. Klinik D/Exp. Nephrologie, Münster, Germany

S 10-01
Organic cation transporters: from structure to function

Harald H. Sitte

Medical University of Vienna, Institute of Pharmacology, Vienna, Austria

Organic cation transporters (OCTs) facilitate the translocation of catecholamines, drugs and xenobiotics across the plasma membrane in various tissues throughout the human body. OCT3 plays a key role in low-affinity, high-capacity uptake of monoamines in most tissues including heart, brain and liver. Its deregulation plays a role in diseases. Despite its importance, the structural basis of OCT3 function and its inhibition has remained enigmatic. In my talk, I will discuss the structure of human OCT3 bound to two prototypical inhibitors, corticosterone and decynium-22. In addition, I will relate the functional characteristics of an extensive collection of human genetic variants to structural features, thereby providing a basis for understanding the impact of OCT3 polymorphisms – and show recent data on how to rescue misfolded variants from the endoplasmic reticulum.

This research was supported by the Vienna Science and Technology Fund (WWTF) [CS 15–28 033] (HHS), Austrian Science Fund (FWF) [W1232] (HHS) and [DOC33-B27] (HHS and JM), Theodor Körner Fonds 2020 (JM), Swiss National Science foundation (SNSF; grant No. 30P400PM_191032) (D.L.), The Lundbeck Foundation (R303-2018-3540, FH).

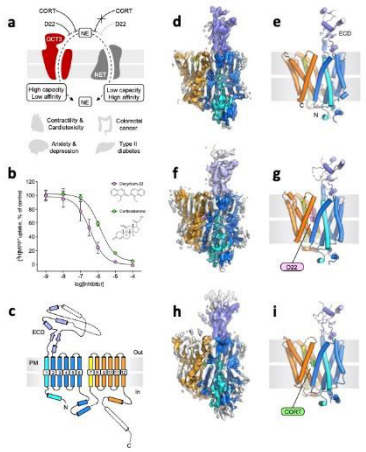

Structure and function of OCT3
a, Schematic representation of OCT3. b, OCT3 transport inhibition by decynium-22 (D22) and corticosterone (CORT). c, A scheme depicting the topology and the secondary structure elements of OCT3. d-e, The cryo-EM map (d) and model of OCT3 in nanodiscs at 3.2 Å resolution. f-g, Same as d-e, for OCT3-D22 complex at 3.6 Å resolution (D22 colored violet). h-i, Same as f-g, for OCT3-CORT complex at 3.7 Å resolution (CORT colored green).

References
[1] Khanppnavar B, Maier J, Herborg F, Gradisch R, Lazzarin E, Luethi D, Yang JW, Qi C, Holy M, Jäntsch K, Kudlacek O, Schicker K, Werge T, Gether U, Stockner T, Korkhov VM, Sitte HH. Structural basis of organic cation transporter-3 inhibition. Nat Commun. 2022 Nov 7;13(1):6714. doi: 10.1038/s41467-022-34284-8.

[2] Angenoorth TJF, Maier J, Stankovic S, Bhat S, Sucic S, Freissmuth M, Sitte HH, Yang JW. Rescue of Misfolded Organic Cation Transporter 3 Variants. Cells. 2022 Dec 22;12(1):39. doi: 10.3390/cells12010039.

S 10-02
Studying organic cation transport using kidneys on chip systems

Roos Masereeuw

Universiteit Utrecht, Utrecht, Netherlands

Adverse effects caused by exposure to foreign compounds, including drugs, often involve the kidney because of its role in maintaining body homeostasis. Early prediction of those effects, such as drug-drug interactions and nephrotoxicity, is imperative for the development of new and safe drugs by the pharmaceutical industry. Current *in vitro* assays do not accurately allow such prediction, predominantly due to inadequate preservation of the organs' microenvironment. The kidney epithelium is highly polarized, and the preservation of this is critical for optimal functioning and responsiveness to environmental signals influencing cell proliferation, migration and differentiation. This presentation will provide an overview of advances in 3D cultures of human kidney cells and organoids in microfluidics, and in particular kidney tubules, thereby improving physiological performance of the tissue. In particular, the activity of the organic cation system in these advanced *in vitro* cultures have been evaluated and will be presented. Kidney-on-a-chip platforms have great potential for drug screenings and provide novel alternative strategies for prediction of renal drug disposition and safety assessment in a human-specific context.

S 10-03
The fruit fly as a model for investigation of solute carrier transporters

Anne T. Nies

Dr. Margarete Fischer-Bosch Institute of Clinical Pharmacology, Stuttgart, Germany

Every living cell is surrounded by a selectively permeable membrane through which substances are exchanged with the environment. Transporter proteins located in the membrane mediate the uptake and efflux of physiological compounds such as amino acids, sugars, nucleosides, vitamins and trace minerals, as well as of therapeutic drugs. Membrane transporters are therefore critically involved in normal human physiology, disease susceptibility and pharmacotherapy. Solute carriers (SLCs) are a large and important superfamily of membrane transporters that are involved in these above described processes.
The organic cation transporters within the SLC22 family are known to mediate the transport of small hydrophilic cationic compounds, including many clinically relevant drugs (e.g. the H_2-receptor antagonist cimetidine and the anti-diabetic drug metformin), across the plasma membrane in a sodium- and proton- independent manner. The driving force for translocation is the concentration gradient of the compound and/or the electrical membrane potential. While OCT2 (encoded by *SLC22A2*) is most highly expressed in the kidney, the two isoforms OCT1 (encoded by *SLC22A1*) and OCT3 (encoded by *SLC22A3*) are expressed in the liver, where they are localized to the sinusoidal membrane of the hepatocytes. The function of organic cation transporters can be studied at many different levels. Using the organic cation transporters OCT1 and OCT2 as examples, I will present how the fruit fly *Drosophila melanogaster* can be used as a novel in vivo model to study function of human OCT transporters.

This work was supported by the Robert-Bosch Foundation, Stuttgart, Germany, and the Interfaculty Centre for Pharmacogenomics and Pharma Research (ICEPHA) Grant Tübingen–Stuttgart, Germany.

S 10-04
The role of lipids in the post-translational regulation and function of OCT2

Michele Visentin

University Hospital Zurich, Clinical Pharmacology and Toxicology, Zurich, Switzerland

Organic cation transporter 2 (OCT2) activity mediates the entry step of the tubular secretion of metabolism product, drugs, and reactive metabolites thereof, exposing the proximal tubular cells to transient high intracellular concentrations of a plethora of harmful molecules, thereby increasing intracellular oxidative stress, ROS production and kidney injury. Among the many changes occurring upon kidney damage, the membrane cholesterol content of the kidney parenchyma is significantly altered. Moreover, a fraction of membrane cholesterol is present in oxidized forms, mainly 7-ketocholesterol. Studies with semisynthetic membranes showed that even subtle changes in cholesterol and 7-ketocholesterol content cause marked molecular-scale biophysical perturbation of membrane structure and properties. It has been proposed that cholesterol content alterations represent adaptive changes secondary to kidney injury that serve to protect proximal tubules from subsequent ischemic or toxic damage. Consistently, we found that OCT2 function is markedly reduced when the overall cholesterol content is reduced, as well as when cholesterol is partly replaced by 7-ketocholesterol. Besides its detoxification role, OCT2 also transports precursors (e.g., choline) and cofactors (e.g., Thiamine) involved in energy metabolism, suggesting that OCT2 activity might be dependent on cellular/systemic metabolic state for rapid control of the systemic and cellular level of these nutrients. We found that OCT2 is S-palmitoylated, a reversible post-translational modification often found in metabolic proteins such as apolipoprotein B, AMP kinase, and glucose transporter 4, suggesting that OCT2 might play an important role in the regulation of the cellular/systemic homeostasis of these nutrients, and might indirectly dictate the pace of the related metabolic pathways (e.g., Kennedy pathway).

S 10-05

Species differences in organic cation transporters

Marleen J. Meyer-Tönnies, Pascale C.F. Schreier, Simon Falk, Sarah Römer, Mladen V. Tzvetkov

Institute of Pharmacology, University Medicine Greifswald, General Pharmacology, Greifswald, Germany

Organic cation transporter OCT1 (*SLC22A1*) is an uptake transporter predominantly expressed in the sinusoidal membrane of hepatocytes. It mediates the first step in hepatic metabolism of weakly basic or cationic drugs. OCT1 is polyspecific and transports a great variety of structurally diverse compounds, among them many clinically relevant drugs. The mechanism and exact amino acids involved in polyspecific substrate binding of OCT1 are not completely clear. Species differences among mammalian OCT1 orthologs are well known. Human and rodent OCT1 differ not only in their organ expression but also in 23% of their amino acid sequence (124 amino acids).

Our aim was to characterize the functional differences among mammalian OCT1 orthologs and paralogs and to utilize them to better understand the mechanisms of OCT polyspecificity. Thirteen out of 27 tested substrates showed significant differences either in transport affinity (K_M) or capacity (v_{max}) between human and mouse OCT1. Using a hypothesis-free approach, we analyzed the transport of human-mouse chimeric OCT1, which enabled narrowing down regions within the protein involved in the species-specific substrate transport. Then we used site-directed mutagenesis of the non-conserved amino acids within the narrowed down regions and were able to identify single amino acids in transmembrane helix 1 to confer the major substrate-specific differences between human and mouse OCT1. Cys/Tyr36 was identified to be responsible for the differences in fenoterol and Phe/Leu32 in trospium kinetics between human and mouse OCT1.

In addition, we extended the species spectrum by cloning and functionally characterizing dog OCT1 and OCT2 (*SLC22A2*). Comparative characterization of the transport kinetics among OCT1 orthologs of human, mouse, and dog revealed similarities and differences that were highly substrate-specific. Analyses of fenoterol and trospium transport confirmed the importance of codons 36 and 32, respectively. This approach can further be extended to other mammalian species.

OCT1 paralogs, OCT2 and OCT3 (*SLC22A3*), also showed substrate-specific differences in their transport affinity and capacity. As a next step, chimeric constructs of OCT1 and OCT2 or OCT3 will be used to identify amino acids conferring paralog differences in transport. The analyses can further be extended to combine ortholog and paralog comparisons. This approach can be combined with the recently published first cryo-EM structures of SLC transporters, OCT1, OCT2, and OCT3, to completely resolve mechanisms of OCT polyspecificity.

In conclusion, ortholog and paralog comparisons can be utilized successfully to better understand the mechanisms of OCT polyspecificity. The outlined strategies are powerful tools and can be extended to other orthologs and paralogs as needed.

S 11 | Protection of the cardiovascular system

S 11-01
NADPH oxidase is protective in carotid artery stenosis

Anja Hofmann[1], Frieda Frank[1], Steffen Wolk[1], Albert Busch[1], Anna Klimova[2], Pamela Sabarstinski[1], Michael Gerlach[3], Dmitry Egorov[4], Irakli Kopaliani[4], Sönke Weinert[5], Bianca Hamann[1], David M. Poitz[6], Coy Brunssen[7], Henning Morawietz[7], Katrin Schröder[8,9], Christian Reeps[1]

[1] University Hospital and Medical Faculty Carl Gustav Carus, Technische Universität Dresden, Division of Vascular and Endovascular Surgery, Department of Visceral, Thoracic and Vascular Surgery, Dresden, Germany
[2] Medical Faculty Carl Gustav Carus, Technische Universität Dresden, Core Unit Data Management and Analytics, National Center for Tumor Diseases Dresden, Partner Site Dresden, University Cancer Center (NCT/UCC), Dresden, Germany
[3] Medical Faculty Carl Gustav Carus, Technische Universität Dresden, Core Facility Cellular Imaging (CFCI), Dresden, Germany
[4] Medical Faculty Carl Gustav Carus, Technische Universität Dresden, Institute for Physiology, Dresden, Germany
[5] Magdeburg University, Internal Medicine, Department of Cardiology and Angiology, Health Campus Immunology, Infectiology and Inflammation, Magdeburg, Germany
[6] University Hospital and Medical Faculty Carl Gustav Carus, Technische Universität Dresden, Institute for Clinical Chemistry and Laboratory Medicine, Dresden, Germany
[7] University Hospital and Medical Faculty Carl Gustav Carus, Technische Universität Dresden, Division of Vascular Endothelium and Microcirculation, Department of Medicine III, Dresden, Germany
[8] Goethe University, Frankfurt am Main, Institute for Cardiovascular Physiology, Frankfurt am Main, Germany
[9] Frankfurt am Main, German Center of Cardiovascular Research (DZHK), partner site RheinMain, Frankfurt am Main, Germany

Carotid artery stenosis (CAS) develops from atherosclerotic lesions and plaques. Plaque rupture or stenosis may result in occlusion of the carotid artery. Accordingly, the asymptomatic disease becomes symptomatic, characterized by ischemic stroke or transient ischemic attacks, indicating an urgent need for better understanding of the underlying molecular mechanisms and eventually prevent symptomatic CAS. NOX4, a member of the NADPH oxidase family has anti-atherosclerotic and anti-inflammatory properties in animal models of early atherosclerosis. We hypothesized that NOX4 is protective in CAS-patients with advanced atherosclerotic lesions as well. Indeed, NOX4 mRNA expression was lower in patients with symptomatic CAS. A low NOX4 expression was associated with an increased risk to become symptomatic. In fact, NOX4 appears to contribute to plaque stability, as apoptosis and plaque hemorrhage, represented by cleaved caspase-3 and glycophorin C, inversely correlated with plaque NOX4 mRNA expression. Even healing of a ruptured plaque appears to be supported by NOX4, as NOX4 mRNA expression correlates to fibrous cap collagen and was reciprocally related to MMP9 activity. In conclusion, low intra-plaque NOX4 mRNA expression is associated with an increased risk for symptomatic outcome and with reduced plaque stabilizing mechanisms suggesting a protective effect of NOX4 in human advanced atherosclerosis.

S 11-02
Acetylcholine as mediator of myocardial ischemia/reperfusion-induced changes in sarcomere function

Martina Krüger

Heinrich Heine University Düsseldorf, Institute of Cardiovascular Physiology, Düsseldorf, Germany

Increasing evidence suggests that stimulation of the vagus nerve is cardioprotective and a possible therapeutic tool for heart conditions such as myocardial ischemia/reperfusion injury (I/R). Previous studies showed that myocardial infarction causes significant release of acetylcholine (ACh) not only in the ischemic, but also in the remote myocardium. Here, we propose that ACh released from vagal efferences is an important mediator of cardioprotective function in the non-ischemic remote myocardium after I/R, by affecting cardiomyocyte passive stiffness. We previously demonstrated in mice that I/R caused rapid protein kinase Cα (PKCα)-dependent phosphorylation of the sarcomere protein titin, thereby increasing cardiomyocyte passive stiffness and contributing to functional remodeling of remote myocardium. Increased myocyte stiffness likely improves stability of the remote myocardium and is beneficial to maintain myocardial function until scar formation is completed. Using biopsies from Göttingen mini pig hearts we tested the impact of acute I/R with or without ischemic preconditioning on passive sarcomere properties in the remote myocardium. During ischemia, relative phosphorylation of PKCα and titin S11878 significantly increased 1.3 and 1.6-fold of baseline values, respectively, and passive tension at sarcomere lengths of 2-2.4 µm was elevated. Brief ischemic preconditioning

caused similar increases of PKCα and titin S11878 phosphorylation within minutes. Importantly, vagotomy prior to I/R inhibited the ischemia-induced alterations of titin and cardiomyocyte passive stiffness, suggesting that vagal signaling is indeed responsible for mediating titin-based functional adaptation in response to ischemia. This idea is further supported by findings from isolated adult rat cardiomyocytes, showing increased titin-based passive stiffness in response to 15 min. incubation with the ACh-analog carbachol. Our in vitro data further suggest that the ACh/Carbachol effect is mediated by M2-, M4- and alpha7n-ACh receptors and can be effectively blocked by inhibition of the downstream target PKCα. In summary, we identified a novel and dynamic mechanism of vagus-induced modification of sarcomere function.

S 11-03
The role of RBCeNOS in myocardial ischemia/reperfusion injury

Miriam M. Cortese-Krott

Heinrich Heine University, Herzinfarktfosrchungslabor, Medizinische Fakultät, Düsseldorf, Germany

Question

Experimental studies have demonstrated the crucial role of endothelial nitric oxide synthase (eNOS) for cardioprotection in vivo. Red blood cells (RBCs) have been found to transport and release nitric oxide (NO) bioactivity and to express an eNOS. We designed a study to specifically differentiate the influence of eNOS in RBCs from that in endothelial cells (ECs).

MethodsWe generated RBC- and EC-specific knock-out (KO) and knock-in (KI) mice, utilizing Cre-induced activation or deactivation of eNOS. In these mice we measured coronary flow responses, systemic hemodynamics, cardiac performance, left ventricular (LV) function before and after ischemia/reperfusion (I/R) injury, and infarct size.

Results

We found that the absence of RBC eNOS did not affect coronary dilatory responses or left ventricular (LV) function. Conversely, the absence of EC eNOS reduced coronary flow response in isolated perfused hearts and increased LV pressure when faced with higher arterial pressure. However, stroke volume remained unaffected. Intriguingly, we observed a significant enlargement of infarct size and worsened LV function, accompanied by decreased stroke volume and cardiac output in the RBC eNOS knockout mice. This aligns with the reduced NO bioavailability and oxygen delivery capacity found in these animals. Importantly, RBC eNOS KI mice demonstrated decreased infarct size and preservation of LV function following AMI. In contrast, EC eNOS KO and KI animals showed no significant differences in infarct size or LV dysfunction after AMI, compared to control groups.

Conclusions

Our data show that EC eNOS controls coronary vasodilator function but does not directly impact infarct size. On the other hand, RBC eNOS plays a vital role in restricting infarct size during AMI. Therefore, signaling of eNOS in RBCs could serve as an innovative target for intervention strategies during ischemia/reperfusion following myocardial infarction.

This work was supported by the German Research Council (SFB1116 TP B06 to M.M.C.-K and Malte Kelm; DFG CO 1305/2-1; the IRTG1902 and by a research grant of the Forschungskommission, Medical Faculty of the Heinrich Heine University Duesseldorf.

S 11-04
nhibition of prolyl-4-hydroxylase domain enzymes during reperfusion in myocardial infarction – a therapeutic option?

Dörthe M. Katschinski

University Medical Center Göttingen, Institute of Cardiovascular Physiology, Göttingen, Germany

Inadequate oxygen supply is a common characteristic for adaptation to high altitudes and various cardiovascular diseases. Manipulation of the cellular oxygen sensors, i.e. prolyl hydroxylase domain (PHD) enzymes, are thought to support the adaptation of the cardiac tissue towards hypoxia and ischemia. We analyzed mice, which mimic PHD inhibitor treatment for the potential of tissue protection (doi: 10.1161/CIRCRESAHA.120.318216). Aside from adaptation to the lack of oxygen, cardiac cells undergo striking changes that are redox-

dependent modifications to regulatory proteins. An imbalance in the production of reactive oxygen species and an altered "redox state" is involved in many cardiac stress reactions that are involved in the development of heart failure. To further characterize the molecular consequences, we apply genetically encoded biosensors and characterize proteins in regard to specific redox modification as well as the consequences for cardiomyocyte metabolism (doi: 10.1038/s41467-023-37744-x.).

S 11-05
A new approach to targeting PI3-Kinase for cardioprotection

Sean Davidson

University College London, The Hatter Cardiovascular Institute, London, UK

Ischaemic heart disease, which often manifests clinically as myocardial infarction, remains a major cause of mortality worldwide. PI3-kinase is a crucial effector of growth factor signalling, and is central to cardioprotection by numerous pharmacological and non-pharmacological interventions, such as ischaemic conditioning. An important component of the cardioprotective effects of the PI3-kinase pathway involves the prevention of mitochondrial permeability transition pore (MPTP) opening and subsequent cardiac cell death. However, these cardioprotective interventions all rely on signalling initiated by receptors in the plasma membrane, and activation of the PI3Kinase pathway is weakened in the setting of common co-morbidities such as diabetes and obesity, which also impair cardioprotection.Although many kinase inhibitors have been developed, we decided to take the opposite approach and investigate if a small molecule could be identified that would directly activate PI3-kinase. After a large high-throughput screen and subsequent medicinal chemistry, we discovered UCL-TRO-1938, a small-molecule activator of the PI3Kα isoform. UCL-TRO-1938 bypasses cellular receptors to allosterically activate PI3Kα through a distinct mechanism by enhancing multiple steps of the PI3Kα catalytic cycle. It is selective for PI3Kα over other PI3K isoforms and transiently activates PI3K signalling in all rodent and human cells tested. In rodent models, acute treatment with UCL-TRO-1938 provides cardioprotection from ischaemia–reperfusion injury. Thus, we have identified a new approach to modulate PI3K activity, widening the therapeutic potential of targeting these enzymes through short-term activation for tissue protection and regeneration. Our findings illustrate the potential of activating kinases for therapeutic benefit, a currently largely untapped area of drug development.

References
[1] Gong, GQ et al, 2013, 'A small-molecule PI3Kα activator for cardioprotection and neuroregeneration', *Nature*, 618, 159-168

S 12 | Teaching Physiology in the future – Challenges and opportunities of the next Approbationsordnung in Germany

S 12-01
Main topics and challenges of the present proposal (Referentenentwurf) for a new Approbationsordnung

Ulrich K. Decking

Heinrich-Heine-University Düsseldorf, Cardiovascular Physiology, Düsseldorf, Germany

In Germany, the medical curriculum is governed by state regulations (Approbationsordnung (AO)), which were created in 2002. In 2017, the outline of a new medical curriculum was defined politically by health and science ministries from both the federal and the state (Länder) level. The current form of the new AO was made public in May 2023 and may become law in autumn 2023. It transforms the classical model of a 2 year preclinical followed by a 3 year clinical phase and a final practical year into an interdisciplinary Z-curriculum.
The "Z" is defined by a simultaneously decreasing portion of basic medical sciences and an increasing portion of clinical content within the 5 year university-based curriculum. About 1/3 of patient contact time (154 hours) will have to be included already in the first 3 years. In this future curriculum, written state examinations governed by a central agency (IMPP) will take place after 3 and 5 years and oral state examinations after 3 and after 6 years of medical studies. A national competency-based learning outcome catalogue (NKLM), developed by

the medical faculties and approved by the federal health ministry, defines the content of the core curriculum, which comprises about 80% of the first 5 years.
The medical faculties will have to design 2 – 3 interdisciplinary modules per semester. Passing the module examinations will be a prerequisite for admission to the state examinations.
In this framework, physiology will be taught from year 1 until year 5 and will remain a major subject in the state examination after year 3 and be present as a minor subject in the exam after 5 years. Within the Z-Curriculum, physiology learning outcomes in each module will enable a better understanding of defined diseases. This may enforce a greater focus on clinical relevance for the physiology curriculum as a whole and will include at the same time pathophysiology into the realm of physiology teaching. Since the core curriculum is reduced compared to the status quo, this is both an opportunity and a challenge.
A further challenge is the fact that passing a subject is no longer a prerequisite for admission to a state examination. Thus in each faculty, physiology departments have to ensure, that their learning outcomes are adequately represented both in the faculty curriculum and module examinations and that a sufficient competence is acquired before entering the state examinations. In the oral exam after the 3rd year, physiology is one out of three clearly defined subjects.
Finally, 20% of the curriculum offer space for studying in depth and by individual choice, with the aim to complete a limited scientific work within 12 weeks. Thus, physiology departments could offer attractive science courses, often in collaboration with other basic science and clinical partners to form longitudinal bundles. How to bring together this scientific work with the classical medical doctoral thesis, often prepared while studying, is still an open question.

S 12-02
Combining basic education in physiology with clinical perspectives and a science track within the first two years of medical school

Anja Meissner

Universität Augsburg, Physiologie - Medizinische Fakultät, Augsburg, Germany

With the foundation of a new Faculty of Medicine at the University of Augsburg, a first cohort of medical students was enrolled in a special competency-based model curriculum in the fall 2019. The first four semesters (previously known as preclinical semesters) of this model curriculum comprise 1) organ-based teaching that integrates basic medical subjects, including Anatomy, Biochemistry, Medical Psychology and Physiology with first clinical aspects, and 2) basic scientific education in a simultaneous special science track.

Within the organ-based teaching each thematic block is commenced by imparting relevant anatomical basics of the respective organs and tissues through the Department of Anatomy. Subsequently, associated biochemical pathways and physiological mechanisms are taught by the Departments of Biochemistry and Physiology, respectively. At the same time, clinicians expose students to relevant diseases to integrate the basic principles taught by the preclinical subjects into more complex clinical problems. This curricular structure creates certain challenges with respect to the combination of preclinical and clinical disciplines as some clinical aspects are already introduced at a stage when not all basic knowledge for each organ system has been taught yet. Thus, clinical reasoning with preferably a holistic view on patients cannot be fully applied at all times during the curriculum. Clinicians rather re-visit example cases throughout the curriculum to continuously add new (patho)mechanistic concepts, and lastly complement with information on therapy and differential diagnostics that connect back to basic physiological and biochemical principles. Although such approach requires a lot of fine tuning between preclinical and clinical teachers, it paves the way for successive learning and a better holistic understanding. In addition to the clinical aspects integrated within the basic education, a separate clinical track focuses on basic clinical skills.

Alongside the basic and initial clinical education runs a basic science track with the overall goal to prepare students for proficiency in evidence-based medicine. During the curriculum, students specifically apply knowledge on basic scientific theory of research design and methods in a clinically oriented science track in semesters 5-9, two laboratory placements in semesters 6 and 8 and a scientific project in semester 10. A particular challenge represents the lack of student involvement in real scientific work at the beginning of their studies, making this course rather

theoretical at first. In order to increase motivation and create more applicability of theoretical concepts, some of the practical courses within biochemistry and physiology have been modified to become part of the science track. Here, the main teaching objectives focus on scientific principles, including generating and testing hypotheses, which helps to implement knowledge obtained during the theoretical courses.

S 12-03
Assessment of knowledge and understanding in physiology within an integrated and interdisciplinary curriculum

Stefan Gründer

RWTH Aachen University, Institute of Physiology, Aachen, Germany

At RWTH Aachen University, since the winter semester of 2003/2004, students of human medicine are enrolled in the Aachener model curriculum of human medicine ("Aachener Modellstudiengang Medizin"). A major goal of introducing the model curriculum was to increase its practical relevance. Teaching in the model curriculum is characterized by an integrated, interdisciplinary concept without strict separation of preclinical and clinical courses. The emphasis of education and training is on understanding organs and organ systems in their anatomy, function, and pathogenetic principles, and less on discipline-specific knowledge of facts. Moreover, 10 % of the curriculum is reserved for elective courses, which allow individual specialization, for example, in biomedical research, various clinical disciplines, or in biomedical engineering.

To account for the integrated and interdisciplinary nature of the curriculum, the first state examination after the 4th semester was replaced by an university examination after the 6th semester. In contrast, the written part of the 2nd state examination is at the end of the 10th semester and the oral part after the practical year is at the end of the 12th semester, as in a regular curriculum. Thus, the Aachener model curriculum contains several key elements that have been recommended in 2014 for the Development of Medical Education in Germany by the German Science and Humanity Council (Wissenschaftsrat): interdisciplinarity, longitudinal and horizontal integration, and a first state examination after the 6th semester.

The Aachener university examination at the end of the 6th semester has two parts: an objective structured practical examination (OSPE) and a classical multiple-choice test. It does not allow benchmarking with students from other universities, for example in the performance in physiology-specific questions. Moreover, many more disciplines contribute to this examination than in a regular curriculum, such that, in principle, it is possible to pass the examination without having a sufficient score for physiology-specific questions. On the other hand, the interdisciplinary courses during the first six semesters finish with obligatory examinations, and physiology contributes to many of them. Thus, knowledge of physiology is regularly examined and is necessary for successful studies.

In the written part of the 2nd state exmination after the 10th semester, students of the Aachener model curriculum regularly perform well above average. In addition, a high percentage of students finishes in the standard time to degree (Regelstudienzeit; ca. 50 % of the students). Students of the Aachener model curriculum also perform well above average in the "Progress Test Medizin", which is organized by Charité. These results demonstrate the high quality of education and training in the Aachener model curriculum for cognitive performance and for gaining knowledge.

S 12-04
Beyond the basics: Deepening of education in physiology and pathophysiology in the later years of a medical curriculum

Alexander P. Schwoerer

University Medical School Hamburg Eppendorf, Institute of Cellular and Integrative Physiology, Hamburg, Germany

In 2012/2013, the integrated medical program (iMED) was implemented at the Faculty of Medicine of the Universität Hamburg. The main features of iMED include the integration of theoretical knowledge and clinical application throughout the curriculum. The core structure comprises 19 modules, which are arranged thematically in seven module groups and cover three stages of a learning spiral. Theoretical

content is taught in a framing context of clinical applications from the first stage of the learning spirals, establishing clinical subjects from the beginning of the curriculum. Conversely, basic medical subjects contribute content also in the second and third stages of the learning spiral.
The focus of physiology during the first three semesters ("normal function") lies on basic principles. In the second stage of the learning spiral ("from symptom to disease"), mainly core diagnostic skills and the relevant basics, e.g. ECG and blood gas analysis, are taught during physiology classes. In the third stage ("disease"), dedicated courses on the pathophysiology of major diseases have been established.
The core concepts of the integrated Z-curriculum, i.e. the integration of theoretical and clinical-practical contents and the application orientation, are highly appreciated by the students and offer opportunities for basic medical subjects. Nevertheless, this approach is associated with different challenges within each study segment. Experiences from the curricular development and from the first ten years of teaching physiology and pathophysiology within the Z-curriculum are discussed during this talk.
Challenges include the reduction of teaching content, and the shift from the subject-related systematic towards a case-related systematic which both becomes necessary during the development of integrated modules. Practical courses in physiology also require a reorientation, e.g. with regard to specific content, and clinical relevance of parameters obtained during the courses. In the third stage of the learning spiral, students are usually well trained in the clinical manifestations and therapeutical options of major diseases. They often, however, lack the understanding of the underlying pathophysiology. Thus, basic physiology and principles of integrative physiology can be revisited and knowledge can be consolidated during these courses. This is regularly appreciated during the students evaluations. On the other hand, pathophysiology courses are demanding, especially for non-medical teaching personnel, as they require in depth understanding of the disease background, of the relevant physiology but also of the broader medical context.
Based on our experiences, the benefits of teaching physiology and pathophysiology beyond the "Physikum" are well worth the challenges which have to be actively addressed during the development of the curriculum.

S 13 | Axons as computational devices in single neurons and networks

S 13-01
Fast hippocampal oscillations tuned by parvalbumin basket cell myelination

David Vandael[1], Cristina Boers Escuder[1], Naomi Petersen[1], Martin Both[3], Andreas Draguhn[3], **Maarten H.P. Kole**[1,2]

[1] Netherlands Institute for Neuroscience, Axonal Signaling, Amsterdam, Netherlands
[2] Utrecht University, Cell biology, Biophysics and Neurobiology, Department of Biology, Utrecht, Netherlands
[3] Heidelberg University, Institute of Physiology and Pathophysiology, Heidelberg, Germany

The author has objected to a publication of the abstract.

S 13-02
Activity–dependent axon initial segment plasticity in interneurons

Elisa Galliano

University of Cambridge, Physiology, Development, and Neuroscience, Cambridge, UK

Dopaminergic (DA) inhibitory interneurons in the olfactory bulb (OB) act at a crucial point in the early olfactory pathway, modulating transmission in OB glomeruli and helping set the gain of incoming inputs. DA neurons are extremely plastic cells, capable of regulating their shape and function in an activity-dependent manner, and even of regenerating throughout life. Long-believed to be a homogeneous population, this talk will explore how recent evidence has instead uncovered a striking heterogeneity in their shape, function and developmental profile – including their ability to undergo adult neurogenesis and of having or lacking an axon. Indeed, only a subclass of axon-bearing, non-regenerating DA cells has been shown to respond to brief sensory deprivation by implementing structural at their axon initial segments and correlated intrinsic plastic changes that result in decreased excitability. Conversely, the axonless DA cells implement synaptic plasticity mechanisms in response to the same deprivation protocols. By differentially acting on one specialised dopaminergic subpopulation, experience-dependent plasticity might act to fine-tune sensory processing in the face of continually fluctuating input.

S 13-03
A neural circuit evolution hypothesis for axon initial segment structure and function

Fred Wolf[1], Andreas Neef[2]

[1] *University of Goettingen & MPI for Dynamics and Self-Organization, Göttingen Campus Institute for Dynamics of Biological Networks, Göttingen, Germany*
[2] *University of Goettingen & MPI for Dynamics and Self-Organization, Göttingen Campus Institute for Dynamics of Biological Networks, Göttingen, Germany*

Action potentials (APs) are the fundamental currency of information flow and interactions in networks of the cerebral cortex. The axon initial segment (AIS) of cortical neurons is the subcellular device that translates the results of continuous intracellular computations in a neuron's dendro-somatic domain into digital AP sequences exchanged between neurons. Intriguingly, in chordate evolution, the molecular architecture of the AIS underwent a major transformation at the origin of the vertebrate forebrain. As the number of forebrain neurons increased dramatically at this evolutionary transition, it likely marked the emergence of genuine neuronal population coding, the representation of information by large groups of neurons interacting through strongly recurrent circuits. Our recent work on the capacity of population coding in mathematical models, in different types of mammalian forebrain neurons, and the dynamics of recurrent cortical circuits suggest that only specific designs of the AIS AP generator can support high-bandwidth, high-capacity population codes. Based on these results, I will discuss whether the transformation of AIS molecular architecture at the origin of vertebrates might represent an adaptation to utilize the newly evolved neuronal coding by large neuronal populations.

S 13-04
Dendritic axon origin enables information gating by perisomatic inhibition in pyramidal neurons

Martin Both

Heidelberg University, Medical Faculty, Institute of Physiology and Pathophysiology, Heidelberg, Germany

Information processing in cortical pyramidal neurons involves the specific activation into functional ensembles. In this process, only a minority of neurons is recruited while the majority remains silent. This sparse activation is believed to result from widespread perisomatic inhibition in conjunction with specific synaptic excitation. We have previously shown that in ~50% of hippocampal pyramidal cells the axon emerges from a basal dendrite. Here, we propose that this particular morphology provides a mechanism for selective activation of participating neurons through these morphologically unique axo-dendritic compartments.
In awake, head-fixed mice, we found that CA1 pyramidal neurons with a dendritic axon origin displayed a ~4-fold higher firing frequency during network activation compared to neurons with somatic axon origin. This difference was absent outside ripples. Extra- and intracellular recordings in mouse brain slices and computer simulations led us to hypothesize that the axon is forming a functional unit together with the axon-carrying dendrite. We show that excitatory input to axon-carrying dendrites remains efficient even during strong perisomatic inhibition. Other dendrites become uncoupled from this compartment, preventing their input to trigger action potentials. This may likewise apply to all neurons with somatic axon origin. Therefore, cells with axon-carrying dendrites may be privileged members of neuronal ensembles during states of strong perisomatic inhibition, such as fast network oscillations. By this mechanism, activation of inhibitory interneurons and targeted excitation of the respective dendrite may dynamically change the functional network topology, resulting in the activation of defined neuronal ensembles.

S 13-05
Development and plasticity of AcD neurons in the mouse whisker/barrel system

Nadja Lehmann[1,2], Stefan Markovic[3], Christian Thome[3,4], Maren Engelhardt[3]

[1] *Medical Faculty Mannheim, Heidelberg University, Instiute of Neuroanatomy, Mannheim, Germany*
[2] *Heidelberg University, Interdisciplinary Center for Neuroscience (IZN), Heidelberg, Germany*
[3] *Johannes Kepler University Linz, Institute of Anatomy and Cell Biology, Linz, Austria*
[4] *Stanford University, Institute for Stem Cell Biology and Regenerative Medicine, Stanford, USA*

The author has objected to a publication of the abstract.

S 14 | Ion channels in immune cell function

S 14-01
Regulation and function of store-operated and mechanosensitive Ca2+ channels in innate immune cells

Camille Rabesahala de Meritens, Nicolas Rosa, Amado Carreras Sureda, **Nicolas Demaurex**

University of Geneva, Department of Cell Physiology and Metabolism, Geneva, Switzerland

Question

The endoplasmic reticulum (ER) transmembrane protein STIM1 mediates the ubiquitous store-operated Ca2+ entry (SOCE) pathway that controls the proliferation of T cells and the development of skeletal muscle. Following the Ca2+ depletion of the ER, STIM1 undergoes a series of conformational changes that open plasma membrane (PM) ion channels of the Orai family, causing an influx of Ca2+ into cells. The entering Ca2+ ions activate essential cell signaling circuits and gene transcription programs as illustrated by the severe combined immunodeficiency and muscle weakness of patients bearing mutations in STIM1 or ORAI1. In innate immune cells, the influx of Ca2+ ions across STIM1-gated Orai1 channels enhances phagocytosis, an evolutionarily conserved cellular process required to eliminate invading pathogens and to maintain tissue homeostasis. We aim to better delineate the regulatory mechanisms of STIM-ORAI coupling and to establish the roles of other ion channels in sustaining phagocytosis and bacterial killing by white blood cells.

Method

We use mouse genetics, electrophysiology, electron microscopy, and a variety of imaging techniques.

Results

We previously used LysM-Cre to delete the Stim1 gene in mouse neutrophils [1-3] but noted partial protein expression and residual SOCE. Using C/EBPα-Cre [4] we can now efficiently ablate genes and express fluorescent proteins in neutrophils and retrieve >10 million labelled bone marrow neutrophils from a single mouse. Using the transgenic Ca2+ reporter Salsa6f developed by the Cahalan lab [5], we performed high-resolution Ca2+ imaging of isolated primary neutrophils. The high affinity and low Ca2+ buffering power of the genetic probe revealed Ca2+ elevations undetected by fluorescent Ca2+ dyes during neutrophil spreading. The Ca2+ elevations were less frequent in neutrophils bearing a targeted disruption in the Stim1/2 genes (p=0.0025), which exhibited negligible SOCE and reduced Ca2+ responses to chemokines. Unexpectedly, the Ca2+ elevations associated with neutrophil spreading persisted in the presence of the Orai1 inhibitor GSK7579a. A pharmacological screen showed that the spreading-associated Ca2+ elevations were inhibited by the tarantula toxin GsMTx4, an inhibitor of PIEZO1 and other stretch-activated ion channels. GsMTx4 inhibited the phagocytosis of opsonized particles by mouse neutrophils and the Ca2+ elevations evoked by the PIEZO1 agonist Yoda1.

Conclusions

These data indicate that PIEZO1 channels are expressed and functional in neutrophils and might contribute to the Ca2+ signals that sustain phagocytosis. The phagocytic process exerts substantial forces on the PM as cells ingest solid particles into intracellular vacuoles. We hypothesize that the mechanical constrains exerted on the cell membrane during the phagocytic process trigger the activation of mechanosensitive channels, enabling the entry of Ca2+ ions that enhance phagocytosis.

Supported by Swiss National Foundation grant N° 310030_189042

References
[1] Nunes, P., et al., STIM1 juxtaposes ER to phagosomes, generating Ca(2)(+) hotspots that boost phagocytosis. Curr Biol, 2012. 22(21): p. 1990-7.
[2] Maschalidi, S., et al., UNC93B1 interacts with the calcium sensor STIM1 for efficient antigen cross-presentation in dendritic cells. Nat Commun, 2017. 8(1): p. 1640.
[3] Carreras-Sureda, A., et al., S-acylation by ZDHHC20 targets ORAI1 channels to lipid rafts for efficient Ca(2+) signaling by Jurkat T cell receptors at the immune synapse. Elife, 2021. 10.
[4] Wolfler, A., et al., Lineage-instructive function of C/EBPalpha in multipotent hematopoietic cells and early thymic progenitors. Blood, 2010. 116(20): p. 4116-25.
[5] Dong, T.X., et al., T-cell calcium dynamics visualized in a ratiometric tdTomato-GCaMP6f transgenic reporter mouse. Elife, 2017. 6.

S 14-02
Channeling Immunity: TRPM7 as regulator of immune homeostasis

Susanna Zierler[1,2]

[1] *JKU Linz, Institute of Pharmacology, Linz, Austria*
[2] *LMU Munich, Walther Straub Institute of Pharmacology and Toxicology, Munich, Germany*

While the immune system protects our body against numerous pathogens, it must not overreach. Otherwise, proinflammatory or autoimmune diseases may develop. Thus, several mechanisms are in place to ensure a suitable immune response at the right time. Using different mouse models as well as primary human immune cells, we deciphered an essential role for the unique channel-kinase, TRPM7 (*transient-receptor-potential melastatin-like 7)*, in cellular signaling and *in vivo* immune reactions. TRPM7 encompasses a cation channel fused with a serine/threonine kinase. We found that its genetic disruption in mice affects innate as well as adaptive immune system responses [1-3]. Using a homozygous kinase-dead mouse model with a single point mutation at the active site of the kinase, *Trpm7*$^{R/R}$, we demonstrated that TRPM7-kinase activity controls proinflammatory T_H17 cell differentiation, but is dispensable for anti-inflammatory, regulatory T cell (T_{reg}) differentiation. Ultimately, we identified SMAD2 as native substrate of the TRPM7-kinase. Notably, genetic disruption of the TRPM7-kinase activity prevented the development of acute graft-*versus*-host-disease in an established mouse model [3]. Likewise, we demonstrated that the TRPM7-kinase is essential for neutrophil transmigration and activity regulating the Akt-signaling hub in an *in vivo* peritonitis model [2]. To date, specific pharmacological modulators of TRPM7-channel orkinase are still limited. Therefore, we are screening for new molecules targeting TRPM7-kinase activity, utilizing artificial intelligence. Previously, we were able to discover the natural compound, waixenicin A, isolated from the Hawaiian soft coral, as first potent and selective TRPM7-channel inhibitor [4]. Using these tools, our translational results imply that TRPM7 is similarly important for the differentiation and activity of primary human T cells as well as for the activation and proliferation of chronic leukemia cells. Our results unravel a fundamental role of the TRPM7-kinase in immune cell function and suggest a therapeutic potential of TRPM-kinase inhibition in averting proinflammatory diseases.

References
[1] Zierler S *et al*., 2016,*The Journal of Physiology*, 2016, doi: 10.1038/s41467-017-01960-z
[2] Nadolni W *et al*., 2021, *Frontiers in Immunology*, doi: 10.3389/fimmu.2020.606893
[3] RomagnaniA *et al*., 2017, *Nature Communications*, doi: 10.1113/JP271564
[4] Zierler S *et al*., 2011, *TheJournal on Biological Chemistry*, doi: 10.1074/jbc.M111.264341

S 14-03
NAADP signaling and calcium microdomains

Andreas H. Guse

University Medical Center Hamburg-Eppendorf, Dept of Biochemistry and Molecular Cell Biology, Hamburg, Germany

The author has objected to a publication of the abstract.

S 14-04
Calcium signaling and cytotoxicity in CTLs during aging

Annette Lis

Saarland University, Biophysics, Center for Integrative Physiology and Molecular Medicine (CIPMM), Homburg, Germany

Aging is associated with reduced functionality and altered distribution of the immune cells from innate and adaptive immunity in humans and mice. Higher incidences of cancer and a higher risk for severe infectious diseases underline the dramatic impact of impaired immunity on the life quality and mortality of elderly individuals. As part of the adaptive immune response, cytotoxic $CD8^+$ T cells are key players in recognizing and killing virus-infected and tumor cells. Various intrinsic and extrinsic factors contribute to the altered efficiency of cytotoxic T lymphocytes (CTLs) in elderly organisms; however, how these changes occur is still largely unknown.

Calcium (Ca^{2+}) is a crucial secondary messenger for proper T cell function, including activation, proliferation, and T cell-mediated cytotoxicity. The ability of T cells to generate Ca^{2+} signals is diminished in elderly individuals, potentially contributing to the decrease in T cell functionality, declining immune competence, and an increased risk for cancer in aging. The main pathway for Ca^{2+} entry into T cells is store-operated Ca^{2+} entry (SOCE), but more research needs to be done on what role Orai channels and stromal interaction molecule proteins (STIM) play as calcium sensors in lymphocyte aging.

Our primary focus is the change accruing during healthy aging in $CD8^+$ T cells from mice. We assessed the molecular repertoire governing Ca^{2+} signals in $CD8^+$ T cells. We investigated the influence of varying $[Ca^{2+}]_{ext}$ on the primary function of these cells, namely the lysis of target cells. Reduced STIM/Orai expression contributes to reduced Ca^{2+} signals in $CD8^+$ T cells of elderly mice. These changes are relevant to immune function as they reduce the Ca^{2+} dependency of CTL cytotoxicity.

Strikingly, we could show that the cytotoxic activity of $CD8^+$ T cells from elderly mice is much faster than those from adult mice if similar CTL numbers or individual cells are compared. Increased perforin and granzyme B expression in CTLs from elderly mice support the notion that cell-intrinsic alterations in the expression of lytic effector molecules cause increased cytotoxicity, replacing granzyme-mediated apoptosis by rapid necrosis induction.

Together, our findings show the crucial contribution of SOCE components to altered Ca^{2+} signals and provide insights into individual cytotoxicity in aged CTLs.

References

[1] Angenendt A, Steiner R, Knörck A, Schwär G, Konrad M, Krause E, Lis A. Orai,STIM, and PMCA contribute to reduced calcium signal generation in $CD8^+$ T cells of elderly mice. Aging (Albany NY). 2020 Feb 12;12(4):3266-3286. doi.org/10.18632/aging.102809

[2] Zöphel, D., Angenendt, A., Kaschek, L., Ravichandran, K., Hof, C., Janku, S., Hoth, M., Lis, A. Faster cytotoxicity with age: Increased perforin and granzyme levels in cytotoxic $CD8^+$ T cells boost cancer cell elimination. Aging Cell. 2022 Aug;21(8):e13668. doi: 10.1111/acel.13668.

[3] Zöphel D, Kaschek L, Steiner R, Janku S, Chang HF, Lis A. Heterozygous OT-I mice reveal that antigen-specific $CD8^+$ T cells shift from apoptotic to necrotic killers in the elderly. Aging Cell. 2023 Jun;22(6):e13824. doi: 10.1111/acel.13824. Epub 2023 Mar 22.

S 14-05
The voltage-gated potassium channel $K_V1.3$ regulates neutrophil functions during acute inflammation

Roland Immler, Monika Pruenster, Markus Sperandio

LMU Munich, Institute for Cardiovascular Physiology and Pathophysiology, Planegg-Martinsried, Germany

Neutrophil functions strongly rely on changes in intracellular calcium concentrations and concomitant calcium signaling. In lymphocytes, sustained Ca^{2+} influx into the cell via Ca^{2+} sensitive ion channels requires a compensatory efflux of potassium via the voltage-gated potassium channel $K_V1.3$ to maintain membrane potential. Although, voltage-gated potassium currents over the plasma membrane have been identified in neutrophils as well, no distinct ion channel could be attributed to these observations for a long time. We started to address the question whether $K_V1.3$ is involved in Ca^{2+} signaling of neutrophils and how it affects neutrophil functions during acute inflammatory processes.

Using *in vitro* and *in vivo* functional assays in combination with electrophysiologicial techniques, we demonstrate that $K_V1.3$ is functionally expressed in neutrophils regulating sustained store operated Ca^{2+} entry (SOCE) through membrane potential stabilizing K^+ efflux. $K_V1.3$ activity is required for multiple neutrophil functions during their recruitment from the vascular compartment to the site of inflammation, including firm

adhesion, post-arrest modifications and intra luminal crawling. In addition, phagocytosis is dependent on $K_V1.3$ activity, as pharmacological inhibition or genetic deletion of $K_V1.3$ impairs phagocytosis of *E. coli* particles.
Besides its role in Ca^{2+} signaling related functions, K^+ efflux via $K_V1.3$ regulates E-selectin-triggered, fast NLRP3 inflammasome activation and downstream gasdermin D pore formation, a process that mediates the release of small cytosolic alarmins such as S100A8/A9 from neutrophils. Our work highlights the role of $K_V1.3$ in key functions of neutrophils and opens up new therapeutic approaches to treat inflammatory disorders characterized by overwhelming neutrophil infiltration.

Supported by DFG SFB914 B11N (MP), TRR332 C2 (MS), and TRR359 B2 (RI, MS)

S 14-06
Kv1.3 potassium channel of myeloid cells controls tumor growth *in vivo*

Tatiana Varanita[1], Beatrice Angi[1], Daniele Bonesso[1], Anna Tosi[5], Mattia Albiero[2,3], Ferenc Erdelyi[6], Gian Paolo Fadini[2,3], Antonio Rosato[4,5], Ildiko Szabo[1]

[1] *University of Padova, Department of Biology, Padova, Italy*
[2] *Veneto Institute of Molecular Medicine, Padova, Italy*
[3] *University of Padova, Department of Medicine, Padova, Italy*
[4] *University of Padova, Department of Surgery, Oncology, and Gastroenterology, Immunology and Oncology Section, Padova, Italy*
[5] *Veneto Institute of Oncology IOV - IRCCS, Padova, Italy*
[6] *KOKI Institute of Experimental Medicine, Budapest, Hungary*

Macrophages are critical mediators of tissue homeostasis crucial in the innate and adaptive immune response in several pathologies including cancer. Tumor-associated macrophages are the most abundant cellular component of the tumor microenvironment (TME). Macrophages in the TME undergo functional changes that actively support tumor growth and progression and associate with poor prognosis. The voltage-gated potassium channel Kv1.3 located in the plasma and inner mitochondrial membranes is highly expressed by macrophages playing important roles in their functionality. Thus, we established a novel mouse model of myeloid-specific Kv1.3 deletion to understand its impact on tumorigenesis. Impaired Kv1.3 in the myeloid lineage leads to increased tumor burden. Tumors from myeloid Kv1.3 depleted mice show higher pro-tumor macrophage infiltration hindering the intratumoral adaptive immune response. Furthermore, Kv1.3 ablation modulates macrophage mitochondrial metabolism and promotes alternative macrophage activation. Therefore, as a regulator of macrophage function, Kv1.3 is required for protection against tumor growth and anti-tumor immunity.

ORAL SESSIONS

OS 01 | Ion Transport: From Physiology to Pathophysiology

OS 01-01
Glucocorticoids improve contractility and excitation-contraction coupling in human failing myocardial slices

Benedikt Pfeilschifter[1], Sophie Sommer[1], Dominik Fiegle[1], Anne Ritzer[1], Victoria Baron[1], Christian Heim[2], Prapassorn Potue[1,5], Zafar Iqbal[1], Michael Weyand[2], Hendrik Milting[3], Roland Tomasi[4], Andreas Dendorfer[4], Tilmann Volk[1], Thomas Seidel[1]

[1] Friedrich Alexander Universität Erlangen, Institut für Physiologie 2, Erlangen, Germany
[2] Friedrich Alexander Universität Erlangen, Herzchirurgische Klinik, Erlangen, Germany
[3] Ruhr-Universität Bochum, Erich und Hanna Klessmann-Institut, Bad Oeynhausen, Germany
[4] Ludwig-Maximilian-Universität München, Walter-Brendel-Centre of Experimental Medicine, München, Germany
[5] Khon Kaen University, Department of Physiology, Khon Kaen, Thailand

Question

Glucocorticoids regulate cardiac development in rodents, improve maturation of stem-cell derived cardiomyocytes, increase the L-type Ca^{2+} current (I_{CaL}) and stabilize the t-system in isolated cardiomyocytes. However, data on direct effects of glucocorticoid activation on human myocardial tissue and human cardiomyocytes are very limited. Here, we investigated the influence of glucocorticoids on contractility, transmembrane currents and excitation-contraction (EC) coupling in living human myocardial slices.

Methods

Precision-cut slices from 18 end-stage failing human heart samples were kept beating in organotypic culture for up to 30 days with either 100nM dexamethasone (DEX), 20nM cortisol, +/- 1µM spironolactone or 1µM mifepristone, or vehicle as control (CTRL). After cultivation, slices were subjected to β-adrenergic stimulation, used for Ca^{2+} imaging (Calbryte), cell isolation to measure whole-cell ionic currents and action potentials, frozen for qPCR or fixed for immunostaining.

Results

Slices treated with DEX exhibited a 2-fold increase in contractile force when compared with CTRL ($p<0.01$), achieved higher beating rates than the CTRL ($p<0.001$) and showed a more positive force-frequency relation. Contraction duration was shorter in DEX-treated LMS than in CTRL. These effects were blunted by mifepristone, but not by spironolactone. Cortisol in concentrations comparable to free plasma levels did not reproduce the effects of DEX. DEX caused a 38±6% increase in CACNA1c mRNA after 2d ($p<0.01$, n=5) and a 23±8% increase after one week ($p<0.05$, n=8). Furthermore, DEX increased mRNA expressions of SERCA, Kv4.3, KChIP2, Kir2.1 and Kir2.3. Fitting to these results, DEX increased I_{CaL} density by 69% ($p<0.05$), I_{to} 2.7fold ($p<0.001$), I_{K1} 1.5fold ($p<0.01$) and caused a slightly more negative membrane potential. Current kinetics remained unchanged. Moreover, the relative increase in contractile force in response to 100 nM isoprenaline was 2fold higher in DEX-treated slices. Ca^{2+} signal upstroke velocity was higher in DEX than in CTRL ($p<0.01$). Ca^{2+} signal amplitudes were unchanged at baseline, but increased in DEX vs CTRL after isoprenaline application ($p<0.05$). Confocal microscopy revealed no difference in cell size and fibrosis, but a slight increase in RyR cluster density in DEX ($p<0.05$).

Conclusions

DEX increases contractility in human failing myocardium via the glucocorticoid receptor and increases current densities of I_{CaL}, I_{to} and I_{K1} in human failing myocardium without affecting kinetic parameters. DEX also increases the expression of the respective ion channel subunits and enhances Ca^{2+} signaling and b-adrenergic response. This suggests increased Ca^{2+} entry and subsequently improved EC coupling as a main mechanism of glucocorticoid-induced increase in inotropy and may oppose the cellular changes in electrophysiology and excitation-contraction coupling commonly observed in human heart failure.

OS 01-02

Cystic fibrosis transmembrane conductance regulator modulators attenuate platelet activation and aggregation in blood of healthy donors and COVID-19 patients

Erik Asmus[1], Weronika Karle[1], Markus C. Brack[2,3], Felix Behrens[1,4], Corey Wittig[1], Leander Reinshagen[5,6], Moritz Pfeiffer[2], Sabrina Schulz[1], Bertina Mandzimba-Maloko[1], Lasti Erfinanda[1], Paul L. Perret[1,4], Laura Michalick[1,5], Patrick J. Smeele[7], Endry H.T. Lim[8,9], Charissa E. van den Brom[8,10], Alexander B.A. Vonk[11], Toralf Kaiser[12], Norbert Suttorp[2,13], Stefan Hippenstiel[2,13], Leif E. Sander[2,13], Florian Kurth[2,13], Ursula Rauch[5,6], Ulf Landmesser[4,5,6], Arash Haghikia[4,5,6], Robert Preißner[1,14], Harm J. Bogaard[7], Martin Witzenrath[2,3,13], Wolfgang M. Kuebler[1,5,15], Robert Szulcek[1,7,15], Szandor Simmons[1,5,15]

[1] Charité - Universitätsmedizin Berlin, corporate member of Freie Universität Berlin and Humboldt-Universität zu Berlin, Institute of Physiology, Berlin, Germany
[2] Charité - Universitätsmedizin Berlin, corporate member of Freie Universität Berlin and Humboldt-Universität zu Berlin, Department of Infectious Diseases and Respiratory Medicine, Berlin, Germany
[3] Charité - Universitätsmedizin Berlin, corporate member of Freie Universität Berlin and Humboldt-Universität zu Berlin, Division of Pulmonary Inflammation, Berlin, Germany
[4] Berlin Institute of Health (BIH), Berlin, Germany
[5] DZHK (German Centre for Cardiovascular Research), Partner site Berlin, Berlin, Germany
[6] Charité - Universitätsmedizin Berlin, corporate member of Freie Universität Berlin and Humboldt-Universität zu Berlin, Department of Cardiology, Berlin, Germany
[7] Amsterdam UMC, Department of Pulmonary Diseases, Amsterdam, Netherlands
[8] Amsterdam UMC, Department of Intensive Care Medicine, Amsterdam, Netherlands
[9] Amsterdam UMC, Department of Neurology, Berlin, Germany
[10] Amsterdam UMC, Department of Anesthesiology, Amsterdam, Netherlands
[11] Amsterdam UMC, Department of Cardiothoracic Surgery, Amsterdam, Netherlands
[12] German Rheumatism Research Centre Berlin (DRFZ), Flow Cytometry Core Facility, Berlin, Germany
[13] German Center for Lung Research (DZL), Partner site Berlin, Berlin, Germany
[14] Charité - Universitätsmedizin Berlin, corporate member of Freie Universität Berlin and Humboldt-Universität zu Berlin, Science-IT, Berlin, Germany
[15] These authors contributed equally to this work., Berlin, Germany

Mutations in cystic fibrosis transmembrane conductance regulator (CFTR) cause the clinical presentation of cystic fibrosis (CF), but have recently also been shown to cause agonist-induced platelet hyperactivation. These findings are reminiscent of platelets from SARS-CoV-2 infected patients since thromboembolic complications represent hallmarks of severe COVID-19. CFTR modulators have recently been introduced as a treatment for patients with various CFTR mutations, but have also been reported to effectively enhance channel function of wild type CFTR. We therefore postulated that CFTR modulators may exert anticoagulant effects on platelets of healthy donors (HD) and COVID-19 patients.

We recruited 36 COVID-19 patients with moderate, and 34 COVID-19 patients with severe disease course (all w/o anti-platelet drugs), and 38 healthy donors (HDs). In line with our hypothesis, pre-treatment with the CFTR modulator ivacaftor significantly reduced platelet agonist-induced CD62p/CD63 expression, Ca^{2+}-mobilization, aggregation, and adhesion of platelets from HDs. In blood of COVID-19 patients, platelet activation correlates with disease severity, as demonstrated by a progressive increase in the proportion of $CD62p^{+}$ platelets from moderate to severe COVID-19 patients relative to HDs. Similarly, the proportion of $CD63^{+}$ platelets in patients with severe COVID-19 was 2-fold higher than in HDs. Retrospective analysis of clinical data from 4,050 CF patients with COVID-19 receiving CFTR modulator therapy in comparison to an untreated cohort revealed that CFTR modulators reduced the relative risk to suffer thromboembolism-associated cardiovascular events such as heart attack or deep vein thrombosis by 50.0% or 61.1%, respectively, suggesting an anti-thrombotic effect of CFTR modulators in CF COVID-19 patients. In line with this observation, e*x vivo* pre-treatment of platelets of acute COVID-19 patients with ivacaftor reduced agonist-induced Ca^{2+} mobilization, adhesion, and aggregation of platelets.

Our results demonstrate an anticoagulant effect of CFTR modulators on platelets of HDs and severe COVID-19 patients and thus, suggest CFTR modulators as promising strategy to reduce the risk of thrombotic events in the clinical management of COVID-19 and similar pro-thrombotic disease states

We would like to thank all medical, paramedical, laboratory and nursing staff involved in the care of the COVD-19 patients and for realising the patient recruitment at Charité – Universitätmedizin Berlin, Germany, and Amsterdam UMC, The Netherlands. Furthermore, the authors would like to thank all the investigators of the Berlin prospective Pa-COVID-19 cohort as well as the investigators of the Amsterdam UMC COVID-19 Biobank.

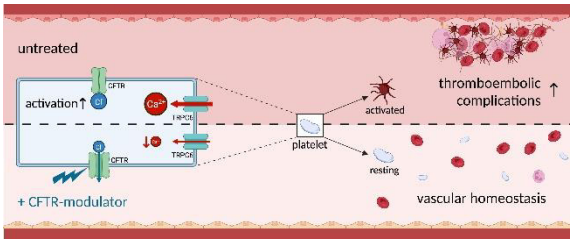

Graphical Abstract
CFTR dysfunction leads to accumulation of Cl^- in platelets and increased Ca^{2+} influx. Ca^{2+} is the most important second messenger in platelets and triggers platelet activation, promoting intravascular coagulation and thrombotic events. Increasing the opening probability of CFTR with ivacaftor, a CFTR-potentiator, enhances Cl^- efflux from platelets, which may reduce Ca^{2+} influx and thus platelet activation, aggregation, and thrombosis.

OS 01-03
Vascular Smooth Muscle BK Channel Activation by Cardiotonic Steroids Is Mediated by Na/K-ATPase, Na/Ca exchanger and Src-Kinase

Anastasia Pyanova[1], Tobias Orth[2], Simon Lux[2], Peter Kaiser[2], Isabel Reinheimer[2], Rudolf Schubert[1]

[1] University of Augsburg, Institute of Theoretical Medicine, Faculty of Medicine, University of Augsburg, Augsburg, Germany
[2] Heidelberg University, European Center of Angioscience (ECAS), Research Division Cardiovascular Physiology, Medical Faculty Mannheim, Heidelberg University, Mannheim, Germany

Question

The supply of blood to organs and tissues is regulated by changes in arterial contractile tone, which is determined by the smooth muscle cells of the vascular wall. Vascular smooth muscle cells express a variety of potassium channels (1), of which calcium-activated potassium channels of high conductance (BK channels) are uniquely important. BK channels are subject to dual regulation by calcium and protein kinases, in particular the Src kinase (2). Interestingly, the sodium-potassium(Na/K)-ATPase has a dual mode of action: an ion transport function by which it can affect the intracellular calcium concentration via the sodium-calcium exchanger (NCX) and a signal transducer function mediated by Src kinase (3, 4). Whether the Na/K-ATPase, as an ion transporter and/or as a signal transducer, is able to regulate BK channel activity and thereby BK channel-dependent arterial tone, is unknown. Thus, the hypothesis was tested that the Na/K-ATPase activates BK channels and thereby regulates vessel tone.

Methods

Endothelium-denuded rat mesenteric arteries were studied by isometric myography and FURA-2 calcium fluorimetry. Na/K-ATP-ase function was challenged by cardiotonic steroids that inhibit the Na/K-ATPase ion transport function and stimulate its signal transducing function.

Results

Methoxamine (Mx) induced concentration-dependent contraction of rat mesenteric arteries. These contractions were enhanced by the specific BK channel inhibitor iberiotoxin (IBTX), showing a contractile effect of IBTX. We did not detect a relevant effect of the cardiotonic steroid ouabain on Mx-induced contractions. However, in the presence of the cardiotonic steroids ouabain and digoxin, the contractile effect of IBTX was enhanced. Moreover, a contractile effect of ouabain and digoxin appeared in the presence of IBTX. Such effects were not observed when ouabain was tested in combination with the Kv7 channel inhibitor XE991. Of note, the ouabain-induced increase in vessel tension in the presence of IBTX was accompanied by an increase of the F340/F380 ratio, representing the intracellular calcium concentration. Furthermore, the contractile effect of ouabain occurring in the presence of IBTX was completely abolished in the presence of the NCX inhibitor SEA0400. In addition, the contractile effect of IBTX was reduced in the presence of SEA0400. Interestingly, the contractile effect of ouabain occurring in the presence of IBTX was also completely abolished in the presence of the Src kinase inhibitor PP2. Finally, the contractile effect of IBTX was reduced in the presence of PP2.

Conclusions

Cardiotonic steroids activate vascular smooth muscle BK channels through its ion transport function (via NCX) as well as the signal transducer function (via Src kinase) of the Na/K-ATPase.

References
[1] Shvetsova AA, Gaynullina DK, Tarasova OS, Schubert R. Remodeling of Arterial Tone Regulation in Postnatal Development: Focus on Smooth Muscle Cell Potassium Channels. Int J Mol Sci. 2021 Jun; 22(11): 5413.
[2] Ling S, Woronuk G, Sy L, Lev S, Braun AP. Enhanced activity of a large conductance, calcium-sensitive K+ channel in the presence of Src tyrosine kinase. J Biol Chem 2000 Sep 29;275(39):30683-9.
[3] Matchkov VV, Gustafsson H, Rahman A et al. Interaction between Na+/K+-pump and Na+/Ca2+-exchanger modulates intercellular communication. Circ Res. 2007 Apr 13;100(7):1026-35.
[4] Nam LB, Keum Y-S. Regulation of NRF2 by Na^+/K^+-ATPase: implication of tyrosine phosphorylation of Src. Free Radic Res. 2020 Dec;54(11-12):883-893.

OS 01-04

The anion channel TMEM16a/Ano1 modulates agonist-activated CFTR activity, but does not function as an apical anion channel in colonic epithelium from cystic fibrosis patients and healthy individuals

Azam Salari[1], Renjie Xiu[1], Mahdi Amiri[1], Sophia-Theres Pallenberg[2], Rainer Schreiber[3], Anna-Maria Dittrich[2], Burkhard Tümmler[2], Karl Kunzelmann[3], Ursula Seidler[1]

[1] *Hannover Medical School, Gastroenterology, Hannover, Germany*
[2] *Hannover Medical School, Pediatric Pulmonology, Hannover, Germany*
[3] *University of Regensburg, Physiology, Regensburg, Germany*

Question

Functional studies in human colonic cell lines and murine intestine suggest the presence of two distinctly different apical anion channels, the cyclic nucleotide-activated CFTR channel and a Ca^{2+}-activated anion channel, presumably TMEM16a. Is there a potential for fluid secretion in patients with severe CF mutations by activating this alternative pathways?

Methods

In order to clarify the expression, localization and potential function as an apical “alternative” anion channel in the human colorectum, we established two-dimensional nondifferentiated colonoid-myofibroblast (CM-CE) cocultures (with the colonic epithelial cells on the transwell filter, and the myofibroblasts on the bottom of the culture dish), resembling transit amplifying/progenitor (TA/PE) cells in the cryptal neck zone, as well as differentiated (DM) cultures resembling surface-near cells, both from healthy controls and from patients with severe functional defects in the CFTR gene who had given informed consent. Ussing-chamber studies were performed to characterize apical agonist-activated Cl^- activity in the TA/PE and the DM monolayers from CF patients and healthy controls, in the absence and presence of TMEM16a channel inhibitors.

Results

The expression levels of the CFTR, NKCC1, and TMEM16a were high in the proliferative CM-CE cocultures, whereas the expression of SLC26A3, NHE3, ALPI, MUC2 were high in the DM monolayers. The mRNA expression levels for the proliferative markers as well as TMEM16a did not differ between CF and healthy controls. CM-CE monolayers from healthy controls displayed a robust, bumetanide-sensitive short circuit current response (ΔIsc) to luminally added UTP (up to 10µM), basolaterally added forskolin (FSK, 10 µM) as well as carbachol (Carb, 100µM), whereas the response was very small and bumetanide-insensitive in DM monolayers. The specific TMEM16a inhibitor Ani9 (up to 30µM) did not alter the response to luminal UTP, significantly decreased FSK-induced ΔIsc, and significantly increased Carb-induced ΔIsc in TA/PE monolayers. The CF monolayers displayed negligible agonist-induced ΔIsc, without a significant effect of Ani9. TMEM16a was localized in intracellular structures, with higher expression in CF than healthy control monolayers; a staining in the apical membrane was not detected.

Conclusions

TMEM16a is highly expressed in human CM-CE cocultures resembling transit amplifying cells of the colonic cryptal neck zone, both from healthy controls and from CF patients. While it may play a role in modulating agonist-induced CFTR-mediated anion currents, it is not localized in the apical membrane, and it has no function as an apical anion channel in CF and healthy human colonic epithelium.

The authors thank the patients and the healthy individuals for their willingness to donate a biopsy to this study. The project was funded by the DFG Sachbeihilfe Se460/21-1 and Se460/22-1

References
1. Li H, Salomon JJ, Sheppard DN, Mall MA, Galietta LJ. Bypassing CFTR dysfunction in cystic fibrosis with alternative pathways for anion transport. Curr Opin Pharmacol. 2017 Jun;34:91-97
[2] Lee B, Hong GS, Lee SH, Kim H, Kim A, Hwang EM, Kim J, Lee MG, Yang JY, Kweon MN, Tse CM, Mark D, Oh U. Anoctamin 1/TMEM16A controls intestinal Cl- secretion induced by carbachol and cholera toxin. Exp Mol Med. 2019 Aug 5;51(8):1-14.
[3] Saha T, Aoun J, Hayashi M, Ali SI, Sarkar P, Bag PK, Leblanc N, Ameen N, Woodward OM, Hoque KM. Intestinal TMEM16A control luminal chloride secretion in a NHERF1 dependent manner. Biochem Biophys Rep. 2021 Jan 22;25:100912
[4] Mall M, Wissner A, Seydewitz HH, Kuehr J, Brandis M, Greger R, Kunzelmann K. Defective cholinergic Cl(-) secretion and detection of K(+) secretion in rectal biopsies from cystic fibrosis patients. Am J Physiol Gastrointest Liver Physiol. 2000 Apr;278(4):G617-24
[5] Control of Ion Transport by Tmem16a Expressed in Murine Intestine. Kunzelmann K, Centeio R, Wanitchakool P, Cabrita I, Benedetto R, Saha T, Hoque KM, Schreiber R. Front Physiol. 2019 Oct 4;10:1262

OS 01-05
Claudin 14 gradually replaces claudin 16 to finetune renal calcium transport

Rozemarijn E. van der Veen[1], Nacéra Mezouar[1], Marie Bieck[1], Henrik Dimke[2], Martin Lehmann[1]

[1] *Leibniz-Forschungsinstitut für Molekulare Pharmakologie, Cellular Imaging, Berlin, Germany*
[2] *University of Southern Denmark, Molecular Medicine - Cardiovascular and Renal Research, Odense, Denmark*

Calcium is essential for many processes in the human body and its levels are therefore tightly regulated through the cooperation of many different organs. The kidney is one of those organs, where calcium is reabsorbed from the pre-urine into the blood. Roughly 20% of this calcium is reabsorbed in the thick ascending limb, where it passes a paracellular ion channel formed by claudin 16 and claudin 19 [1,2]. Claudin 14 is known to finetune this transport: it gets expressed upon hypercalcemia and blocks calcium transport through claudin 16/19 [3,4]. Correspondingly, claudin 14 has been associated with kidney stone formation and hypercalciuria in genome-wide association studies [5]. In this study we aimed to understand the mechanism by which claudin 14 blocks the claudin 16/19 calcium pore. With super-resolution microscopy of reconstituted tight junction meshworks, we could show that claudin 16 on its own cannot form a meshwork, but can incorporate into the meshwork of claudin 19. Interestingly, upon introduction of claudin 14, claudin 16 is lost from the meshwork and claudin 14 takes its place. We validated these findings in mice that were subjected to hypercalcemia for different timeframes. Hypercalcemia led to an upward trend in claudin 14 and a corresponding downward trend in claudin 16, indicating a gradual replacement. Moreover, longer timeframes of hypercalcemia led to the development of hypercalciuria. Finally, we linked these findings to tight junction calcium fluxes and barrier formation through the reconstitution of the different claudins in a claudin-free kidney epithelial cell line. Our data collectively show how calcium transport and barrier maintenance are balanced in the tight junction of the thick ascending limb through a gradual increase in claudin 14 which goes on to replace claudin 16 in its tight junction association with claudin 19.

References
[1] Hou, J, Renigunta, A, Konrad, M, Gomes, AS, Schneeberger, ES, Paul, DL, Waldegger, S, Goodenough DA, 2008, 'Claudin-16 and claudin-19 interact and form a cation-selective tight junction complex', *J Clin Invest*, 118 (2), 619-628
[2] Hou, J, Renigunta, A, Gomes, AS, Hou, M, Paul, DL, Waldegger, S, Goodenough, DA, 2009, 'Claudin-16 and claudin-19 interaction is required for their assembly into tight junctions and for renal reabsorption of magnesium', *PNAS*, 106 (36), 15350-15355
[3] Gong, Y, Renigunta, V, Himmerkus, N, Zhang, J, Renigunta, A, Bleich, M, Hou, J, 2012, 'Claudin-14 regulates renal Ca^{++} transport in response to CaSR signalling via a novel microRNA pathway', *EMBO J*, 31, 1999-2012
[4] Dimke, H, Desai, P, Borovac, J, Lau, A, Pan, W, Alexander, RT, 2013, 'Activation of the Ca^{2+}-sensing receptor increases renal claudin-14 expression and urinary Ca^{2+} excretion', *Am J Physiol Renal Physiol*, 304 (6), F761-769
[5] Thorleifsson, G, Holm, H, Edvardsson, V, Walters, GB, Styrkarsdottir, U, Gudbjartsson, DF, Sulem, P, Halldorsson, BV, de Vegt, F, d'Ancona, FC, den Heijer, M, Franzson, L, Christiansen, C, Alexandersen, P, Rafnar, T, Kristjansson, K, Sigurdsson, G, Kiemeney, LA, Bodvarsson, M, Indridason, OS, Palsson, R, Kong, A, Thorsteinsdottir, U, Stefansson, K, 2009, 'Sequence variants in the CLDN14 gene associate with kidney stones and bone mineral density', *Nat Genet*, 41 (8), 926-930

OS 01-06
Renal Basolateral Potassium Channels in Salt Handling and Blood Pressure Control

Adrian Zietara[1], Christine Klemens[1,2], Biyang Xu[1], Ruslan Bohovyk[1], Vladislav Levchenko[1], Oleg Palygin[3], **Alexander Staruschenko**[1,2]

[1] *University of South Florida, Molecular Pharmacology and Physiology, Tampa, USA*
[2] *University of South Florida, Hypertension and Kidney Research Center, Tampa, USA*
[3] *Medical University of South Carolina, Division of Nephrology, Charleston, USA*

Salt and waterhandling by the kidney directly impact blood pressure and is tightly controlled by electrolyte homeostasis maintained through ion channel function. Inwardly rectifying potassium (K_{ir}) channels, including apical $K_{ir}1.1$ and basolateral $K_{ir}2.1$, $K_{ir}4.1$, $K_{ir}5.1$, and $K_{ir}7.1$, are expressed in the kidney. K_{ir} channels, specifically $K_{ir}4.1$ and $K_{ir}5.1$ (encoded by *Kcnj10* and *Kcnj16*), are considered major players in controlling basolateral membrane potential and recycling potassium in the aldosterone-sensitive distal nephron. To understand the role of basolateral K_{ir} channels in blood pressure control and kidney function, we have created $SS^{Kcnj10-/-}$, $SS^{Kcnj16-/-}$, $SS^{Kcnj13+/-}$, and $SS^{Kcnj2+/-}$ models on the Dahl Salt-sensitive (SS) rat background. $SS^{Kcnj16-/-}$ rats revealed lower blood pressure and hypokalemia when fed a normal (0,4% NaCl) salt diet. Change of the diet to a high salt (4%) causes rapid mortality of $SS^{Kcnj16-/-}$ (majority of animalsdid not survive more than 48 hrs) triggered by severe hypokalemia, which was prevented with the supplementation of the diet with high potassium or inhibition of ENaC with benzamil. Furthermore, we revealed that knockout of *Kcnj16* markedly altered renin-angiotensin-aldosterone system (RAAS) regulation and function, suggesting $K_{ir}5.1$ as a key regulator of the RAAS, particularly when exposed to changes in dietary sodium and potassium content. Importantly, HS-induced mortality in $SS^{Kcnj16-/-}$rats and salt-induced increase in blood pressure seen in SS rats can be prevented by high K^+ diet supplementation. $SS^{Kcnj10-/-}$ rats survived approximately three weeks even when the diet was supplemented with high K^+. $SS^{Kcnj10+/-}$ rats also had a shortened life span. When fed a high salt diet, $SS^{Kcnj10+/-}$ rats had lower blood pressure and albuminuria than wild-type littermates. Knockout of *Kcnj13* and *Kcnj2* resulted in embryonic lethality. Heterozygous $Kcnj13^{+/-}$ rats revealed an increase in potassium excretion on a normal salt diet but did not exhibit a difference in blood pressure development or plasma electrolytes after three weeks of a high salt diet. Heterozygous $Kcnj2^{+/-}$ rats also revealed some vascular dysfunction. The current study provided essential information about the role of basolateral K_{ir} channels on potassium homeostasis in the kidney and blood pressure, specifically in the setting of salt-induced hypertension.

This research was supported by the National Institute of Health grants R35 HL135749 (to AS), R01 DK126720 (OP), and R01 DK129227 (to AS and OP).

OS 01-07

Role of transmembrane serine protease 2 (TMPRSS2) in proteolytic processing and activation of the epithelial sodium channel (ENaC) in kidney and lung epithelia

Florian Sure[1], Sara Afonso[1], Paul Schmidt[2], Daniel Essigke[2], Alicia Kißler[1], Marko Bertog[1], Ralf Rinke[1], Sabine Wittmann[3], Thomas Gramberg[3], Ferruh Artunc[2], Christoph Korbmacher[1], Alexandr V. Ilyaskin[1]

[1] *Friedrich-Alexander-Universität Erlangen-Nürnberg, Institute of Cellular and Molecular Physiology, Erlangen, Germany*
[2] *University Hospital Tübingen, Division of Endocrinology, Diabetology and Nephrology, Department of Internal Medicine, Tübingen, Germany*
[3] *Friedrich-Alexander-Universität Erlangen-Nürnberg, Universitätsklinikum Erlangen, Institute of Clinical and Molecular Virology, Erlangen, Germany*

The appropriate regulation of ENaC is functionally important in lung epithelia for maintaining surface liquid homeostasis and alveolar fluid clearance and in the distal nephron for long-term control of sodium balance and blood pressure. A unique feature of ENaC is its complex proteolytic processing and activation. Cleavage by proteases releases inhibitory tracts from the α- and γ-subunits of ENaC, which ultimately results in channel activation. However, the proteases involved in ENaC cleavage *in vivo* remain largely unknown. Using the *Xenopus laevis* oocytes expression system, we recently demonstrated that TMPRSS2 can activate ENaC by cleaving the channel's γ-subunit [1]. ENaC and TMPRSS2 are endogenously expressed in human distal lung epithelial cells (H441 cell line) and mouse cortical collecting duct cells ($mCCD_{cl1}$ cell line). Thus, TMPRSS2 may be involved in proteolytic ENaC activation in these cells. To investigate this, we generated TMPRSS2 knockdown H441 and $mCCD_{cl1}$ cell lines with CRISPR/Cas9 technology. Cells were grown on permeable supports, and transepithelial short circuit currents (I_{SC}) were measured in modified Ussing chambers. Interestingly, apical application of the prototypical protease chymotrypsin significantly increased ENaC-mediated I_{SC} in TMPRSS2-knockdown H441 cells. In contrast, no increase of I_{SC} was observed in control H441 cells. Similar results were obtained in $mCCD_{cl1}$ cells, where chymotrypsin applied apically stimulated I_{SC} in TMPRSS2-knockdown but not in control cells. These findings indicate that TMPRSS2 deficiency impairs proteolytic ENaC activation in H441 and $mCCD_{cl1}$ cells. To investigate the relevance of TMPRSS2 for ENaC regulation *in vivo*, we used constitutive TMPRSS2 knockout mice ($Tmprss2^{-/-}$). Using western blot analysis, we demonstrated that the fully to partially cleaved γ-ENaC ratio was significantly reduced in $Tmprss2^{-/-}$ mice compared to $Tmprss2^{+/+}$ mice in lysates from kidney cortex. To investigate the functional role of TMPRSS2 in renal sodium handling, mice were challenged with a 4-day low sodium diet. $Tmprss2^{-/-}$ and $Tmprss2^{+/+}$ mice similarly reduced urinary sodium excretion in response to low sodium intake. Importantly,

plasma aldosterone increased to significantly higher levels in *Tmprss2*$^{-/-}$ mice compared to controls under low sodium conditions. This can be interpreted as a compensatory response to compromised proteolytic ENaC activation due to TMPRSS2 deficiency. We conclude that in the kidney TMPRSS2 is likely to contribute to proteolytic ENaC activation under baseline conditions and when animals are challenged with a low sodium diet. Moreover, our findings in H441 cells suggest that TMPRSS2 may also be involved in proteolytic ENaC processing and activation in lung epithelia. Future studies are needed to elucidate a possible role of TMPRSS2 in proteolytic ENaC activation in native lung tissue under physiological conditions.

Funded by the Deutsche Forschungsgemeinschaft (DFG, German Research Foundation), project number 357509280, SFB 1350 (subproject A4 to C.K.) and project number 509149993, TRR 374 (subproject A4 to A.I. and C.K.) and the Bayerisches Staatsministerium für Wissenschaft und Kunst (Bavarian Ministry of Art and Science), project VI-Corona-Forschung (subproject 07 to M.B. and T.G). A.K. was supported by the Interdisziplinäres Zentrum für klinische Forschung (IZKF) Erlangen. S.W. was supported by the Bundesministerium für Bildung und Forschung (BMBF, Federal Ministry of Education and Research, Germany), project SENSE-CoV2, 01KI20172A. P.S. and F.A. were funded by the IZKF Tübingen.

References
[1] Sure, F., Bertog, M., Afonso, S., Diakov, A., Rinke, R., Madej, M.G., Wittmann, S., Gramberg, T., Korbmacher, C., Ilyaskin, A.V. 2022, 'Transmembrane serine protease 2 (TMPRSS2) proteolytically activates the epithelial sodium channel (ENaC) by cleaving the channel's γ-subunit', *J Biol Chem*, 298(6):102004.

OS 01-08
T- and L-type calcium channels maintain calcium oscillations in the murine zona glomerulosa

Hoang A. Dinh, Marina Volkert, Ali K. Secener, Ute Scholl, Gabriel Stölting

Berlin Institute of Health at Charité – Universitätsmedizin Berlin, Center of Functional Genomics, Berlin, Germany

The zona glomerulosa (ZG) of the adrenal gland is responsible for the synthesis and release of the mineralocorticoid aldosterone. This steroid hormone regulates salt reabsorption in the kidney and blood pressure [1]. The most important stimuli of aldosterone synthesis are the serum concentrations of angiotensin II and potassium. In response ZG cells depolarize from the resting membrane potential causing influx of calcium via voltage-gated calcium channels which provides the signal for aldosterone synthesis [1].
In murine ZG cells, these depolarizations occur in oscillations that increase upon stimulation [2]. We and other groups have shown that the intracellular concentration of calcium fluctuates with a similar pattern and frequency [3, 4]. It was proposed that the voltage-gated T-type calcium channel $Ca_V3.2$ (encoded by the *Cacna1h* gene) is necessary for the generation of these oscillations by maintaining voltage oscillations [2].
However, *Cacna1h* knockout mice did not show altered systemic aldosterone or renin levels, suggesting additional calcium entry pathways [3, 5].
We used a combination of calcium imaging, patch clamp and RNA-seq to investigate these pathways.

Cacna1h$^{-/-}$ mice showed similar calcium levels as wild-type mice in response to stimulation with angiotensin II or potassium. No calcium channels or transporters were upregulated to compensate for the loss of $Ca_V3.2$. The calcium oscillations observed in the ZG of *Cacna1h*$^{-/-}$ mice were instead dependent on L-type voltage-gated calcium channels, likely $Ca_V1.2$ and $Ca_V1.3$. Also in WT, only inhibition of both, T- and L-type calcium channels abolished the increase of intracellular calcium caused by angiotensin II.

Our study demonstrates that T-type calcium channels are not required to maintain glomerulosa calcium oscillations. This implicates that T-type calcium channels are dispensable for aldosterone production in the long term. Furthermore, we conclude that the combination of T- and L-type calcium channels mediate oscillatory angiotensin II-dependent Ca^{2+} influx.

References
[1] Spaet, A., Hunyady, L. 2004 *Physiol Rev*. 84, 489–539.
[2] Hu, C., Rusin, C. G., Tan, Z., Guagliardo, N. A., and Barrett, P. Q. 2012 *J Clin Invest*. 122, 2046–2053.
[3] Seidel, E., Schewe, J., Zhang, J., Dinh, H. A., K Forslund S. K., Markó, L., Hellmig, N., Peters J., Muller, D. N., Lifton, R. P., Nottoli, T., Stölting, G., and Scholl, U.I. 2021 *PNAS* 118.
[4] Guagliardo, N. A., Klein, P. G., Gancayco, C. A., Lu, A. C., Leng, S., Makarem, R. R., Cho, C., Rusin, C. G., Breault, D. T., Barrett, P. M., and Beenhakker, M. P. 2020 *Nat Commun* 11, 1679.

[5] Thuesen, A.D., Finsen, S.H., Rasmussen, L.L., Andersen, D. T., Jensen, B. L., and Hansen, P.B.L., 2019 *Am. J. Physiol. Renal Physiol.* 317, F254–F263.

OS 02 | Best Abstract Session

OS 02-01
Renal compartment-specific proteasome alterations in a murine type-2 diabetes model

Lukas Blume[1], Man Wang[1], Shuya Liu[2], Yu Zhao[3], Johannes Brand[1], Stephanie Zielinski[1], Tobias Huber[2], Desirée Loreth[1], Wiebke Sachs[1], Catherine Meyer-Schwesinger[1]

[1] *University Medical Center Eppendorf, Institute of Cellular and Integrative Physiology, Hamburg, Germany*
[2] *University Medical Center Eppendorf, III. Medical Clinic, Hamburg, Germany*
[3] *University Medical Center Eppendorf, ZMNH Institute of Medical Systems Biology, Hamburg, Germany*

Question

In contrast to the significance of autophagy in diabetic nephropathy (DN), little is known about the involvement of the ubiquitin-proteasome system (UPS). Therefore, this study aims to characterise the changes in compartment-specific proteasome levels and activity in the development of type-2 DN using BTBR *ob/ob* mice and to assess the efficiency of Empagliflozin (EMPA) treatment in reverting underlying proteasome alterations.

Methods

Kidney tissue, isolated glomeruli, urine and sera from 8- and 20-week-old BTBR *ob/ob* and control mice were collected. Transcript and protein levels of proteasome subunits were assessed *via* scRNAseq and Western blot analysis. Proteasome subtype composition and activity were quantified *via* in-gel activity assays and activity-based probes targeting the proteolytic subunits. Immunohistochemical analyses in mice and patient biopsies with DN were used to localize proteasome alterations to renal cell-types. The effect of EMPA treatment (6-week treatment starting at 15 weeks of age) on proteasome functionality in BTBR *ob/ob* mice was assessed.

Results

A with clinical disease progression exacerbating decrease in proteasome subunit expression was present in diabetic kidneys, both for subunits of the regulatory caps and of the proteolytic 20S particle. scRNAseq showed the strongest downregulation of the proteasome system in proximal tubular segments. This downregulation impacted kidney proteasome functionality at multiple levels. 26S proteasomes were lost, thereby shifting protein degradation towards 20S proteasomes, which favour ubiquitin- and ATP-independent degradation. Further, the proteolytic activity of individual 20S proteasomes was impaired in progressive disease, suggesting alteration of proteasome functionality at the molecular level. In line, exposure of purified 20S proteasomes to high glucose decreased proteolytic activity. In BTBR *ob/ob* kidneys, impaired 20S proteasome activity correlated to albuminuria. Contrasting whole kidney tissue, an early proteasome switch towards the immunoproteasome was observed in isolated glomeruli, a constitution which is thought to relieve proteostatic stress through a higher proteolytic activity. In humans and mice, the proteasome switch was strongest in glomerular endothelial cells followed by podocytes, however, did not relate to an enhanced glomerular proteasome activity. Persistent high levels of 20S proteasomes were present in sera of BTBR *ob/ob* mice, which were normalized by EMPA treatment in conjunction with amelioration of serum glucose levels, proteinuria, and weight-gain.

Conclusions

Compartment-specific proteasome alterations are present in type 2 DN, mostly relating to loss of ubiquitin- and ATP-dependent degradation in tubular cells and a proteasome switch in glomerular cells. High glucose directly impairs 20S proteasome functionality, which correlates to albuminuria, indicating that proteasome impairment plays a major part in the pathogenesis of type-2 DN.

OS 02-02
Role of pericardial cells in myocardial infarction.

Olesia Omelchenko[1], Rianne Nederlof[1], Andre Heinen[1], Stefanie Gödecke[1], Tobias Lautwein[2], Axel Gödecke[1]

[1] *Heinrich-Heine University, Cardiovascular Physiology, Düsseldorf, Germany*
[2] *Biologisch-Medizinisches Forschungszentrum (BMFZ), Genomics and Transcriptomics Laboratory, Heinrich-Heine University, Düsseldorf, Germany*

Pericardium is generally viewed as a fibrous sac that protects the heart from excessive filling and it secretes pericardial fluid serving as a lubrication to reduce friction between the heart and surrounding organs. Moreover, its visceral layer (epicardium) serves as a source of progenitor cells and paracrine factors during embryonic development and after myocardial infarction (MI). Meanwhile, its adjacent parietal and fibrous layers were studied to a minor extent. Therefore, we aimed to examine the pericardium, its cell composition and response to MI.
Histological analysis revealed that apart from the mentioned sublayers, the murine pericardium contains integrated fat depots and fat-associated lymphoid clusters (FALCs). To describe their cellular composition, we used the lineage-tracing model WT1CreERT2;Rosa26^{Tomato}, where WT1 (Wilms' tumor 1) is commonly known as epicardial cell marker. We showed that, in contrast to the postnatal epicardium, the pericardium contains a multitude of WT1 expressing cells already under basic conditions. This observation was confirmed by qPCR analysis and cultivation of the pericardial cells. The fat depots and FALCs contained, in addition to WT1$^+$ cells, CD68$^+$ and F4/80$^+$ macrophages, CD19$^+$ B-cells and CD31$^+$ cells. According to FACS analysis, the amount of pericardial cells under basic conditions was 80218±*17428* cells per pericardium (c/p), among them CD45$^+$ immune cells(36040±6371 c/p), CD31$^+$ cells(2944±2036 c/p), and MEFSK4$^+$ fibroblasts (11687±5460 c/p).
To examine the pericardial response to MI we conducted a surgical induction of ischemia/reperfusion (I/R) injury in mouse models with closed pericardium and analyzed the tissue on day 6 after surgery. Pericardial thickness increased from 10±3 µm (control mice) up to 147±45 µm (the scar vicinity) and 17±14 µm (the remote area) after I/R. However, in sham experiments the thickness expanded up to 113±14 µm and 12±0.3 µm along the left and the right ventricles respectively. Moreover, we observed a 3-fold increase in FALCs number and found integration of adipocytes into FALCs as well as in the fibrous pericardium.
Single-cell RNA-sequencing analysis revealed 20 cell clusters, among them are B- and T-cells, plasma cells, neutrophils, macrophages, conventional and plasmacytoid dendritic cells, endothelial cells and, interestingly, two populations of WT1+ cells, positive for the epicardial markers (*Tbx18, Sema3d, Aldh1a2,Gata5*, and *Tcf21)* and markers indicating the mesothelial origin: *Upk3b, MSLN* and*Lrrn4*.
We have shown that the pericardium, composed of the visceral, parietal and fibrous layers, fat depots and FALCs is a complex tissue containing various cell types. It can be activated upon damage suggesting that it may substantially modulate cardiac inflammation and repair upon injury. The presence of WT1+ cells rises a question, if the pericardium is also a source of cells, able to differentiate into other cell types.

This work was supported by Grant IRTG 1902 and the Dr. Sigrid Worch-Pöhler-Stiftung to AG, Düsseldorf, Germany.

OS 02-03
Relaxin' cortical circuits: Understanding the effect of relaxin on synaptic transmission within cortical circuits

Sadat Hodzic[1], Andrew Gundlach[3], Marc Landry[4], Beate Averbeck[2], Therese Riedemann[1], LMU-Bordeaux Research Cooperation Program

[1] *Biomedical Center Munich, Physiological Genomics, Planegg-Martinsried, Germany*
[2] *Biomedical Center Munich, Cardiovascular Physiology and Pathophysiology, Planegg-Martinsried, Germany*
[3] *The Florey Institute of Neuroscience and Mental Health, Anatomy and Physiology, Melbourne, Australia*
[4] *University of Bordeaux, CNRS, IMN, Bordeaux, France*

Relaxin is a heterodimeric peptide whose biological effect is mediated via the family of G-protein coupled receptor Relaxin Family Peptide Receptor 1 (RXFP1). Relaxin was initially described as facilitator of parturition in reproductive endocrinology. Although studies suggest a wide distribution of RXFP1 in different brain areas, little is known about the biological actions of the peptide on the brain.

Single-cell sequencing data show robust mRNA levels of relaxin-1 in a subgroup of GABAergic interneurons, namely somatostatin-expressing

interneurons (SOM-INs), suggesting that relaxin-1 might act as a neuropeptide inside the brain. This hypothesis is supported by the finding that intracerebroventricular injection of the synthetic peptide human relaxin-2 (H2-relaxin) has analgesic effects on thermic and mechanic pain perception in mice. The anterior cingulate cortex (aCC) is at the core of the pain matrix and plays a prominent role in nociception and pain processing. Interestingly, RXFP1 is expressed by around 80% of all excitatory neurons of that brain region suggesting that H2-relaxin might well act as a neuromodulator of pain processing.

Therefore, we studied the effect of H2-relaxin on synaptic transmission within the aCC using whole-cell patch clamp recordings. To this end, we prepared 300 µm-thick acute coronal brain slices containing the aCC and obtained recordings from infragranular pyramidal cells (PCs) or from 2 different types of GABAergic interneurons namely parvalbumin-expressing interneurons (PV-INs) or SOM-INs. Experiments were performed on wild-type mice and on two different transgenic mouse lines: 1) the GIN mouse line where a subset of SOM-INs expresses the enhanced green fluorescent protein (eGFP), 2) a PV-Cre mouse line where PV-INs express robust tdTomato fluorescence following Cre-mediated recombination. All animals used in this study were older than 4 weeks.

In the majority of PCs, we found that exposure to H2-relaxin caused a sustained and reversible inward current suggesting a direct postsynaptic effect. In agreement with that, we found that H2-relaxin resulted in a depolarization of the resting membrane potential and an increase in the action potential discharge frequency. In contrast, no such inward current was observed in SOM-INs nor in PV-INs. Nonetheless, H2-relaxin exposure resulted in a robust activity-dependent increase in the firing frequency of SOM-INs. Interestingly, we did not detect a strong postsynaptic H2-relaxin effect on PV-INs. In line with above findings, RXFP1 expression could only be detected in a small fraction of SOM-INs and PV-INs of the aCC.

In addition, initial evidence suggests that H2-relaxin enhances excitatory synaptic inputs onto SOM-INs and PV-INs but not onto PCs. However, we report increased inhibitory inputs onto a subset of ingragranular PCs upon exposure to H2-relaxin.
Altogether, these data suggest that H2-relaxin acts as a powerful neuromodulator of cortical circuits.

We thank Prof. Mike Myoga, Dr. Diana Rodrigues and Dr. Sarah Gleiss for helpful discussions and support.
In addition, we thank Gabi Horn for excellent technical assistance.

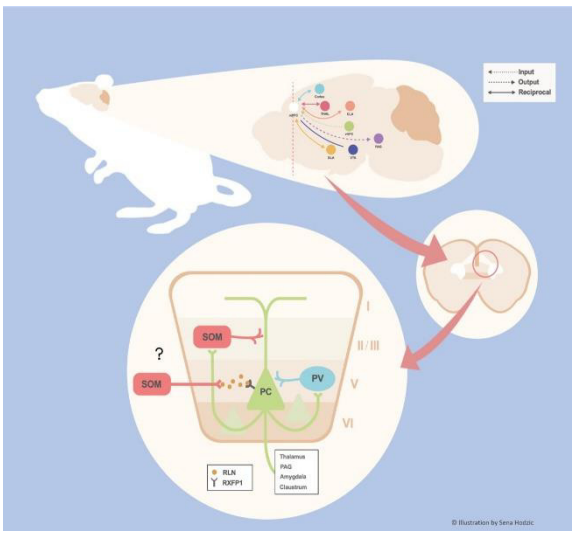

Working model

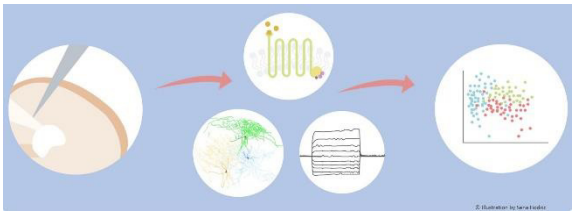

Methodological approach

OS 02-04
Gain-of-function mutations in *CLCN6* cause early-onset neurodegeneration

Maya M. Polovitskaya[1], Carlo Barbini[1], Daniel J. Wegner[2], Kerstin Kutsche[3], Marco Tartaglia[4], Thomas J. Jentsch[1]

[1] *Leibniz-Forschungsinstitut für Molekulare Pharmakologie, Physiology and Pathology of Ion Transport, Berlin, Germany*
[2] *Washington University School of Medicine and St. Louis Children's Hospital, Division of Newborn Medicine, Edward Mallinckrodt Department of Pediatrics, St. Louis, USA*
[3] *University Medical Center Hamburg-Eppendorf, Institute for Human Genetics, Hamburg, Germany*
[4] *Ospedale Pediatrico Bambino Gesu, Genetics and Rare Diseases Research Division, Rome, Italy*

ClC-6 is a late endosomal $2Cl^-/H^+$-exchanger predominantly expressed in neurons. It is the least explored of the mammalian CLCs and its role in endolysosomal ion homeostasis remains poorly understood. Disruption of ClC-6 in mice leads to a mild form of lysosomal storage disease in which storage material accumulates specifically in initial axon segments [1]. Loss-of-function character of a variant previously associated with late-onset neuronal ceroid lipofuscinosis has recently been established [2].

We identified three unrelated subjects carrying the same *de novo* c.1658A>G (Y553C) mutation in the *CLCN6* gene with a severe early-onset neurological disorder characterized by developmental delay, generalized hypotonia, respiratory insufficiency, and variable neurodegeneration and diffusion restriction in cerebral peduncles, midbrain, and/or brainstem in MRI scans [3].

Whole-cell patch clamp of the plasma membrane-targeted GFP-ClC-6^{Y553C} showed a strong gain-of-function phenotype with a shift in voltage dependency towards less depolarized voltages and accelerated activation kinetics.

Heterologous expression of ClC-6^{Y553C}, but not of WT ClC-6, generated giant LAMP-1-positive vesicles that were poorly acidified. Their generation required ion transport by ClC-6, as combining the Y553C variant with the transport-deficient mutation of the 'proton-glutamate' E267A abolished vesicular swelling. Vesicular enlargement also depended on the Cl^-/H^+-exchange, while the double E200A,Y553C mutation, as well as the single E200A mutation in the 'gating glutamate', which turns the exchanger into a pure Cl^- channel, both caused only a moderate enlargement of vesicles. Interestingly, E200A variant was found in a patient with infantile spasms and microcephaly [4]. We propose that H^+-driven Cl^- accumulation drives osmotic swelling of vesicles, as preemptive bafilomycin treatment prevented vesicle enlargement, and its application to cells with giant vesicles caused vesicular shrinkage.

Our work established *CLCN6* involvement in human neurological disease [3]. Later we identified two further subjects with *de novo* mutations in a residue predicted to interact with Y553, showing a similar clinical, electrophysiological, and cell-biological phenotype, and extended our studies to gain-of-function variants in other endolysosomal CLC transporters [5].

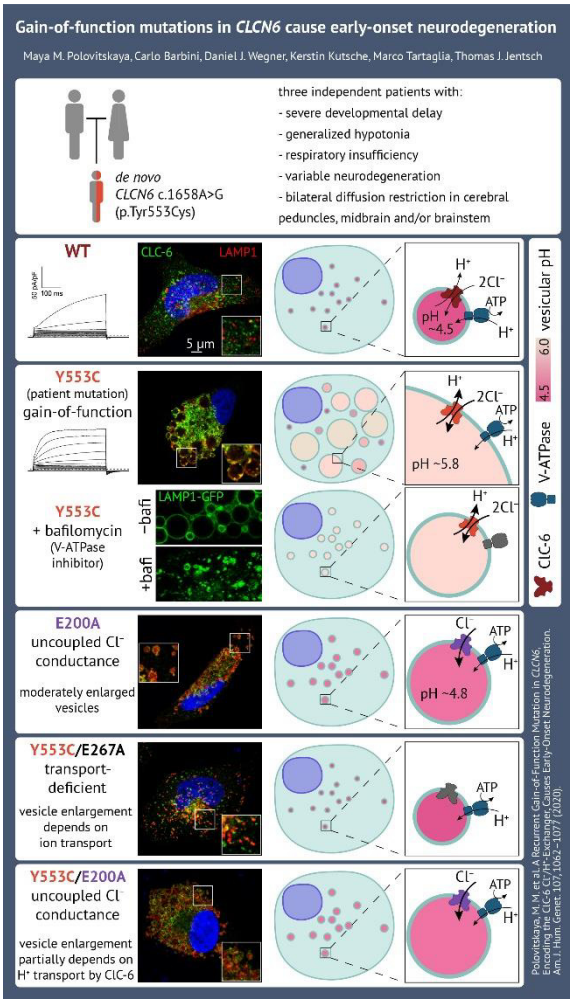

Graphical abstract

References

[1] Poët, Kornak, Schweizer, Zdebik, Scheel, Hoelter, … Jentsch. (2006). Lysosomal storage disease upon disruption of the neuronal chloride transport protein ClC-6. *Proceedings of the National Academy of Sciences of the United States of America*, *103*(37), 13854–13859. https://doi.org/10.1073/pnas.0606137103

[2] Zifarelli, Pusch, & Fong. (2022). Altered voltage-dependence of slowly activating chloride-proton antiport by late endosomal ClC-6 explains distinct neurological disorders. *The Journal of Physiology*, *600*(9), 2147–2164. https://doi.org/10.1113/JP282737

[3] Polovitskaya, Barbini, Martinelli, Harms, Cole, Calligari, … Jentsch. (2020). A Recurrent Gain-of-Function Mutation in CLCN6, Encoding the ClC-6 Cl−/H+-Exchanger, Causes Early-Onset Neurodegeneration. *American Journal of Human Genetics*, *107*(6), 1062–1077. https://doi.org/10.1016/j.ajhg.2020.11.004

[4] He, Cao, Yin, Wu, Stauber, & Peng. (2021). West Syndrome Caused By a Chloride/Proton Exchange-Uncoupling CLCN6 Mutation Related to Autophagic-Lysosomal Dysfunction. *Molecular Neurobiology*, *58*(6), 2990–2999. https://doi.org/10.1007/s12035-021-02291-3

[5] Duncan, Polovitskaya, Gaitán-Peñas, Bertelli, VanNoy, Grant, … Agrawal. (2021). Unique variants in CLCN3, encoding an endosomal anion/proton exchanger, underlie a spectrum of neurodevelopmental disorders. *The American Journal of Human Genetics*, *108*(8), 1450–1465. https://doi.org/10.1016/j.ajhg.2021.06.003

OS 02-05

Renin versus erythropoietin – the endocrine plasticity of renal vascular smooth muscle cells is influenced by the prolyl-4-hydroxylases 2 and 3

Katharina A.-E. Broeker, Michaela Fuchs, Julia Schrankl, Armin Kurtz

Universität Regensburg, Institut für Physiologie, Regensburg, Germany

Question

The production of renin and erythropoietin (EPO) is an essential task of renal stromal cells. Under physiological conditions, both hormones are expressed by different stromal cell types. However, in stressful situations high endocrine plasticity is evident regarding the expression of renin and EPO within stromal cells: Under hypotension vascular smooth muscle cells (VSMCs) are recruited to produce renin, interstitial fibroblasts

simultaneously express renin and EPO after blood loss or juxtaglomerular renin-producing cells are transformed into EPO-producing cells upon chronic hypoxia. Due to these findings, the question arose whether VSMCs can also be transformed into EPO-expressing cells upon activation of the hypoxia inducible signaling pathway (HIF-2α stabilization) and whether prolyl-4-hydroxylases (PHD) 2 and 3 play a role in the endocrine identity of these cells, as has been shown for the transformation of juxtaglomerular renin cells?

Methods

To address these questions mice with an inducible deletion of PHD2 and PHD3 were generated to stabilize HIF-2α specifically in VSMCs ($SMMHC^{CreERT2/+}$ $PHD2^{ff}$ $PHD3^{ff}$ mice). To analyze whether PHD2/3 deficiency affects the recruitment of VSMCs for renin production, a second group received an additional low salt diet combined with enalapril (LSE) for 14 days after PHD2/PHD3 deletion to stimulate renin expression. Then, renal EPO and renin mRNA abundances as well as plasma concentrations were determined. In addition, EPO^+ and $renin^+$ cells were localized by RNAscope or immunofluorescence and their number quantified.

Results

VSMC specific HIF-2α stabilization led to polycythemia with significantly increased plasma EPO concentrations (767.5±82.0 pg/ml vs. 236.2±17.4 pg/ml in controls). Renal EPO mRNA abundance was about 6-fold elevated. RNAscope analysis revealed though that EPO expression was mostly induced in contractile interstitial cells, which are also positive for SMMHC but only sporadically in VSMCs of renal vessels. However, after 14 days LSE treatment clear EPO mRNA expression could be detected in VSMCs of $SMMHC^{CreERT2/+}$ $PHD2^{ff}$ $PHD3^{ff}$ mice that led to a further increase in the plasma EPO concentrations (1293.6±96.4 pg/ml). In parallel, renin mRNA abundance as well as plasma renin concentrations were significantly less induced compared to controls with 14d LSE treatment. RNAscope analysis revealed that VSMCs were no longer recruited to produce renin but instead EPO.

Conclusions

Taken together, we could show that VSMCs show endocrine plasticity and possess the potential to not only produce renin but also EPO under certain conditions. Moreover, their endocrine identity seems to be influenced by PHD2 and PHD3. To identify signaling pathways involved in the endocrine transformation, additional cell markers and regulatory factors will be analyzed in more detail. Moreover, the effect of PHD inhibitors on the endocrine plasticity of renal stromal cells will be investigated.

Funded by the Deutsche Forschungsgemeinschaft (DFG, German Research Foundation) – Project-ID 509149993, TRR 374 Project B1

OS 02-06

Alterations in extracellular vesicle microRNAs drive loss of endothelial homeostasis in chronic kidney disease

Felix Behrens[1,2,3], Johannes B. Holle[2,4,5], Chia-Yu Chen[5,6], Laura F. Ginsbach[1], Benjamin C. Krause[7], Ulrike Bruening[3,6], Fabian Kriegel[7,8], Toralf Kaiser[9], István A. Szijártó[5,10], Katrin Lehmann[11], Pawel Durek[11], Lisa Peters[1,4], Andreas Luch[7], Laura Michalick[1,2,3], Jennifer Kirwan[3,6], Sofia K. Forslund[4,5,6], Dominik Müller[2], Nicola Wilck[4,10,5], Hendrik Bartolomaeus[4,10,5], Mir-Farzin Mashreghi[11,3], Ulrike Löber[4,5,6], Wolfgang M. Kübler[1,4,12], **Szandor Simmons**[1,4]

[1] Charité - Universitätsmedizin Berlin, Institute of Physiology, Berlin, Germany
[2] Charité - Universitätsmedizin Berlin, Department of Pediatric Gastroenterology, Nephrology and Metabolic Diseases, Berlin, Germany
[3] Berlin Institute of Health (BIH) at Charité – Universitätsmedizin Berlin, Berlin, Germany
[4] German Centre for Cardiovascular Research (DZHK), partner site Berlin, Berlin, Germany
[5] Experimental and Clinical Research Center (ECRC), a cooperation of Charité – Universitätsmedizin Berlin and Max Delbrück Center for Molecular Medicine (MDC), Berlin, Germany
[6] Max Delbrück Center for Molecular Medicine (MDC), Berlin, Germany
[7] German Federal Institute for Risk Assessment (BfR), Department of Chemical and Product Safety, Berlin, Germany
[8] Carl Zeiss Meditech, Berlin, Germany
[9] German Rheumatism Research Centre (DRFZ), Flow Cytometry and Cell Sorting Core Facility, Berlin, Germany
[10] Charité - Universitätsmedizin Berlin, Department of Nephrology und Intensive Medical Care, Berlin, Germany
[11] German Rheumatism Research Centre (DRFZ), Laboratory of Systems Rheumatology & Therapeutic Gene Regulation, Berlin, Germany
[12] University of Toronto, Departments of Physiology and Surgery, Toronto, Canada
[13] St. Michael's Hospital, Keenan Research Centre for Biomedical Science, Toronto, Canada

Background: Cardiovascular disease (CVD) is the main cause of death in chronic kidney disease (CKD). However, the pathogenesis of CVD in CKD remains incompletely understood. Extracellular vesicles (EVs) have emerged as mediators of organ cross-talk and specifically endothelial EVs are associated with CVD. We hypothesized that CKD drives endothelial cell (EC) EV release in CKD and that these EC-EVs drive CVD in CKD.

Results: We recruited a cohort of 94 children (mean age 10.9 years) at different stages of CKD (patients with or without dialysis and after kidney transplantation (KTx)) and age-matched healthy donors, offering the unique opportunity to analyze cardiovascular effects of CKD and EV dynamics in the absence of age-related confounders like diabetes and hypertension[KW1] . Nanoparticle tracking analyses yielded elevated total plasma EVs in peritoneal dialysis (PD) patients compared to healthy donors and KTx patients . EV flow cytometry revealed increased macrophage- (3-fold) and T-cell-derived EVs (6-fold) in CKD without dialysis compared to healthy donors, while EC-EVs were reduced after KTx in longitudinal follow-ups and cross-sectional comparison of hemodialysis (HD) and KTx patients (3-fold). EV small RNA sequencing showed lower abundance of several microRNAs (miRNAs) in EVs from CKD patients, with most pronounced changes in HD patients. Downregulation of let-7d-5p, miR-19a-3p, miR-24-3p, miR-103a-3p and miR-142-3p in dialysis patients was confirmed by RT-qPCR. Gene enrichment analyses predicted multiple processes related to CVD pathogenesis as targets of differentially regulated miRNAs in CKD. In parallel, tryptophan metabolomics showed stage-dependent increases in uremic toxins of indole and kynurenine pathways in children with CKD, with highest levels in dialysis patients and almost normal levels after KTx. *In vitro*, uremic toxins alone were not sufficient to trigger EV release from aortic EC, but in combination with high shear stress the uremic toxin[KW2] indoxyl sulfate increased EV release from venous[KW3] EC corresponding to higher EC-EV concentrations in HD patients with arterio-venous fistulas (AVF), and recapitulated EV miRNA changes observed in CKD (lower abundance of let-7d-5p and miR-24-3p).**Conclusion:** EC-EV release and decreased EV miRNA associate with advanced CKD and may be driven by increased EC shear stress in combination with uremia. Dysregulated EV miRNAs may drive CVD and could form novel therapeutical targets to prevent CVD in CKD.

OS 02-07
An ultrasensitive genetically encoded voltage indicator reveals the endogenous electrical activity of non-excitable cells

Philipp Rühl, Anagha G. Nair, Roland Schönherr, Stefan H. Heinemann

Friedrich Schiller University Jena, Department of Biophysics, Jena, Germany

The membrane potential (V_m) is a crucial parameter for excitable and non-excitable cells with implications in cell-cycle progression, tissue development, and tumorigenesis. Alterations in the expression level of ion transport proteins, including channels, carriers, and pumps, were reported to contribute to the development of various cancer types, such as breast and prostate carcinoma, glioma, and melanoma.[1]

To study the electrical signaling of non-excitable cells, we developed rEstus, a calibratable, ultrasensitive genetically encoded voltage indicator (GEVI) based on the green fluorescent GEVI ASAP3.[2-4] We designed rEstus to place its sensitivity optimum (-32 mV) into the voltage range of non-excitable cells, such as dividing tumor cells (0 to -50 mV).[1] At this voltage, rEstus features a 4.6-fold improvement in molecular brightness change per mV (0.55% EGFP/mV) over ASAP3 (0.12% EGFP/mV) without marked compromises in sensor speed. Furthermore, the fluorescence signal of rEstus can be calibrated by using the equilibrium of the chromophore's neutral and phenolate state. Thus, alternating measurements of fluorescence with 480-nm and 400-nm excitation allows for simultaneous and quantitative imaging of V_m in many cells with high time resolution.

We generated a HEK293T cell line stably expressing rEstus and recorded the membrane voltage by imaging F_{480} and F_{400} at 10 Hz. Remarkably, we found that the resting membrane potential of HEK293T is far from stable but V_m fluctuated with a cut-off frequency of ≈1 Hz and an average rms amplitude of 2 mV. To determine whether these fluctuations are a unique feature of HEK293T cells, we also examined MCF7 breast cancer cells transiently expressing rEstus. MCF7 cells exhibited fluctuations in V_m with similar characteristics to those found for HEK293T cells.

Using such endogenous electrical activity, we measured the correlation among cells in culture. V_m fluctuations were strongly correlated between neighboring HEK293T cells (linear correlation coefficient r: 0.80 ± 0.05, n = 19 cell pairs), indicating a strong electrical coupling. In

contrast, the fluctuations in the fluorescence signal inside clusters of MCF7 cells were only weakly correlated (r: 0.49 ± 0.09, n = 13 cell pairs), suggesting that they largely act as independent electrical entities.
Our study demonstrates that V_m of non-excitable cells is dynamic and changes over time on a timescale of seconds, and that these fluctuations in the range of a few mV can be measured with rEstus in a fluorescence imaging approach suited for high-throughput applications. rEstus is a new tool to study the resting membrane potentials of single cells and electrical connectivity between cells. Further studies promise to provide insight into the electrical signaling of non-excitable cells and to unravel the implications of V_m and changes in V_m for the physiology and pathophysiology in cell development and cancer cell progression.

German Academic Exchange Service (A.G.N., 91819480)

Simons Foundation Autism Research Initiative (SFARI) (S.H.H, 705944SH)

References

[1] Kadir, L. A., Stacey, M. & Barrett-Jolley, R. Emerging roles of the membrane potential: Action beyond the action potential. *Frontiers in Physiology***9**, 1661 (2018).
[2] Villette, V. *et al.* Ultrafast two-photon imaging of a high-gain voltage indicator in awake behaving mice. *Cell***179**, 1590-1608.e23 (2019).
[3] Rühl, P. *et al.* Monitoring of compound resting membrane potentials of cell cultures with ratiometric genetically encoded voltage indicators. *Communications Biology***4**, 1–11 (2021).
[4] Rühl, P. *et al.* Genetically encoded voltage indicators optimized for measuring the cellular resting membrane potential. *ACTA PHYSIOLOGICA* 236, 157-157 (2022)

OS 03 | Molecular & Cellular Neurosciences

OS 03-01

Synergistic and distinct roles of GluA1-receptors in the dorsal and ventral hippocampus in schizophrenia-related sensory and cognitive processing

Sampath Kumar Kapanaiah[1], Daniel Strahnen[1], Rolf Sprengel[2], David Bannermann[3], Dennis Kätzel[1]

[1] *Ulm University, Institute of Applied Physiology, Ulm, Germany*
[2] *Max-Planck-Institute for Medical Research, Heidelberg, Germany*
[3] *University of Oxford, Dept. of Experimental Psychology, Oxford, UK*

Schizophrenia is a debilitating brain disorder that affects almost 1% of the general population and involves aberrant assignment of salience and attention as core deficits which may drive psychotic and cognitive symptoms of this disease. Ionotropic glutamate receptors of the AMPA-type (AMPAR) that contain the subunit GluA1 have been linked to schizophrenia at the level of genetics, protein expression (particularly in the hippocampus) and neuropsychology. GluA1-containing AMPARs mediate the fast and early phase of synaptic long-term potentiation, that is likely involved not only in long-term memory, but also in more transient cognitive processing including short-term habituation, selective attention, and working memory, which are impaired in schizophrenia. Mice with a global knockout of the GluA1-encoding gene *Gria1* (*Gria1*$^{-/-}$ mice) have been used as a tool to study the mechanistic role of GluA1-AMPARs in such sensory and cognitive processing with relevance to the pathomechanism of schizophrenia. We have previously shown, that the selective restoration of GluA1-expression in the CA2/CA3 subfields of the hippocampus of *Gria1*$^{-/-}$ mice is sufficient to rescue their deficit in spatial short-term habituation – a key mechanism to regulate attention paid to spatial cues – and in hippocampal-prefrontal coherence in the theta-frequency range - which is likely a correlate of this process. In our current study, we have extended and refined this approach by re-constituting GluA1 in *Gria1*$^{-/-}$ mice with viral vectors selectively either only in the dorsal or the ventral hippocampus, in order to reveal the distinct roles of both, these two *hippocampal subdivisions* and the *GluA1-AMPAR populations* within them for a broad range of schizophrenia-related sensory and cognitive processing. We have conducted a comprehensive battery of assays assessing spatial and object-related short-term habituation, working memory, sociability, and auditory sensory processing with concomitant multi-site field potential recordings in dorsal and ventral hippocampus, mediodorsal thalamus, prefrontal and auditory cortex. We found that several impairments in sensory and cognitive processing could be rescued either by restoration of GluA1-expression in only *one* of the two hippocampal subdivisions alone or by restoration *in either one* of the two regions. The findings suggest a certain – and surprising - level of redundancy between the role of GluA1 in dorsal and ventral hippocampus.

Funding: Else-Kröner-Fresenius-Foundation/German-Scholars-Organization (programme for excellent medical scientists from abroad; GSO/EKFS 12, to D.K.), Ministry of Arts and Science of Baden Württemberg (Junior-Professorship Programme; to DK) and DFG (KA 4594/2-1; to DK)

OS 03-02
Postsynaptic plasticity of cholinergic synapses underlies the induction and expression of appetitive and familiarity memories in *Drosophila*

Carlotta Pribbenow[1], Yi-chun Chen[1], Michael-Marcel Heim[1], Desiree Laber[1], Silas Reubold[1], Eric Reynolds[1], Isabella Balles[1], Tania Fernández-d.V. Alquicira[1], Raquel Suárez Grimalt[1,2], Lisa Scheunemann[1,3,5], Carolin Rauch[1], Tanja Matkovic[1,5], Gregor Lichtner[1], Sridhar R. Jagannathan[1], Jörg Rösner[1,4], David Owald[1,2,3]

[1] *Charité- Universitätsmedizin Berlin, Institut für Neurophysiologie, Berlin, Germany*
[2] *Einstein Center for Neurosciences Berlin, Berlin, Germany*
[3] *NeuroCure, Charité – Universitätsmedizin Berlin, corporate member of Freie Universität Berlin and Humboldt-Universität zu Berlin, and Berlin Institute of Health, Berlin, Germany*
[4] *NWFZ, Charité – Universitätsmedizin Berlin, corporate member of Freie Universität Berlin and Humboldt-Universität zu Berlin, and Berlin Institute of Health, Berlin, Germany*
[5] *Freie Universität Berlin, Institut für Biologie, Berlin, Germany*
[6] *Universitätsmedizin Greifswald, Department of Anesthesia, Critical Care, Emergency and Pain Medicine, Greifswald, Germany*

In vertebrates, several forms of memory-relevant synaptic plasticity involve postsynaptic rearrangements of glutamate receptors. In contrast, previous work indicates that *Drosophila* and other invertebrates store memories using presynaptic plasticity of cholinergic synapses. Here, we provide evidence for postsynaptic plasticity at cholinergic output synapses from the *Drosophila* mushroom bodies (MBs). We find that the nicotinic acetylcholine receptor (nAChR) subunit α5 is required within specific MB output neurons (MBONs) for appetitive memory induction, but is dispensable for aversive memories. In addition, nAChR α2 subunits mediate memory expression and likely function downstream of α5 and the postsynaptic scaffold protein Dlg. We show that postsynaptic plasticity traces can be induced independently of the presynapse, and that *in vivo* dynamics of α2 nAChR subunits are changed both in the context of associative and non-associative (familiarity) memory formation, underlying different plasticity rules. Therefore, regardless of neurotransmitter identity, key principles of postsynaptic plasticity support memory storage across phyla.

OS 03-03
Parkinson's related alterations in the α-synuclein protein network

James Conway[1], Helia Weiberlen[2], Karsten Tillack[2], Michele Kiernan[1], Edgar R. Kramer[1,2,3]

[1] *University of Plymouth, Faculty of Health, Plymouth, UK*
[2] *Hamburg University, Center for Molecular Neurobiology Hamburg, Hamburg, Germany*
[3] *HMU, Medical Faculty, Potsdam, Germany*
[4] *Professor für Physiologie, HMU Potsdam, Potsdam, Germany*

Introduction

In Parkinson's disease patients, the small protein α-synuclein frequently accumulates and aggregates via toxic oligomers to large Lewy bodies and neurites, leading to midbrain dopaminergic cell death. The molecular mechanism of how oligomeric α-synuclein interferes with the physiological processes of dopaminergic neurons is still under debate, as well as what the optimum strategy to prevent α-synuclein accumulation and aggregation is. Currently, targeting α-synuclein expression or aggregation is believed to be a promising therapeutic approach to prevent or slow the progression of Parkinson's disease .

Here we investigated *in vivo* and *in vitro* the effects of disease-relevant accumulation of α-synuclein on physiological processes related to dopaminergic neuron survival. In addition, we evaluated *in vivo* and *in vitro* how the deficiency of endogenous ubiquitin ligases that can target α-synuclein for degradation affects the physiology of dopaminergic neurons.

Results

We have found, for example in mice, that contrary to previously reported data, the accumulation of α-synuclein does not lead to downregulation of the receptor tyrosine kinase RET, an important survival signaling receptor for dopaminergic neurons. However, α-synuclein seems to influence autophagy and mitochondrial integrity. Surprisingly, while the absence of the ubiquitin-protein ligase NEDD4-1 in mice increases the amount of endogenous α-synuclein protein, it is the absence of the ubiquitin-protein ligase NEDD4-2 that leads to the loss of dopaminergic neurons without altering the amount of α-synuclein protein. At the meeting, we will present a comprehensive characterization of our mouse models as well as data from cell culture experiments and histological stainings of patient brain sections.

Conclusions

Taken together, our data support the clinical trials using RET receptor ligands to support dopaminergic neuron survival in Parkinson's disease and dementia with Lewy body patients, as well as define NEDD4-1 and NEDD4-2 as novel therapeutic targets to prevent α-synuclein accumulation and dopaminergic cell death.

We acknowledge funding from BRACE, ARUK, Northcott Devon Medical Foundation, University of Plymouth and Hamburg University.

References

[1] Conway JA, Kramer ER (2021). Is activation of GDNF/RET signalling the answer for successful treatment of Parkinson's disease? A discussion of data from culture dish to clinic. Neural Regen Res. doi: 10.4103/1673-5374.327330.

[2] Conway JA, Kinsman G, Kramer ER (2022). The Role of NEDD4 E3 Ubiquitin-Protein Ligases in Parkinson's Disease. Genes. doi.org/10.3390/genes13030513

OS 03-04
Human iPSC-derived neurons with reliable synapses and large presynaptic action potentials

Torsten Bullmann[1], Andreas Ritzau-Jost[1], Thomas Kaas[1], Toni Kirmann[1], Anne Wöhner[1], Filiz S. Rizalar[2], Max Holzer[4], Jana Nerlich[1], Dmytro Puchkov[2], Christian Geis[5], Jens Eilers[1], Robert J. Kittel[6], Volker Haucke[2,3], Thomas Arendt[4], Stefan Hallermann[1]

[1] *University of Leipzig, Carl-Ludwig-Institute for Physiology, Leipzig, Germany*
[2] *Leibniz-Forschungsinstitut für Molekulare Pharmakologie (FMP), Berlin, Germany*
[3] *Free University of Berlin, Department of Biology, Chemistry, and Pharmacy, Berlin, Germany*
[4] *University of Leipzig, Paul-Flechsig-Institute for Brain Research, Leipzig, Germany*
[5] *Jena University Hospital, Department of Neurology, Section Translational Neuroimmunology, Jena, Germany*
[6] *University of Leipzig, Institute of Biology, Department of Animal Physiology, Leipzig, Germany*

Question

Understanding the function of the human brain requires the determination of fundamental parameters of synaptic transmission in human neurons. One of the most basic parameters controlling neurotransmitter release is the presynaptic action potential, but controversy remains its amplitude and duration. Presynaptic action potentials have so far only been measured with high temporal resolution in a limited number of vertebrate but not in human neurons.

Methods and Results

To uncover properties of human presynaptic action potentials, we exploited recently developed tools to generate human glutamatergic neurons by based on forced expression of Neurogenin 2 (Ngn2) in pluripotent stem cells. We characterized the structural, molecular, and functional properties of these neurons and their synapses after 3 to 9 weeks of culturing in different established media. During maturation, the proportion of cells with multiple axon initial segments decreased and the amount of axonal Tau protein increased. Whole-cell patch-clamp recordings revealed increased human neuronal excitability, decreased resting membrane potential, and somatic action potentials became shorter during maturation. Super-resolution and electron microscopy indicated mature synaptic contacts. Synaptic transmission in 6- to 9-weeks-old cells was reliable and synchronous up to a frequency of 100 Hz. Induced human neurons thus form mature high-fidelity synapses. To analyze

presynaptic action potentials, we performed direct presynaptic patch-clamp recordings at physiological temperature and with high temporal resolution. These revealed large overshoots to +40 mV and short durations of 0.5 ms.

Conclusions

Our results establish human induced excitatory neurons as a model for high-resolution structural-functional analyses of synaptic transmission and suggest that in humans glutamatergic transmission is mediated by large and rapid presynaptic action potentials.

OS 03-05
Observing single Dynamin-mediated fission events in TIRFM-amenable synapses

Sai Krishnan, Julia Lehrich, Yaroslav Tsytsyura, Jürgen Klingauf

Institut für Medizinische Physik und Biophysik, Münster, Germany

The presynapse features a unique tight coupling of exo- and endocytosis resulting in the formation of synaptic vesicles with uniform morphology. The difficulty in accessing the pre-synapse has hampered attempts to directly visualize the functionality of presynaptic proteins which enable such exquisite pairing.

To this end our lab has developed “Xenapses”, TIRFM-able synapses, formed by mouse hippocampal neurons cultured on micropatterned host substrates coated with synaptogenic proteins. Xenapses show all the characteristics of a synapse and allow us to directly observe the behavior of proteins involved in compensatory endocytosis. Xenapses lend themselves to unroofing, revealing via SEM the membrane surface to be studded with pre-assembled Clathrin structures, consistent with a pre-sorted and pre-assembled readily retrievable pool (RRetP) of endocytic structures.

We have further combined this preparation with CRISPR-Cas9 to endogenously label Dynamin I. This enabled the study of triggered compensatory endocytosis at an unprecedented spatial and temporal resolution. Dynamin-dependent fission occurred as discreet, quantal events, demonstrating the rate of endocytosis to be determined by the number of vesicles retrieved within a unit of time rather than by an intrinsic value. While Dynamin was recruited to the membrane within subsecond timescale following a single action potential, the subsequent assembly and fission, evidenced by gradual increase in fluorescence followed by rapid collapse, occurred over many seconds with a median duration of ~ 4 seconds at physiological temperature (Figure 1).

Disruption of actin polymerization by Latrunculin A increased the pinch off time to ~6 seconds, suggesting a role for actin as a force-generator during the scission process. Finally, cross-correlational analysis with overexpressed and orthogonally labelled Clathrin revealed Dynamin-dependent fission to be Clathrin-mediated. These results taken together cast a shadow over the existence of the Dynamin-dependent and Clathrin-independent ultrafast endocytic mode proposed to predominate at physiological temperature.

These observations advance Dynamin-mediated vesicle scission as the rate-limiting step in endocytosis, with the preassembled RRetP providing an element of speed advantage for the rapid, high fidelity retrieval of synaptic vesicles. The full potential of our system will be realized by investigating the choreography of other key endocytic proteins relative to Dynamin.

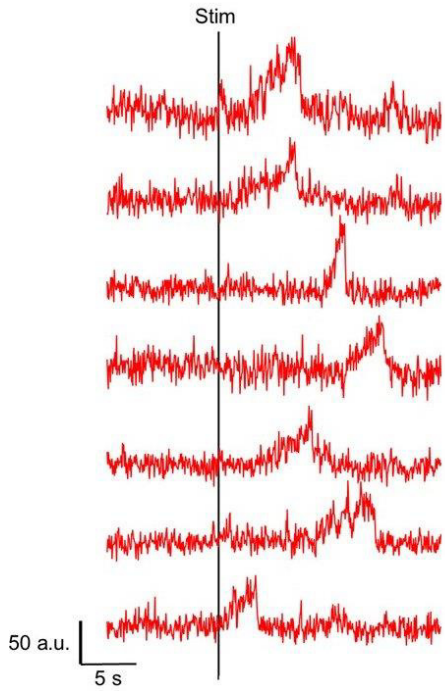

Figure 1
Sample traces of single Dynamin-mediated fission events in response to stimulus (1 AP).

OS 03-06
A Noelin-organized extracellular network of proteins required for constitutive and context-dependent anchoring of AMPA-receptors.

Jochen Schwenk[1], Sami Boudkkazi[1], Aline Brechet[1], Naoki Nakaya[2], Wolfgang Bildl[1], Astrid Kollewe[1], Uwe Schulte[1], Akos Kulik[1], Stanislav Tomarev[2], Bernd Fakler[1,3]

[1] *University of Freiburg, Institute of Physiology II, Freiburg, Germany*
[2] *National Institutes of Health, National Eye Institute, Section of Retinal Ganglion Cell Biology, Bethesda, USA*
[3] *University of Freiburg, Signaling Research Centers BIOSS and CIBSS, Freiburg, Germany*

Question

Fast excitatory neurotransmission and its context-dependent dynamics that are fundamental for processing, propagation and storage of information in the brain are mediated by AMPA-type glutamate receptors (AMPARs). They must be precisely localized into synaptic and extra-synaptic sites and finally be stabilized by distinct anchoring mechanisms. Best characterized is anchoring on the cytoplasmic side, where AMPARs may bind to various constituents of the postsynaptic density (PSD) via PDZ-interactions of their auxiliary TARP subunits. The molecular nature of a 'universal' and brain-wide active extra-cellular anchor that controls positioning and stabilization of AMPARs independent of their GluA-composition and is expected to be fundamental for constitutive and activity-dependent excitatory synaptic transmission has so far remained unresolved.

Methods

Here, we used high-resolution proteomics together with functional (electrophysiology in acute brain slices) and morphological analyses (immuno-EM and light microscopy) to identify the Noelin-family of secreted proteins as critical elements for stabilizing AMPARs at synaptic membranes.

Results

We found that distribution and dynamics of AMPARs in the plasma membrane are controlled by Noelins, a three-member family of conserved secreted proteins expressed throughout the brain. Noelin tetramers bind to the extracellular portion of all GluA proteins, albeit with some distinction for GluA4 versus GluAs1-3 and interconnect them in a network-like configuration with a variety of secreted and membrane-anchored proteins including Neurexin1, Neuritin1, and Seizure 6-like. Distribution of AMPARs was analyzed in freeze-fracture replicas from the CA1 region using electron-microscopy combined with immunogold-labelling by an *anti-GluA1-4* antibody in knockouts of Noelins1-3. In the absence

of Noelins the number of AMPARs in the surface membrane was largely reduced both in synapses, as well as in extra-synaptic sites of dendrites and the number of silent synapses increased by two-fold. Similarly, amplitudes of spontaneous and miniature EPSCs (sEPSC, mEPSC) were reduced in the hippocampus and the cerebellum in a cell-type dependent manner by 35-70%. Different from AMPAR currents, sEPSCs mediated by NMDA-type glutamate receptors (NMDARs) or sIPSCs through $GABA_A$ receptors were not affected by the deletion of Noelin1-3. Furthermore, Noelins are required for activity dependent plasticity. The stimulation of Schaffer collaterals (CA3-to-CA1) failed to trigger a stable LTP in the absence of Noelin1 or Noelin1-3.

ConclusionsOur results uncover an endogenous mechanism for extracellular anchoring of AMPARs and establish Noelin-organized networks as versatile determinants of constitutive and context-dependent neurotransmission.

References
[1] Diaz-Alonso, J., and Nicoll, R.A. 2021, AMPA receptor trafficking and LTP: Carboxy-termini, amino-termini and TARPs. Neuropharmacology *197*, 108710.
[2] Watson, J.F., Pinggera, A., Ho, H., and Greger, I.H. 2021, AMPA receptor anchoring at CA1 synapses is determined by N-terminal domain and TARP gamma8 interactions. Nat Commun *12*, 5083.
[3] Greger, I.H., Watson, J.F., and Cull-Candy, S.G. 2017, Structural and Functional Architecture of AMPA-Type Glutamate Receptors and Their Auxiliary Proteins. Neuron *94*, 713-730.
[4] Huganir, R.L., and Nicoll, R.A. 2013, AMPARs and synaptic plasticity: the last 25 years. Neuron *80*, 704-717.

OS 03-07
The lipid transporter ORP2 regulates synaptic neurotransmitter release via two distinct mechanisms

Marion Weber-Boyvat[1], Jana Kroll[1], Thorsten Trimbuch[1], Vesa M. Olkkonen[2,3], Christian Rosenmund[1]

[1] Charité - Universitätsmedizin Berlin, Institut für Neurophysiologie, Berlin, Germany
[2] Minverva Foundation Institute for Medical Research, Helsinki, Finland
[3] University of Helsinki, Helsinki, Finland

Cholesterol is crucial for neuronal synaptic transmission, assisting in the molecular and structural organization of lipid rafts, ion channels, and exocytic proteins. Although cholesterol absence was shown to result in impaired neurotransmission, how cholesterol locally traffics, and its route of action is still under debate. Here, we characterized the lipid transfer protein ORP2 in murine hippocampal neurons. We show that ORP2 preferentially localizes to the presynapse. Loss of ORP2 reduced presynaptic cholesterol levels by 50%, coinciding with a profoundly reduced release probability, enhanced facilitation and impaired presynaptic calcium influx. In addition, ORP2 displayed a cholesterol transport-independent function in regulating vesicle priming and spontaneous release, likely by competing with Munc18-1 to Syntaxin1A binding. To conclude, we identified a dual function of ORP2 as a physiological modulator of the synaptic cholesterol content, and a novel regulator of neuronal exocytosis.

OS 03-08
TRPV1-dependent nocifensive behavior in larval zebrafish reveals thermal hyposensitivity as a sensory marker of diabetic peripheral neuropathy

Jonathan R. Husk[1], Katrin Bennewitz[2], Uta Binzen[3], Jens Kroll[2], Rolf-Detlef Treede[1], Wolfgang Greffrath[1]

[1] Mannheim Center for Translational Neuroscience, Medical Faculty Mannheim, Heidelberg University, Department of Neurophysiology, Mannheim, Germany
[2] European Center for Angioscience, Medical Faculty Mannheim, Heidelberg University, Department of Vascular Biology and Tumor Angiogenesis, Mannheim, Germany
[3] European Center for Angioscience, Medical Faculty Mannheim, Heidelberg University, Department of Cardiovascular Biology, Mannheim, Germany

Introduction
Diabetic peripheral neuropathy (DPN) affects 30 % of diabetes patients and is characterized by numbness, paresthesia and in some cases spontaneous pain (Sun et al., 2020). While most rodent models of DPN develop a gain of function, in quantitative sensory testing most DPN

patients present a loss of small fiber function defined by increased thermal thresholds (Themistocleous et al., 2016). Here, we present a novel method to quantitatively analyze nocifensive responses to radiant heat stimuli in larval zebrafish. We examined the role of TRPV1 for the detection of noxious heat and the change in thermal threshold in different zebrafish models of diabetes mellitus.

Methods

We stimulated zebrafish larvae at 96 hours post fertilization (hpf) with a near-infrared diode laser (Schäfter+Kirchhoff, Germany) at five different intensities (150 ms, 18-88 mW, 5 stimuli each) to determine a stimulus response function. Wildtype embryos were injected with trpv1, pdx1, glo1 or control morpholino oligonucleotides to study the role of TRPV1 in vivo, or model diabetes by impaired pancreatic development (pdx1) or methylglyoxal scavenging (glo1). Larvae were also incubated in 10, 20 or 40 mM glucose or mannitol, or 50, 200 or 500 mM methylglyoxal (MG) from 24 to 96 hpf. For rescue, pdx1 morphants and glucose incubated larvae were immersed in the antihyperglycemic compound PK11195 (10 mM). Extra sum-of-squares F test was conducted with Prism 9 (GraphPad, USA).

Results

TRPV1 knockdown (threshold (mean ± SD) 62.5±6.5 mW) results in an increased heat pain threshold as compared to control morphants (threshold 28.6±4.4 mW, $p<0.0001$), stressing its relevance for the transduction of noxious heat in vivo. Both pdx1 morphants (50.1±4.9 mW) as well as glucose incubated larvae (10 mM: 42.3±4.7 mW, 20 mM: 40.8±4.6 mW, 40 mM: 44.5±4.9 mW) show increased heat pain thresholds as compared to control morphants (33.3±3.6 mW), wildtype (31.2±3.5 mW) or mannitol incubated animals (10 mM 33.5±3.6 mW, 20 mM 36.0±3.8 mW, 40 mM 39.2±4.3 mW, all $p<0.0001$). Since glucose-dependent effects were prevented by PK11195, and a similar phenotype was observed in glo1 knockdowns (45.5±4.9 mW) and MG incubated larvae (50 mM 47.3±4.9 mW, 200 mM 39.5±4.4 mW, 500 mM 36.8±4.0 mW; all $p<0.0001$), MG seems to cause sensory loss downstream from glucose.

Discussion

Nocifensive behavior in response to radiant heat in larval zebrafish depends on TRPV1 as marked thermal hyposensitivity occurs in knockdown animals. Further, all tested zebrafish diabetes models display a loss of small fiber function as measured in most DPN patients stressing their potential as a translational model in contrast to rodents. MG acts as an important downstream mediator in the development of small fiber sensory loss in DPN. This loss of function contrasts with thermal hyperalgesia in MG-driven rodent models of diabetes, which was proposed to be driven by a facilitation of nociceptive neuron firing (Bierhaus et al., 2012).

References

[1] Bierhaus, A., Fleming, T., Stoyanov, S., Leffler, A., Babes, A., Neacsu, C., Sauer, S.K., Eberhardt, M., Schnölzer, M., Lasitschka, F., *et al.* (2012). Methylglyoxal modification of Nav1.8 facilitates nociceptive neuron firing and causes hyperalgesia in diabetic neuropathy. Nat Med *18*, 926-933.

[2] Sun, J., Wang, Y., Zhang, X., Zhu, S., and He, H. (2020). Prevalence of peripheral neuropathy in patients with diabetes: A systematic review and meta-analysis. Prim Care Diabetes *14*, 435-444.

[3] Themistocleous, A.C., Ramirez, J.D., Shillo, P.R., Lees, J.G., Selvarajah, D., Orengo, C., Tesfaye, S., Rice, A.S.C., and Bennett, D.L.H. (2016). The Pain in Neuropathy Study (PiNS): a cross-sectional observational study determining the somatosensory phenotype of painful and painless diabetic neuropathy. Pain *157*, 1132-1145.

OS 04 | At the Heart of the Matter: Cardiac Physiology and Pathophysiology

OS 04-01

In left heart disease, elastin degradation impairs pulmonary arterial biomechanics and promotes pulmonary hypertension

Mariya M. Kucherenko[1,2,3], Pengchao Sang[1,2], Juquan Yao[1,2], Tara Gransar[1,2], Saphala Dhital[4], Jana Grune[1,2,3], Szandor Simmons[2,3], Laura Michalick[2,3], Dag Wulsten[5], Mario Thiele[5], Orr Shomroni[6], Felix Hennig[1], Ruhi Yeter[1], Natalia Solowjowa[1], Gabriela Salinas[6], Georg N. Duda[5], Volkmar Falk[1], Narendra Vyavahare[4], Wolfgang M. Kuebler[2,3], Christoph Knosalla[1,3]

[1] *Deutsches Herzzentrum der Charite, Department of Cardiothoracic and Vascular Surgery, Berlin, Germany*

[2] *Institute of Physiology, Charité-Universitätsmedizin Berlin, Berlin, Germany*

[3] *DZHK (German Centre for Cardiovascular Research), partner site Berlin, Berlin, Germany*

[4] *Clemson University, Department of Bioengineering, Clemson, USA*

[5] *Julius Wolff Institute for Biomechanics and Musculoskeletal Regeneration, Berlin, Berlin, Germany*

[6] *NGS Integrative Genomics (NIG), Göttingen, Goettingen, Germany*

Left heart failure is a global pandemic that affects 20% of all adults >40 years of age worldwide. Pulmonary hypertension secondary to left heart disease (PH-LHD) is a common complication that contributes relevantly to left heart disease (LHD) morbidity and mortality and accounts for 65-80% of all pulmonary hypertension (PH) cases. However, compared to other forms of PH, vascular remodeling in PH-LHD is poorly understood, and pharmacological interventions are lacking. In addition to increased pulmonary arterial pressure (PAP) and pulmonary vascular resistance (PVR), stiffening of pulmonary arteries (PAs) can aggravate PH by amplifying systolic pulse pressure and reducing diastolic flow, thus causing a further increase in right ventricular (RV) afterload and distal vessel injury.
We assessed PA stiffening and underlying molecular mechanisms in PA samples of left heart disease (LHD) patients with and without PH. Biomechanical testing revealed a 1.7-fold increase in stiffness and 1.4-fold reduction in strain in PH-LHD patients compared to healthy controls. Altered PA mechanics correlated positively with mean PAP. Extracellular matrix (ECM) remodeling in the PA wall preceded the onset of PH in LHD patients, as PAs of LHD patients which had not yet developed PH already showed marked dysregulation of genes implicated in elastic fiber fragmentation and degradation, while further deterioration of elastic fibers in PH-LHD patients was associated with increased expression of fibrillar collagens crosslinked by advanced glycation end-products (AGEs). In ex vivo cultured human PAs, elastin stabilization with the polyphenolic compound pentagalloyl glucose (PGG) protected fibers from elastolysis and improved PA mechanical properties. In a rat model of PH-LHD, nanoparticle-based targeted delivery of PGG improved PA biomechanics and normalized RV and pulmonary hemodynamics. Our findings identify PA stiffening as a characteristic feature of LHD that contributes relevantly to the development and progression of PH. Targeting extracellular matrix remodeling may present a promising therapeutic approach in PH-LHD.

Supported by the DZHK (German Centre for Cardiovascular Research) and the BMBF (German Ministry of Education and Research).

OS 04-02
Pro-regenerative Feature of Fibroblasts During Early Postnatal Phase

Adrian Goldspink[1], Julia Nicke[1], Fabian Ebach[1,2], Mauro Giacca[3], Bernd Fleischmann[1], **Mona Malek Mohammadi**[1]

[1] Medical Faculty, University of Bonn, Physiology I, Life & Brain Center, Bonn, Germany
[2] Medical Faculty, University of Bonn, Department of Neonatology and Paediatric Intensive Care, Children's Hospital, Bonn, Germany
[3] King's College London, School of Cardiovascular and Metabolic Medicine & Sciences and British Heart Foundation Centre of Research Excellence, London, Germany

Cardiovascular disease is the leading cause of death worldwide. A main reason is the insufficient regenerative capacity of the human heart to replace dead cardiomyocytes. Loss of these contractile cells and their replacement with non-contractile fibrotic tissue leads to reduced cardiac function and heart failure. In case the adult heart is exposed to pressure overload, cardiomyocytes become hypertrophic and cardiac fibroblasts strongly proliferate, differentiate into myofibroblasts, and secrete collagen. This leads to cardiac hypertrophy and interstitial and perivascular fibrosis resulting in comprised function.In clear contrast, neonatal mice, have the ability to regenerate the heart after injury. In fact, we have shown in earlier work that neonatal mice at postnatal day 1 (P1) are able to adapt to pressure overload via prominent cardiomyocyte proliferation. This capacity, however, is lost 7 days after birth when cardiomyocytes exit the cell cycle and pressure overload leads to cardiomyocyte hypertrophy and deterioration of cardiac function. Besides cardiomyocytes, fibroblasts, and endothelial cells also respond in a different fashion to pressure overload when induced at P1 compared to P7 and adult mice. We found that 14 days of pressure overload induced in P1 mice did neither cause fibrosis nor an increase in the number of fibroblasts in the heart, but enhanced angiogenesis. Herein, we investigated the different response of cardiac fibroblasts to pressure overload at P1 and P7 and their contributions to the adaptive response of the heart at P1. To this aim bulk RNAseq analysis was performed and analysis of the transcriptome of fibroblasts shortly after induction of pressure overload at P1 revealed strong expression of pro-angiogenesis and po-survival genes. The transcriptomic response of fibroblasts in P7 mice upon pressure overload was completely different and was mainly associated with enhanced cell cycle activity. Bioinformatic analysis revealed many genes related to secreted factors, which were upregulated in P1 fibroblasts. Gene ontology of these genes indicated a role in regulating angiogenesis, endodermal cell differentiation, the ERBB-2 signaling pathway, and anti-apoptosis effects. We explored some of the pathways by treating cardiomyocytes and endothelial cells with some of the P1 fibroblast secreted factors *in vitro* and could corroborate the pro-proliferative, pro-survival and pro-angiogenesis effects of these factors. We identified, similar to a recent report on heart regeneration in zebrafish, activation of collagen 11 and 12 in fibroblasts upon induction of pressure overload in P1, but not in P7 mice. Similarly, this was associated with endodermal differentiation and activation of Wnt signaling suggesting preserved fibroblast features and a role for cardiac

regeneration in neonatal mice. Thus, our results support a critical role of neonatal fibroblasts in the adaptive response of the neonatal mouse heart to pressure overload.

OS 04-03
Cardiac fatty acid oxidation after myocardial infarction is restored by insulin-like growth factor 1 treatment.

Andre Heinen, Eva Köster, Axel Gödecke

Institut für Herz- und Kreislaufphysiologie, Heinrich-Heine-Universität Düsseldorf, Düsseldorf, Germany

Question

Cardiac remodelling after myocardial ischemia and reperfusion (I/R) is accompanied by alterations in substrate metabolism affecting heart failure development. However, the exact nature of the metabolic disturbances is incompletely understood. Disease- and time-dependent effects as well as regional differences within the heart might contribute to this lack of clarity. We and others described that administration of insulin-like growth factor 1 (IGF1) preserves cardiac function after I/R, but it is unknown whether IGF1-treatment also affects cardiac substrate metabolism after I/R.

Methods

Male C57Bl6J mice underwent 45 minutes of LAD-occlusion or sham, respectively. Myocardial tissue was harvested 3, 7, or 28 days after I/R to determine kinetics of metabolic alterations. In addition, IGF1 was administered for three days after ischemia by osmotic pumps to investigate the effect of IGF1 on substrate metabolism; and tissue was harvested at day 3 or day 7. Substrate metabolism was analysed in tissue obtained from the interventricular septum, i.e. remote myocardium, by extracellular flux analysis in vibratome-cut intact cardiac tissue pieces. Oxygen consumption rates (OCR) were measured at baseline and after FCCP-stimulation in palmitate, glucose, and glutamine enriched medium using a Seahorse XFe24 analyser. To determine long-chain fatty acid (LCFA) metabolism, CPT1 was inhibited by etomoxir, and glucose metabolism by inhibition of mitochondrial pyruvate carrier (MPC) with UK5099. Data are mean±SD; n=5-6 animals per group.

Results

At day 3, I/R injury caused an increase in both basal OCR (66±8 vs. 51±8 pmol/min; p=0.02) as well as uncoupled OCR (107±7 vs. 84±12 pmol/min; p=0.01) compared to sham, whilst no effect was observed at day 7 and 28, respectively. CPT1 inhibition by etomoxir caused a larger reduction of uncoupled OCR in I/R compared to sham (62±9 vs. 49±11 pmol/min; p=0.09) at day 3. This increased contribution of long-chain fatty acids (LCFA) to overall metabolism in the I/R group was not found at day 7, and reverted at day 28 (I/R: 37±18, sham: 58±16 pmol/min; p=0.07). Administration of IGF1 increased basal OCR at day 7 by 39% compared to I/R group. With respect to substrate contribution, IGF1 treatment did not influence the effect of MPC inhibition at day 7 compared to I/R (49±19 vs. 47±17 pmol/min; ns). In contrast, IGF1 increased the effect of CPT1 inhibition at day 7 by 80% (64±21 vs. 36±7 pmol/min; p=0.02).

Conclusions

Acute myocardial infarction affects substrate metabolism in the remote myocardium in a time-dependent manner as seen by an increased LCFA oxidation in the early phase, and reduced LCFA oxidation at day 28, i.e. the chronic phase of cardiac remodelling. IGF1 treatment strongly improves LCFA oxidation at day 7 after I/R, and thereby potentially contributing to the beneficial effect of IGF1 on cardiac remodelling.

Funding: DFG SFB1116, A06 and S01

OS 04-04
Electrical auricular tragus stimulation induces release of circulating cardioprotective factors in healthy human volunteers.

Helmut Lieder, Umut Paket, Andreas Skyschally, Petra Kleinbongard, Gerd Heusch

Universität Duisburg-Essen, Institut für Pathophysiologie, Essen, Germany

Question

Remote ischemic conditioning (RIC) induces vagal activation with subsequent release of cardioprotective factors from the spleen into the circulation and reduces infarct size. These humoral cardioprotective factors can be transferred with plasma-dialysate from human donors undergoing RIC to isolated rodent recipient hearts where they reduce infarct size. Electrical auricular tragus stimulation (ATS) has been demonstrated to reduce myocardial injury and to improve contractile function in patients with acute myocardial infarction. Whether ATS, as RIC, induces release of cardioprotective factors into the circulation is unknown.

Methods

Healthy volunteers (3 females, 7 males, 26±5 years) were randomized to receive ATS or RIC, respectively, with an interval of at least two weeks between protocols. ATS was induced by bipolar electrical rectangular pulses of 200 µs width and a frequency of 30 Hz. The amplitude (5.5±0.81 mA) was set for each volunteer to not be perceived as uncomfortable. A microprocessor-controlled circuit periodically interrupted the stimulation signal after 5 s of stimulation for 5 s. ATS was continued over 30 min. RIC by 3 x 5 min blood pressure cuff inflation at 200 mmHg on the left upper arm/ 5 min deflation served as a reference to induce the release of cardioprotective factors. Venous blood samples were taken before and 60 min after ATS or RIC, respectively, and used to prepare plasma-dialysates (1:10 dialysis against buffer for 24 h, cut-off 12-14 kDa). Plasma-dialysates from samples taken before and 60 min after ATS or RIC, respectively, were infused for 8 min into isolated pressure-constant perfused rat hearts followed by 2 min washout before global 30 min ischemia/ 120 min reperfusion. Infarct size was demarcated by triphenyl tetrazolium chloride staining and calculated as percent of ventricular mass.

Results

With infusion of plasma-dialysate before ATS, infarct size was 30.9±4.5% of ventricular mass and not different from that with infusion of plasma-dialysate before RIC (35.8±5.8%). Infusion of plasma-dialysate after ATS reduced infarct size to 18.3±3.9%. This cardioprotective effect was similar to that seen with infusion of plasma-dialysate after RIC (20.1±3.5%).

Conclusions

ATS induces the release of cardioprotective factors into the circulation of healthy volunteers. Plasma-dialysates after ATS or RIC, respectively, reduce myocardial infarct size by the same magnitude in ex vivo isolated perfused rat hearts with global ischemia/ reperfusion.

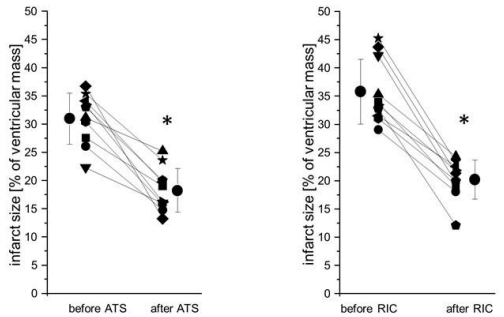

Figure: Infarct size in isolated perfused rat hearts with infusion of plasma-dialysate from samples taken before and after electrical auricular tragus stimulation (ATS) or remote ischemic conditiong (RIC), respectively, in healthy young volunteers. Plasma-dialysates were infused into isolated perfused rat hearts for 8 min before hearts were subjected to 30 min global ischemia/ 120 min reperfusion. Individual symbols indicate samples taken from the same individuum. Each volunteer was subjected to ATS or RIC protocols performed in random sequence with a minimum interval of two weeks betweeen the respective protocols. *p<0.001 versus before ATS or before RIC, respectively; one-way ANOVA for repeated measurements with Fisher's least significant differences post-hoc tests.

Infarct size in isolated perfused rat hearts with infusion of plasma-dialysate from samples taken

Plasma-dialysates were infused into isolated perfused rat hearts for 8 min before hearts were subjected to 30 min global ischemia/ 120 min reperfusion. Individual symbols indicate samples taken from the same individuum. Each volunteer was subjected to ATS or RIC protocols performed in random sequence with a minimum interval of two weeks betweeen the respective protocols. *p<0.001 versus before ATS or before RIC, respectively; one-way ANOVA for repeated measurements with Fisher's least significant differences post-hoc tests.

References

[1] Lieder HR, Tsoumani M, Andreadou I, Schrör K, Heusch G, Kleinbongard P. Platelet-Mediated Transfer of Cardioprotection by Remote Ischemic Conditioning and Its Abrogation by Aspirin But Not by Ticagrelor. Cardiovasc Drugs Ther. 2022 May 21. doi: 10.1007/s10557-022-07345-9.

[2] Lieder HR, Tüller P, Braczko F, Zandi A, Kamler M, Thielmann M, Heusch G, Kleinbongard P. Bioassays of Humoral Cardioprotective Factors Released by Remote Ischemic Conditioning in Patients Undergoing Coronary Artery Bypass Surgery. J Cardiovasc Pharmacol Ther. 2022 Jan-Dec;27:10742484221097273. doi: 10.1177/10742484221097273.
[3] Yu L, Huang B, Po SS, Tan T, Wang M, Zhou L, Meng G, Yuan S, Zhou X, Li X, Wang Z, Wang S, Jiang H. Low-Level Tragus Stimulation for the Treatment of Ischemia and Reperfusion Injury in Patients With ST-Segment Elevation Myocardial Infarction: A Proof-of-Concept Study. JACC Cardiovasc Interv. 2017 Aug 14;10(15):1511-1520. doi: 10.1016/j.jcin.2017.04.036.
[4] Lieder HR, Kleinbongard P, Skyschally A, Hagelschuer H, Chilian WM, Heusch G. Vago-Splenic Axis in Signal Transduction of Remote Ischemic Preconditioning in Pigs and Rats. Circ Res. 2018 Oct 26;123(10):1152-1163. doi: 10.1161/CIRCRESAHA.118.313859.

OS 04-05
Hypertrophic Cardiomyopathy mutation R723G enhances *MYH7*-mRNA stability

Kathrin Kowalski, Jirka Baustian, Julia Rose, Valentin Burkart, Theresia Kraft, **Judith Montag**

Hannover Medical School, Molecular and Cell Physiology, Hannover, Germany

Hypertrophic Cardiomyopathy (HCM) is mainly caused by mutations in sarcomeric proteins. More than a third of the patients are heterozygous for mutations in the *MYH7*-gene encoding for the β-myosin heavy chain (β-MyHC). Patients can express unequal fractions of mRNA and protein from mutant and wildtype alleles. High fractions of mutant mRNA can be associated with severe disease courses. Heterozygous patients with mutation R723G exhibit such a so-called allelic imbalance of on average 67% mutant and 33% wildtype *MYH7*-mRNA. This increased fraction of R723G-mRNA could either be caused by enhanced production or by decreased degradation.
Preliminary RNA-FISH analysis on patient-derived hiPSC-CMs with mutation R723G using a mutation-specific probe indicated that 46%±9% of the transcribed alleles encoded for the R723G-allele. In addition, co-transfection of expression-vectors for R723G- and wildtype-mRNA in HeLa cells with subsequent allele-specific RT-PCR showed that both mRNAs were produced in comparable amounts. These results suggest that mutation R723G has no effect on *MYH7*-mRNA production rate. To address RNA-degradation, we inhibited mRNA production by Actinomycin D and subsequently quantified non-degraded R723G- and wildtype-mRNA by RT-qPCR. We show an increase in R723G- relative to wildtype-mRNA over time, corresponding to a 1.5-fold increase in R723G-mRNA half-life. This prolonged life-time is associated with an altered secondary structure of the mRNA with mutation R723G as shown by *Selective 2'-hydroxyl acylation analyzed by primer extension* (SHAPE) analysis. Our results suggest that mutation R723G in *MYH7* alters mRNA-secondary structure, which enhances R723G-mRNA stability and thereby causes allelic imbalance in HCM-patients.

OS 04-06
Dysfunction of human cardiac ventricular myosin due to light chain-2 mutation D166V associated with Hypertrophic cardiomyopathy (HCM)

Faris Mehdawi, Tianbang Wang, Emrulla Spahiu, Petra Uta, Theresia Kraft, Arnab Nayak, Mamta Amrute-Nayak

Medizinische Hochschule Hannover, Institut für Molekular- und Zellphysiologie, Hannover, Germany

Hypertrophic cardiomyopathy (HCM) is an autosomal-dominant genetic disease of the heart muscle characterized by hypertrophy of the left ventricular wall and interventricular septum, often causing diastolic dysfunction. Clinical phenotype encompasses symptoms such as dyspnea, cardiac arrhythmia, syncope or even sudden cardiac death (SCD) in young individuals. Mutations in the *MYL2* gene that encodes ventricular myosin light chain-2 (MLC2v) are linked to HCM. MLC2v is a key component of the ventricular force-generating motor protein b-cardiac myosin. Point mutation Asp166Val (D166V) in MLC2v (D166V-MLC2v) is associated with a severe HCM phenotype and even SCD at a young age. Our aim is to understand how the mutation causes motor dysfunction that leads to left ventricular hypertrophy and impaired heart function in affected patients.
To investigate mutation-induced changes in motor function, we established a reconstitution approach and generated myosin motors bearing mutant MLC2v of human origin. The function of the wild type and mutant motors is studied using actin filament motility assay under predefined conditions. In this assay, the movement of fluorescently marked actin filaments (F-actin) on the lawn of mutant (MUT) or wild-type (WT) motors is similar to the unloaded shortening velocity at the sarcomere level in cardiomyocytes. Our preliminary results suggested an increased velocity of F-actin driven by D166V-MLC2v MUT motors. Furthermore, native thin filaments (comprising actin: tropomyosin: troponins) from human

ventricular tissue were used to assess the calcium sensitivity of the thin filaments driven by MUT motors. Changes in gliding speed are a result of altered chemomechanical features of MUT motors, which will be probed using optical trapping-based single-molecule studies. Probing functional defects in MUT ventricular myosin comprising myosin heavy and light chains of human origin are expected to reveal the primary trigger for disease development.

A comprehensive understanding of the mutation-specific impairment of overall motor function is fundamental to developing effective pharmacological therapies for HCM to curb disease progression.

OS 04-07

Neonatal model of pulmonary artery banding – a unique model to investigate right ventricular plasticity and intraventricular crosstalk in neonatal mice

Fabian Ebach[1,2], Julia Nicke[2], Tianyuan Hu[2], Bernd Fleischmann[2], Mona Malek Mohammadi[2]

[1] *University Hospital Bonn, Department of Neonatology and Paediatric Intensive Care, Bonn, Germany*
[2] *University of Bonn, Institute of Physiology I, Bonn, Germany*

Question

The capacity of neonatal left ventricular (LV) myocardium for adaptive regeneration following injury or pressure overload has been widely recognized[1,2]. However, it is unclear whether the right ventricular (RV) myocardium has similar plasticity in the neonatal period and how injury and regenerative response of one ventricle affects the other ventricle. RV pressure overload of varying degrees is a common symptom in neonatology and pediatric cardiology that can lead to severe disease or even death[3]. In contrast, surgically induced elevation of RV pressure by pulmonary artery banding has been shown to enhance LV function in young children with dilated cardiomyopathy[4]. Although the molecular mechanisms by which pressure overload of the RV can improve the LV function remain unknown, this evidence indicates a great plasticity of the RV and the existence of ventricular crosstalk shortly after birth. To investigate the plasticity and regenerative potential of the RV compared to the LV and to explore “interventricular” effects, we established a surgical neonatal mouse model of pulmonary artery banding (nPAB).

Methods

In CD1 mice at P1, anesthesia was induced by isoflurane and maintained by hypothermia. For nPAB, the main pulmonary artery (MPA) and the aorta were carefully separated. A suture was placed around the MPA (Fig. 1) and then tied around a placeholder needle, constricting the lumen to the size of the needle. As controls, either LV pressure overload was induced by neonatal transverse aortic constriction[5] (nTAC) or mice were Sham-operated. In all groups, echocardiography was performed at P7 and P14 to confirm the positioning of the constriction and to assess RV and LV function. At P14, hearts were collected for histological analysis.

Results

Echocardiography confirmed a constriction of the MPA with Doppler measurements showing a markedly increased flow velocity across the banding. As a result, the RV wall was thickened and the septum was deviated to the left (Fig. 2). Interestingly, we also found a thickening of the LV of about the same extent as after nTAC. In mice after nTAC, however, RV wall thickness remained unchanged. Interestingly, 14 days of nPAB or nTAC did not induce cardiomyocyte hypertrophy or fibrosis in the RV and the LV but enhanced angiogenesis in both ventricles.

Conclusions

We established nPAB in CD1 mice at P1. In echocardiography and post-mortem imaging, we observed a thickening of both ventricles without cardiomyocyte hypertrophy or increased fibrosis. This suggests that RV pressure overload not only leads to an adaptive response of the RV, but also triggers a response in the LV, indicating interventricular crosstalk. With nPAB, we are able to recreate the clinical situation of neonatal RV pressure overload in an animal model. Using this model, we aim to further understand the molecular mechanisms of RV plasticity and ventricular crosstalk, which may ultimately be therapeutic targets for children with RV pathologies.

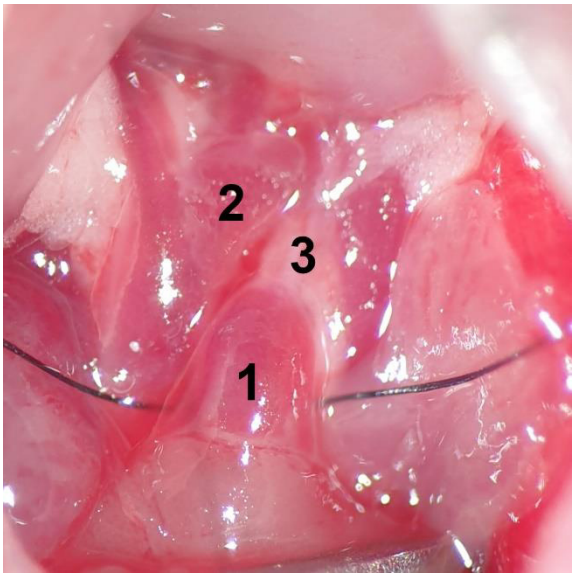

Figure 1
Intraoperative view after passing a thread beneath the main pulmonary artery **1**: main pulmonary artery, **2**: aortic arch, **3**: ductus arteriosus (obliterated)

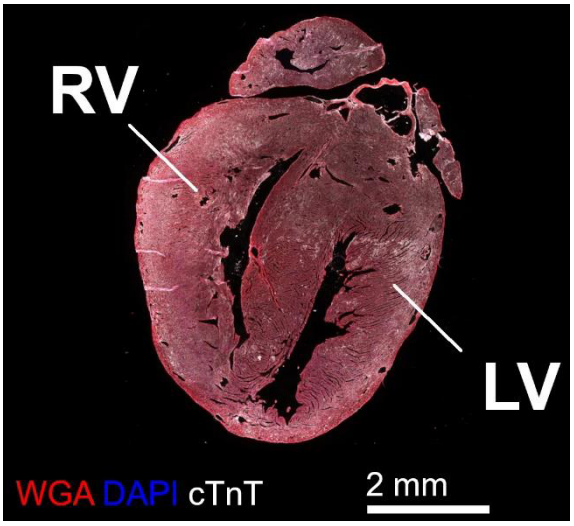

Figure 2
Increased right ventricular wall thickness and deviation of the intraventricular septum. **RV**: right ventricle, **LV**: left ventricle

References
[1] Lam NT, Sadek HA. Neonatal Heart Regeneration: Comprehensive Literature Review. *Circulation* 2018;138:412–23.
[2] Malek Mohammadi M, Abouissa A, Azizah I, et al. Induction of cardiomyocyte proliferation and angiogenesis protects neonatal mice from pressure overload-associated maladaptation. *JCI Insight* 2019;5:e128336.
[3] Malowitz JR, Forsha DE, Smith PB, Cotten CM, Barker PC, Tatum GH. Right ventricular echocardiographic indices predict poor outcomes in infants with persistent pulmonary hypertension of the newborn. *Eur Heart J Cardiovasc Imaging* 2015;16:1224–31.
[4] Schranz D, Recla S, Malcic I, Kerst G, Mini N, Akintuerk H. Pulmonary artery banding in dilative cardiomyopathy of young children: review and protocol based on the current knowledge. *Transl Pediatr* 2019;8:151–60.
[5] Malek Mohammadi M, Abouissa A, Heineke J. A surgical mouse model of neonatal pressure overload by transverse aortic constriction. *Nat Protoc* 2020:1–16.

OS 04-08
Implementing peer-assisted cardiac ultrasound demonstration in the practical heart physiology class

Vivian Blechschmidt[1], Uta Binzen[2], Jörg Heineke[2], Simon Wiegert[1], **Wolfgang Greffrath**[1]

[1] *Medical Faculty Mannheim, University Heidelberg, Department of Neurophysiology, Mannheim Center for Translational Neuroscience, Mannheim, Germany*
[2] *Medical Faculty Mannheim, University Heidelberg, Department of Cardiovascular Physiology, European Center for Angioscience, Mannheim, Germany*

Question

Previous studies have successfully used ultrasound to demonstrate concepts of cardiac physiology (1, 2). However, these teaching formats have only been offered to a limited number of students. The goal of this project was to implement a teaching format into the curriculum that could be made available to a full cohort of 270 students.

Methods

A 30-minute cardiac ultrasound demonstration was integrated into the mandatory physiology laboratory course "cardiac function" in the theme block "heart physiology" of the second semester. 20 groups of 10-15 students each attended the demonstration on a rotating basis, so only one ultrasound machine was needed. The demonstration was performed by a trained student tutor. The focus of the course unit was on the dynamic changes of the left side of the heart. Topics covered included diastolic and systolic characteristics, volume changes, mitral valve and aortic valve dynamics. The concepts of end-diastolic volume and end-systolic volume were also demonstrated and used to explain the calculations of stroke volume, cardiac output, and ejection fraction. The relationship of E/A ratio (representing ventricular filling) at normofrequency as well as tachycardia were used to demonstrate diastolic function.

Students were asked to report their level of agreement to eight statements on a scale of *1–5* (where 1 = strongly agree, *2* = agree, *3* = neutral, *4* = disagree, and *5* = strongly disagree) after the ultrasound demonstration. They could also leave additional comments. The ultrasound practical was conducted two years in a row. Year 1 (Y1) received the questionnaire 6 weeks after the practical, year 2 (Y2) received the questionnaire on the day of the practical. The mean agreement score (MAS) was calculated by summing the ratings (1-5) of all answers and dividing by the number of students. MAS is given in brackets for both years (Y1, Y2) separately.

Results

68 students of Y1 (response rate 29%) and 93 students of Y2 (response rate 36%) fully completed the questionnaire. Most students found the practical interesting (Y1 = 1.49, Y2 = 1.08). The course contributed to a better understanding of (Y1 = 1.81, Y2 = 1.33) and higher interest (Y1 = 1.65, Y2 = 1.38) in cardiac physiology. The amount of time (Y1 = 1.79, Y2 = 1.37) and content (Y1 = 1.75, Y2 = 1.23) were considered appropriate. The student tutors provided the content competently (Y1 = 1.65, Y2 = 1.06). Most students agreed that the course was useful in their medical training (Y1 = 1.63, Y2 = 1.22) and that the practical should also be offered to future years (Y1 = 1.39, Y2 = 1.01).

Conclusions

The cardiac ultrasound demonstration was well received by students and tutors, respectively, and should be offered to future years. Even with limited resources (one ultrasound machine; student tutor; 30 minutes of time) ultrasound can be implemented in the physiology practical to enhance interest and understanding of the heart dynamics.

References

[1] Bell FE 3rd, Wilson LB, Hoppmann RA. 2015, Using ultrasound to teach medical students cardiac physiology, Adv Physiol Educ, 39(4):392-396.

[2] Johnson CD, Montgomery LEA, Quinn JG, Roe SM, Stewart M, & Tansey EA. 2016, Ultrasound imaging in teaching cardiac physiology, *Adv Physiol Educ,* 40(3):354-358.

OS 05 | Vascular Reactivity

OS 05-01

Endothelial basement membrane remodeling regulates smooth muscle cell hyperplasia in pulmonary hypertension due to left heart disease

Netra Nambiar Veetil[1,2,3], Tara Gransar[1,2], Shao-Fei Liu[1,3], Robert Szulcek[1,2], Volkmar Falk[2,3], Mariya M. Kucherenko[1,2,3], Wolfgang M. Kübler[1,3,4], Christoph Knosalla[2,3]

[1] *Charité - Universitätsmedizin Berlin, Institute of Physiology, Berlin, Germany*
[2] *Charité – Universitätsmedizin Berlin, Department of Cardiothoracic and Vascular Surgery (DHZC), Berlin, Germany*
[3] *DZHK (German Centre for Cardiovascular Research), Partner site Berlin, Berlin, Germany*
[4] *DZL (German Centre for Lung Research), Partner site Berlin, Berlin, Germany*

Introduction: Pulmonary hypertension due to left heart disease (PH-LHD) is first initiated by passive congestion of blood from the left heart into the pulmonary vasculature, but subsequently progresses by pulmonary arterial (PA) remodeling. The latter is characterized by smooth

muscle cell (SMC) hyperplasia (SH), yet underlying pathomechanisms are so far little understood. Here, we addressed the role of the endothelial cell (EC)-derived basement membrane (BM) in regulating the SMC phenotype in PH-LHD.

Methods and Results: By histological analysis of human PA samples collected during heart transplantation, we identified intimal SH as a hallmark of PH-LHD. SH increased PA wall thickness up to 10% and correlated with mean pulmonary arterial pressure indicating a potential role in PH pathogenesis. *In vitro* evaluation of SMCs isolated from PAs of PH-LHD patients revealed a significant increase in cell migration and proliferation as compared to control SMCs. Further transcriptome analyses and immunohistological detection of BM markers collagen IV and laminin in PAs identified BM remodeling as an early event in PA remodeling in LHD patients prior to pulmonary hypertension (PH) and SH. Based on these findings we hypothesized that early remodeling of the endothelial BM may trigger SH by enhancing SMC migration and proliferation. Consistent with this idea, EC-produced decellularized BM from PAs of LHD patients without PH increased proliferation and migration in control SMCs, while control BM inhibited these responses in PH-LHD SMCs. We next considered YAP-1, a mechanosensitive transcriptional co-activator of the Hippo signaling pathway, as potential mediator of BM effects on SMCs. Increased nuclear (active) YAP-1 was detected in LHD without PH and PH-LHD SMCs. Concomitant *in vitro* experiments showed that decellularized BM produced by ECs of LHD patients with or without PH increased nuclear YAP-1 in control SMCs, while control BM decreased it in PH-LHD SMCs. YAP-1 inhibition by Verteporfin decreased YAP-1 nuclear translocation in isolated primary SMCs and attenuated the BM-induced increase in SMC proliferation and migration.

Conclusion: Our findings identify remodeling of the endothelial BM as an early event in PH-LHD development that drives SMC proliferation and migration via YAP-1 activation, thus promoting SH. BM remodeling and downstream YAP-1 activation present promising therapeutic targets for preventing SH in PH-LHD.

This research was supported by the DZHK, the BMBF, the DSHF, the DGK, and the DFG.

OS 05-02
Piezo1 in Pulmonary Arterial Smooth Muscle Cells – a critical player for the Development of Pulmonary Hypertension

Fenja Knoepp[1], Shariq Abid[2], Amal Houssaini[2], Emmanuelle Born[2], Elisabeth Marcos[2], Larissa Lipskaia[2], Malika Arhatte[3], Edyta Glogowska[3], Nora Vienney[2], Simone Kraut[1], Karin Quanz[1], Dagmar Fenner-Nau[1], Norbert Weissmann[1], Eric Honoré[3], Serge Adnot[2,4]

[1] *Justus Liebig University, Excellence Cluster Cardio-Pulmonary Institute (CPI), Giessen, Germany*
[2] *INSERM U955, Département de Physiologie-Explorations Fonctionnelles and DHU A-TVB Hôpital Henri Mondor, APHP, Crétail, France*
[3] *Université Côte d'Azur, Centre National de la Recherche Scientifique, Institut national de la santé et de la recherche médicale, Institut de Pharmacologie Moléculaire et Cellulaire, Labex ICST, Valbonne, France*
[4] *Justus Liebig University, Institute for Lung Health (ILH), Giessen, Germany*

Question

Pulmonary hypertension (PH) is a life-threatening and progressive, but yet incurable disease. The hallmarks of PH comprise i) sustained contraction and ii) excessive proliferation of pulmonary arterial smooth muscle cells (PASMCs). A major stimulus to which PASMCs are exposed during PH development is altered mechanical stress, originating from increased blood pressure, changes in blood flow velocity and a progressive stiffening of pulmonary arteries. Mechanosensitive ion channels, e.g. Piezo1, perceive such mechanical stimuli and translate them into a variety of cellular responses, including contractility or proliferation. Thus, the objective of the present study was to elucidate the specific role of Piezo1 in PASMCs for PH-development and progression.

Methods

The role of Piezo1 in PH-development was assessed in a) PASMCs and lung tissues from pulmonary hypertension (PH)-patients as well as b) two mouse strains characterized by SMC-specific, conditional Piezo1 knock-out. Taking advantage of these strains, the SMC-specific role of Piezo1 in PH-development and progression was assessed *via* experiments in isolated, perfused and ventilated mouse lungs, wire myography and proliferation assays. Finally, *in vivo* function of SMC-specific Piezo1 knockout was evaluated upon induction of chronic hypoxia-induced PH (CHPH) in these mice.

Results

Piezo1 expression and proliferation was enhanced in PASMCs from PH-patients. SMC-specific Piezo-deletion, as confirmed via qPCR and patch clamp recordings, prevented the hypoxia-induced increase in proliferation. Moreover, Piezo1-knockout reduced vasoconstriction, hypoxic pulmonary vasoconstriction (HPV) in particular, in isolated, perfused and ventilated mouse lungs, endothelial-denuded pulmonary arteries and hemodynamic measurements *in vivo*. Consequently, Piezo1-deficient mice were significantly protected against CHPH-development with ameliorated right heart hypertrophy and improved hemodynamic function.

Conclusions

This study provides evidence for Piezo1 expressed in PASMCs being critically involved in the pathogenesis of PH - most likely by controlling pulmonary vascular tone and arterial remodeling.

OS 05-03

The role of the Secreted Modular Calcium Binding protein 1 (SMOC1) in endothelial-to-mesenchymal transition and myocardial infarction

Fredy Delgado Lagos[1], Bardia Amirmiran[2], Urün Ukan[1], Beate Fisslthaler[1], Ralf Brandes[2], Mauro Siragusa[1], Ingrid Fleming[1]

[1] *Goethe Universität, Institute for Vascular Signalling, Goethe Universität, Frankfurt am main, Germany*
[2] *Goethe Universität, Institute for Cardiovascular Physiology, Frankfurt am Main, Germany*

The author has objected to a publication of the abstract.

OS 05-04

The long non-coding RNA *HIF1α-AS1* forms DNA:DNA:RNA triplexes to regulate endothelial cell function

Matthias S. Leisegang[1], Jasleen K. Bains[2], Timothy Warwick[1], James A. Oo[1], Nina M. Krause[2], Sandra Seredinski[1], Chao-Chung Kuo[3], Stefan Günther[4], Nevcin Sentürk Cetin[5], Frederike Boos[1], Soni S. Pullamsetti[6], Flavia Rezende[1], Ralf Gilsbach[1], Ilka Wittig[1], Ingrid Grummt[5], Teodora Ribarska[5,7], Ivan G. Costa[3], Harald Schwalbe[2], Ralf P. Brandes[1]

[1] *Goethe University Frankfurt, Institute of Cardiovascular Physiology, Frankfurt am Main, Germany*
[2] *Goethe University Frankfurt, Institute for Organic Chemistry and Chemical Biology, Center for Biomolecular Magnetic Resonance (BMRZ), Frankfurt am Main, Germany*
[3] *RWTH Aachen Medical Faculty, Institute for Computational Genomics, Joint Research Center for Computational Biomedicine, Aachen, Germany*
[4] *Max Planck Institute for Heart and Lung Research, Bad Nauheim, Germany*
[5] *German Cancer Research Center DKFZ-ZMBH, Division of Molecular Biology of the Cell II, Heidelberg, Germany*
[6] *Justus Liebig University, Department of Internal Medicine, Gießen, Germany*
[7] *Oslo University Hospital, Oslo, Norway*

Question

The phenomenon of DNA:DNA:RNA triplex formation through Hoogsteen base-pairing has been observed in *in vitro* systems, but its occurrence and potential impact on cellular function remain subject to debate [1]. Additionally, the physiological relevance, mechanistic mode of action, and associated protein complexes of triplex-forming long non-coding RNAs (lncRNAs) are not understood [1, 2]. Our objective was to identify lncRNAs that are functionally significant in human endothelial cells by investigating those that have the ability to form DNA:DNA:RNA triplexes.

Methods & Results

We used bioinformatic techniques, RNA/DNA pulldown, and biophysical studies to identify significant DNA:DNA:RNA triplex-forming lncRNAs in human endothelial cells. The lncRNA *HIF1α-AS1*, which is positioned antisense to the important Hypoxia-inducible factor 1α gene, was identified as a top hit. Knockdown or CRISPRi of the lncRNA in endothelial cells enhanced angiogenic capacity, while overexpression or CRISPRa had the opposite effect. The lncRNA was decreased in endothelial cells from glioblastoma and from lungs of pulmonary arterial

hypertension patients. In contrast, reoxygenation after hypoxia induced *HIF1α-AS1*. The lncRNA reduced the expression of numerous genes, including EPH Receptor A2 (EPHA2) and Adrenomedullin (ADM), through DNA:DNA:RNA triplex formation. Exchange of the triplex-forming region of *HIF1α-AS1* with other known triplex-forming regions by CRISPR Architect abolished its effects on gene expression. Protein interaction studies revealed that *HIF1α-AS1* binds to MPP8, a subunit of the repressive human silencing hub complex. *In vitro* binding experiments provided evidence that Exon1 of *HIF1α-AS1* is crucial for its interaction with the C-terminal domain of MPP8. ATAC-Seq analysis subsequent to *HIF1α-AS1* knockdown, CRISPRi, CRISPRa, or LentiCRISPR KO revealed that the lncRNA functions as an adaptor for the HUSH complex on *EPHA2* and *ADM*.

Conclusions

As demonstrated by *HIF1α-AS1* [3], DNA:DNA:RNA triplex formation plays a role in vascular tissue by regulating the angiogenic response and is essential for controlling trans-acting gene expression through the recruitment of epigenetic silencing complexes.

References

[1] Warwick T, Brandes RP, Leisegang MS. Computational Methods to Study DNA:DNA:RNA Triplex Formation by lncRNAs. *Noncoding RNA*. 2023

[2] Oo JA, Brandes RP, Leisegang MS. Long non-coding RNAs: novel regulators of cellular physiology and function. *Pflugers Arch*. 2022;474:191–204.

[3] Leisegang MS, Bains JK, Seredinski S, Oo JA, Krause NM, Kuo CC, Günther S, Sentürk Cetin N, Warwick T, Cao C, Boos F, Izquierdo Ponce J, Haydar S, Bednarz R, Valasarajan C, Fuhrmann D, Preussner J, Looso M, Pullamsetti SS, Schulz MH, Jonker HRA, Richter C, Rezende F, Gilsbach R, Pflüger-Müller B, Wittig I, Grummt I, Ribarska T, Costa IG, Schwalbe H, Brandes RP. HIF1α-AS1 is a DNA:DNA:RNA triplex-forming lncRNA interacting with the HUSH complex. *Nat Commun*. 2022;13:6563.

OS 05-05
Differential cGMP-reactivity of large and small vessels of mesenteric and renal vascular tree

Lubomir T. Lubomirov[1], René Mantke[2,3], Thomas Enzmann[4], Hendrik Borgmann[4], Olaf Grisk[1]

[1] *Brandenburg Medical School Theodor Fontane, Institute of Physiology, Neuruppin, Brandenburg an der Havel, Germany*
[2] *General and Visceral Surgery Clinic, Brandenburg Medical School Theodor Fontane, Brandenburg an der Havel, Germany*
[3] *Faculty of Health Brandenburg, Brandenburg Medical School Theodor Fontane, Brandenburg an der Havel, Germany*
[4] *Urology and Children Urology Clinic, Brandenburg Medical School Theodor Fontane, Brandenburg an der Havel, Germany*

Question

The adequate response of the vasculature to stimulation of cGMP/PKG-system ensures the precise regulation of blood flow and organ perfusion. The present study was undertaken to explore the cGMP-reactivity of large mesenteric arteries (LMA, diameter >500µm), small mesenteric arteries (SMA, <500µm), large medullary renal arteries (MRA, >500µm) and cortical renal arteries (CRA, <500µm), obtained from patients recruited for surgical colon resection or nephrectomy.

Methods

Vascular diameter and contractility were measured by wire myography. Phosphorylation of the regulatory 20-kDa light-chain-of-myosin at serin19 (MLC_{20}-S19) and targeting-subunit-of-myosin-phosphatase at phsphosites threonine 853 and serine 668 (MYPT1-T853 and MYPT1-S668) were determined by western blotting.

Results

Median vascular diameter, under pressure of ~100 mmHg was 404µm in CRA, 837µm in MRA, 475µm in SMA and 2824 µm in LMA. Maximal force, obtained under stimulation by 1 µmol/l tromboxaneA2-analogue, U46619 was 15.2±1.9 mN, 32.4±5.5 mN, 21.2±3.0 mN and 94.7±4.7 mN, respectively. Submaximal force evoked by 60 mmol/l K^+ (K60) was ~85% in all groups. Application of increasing concentrations of the NO-independent soluble guanylyl cyclase (sGC) activator, cinaciguat (10^{-10}-10^{-5} mol/l) induced concentration-dependent relaxation in all groups. The dose responsiveness was similar in the mesenteric vessels (pD_2=7.5±0.2 SMA vs. 7.9±0.2 LMA), but the maximal relaxation (F_{max}) was significantly attenuated in LMA (41.2±4.3% vs. 65.0±4.1% respectively; p<0.001). In renal vessels pD_2-values were also similar in MRA and CRA, (7.0±0.4 vs. 6.7±0.5), but F_{max} was attenuated to a smaller extent (68.2±3.6% vs. 55.9±3.9%; p<0.05). While under K60, a treatment by 1 µmol/l cinaciguat reduced MLC_{20}-S19 by ~twofold in SMA (p<0.05), in LMA the same treatment reduced this phosphorylation insignificantly (p=0.4). In SMA cinaciguat also increased the phosphorylation of the PKG site of MYPT1, MYPT1-S668. By contrast, the dephosphorylating effect of the compound on RhoA-protein kinase (ROK) site, MYPT1-T853 was equal.

Conclusions

The present work reports a blunted LMA reactivity to cinaciguat. The underlying mechanism involves impaired ability of the compound to dephosphorylate MLC_{20}-S19. Interestingly, cinaciguat is still able to reduce the ROK-pathway in LMA, but its ineffectiveness to reduce force, point out the importance of ROK-independent pathways of myosin phosphorylation for maintenance of tone of large vessels.

OS 05-06

Impaired vasomotor function in mesenteric arteries of Ossabaw minipigs with a genetic predisposition to, but without the phenotype of the metabolic syndrome

Chantal Eickelmann[1], Michael Sturek[2], Gerd Heusch[1], Petra Kleinbongard[1]

[1] *Institute for Pathophysiology, West German Heart and Vascular Center, University of Essen Medical School, Essen, Germany*
[2] *CorVus Biomedical LLC and CorVus Foundation Inc, Crawfordsville, USA*

Question

The metabolic syndrome plays a major role in the development and progression of atherosclerosis. An early manifestation of atherosclerosis is endothelial dysfunction, which results in increased arterial contractile function due to an imbalance between relaxing and contractile factors [1]. The minipig strain "Ossabaw" is characterized by a genetic predisposition to develop a metabolic syndrome upon high fat diet [2-3]. We have investigated whether Ossabaw minipigs exhibit an impaired vasomotor function even before they develop a metabolic syndrome. Therefore, we used isolated arteries of adult lean Ossabaw minipigs and, for comparison, adult Göttingen minipigs without such genetic predisposition.

Methods

In terms of the 3Rs of animal use in research [4-5], we included pigs which originally underwent cardioprotection studies. Mesenteric arteries are characterized by a comparable receptor arrangement as arteries of other vascular territories, e.g. coronary arteries and therefore provide a useful bioassay preparation. Isolated mesenteric arteries of both minipig strains were harvested post mortem, dissected, and mounted on a wire small vessel myograph for isometric force measurements. Vasoconstriction to potassium chloride (KCl)-induced depolarization of the vascular smooth muscle cells was induced (twice 0.6×10^{-1} mol/L and twice 1.2×10^{-1} mol/L), and maximal vasoconstriction to KCl (KCl_{max}) quantified. Cumulative concentration-response curves were determined in response to 1×10^{-9} mol/L – 1×10^{-4} mol/L norepinephrine. Endothelium-dependent and -independent vasodilation was measured in response to carbachol and nitroprusside (1×10^{-9} mol/L – 1×10^{-4} mol/L, each) after pre-constriction with norepinephrine (1×10^{-4} mol/L).

Results

Vasoconstriction in response to KCl was comparable between Ossabaw and Göttingen minipigs (Figure 1A). In vessels from Ossabaw minipigs vasoconstriction in response to norepinephrine was more pronounced than in those from Göttingen minipigs (Figure 1B), there was less endothelium-dependent (Figure 2A) and -independent vasodilation (Figure 2B).

Conclusion

Even before development of the metabolic syndrome, vasomotor function is impaired in Ossabaw minipigs, suggesting a genetic predisposition for the early development of a vascular dysfunction. Thus, Ossabaw minipigs may resemble the human situation.

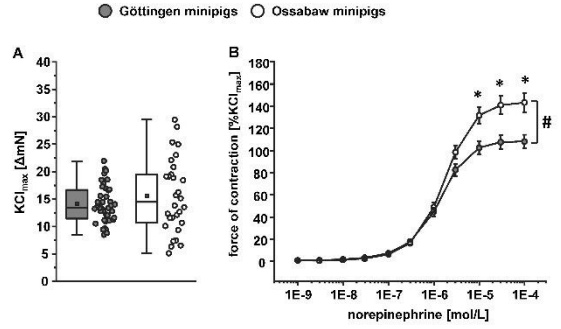

Figure 1: Vasoconstriction in response to potassium chloride and norepinephrine
Data are presented as (A) boxplots and as (B) means ± standard errors. The means ± standard errors were calculated from averages of 1-6 vessels per pig, respectively; 184 vessels from n=40 Göttingen minipigs and 118 vessels from n=30 Ossabaw minipigs; (A) unpaired students t-test: p=0.23 Göttingen minipigs vs. Ossabaw minipigs; (B) two-way analysis of variance for repeated measures: #p=0.0012 Göttingen minipigs vs. Ossabaw minipigs, Fisher's least significant difference post hoc test: *p<0.05 vs. Göttingen minipigs.

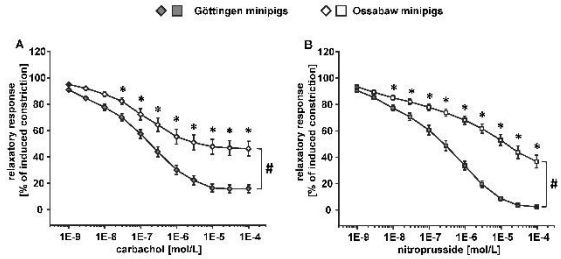

Figure 2: Endothelium-dependent and -independent vasodilation
Data are presented as means ± standard errors. The means ± standard errors were calculated from averages of 1-3 vessels per pig, respectively; (A) 97 vessels from n=37 Göttingen minipigs and 60 vessels from n=29 Ossabaw minipigs; (B) 87 vessels from n=38 Göttingen minipigs and 58 vessels from n=27 Ossabaw minipigs; two-way analysis of variance for repeated measures: #p<0.001 Göttingen minipigs vs. Ossabaw minipigs, Fisher's least significant difference post hoc test: *p<0.05 vs. Göttingen minipigs.

References
[1] Libby, P., Buring, J. E., Badimon, L., Hansson, G. K., Deanfield, J., Bittencourt, M. S., Tokgözoğlu, L., & Lewis, E. F. (2019). Atherosclerosis. Nature reviews. Disease primers, 5(1), 56.
[2] Sturek, M., Alloosh, M., & Sellke, F. W. (2020). Swine Disease Models for Optimal Vascular Engineering. Annual review of biomedical engineering, 22, 25–49.
[3] Kleinbongard, P., Lieder, H. R., Skyschally, A., Alloosh, M., Gödecke, A., Rahmann, S., Sturek, M., & Heusch, G. (2022). Non-responsiveness to cardioprotection by ischaemic preconditioning in Ossabaw minipigs with genetic predisposition to, but without the phenotype of the metabolic syndrome. Basic research in cardiology, 117(1), 58.
[4] Burden, N., Chapman, K., Sewell, F., & Robinson, V. (2015). Pioneering better science through the 3Rs: an introduction to the national centre for the replacement, refinement, and reduction of animals in research (NC3Rs). Journal of the American Association for Laboratory Animal Science : JAALAS, 54(2), 198–208.
[5] Yosten, G. L. C., Adams, J. C., Bennett, C. N., Bunnett, N. W., Scheman, R., Sigmund, C. D., Yates, B. J., Zucker, I. H., & Samson, W. K. (2018). Revised guidelines to enhance the rigor and reproducibility of research published in American Physiological Society journals. American journal of physiology. Regulatory, integrative and comparative physiology, 315(6), R1251–R1253.

OS 05-07

Vascular smooth muscle epidermal growth factor receptor increases obesity-induced vascular alterations and renal end organ damage.

Barbara Schreier, Christian Stern, Sindy Rabe, Sigrid Mildenberger, Virginie Dubourg, Alexander Nolze, Michael Gekle

Martin Luther University Halle-Wittenberg, Julius Bernstein Institute of physiology, Halle, Germany

Question

Diabetes mellitus type 2 as well as metabolic syndrome are associated with hypertension, most probably because of endocrine dysregulation of the adrenergic and the renin-angiotensin-aldosterone-system. It has been demonstrated, that the epidermal growth factor receptor (EGFR) contributes - as an important signaling hub - to cardiovascular function and disease. In this study we investigate the role of smooth muscle cell (VSMC) and endothelial cell (EC) EGFR for blood pressure homeostasis, acute vascular reactivity and renovascular dysfunction.

Methods

We generated mouse models with deletion of the EGFR in EC or VSMC. After 18 weeks of high fat (HFD) or standard fat diet (SFD) various structural (organ weight, vessel morphology, kidney morphology) and functional variables (Mulvany myography, pressure myography) as well as transcriptome changes were assessed. In an additional cohort of anaesthetized (Ketamine/Xylazin) animals intravascular blood pressure and heart rate was measured via millar catheter upon volume load, angiotensin II (ang II) and phenylephrine (PE) stimulation.

Results

We show that VSMC-EGFR mediates obesity/ diabetes type 2-induced vascular dysfunction, remodelling and transcriptome dysregulation preceding renal damage. EGFR deletion in VSMC protects the animals from HFD-induced endothelial dysfunction, creatininaemia and albuminuria. Furthermore, we demonstrate that HFD leads to marked changes of the aortic transcriptome in VSMC wild-type but not knockout animals. We confirmed that deletion of the EGFR in VSMC leads to reduced blood pressure and a heart rate increase. Furthermore, volume load induced larger increases in blood pressure in VSMC EGFR KO animals than in VSMC EGFR WT animals and counteracted the blood pressure changes induced by high fat diet, thereby indicating a higher acute blood pressure response.

EC-EGFR deletion did not alter heart and lung weight, baseline blood pressure and aortic transcriptome (determined by RNA-seq). Regarding vasoactive substances, the EGFR in EC seems to be without importance for ang II action and to counteract HFD-induced blood pressure increase upon PE stimulation.

Conclusions

VSMC-EGFR contributes to HFD-induced vascular and subsequent renal alterations. Our results indicate that EC-EGFR, in comparison to VSMC-EGFR, is of minor and opposite importance for basal renovascular function as well as for high fat diet-induced vascular remodeling and renal endorgan damage. We demonstrate that EGFR VSMC, but not EC EGFR, is of major importance for shorttime vascular reactivity to angiotensin II, catecholamines and volume as well as obesity-induced alterations of vascular reactivity.

This research was funded by the Deutsche Forschungsgemeinschaft with the grants GE905/19-2 & SCHR1450/2-4.

References

[1] Stern, C, Schreier, B, Nolze, A, Rabe, S, Mildenberger, S, Gekle, M (2020) 'Knockout of vascular smooth muscle EGF receptor in a mouse model prevents obesity-induced vascular dysfunction and renal damage in vivo' *Diabetologia* 63, 2218–2234, doi:10.1007/s00125-020-05187-4.

[2] Schreier, B, Stern, C, Dubourg, V, Nolze, A, Rabe, S, Mildenberger, S, Wickenhauser, C, Gekle, M. (2021) 'Endothelial epidermal growth factor receptor is of minor importance for vascular and renal function and obesity-induced dysfunction in mice.' *Sci. Rep.* 11, 7269, doi:10.1038/s41598-021-86587-3.

OS 05-08
The role of promyelocytic leukemia protein in vascular inflammation and atherosclerosis

Gustav Steinemann, Janine Berkholz

Institut für Physiologie, Universitätsmedizin Charite Berlin, Berlin, Germany

Promyelocytic Leukemia Protein (PML) is a multifunctional protein involved in many cellular processess such as gene regulation, DNA repair, cellular senescence, and tumor suppression. It forms so called nuclear bodies and interacts with various proteins, impacting a variety of cellular activities. PML's roles in stress response and inflammation contribute to its significance in disease and therapeutic potential.

Vascular inflammation is a complex physiological response that plays a critical role in the pathogenesis of various cardiovascular disorders, including atherosclerosis. Inflammation within the vascular wall involves the activation of various immune cells, endothelial dysfunction, and the release of pro-inflammatory cytokines and chemokines. Within this process, PML has emerged as a potential regulator of vascular inflammation, presenting an intriguing avenue for further exploration.

Our aim is to shed light on the specific role of PML in vascular inflammation, with a focus on its interplay with low-density lipoprotein (LDL) and the intricate relationship with select chemokines and cytokines.

Our research highlights the specific relationship between PML, LDL, and interleukin-6 (IL-6) in human endothelial cells (ECs) such as human umbilical vein endothelial cells (HUVECs) and EA.hy926 cells. We showed that LDL treatment induces the upregulation of PML expression in ECs. Subsequently, the elevated PML levels modulate IL-6 production and secretion in response to LDL. This intricate interplay between LDL, PML, and IL-6 in human ECs contributes to the inflammatory response within the endothelium, a critical event in the development of atherosclerosis.

Additionally we explored the interplay between PML, inflammation, and atherosclerosis, with a particular focus on specific chemokines and cytokines. Inflammatory stimuli, such as interleukin-1β (IL-1β) and interleukin-6 (IL-6), can induce the expression of PML and modulate its interaction with chemokines, like interleukin-8 (IL-8). PML, in turn, can regulate the expression of pro-inflammatory genes, such as vascular cell adhesion molecule-1 (VCAM-1) and intercellular adhesion molecule-1 (ICAM-1), thereby facilitating the recruitment and activation of immune cells within atherosclerotic lesions.

Moreover, understanding the intricate role of PML in atherosclerosis, particularly in the context of LDL metabolism and inflammation, holds great clinical significance. Dysregulation of PML-mediated processes can lead to enhanced LDL accumulation, foam cell formation, and perpetuation of the inflammatory response within plaques.

Understanding the precise regulatory mechanisms by which PML modulates chemokines and cytokines provides crucial insights into the pathogenesis of chronic vascular diseases. Targeting PML-mediated pathways may hold promise for developing therapeutic interventions aimed at modulating the inflammatory response and mitigating disease progression.

OS 06 | Kidney & Gastrointestinal Physiology

OS 06-01

Analysis of molecules perturbed by SGLT2 inhibition reveals kidney reconfiguration and metabolic interorgan communication.

Anja Billing[1], Young Kim[2], Volker Vallon[2], Markus Rinschen[1,3]

[1] *Aarhus University, Aarhus, Denmark*
[2] *UCSD, San Diego, USA*
[3] *University Medical Center Hamburg-Eppendorf, Hamburg, Germany*

Question

SGLT2 inhibitors, originally employed for hyperglycemia management, exhibit protective effects against renal and cardiovascular complications, irrespective of diabetes presence. The precise molecular mechanisms underlying these effects remain largely unknown and cannot be solely attributed to their primary function of inhibiting renal glucose re-absorption. SGLT2 inhibitors, originally employed for hyperglycemia management, exhibit protective effects against renal and cardiovascular complications, irrespective of diabetes presence. The precise molecular mechanisms underlying these effects remain largely unknown and cannot be solely attributed to their primary function of inhibiting renal glucose re-absorption.

Methods

To gain insights into these mechanisms, we employed LC-MS/MS to investigate various aspects, including the proteome, phosphoproteome, gut metaproteome, metabolome, and SGLT2 interactome. For proteomics/phosphoproteomics analysis, we used TMT16-plex labeling or label-free approaches with an Exploris 480 mass spectrometer (Thermo Fisher Scientific) connected to an UltiMate3000 RSLC (Thermo Fisher Scientific) system. For untargeted metabolomics, we utilized a quadrupole time-of-flight Impact II instrument (Bruker) connected to either a Bruker Elute HPLC or an Agilent 1290 infinity HPLC device. Targeted metabolomics was conducted using a 6495C triple-quadrupole coupled to an Agilent 1290 Infinity HPLC.

Results

We performed an extensive analysis of the proteome, phosphoproteome, and metabolome following one week of SGLT2 inhibitor treatment in non-diabetic and early diabetic mice. We integrated data from multiple metabolic organs and body fluids, including the kidney, liver, heart, white adipose tissue, skeletal muscle, plasma, urine, and gut microbiota. The kidney exhibited the strongest and most significant response to SGLT2 inhibitors in terms of metabolic signaling and transporter reconfiguration. Additionally, the gut microbiome displayed a reduction in bacteria taxa capable of fermenting aromatic amino acid levels and tryptophan, resulting in lower plasma levels of uremic toxins. Among the most prominently affected metabolites was p-cresol sulfate, a finding confirmed in cohort studies involving diabetic and heart failure patients with reduced ejection fraction.

Conclusions

The metabolic communication facilitated by SGLT2 inhibitors reduced the presence of circulating waste products such as p-cresol sulfate, consequently reducing the need for renal detoxification. This, combined with decreased glucotoxicity in the proximal tubules and a broad downregulation of apical transport activity, provides a metabolic explanation for the kidney and cardiovascular protection observed.

OS 06-02
TYK2 is required for LIF-induced augmentation of vascular calcification

Mehdi Razazian[1], Ioana Alesutan[1], Trang T. Luong[1], Misael Estepa[2], Lakmi Pitigala[1], Laura Henze[2], Jakob Obereigner[1], Gregor Mitter[1], Daniel Zickler[3], Mirjam Schuchardt[3], Christine Deisl[1], Manousos Makridakis[4], Can Gollmann-Tepeköylü[5], Andreas Pasch[1,6], Daniel Cejka[7,9], Susanne Suessner[8], Marlies Antlanger[9], Bernhard Bielesz[10], Matthias Müller[11], Antonia Vlahou[4], Johannes Holfeld[5], Kai-Uwe Eckardt[3], Jakob Voelkl[1,3,12]

[1] *Johannes Kepler University Linz, Institute for Physiology and Pathophysiology, Linz, Austria*
[2] *Charite Berlin, Department of Internal Medicine and Cardiology, Berlin, Germany*
[3] *Charite Berlin, Department of Nephrology and Medical Intensive Care, Berlin, Germany*
[4] *Biomedical Research Foundation of the Academy of Athens, Biotechnology Laboratory, Athens, Greece*
[5] *Medical University of Innsbruck, University Clinic of Cardiac Surgery, Innsbruck, Austria*
[6] *Calciscon, Biel, Switzerland*
[7] *Ordensklinikum Linz, Internal Medicine III - Nephrology, Transplantation Medicine, Rheumatology, Linz, Austria*
[8] *Red Cross Transfusion Service of Upper Austria, Linz, Austria*
[9] *Department of Internal Medicine 2, Kepler University Hospital and Johannes Kepler University, Linz, Austria*
[10] *Medical University of Vienna, Division of Nephrology and Dialysis, Vienna, Austria*
[11] *University of Veterinary Medicine Vienna, Institute of Animal Breeding and Genetics, Vienna, Austria*
[12] *DZHK, Berlin, Germany*

Question

Hyperphosphatemia in chronic kidney disease (CKD) is associated with medial vascular calcification and cardiovascular mortality. Inflammatory pathways have been linked to the pro-calcific effects of phosphate in vascular smooth muscle cells (VSMCs). Interleukin-6 family members are involved in vascular calcification, but the role of leukemia inhibitory factor (LIF) has not been investigated.

Methods

Experiments were performed in primary human aortic VSMCs, mouse aortic rings, mice treated with cholecalciferol as well as serum samples from CKD patients and healthy controls.

Results

Phosphate exposure increased LIF expression in VSMCs. Silencing of endogenous LIF reduced calcification and expression of calcification markers after phosphate treatment. Addition of LIF to the medium aggravated VSMC calcification. Soluble LIFR acted as LIF antagonist and reduced VSMC calcification. LIF exposure increased STAT3 phosphorylation and activity, effects blunted after pharmacological TYK2 inhibition. Silencing or inhibition of TYK2 or STAT3 was sufficient to reduce VSMC calcification. Conversely, overexpression of TYK2 increased VSMC calcification. In phosphate-treated mouse aortic rings, calcification and expression of calcification markers was reduced by TYK2 inhibition or genetic deficiency. Also in vivo, calcification and calcification marker expression in mouse aortic tissue was reduced after TYK2 inhibition or genetic deficiency. In a pilot study, soluble LIFR levels were reduced in patients with renal disease as compared to healthy controls. In a subgroup of these patients, soluble LIFR levels were correlated to pulse wave velocity.

Conclusion

LIF augments VSMC calcification, identifying a central role for TYK2 in the pro-calcific signalling pathways. Interference with this pathway may provide benefits for patients at risk beyond IL-6 blockade.

OS 06-03

Effects of creatine supplementation on expression and protein aggregate formation in a mouse model of GATM-associated kidney disease

Allein Plain[1], Vanessa Mikicz[1], Katrin Meindl[1], Eva Wacker[1], Ines Tegtmeier[1], Ralph Witzgall[1], Ben Davies[2], Detlef Böckenhauer[3], Robert Kleta[3], Markus Reichold[1], Felix Knauf[4], Richard Warth[1]

[1] *University of Regensburg, Regensburg, Germany*
[2] *The Francis Crick Institute, London, UK*
[3] *University College London, London, UK*
[4] *Charité – Universitätsmedizin Berlin, Berlin, Germany*

Question

GATM is a mitochondrial enzyme involved in creatine biosynthesis. In GATM-associated autosomal dominant nephropathy, the T336A mutant of the GATM protein forms filamentous aggregates in mitochondria. The aggregates lead to giant mitochondria that can hardly be degraded by the cell and trigger fatal signals towards inflammation, cell death, and fibrosis. This leads to chronic kidney failure in affected patients. The exact signaling pathways of GATM-associated kidney disease are still unknown. Here, we have begun to study the renal phenotype of a Gatm-T336A knockin mouse. Furthermore, we tested dietary supplementation with creatine as a strategy to suppress Gatm expression.

Methods

WT and Gatm-T336A knockin C57Bl/6J mice received dietary supplementation with creatine and sucrose or sucrose alone. Urine, blood, and kidney samples were collected for analysis. Gatm mRNA expression was determined by RT-qPCR and protein expression by Western blot. Histology of the kidney and localization of Gatm were examined by immunofluorescence and electron microscopy.

Results

The Gatm-T336A knockin mouse showed a mild phenotype without renal failure in contrast to affected patients. There was no evidence of renal fibrosis or increased numbers of macrophages in the kidney. However, immunofluorescence and electron micrographs showed giant pathological mitochondria in the proximal tubular cells. We next examined the expression levels of Gatm, as it appears to be a critical factor for filament formation in knockin mice. Interestingly, mRNA expression of Gatm was higher in homozygous knockin mice than in WT mice. As expected from the literature, creatine supplementation decreased Gatm mRNA expression in WT mice and, more importantly, in knockin mice. Western blots showed decreased Gatm protein expression in WT and knockin mice after creatine supplementation.

Conclusions

We conclude that dietary supplementation with creatine may also be a strategy to suppress mutant GATM expression in humans, thereby slowing protein aggregate formation in mitochondria and the progression of kidney disease.

OS 06-04

Optical and quantitative analysis of diclofenac-induced changes of cellular and nuclear morphology in renal organoids

Jasmin Dilz, Isabel Auge, Kathrin Groeneveld, Ralf Mrowka

Universitätsklinikum Jena, Exp. Nephrologie, KIM III, Jena, Germany

Introduction

Renal organoids are emerging as valuable tools for screening drug toxicity. In this study, we investigated the impact of diclofenac, a nonsteroidal anti-inflammatory drug, on organoid viability and morphological changes associated with cell death. Cell death can occur through different pathways, including apoptosis and necrosis. Apoptosis involves cell shrinkage, nuclear condensation, deformation, fragmentation, and the formation of apoptotic bodies. Necrosis, on the other hand, involves cell swelling, nuclear and cell membrane disintegration, and release of cellular contents. Apoptotic cells in vitro can undergo a late stage of necrosis characterized by cell membrane damage. To analyze nuclear morphological changes associated with apoptosis, we utilized the nuclear area factor (NAF). A low NAF value indicates early signs of cell death, based on previous studies.

Methods

Human induced pluripotent stem cells were differentiated into 3D kidney organoids and cultured for 11 days. The organoids were treated with different concentrations of diclofenac (25 - 400 µg/mL) for 48 hours. Cell viability was assessed using a luciferase-ATP assay. The treated organoids were visualized through whole-mount fluorescence staining and confocal imaging. The built-in positive cell detection tool of QuPath v0.4.2 was used to measure the cells and nuclei of the organoids. The parameters were adjusted to allow for the detection of both larger and smaller nuclear fragments. The NAF was calculated by dividing the nuclear area by nuclear circularity. At least 7 images were analyzed per concentration.

Results and Discussion

The ATP-luciferase assay demonstrated a dose-dependent decrease in organoid viability, with a minimum viability of approximately 28% compared to untreated controls. Confocal microscopy analysis further supported these findings, showing renal tubule loss, membrane disintegration, and nuclear fragmentation in organoids treated with 200 and 400 g/mL diclofenac. Analysis of cellular and nuclear morphology revealed a decrease in nuclear area with higher diclofenac concentrations, further indicating increased nuclear fragmentation. Additionally, a dose-dependent decrease in cell area, perimeter, and NAF was observed with higher diclofenac doses, suggesting involvement of apoptotic events. These results imply that our model setup could potentially be utilized to identify apoptotic processes during drug toxicity screenings in renal organoids.

We thank Silke Noßmann, Christiane Pilz and Konrad Fischer for technical assistance in stem cell culture. A part of the project on which these results are based was funded by the Free State of Thuringia under the number 2019 FGR 0083 (Morphotox) and co-financed by funds from the European Union within the framework of the European Social Fund (ESF). A part of the project on which these results are based was funded by the Free State of Thuringia under the number 2018 IZN 0002 (Thimedop) and co-financed by funds from the European Union within the framework of the European Regional Development Fund (EFRE).

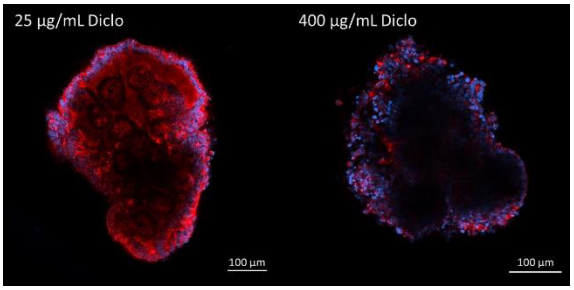

Comparison of diclofenac-treated organoids
Confocal imaging of organoids treated with different concentrations of diclofenac. Staining: WGA 633, Hoechst 33342.

OS 06-05
Dysregulation of renal polyamine levels after kidney injury

Tobias Sieckmann, Holger Scholz, **Karin M. Kirschner**

Chartié - Universitätsmedizin Berlin, Inst. für Translationale Physiologie, Berlin, Germany

Question

Polyamines are organic polycations, which regulate a plethora of biological processes including ion channel gating, cellular stress responses, gene expression and cell survival. As such, the polyamines spermidine and spermine and their common precursor, the diamine putrescine, are also involved in tissue injury and repair. In our previous work, we showed that impaired polyamine homeostasis is shared by various kidney pathologies.[1] Most kidney pathologies displayed remarkably similar changes in polyamine regulation with reduced expression of enzymes involved in polyamine synthesis (*Odc1*, *Srm* and *Sms*) and increased expression of polyamine degrading enzymes (*Sat1* and *Aoc1*). Knockout of *Sat1* has been shown to be protective in kidney injury. Here, we examine whether reconstitution of normal putrescine levels by deletion of the degrading enzyme AOC1 protects mice against kidney injury.

Methods

We analyzed renal levels of the polyamines putrescin, spermidine and spermine in rodent models of ischemia-reperfusion kidney injury, adenine-induced nephropathy and kidney transplantation. A knockout model of putrescine degrading enzyme *Aoc1* was used to reconstitute putrescine levels after kidney injury.

Results

All three models showed changes in polyamine levels. After kidney ischemia-reperfusion injury, renal putrescine and spermine were significantly reduced and spermidine was increased. Reduced spermidine was observed in adenine-induced nephropathy. Reduced putrescine and increased spermidine could be measured after kidney transplantation. These data indicate a similar tendency of changed polyamine levels after kidney injury although with slight differences between the models. Knockout of *Aoc1* was able to reconstitute renal putrescine levels after ischemia-reperfusion injury but did not significantly attenuate ischemic kidney damage. Renal putrescine levels were unaffected in adenine-induced nephropathy and knockout of *Aoc1* increased renal putrescine levels significantly in adenine-induced nephropathy. Knockout of *Aoc1* did not modify the observed changes of spermidine and spermine after kidney ischemia-reperfusion injury and adenine nephropathy.

Conclusions

The kidneys respond to heterogeneous types of injury with down-regulation of polyamine synthesis and activation of the polyamine breakdown pathway. Reconstitution of putrescine by *Aoc1* knockout alone does not significantly improve kidney injury. Therefore, a combined approach of inhibition of polyamine degradation and activating polyamine synthesis might be necessary to fully restore normal polyamine levels after kidney injury.

The expert technical assistance of Ulrike Neumann and Gabriele N'diaye is highly appreciated. The authors acknowledge the financial support provided by the Deutsche Forschungsgemeinschaft (DFG, German Research Foundation), Project-ID 394046635, SFB 1365 Renoprotection. TS received a fellowship from Wilhelm Sander-Stiftung (grant no. 2018.015.1).

References

[1] Sieckmann T, Schley G, Ögel N, Kelterborn S, Boivin FJ, Fähling M, Ashraf MI, Reichel M, Vigolo E, Hartner A, Lichtenberger FB, Breiderhoff T, Knauf F, Rosenberger C, Aigner F, Schmidt-Ott K, Scholz H, Kirschner KM. Strikingly conserved gene expression changes of polyamine regulating enzymes among various forms of acute and chronic kidney injury. Kidney Int. 2023 Apr 28:S0085-2538(23)00310-1.

OS 06-06

Activation of soluble guanylate cyclase attenuates the progression from acute kidney injury to chronic kidney disease in a rat model

Falk B. Lichtenberger, Minze Xu, Cem Erdogan, Pontus B. Persson, Erdmann Seeliger, Andreas Patzak, Kathleen Cantow, Pratik Khedkar

Charité, Translational Physiology, Berlin, Germany

Question

Acute kidney injury (AKI) is associated with high morbidity and mortality due to frequent progression to chronic kidney disease (CKD).[1] Rapid restoration of an adequate blood supply can prevent critical renal tissue hypoxia and nephron loss.[2] Soluble guanylate cyclase (sGC) is a key enzyme mediating vasodilation.[3] Therefore, the present study investigates the hypothesis that pharmacological activation of sGC after AKI can improve renal tissue perfusion in areas at risk of hypoxic damage, thereby preventing the development of CKD.

Methods

Kidney examinations were performed 3, 7, 14 (acute phase) and 84 days (late phase) after unilateral ischemia reperfusion injury (IRI) in rats. Animals received daily orally sGC activator Bay 60-2770 (1 mg/kg body weight) or vehicle. A sham-operated group served as handling control. In addition to histological and immunohistochemical analyses, *ex vivo* experiments were performed on isolated perfused renal microvessels. Furthermore, an *in vivo* study was conducted to examine control of renal haemodynamics and oxygenation.

Results

Compared to sham-operated animals, the kidneys of vehicle-treated IRI rats developed signs of sterile inflammation and fibrosis, reflected in the invasion of monocytes, significantly increased expression of pro-inflammatory and pro-apoptotic cytokines (*Il-6, Tnf-α, Tgf-β1*), increased expression of renal injury markers (*Kim-1, Ngal*), and progressive collagen accumulation over time. Analysis of vascular morphology and function revealed a reduction in the diameter of medullary vessels along with hypertrophic inward remodelling of cortical vessels, particularly

in the chronic phase. Treatment with Bay 60-2770 significantly attenuated the proinflammatory and profibrotic responses in the acute and chronic phases, prevented kidney weight loss in the acute phase and preserved the largely intact vascular architecture in the chronic phase. Furthermore, *ex vivo* assessment of vascular reactivity of perfused renal microvessels showed positive effects of sGC activation on angiotensin and acetylcholine responses. Similarly, *in vivo* total renal blood flow was higher, and the response of renal tissue perfusion and oxygenation to a haemodynamic challenge improved, following sGC activation vs. vehicle.

Conclusions

The results demonstrate the short- and long-term benefits of sGC activation in reducing AKI and lowering the risk of subsequent CKD. Our models also provide morphological and functional details on the dynamics of the transition from AKI to CKD.

We would like to thank the Deutsche Forschungsgemeinschaft (DFG, German Research Foundation) for funding our project (number 394046635) within the CRC1365 "Renoprotection".

References

[1] Su C-C, Chen J-Y, Chen S-Y, et al. Outcomes associated with acute kidney disease: A systematic review and meta-analysis. *EClinicalMedicine*. 2023;55:101760. doi:10.1016/j.eclinm.2022.101760

[2] Cantow K, Flemming B, Ladwig-wiegard M, Persson PB. Low dose nitrite improves reoxygenation following renal ischemia in rats. *Sci Rep*. 2017;(October):1-7. doi:10.1038/s41598-017-15058-5

[3] Wennysia IC, Zhao L, Schomber T, et al. Role of soluble guanylyl cyclase in renal afferent and efferent arterioles. *Am J Physiol Ren Physiol*. 2021;320(2):F193-F202. doi:10.1152/AJPRENAL.00272.2020

OS 06-07

The enriched expression of aquaporin-2 in the renal inner medulla is mediated by increased chromatin accessibility

Kristina Engel[2], Dmitry Chernyakov[2], **Bayram Edemir**[1,2]

[1] *Universität Witten/Herdecke, Lehrstuhl für Physiologie, Pathophysiologie und Toxikologie, Witten, Germany*
[2] *Martin-Luther-Universität Halle-Wittenberg, Klink für Innere Medizin IV, Halle, Germany*

Question

The osmotic gradient between renal cortex (CTX) and renal inner medulla (IM) is important for the generation of a concentrated urine. In addition, the unique hypertonic environment in the IM induces a specific gene expression pattern. For example the expression of aquaporin-2 (*Aqp2*) is enriched in the IM compared to CTX. We postulated that these changes must be associated with epigenetic mechanisms that could regulate the spatial expression pattern in CTX and IM. We performed assay for transposase-accessible chromatin (ATAC) sequencing to identify genomic regions with differences in accessibility in CTX and IM.

Methods

We used kidneys from control mice and collecting duct principal cell specific nuclear factor of activated t cells *(Nfat5)*-KO mice and dissected CTX and IM. These samples were subjected for ATAC-seq analysis. Accessible genomic regions were identified with MACS2. We next compared differentially accessible regions between CTX and IM in control mice and between control and *Nfat5*-KO mice. The results were correlated with corresponding gene expression profiles that have been analyzed in a former study.

Results

There are massive differences in the accessibility of genomic regions between CTX and IM. In CTX, more than 100,000 regions are differentially accessible compared to IM, with 48,698 regions having higher accessibility and 55,453 regions having lower accessibility. Genes with higher accessibility in CTX show also higher or even specific gene expression in CTX and vice versa. Since loss of NFAT5 is associated with a massive change in gene expression in kidneys from *Nfat5*-KO mice, we analyzed if this is affected by differences in chromatin accessibility. Our data shows that not only spatial localization in the kidney affects chromatin accessibility, but also the function of NFAT5. Loss of NFAT5 results in 10,456 regions with higher accessibility and 3,858 regions with closed chromatin in the CTX and 16,452 regions losing accessibility and 9,494 regions with increased accessibility in the IM. The accessibility of the *Aqp2* gene is higher in IM compared with CTX. The open chromatin of the *Aqp2* promoter region correlates with higher expression of *Aqp2* in the IM. This suggests that hypertonicity leads to an improvement in the accessibility of the promoter region of *Aqp2*. In *Nfat5*-KO IM the accessibility of this region was decreased, which could explain the reduced *Aqp2* expression in *Nfat5*-KO mice.

Conclusions

To date, studying hypertonicity-dependent regulation of chromatin accessibility and associated gene expression in CTX and IM in the kidney were missing. Here we show that the differences in gene expression between CTX and IM might be due to changes in accessibility of genomic regions. We also show that the renal expression of *Aqp2* might be a result of an epigenetic mechanism. In this context, NFAT5 was found to be an important regulator of chromatin accessibility and gene expression in the kidney.

OS 06-08
Role of NHE1 in renal function

Oleh Pochynyuk[3], Jessica A. Dominguez Rieg[1,2], Jianxiang Xue[1], Gabriella Blanco[1], Sima Al-Masri[1], Linto Thomas[1], **Timo Rieg**[1,2]

[1] *University of South Florida, Molecular Pharmacology and Physiology, Tampa, USA*
[2] *Department of Veterans Affairs, James A. Haley VA, Tampa, USA*
[3] *Department of Integrative Biology and Pharmacology, University of Texas Health Science Center at Houston, Houston, USA*

Question

The sodium-hydrogen exchanger isoform 1 (NHE1) is a transporter with roles in transepithelial Na^+/H^+ transport, intracellular pH (pH_i) and cell volume regulation. Within the kidney, NHE1 was previously documented to be expressed in all nephron segments but all recent transcriptomic and proteomic analyses consistently find no, or very low, expression of NHE1 in the proximal tubule or thick ascending limb, but high expression in the distal nephron, including distal convoluted tubule (DCT), connecting tubule (CNT), and collecting duct (CD). Due to these published discrepancies in NHE1 localization and lack of its functional role we generated kidney-specific NHE1 knockout ($NHE1^{KS\text{-}KO}$) mice and hypothesized that, based on recent data on its localization, basolateral NHE1 in the DCT, CNT and CD plays an important role in acid-base homeostasis.

Methods

$NHE1^{KS\text{-}KO}$ mice were created by crossing $NHE1^{loxlox}$ mice with $Pax8^{Cre}$ mice. Fluid and food intake was determined in their home cages. Blood was collected and analyzed after brief isoflurane anesthesia by an OPTI CCA-TS2 analyzer. Urine was collected spontaneously and analyzed using commercial available assays. Kidneys were harvested for Western blotting and immunofluorescence labeling. To study the role of NHE1 for pH_i regulation we used confocal microscopy of acutely isolated and split-open cortical CD where pH_i recovery was determined after employing a NH_4Cl prepulse. The split-open method allows for the analysis of a vast number of PC and IC simultaneously.

Results

$NHE1^{KS\text{-}KO}$ mice were born at predicted Mendelian frequencies, appeared grossly indistinguishable from control mice, and developed normally. $NHE1^{KS\text{-}KO}$ mice completely lack renal NHE1 protein expression compared to their control littermates (n=6 male mice/genotype). In control mice, NHE1 was localized to distal parts of the nephron and CD (co-labelling with H^+-ATPase B1 subunit, labeling all 3 types of intercalated clls (IC): type A, B, and non-A-non-B). Physiological analysis revealed no differences in body weight, food and water intake or concentrations of blood Na^+, K^+, Ca^{2+}, pH or HCO_3^-. Urine analysis showed no significant differences in electrolytes, minerals or pH. Intracellular pH recovery in PC (n=171) was significantly slower (~50%) in $NHE1^{KS\text{-}KO}$ mice compared to controls (n=85). Similar to PC, pH_i recovery in type B IC of $NHE1^{KS\text{-}KO}$ mice (n=38) was significantly slower (~35%) compared to controls (n=40). No differences in type A IC were observed between $NHE1^{KS\text{-}KO}$ mice (n=35) and controls (n=29). Inhibition of ClC-K2 via NPPB (Cl^- channel blocker) was used to confirm cell types: PC did not respond with a change in pH_i but NPPB increased pH_i in type A and decreased pH_i in type B ICs.

Conclusions

Our results identify that under baseline conditions NHE1 is dispensable or its loss can be compensated for. However, NHE1 is important for pH_i regulation particularly in PCs and type B ICs.

Funding was provided by grants: 1R01DK110621, IBX004968A, 19TPA34850116, DK076169 and DK115255 to TR, DK095029 and DK117865 to OP, and 828731 to LT.

OS 07 | Ion Transport: From Biophysics to Physiology

OS 07-01

Mechanosensitive ion channels are key sensors and transducers for durotaxis in pancreatic stellate cells

Ilka Budde[1], David Ing[1], Joelle Romac[2], Sandip Swain[2], Rodger Liddle[2], Andre Schlichting[3], Angela Stevens[3], Albrecht Schwab[1], Zoltan Pethö[1]

[1] *University of Münster, Physiology II, Münster, Germany*
[2] *Duke University, Department of Medicine, Durham, USA*
[3] *University of Münster, Institute for Analysis and Numerics, Münster, Germany*

Question

Pancreatic ductal adenocarcinoma (PDAC) is characterized by an increased tissue stiffness that creates a rigidity gradient between healthy and tumorous tissue. Cells recognize this gradient and undergo durotaxis, a process where cells migrate toward the areas of higher stiffness. Pancreatic stellate cells (PSCs) play a major role in producing the rigid environment in PDAC promoting cancer invasiveness. The molecular sensors behind durotaxis are largely unknown. This study aimed to examine the importance of mechanosensitive ion channels in the durotaxis of PSCs.

Methods

We created a two-dimensional model system using ultraviolet polymerized polyacrylamide gels with a linear rigidity gradient. The role of ion channels Piezo1, TRPC1, and TRPV4 on durotaxis was studied using pharmacological and genetic methods in primary murine PSCs. For overall mechanosensitive ion channel inhibition, the peptide toxin GsMTx-4 was applied. Piezo1 opening was facilitated using Yoda-1, TRPV4 was activated using GSK-1016790A, and inhibited using HC-067047. Moreover, PSCs were isolated from global TRPC1-knockout as well as Piezo1-cKO mice.

Results

Our results indicate that PSCs migrate towards a more rigid substrate. Inhibiting or activating Piezo1 suppresses durotaxis. We recapitulated these findings with a mathematical model. This model also predicted that durotaxis is optimal with an intermediary level of mechanosenstive channel activity. To test this prediction, we extended our model to TRPV4 and TRPC1 that are prominent mechanosensors and mechanotransducers in PSCs. Indeed, knocking out the TRPC1 channel with simultaneous TRPV4 inhibition also abolishes PSC durotaxis even when Piezo1 function is unaltered.

Conclusions

Our findings indicate that mechanosensitive ion channels, particularly Piezo1, are involved in sensing and transmitting the mechanical microenvironment to guide the migration of PSCs. However, Piezo1 relies on TRPC1 or TRPV4 for mediating the stiffness-directed migration of the cells.

OS 07-02

Electrophysiological characterization of the interaction between secreted protein 1 (SEP1) and acid-sensing ion channel 1a (ASIC1a)

Sven Kuspiel, Stefan Gründer, Dominik Wiemuth

Uniklinik RWTH Aachen, Institute of Physiology, Aachen, Germany

Acid-sensing ion channel 1a (ASIC1a) is a postsynaptic Na^+ channel that is directly activated by a fast increase in the extracellular proton concentration.[1] It is a trimeric ion channel and highly abundant in the central nervous system (CNS).[2] ASIC1a plays a pivotal role in several physiological and pathophysiological processes e.g. synaptic transmission, long-term potentiation and stroke.[3-5] So far the interactome of ASIC1a has not been elucidated and specific interaction partners of ASIC1a are largely unknown. A knockout-controlled proteomic screen of mice brain revealed secreted protein 1 (SEP1) as a putative interaction partner of ASIC1a. We verified the direct interaction of SEP1 with ASIC1a via co-immunoprecipitation. Overexpression of ASIC1a and SEP1 in heterologous expression systems increased current density of ASIC1a by a factor 3-5, while its biophysical properties remained unchanged. Knockdown of mSEP1 in isolated cortical neurons reduced ASIC1a amplitude. Moreover, cortical neurons from $SEP1^{-/-}$ mice exhibited no detectable ASIC1a currents, while overexpression of mSEP1 in

SEP1$^{-/-}$ neurons recovered ASIC1a currents. These results suggest that SEP1 represents an essential auxiliary subunit of ASIC1a. SEP1 is a secreted protein and most likely binds to the extracellular site of ASIC1a. The exact functional mechanism and the interaction site of SEP1 and ASIC1a are currently under investigation. In addition, we currently study the role of SEP1 in long-term potentiation (LTP) in freshly isolated mouse brain slices.

References
[1] Waldmann, R., Champigny, G., Bassilana, F., Heurteaux, C. & Lazdunski, M. A proton-gated cation channel involved in acid-sensing. *Nature***386**, 173–177 (1997)
[2] Sherwood, T. W., Lee, K. G., Gormley, M. G. & Askwith, C. C. Heteromeric Acid-Sensing Ion Channels (ASICs) Composed of ASIC2b and ASIC1a Display Novel Channel Properties and Contribute to Acidosis-Induced Neuronal Death. *Journal of Neuroscience***31**, 9723–9734 (2011)
[3] Du, J. *et al.* Protons are a neurotransmitter that regulates synaptic plasticity in the lateral amygdala. *Proceedings of the National Academy of Sciences***111**, 8961–8966 (2014)
[4] Wemmie, J. A. *et al.* The Acid-Activated Ion Channel ASIC Contributes to Synaptic Plasticity, Learning, and Memory. *Neuron***34**, 463–477 (2002)
[5] Xiong, Z.-G. *et al.* Neuroprotection in Ischemia. *Cell***118**, 687–698 (2004)

OS 07-03
Learning About Properties of the Voltage-Gated Proton Channel from in silico Methods

Christophe Jardin[1], Gustavo Chaves[1], Niklas Ohlwein[1,2], Boris Musset[1]

[1] *KNMS PMU Nuremberg, Center of Physiology, Pathophysiology and Biophysics, Nuremberg, Germany*
[2] *KNMS PMU Nuremberg, Klinik für Anästhesie und operative Intensivmedizin, Nuremberg, Germany*

Voltage-gated proton channels (H_V) are key players in a multitude of physiological processes, widely distributed in human and many other organisms. The proton channels are atypical channels, to date probably the most unique in the superfamily of voltage-gated ion channels. They are the most selective ion channels described so far (almost perfectly selective for hydrogen ions), their activity is dependent on the voltage across the membrane, and this voltage-dependence is strongly controlled by the pH gradient across the membrane. Unlike traditional ion channels, like K_V or Na_V channels, that have distincts voltage-sensing (transmembrane helices S1-S4) and ion conducting pore (S5-S6) domains, the voltage-sensing and pore domains of H_V channels are fused in one single domain, S1-S4. The main function of proton channels is to extrude (with only a few exceptions) protons from the cytoplasm, thereby regulating the intracellular pH.
Since the identification of the HVCN1 gene in 2006, some progress has been made in understanding the molecular determinants of proton channel's properties from experimental studies. However, still little is known about how the structure of the channel accomplishes its functions and most of the molecular determinants determining the function and inhibition are still elusive. In fact, many of the known aspects of H_V channel functions have been clarified using in silico methods. In our lab, besides patch-clamp experiments, we use such methods, e.g. (multiple conventional or constant pH with replica exchange) molecular dynamics simulations, to investigate properties of proton channels. We will show that the application of these methods allowed us to unveil the structural determinants of, e.g., the binding of Zn^{2+} cations (Figure 1), that inhibit the channels, or the pH-dependent gating (Figure 2) in the case of the human voltage-gated proton channel hH_V1 [1,2].

The authors thank Yuan-Ping Pang for technical support and interpretation of the results of the simulations using the cationic dummy atom approach.
Research was supported by grants from the Paulmanns-Wunschkinder Stiftung and the Förderverein der Paracelsus Medizinische Privatuniversität (PMU) Nürnberg to Christophe Jardin, the W. Lutz Stiftung to Gustavo Chaves, and the Deutsche Forschungsgemeinschaft (MU 3574/4-1) to Boris Musset.

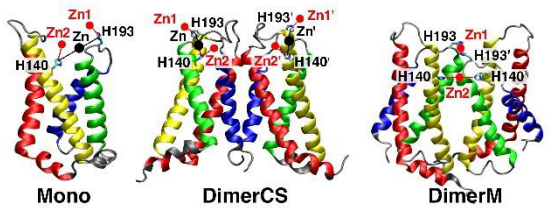

Putative zinc binding site(s) were investigated using multiple molecular dynamics simulations
The putative binding site(s) involve the two essential histidines, H140 and H193. DIfferent putative binding conformations, shown respectively in red and in black, were investigated using multiple MD simulations for their respective potential to coordinate zinc cations in different conformations of the human H_V1 proton channel: the monomer (Mono) and two plausible dimer (DimerCS and DimerM) structures. The results of this study have been published in [1].

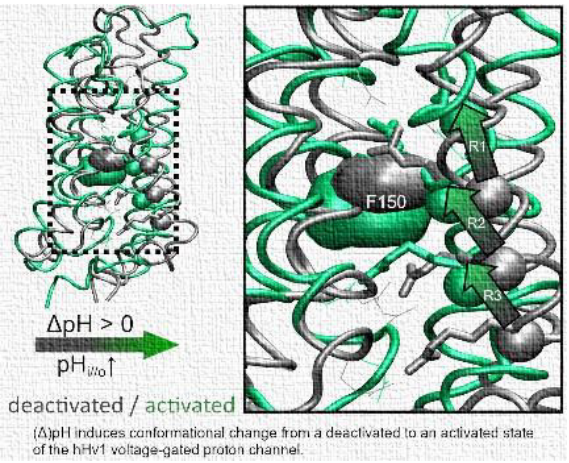

The pH- and ΔpH-dependent gating of hHv1 channel from constant pH MD simulations

The pH- and ΔpH-dependent gating of the human H_V1 channel was investigated using constant pH molecular dynamics simulations in symmetrical and asymmetrical pH conditions across the membrane. A conformational change from a deactivated to an activated state was captured by the MD simulations that moves the voltage-sensing arginines (R1-R3) in helix S4 outwards. The results of this study have been published in [2].

References

[1] Jardin, C, Chaves, G, Musset, B 2020, 'Assessing structural determinants of Zn2+ binding to human Hv1 via multiple MD simulations', *Biophys. J.*, 118, 1221-1233

[2] Jardin, C, Ohlwein, N, Chaves, G, Musset, B, 2022, 'The pH-dependent gating of the human voltage-gated proton channel from computational simulations', *Phys. Chem. Chem. Phys.*, 24, 9964-9977

OS 07-04

An integrated microsystems approach towards enhanced resolution and multimodal single-molecule analysis of ion-channels and membrane pores

Tobias Ensslen[1], Mohammad Amayreh[2], Gerhard Baaken[3], Sönke Petersen[3], Markus Kuderer[2], **Jan C. Behrends**[1]

[1] *University of Freiburg, Dept. of Physiology, Freiburg, Germany*
[2] *Hahn-Schickard-Society, Institute for Micro- and Information Technology, Villingen-Schwenningen, Germany*
[3] *Ionera Technologies GmbH, Freiburg, Germany*

Nearly 50 years ago, voltage clamp analysis in the form of patch clamp single channel recording was the first biophysical technique to attain single molecule resolution. Currently, single ion channel analysis is still constrained to one modality (electric current recording) and limited in bandwidth by noise due to stray capacitance and amplifier electronics. As miniaturization was key in developing the patch-clamp, it has been suggested an integrated microsystems approach might both overcome bandwidth/ noise limitations (Sigworth & Klemic 2005) and pave the way towards multimodal, e.g. simultaneous optical-electrical recordings from single ion-conducting membrane proteins (Borisenko et al. 2003). Here, we present recent advances in these directions as part of an integrated approach towards simultaneous electrical recording with enhanced bandwidths and single photon counting from free-standing lipid bilayers with reconstituted ion channels.
First, we have developed a chip-based platform for simultaneous single-channel electrical recording and time-resolved single photon counting (Fig. 1) based on the microelectrode cavity array (MECA) device (Baaken et al. 2008, Ensslen et al. 2022). Second, we have produced and tested a novel integrated CMOS-ASIC-MECA device with optimized flat noise characteristics that allows resolution of current steps in the 10pA range with > 500 kHz bandwidth while preserving low noise at low bandwidths (Fig. 2). Importantly, both developments are amenable to parallelization in array-formats and to automated formation of bilayers, as required to make multimodal experiments practical and productive. Combining these two developments into an integrated device seems feasible by replacing traditional microscope-based optics with microoptoelectromechanical excitation and local photon detectors.

This work was funded by the German Ministry for Research and Education through Project Management PTJ (TseNareo, FKZ 031B0864A), by the BW-Foundation through Project Management VDI (MSDS-BioMem) and by the Ministry of Commerce of the State of Baden-Württemberg in the Framework of the Forum Gesundheitsstandort Baden- Württemberg (TechPatNano) andby a Major Research Instrumentation Grant from the DFG (project No. 290424854) and by the BW-Foundation (project BITS).

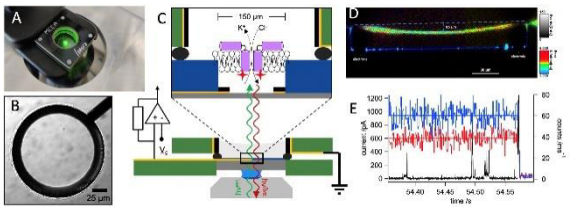

Fig. 1 MECA-OPTO device for simultaneous membrane fluorescence and voltage clamp recording
A: MECA-OPTO on microscope stage; B: circular ring electrode; C: schematic of set-up; D: x-z-fluorescence lifetime scan, E: dual channel polarization resolved photon counting (colored races) witH simultaneous recording of ceratotoxin channel activity (black trace).

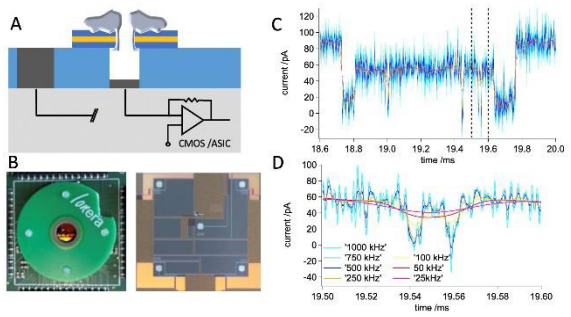

Fig. 2: ASIC-CMOS_MECA-Array for high-resolution electrical recording
A: Schematic of one element, B: top view and close-up. C, D: example current traces of 1.4 and 0.1 ms duration, respectively, during block of aerolysin pore by an adenine-trinucleotide, digitally Bessel-filtered at -3 dB cut-off frequencies indicated.

References
[1] Sigworth, F.J., and K.G. Klemic. 2005. Microchip Technology in Ion-Channel Research. *IEEE Trans. NanoBiosci.* 4:121–127.
[2] Borisenko, V., T. Lougheed, J. Hesse, E. Fureder-Kitzmuller, N. Fertig, J.C. Behrends, G.A. Woolley, and G.J. SchÜz. 2003. Simultaneous optical and electrical recording of single gramicidin channels. *Biophys. J.* 84:612–622.
[3] Baaken, G., M. Sondermann, C. Schlemmer, J. Rühe, and J.C. Behrends. 2008. Planar microelectrode-cavity array for high-resolution and parallel electrical recording of membrane ionic currents. *Lab Chip*. 8:938–944. doi:10.1039/b800431e.
[4] Ensslen, T., and J.C. Behrends. 2022. A chip-based array for high-resolution fluorescence characterization of free-standing horizontal lipid membranes under voltage clamp. *Lab Chip*. 22:2902–2910. doi:10.1039/D2LC00357K.

OS 07-05

Bayesian filtering for macroscopic Hidden Markov Models (HMM): Potential and limits of minimal informative priors to improve parameter inference

Jan L. Münch, Ralf Schmauder, Klaus Benndorf

Uniklinikum Jena, Physiology 2, Jena, Germany

Inferring the functional dynamics of ion channels from ensemble currents or combined with fluorescence data is daunting because the chemical reaction network is only partially observable. We addressed this problem by applying a parallelized Bayesian filter to specify kinetic schemes for macroscopic current and fluorescence data leading to a more accurate likelihood for first-order kinetic schemes (Muench 2022 *eLife***11**:e62714) than previous gold-standard algorithms.

We generalized the signal model of previous work: We can report closed-form filtering equations beyond the Kalman filter solution of (Moffatt, *Biophysical journal* 93.1 (2007): 74-91.) even if state-dependent noise contributions in the signal are present. Incorporating the details of the single-channel Markov dynamics into a Gaussian Markov kernel for the macroscopic signal supersedes classical approaches with rate equations in two ways. Firstly, the posterior is closer located to the true parameter values. Secondly, using the Gaussian Markov kernel produces correct uncertainty quantification, while posteriors from a deterministic algorithm fail to cover the true values even for large ensembles of chemically reacting molecules. The likelihood misspecification generated by the often-used rate equations causes p-values, confidence regions, or posteriors to be too confident for any finite data amount.

Using Bayesian statistics requires defining a prior distribution. When little information about the parameter is known, and information contained in the data is poor, a minimal informative prior is crucial to make the posterior as sensitive as possible to the data. Applying such a prior reduces the number of channels required for a reasonable inference by one order of magnitude compared to the standard uniform prior, which is often considered mistakenly uninformative.

Generally, ion currents from patch-clamp experiments report only partially the dynamics of interest in the chemical network. We show by simulated patch-clamp data that this partial observability causes a degree of practical parameter non-identifiability (non-PI) for most non-trivial HMMs. The minimal informative prior desensitizes the posterior to the non-PI problem of the likelihood for some part of the parameter space. Nevertheless, the posterior will always be dominated by the prior shape in the rest of the parameter space. Thus, all posteriors of HMM models will be improper if equipped with minimal informative improper prior distributions.

We discuss how to treat this practical parameter non-PI problem inherent in most HMMs and any statistical framework used. Also, we consider model selection strategies to avoid overfitting kinetic schemes. Nevertheless, the likelihood has to be specified accurately enough (Muench et al., *eLife***11**, 2022, e62714) to become a meaningful parameter and model inference.

OS 07-06

The TRPV4 channel mutants E278K and N302Y show differential effects on cell adhesion and cytoplasmic calcium levels in HEK 293 cells

Philipp Lutze[1], Emily Nothnik[1], Lena Teske[1], Mirjam Krautwald[1], Martin Landsberger[2], **Heinrich Brinkmeier**[1]

[1] *University Medicine Greifswald, Institute ofPathophysiology, Greifswald, Germany*
[2] *Universität Osnabrück, Abteilung für Biomedizinische Grundlagen/ Institut für Gesundheitsforschung und Bildung, Osnabrück, Germany*

Question

The transient receptor potential channel TRPV4 is a Ca^{2+} permeable cation channel in the plasma membrane of various cell types. TRPV4 missense mutations are known to cause skeletal dysplasias and peripheral neuropathies in humans. TRPV4-related diseases show an autosomal dominant inheritance indicating gain of function of the mutant channels. Though it is likely that altered Ca^{2+} influx plays a role for the disease pathology in some cases, the precise pathomechanisms of most the TRPV4 mutations are still unknown. The current study was undertaken to investigate physiological and cell biological abnormalities caused by the TRPV4 mutants E278K and N302Y (coding sequence NM_022017.3).

Methods

To this end YFP-tagged mutant and wildtype (WT) TRPV4 proteins were expressed in HEK 293 cells using an inducible promotor system (Flp-In™ T-REx™). Cell growth and viability were analysed with the Trypan Blue assay. Intracellular Ca^{2+} concentrations were monitored with the fluorescent Ca^{2+} indicator Fura-2.

Results

TRPV4 gene expression was reproducibly induced by 0.01 µM doxycycline. While the growth rate of non-induced cells was identical for all three clones, the growth rate of cells expressing the E278K mutant was reduced by about 50% (n=6 independent tests, 72 h). In addition, cells expressing the E278K mutant tended to detach from the surface of the culture dish. After *TRPV4* gene expression for 72 h, 90% of the cells with the E278K mutant were found in the supernatant, while only 1-2% of the cells expressing the WT channel and 7% of the cells with the N302Y mutant channel showed this behaviour (n=6). All cell types showed slight YFP fluorescence at the plasma membrane and in addition bright intracellular patches, suggesting the presence of the TRPV4 proteins in organelles. Cytoplasmic Ca^{2+} concentrations (given as fura-2 fluorescence ratios) rose to a plateau in doxycycline-induced cells in response to the application of the TRPV4 activator GSK1016790A (10 nm). Cells expressing the WT-TRPV4 channel showed an average resting ratio of 0.14 ± 0.05 (n=91 cells) that increased to 0.66 ± 0.15 upon application of GSK1016790A. HEK 293 cells expressing the E278K mutant had significantly higher resting ratios (0.29 ± 0.15, n=49) that rose to the same plateau in the presence of GSK1016790A (0.56 ± 0.18; means ± STD given in all cases). The increased resting ratios observed in cells expressing the E278K mutant were significantly lowered by application of the TRPV4 channel blocker HC-067047 (1 µM). The results obtained for the E278K mutant could not be reproduced with the N302Y mutant (fura-2 fluorescence ratio at rest: 0.12 ± 0.04, n=87).

Conclusions

The TRPV4 channel mutants E278K and N302Y can be functionally expressed in HEK 293 cells, but only the E278K mutant causes increased cytoplasmic Ca^{2+} levels and disturbs cell adhesion, probably due to an increased open probability of the TRPV4 channel allowing excessive Ca^{2+} influx.

This work was supported by the German Bundesministerium für Wirtschaft und Energie (BMWi), grant No. KF2870604TS4 to HB.

OS 07-07
Proton-gated anion transport governs macropinosome shrinkage

Mariia Zeziulia[1,2], Sandy Blin[1,2], Franziska W. Schmitt[1,2], Martin Lehmann[1], Thomas J. Jentsch[1,2,3]

[1] *Leibniz-Forschungsinstitut für Molekulare Pharmakologie (FMP), Berlin, Germany*
[2] *Max-Delbrück-Centrum für Molekulare Medizin (MDC), Berlin, Germany*
[3] *NeuroCure Cluster of Excellence, Charité Universitätsmedizin, Berlin, Germany*

Intracellular organelles undergo changes in their size during trafficking and maturation. Such changes require transport of ions and water across organellar membranes. Macropinocytosis is a form of endocytosis that results in generation of large vesicles and is of particular importance for immune and cancer cells [1]. These vacuoles shrink in the course of 15 minutes, which is necessary for their further trafficking. Water efflux and hence shrinkage of macrophage macropinosomes depends on Na^+ and Cl^- efflux since these are the only ions that have appropriate gradients to leave the vesicle. While it has been shown that Na^+ exits the macropinosomes through TPC channels, Cl^- exit pathway had remained unknown [2].

Using bone marrow derived macrophages from various knock-out mice in live imaging spinning disk microscopy, we identified the missing Cl^- channel as ASOR/TMEM206, a widely expressed proton-activated Cl^- channel earlier shown to be involved in acid-induced cell death and stroke [3, 4]. ASOR knock-out macrophages displayed delayed macropinosome shrinkage, which could be fully rescued by protein overexpression. ASOR is perfectly suited for this role since it localizes to the plasma membrane, where it normally remains inactive due to its voltage- and pH-dependencies. Plasma membrane localization leads to early ASOR incorporation into macropinosomes, placing it in the environment appropriate for its activation. This involves Na^+-mediated depolarization and luminal acidification by redundant transporters including H^+-ATPases and CLC $2Cl^-/H^+$-exchangers. Electrically coupled Na^+ and Cl^- efflux through TPCs and ASOR, respectively, induces osmotic shrinkage of the vesicle. We also showed that ASOR-dependent macropinosome shrinkage plays a role in cancer cells' nutrition, which depends on macropinocytosis of extracellular proteins. Due to decreased albumin recycling, *TMEM206* disruption increased albumin-dependent growth of cancer cells under nutrient starvation. We also integrated our results in a mathematical model that semi-quantitatively reproduces our experimental results and can be used to infer the value of parameters such as vesicle voltage that are experimentally inaccessible. Our work suggests a function for the voltage- and pH-dependence of ASOR and CLCs, offers a thorough model for ion transport-dependent vacuole maturation, and reveals biological roles of ASOR.

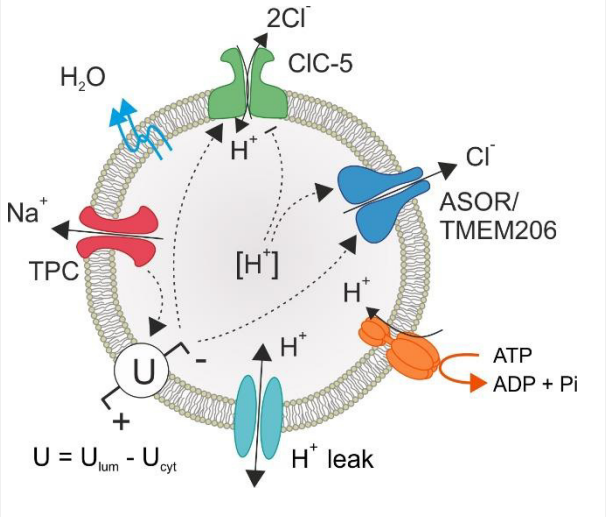

The proposed model of macropinosome shrinkage.
Na^+ efflux through TPC renders inside negative macropinosome potential, which activates ClC-5 and is permissive for ASOR. Additionally necessary for ASOR activation lumenal acidic pH is provided by ClC-5 and H^+-ATPAse. Electrically coupled Na^+ and Cl^- efflux leads to osmotic shrinkage.

References
[1] King, J. S. & Kay, R. R. The origins and evolution of macropinocytosis. *Philos. Trans. R. Soc. Lond. B. Biol. Sci.***374**, 20180158 (2019).
[2] Freeman, S. A. *et al.* Lipid-gated monovalent ion fluxes regulate endocytic traffic and support immune surveillance. *Science***367**, 301–305 (2020).
[3] Ullrich, F. *et al.* Identification of TMEM206 proteins as pore of PAORAC/ASOR acid-sensitive chloride channels. *eLife***8**, e49187 (2019).
[4] Yang, J. *et al.* PAC, an evolutionarily conserved membrane protein, is a proton-activated chloride channel. *Science***364**, 395–399 (2019).

OS 07-08
cAMP binding to resting pacemaker channels – a single molecule approach in native membranes

Stefan Kuschke, Susanne Thon, Tina Schwabe, Klaus Benndorf, Ralf Schmauder

Jena University Hospital, Institute for Physiology II, Jena, Germany

Pacemaker channels are tetrameric ion channels that facilitate rhythmic generation of action potentials in the heart as well as in the central nervous system. The frequency of these rhythms is altered by cAMP binding to the subunits of these hyperpolarization activated cyclic nucleotide-modulated (HCN) ion channels by changing both their activation kinetics and open-probability. Earlier investigations revealed that for the activated channel the binding of cAMP is cooperative in a complex manner. However, for the resting channel there are conflicting results on whether binding of cAMP is cooperative or not. While macroscopic data recorded in native cell membranes showed cooperativity[1], single-molecule studies in artificial micelles reported non-cooperative binding of fluorescently labeled cAMP binding to resting channels[2].
To settle these conflicting results, we combined the accuracy of microscopic single-molecule measurements with channels in native cell membranes to observe binding of individual fluorescently labelled cAMP molecules (fcAMP) to resting mHCN2 channels. Binding was recorded by total internal reflection microscopy (TIRFM) in supported membranes from HEK293 cells expressing low amounts of eGFP tagged mHCN2 channels. Ligand binding to the membrane was matched to localization of the eGFPmHCN2 channels to reduce false positive signals from endogenous cAMP binding proteins. Additionally, a cocktail of competitive inhibitors suppressed binding to endogenous cAMP binders. From the obtained data we could infer the number of fcAMP molecules binding to the channel at any given time point.
Comparing the observed population of occupied binding sites to binomial predictions for independent binding sites directly revealed cooperativity in binding. Furthermore, these data confirm earlier findings on the existence of a flip state. Modeling of the data shows an increased population of the flip state upon progressive binding of ligands, a monotone increase off affinity and a higher affinity for the flip compared to the ground state.
Together with the earlier study suggesting no cooperativity in artificial micelles, our results suggest that the native membrane surrounding of the mHCN2 channel is required for cooperative ligand binding.

References
[1] Thon S, Schulz E, Kusch J, Benndorf K. Conformational Flip of Nonactivated HCN2 Channel Subunits Evoked by Cyclic Nucleotides. *Biophys J*. 2015 Dec 1;109(11):2268-76. doi: 10.1016/j.bpj.2015.08.054. PMID: 26636938; PMCID: PMC4675818.
[2] White DS, Chowdhury S, Idikuda V, Zhang R, Retterer ST, Goldsmith RH, Chanda B. cAMP binding to closed pacemaker ion channels is non-cooperative. *Nature*. 2021 Jul;595(7868):606-610. doi: 10.1038/s41586-021-03686-x. Epub 2021 Jun 30. PMID: 34194042; PMCID: PMC8513821

OS 08 | Network & System Neuroscience

OS 08-01
Enhanced *in vivo* firing in chemogenetically identified dopamine midbrain neurons projecting to dorsal medial striatum in freely moving 22q11.2 mice, a genetic model of Schizophrenia

Solmaz Bikas, Jochen Roeper, Anastasia Diamantopoulou

Goethe University Frankfurt am Main, Institute of Neurophysiology, Frankfurt am Main, Germany

Dopamine (DA) dysregulation and, region-specific striatal DA elevation, has been at the focus of schizophrenia (SCZ) psychopathology for decades, but its mechanistic contributions to disease manifestations have not yet been resolved. To study DA dysregulation relevant to human disease, we made use of the *Df(16)A*$^{+/-}$mouse model of the 22q11.2 Deletion Syndrome. The hemizygous microdeletions of the 22q11.2 locus are the most common chromosomal microdeletions and the highest genetic risk factor for the development of SCZ. Previous work on the *Df(16)A*$^{+/-}$ mouse model revealed schizophrenia-like associated abnormalities on cellular, neurocircuitry, cognitive and behavioral levels. Here, we looked at the function of the DA midbrain system as a source of DA dysregulation relevant for schizophrenia. Initially, we characterized the electrical *in vivo* properties of pharmacologically identified DA midbrain neurons by chronic *in vivo* single-unit extracellular recordings during open field exploration in awake freely moving male and female *Df(16)A*$^{+/-}$mice and wild type littermates. We detected persistent electrophysiological hyperactivity in DA neurons in the medial substantia nigra (SN) in both male and female *Df(16)A*$^{+/-}$mice in comparison to

controls. This was characterized by increased firing frequencies (WT median FR: 4.35 Hz; *Df(16)A*$^{+/-}$ median FR: 7.51 Hz; 1.5–fold; $p = 0.0002$, WT: = 53, N = 7; *Df(16)A*$^{+/-}$: n = 97, N = 7) and elevated bursting activity (WT median SFB: 40.3; *Df(16)A*$^{+/-}$ median SFB: 71.5, 1.7-fold; $p < 0.0001$, WT: n = 53, N = 7; *Df(16)A*$^{+/-}$: n = 97, N = 7). In contrast to DA neurons in the medial SN, *in vivo* recordings of DA neurons in the ventral tegmental area (VTA), the main source of the mesolimbic dopamine system, revealed no differences between *Df(16)A+/-* and controls (WT median FR: 7.21 Hz & SFB: 61.8; *Df(16)A*$^{+/-}$ median FR: 7.46 Hz & SFB 61.2; WT: n = 107, N = 7; *Df(16)A*$^{+/-}$: n = 151, N = 7). We then used AAV-based retrograde chemogenetic tagging to better define the neuronal identity of hyperactive DA neuron subtypes. DA neurons projecting to the dorsomedial striatum (DMS),weretagged by expression of an inhibitory DREADD receptor in DAT-Cre X *Df(16)A+/-* double transgenic mice and identified *in vivo* by an inhibitory response to a systemic application of 100 µg/kg Deschloroclozapine (DCZ) showed increased firing frequencies(DAT-Cre median FR: 5.00 Hz; DAT-Cre X *Df(16)A+/-* median FR: 7.13 Hz; 1.4–fold; $p = 0.0007$, DAT-Cre: = 21, N = 5; DAT-Cre X *Df(16)A+/-* : n = 36, N = 5) and elevated bursting activity (DAT-Cre median SFB: 43.7; DAT-Cre X *Df(16)A+/-* median SFB: 59.5, 1.4-fold; $p < 0.0001$, DAT-Cre: n = 21, N = 5; DAT-Cre X *Df(16)A+/-* : n = 36, N = 5). In summary, our experiments identified the selective *in vivo* hyperactivity of DMS-projecting DA neurons in the 22q11.2 mouse model of Schizophrenia.

OS 08-02
Subfield-specific interneuron circuits govern the hippocampal response to novelty

Aurore Cazala[1], Thomas Hainmueller[2,3], Li-Wen Huang[1], Marlene Bartos[1]

[1] *Universitätsklinikum Freiburg, Freiburg, Germany*
[2] *NYU Neuroscience Institute, New York, USA*
[3] *Department of Psychiatry, New York, USA*

The hippocampus is the brain's center for episodic memories and is critical for spatial navigation and novelty-detection, among others. Its subregions, the dentate gyrus (DG), CA2/3, and 1, are involved in these functions in distinct ways. DG is crucial for discriminating novel contents from similar familiar ones while CA3 aids fast encoding of novel information. Hippocampal principal cells (PC) represent episodic features like movement, space, and context but little is known about GABAergic interneurons (IN) and how they influence on PCs activity and contribute to hippocampal function. Here, we performed two-photon calcium imaging of parvalbumin (PV)- and somatostatin (SOM)-expressing INs in the DG and CA1-3 of mice exploring virtual environments. PV-INs throughout the hippocampus increased activity with running-speed and reduced it in novel environments. SOM-INs displayed a dichotomy: CA1-3 SOM-INs behaved similar to PV-INs, but their DG counterparts increased activity during immobility and in novel environments. Congruently, chemogenetic silencing of DG SOM-INs caused increased activation of DG granule cells (GC) in novel environments and decreased context selectivity, while silencing of DG PV-INs had opposite effects. Our data indicate unique roles for DG PV- and SOM-INs that are distinct from their CA1-3 counterparts and may support novelty-dependent, dynamic routing of information through the hippocampus.

We thank K. Winterhalter and K. Semmler for technical support. We further thank Drs. Antje Kilias, Thibault Cholvin, Claudio Elgueta and Antonio Fernández-Ruiz for comments on versions of this manuscript. This work was funded by the German Research Foundation (DFG BA1582/12-1 M.B.; FOR2143 M.B.; HA 8939/1-1 T.H.), EMBO (ALTF 6-2019 T.H.) and by the ERC-AdG 787450 (M.B.).

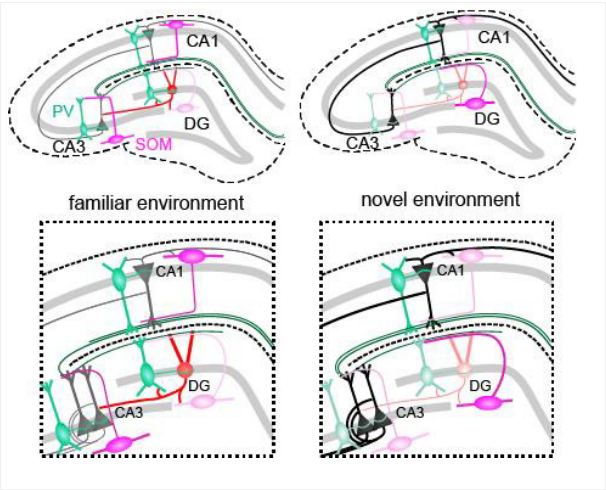

Context-discrimination is differentially affected by DG SOM and PV INs.
Schematic of the observed activity differences between familiar and novel environments. Opacity of symbols indicates strength of activation. Blue cells represent PV-INs, brown cells SOM-INs, red- and black cells depict DG GCs and hippocampal pyramidal cells, respectively.

OS 08-03

Human layer 2-3 pyramidal neurons are functionally diverse and differentially embedded in the local network

Franz Xaver Mittermaier[1], Henrike Planert[1], Sabine Grosser[2], Pawel Fidzinski[3], Ulf C. Schneider[4], Helena Radbruch[5], Julia Onken[4], Martin Holtkamp[6], Dietmar Schmitz[3], Henrik Alle[1], Imre Vida[2], Jörg R.P. Geiger[1], Yangfan Peng[1]

[1] *Charité - Universitätsmedizin Berlin, Institute of Neurophysiology, Berlin, Germany*
[2] *Charité - Universitätsmedizin Berlin, Institute for Integrative Neuroanatomy, Berlin, Germany*
[3] *Charité - Universitätsmedizin Berlin, NeuroCure Cluster of Excellence, Berlin, Germany*
[4] *Charité - Universitätsmedizin Berlin, Department of Neurosurgery, Berlin, Germany*
[5] *Charité - Universitätsmedizin Berlin, Department of Neuropathology, Berlin, Germany*
[6] *Charité - Universitätsmedizin Berlin, Department of Neurology, Berlin, Germany*

Recent studies have revealed that human pyramidal cells in the neocortical layer 2-3 display high molecular, anatomical and electrophysiological diversity. Using advanced multineuron patch-clamp recordings, we demonstrate that this diversity is a fundamental principle observed in every human individual. By employing exploratory cluster algorithms, we show that this diversity can be described by functional subtypes. Moreover, we provide evidence that pyramidal cell subtypes exhibit differences in both anatomy and synaptic connectivity within the local network. Our dataset provides a unique insight into the complex and heterogeneous pyramidal cell network of the human layer 2-3, serving as a critical foundation for future experimental and theoretical studies.

OS 08-04

A persistent prefrontal reference frame across time and task rules

Hannah Muysers[1,2], Hung-Ling Chen[1], Johannes Hahn[3,4], Torfi Sigurdsson[3], Jonas-Frederic Sauer[1], Marlene Bartos[1]

[1] *University of Freiburg, Medical Faculty, Institute of Physiology I, Freiburg im Breisgau, Germany*
[2] *University of Freiburg, Faculty of Biology, Freiburg im Breisgau, Germany*
[3] *Goethe University Frankfurt, Institute of Neurophysiology, Frankfurt am Main, Germany*
[4] *Max Planck Institute for Brain Research, IMPRS for Neural Circuits, Frankfurt am Main, Germany*

The medial prefrontal cortex (mPFC) is activated during the recall of long-term contextual memories. However, how these memories are maintained over a long period of time is still unknown. To shed light on this, we asked three main questions: (1) how stable or dynamic is the representation of a contextual task in the mPFC over the time-course of weeks? (2) what kind of stimuli influence the representation? And (3) how is the task represented during learning? To address these questions, we used 1-photon calcium imaging in Thy1-GCaMP6f mice, which predominantly express the calcium indicator in layer V of the mPFC. We recorded mice during an olfaction guided spatial memory task, in which the mice needed to associate an odour (presented in the centre-arm of an M-maze), with a specific reward location (left or right side-

arm). For question 1) our results show that a majority of active cells are spatially tuned to a specific position on the trajectory (left or right trials respectively) and reliably keep their spatial tuning across several weeks with only a mild drift. Moreover, when we trained a decoder on neuronal data from the first day, we were able to predict trial identity and the animal's linearized position in the maze over the full experimental period of 24 days. Furthermore, with a generalized linear model we identified the animals linearized position as the most prominently and abundantly encoded behavioural variable in the imaged cell population. Compared across days, cells that encoded 'position' were more likely to keep this property as opposed to goal- or speed encoding cells. Taken together, this reveals a stable, long-term encoding of contextual memories in the mPFC. With regard to question 2) the stability of the trajectory specific representation was unperturbed during introduction of breaks in task-exposure, during visual modification of the arena or switching of the cue-location pairing. This suggests a rather abstract and robust representation of the task structure. Investigating question 3) showed that spatial tuning stability was lower in the initial phase of task exposure, indicating that the stability of the representation emerges during learning. Taken together, such a coding may provide a stable reference frame, which might support the animal's navigation in the task-context and might allow for quick task-related decisions.

OS 08-05
Bacterial infection and behavior: The role of theAMPs and neuromodulation in brain-body communication

Ilona Grunwald Kadow, Yujie Wang

Institute of Physiology, Faculty of Medicine, University of Bonn, Bonn, Germany

Pathogen ingestion can lead to physiological consequences such as infection and tissue damage. However, animals can learn from the consequences of pathogen feeding and modify their behavior to avoid future exposure (Garcia et al., 1955; Wright et al., 2010;). While the fundamental mechanisms seem conserved across species, the mechanisms are not fully understood.
Recent work implicates the immune system as a central mechanism (Gonzalez-Santana and Diaz Heijtz, 2020) since bacterial peptidoglycans (PGNs) are recognized by peptidoglycan-recognizing proteins (PGRPs) in various tissues, including the nervous system; PGN recognition can activate the downstream expression of antimicrobial peptides (AMPs) (Pean and Dionne, 2014). Previous studies revealed that AMPs are required for learning and memory (Barajas-Azpeleta et al., 2018).
Recent work from our lab showed that the flies acquire the CFA through a mushroom body-dependent neural circuit, AMPs and PGRP-LC in octopaminergic (fly equivalent of noradrenaline) neurons (OANs) are essential parts of this mechanism (Kobler et al., 2020).
In a current study, we aimed at identifying the involved AMPs and their roles in CFA. To this end, we tested flies mutant for different AMPs or lacking specific AMPs in specific neurons and tissues by testing their preference for two Gram-negative pathogenic bacterial strains, Erwinia Carotovora 15 (Ecc15) and Pseudomonas entomophila (Pe) post-ingestion. First, we identify specific AMPs necessary and sufficient for CFA, specifically in the head fatbody and OANs. Second, RNAseq data confirms that pathogens ingestion leads to the upregulation of AMPs and other candidate genes in the head and fatbody. Finally, our preliminary data suggest that octopamine and dopamine receptors are involved in this behavior.
Current experiments aim at characterizing (i) the functional relationship between AMPs, dopamine and octopamine receptors signaling and (ii) the interaction between the fatbody and the nervous system by using a combination of feeding assays, genetics and imaging approaches.

OS 08-06
BDNF-expressing neurons of the lateral hypothalamus limit feeding in an obesogenic environment

Anne Petzold[1,2], Carolin Schumacher[1,2], Tatiana Korotkova[1,2]

[1] *University of Cologne, Institute for Systems Physiolgy, Cologne, Germany*
[2] *Max Planck Institute for Metabolism Research, Cologne, Germany*

The author has objected to a publication of the abstract.

OS 08-07
Global neuron population dynamics predict goal approach

Yangfan Peng[1], Carl Lindersson[1], Sasha Tinelli[1], Jeffrey Stedehouder[1], Armin Lak[2], Charlotte Stagg[1], Andrew Sharott[1]

[1] University of Oxford, MRC Brain Network Dynamics Unit, NDCN, Oxford, UK
[2] University of Oxford, Department of Physiology, Anatomy and Genetics, Oxford, UK

Large-scale recordings have revealed that movement modulates neuronal activity throughout the brain. Within the motor cortex, individual neurons have been shown to encode movement kinematics, while distinct lower-dimensional dynamics are exhibited by the population activity during preparation and execution of movement. However, the relationship between brain wide neuronal activation and these established neural representations of motor control remains unclear.
To elucidate this relationship, we simultaneously recorded the spiking activity of over thousand neurons across 20 cortical and subcortical brain regions during a goal-directed reaching task in mice using Neuropixels probes. Our results show robust latent population dynamics, displaying remarkable consistency across all recorded regions, animals, and sessions. We further found that these global population dynamics represent a time-varying signal, which continuously predicts the onset, approach, and successful completion of the goal-directed reach. Moreover, this signal is modulated by the anticipated likelihood of success. Together, our findings provide evidence for a distributed, continuous, and adaptive neural representation of goal-directed movements at millisecond timescale that could serve as a global reward prediction signal.

We thank Brook Perry, Robert Toth, Ben Micklem, Melissa Serrano, Colin McNamara, Julien Carponcy, Naomi Berry, Shiva Mahdian, and Jessica Myatt for technical and experimental assistance.
This research was supported by the Deutsche Forschungsgemeinschaft (DFG): Walter Benjamin Fellowship to Yangfan Peng (451242556) and the Medical Research Council UK (MRC) to Andrew Sharott (MC_UU_00003/6).

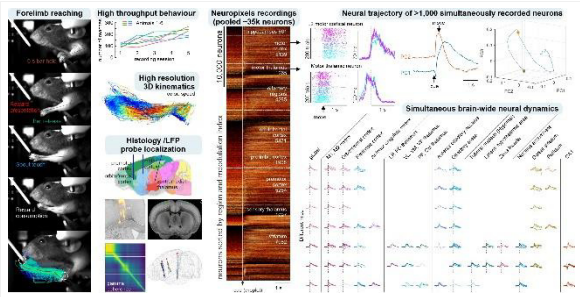

Large-scale Neuropixels recordings uncover consistent population dynamics across regions and animals
Depiction of head-fixed forelimb reaching task for a water droplet. Mice perform up to 200 reaches within a single session. The reach trajectories are captured via two high-speed cameras allowing reconstruction of 3D trajectories using DeepLabCut. We inserted up to three Neuropixels probes into multiple motor and non-motor brain regions to simultaneously record over thousand single neurons during the task. PSTH depicts task-modulated neurons across all regions. PCA analysis of population activity uncovers robust and consistent dynamics during reach across regions, animals and sessions.

OS 08-08
DBS in GPi modulates spontaneous cerebellar activity in a dystonic hamster.

Fabiana S. Kragelund[1], Denise Franz[1], Marco Heerdegen[1], Anika Lüttig[2], Stefanie Perl[2], Angelika Richter[1], Rüdiger Köhling[2]

[1] Universität Rostock, Oscar Langendorff Institut für Physiologie, Rostock, Germany
[2] Universität Leipzig, Institut für Pharmakologie, Pharmazie und Toxikologie, Leipzig, Germany

Question

[Dystonia is a neurological syndrome that alters muscle control for voluntary movement and sustained posture. Although the basal ganglia play a role in dystonia, an abnormal cerebellar function is also involved. Deep brain stimulation (DBS) is a standard treatment option for drug-refractory dystonia, and the most promising targets are the Globus Pallidus internus (GPi) or the subthalamic nucleus. The mechanisms of DBS, however, are as yet unclear. In this context, we were interested in the impact of DBS on cerebellar activity and, specifically, the role of glutamatergic transmission in DBS-induced changes.]

Methods

[We explored this question in a genetic animal model of primary paroxysmal dystonia (dtsz mutant hamster) and appropriate controls, bilaterally implanted with bipolar DBS electrodes in the entopeduncular nucleus (homolog to the GPi in humans).
The dtsz hamster is known for alteration in the ganglia–thalamocortical circuit, cortico-striatal circuit, and limbic structures. These further support us in investigating the cerebellum network, especially the synapse plasticity and the expression of NR2A subunits of NMDA since we already know that the NR2A/NR2B ratio is increased in the striatum of dystonic hamsters.
To gauge cerebellar activity, parasagittal slices were recorded with a high-density microelectrode array (200 µm thick) (HD-MEA; 3Brain AG). To analyze the involvement of the glutamatergic system, cerebellar slices were treated with 50 µM of PEAQX, an antagonist selective GluN2A, and their activity compared to baseline recordings in ACSF solution (10 minutes, 2 mL/min, at room temperature).]

Results

[Our preliminary results indicate that blocking the subunit GluN2A of the NMDA receptor with PEAQX modulates cerebellar activity. The results suggest changes in the %mean firing rate of Purkinje cells, on the cerebellar slices of wild type. Furthermore, the DBS in the GPi at 130 Hz seems effective against generalized dystonia in the dtsz mutant.]

Conclusions

[Our previous results indicate that blocking the NMDA receptor with PEAQX might modulate the Purkinje cell spike firing concerning the % of mean firing rate differentially between control and dystonic hamster. In addition, DBS in GPi seems to increase synaptic efficiency in the cerebellum of the dystonic model.]

This study was supported by the German Research Foundation (DFG) within the Collaborative Research Centre (SFB 1270/1 ELAINE 299150580). We also thank Tina Sellmann and Anna Einsle for all their support.

OS 09 | Oxygen, Metabolism & Inflamation

OS 09-01
The Omega Amidase NIT2 is a novel redox-sensitive key regulator of glutamine metabolism in endothelial cells

Niklas Müller[1,2], Pedro Malacarne[1,2], Sarah Wionski[1,2], Stephan Klatt[3,2], Ilka Wittig[1,2], Katrin Schroeder[1,2], Ralf Gilsbach[4,2], Travis Denton[5], Timothy Warwick[1,2], Arthur Cooper[6], Ralf Brandes[1,2], **Flávia Rezende**[1,2]

[1] *Goethe-University, Institute for Cardiovascular Physiology, Frankfurt, Germany*
[2] *DZHK, Rhein Main, Germany*
[3] *Goethe-University, Institute for Vascular Signaling, Frankfurt, Germany*
[4] *Heidelberg University Hospital, Institute of Experimental Cardiology, Heidelberg, Germany*
[5] *Washington State University, Department of Pharmaceutical Sciences, Spokane, Germany*
[6] *New York Medical College, Department of Biochemistry and Molecular Biology, NYC, Germany*

The author has objected to a publication of the abstract.

OS 09-02
Hypoxia induces MEK/ERK signaling via primary cilia - An unexpected function of the hypoxia-inducible factor-2alpha

Tristan Leu, Jannik Denda, Anna Wrobeln, Joachim Fandrey

University Duisburg-Essen / University Hospital Essen, Institute of Physiology, Essen, Germany

Primary cilia, which are antenna-like structures on the surface of most mammalian cell types, receive signals on the cell surface and transmit them to the interior implementing signal transduction. These organelles enable the cell to communicate and realize essential processes such as proliferation, migration and differentiation by controlling cellular signaling via Hedgehog, Wnt, TGF-β and much more. Disruption of signal

transmission in these pathways will lead to a multitude of serious human diseases and developmental disorders, called ciliopathies. Well-known ciliopathies are the Joubert syndrome (JBTS), the Meckel–Gruber syndrome (MKS), or the Bardet-Biedl syndrome (BBS), which are all linked to malformations of the central nervous system.

Ciliopathies often present with abnormalities in cilia length, in part controlled by the activity of intraflagellar transport (IFT), which is a parameter for adequate function of primary cilia. Especially in situations when oxygen supply falls short, e.g. during an ischemic stroke, it is necessary to provide relevant signals for counter-regulations quickly, as sufficient oxygen supply is required for proper cell function and survival. According to this, the formation and function of primary cilia has already been linked to the oxygen supply of the cell [1].

Key factors in the hypoxic response are hypoxia-inducible factors (HIFs). Especially the HIF-2 isoform promotes neurogenesis and has a protective effect on neuronal stem cells [2]. Through its influence on the physiological formation of new nerve cells and the production of apoptosis inhibitors, HIF-2 is a relevant factor in the regeneration of cerebral pathologies [3].

We now showed, by Immunofluorescence, the localization of hypoxia-inducible factor-2alpha (HIF-2α) in the axoneme of murine neuronal primary cilia under hypoxic conditions [4]. This entails an elongation of the ciliary axoneme, realized by the direct interaction of HIF-2a with the intraflagellar transport protein 88 homolog (IFT88), shown by Co-Immunoprecipitation. Quantitative PCR analyses confirmed the induction of *Mek1/2*, *Erk1/2* and associated target genes only in presence of primary cilia and HIF-2α. By increasing MEK/ERK signaling via primary cilia, HIF-2 seems to promote processes to increase the regenerative abilities of the cell and consequently improves the outcome of diseases such as stroke by means of signals mediated by primary cilia. Therefore, we propose that HIF-2, which otherwise acts as a transcription factor, plays a functional role in the signal transmission of primary cilia representing an unexpected and far more extensive function of HIF-2α than described before.

References
[1] Lavagnino, M, Oslapas, AN, Gardner, KL, Arnoczky, SP. Hypoxia inhibits primary cilia formation and reduces cell-mediated contraction in stress deprived rat tail tendon fascicles. Muscle Ligaments and Tendons J. 2019; 06:193–197. doi:10.32098/mltj.02.2016.05.
[2] Leu, T, Fandrey, J, Schreiber, T. (H)IF applicable: promotion of neurogenesis by induced HIF-2 signalling after ischaemia. Pflugers Arch. 2021;473: 1287–1299. doi:10.1007/s00424-021-02600-8.
[3] Nasyrov, E, Nolan, KA, Wenger, RH, Marti, HH, Kunze, R. The neuronal oxygen-sensing pathway controls postnatal vascularization of the murine brain. faseb J. 2019;33:12812–12824. doi:10.1096/fj.201901385RR.
[4] Leu, T, Denda, J, Wrobeln, A, Fandrey, J. Hypoxia-Inducible Factor-2alpha Affects the MEK/ERK Signaling Pathway via Primary Cilia in Connection with the Intraflagellar Transport Protein 88 Homolog. Mol Cell Biol. 2023;43(4):174-183. doi: 10.1080/10985549.2023.2198931.

OS 09-03
Differential miR expression during macrophage differentiation

Gerhild Euler[1], Oezden Tastan[1], Abdullah Al-Najjar[1], Rainer Schulz[1], Mariana Parahuleva[2]

[1] *Justus Liebig Universität, Institute of Physiology, Gießen, Germany*
[2] *UKGM, Clinic of Cardiology, Angiology and Internal Intensive Medicine, University Hospital Giessen und Marburg GmbH, Gießen, Germany*

In atherosclerosis, macrophages lodge in the intima and subintima of arteries, leading to the formation of obstructive atherosclerotic plaques that are prone to rupture. Recently, we identified eight differentially expressed miRs, either in monocytes from myocardial infarction patients or in atherosclerotic plaques. Since differentiation of monocytes to M0 macrophages or pro-inflammatory M1 macrophages is a prerequisite for their invasion in the atherosclerotic plaque, we now analyzed expression of those eight miRs during the process of monocyte/macrophage differentiation.

For induction of macrophage differentiation to M0, THP1 cells were stimulated with PMA (phorbol-12-myristate-13-acetate). mRNA expression of CD14, a marker of macrophage differentiation, was upregulated 31-times compared to non-stimulated cells after three days (n=4, $p<0.05$). At the same time, morphology of round, non-adherent THP-1 monocytes changed to a macrophage-like phenotype with enhanced granularity, formation of pseudopodia, and adherence to the culture dish. let-7f and miR92a expression decreased under PMA stimulation and the expression of miR1 and miR143 increased within 3 days, whereas four of the eight miRs under study remained unchanged (n=5-10, $p<0.05$ vs. unstimulated control). Treatment of THP-1 cells with agomiR92a attenuated enhancement of CD14-mRNA expression and thus M0-differentiation under PMA stimulation. In contrast, treatment with agomiR-let-7f amplified CD14-mRNA expression under PMA. For M1 differentiation, M0 macrophages were treated with IFN-γ and LPS. Marker genes of M1 polarization, IL-1β and TNFα, increased within 3 days (n=9, $p<0.05$ vs. unstimulated control). In addition, expression of miR21 increased, while miR143 and -223 decreased (n=13, $p<0.05$ vs.

unstimulated control). Under those conditions, treatment of cells with agomiR223 and antagomiR21 enhanced TNFα mRNA expression and thus M1-differentiation, whereas agomiR143 had no influence.
In conclusion, let-7f and miR223 promote the differentiation of monocytes into proatherogenic M0 or M1 macrophages, whereas miR92a and miR21 counteract these processes. Modulation of these miRs in vivo may therefore represent useful targets in the treatment of atherosclerosis in the future.

OS 09-04
Androglobin, a chimeric mammalian globin, is associated with ciliogenesis and sonic hedgehog signaling

Anna Keppner[1], Océane Derivaz[1], Darko Maric[1], Saar Adriaensen[2], Miguel Correia[1], David Hoogewijs[1]

[1] *University of Fribourg, Endocrinology, metabolism and cardiovascular system, Fribourg, Switzerland*
[2] *University of Antwerp, Antwerp, Belgium*

The author has objected to a publication of the abstract.

OS 09-05
5000 m Above Sea Level: Experiencing Integrative Exercise Physiology

Oliver H. Wittekindt, Michael Fauler, Paul Dietl

University of Ulm, Institute of General Physiology, Ulm, Germany

Teaching in physiology should provide students with the scientific knowledge and skills to enable independent solving of clinical problems. This forces medical students to grasp a large amount of information, structure and integrate it in an interdisciplinary framework that is beyond the capabilities of most current curricular teaching sessions. Therefore, we established an elective course which leads attendees through a fast-learning experience. It takes the students from the basics of vegetative physiology over practical aspects to a challenging integrative application in exercise physiology. It culminates in a field trip to the Eurac Research facility terraXcube in Bozen, Italy, where students perform cardiopulmonary exercise tests at environmental pressure conditions according to altitudes of 5000 m above sea level, but at safe and controlled laboratory conditions.
Our course consists of a seminar that follows an inverted classroom approach. It addresses vegetative-physiology and basics for height adaptation. A subsequent practical course covers lung function testing and breath-by-breath gas analysis, lung biomechanics and artificial ventilation, assessing cardiopulmonary function at different conditions (orthostasis and exercise), basics of echocardiography, blood gas analysis and cardiopulmonary exercise testing. The last part of the course is the field trip, during which the students perform cardiopulmonary exercise testing at altitude conditions of 5000 m above sea level. The students analyze their experimental data, compare their results obtained at 5000 m with their measurements performed at Ulm University (620 m above sea level) and finally discuss their results during a closure seminar.
Our elective course requires a high degree of direct active participation by students. Performing those experiments at 5000 m altitude contributes massively to student's motivation and learning performance. It trains their ability to recognize physical symptoms and educates their psychosocial skills. By design, the course attracts heterogenous groups of students, motivates them not as a best-grade-strategy but through subject-oriented curiosity. Despite disadvantages from high expenditure of faculty time and per-student costs, we are excited about the overall engagement of students and the high levels of performance. We further recognize that most attendees ask for positions as tutors as well as for MD projects.

We thank C. Steurer and his team from terraXcube as well as Prof. Dr. Jürgen Steinacker and PD Dr. Gunnar Treff (Section Sports and Rehabilitation Medicine) for their support and help.

OS 09-06
B lymphocyte autoimmunity in patients with mitral valve disease and secondary pulmonary hypertension

Teresa C. Funk-Hilsdorf[1,2,3], Jan Klages[4], Nikolay Dranishnikov[4], Raimund Rutenberg[4], Nicolas Merke[5], Weronika Karle[1], Matthias Hommel[4], Toralf Kaiser[6], Jenny Kirsch[6], Christian E. Busse[7], Hermann Kuppe[4], Jana Grune[1,3], Benjamin O'Brien[4], Wolfgang M. Kübler[1,3,9], **Szandor Simmons**[1,3]

[1] *Charité - Universitätsmedizin Berlin, Institute of Physiology, Berlin, Germany*
[2] *Berlin Institute of Health (BIH), Berlin, Germany*
[3] *German Centre for Cardiovascular Research (DZHK), partner site Berlin, Berlin, Germany*
[4] *German Heart Center Berlin (DHZC), Department of Cardiac Anesthesiology and Intensive Care Medicine, Berlin, Germany*
[5] *German Heart Center Berlin (DHZC), Department of Cardiothoracic and Vascular Surgery, Berlin, Germany*
[6] *German Rheumatism Research Centre Berlin (DRFZ), Flow Cytometry and Cell Sorting Core Facility, Berlin, Germany*
[7] *German Cancer Research Center, Division of B Cell Immunology, Heidelberg, Germany*
[8] *German Center for Lung Research (DZL), partner site Berlin, Berlin, Germany*
[9] *St. Michael's Hospital, The Keenan Research Centre for Biomedical Science, Toronto, Canada*
[10] *University of Toronto, Departments of Surgery and Physiology, Toronto, Canada*

Pulmonary hypertension (PH), a common complication of left heart disease (LHD), negatively impacts on LHD patients´ morbidity and mortality. PH-LHD represents the most common type of PH and is defined as mean pulmonary arterial pressure (mPAP) >20 mmHg and a mean pulmonary arterial wedge pressure >15 mmHg. Recent work by us and others stressed the role of dysregulated immunity in PH including changes in B-cell homeostasis in animal models of PH-LHD. In inflammatory conditions, autoreactive B-cells can escape central and peripheral tolerance mechanisms, conducing to the genesis of autoimmunity, a so far unrecognized pathomechanism in PH-LHD. Deeper insight into the contribution of B-cell immunity to PH-LHD may provide for a better understanding of pathophysiological processes and thus, for the identification of novel cellular therapeutic targets. We hypothesized that PH-LHD may be associated with changes in B-cell homeostasis and autoreactivity as potential drivers of disease development and severity.

To test this hypothesis, we analyzed whole blood samples of patients with mitral valve (MV) replacement/repair with and without PH as assessed by echocardiography according to the 2015 ESC/ERS guidelines allowing for classification of patients into groups of low (n=34), intermediate (n=8) or high probability (n=21) of PH. B-cell subpopulations in the blood of patients with MV disease were identified by flow cytometry, correlated with the total number of B-cells, and compared to a group of age and sex matched healthy controls (n=35).

No differences could be detected in concentrations of peripheral total plasmablasts (CD19+ CD27+ CD38+), plasma cells (CD19+ CD27+ CD38+ CD138+), as well as total non-switched memory B-cells (CD19+ CD27+ CD38- IgD+) and total switched memory B-cells (CD19+ CD27+ CD38- IgD-). In line with these findings, immunoglobulin isotyping analyses revealed no significant differences between patients with MV disease and healthy controls. Autoimmunity was tested by using indirect immunofluorescence assays on Kallestad rat tissue slides. In their plasma 75% of patients with a high probability of PH carried IgG and IgA anti-nuclear or anti-cytoplasmatic autoantibodies, compared to 0% of healthy controls and 29% of patients with a low probability of PH. These results highlight the association of B-cell autoreactivity with PH-LHD and point to the potential relevance of autoantibodies as targetable pathomechanisms and prognostic marker in PH-LHD.

OS 09-07
cAMP-dependent Modulation of Calcium Oscillations in Pancreatic Beta Cells

Johannes U. Pfabe[1], Nastja Sluga[2], Sandra Postic[1], Marjan Slak Rupnik[1]

[1] *Medical University of Vienna, Institute of Physiology, Vienna, Austria*
[2] *University of Maribor, Faculty of Medicine, Maribor, Slovenia*

Objective

Many intracellular processes in beta cells are influenced by cAMP concentration ($[cAMP]_i$), the best described is exocytosis of insulin granules. The direct effects of cAMP-dependent mechanisms on intracellular Ca^{2+} release are less well described. Commonly used compunds to modulate cAMP, e.g., caffeine, exert dual effects. Caffeine acts on both Ca^{2+} release from the endoplasmic reticulum (ER), or as an inhibitor

of phosphodiesterase activity, directly rising $[cAMP]_i$. In this study, we aim to primarily address the effects of manipulation of $[cAMP]_i$ on the pattern of Ca^{2+} oscillations in beta cells in acute pancreatic tissue slices.

Methods

Acute pancreatic tissue slices were produced from male C57BL/6J mice as previously described [1]. After staining the slices with a low-affinity calcium indicator dye, we performed high-temporally resolved confocal microscopy. The identity of beta and delta cells within the islets was confirmed by immunocytochemistry. We investigated the effect of $[cAMP]_i$ pharmacologically using forskolin, caffeine, adrenaline, somatostatin, or a soluble cAMP analogue. A custom-made open-source high-throughput analysis pipeline was used to analyze the events of Ca^{2+} oscillations [2].

Results

We observed that the amount of Ca^{2+} released by caffeine has been overestimated in previous experiments using high-affinity Ca^{2+} indicators. In addition, event halfwidths got prolonged during caffeine and forskolin treatment. This is caused by temporal summation of short events in a concentration-dependent manner, an effect also observed with glucose-stimulation above 10 mM. Interestingly, during treatment where cAMP sources got combined, we observed a shift towards events with shorter halfwidth. Lowering cAMP levels with somatostatin or adrenaline, on the other hand, resulted in concentration-dependent inhibition of beta cell activity.

References
[1] Speier, S. & Rupnik, M. A novel approach to in situ characterization of pancreatic β-cells. *Pflugers Arch - Eur J Physiol* 446, 553–558 (2003).
[2] Postić, S., Sarikas, S., Pfabe, J., Pohorec, V., Bombek, L., Sluga, N., Skelin Klemen, M., Dolenšek, J., Korošak, D., Stožer, A., Evans-Molina, C., Johnson, J. D., & Slak Rupnik, M. (2023). Physio_Ca - islets framework (Version 0.8.0) [Computer software]. https://doi.org/10.1152/ajpendo.00165.2022

OS 09-08
The loss of gap junctions in excitable cells promotes mitochondrial stress-induced longevity in Caenorhabditis elegans

Daniel-Cosmin Marcu[1], Nathalie A. Vladis[2,3], Katharina E. Fischer[3], Karl E. Busch[1,3]

[1] *HMU Health and Medical University Potsdam, IMBB Institute for Mind, Brain and Behavior, Potsdam, Germany*
[2] *Brandeis University, Waltham, USA*
[3] *University of Edinburgh, Centre for Discovery Brain Sciences, Edinburgh, UK*

The nervous system is a central regulator of longevity, but how communication between excitable cells influences lifespan and ageing is poorly understood. We investigated whether gap junctions play a role in regulating longevity and ageing, and found that loss of the genes that encode gap junction proteins in the nematode *Caenorhabditis elegans* has extensive and diverse effects on lifespan. Loss of the innexin *unc-9* from either the nervous system or muscles, for example, increases longevity by a third and also improves healthspan. This *unc-9*-dependent extension of lifespan requires reactive oxygen species. The loss of intercellular coupling by UNC-9 increases mitochondrial respiration and triggers a systemic induction ofq the mitochondrial-specific unfolded protein response (UPRmt) to promote longevity. Thus, the coupling by gap junctions in excitable cells regulates lifespan and ageing through altering mitochondrial respiration.

Roderick N. Carter and Nicholas Morton contributed to microrespiration measurements, Peter Askjaer contributed to strain generation, and María Goya and Maria Doitsidou contributed to qPCR assays. We gratefully acknowledge financial support by the Wellcome Trust (109614/Z/15/Z) and the Medical Research Council (MR/N004574/1).

OS 10 | Cell Biology & Signal Transduction

OS 10-01
Ventricular and slow skeletal β-myosin molecules exhibit dissimilar chemomechanical properties due to deceleration by myosin essential light chain 1sa

Jennifer Osten, Tianbang Wang, Maral Mohebbi, Petra Uta, Arnab Nayak, Theresia Kraft, Mamta Amrute-Nayak, **Tim Scholz**

Hannover Medical School, Molecular and Cell Physiology, Hannover, Germany

Myosin-II molecules are ATP-powered force-generating machines driving cardiac and muscle contraction. They consist of two myosin heavy chains (MyHC) and two pairs of associated essential (ELC) and regulatory (RLC) light chains. Ventricular and slow-twitch skeletal *M. soleus* myosin-II molecules are often regarded functionally equivalent as their heavy chains are both expressed from gene *MYH7*. Consequently, *M. soleus*–derived myosin-II is often used as an alternative source to study functional effects of disease-associated mutations in ventricular β-cardiac myosin in hypertrophic cardiomyopathy (HCM).
We examined the mechanochemical properties of native myosin molecules isolated from rabbit ventricle and soleus muscles both in ensembles and at the single-molecule level using *in vitro* actin gliding assays and optical trapping. We found that myosin from these two tissues, despite expressing the same MyHC isoform, displayed distinct motile and ATPase kinetic properties. *M. soleus* myosin moved actin filaments approximately threefold slower than ventricular myosin. Slower actin gliding was associated with the presence and relative content of the long-type ELC MLC1sa in *M. soleus* myosin. While the power stroke size and actomyosin (AM) rigor stiffness derived in single-molecule assays were comparable for both myosins, the AM detachment rate was reduced approximately threefold in *M. soleus* myosin, corresponding to decelerated ADP release rates, thus explaining the observed differences in the motility driven by these myosins.
Long-type ELC isoforms contain a positively charged N-terminal extension, which can transiently interact with the MyHC close to the ATPase domain or with acidic residues on actin, thereby bridging the actin filament and the myosin motor domain. We propose that the, compared to the ventricular ELC, longer and more positively charged MLC1sa decelerates actin gliding either due to a higher affinity to actin associated with a decreased dissociation rate or by decelerated actomyosin cycling kinetics. In previous studies, *M. soleus* fibers from HCM patients were compared to fibers from healthy individuals. Possible differences between HCM patient and healthy control samples are likely to reflect mutation-specific effects as long as samples from the same muscle tissue are compared. However, tissue-specific differences in key functional parameters suggest the use of e.g. ventricular myosin, myofibrils or cardiomyocytes in future studies on HCM-associated mutations in ventricular myosin.

OS 10-02

Liver X Receptors Alpha and Beta Modulate Skeletal Muscle Adaptations in Sedentary and Loading Conditions: Insights from Mice Studies

Frank Suhr[1,2], Florian Blaschke[3], Wiljelm Bloch[4]

[1] *University of Bayreuth, Faculty of Life Sciences: Food, Nutrition and Health, Division of Molecular Exercise Physiology, Kulmbach, Germany*
[2] *Uniklinik RWTH Aachen, RWTH Aachen University, Institute of Anatomy and Cell Biology, Aachen, Germany*
[3] *Charité-Universitaetsmedizin Berlin, Department of Cardiology, Berlin, Germany*
[4] *German Sport University Cologne, Department of Molecular and Cellular Sports Medicine, Cologne, Germany*

The author has objected to a publication of the abstract.

OS 10-03

Proteo-genomic identification of functional endothelial microproteins encoded by non-canonical small open reading frames.

Mauro Siragusa[1], Johannes Graumann[2,3], Carsten Künne[4], Stefan Günther[4], Sylvia Jeratsch[2], Bethlehem Bezuneh[1], Sebastian Süsser[5], Xiaozhu Zhou[1], Haaglim Cho[6], Manuel Kaulich[5], Mario Looso[4], Stefan Offermanns[6], Ingrid Fleming[1]

[1] Goethe University, Institute for Vascular Signalling, Frankfurt am Main, Germany
[2] Max Planck Institute for Heart and Lung Research, Biomolecular Mass Spectrometry, Bad Nauheim, Germany
[3] Philipps-Universität Marburg, Institute of Translational Proteomics, Marburg, Germany
[4] Max Planck Institute for Heart and Lung Research, Bioinformatics and Deep Sequencing Platform, Bad Nauheim, Germany
[5] Goethe University, Institute of Biochemistry II, Frankfurt am Main, Germany
[6] Max Planck Institute for Heart and Lung Research, Department of Pharmacology, Bad Nauheim, Germany

Background and Aim. The study of non-canonical small open reading frames (smORFs)-encoded microproteins (miPs; <100 amino acids) has been hampered by technical challenges associated with the detection of small peptides by mass spectrometry. Since the relevance of miPs in endothelial cells is mostly unknown, the aim of this study was to identify and characterize endothelial cell smORF-encoded miPs.
Methods and Results. We combined deep RiboTag-RNA sequencing and bioinformatic pipelines optimized for downstream proteomic studies to identify miPs in endothelial cells by mass spectrometry. This approach led to the identification of 728 *bona fide* miPs encoded by previously non-annotated smORFs in human endothelial cells. Endothelial cell activation by interleukin-1β was associated with profound alterations in endothelial miP expression *in vitro* (698 differentially expressed miPs). The release of miPs was demonstrated under homeostatic conditions (210) as well as after stimulation with interleukin-1β (297). RNA-seq of ribosome associated RNAs from endothelial cell-specific RiboTag mice combined with proteomic analyses revealed that 408 endothelial miPs were differentially expressed in response to inflammation and endothelial dysfunction in mice (AAV-PCSK9 injection/high cholesterol diet combined with partial carotid artery ligation). Large-scale CRISPR screening demonstrated the relevance of numerous smORFs for endothelial cell survival. The detailed functional characterization of selected miPs was performed combining gain- and loss-of-function approaches with multi-omic analyses. These studies revealed the ability of human endothelial cell miPs to interact with other proteins to affect cell proliferation, cytoskeleton dynamics, migration and transcriptional regulation, in line with their diverse cellular localization, including the cytosol, the cytoskeleton, the endoplasmic reticulum or the nucleus.
Conclusions. We identified previously non-annotated endothelial cell smORFs and their encoded miPs under homeostatic conditions as well as their alterations in response to endothelial cell activation. A pool of endothelial miPs is secreted and may exert autocrine or paracrine functions, potentially relevant for human cardiovascular disease. Finally, similar to large proteins, miPs are involved in a plethora of biological processes and represent an unexplored new class of molecular players.

OS 10-04
Unc13A dynamically stabilizes vesicle priming at synaptic release sites for short-term facilitation and homeostatic potentiation

Meida Jusyte[2], Natalie Blaum[1], Mathias A. Böhme[2,4], Manon M. Berns[1], Alix E. Bonard[1], Abel B. Vamosi[1], Kavya V. Pushpalath[1], Janus R. Kobbersmed[3], Alexander M. Walter[1,2]

[1] University of Copenhagen, Department of Neuroscience, Copenhagen, Denmark
[2] Leibniz-Forschungsinstitut für Molekulare Pharmakologie, Molecular and Theoretical Neuroscience, Berlin, Germany
[3] University of Copenhagen, Department of Mathematical Sciences, Copenhagen, Denmark
[4] Leipzig University, Rudolf Schönheimer Institute for Biochemistry, Leipzig, Germany

Question
Chemical synaptic transmission relies on neurotransmitter release from presynaptic release sites and on transmitter-sensing by the postsynaptic cell. Presynaptic plasticity increasing neurotransmitter release achieves two fundamental nervous system functions: It tunes some synapses to be more responsive to millisecond repetitive activation and it maintains signals when postsynaptic transmitter sensitivity is reduced. How enhanced neurotransmitter release is achieved in these phenomena, termed short-term facilitation and homeostatic potentiation, remains unknown.

Methods
We combine mathematical modeling and experimental analysis of *Drosophila* neuromuscular junction model synapses to elucidate the molecular mechanisms underlying these forms of plasticity.
Results

Despite their eminence on different timescales, our analysis revealed functional communalities and shared molecular dependence of short-term plasticiy and homeostatic potentiation on the release site protein Unc13A. Mutating Unc13A's Calmodulin binding (CaM) domain increased baseline transmission while blocking short-term facilitation and homeostatic potentiation. Mathematical modeling suggested that Ca^{2+}/Calmodulin binding to Unc13A plastically stabilizes vesicle priming at release sites and that mutation of the CaM domain blocked plasticity by causing constitutive stabilization. Super-resolution STED microscopy revealed higher signals for Unc13A's functionally essential MUN domain closer to release sites in CaM-domain mutants which might contribute. Akin to effects of CaM domain mutation, acute treatment of synapses expressing wildtype Unc13A with phorbol esters (that can activate the neighboring Unc13A C1 domain) enhanced transmission and blocked both short-term facilitation and homeostatic potentiation. This effect was not seen in synapses expressing CaM domain mutants, indicating a common downstream effect.

Conclusions

Our findings indicate that Unc13A regulatory domains are tuned to integrate a multitude of signals on various timescales to switch release site participation for synaptic plasticity.

This work was supported by grants from the Deutsche Forschungsgemeinschaft (DFG) to A.M.W. (Emmy Noether Programme, Project Number 261020751 and the TRR 186, Project Number 278001972) and the Novo Nordisk Foundation (Young Investigator Award NNF19OC0056047 to A.M.W.). M.J. was supported by the Einstein Foundation Berlin (grant EZ-2014-226). We thank Dr. Stephan Sigrist for helpful comments and sharing antibodies.

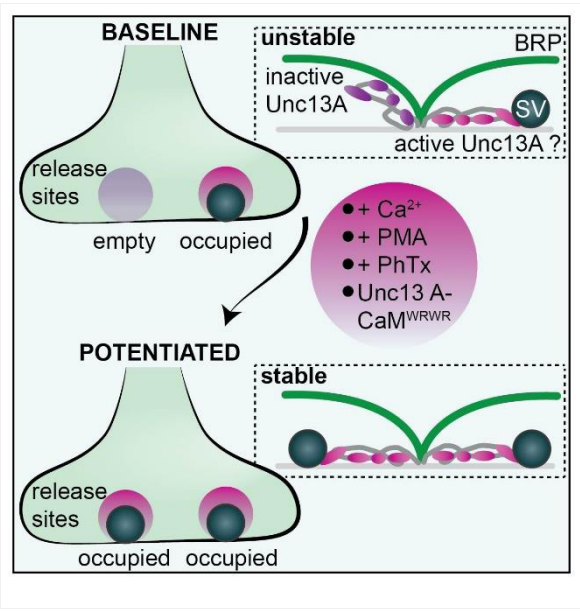

Acute and intermediate presynaptic plasticity targets Unc13A at neurotransmitter release sites

We find joint dependence of millisecond and minute's presynaptic plasticity on the conserved Unc13A protein. Constituative mutation of its Ca^{2+}/calmodulin binding domain or acute phorbol-ester treatment blocked plasticity by over-activating Unc13A, possibly by enhancing neurotransmitter release site occupation through its subsynaptic re-distribution. Converging signals on Unc13A dynamically control synaptic output from neurotransmitter release sites.

OS 10-05
S-acylation of Stromal Interaction Molecule 1 (STIM1) enhances store-operated Ca^{2+} entry (SOCE)

Raphaël Néré[1], Sana Kouba[1], Amado Carreras-Sureda[1], Laurence Abrami[2], Gisou Van Der Goot[2], Nicolas Demaurex[1]

[1] *UNIGE, Physiology & Medicine, Geneva, Switzerland*
[2] *EPFL, Lausanne, Switzerland*

STIM1 is an endoplasmic reticulum (ER) Ca^{2+} sensing protein that mediates the ubiquitous SOCE pathway by activating plasma membrane (PM) channels of the ORAI and TRPC families, thereby enabling Ca^{2+} entry into cells. Upon Ca^{2+} depletion of the ER, STIM1 undergoes a sequence of conformational changes, oligomerizes and migrates to ER-PM membrane contact sites where it traps and gates PM channels. This process is critical for T cell activation and differentiation and loss-of-function mutations in STIM1 or ORAI1 are linked to severe combined immunodeficiencies. SOCE can be modulated by post translational modifications, including phosphorylation and redox-mediated modifications

of cysteine residues. Here, we investigate whether STIM1 is also regulated by S-acylation, the attachment of a long chain fatty acid on cysteines.

A STIM1-immunoreactive band was detected by acyl-resin assisted capture (Acyl-RAC) of HEK-293 cells, indicating that endogenous STIM1 is S-acylated. Cys mutagenesis revealed that substitutions at Cys_{437} abolished the binding of RFP-STIM1 to the acyl resin, indicating that STIM1 is S-acylated at residue Cys_{437}. GFP-STIM1 was similarly acyl-captured when expressed in WT VeroE6 cells, but not following CRISPR-Cas editing of the palmitoyl acyltransferase (PAT) enzyme *DHHC20* (PAT20), indicating that this PAT isoform is required for STIM1 S-acylation. CFP-STIM1 lacking the polybasic C-terminal domain was also acyl-captured when expressed in cells lacking the three isoforms of the ORAI1 channel, indicating that binding to ORAI channels or to negatively charged PM lipids is dispensable for the S-acylation reaction. A robust Ca^{2+} elevation was observed by fura-2 imaging upon Ca^{2+} readmission to thapsigargin-treated cells lacking both STIM1 and STIM2 isoforms and re-expressing RFP-STIM1 along with YFP-ORAI1. Both the slope and amplitude of the SOCE component were reduced by 50% when the S-acylated Cys_{437} residue was mutated to alanine or serine (RFP-$STIM1^{C437A}$ or RFP-$STIM1^{C437S}$), linking the S-acylation to a gain-of-function of STIM1. Accordingly, PAT20 overexpression enhanced SOCE 4-fold when co-expressed with RFP-STIM1 but had no effect when co-expressed with RFP-$STIM1^{C437A}$.These data show that STIM1 is S-acylated at Cys-437 independently of ORAI channels or its polybasic domain. STIM1 S-acylation requires PAT20, whose expression enhances SOCE only when Cys-437 is present, indicating that the addition of a lipid to STIM1 enhances channel gating. The STIM1 conformational step impacted by this lipidation as well as the nature of the lipids added to STIM1 and the functional impact of this post-translational modification for immune cells are currently under investigation.

OS 10-06

Ferroptosis resistance is associated with abated iron transport and increased tumorigenic hypoxia-inducible factor signalling in *VHL*-deficient renal cancer cells.

Wing-Kee Lee[1], Marie Bergmeier[1], Daniel Hebrok[1], Teresa Kern[1], Calista Ow[2,3], Frank Thévenod[1]

[1] *Bielefeld University, Medical School OWL, Physiology & Pathophysiology of Cells and Membranes, Bielefeld, Germany*
[2] *Witten/Herdecke University, Institute for Physiology, Pathophysiology and Toxicology, Witten, Germany*
[3] *University of Manchester, Faculty of Biology, Medicine and Health, Manchester, UK*

Ferroptosis is a mode of programmed cell death dependent on iron (Fe) that is characterised by a defective antioxidant system, elevated membrane polyunsaturated fatty acids and lipid peroxidation. It is elicited by Fe-induced generation of reactive oxygen species (ROS), resulting in membrane damage and cell death. Though cancer cells are particularly susceptible to ferroptosis, recent data suggest renal cancers accumulate less iron with pathological progression, thus decreasing ferroptosis susceptibility [1]. We therefore hypothesised Fe transport and Fe-dependent cell death signalling are altered in renal cancer cells (RCCs). Cell culture models for normal renal proximal tubule (HPCT) and RCCs with a drug-resistant and inactive Von-Hippel-Lindau (VHL) phenotype (A498, 786-O) were used. Loss-of-function *VHL* mutations are commonly found in RCCs, leading to a persistent pseudohypoxic state due to increased stability of tumorigenic hypoxia-inducible factors (HIFs). Both A498 and 786-O cells harbour elevated HIF2A. The ferroptosis inducer, erastin (5 µM, 24 h), was more effective in decreasing cell viability by MTT assay in HPCT (EC_{50} 0.66 µM) compared to A498 (EC_{50} 1.76 µM) after 24 h. Trypan blue staining, electrophysiological (ECIS) and ATP assays revealed cell proliferation is diminished by erastin in HPCT. H_2O_2 augmented ROS measured with CellROX by ~300% in HPCT versus ~50% in A498. Expression of the Fe efflux transporter FPN1 increased in HPCT after Fe loading by ferric ammonium citrate for 30 h, but not in RCCs, despite lower basal expression. Compared to HPCT, receptor-mediated Fe transport pathways in RCCs showed diminished transferrin receptor 1 (TFR1) (by 50-60%) expression, but increased cellular expression and secretion of Fe-sequestering lipocalin-2 (LCN2) (4-fold) and its receptor (LCN2-R) (3-fold). Transient transfection of *HIF2A* siRNA (20 nM, 72 h) resulted in increased *LCN2* (~6-fold) and renal mesenchymal-to-epithelial transformation regulator *WNT4* (~2-fold) mRNA, yet attenuated cell proliferation gene cyclin D1 (*CCND1*, >60%) in addition to FPN1 (up to 50%) and LCN2-R (up to 20%) at the protein level. Both TFR1 mRNA and protein were not affected by *HIF2A* siRNA.

Taken together, these data imply deregulation of Fe-sensing pathways as well as uptake and efflux mechanisms occurs in RCCs is partly driven by HIF2A. We posit lower cellular Fe levels and diminished responsiveness in Fe-sensing imparts resistance to ferroptosis in RCCs with increased metastatic potential, impacting therapeutic strategies.

References
[1] Greene, C.J. *et al.* 2022, Iron accumulation typifies renal cell carcinoma tumorigenesis but abates with pathological progression, sarcomatoid dedifferentiation, and metastasis. *Front. Oncol.* 12:923043.

OS 10-07
Extracellular acidosis induces G0/G1 cell cycle arrest in tumor cells via Ca^{2+} signaling

Anne Riemann, Mandy Rauschner, Virginie Dubourg, Sarah Reime, Oliver Thews

Martin-Luther-Universität Halle-Wittenberg, Julius-Bernstein-Institut für Physiologie, Halle, Germany

Question

The tumor microenvironment is characterized by deprivation of nutrients like glucose, shortage of oxygen (hypoxia) and a reduction of the tissue pH (acidosis). Acidosis has an impact on tumor promotion as well as progression, resulting in increased risk of metastases formation and therapy resistance. On the cellular level acidosis affects tumor cell growth, but the precise mechanisms remain to be elucidated.

Methods

We analyzed the impact of acidosis on proliferation of rat prostate tumor cells (AT1) with flow cytometry and propidium iodide staining. Therefore, cells were exposed either to a control (pH 7.4) or an acidic extracellular environment (pH 6.6) for 24 h prior to the measurements. The role of various signaling pathways was elucidated using the respective inhibitors during the incubation period. The level of reactive oxygen species (ROS) was reduced by the cell permeable ROS scavenger Tiron (disodium 4,5-dihydroxy-1,3-benzenedisulfonate), while intracellular calcium was reduced using Ca^{2+}-free medium. Acidosis-induced changes in gene expression were studied by Next Generation Sequencing and Ingenuity Pathway Analysis.

Results

We found that acidosis reduced the amount of tumor cells in S phase, while increasing cells in G1 phase. No changes were found concerning G2 phase, when comparing control and acidic extracellular pH. Mechanistically, acidosis did not affect cell cycle by signaling pathways relying on mTOR, c-Myc or ROS, but via changes in Ca^{2+} signaling. Acidosis regulated gene expression patterns in prostate tumor cells, and many of these groups of genes were involved in cell cycle and cell cycle control. The expression of genes promoting proliferation was markedly reduced by acidosis, including E2F transcription factors, cyclins, cyclin dependent kinase 1 and cell division cycle proteins. In line with this, gene expression of cell cycle inhibitors like p21 and p27 was increased.

Conclusions

Our findings indicate that targeting the acidic tumor environment might thus restore cell growth and could improve tumor therapy targeting proliferating cells.

POSTER SESSION A

A 01 | K+ & Cl- Transport Across Membranes

A 01-01
Molecular Basis of TREK K_{2P} Channel Gating

Marcus Schewe[1], Kristin Rathje[1], Elena B. Riel[2], Friederike Schulz[1], Marianne A. Musinszki[1], Sönke Cordeiro[1], Thomas Baukrowitz[1]

[1] *Kiel University, Medical Faculty, Institute of Physiology, Kiel, Germany*
[2] *Weill Cornell Medical College, 2Department of Anesthesiology, New York, USA*

Two-pore domain K^+ (K_{2P}) channels play a crucial role in regulating electrical cell excitability and thereby are important mediators of biological processes like neurotransmission, hormone secretion, K^+ homeostasis or temperature and pain perception. Particularly, TREK K_{2P} channel gating is complex as a wide range of stimuli and small chemical compounds, partner proteins and second messenger molecules modulate channel activity. Moreover, two crystallographic conformations of TREK-2 K_{2P} channels (i.e. the up and down state) have been resolved and their main difference lies in the position and orientation of the transmembrane helix TM4. In the down state (but not in the up state) large side fenestrations -branching off from the central cavity- exist that are also targeted by drugs such as the norfluoxetine (NFx). NFx is thought to inhibit TREK-2 K_{2P} activity by preventing the transition from the down into the up state. Because of this, the down state is thought to represent a low activity state while the up state is thought to have a high open probability. However, direct functional data linking the two states to the physiological regulation such as pH regulation, PIP_2 regulation or phosphorylation is still largely missing.
Here, we used a functional mutagenesis screen of the TREK-1 transmembrane helices TM2, TM3 and TM4 and the proximal C-terminus (pCT), cysteine modification experiments in TREK and TRAAK channels and a NFx inhibition assay as well as molecular dynamics (MD) simulations of TREK channels to gain structural insights into the gating mechanism of these K_{2P} channels. Scanning mutagenesis identified several residues that strongly activate TREK-1 K_{2P} channels including three homolog residues in the different TM helices of TREK-2 that are in close proximity in the down state but break apart in the up state indicating that this triad stabilizes the down state conformation. Moreover, disrupting the triad resulted in channels with strongly reduced NFx sensitivity consistent with the closed side fenestrations observed in the crystallographic up state. The activation of TREK-1/-2 K_{2P} channels by intracellular acidification, PIP_2 and dephosphorylation mimicking mutations that are thought to act via the pCT, also resulted in markedly decreased NFx affinities suggesting that these stimuli also induce the up state. The involvement of pCT in TREK K_{2P} channel gating was further investigated via cysteine mediated attachment of either hydrophobic moieties (decyl-groups) or hydrophilic moieties (charged groups). The results are consistent with the pCT forming an amphipathic helix that dips into the membrane at acidic pH or upon PIP_2 binding and, thereby, favoring the highly active up state.Collectively, the results draw a consistent structural mechanism of TREK K_{2P} channel gating based on crystallographic as well as now also on comprehensive functional data.

We thank the members of our laboratories for technical support and helpful comments.

A 01-02
Essential role of conserved alanine residues in CLC channel proteostasis

Chia-Ying You[1], Ciao-Yu Zhung[1], Chung-Jiuan Jeng[2], Chih-Yung Tang[1]

[1] *National Taiwan University, Graduate institute of physiology, Taipei City, Taiwan*
[2] *National Yang Ming Chiao Tung University, Institute of Anatomy and Cell Biology, Taipei City, Taiwan*

The voltage-dependent chloride channels ClC-1 and ClC-2 are members of the CLC channel/transporter superfamily. A functional CLC channel/transporter comprises a dimeric structure, with each monomer containing an intracellular α-helix (helix A) as well as 17 transmembrane α-helices (helices B to R). Loss-of-function mutations in the human gene encoding ClC-1 (*CLCN1*) and ClC-2 (*CLCN2*) channels are associated with myotonia congenita and leukodystrophy, respectively. Disease-causing ClC-1 and ClC-2 mutations may manifest aberrant voltage-

dependent gating, as well as defective protein homeostasis (proteostasis). Significant defect in CLC channel proteostasis has been demonstrated for two disease-causing alanine-to-valine mutations in the transmembrane helix O: ClC-1 A531V and ClC-2 A500V. Importantly, these two locations correspond to the highly conserved helix O alanine residues present in virtually all members of the CLC channel/transporter superfamily. To further understand their proteostatic significance in CLC channels, we generated a series of different mutations of these highly conserved alanine residues in helix O of ClC-1 and ClC-2 channels. Our biochemical analyses indicate that a modification of the side-chain volume at these helix O locations notably disrupts protein stability and membrane trafficking of ClC-1 and ClC-2 channels. In contrast, an alanine-to-valine mutation in the nearby helix Q, as well as a disease-causing alanine-to-threonine mutation in helix E, fails to discernibly affect ClC-1 protein level. These observations suggest that a minor change in the side-chain volume at the highly conserved helix O alanine residues may lead to substantial interference of CLC channel proteostasis, consistent with the idea that helix O plays an essential role in protein folding during CLC channel biogenesis in the endoplasmic reticulum.

We thank Dr. Chen Tsung-Yu for his helpful suggestions and advice on this project, and Dr. Fu Ssu-Ju for the technical support during the experiments. Additionally, we express our gratitude to the staff of the Biomedical Resource Core at the First Core Labs, National Taiwan University College of Medicine, for their technical assistance.

References

[1] Papponen, H., Nissinen, M., Kaisto, T., Myllylä, V. V., Myllylä, R., & Metsikkö, K. (2008). F413C and A531V but not R894X myotonia congenita mutations cause defective endoplasmic reticulum export of the muscle-specific chloride channel CLC-1. *Muscle & Nerve, 37*(3), 317-325.
[2] Tang, C.-Y., & Chen, T.-Y. (2011). Physiology and Pathophysiology of CLC-1: Mechanisms of a Chloride Channel Disease, Myotonia. *Journal of Biomedicine and Biotechnology, 2011*, 685328.
[3] Gaitán-Peñas, H.; Apaja, P.M.; Arnedo, T.; Castellanos, A.; Elorza-Vidal, X.; Soto, D.; Gasull, X.; Lukacs, G.L.; Estévez, R. (2017). Leukoencephalopathy-causing CLCN2 mutations are associated with impaired Cl^- channel function and trafficking. *Journal of Physiology-London, 595*(22), 6993-7008.
[4] Fu, S. J., Hu, M. C., Hsiao, C. T., Cheng, A. T., Chen, T. Y., Jeng, C. J., & Tang, C. Y. (2021). Regulation of ClC-2 Chloride Channel Proteostasis by Molecular Chaperones: Correction of Leukodystrophy-Associated Defect. *International Journal of Molecular Sciences, 22*(11), 20.

A 01-03
Exploring basics of ion channel gating in viral proteins

Nils Drexler[1], Lena Diederich[1], Oliver Rauh[2], Jennifer Opper[2], Maximilian Sturm[2], Deborah Scheub[2], Gerhard Thiel[2], Ulf-Peter Hansen[3], **Indra Schroeder**[1]

[1] *University Hospital Jena, Friedrich Schiller University Jena, Physiology II, Jena, Germany*
[2] *Technical University Darmstadt, Plant Membrane Biophysics, Darmstadt, Germany*
[3] *Kiel University, Department of Structural Biology, Kiel, Germany*

The selectivity filter gate in potassium (K^+) channels is regulated by a complex interaction network anchoring it to the rest of the channel, as well as by the ion occupancy in the (K^+) binding sites in the filter. Cellular signals and the state of other gates are communicated to the filter through this network. Despite decades of research, this gate is still not fully understood. The minimal viral Kcv channels are an ideal system to study an “autonomous” filter gate, since they are devoid of regulating domains and have no bundle-crossing gate. By changing the ion species in the recording solutions in single-channel recordings in planar lipid bilayers and via mutations, we explore the regulation of this still not well-understood channel region.

A 01-04
Understanding the role of individual subunits in concatenated heteromeric Kv2.1/Kv6.4 channels.

Debanjan Tewari, Christian Sattler, Klaus Benndorf

University Hospital FSU Jena, Institute of Physiology II, Jena, Germany

Question

Voltage-gated potassium channels (Kv) are membrane proteins allowing the transport of K^+ ions across the membrane in response to the voltage. During activation, the S4 segment in the voltage-sensing domain (VSD) is moving across the hydrophobic core of the membrane. A conserved phenylalanine in the trans-membrane S2 helix is the charge transfer center that interacts with the positive arginine of the S4 helix

essentially involved in the opening of the pore. This phenylalanine is highly sensitive to diverse substitutions. Within the family of Kv subunits, there are several that do not form functional channels on their own but can form functional heteromeric channels with other Kv subunits. We used the approach of subunit concatenation to define the number and position of the Kv2.1 and Kv6.4 subunits in hetero-tetrameric channels. Kv2.1 subunits can form functional channels independently whereas 'silent' Kv6.4 subunits are electrically silent. Mutations of the respective phenylalanine (F290 in related Shaker channels) were introduced in individual subunits of the concatemers.

Methods

The constructs were expressed and measured from *Xenopus laevis* oocytes and the elicited current was characterized with the two-electrode voltage-clamp (TEVC) technique.

Results

Our results show the following: 1. The silent subunit Kv6.4 decreases the steepness in the voltage-activation relationships and shifts inactivation approximately by 50 mV to hyperpolarized potentials as compared to homomeric Kv2.1 channels. 2. Kv2.1/Kv6.4 channels express in a 2:2 stoichiometry with an alternating sequence. 3. Mutations of phenylalanine to different amino acids at the charge transfer center shift voltage-dependent activation to either hyperpolarized or depolarized potentials depending on the property of the amino acids in both monomers and concatenated dimers. 4. Kv2.1/6.4 channels undergo slow type inactivation shifting the inactivation curve towards hyperpolarizing potentials. Mutating the charge transfer center of the Kv6.4 subunit only shifts the inactivation curve for channels formed by monomers as well as concatenated dimers towards depolarizing potentials if compared to Kv2.1/6.4 channels formed by coexpressed wild-type subunits.

Conclusions

This result tells that the mutation in Kv6.4 recovers the channel from closed-state inactivation.

Uta Enke, Claudia Ranke, Sandra Bernhardt and Karin Schoknecht

References
[1] E. Bocksteins, A. J. Labro, D. J. Snyders, D. P. Mohapatra. The electrically silent Kv6.4 subunit confers hyperpolarized gating charge movement in Kv2.1/Kv6.4 hetero-tetrameric channels. PLoS One 7 (2012), e37143.
[2] A. Pisupati et al., The S6 gate in regulatory Kv6 subunits restrict heteromeric K+ channel stoichiometry. J. Gen. Physiol. 150, 1702–1721 (2018).
[3] E. Bocksteins. Kv5, Kv6, Kv8, and Kv9 subunits: No simple silent bystanders. J. Gen. Physiol. 147, 105–125 (2016).
[4] Lena Möller, Glenn Regnier, Alain J Labro, Rikard Blunck, and Dirk J Snyders. Determining the correct stoichiometry Kv2.1/Kv6.4 heterotetramers, functional in multiple stoichiometrical configurations. PNAS. 117, 17, 9365-9376 (2020).
[5] Bocksteins, E., D.J. Snyders, and M. Holmgren. Independent movement of the voltage sensors in KV2.1/KV6.4 heterotetramers. Sci. Rep. 7:41646 (2017).

A 01-05
Mechanism of voltage sensing in Ca^{2+}- and voltage-activated K^+channels

Ignacio Segura[1], Willy Carrasquel-Ursulaez[2], Ignacio Diaz-Franulic[4,3], Jose A. Garate[3], Fernando Gonzalez-Nilo[4,3], Ramon Latorre[3]

[1] *Forschungszentrum Jülich, Institut für Biologische Informationsprozesse Molekular- und Zellphysiologie (IBI-1), Jülich, Germany*
[2] *Washington University in St Louis, Department of Anesthesiology, St Louis, USA*
[3] *Centro Interdisciplinario de Neurociencias de Valparaiso, Facultad de Ciencias, Universidad de Valparaiso, Valparaiso, Chile*
[4] *Centro de Bioinformatica y Biologia Integrativa, Facultad de Ciencias de la Vida, Universidad Andres Bello, Santiago, Chile*

Excitable tissues accomplish their signalling functions thanks partly to the interplay of voltage-sensitive ion channels. Therefore, it is necessary to establish how voltage-sensitive ion channels sense changes in the electric field across the cell membrane. In particular, allosteric communication between the voltage sensors and Ca^{2+} binding in BK channels is crucially involved in damping excitatory stimuli. For example, these channels must be precisely tuned for the neurosecretion process to work properly. Although the specific voltage-sensing mechanism of BK channels is still under debate, the most accepted mechanism proposes the existence of voltage-sensor domains (VSDs), which undergo two or more discrete conformational states in response to changes in the membrane voltage. The simplest model considers two states: active (A), which promotes channel opening, and resting (R), which promotes channel closing, a process called on consensus voltage gating of ion channels. To accomplish its function, VSDs contain charged residues that move across the membrane borders in response to changes in the electric field. Here, based on gating current measurements, we demonstrated that two arginines in the transmembrane segment S4, R210 and R213, function as the BK channel gating particles. Significantly, the energy landscape of the gating particles is electrostatically tuned by a network of salt bridges contained in the voltage sensor. The neutralization of other VSD charges exclusively points to roles in tuning the half-

activation voltage of the VSD and its allosteric coupling with the pore domain. Moreover, molecular dynamics simulations based on the cryo-EM structures of the human BK channel as templates suggested that R210 and R213 lie in a narrow septum separating intra- and extracellular water-filled vestibules whose boundaries are defined by these gating charges. This interpretation is consistent with the hyperpolarization-activated proton currents generated by BK channels when R210 is mutated to the protonable amino acid histidine (R210H). The overall results point to a unique and distinctive mode of BK channel activation. In canonical voltage-activated K^+ (K_V) channels, positive charges move one by one through a charge transfer center (absent in BK channels) that spans the entire electric field. In contrast, charge movement in BK channels is limited to a small displacement of the guanidinium moieties of R210 and R213 in a narrow septum where the electric field drops without a significant movement of the S4 transmembrane segment.

We thank Mrs. Luisa Soto (Universidad de Valparaiso) for excellent technical assistance and Drs. Francisco Bezanilla and John Ewer for their careful reading of the published manuscript. This research was supported by the Fondo Nacional de Desarrollo Cientifico y Tecnologico (FONDECYT) Regular Grant Nos. 1190203 (To R.L.), 1170733 (To F.G.-N.) and 1221260 (to J.A.G.); US Air Force Office of Scientific Research grant under award FA9550-16-1-0384 (To R.L.); and NIH Grant No. GM030376 (To R.L.). The Centro Interdisciplinario de Neurociencias de Valparaiso (CINV) is supported by the Iniciativa Cientifica Milenio-Agencia Nacional de Investigacion y Desarrollo (ICM-ANID), Project P09-022-F (CINV).

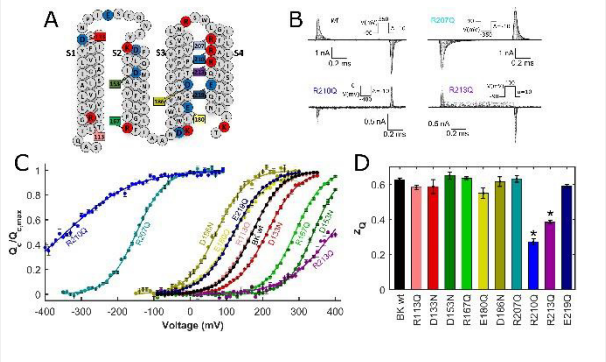

Gating chage displacement for neutralization mutants in the VSD of the human BK channel.
(*A*) Primary amino acid sequence of the VSD (S1 to S4). Positively charged residues are colored blue, and negatively charged residues are colored red. Residues that were neutralized are highlighted. (*B*) Representative records of gating current of BK wt and neutralization mutants R207Q, R210Q, and R213Q. (*C*) Gating charge versus voltage ($Q(V)$) curves at zero internal calcium. (*D*) Half-activation voltage (V_0) and the apparent number of gating charges (z_Q) for the BK wt and mutants were obtained from the fitting of the ($Q(V)$) data with a Boltzmann function.

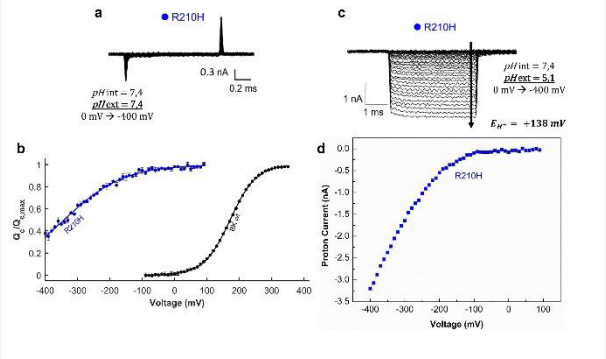

Hyperpolarization-activated proton pore reveals a distinctive VSD activation mechanism
(*A*) Representative gating current recording for R210H channel under symmetrical pH conditions. (*B*) External acidification protonates the histidine at this position, forming an inward rectifying proton channel. Error bars = SD. (*C*) $Q(V)$ relationship for R210H mutant obtained at symmetrical pH = 7.4. (*D*) Steady-state current versus voltage curve obtained from current records such as those shown to the left.

References
[1] Horrigan, F, and Aldrich, R 2002, Coupling between voltage sensor activation, Ca^{2+} binding and channel opening in large conductance (BK) potassium channels, J Gen Physiol, 120, 267-305.
[2] Starace, D, and Bezanilla, F 2004, A proton pore in a potassium channel voltage sensor reveals a focused electric field, Nature, 427, 548-553.
[3] Ma, Z, Lou, X, and Horrigan, F 2006, Role of Charged Residues in the S1–S4 Voltage Sensor of BK Channels, J Gen Physiol, 127, 309-328.
[4] Tao, X, Hite, R, MacKinnon R 2017, Cryo-EM structure of the open high-conductance Ca^{2+}-activated K^+ channel, Nature, 541, 46-51.

A 01-06
Unraveling the role of the Ca^{2+}-activated K^+ channel $K_{Ca}3.1$ in pancreatic ductal adenocarcinoma

Benjamin Soret[1,2], Zoltan Pethö[2], V'yacheslav Lehen'kyi[1], Albrecht Schwab[2]

[1] *University of Lille, Laboratory of Cell Physiology – PHYCELL - INSERM U1003, Villeneuve d'Ascq, France*
[2] *Westfälische Wilhelms-Universität Münster, Institut für Physiologie II, Münster, Germany*

Pancreatic ductal adenocarcinoma (PDAC) is the fourth leading cause of cancer-related deaths in Western countries. The molecular mechanisms that give rise to PDAC are far from being clear and have not yet delivered efficient therapies. PDAC is linked to the physiology and microenvironment of the exocrine pancreas. Ca^{2+} signals are particularly relevant in cancer. The cellular "Ca^{2+} toolkit" includes ion channels that indirectly affect Ca^{2+} signaling such as the Ca^{2+}-activated K^+ channel $K_{Ca}3.1$. In PDAC, this channel is massively overexpressed and indicates a poor prognosis. Despite some *in vitro* information on the role of $K_{Ca}3.1$ channels on individual cell types of the PDAC cancer tissue, its role is still poorly characterized, and *in vivo* data are missing. The current project is aimed at reducing this gap of knowledge.
In vivo experiments were performed using the$Kras^{LSL-G12D/+}Trp53^{fl/fl}Pdx1^{Cre/+}$ (KPfC) PDAC mouse model. Mice were treated with vehicle, gemcitabine, the $K_{Ca}3.1$ inhibitor TRAM-34 or a combination of the two. Retrieved pancreata were sliced, stained, and analyzed to assess tumor size and the extent of fibrosis. This was complemented through the evaluation of $K_{Ca}3.1$ inhibition on migration in a spheroid model of PDAC composed of pancreatic tumor cells (PANC-1) and pancreatic stellate cells (PS-1).
The inhibition of $K_{Ca}3.1$ in combination with gemcitabine leads to a moderate decrease in tumor size and a reduction of gemcitabine-induced fibrosis. This could mean that the combined effect makes the tumor tissue more accessible to treatment. In mixed spheroids, $K_{Ca}3.1$ inhibition in combination with gemcitabine decreases the invasive potential. This is accompanied by a change from an elongated to a round morphology of the migrating cells. Nevertheless, this inhibition does not reach the level of inhibition of gemcitabine alone. More interestingly, the inhibition of plasma membrane $K_{Ca}3.1$ by maurotoxin decreases the invasive potential of the PANC-1/PS1 spheroids more efficiently than the combination of TRAM-34 and gemcitabine suggesting that plasma membrane and intracellular $K_{Ca}3.1$ have distinct effects in PDAC.
Collectively these results point to a function of $K_{Ca}3.1$ channels in complex tumor models that goes beyond the well described roles of the channels in individual cell types from the tumor microenvironment.

A 01-07
The natural polyphenolic compound α-Mangostin modulates diverse potassium channel classes

Marianne Musinszki, **Sönke Cordeiro**, Thomas Baukrowitz

Christian-Albrechts-Universität zu Kiel, Institute of Physiology, Kiel, Germany

Question
Traditional far eastern medicine suggests that Mangostin, a natural extract from the fruit of *Garcinia mangostana*, exhibits a wide range of beneficial pharmacological activities, including antioxidant, anti-inflammatory, anti-cancer, anti-microbial and cardioprotective properties. The predominant compounds of this fruit peel extract are the xanthones α- and γ-Mangostin that have been investigated in various physiological and pathological contexts. Recent research showed that α-Mangostin also modulates ion channels, including members of the Two-Pore Domain Potassium (K_{2P}) channels.
Methods
We used electrophysiological whole-cell recordings of different potassium channels heterologously expressed in HEK293 cells to screen for modulatory effects of α-Mangostin in all K^+ channel subfamilies (K_v, K_{Ca} and K_{ir}, and K_{2P} potassium channels).
Results
First, we could corroborate the strong activation of TREK-1, TREK-2 and TRAAK channels. We further demonstrated that also most other members within the K_{2P} channel family are strongly modulated by application of α-Mangostin, resulting either in strong activation comparable to the reported TREK/TRAAK activation, or, conversely, in pronounced inhibition by the compound. Interestingly, α-Mangostin activated a K_{Ca} potassium channel (BK channel) which play a crucial role in regulating cardiovascular function by regulating smooth muscle tone, vascular tone, and cardiac action potentials.

We hypothesize that the activation of BK channels, leading to smooth muscle relaxation and vasodilation, has significant implications i.e. for blood pressure control and could pose the underlying molecular mechanism of the reported beneficial cardiovascular action of the mangostin extracts. We therefore investigated the mechanism of action of α-Mangostin and explored the possible binding site in TREK-1 and BK channels by site-directed mutagenesis and by *in silico* docking experiments.

Conclusions

Our study scrutinized therapeutic implications of α-Mangostin in cardiovascular health by elucidating its effects on BK channel activity and provides mechanistic insights into how this natural compound may modulate cardiovascular function, warranting further investigation into its clinical relevance.

A 01-08
K_{Ca}channels as amplifiers of TRPV4-mediated pulmonary edema formation

Mei Li[1], Jorge Blázquez-Prieto[2], Guillermo M. Albaiceta[2,3], Wolfgang M. Kuebler[1,4,5], Laura Michalick[1,6]

[1] *Charité - Universitätsmedizin Berlin, Institut für Physiologie - Charité, Berlin, Germany*
[2] *Instituto Universitario de Oncología (IUOPA), Department of Biología Funcional, Universidad de Oviedo, Oviedo, Spain*
[3] *CIBER-Enfermedades respiratorias, CIBER-Enfermedades respiratorias, Madrid, Spain*
[4] *St. Michael's Hospital, Toronto, Keenan Research Centre for Biomedical Science, Ontario, Canada*
[5] *University of Toronto, Departments of Surgery and Physiology, Ontario, Canada*
[6] *partner site Berlin, DZHK (German Centre for Cardiovascular Research), Berlin, Germany*
[7] *partner site Berlin, DZL (German Centre for Lung Research), Berlin, Germany*

Question

[Mechanical ventilation is life-saving in patients with acute respiratory failure, but can also inflict ventilator-induced lung injury (VILI) and exacerbate endothelial barrier failure. The mechanosensitive transient receptor potential vanilloid 4 (TRPV4) channel i) mediates Ca^{2+}-dependent endothelial leak in overventilated lungs and ii) activates Ca^{2+}-activated K^+ (K_{Ca}) channels, which iii) may in turn increase the electrochemical gradient for TRPV4-mediated Ca^{2+} influx. As such, K_{Ca} channels may promote stretch-induced barrier failure and aggravate VILI.]

Methods

[Male mice were ventilated for 2 h with low or high tidal volumes in the presence or absence of K_{Ca} antagonists (apamin, charybdotoxin, TRAM34). Changes in endothelial Ca^{2+} concentration ($[Ca^{2+}]_i$) were quantified by ratiometric imaging of isolated-perfused mouse lungs at different levels of airspace pressure, or in human pulmonary microvascular endothelial cells (HPMECs) in response to TRPV4 activation with or without inhibition of K_{Ca} channels. Analogously, changes in endothelial K^+ concentration ($[K^+]_i$) and membrane potential were imaged *in vitro*.]

Results

[Inhibition of K_{Ca} channels, specifically the intermediate Ca^{2+}-activated K^+ channel ($IK_{Ca}1$) attenuated characteristic features of lung injury *in vivo*. Analogously, inhibition of $IK_{Ca}1$ channels in isolated lungs reduced the sustained $[Ca^{2+}]_i$ response to elevated airspace pressure. In HPMECs, TRPV4-mediated Ca^{2+} influx decreased $[K^+]_i$ and caused membrane hyperpolarization. This response was prevented by inhibition of K_{Ca} channels, whereby inhibition of $IK_{Ca}1$ channels showed the most pronounced effect. Inhibition of K_{Ca} channel downstream of TRPV4 activation reduced endothelial $[Ca^{2+}]_i$ *in vitro*.]

Conclusions

[K_{Ca} channels, specifically $IK_{Ca}1$, act as amplifiers of TRPV4-mediated Ca^{2+} influx in the lung endothelium and can establish a feed-forward cycle that drives endothelial barrier failure and the progression of VILI.]

We thank the Advanced Medical Bioimaging Core Facility (AMBIO) of the Charité-Universitätsmedizin Berlin for support in the acquisition of real-time fluorescence imaging data. We thank Dr. Stefan Heller, Stanford University, for kindly providing the rabbit anti-TRPV4 antiserum used for Western blotting in HPMECs.

A 01-09
The Role of *Clcn2* in the Murine Zona Glomerulosa

Marina Volkert, Ute Scholl, Gabriel Stölting

Berlin Institute of Health at Charité – Universitätsmedizin Berlin, Center of Functional Genomics, Berlin, Germany

Question

The zona glomerulosa (ZG) comprises the outer layer of the adrenal cortex, which synthesizes aldosterone. This steroid hormone regulates the volume and salt balance of the body in response to the serum concentrations of potassium and angiotensin II (Ang II). Stimulation of the ZG leads to oscillatory membrane depolarizations and calcium influx, which is required for aldosterone synthesis. Heterozygous gain-of-function mutations in *CLCN2*, which encodes the chloride ion channel ClC-2, lead to familial hyperaldosteronism through increased calcium signaling of the ZG. The role of ClC-2 in the healthy ZG, however, is still unclear.

Methods

In order to determine the role of ClC-2 in the ZG, we compared *Clcn2*$^{-/-}$(KO) and wild type (WT) mice. Using fluorescent indicators, we studied changes in cytosolic calcium signaling (using Calbryte 520) and in the chloride homeostasis (using 6-methoxy-N-ethylquinolinium iodide (MEQ)) in acute slice preparations of murine adrenal glands. As it was reported that ClC-2 and aldosterone synthesis are both activated by extracellular hypotonicity, we investigated several osmolar conditions.

Results

After an acute change (minutes) to a hypotonic solution, WT and KO showed a similar increase of calcium spiking in the ZG. However, under a sustained exposure (hours) to an extracellular hypotonic condition, calcium spiking in the ZG of KO mice remained stronger compared to WT. The number of calcium oscillations in the ZG of KO mice were higher across several tested concentrations of potassium and Ang II. This indicates that ClC-2 might only be active following prolonged hypotonic stress. This hypothesis is further supported by our finding that chloride concentrations in WT and KO were similar under isotonic conditions, whereas the chloride concentration was higher in KO ZG cells under prolonged hypotonic stress.

Conclusions

Our results suggest that ClC-2 plays a role in the long-term response of the ZG to changes in extracellular osmolality.

A 01-10
Activation of TMEM16A channels by methionine oxidation

Rama A. Hussein[1], Jinshi Wang[2], Yutao Tian[2], Roland Schönherr[1], Stefan H. Heinemann[1], Toshinori Hoshi[3]

[1] *Friedrich Schiller University Jena & Jena University Hospital, Center for Molecular Biomedicine (CMB)- Department of Biophysics, Jena, Germany*
[2] *Tianjin University, Academy of Medical Engineering and Translational Medicine (AMT) & Tianjin Key Laboratory of Brain Science and Neural Engineering, Tianjin, P.R. China, 300072, China*
[3] *University of Pennsylvania, Department of Physiology, Philadelphia PA 19104, USA, USA*

The author has objected to a publication of the abstract.

A 01-11
Current clamp Ussing chamber measurements show different effects of modulators depending on CFTR mutation

Vanessa Mete[1,2], Heymut Omran[2], Jörg Große-Onnebrink[2], Wolf-Michael Weber[1]

[1] Westfälische Wilhelms-Universität Münster, Institute of Animal Physiology, Münster, Germany
[2] Universitätsklinikum Münster, Department of General Paediatrics, Münster, Germany

Cystic fibrosis (CF) is caused by the malfunction of the chloride channel cystic fibrosis transmembrane conductance regulator (CFTR). It is the most common genetic disorder in the Caucasian population. Decreased CFTR function leads to an imbalance in homeostasis of ion and water transport in secretory epithelia. Particularly in the lung, this defect impairs mucociliary clearance leading to the common clinical picture. Modulators, a new type of drug and the first to allow for causal treatment of CF, greatly improved patient's quality of life. However, with its pleiotropic nature and over 300 mutations causing the disease, not all patients get the right combination of modulators if their genotype is even approved for treatment. Here we measured the efficacy of the modulators Ivacaftor, Lumacaftor, Tezacaftor and Elexacaftor developed by Vertex on primary cell culture in a state-of-the-art current clamp Ussing chamber (EP Devices).The Ussing chamber turned out to be sensitive enough to measure the effect of the rescued but still malfunctioning CFTR proteins in the nasal epithelial cell collected from patients. Influence on the conductance was dependent on the functionality of the rescued protein, for the conductance reflects the properties of the membrane. For cells with ΔF508 mutation the effects of all correcting modulators were low in conductance. Especially compared to previously conducted transfection experiments with experimentally developed chitosan-nanocapsules as vectors in which CF cells turned out indistinguishable from healthy controls. However, the voltage measured at current clamp conditions reflected the true ion transport through the epithelium and was much improved after 24 h by the correcting modulators and acutely by the potentiator Ivacaftor. These results bring a future with further personalized medicine closer and will make treatment available for patients whose mutations are not approved of by FDA or EMA.

We greatfully acknowledge finacial support from Deutsche Förderungsgesellschaft zur Mukoviszidoseforschung e. V.

A 01-12
Analysis of the transport mechanism of SLC26A3 and SLC26A6

Annalisa Questino, Dominik Lenz, Dominik Oliver

Philipps-Universität Marburg - Institute of Physiology and Pathophysiology, Department of Neurophysiology, Marburg, Germany

Question

Solute Carrier Family 26 (SLC26) is a conserved anion transporter family with 10 members in humans. The SLC26 genes (except for SLC26A5) encode multifunctional anion exchangers and anion channels that transport a broad range of substrates with important roles in electrolyte transport and homeostasis throughout the body. Among the ten human SLC26 paralogs, SLC26A3 and A6 are important in normal function and disease states of the intestine. They are Cl^-/HCO_3^- exchangers but SLC26A6 can also mediate the transport of divalent anions such as sulfate and oxalate. Transport mode appears to be electrogenic in some studies, with a stoichiometry monovalent: monovalent of 1:2 and divalent: monovalent of 1:1 [3]. In other studies, the transport mode appears to be electroneutral [1][4], so both transport mode and stoichiometry are still controversial. These differences may have technical reasons but may as well indicate differences in transport stoichiometry between species [1][2]. In this study, we aim, at first, to solve this controversy and clarify the stoichiometry and transport differences in between human and mouse orthologous of both SLC26A3 and A6.

Methods

Confocal microscopy was used to assess membrane localization of the GFP-fused expression constructs, which was required to allow for subsequent transport current recording by whole-cell patch-clamp. Transport currents were recorded in the presence of the proposed substrates oxalate or bicarbonate in the extracellular solution, while varying the concentration gradient of counter-transported chloride. Currents were recorded using voltage ramp protocols and reversal potential (Vrev) and the current at 0 mV were used as a measure of transport activity and transport mode.

Results

Our imaging data showed a predominant plasma membrane (PM) localization of both human and mouse SLC26A6 in Chinese hamster ovary (CHO) cells, whereas human SLC26A3 was poorly targeted to the PM in CHO cells. Patch clamp experiments from CHO cells expressing mSLC26A6 yielded robust transport currents both in the presence of either oxalate or $HCO3^-$.

Conclusions

These data show an electrogenic Cl^-/oxalate and Cl^-/ HCO_3^- exchange with 1 Cl^- : 2 HCO_3^- exchange stoichiometry of the monovalent

substrates madiated by mSLC26A6. We will further perform the same analysis on hSLC26A6 and SLC26A3. To this end, we are engineering C-terminal truncation constructs of hSLC26A3 in order to improve membrane targeting, as previously successfully demonstrated for SLC26A9 [5].

References
[1] Chernova, M. N., Jiang, L., Friedman, D. J., Darman, R. B., Lohi, H., Kere, J., Vandorpe, D. H., & Alper, S. L. (2005). Functional comparison of mouse slc26a6 anion exchanger with human SLC26A6 polypeptide variants: differences in anion selectivity, regulation, and electrogenicity. *The Journal of biological chemistry*, *280*(9), 8564–8580. https://doi.org/10.1074/jbc.M411703200
[2] Clark, J. S., Vandorpe, D. H., Chernova, M. N., Heneghan, J. F., Stewart, A. K., & Alper, S. L. (2008). Species differences in Cl- affinity and in electrogenicity of SLC26A6-mediated oxalate/Cl- exchange correlate with the distinct human and mouse susceptibilities to nephrolithiasis. *The Journal of physiology*, *586*(5), 1291–1306. https://doi.org/10.1113/jphysiol.2007.143222
[3] Shcheynikov, N., Wang, Y., Park, M., Ko, S. B., Dorwart, M., Naruse, S., Thomas, P. J., & Muallem, S. (2006). Coupling modes and stoichiometry of Cl-/HCO3- exchange by slc26a3 and slc26a6. *The Journal of general physiology*, *127*(5), 511–524. https://doi.org/10.1085/jgp.200509392
[4] Stewart, A. K., Shmukler, B. E., Vandorpe, D. H., Reimold, F., Heneghan, J. F., Nakakuki, M., Akhavein, A., Ko, S., Ishiguro, H., & Alper, S. L. (2011). SLC26 anion exchangers of guinea pig pancreatic duct: molecular cloning and functional characterization. *American journal of physiology. Cell physiology*, *301*(2), C289–C303. https://doi.org/10.1152/ajpcell.00089.2011
[5] Walter, J. D., Sawicka, M., & Dutzler, R. (2019). Cryo-EM structures and functional characterization of murine Slc26a9 reveal mechanism of uncoupled chloride transport. *eLife*, *8*, e46986. https://doi.org/10.7554/eLife.46986

A 01-13
The p53-p21 DREAM signaling pathway regulates the TMEM206 ion channel

Korollus Melek[1,2], Barbara Hauert[1], Christine Peinelt[1], Sven Kappel[1]

[1] *University of Bern, Institute for Biochemistry and Molecular Medicine, Bern, Switzerland*
[2] *University of Bern, Graduate School for Cellular and Biomedical Sciences, Bern, Switzerland*

The author has objected to a publication of the abstract.

A 01-14
Regulation of selectivity filter gating in the model system of minimal viral potassium channels

Nils Drexler[1], Ulf P. Hansen[2], Indra Schroeder[1]

[1] *University Hospital Jena, Friedrich Schiller University Jena, Physiology II, Jena, Germany*
[2] *Christian-Albrechts-Universität zu Kiel, Department of Structural Biology, Kiel, Germany*

The selectivity filter (SF) gate in potassium channels (K^+-channels) is regulated by K^+ occupancy as well as a complex interaction network between the SF and the surrounding protein helices. Recent work on the minimal viral K^+ channel Kcv_{NTS} has revealed that while the SF is highly conserved in the family of K^+ channels, the interactions between the SF and the surrounding protein structures seems to vary.
To gain an overview of the structures involved in SF gating, we performed an alanine scan of the pore helix, the outer pore mouth, and a section of the transmembrane helix 2 (TM2). The single-channel recordings in planar lipid bilayers demonstrated that the importance of some residues and even their chemical nature is conserved among different K^+ channels, while this is not the case for others. We discovered an intriguing interaction between position T45, which is adjacent to the most cytosolic K^+ binding site (S4 site) in the SF, and residues on TM2. Further mutational studies indicate that this interaction seems to be of a predominantly (allo)steric nature. This observation reminds of the allosteric interactions between a different part of TM2 and the SF reported for the bacterial K^+ channel KcsA. Furthermore, these residues appear to be changing the gating behavior in a complex manner, involving both ion occupancy and other mechanisms.
In conclusion, Kcv channels can provide an ideal and easily manipulable model system for studying the peculiar mixture of conserved and non-conserved mechanisms and interactions that regulate SF gating in K^+ channels.

A 01-15
Exploring the pore structure of THIK1 channels (KCNK13) with blockers and chemical cysteine modification

Bisher Eymsh, Marcus Schewe, Sönke Cordeiro, Thomas Baukrowitz

Kiel University, Institute of Physiology, Kiel, Germany

The two-pore domain potassium channels (K2P) are the most recently discovered subgroup of potassium channels consisting of 15 mammalian members are composed of two subunits each containing four transmembrane domains with two pore forming domains. K2P channels are gated by a multitude of stimuli including physical (temperature, tension), chemical (lipids, H+, small molecule drugs) and intracellular signaling pathways. THIK-1 is a member of this K2P family and widely expressed in CNS but its physiological functions are mostly unknown with the exception of microglia cells where THIK-1 activation was shown to be involved in microglial immune surveillance und inflammatory cytokine release. The mechanisms that regulate THIK-1 channel activity are also poorly understood.
In this study, we explore the inhibition of THIK-1 channels by classical K+ channel pore blocking molecules such as tetrapentylammoniumchlorid (TPA). We report that the kinetics of TPA pore blockade are exceptional slow and identified pore residues that control the blocking kinetics possibly via a hydrophobic barrier. Further, we provide evidence for a gated permeation constriction below the central pore cavity by studying the time course for chemical modification of introduced pore cysteines for high and low activity states of the THIK-1 channel that were induced by various ligands (i.e. lipids and pharmacological compounds).
These results are discussed in the context of a THIK-1 homology model and provide first mechanistic insights into the structural mechanism of activity regulation of these channels.

A 02 | Non-Selective Cation Channels

A 02-01
HCN channels in the context of a potential *Retinitis Pigmentosa* therapy

Laura Karwehl, Anna Hahnefeld, Jana Kusch

Universitätsklinikum Jena, Institut für Physiologie II, Jena, Germany

Question
Retinitis Pigmentosa (RP), a genetically heterogeneous group of inherited retinal dystrophies, is one of the leading causes of visual disability. It manifests temporally and symptomatically in a variable manner and may lead to the complete loss of vision. An increased intracellular concentration of guanosine 3',5'-cyclic monophosphate (cGMP) in rods and the resulting increased activation of cGMP target proteins such as protein kinase G (PKG) and CNG channels, has been described as the cause for the primary death of rod photoreceptors in the retina. Thus, a plausible therapeutic approach is the application of cGMP derivatives that antagonizes the effect of the cGMP on those target proteins.
Besides PKG and CNG channels, another cGMP-dependent protein is expressed in photoreceptors, the hyperpolarization-activated and cyclic nucleotide-modulated (HCN) channel. These channels have a protective effect on dysfunctional photoreceptors, thus PKG and CNG channel antagonists should have either no or an agonistic effect on HCN channels (Schön et al. 2016). For the cGMP-derivative Rp-8-Br-PET-cGMPS it has been shown recently, that it acts as competitive inhibitor in PKG as well as on CNG channels (Vighi et al. 2018). Therefore, we studied this compound and four other related derivatives, modified at the ribose cyclic phosphate moiety and/or the guanine moiety, with respect to their ability to interact with HCN channels.
Methods
We heterologously expressed mHCN2 in *Xenopus laevis* oocytes and performed electrophysiological patch-clamp experiments in macropatches. The current responses in the presence of 50 µM of the respective derivatives were used to determine the efficacy values (1) as the ability to increase the current amplitude and (2) as the ability to shift the steady-state activation curve to more depolarized voltages.
Results
We could show that all five derivatives acted either as full or partial agonists on HCN2 channels and that the type of agonistic behavior can be attributed to the type of chemical modification of the ligand molecule.

Conclusions

Thus, this data shown herein contribute to a better understanding of the structure-function relationship of cyclic nucleotides as HCN channel ligands representing a significant step towards a pharmacological therapy for *Retinitis pigmentosa*.

References

[1] Schön C, Asteriti S, Koch S, Sothilingam V, Garcia Garrido M, Tanimoto N, Herms J, Seeliger MW, Cangiano L, Biel M, Michalakis S., 2016, 'Loss of HCN1 enhances disease progression in mouse models of CNG channel-linked retinitis pigmentosa and achromatopsia', *Hum Mol Genet*, 25 (6), 1165-1175

[2] Vighi E, Trifunovic D, Veiga-Crespo P, Rentsch A, Hoffmann D, Sahaboglu A, Strasser T, Kulkarni M, Bertolotti E, van den Heuvel A, Peters T, Reijerkerk A, Euler T, Ueffing M, Schwede F, Genieser HG, Gaillard P, Marigo V, Ekstrom P, Paquet-Durand F., 2018, 'Combination of cGMP analogue and drug delivery system provides functional protection in hereditary retinal degeneration', *Proc Natl Acad Sci U S A*, 115 (13), E2997-e3006

A 02-02
Voltage and time dependent gating of endo-lysosomal hTPC2 channels

Leon-Patrick Sprenger[1], Birgit Begemann[1], Martin Fischer[1], Christian Wahl-Schott[2]

[1] *Hannover Medical School (MHH), Institute for Neurophysiology, Hannover, Germany*
[2] *Ludwigs-Maximilians-Universität (LMU), Institute for Cardiovascular Physiology and Pathophysiology (Biomedical Center), Munich, Germany*

Question

The endo-lysosomal system mediates degradation of extra- and intracellular substrates. It is essential for intracellular cargo and membrane trafficking and regulates the cell's ionic homeostasis. Dysfunction causes lysosomal storage disease, metabolic or infectious disorders. Fusion or fission of endosomes and lysosomes appears to be regulated by cation-selective Two-Pore channels (hTPC1 and hTPC2) that are activated by ligands like phosphatidylinositol 3,5-bisphosphate ($PI(3,5)P_2$) and nicotinic acid adenine dinucleotide phosphate (NAADP). Unlike hTPC1, hTPC2 is thought to gate voltage-independently, according to a linear current/voltage relationship as obtained by short patch clamp ramp protocols. Applying extended step protocols, however, we here find a strong voltage dependence of hTPC2 and ask for the origin of this time-dependent gating.

Methods

Wild-type or mutant isoforms of hTPC2 channels were heterologously expressed in human embryonal kidney (HEK293) cells and hTPC2 currents were recorded in the lysosomal patch clamp configuration.

Results

Using long-lasting voltage step protocols, wild-type hTPC2 channels display extensive voltage-dependent gating after activation by $PI(3,5)P_2$ (Fig.). Current amplitudes increase with depolarization and decrease with hyperpolarization, reaching very low minimal relative open probabilities (< 10%) at -160 mV after 5 seconds (mean time constant = 2.6 ± 1.7 sec). Half-maximal activation is found at +20 mV. Cryo-EM data shows that hTPC2 channels harbor two constriction sites[1], i.e. the selectivity filter at the luminal side and a hydrophobic gate at the cytosolic side of the pore. We here widened the selectivity filter by a single point mutation N653A or a double mutation N653A/N654A. Besides vanishing of the predominant permeability of sodium over potassium, these mutations additionally attenuated voltage dependence of hTPC2 gating (Fig.). Minimal relative open probabilities at negative potentials increased to 37% for N653A hTPC2 and to 52% for N653A/N654A hTPC2. Mutations of the hydrophobic gate (residues T308 & Y312 and L690 & L694) less affectively altered gating of hTPC2.

Conclusions

We conclude that hTPC2 channels are strongly regulated by the potential difference over the lysosomal membrane with time constants in the range of seconds. The origin of this slow gating process seems to be located mainly in the selectivity filter. Comprehending the gating mechanisms will aid the understanding of the physiological role of hTPC2 channels and provide the basis for treatment of associated diseases.

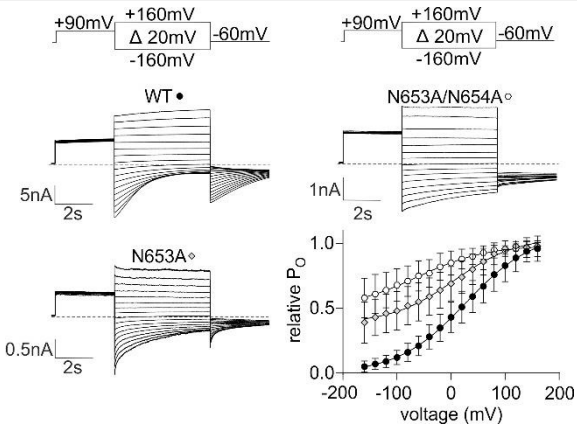

The selectivity filter contributes to voltage dependent gating of hTPC2 channels
Representative current recordings as response to long lasting voltage steps from enlarged lysosomes of transiently transfected HEK cells after activation of WT or mutant hTPC2 channels by $PI(3,5)P_2$ [1µM]. Relative open probabilities as obtained from tail current amplitudes reveal reduced voltage dependence for hTPC2 channels that harbor mutations N653A or N653A/N654A in their selectivity filter (n_{WT}= 14; n_{N653A} = 10; $n_{N653A/N654A}$ = 9).

References
[1] She et al, 2019, 'Structural mechanisms of phospholipid activation of the human TPC2 channel', eLife, Structural Biology and Molecular Biophysics

A 02-03
Identification of residues in TRPM3 channels important for the agonist action of pregnenolone sulfate

Nuwar Harb, Margarete Fitzner, Deniz Harms, Christian Goecke, Doris Newel, Raissa Enzeroth, Johannes Oberwinkler

Philipps-Universität Marburg, Institut für Physiologie und Pathophysiologie, Marburg, Germany

TRPM3 channels are expressed in primary afferent nociceptive neurons and have been implicated in the detection of noxious heat stimuli. However TRPM3 channels are also expressed in other tissues, such as the pancreatic β cells, in which a role in thermo-sensory processes is less likely. In these cells, it is unknown how TRPM3 channels are activated physiologically, but one candidate agonist is the endogenously produced steroid pregnenolone sulfate (PregS, ref. 1). While PregS is the best characterized chemical agonist of TRPM3 channels, it is nevertheless unknown how PregS activates TRPM3. In a recently published 3D-structure of TRPM3 channels, PregS, although present during protein preparation, was not resolved in the resulting CryoEM structures [2]. TRPM3 channels can also be activated by the non-steroidal and chemically unrelated substance nifedipine (Nif). Nif has been previously shown not to compete with PregS for their respective agonist action on TRPM3 channels [3].

We used molecular docking on the CryoEM structure of TRPM3 [2] to identify potential binding sites of PregS and observed an intersubunit cleft capable of accommodating PregS. In the CryoEM structure of TRPM3, this cleft is occupied by a lipid used for solubilization of the channel protein complexes [2]. Docking PregS to this cleft allowed the identification of several potential amino acid residues interacting with PregS from both subunits forming the cleft. We mutated the 10 amino acids having the strongest interaction with PregS in the docked pose and analyzed the resulting mutant ion channels after overexpression in HEK293T cells by whole-cell patch-clamp recordings. We measured dose-response curves for the agonists PregS and Nif, but also tested other steroidal substances with weaker agonist properties, such as pregnenolone, pregnenolone hemisuccinate and DHEAS [3].

All tested mutant proteins produced functional ion channels that could be activated by PregS and Nif, although the current densities observed were generally smaller in the mutated ion channels compared to wild-type TRPM3. Upon quantitative analysis, our results show that some (but not all) residues tested severely affect the pharmacological properties of the channel when mutated. We identified several mutations that strongly reduced the agonistic effect of PregS while apparently not (or less) affecting the activating effect of Nif. Most of the mutants tested showed abnormalities compared to wild-type channels when tested with steroidal analogues of PregS. The mutations with the strongest effects on steroid activation were located on transmembrane helices 1 and 4.

These data indicate that PregS might bind to TRPM3 channels in a cleft which is formed by transmembrane helices 1 and 4 from different subunits and is accessible from the membrane lipids surrounding the channels. This unique location on TRPM3 channels might therefore play an important role during the binding and activation of TRPM3 channels by PregS.

References
[1] Wagner TF et al. (2008) Transient receptor potential M3 channels are ionotropic steroid receptors in pancreatic beta cells, *Nat Cell Biol* 10:1421-1430
[2] Zhao C, MacKinnon R (2023) Structural and functional analyses of a GPCR-inhibited ion channel TRPM3, *Neuron* 111:81-91
[3] Drews A et al. (2014) Structural requirements of steroidal agonists of transient receptor potential melastatin 3 (TRPM3) cation channels, *Br J Pharmacol* 171:1019-1032

A 02-04
On the subunit arrangement in heterotetrameric olfactory CNG channels

Taulant Kukaj, Jana Schirmeyer, Ralf Schmauder, Tina Schwabe, Günther Ehrlich, Christian Sattler, Thomas Zimmer, Klaus Benndorf

Friedrich-Schiller-Universität Jena, Institute of Physiology II, Faculty of Medicine, Jena, Germany

Olfactory cyclic nucleotide-gated (CNG) ion channels are composed of two A2 subunits, one A4 subunit, and one B1b subunit, arranged in a tetrameric structure. Each subunit possesses a cyclic nucleotide-binding domain (CNBD) in the C-terminus. These CNBD domains facilitate the binding of cyclic nucleotides cAMP or cGMP, resulting in the activation of the channels. However, the precise arrangement of the subunits within these channels and the mechanisms of activation and cooperativity are not yet fully understood.

To gain a deeper understanding of the activation and cooperativity of CNG channel subunits, we conducted experiments to manipulate the subunit arrangement. This involved generating specific subunit sequences through concatenation and disabling their CNBD. By examining channel activation at different concentrations of cGMP, we aimed to investigate the impact of the subunit arrangement on the mechanisms of activation and cooperativity.

In our study, we utilized the subunit sequences A4-A2-B1b-A2, A4-B1b-A2-A2, and B1b-A4-A2-A2, and measured the resulting currents to analyze the activation and cooperativity mechanisms of the channels. Surprisingly, when stimulated with cGMP, the currents and concentration-activation relationships produced by two complete sets of concatamers (A4-A2-B1b-A2, A4-B1b-A2-A2) and a portion of a third set (B1b-A4-A2-A2) were similar. This finding can be interpreted in two ways: (1) The subunits consistently assemble in a fixed sequence within the concatamers, regardless of the order of concatenation, or (2) the functionality of the channels is independent of the specific arrangement of the subunits.

To further investigate this question, we incorporated FRET (Fluorescence Resonance Energy Transfer) techniques to determine the distances between subunits. By differentiating between neighboring and opposing positions of A2 subunits within the CNG heterotetramer, we can assess variations in distances between these different positions. These experiments are currently underway. To accomplish this, we developed FRET sensors using click chemistry to integrate unnatural amino acids into the extracellular side of the A2 subunits. This labeling technique allows for efficient labeling while minimizing any potential impact on the binding site. So far we have successfully incorporated unnatural amino acids into the extracellular side of the A2 subunits. Currently we identify optimal dyes to serve as FRET partners.

Through these ongoing experiments, we aim to shed light on the subunit arrangement and the mechanisms underlying activation and cooperativity in CNG channels.

A 02-05
Hearing loss mutations in human P2X2 receptor channels

Paula-Luise Wand, Xenia Brünings, Thomas Zimmer, Klaus Benndorf, Christian Sattler

University Hospital Jena, Physiology 2, Jena, Germany

ATP is not only an energy source, it is also a signaling molecule and a player in the purinergic system. P2X receptors (P2XRs) are cation channels that belong to this system. They are permeable for cations like sodium, potassium and calcium. They are expressed in various tissues and are found in neuronal and immune cells. P2X2 receptors play important roles in cochlea adaptation to elevated sound levels. Three mutations have been identified that cause inherited progressive hearing loss. Structures of related P2X receptors suggest that these mutations localize to transmembrane domain 1 (V60L), transmembrane domain 2 (G353R) and a b-sheet linking the ATP binding site to the pore (D273Y). Previous results from other groups concluded contradictorily that these channels are either not functional or constitutively active without binding of ATP.

We developed inducible HEK293 cells stably expressing the three human P2X2 mutations and measured the localization on the plasma membrane by a red fluorescent protein (RFP) attached to the C-terminus and the binding of a fluorescently labeled ATP derivative (fATP). The constructs were functionally characterized with the patch-clamp technique in the whole-cell configuration using a ligand-application as well as a voltage-step protocol.

Conclusions from our results are: (1) The mutations in the transmembrane domains V60L and G353 show robust localization on the plasma membrane and binding of fATP. (2) Compared to wildtype, the affinity for fATP was increased in V60L channels whereas it was unchanged in G353 channels. (3) The expression of V60L channels has a destructive effect on the cell viability leading to cell death after the second day of expression. This effect may support the role in the pathogenesis of hearing loss.

A 02-06
Salivary gland dysfunction is a major factor driving the phenotype of claudin-10b deficient mice

Selma Dib[1], Tilman Breiderhoff[2], Ahmad Mouna[1], Jenny Fürstenau[3], Olivia Kershaw[3], Susanne Krug[1], Anja Fromm[1], **Luca Meoli**[1], Dorothee Günzel[1]

[1] *Charité--University Medicine Berlin, Clinical Physiology/ Nutritional Medicine, Berlin, Germany*
[2] *Charité--University Medicine Berlin, Department of Pediatrics, Division of Gastroenterology, Nephrology and Metabolic Medicine, Berlin, Germany*
[3] *Free University of Berlin, Institute of Veterinary Pathology, Berlin, Germany*

Claudin-10b is a tight junction protein that confers cation selectivity to the paracellular pathway and is ubiquitously expressed. To investigate its *in vivo* role, we generated different mouse models and used different methods, including immunohistochemistry, real-time PCR, western blotting, and metabolic cage experiments.

Constitutive knockout of claudin-10b (C10bKO) mice resulted in perinatal lethality. While histopathological examination did not reveal any significant differences between control and knockout mice in several organs, alterations in the PAS-based histology of the salivary glands of newborn C10bKO mice were observed. Consistently, C10bKO mice had reduced stomach milk content and decreased blood glucose levels, suggesting that xerostomia (i.e., dry mouth) and severe eating difficulties may have contributed to the lethal phenotype. This was supported by the finding that targeted *Cldn10* deletion in the salivary gland, but not in the kidney (1), intestine and pancreas, resulted in perinatal death. Moreover, postnatal deletion of *Cldn10* in the lungs did not lead to lethality, further corroborating the hypothesis that the lethal phenotype in C10bKO mice was primarily driven by xerostomia.

C10biKD mice, with inducible knockdown (iKD) of claudin-10b in adult mice, exhibited reduced food intake and body weight loss, as well as impaired saliva secretion in response to pilocarpine stimulation. The introduction of moist food pellets partially rescued the phenotype. Additionally, the tissue-specific deletion of Cldn10b in the intestine and pancreas did not result in body weight loss, ruling out malabsorption effects and suggesting that the reduced food intake and weight loss in C10biKD mice were secondary to xerostomia. These results pointed to a role of dysfunctional salivary glands driving the phenotype of C10biKD mice.

Our models and results may have translational implications for HELIX syndrome, which is caused by mutations in CLDN10b and is characterized by xerostomia and other epithelial abnormalities (2–3). By providing an *in vivo* tool for HELIX syndrome research, our findings could potentially improve our understanding of this disease and ultimately lead to new treatments for patients.

Funded by the DFG GU 447/14-2 (project ID 318374368) and DFG GRK 2318 (project ID 318905415).

References
[1] **Breiderhoff T, Himmerkus N, Stuiver M, Mutig K, Will C, Meij IC, Bachmann S, Bleich M, Willnow TE, Müller D.** Deletion of claudin-10 (Cldn10) in the thick ascending limb impairs paracellular sodium permeability and leads to hypermagnesemia and nephrocalcinosis. *Proc Natl Acad Sci U S A* 2012;109(35):14241–14246.
[2] **Klar J, Piontek J, Milatz S, Tariq M, Jameel M, Breiderhoff T, Schuster J, Fatima A, Asif M, Sher M, Mäbert K, Fromm A, Baig SM, Günzel D, Dahl N.** Altered paracellular cation permeability due to a rare CLDN10B variant causes anhidrosis and kidney damage. *PLoS Genet* 2017;13(7). doi:10.1371/journal.pgen.1006897.
[3] **Hadj-Rabia S, Brideau G, Al-Sarraj Y, Maroun RC, Figueres ML, Leclerc-Mercier S, Olinger E, Baron S, Chaussain C, Nochy D, Taha RZ, Knebelmann B, Joshi V, Curmi PA, Kambouris M, Vargas-Poussou R, Bodemer C, Devuyst O, Houillier P, El-Shanti H.** Multiplex epithelium dysfunction due to CLDN10 mutation: The HELIX syndrome. *Genetics in Medicine* 2018;20(2):190–201.

A 02-07
Selectivity filter mutation N648A alters voltage-dependence of endo-lysosomal mTPC1 channels

Oemer Kocdölü[1], Birgit Begemann[1], Petra Killian[1], Christian Wahl-Schott[2], Martin Fischer[1]

[1] *Hannover Medical School, Neurophysiology, Hannover, Germany*
[2] *Ludwig-Maximilian-University Munich, Cardiovascular Physiology and Pathophysiology, Munich, Germany*

Question: The cation-selective two-pore channels (TPC1 and TPC2) of the endo-lysosomal system belong to the superfamily of voltage-gated ion channels. Dysfunction of TPCs impairs subcellular trafficking of vesicles resulting in accumulation of different "cargo". Previous studies report that pharmacological inhibition or deletion of TPC2 result in increased susceptibility of non-alcoholic fatty liver disease due to hepatic cholesterol accumulation, altered exosome formation, and altered entry of pathogens. TPC1 is less investigated on the systemic level. On the cellular level, however, voltage and pH dependence of TPC1 indicate that this channel regulates vesicular membrane excitability, pH homeostasis and membrane trafficking. TPC1 is activated upon depolarization and deactivated upon hyperpolarization of the endo-lysosomal membrane only in presence of ligands ($PI(3,5)P_2$). Opening of a hydrophobic gate at the cytosolic side of the pore thus relies on movement of a voltage-sensing domain and combined conformational changes by ligand binding. A further constriction side at the luminal end of the pore is the selectivity filter [1]. We here report on a point mutation N648A in this filter with unexpected impact on voltage-dependent gating of mouse TPC1.

Methods: WT or mutant mTPC1 channels were transiently expressed in HEK293T cells. After enlargement by treatment with vacuolin-1, endo-lysosomes were isolated and investigated using whole-lysosome patch-clamp technique under physiological ion concentrations (luminal: 145 mM Na^+, pH 4.6; cytosolic: 145 mM K^+, pH 7.2).

Results: Starting from a holding potential of +70 mV, WT mTPC1 channels display voltage-dependent current increase at more positive voltages and strong decrease at negative potentials (Fig.). Substitution of asparagine by alanine at position 648, which widens the narrowest constriction site of the selectivity filter, vanished the predominant permeability of sodium over potassium. Furthermore, current amplitudes are reduced and inward currents at negative potentials are abolished. While western blot analysis suggests unaltered expression of the mutant channel, tail current analysis revealed a dramatic rightward shift of the activation curve from 75 mV to around 143 mV contributing to the poor conductance upon hyperpolarization.

Conclusions: Our findings indicate a complex gating mechanism for mTPC1 channels, involving not only the opening of a hydrophobic gate by combined $PI(3,5)P_2$ binding and depolarization of the vesicular membrane. Additional interactions with the selectivity filter of the pore might participate in the voltage-dependence of gating. Detailed knowledge of gating mechanisms will help to understand the physiological role of TPC1 in the endo-lysosomal system.

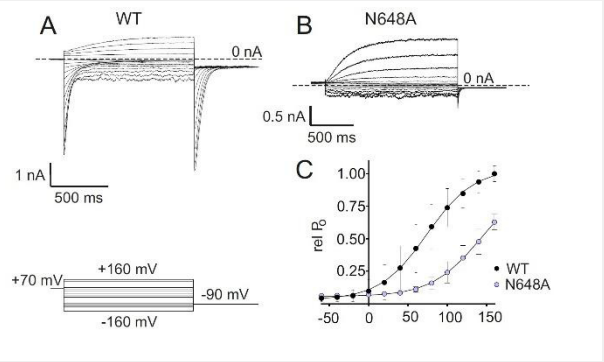

Fig.: Voltage dependence of WT and N648A mTPC1 channels.
(**A-B**) Representative current recordings of WT (**A**) or mutant N648A (**B**) mTPC1 channels elicited by voltage steps as indicated using the whole-endolysosome patch clamp technique. (**C**) Voltage dependence of relative open probabilites displays a strong rigthward shift of activation for N648A mTPC1 (WT: n= 16; N648: n = 3).

References
[1] She et al. 2018, Structural insights into the voltage and phospholipid activation of the mammalian TPC1 channel., *Nature*, 556 (7699), p. 130-134, Dallas Texas USA.

A 02-08
Ionic selectivity of the permeation pathways in TRPM3 channels

Homa G. Samani, Mara Hansen, Sandeep Dembla, Júlia Castro Marsal, Raissa Enzeroth, Doris Newel, Johannes Oberwinkler

Philipps-Universität Marburg, Institut für Physiologie und Pathophysiologie, Marburg, Germany

TRPM3 channels are involved in diverse cellular processes, such as insulin secretion and perception of painful heat. TRPM3 channels itself can be activated by heat or by chemical agonists such as the endogenous steroid pregnenolone sulfate. In addition to the traditional central ion conduction pathway, recent studies have proposed the presence of a non-canonical permeation pathway, also known as Ω-pore, that can be opened by co-application of clotrimazole and pregnenolone sulfate [1] or by pathogenic gain-of-function mutations [2]. The Ω-pore has been reported to be activated at hyperpolarizing membrane potentials and to support large sodium currents [1].
Here, we aimed to investigate the selectivity property of Ω-pores in TRPM3 channels in more detail. We recorded currents during voltage ramps in whole-cell patch-clamp recordings of HEK293T cells overexpressing wild-type TRPM3 channels and point mutations located in the central pore using combinations of pregnenolone sulfate and clotrimazole as agonists. We used a variety of extracellular solutions with a simplified composition (e.g. for bi-ionic conditions) and analyzed the reversal potentials of the resulting currents. In addition, we also investigated the ionic-selectivity of a gain-of-function mutation (V992M, ref. 2).
Our results confirm the previous studies inasmuch as co-application of clotrimazole strongly potentiated inward currents through TRPM3 channels. Surprisingly however, our data indicate that the clotrimazole-enhanced inward current can also be carried by divalent cations. Furthermore, our data demonstrate that the reversal potentials of TRPM3 currents were not significantly altered by the addition of clotrimazole, indicating that the ion selectivity of TRPM3 channels were not altered by this substance. This result was confirmed under a large variety of ionic conditions. Importantly, replacing a glutamate (E1057) in the central pore by cysteine or glutamine strongly reduces the divalent permeability of this central pore, but also of the clotrimazole-enhanced currents. Finally, we show that the inward current through the pathogenic mutant V992M is at least partially carried by divalent cations and has a similar ionic selectivity profile as wild-type TRPM3 channels.

Together, our results do not support the notion that TRPM3 channels exhibit two distinct ion-conducting pathways with different ionic selectivities. Rather, our data are consistent with the traditional assumption of the exclusive presence of a central pore in TRPM3 channels, with a greater permeability to divalent cations than monovalent cations. This conclusion has important implications for the pathophysiology of TRPM3-related disorders, such as juvenile epilepsy and mental retardation associated with gain-of-function mutations in TRPM3 channels.

References
[1] Vriens J et al. (2014) Opening of an alternative ion permeation pathway in a nociceptor TRP channel. *Nat Chem Biol* 10:188-195
[2] Van Hoeymissen E et al. (2020) Gain of channel function and modified gating properties in TRPM3 mutants causing intellectual disability and epilepsy, *eLife* 9:e57190

A 02-09
Negative charges in the S2-S3 linker are involved in voltage-dependent gating of hyperpolarization-activated, cyclic nucleotide-modulated channels

Inga Saß, Christian Sattler, Klaus Benndorf, Jana Kusch

University Hospital Jena / Friedrich Schiller University Jena, Institute of Physiology II, Jena, Germany

Hyperpolarization-activated cyclic nucleotide-modulated (HCN) channels are key regulators of rhythmic electrical activity in the nervous system and heart. Channel opening requires membrane hyperpolarization and is further enhanced by the binding of intracellular cyclic nucleotides.
Each subunit of the tetrameric channel comprises defined structural domains. The C-linker directly connects the cyclic nucleotide-binding domain (CNBD) with the transmembrane regions, while the HCN domain (HCND) is thought to be crucial for integrating voltage- and ligand-dependent gating mechanisms. The interaction between HCND and C-linker of the opposite subunit has been shown to be important for voltage-dependent gating of the channel (Kondapuram et al., 2022).
A flexible region connecting helices S2 and S3 is positioned in a hollow between HCND, C-linker and the main voltage-sensing helix S4 (Lee and MacKinnon, 2017; Saponaro et al., 2021). This S2-S3 linker includes a series of negative charges, highly conserved across isoforms and species. This suggests a role of these negative charges in voltage-dependent activation.
To study the effects of both charge neutralization and reversion at positions E243, D244 and E247 of the S2-S3 linker, mutant mHCN2 channels were heterologously expressed in *X. laevis* oocytes and characterized by electrophysiological methods. At cAMP-free conditions, the constructs showed a systematic shift of the voltage-dependence towards hyperpolarizing potentials. This shift was most substantial in a mutant including two charge reversals. Furthermore, while the voltage-dependence at cAMP-saturation was comparable to that of the wildtype channel, all charge reversal mutants showed a reduction of the apparent gating charge.
To summarize, the loss of negative charges inside the S2-S3 linker seems to further stabilize the autoinhibited state of the unliganded mutant channels, shifting channel opening to very low hyperpolarized potentials. Binding of cAMP is able to re-establish wild type-like voltage-dependence. However, the loss of negative charges seems to impair the voltage-sensitivity of cAMP-bound mutant channels.
While not fully understood, our data contribute to a better understanding of the complex voltage- and ligand-dependent gating behaviour of HCN pacemaker channels.

References
[1] Kondapuram, M., et al. (2022). Functional and structural characterization of interactions between opposite subunits in HCN pacemaker channels. *Communications Biology*, 5(1), 430.
[2] Lee, C. H., & MacKinnon, R. (2017). Structures of the Human HCN1 Hyperpolarization-Activated Channel. *Cell*, 168(1-2), 111–120.e11.
[3] Saponaro, A., et al. (2021). Gating movements and ion permeation in HCN4 pacemaker channels. *Molecular Cell,* 81(14), 2929–2943.e6.

A 02-10
The bile acid-sensitive ion channel (BASIC) affects the morphology of pancreatic islets and glucagon secretion

Jingyu Yang, Stefan Gründer, Dominik Wiemuth

RWTH Aachen University, Institute of Physiology, Aachen, Germany

The bile acid-sensitive ion channel (BASIC), an ion channel related to acid-sensing ion channels (ASIC), is found in a variety of tissues including liver, brain, intestine, lungs, and testis. It is currently unclear whether BASIC is also expressed in the pancreas. To investigate this, we conducted histological, transcriptomic, and biochemical analyses of BASIC expression in pancreatic tissue from both BASIC$^{+/+}$ and BASIC$^{-/-}$ mice. Our findings demonstrate that BASIC is expressed at low levels in pancreatic islets and specifically localizes to pancreatic α-cells. Histological, protein and nucleic acid analyses revealed that the absence of BASIC resulted in a decrease in α-cell number and changes in pancreatic islet morphology. We are currently assessing the secretion of glucagon from islets isolated from a-cells of BASIC$^{+/+}$ and BASIC$^{-/-}$ mice. This study provides the first evidence that BASIC is expressed in pancreatic α-cells and suggests that it may play a role in regulating α-cell proliferation and glucagon secretion.

A 02-11

Selectively targeting rod CNG channels for limiting photoreceptor degeneration in *retinitis pigmentosa*

Sandeep Kesh[1], Palina Pliushcheuskaya[2,3], Sophie Wucherpfennig[1], Frank Schwede[4], François Paquet-Durand[5], Georg Kuenze[3,2], Vasilica Nache[1]

[1] *Universitatsklinikum Jena, Physiologie 2, Jena, Germany*
[2] *Leipzig University Medical School, Interdisciplinary Center for Bioinformatics, Leipzig, Germany*
[3] *Leipzig University Medical School, Institute for Drug Discovery, Leipzig, Germany*
[4] *BIOLOG Life Science Institute GmbH & Co KG, Bremen, Germany*
[5] *University of Tübingen, Institute for Ophthalmic Research, Tübingen, Germany*

Retinitis pigmentosa (RP) is a progressive eye disease and the primary cause of inherited blindness. The condition is the result of mutations in over 80 genes that play a critical role in the visual pathway. RP is characterized by the degeneration of rod photoreceptors, followed by cone photoreceptors, which eventually leads to complete blindness. The retina contains two types of CNG (cyclic nucleotide-gated) channels, namely rod and cone CNG channels, which share ~80% sequence similarity. Despite this, the two types of channels exhibit significant differences in structure and function. They also have different affinity towards cyclic guanosine monophosphate (cGMP), which is responsible for activation of rod and cone CNG channels[1]. Previous research has revealed that elevated levels of cGMP in the retina of individuals with RP lead to over-activation of the CNG channels, resulting in the degeneration of photoreceptor cells. Achieving a rod-selective modulation of these pathways has remained a challenge[2]. We seek to identify compounds that selectively inhibit rod CNG channels, rather than inhibiting both rod and cone CNG channels. We additionally strive to investigate the interactions between ligands and the cyclic nucleotide-binding domain, aiming to enhance our comprehension of the gating mechanism in CNG channels.
For this, we expressed the rod and cone CNG channels in *Xenopus laevis* oocytes and we measured their efficacy and potency in the presence of different cGMP analogues using the patch-clamp technique. The tested cGMP analogues were differentiated based on modifications to the guanosine moiety and exocyclic oxygen. Additionally, binding of cGMP analogues was evaluated using ligand docking, MD simulations and MM/GBSA (Molecular mechanics with generalized Born and surface area solvation) analysis.
In our study 16 cGMP analogues were evaluated, out of which a Rp modification (Sulphur modification at equatorial exocyclic position) in RP-cGMPS induced the highest level of selectivity among both rod and cone CNG channels. The computational analysis (binding energy and docking scores) revealed comparable binding modes for cGMP in both rod and cone CNG channels. However, the computational data, did not establish a conclusive correlation with the experimental results concerning channel activity triggered by the respective cGMP analogs. Therefore, we believe that, in addition to ligand binding strength, other factors such as ligand efficacy, spontaneous channel opening, and alterations in binding affinity following channel opening may have a significant impact in determining ligand efficiency. Consequently, gaining a more comprehensive understanding of these factors is crucial for achieving selective modulation of rod CNG channels and developing successful RP-treatments.

References
[1] Varnum, Michael, Zagotta, Wiliam N. 1995, Molecular mechanism for ligand discrimination of cyclic nucleotide-gated channels, Neuron, 15, 3, 619-625
Wucherpfennig, S, Haq, W, Popp, V, Kesh, S, Das, S, Melle, C, Rentsch, A, Schwede, F, Durand, F, Nache, V 2022, cGMP Analogues with Opposing Actions on CNG Channels Selectively Modulate Rod or Cone Photoreceptor Function, MDPI Pharmaceutics, 14, 10.

A 02-12

Human monoclonal autoantibody blocks N-methyl-D-aspartate receptors within seconds

Shang Yang[1,2], **Johanna R. Heckmann**[1,3], Abdulla Taha[3], Shiqiang Gao[1], Christian Geis[3], Manfred Heckmann[1], Jing Yu-Strzelczyk[1]

[1] *Wuerzburg university, Physiology Institute, Würuburg, Germany*
[2] *Howard Hughes Medical Institute, Janelia Research Campus, Ashburn, USA*
[3] *Jena University Hospital, Department of Neurology/Section of Translational Neuroimmunology, Jena, Germany*

Question

Autoantibodies against ionotropic N-methyl-D-aspartate receptors from patients with autoimmune encephalitis are pathogenic and induce typical disease signs upon passive-transfer[1]. Receptor internalization is a critical long-term antibody effect in this disease[2]. Here we focus on direct and acute effects of a specific patient autoantibody on N-methyl-D-aspartate receptor function. Acute effects are relevant since receptors could be directly blocked, modulated or even activated by binding an antibody.

Methods

We performed cell-attached single channel recordings in human embryonic kidney cells transfected with the GluN1 and GluN2A subunit of the N-methyl-D-aspartate receptor and investigated direct effects of a specific and well-characterized monoclonal patient autoantibody (immunoglobulin G #003-102) against the amino-terminal domain of the glycine-binding GluN1 subunit of the receptors[3]. Antibodies were applied via recording electrodes and subsequent receptor activity was monitored for 300 seconds.

Results

Immunoglobulin #003-102 reduced simultaneous receptor openings significantly compared to control immunoglobulin (P = 0.038) at low concentrations of glutamate and glycine (median 2 versus 3 in 23 measurements with #003-102 and 30 controls, respectively). Similarly, at high concentrations of glutamate and glycine, simultaneous receptor openings were highly significantly reduced with patient-derived compared to control antibodies (P = 0.003). However, antigen-binding fragments of immunoglobulin G #003-102 did not reduce receptor opening.

Conclusions

In conclusion acute binding of monoclonal immunoglobulin G #003-102 blocks N-methyl-D-aspartate receptors rapidly and thus is functionally relevant even prior to receptor internalisation. Complete immunoglobulin G is necessary for the acute blocking effect.

References
[1] Dalmau J, Lancaster E, Martinez-Hernandez E, Rosenfeld MR, Balice-Gordon R. Clinical experience and laboratory investigations in patients with anti-NMDAR encephalitis. *Lancet Neurol* 2011; 10: 63-74. Elsevier
[2] Hughes EG, Peng X, Gleichman AJ, et al. Cellular and synaptic mechanisms of anti-NMDA receptor encephalitis. *J Neurosci* 2010; 30: 5866-75. Society for Neuroscience
[3] Kreye J, Wenke NK, Chayka M, et al. Human cerebrospinal fluid monoclonal N-methyl-D-aspartate receptor autoantibodies are sufficient for encephalitis pathogenesis. *Brain* 2016; 139: 2641-2652. Oxford University Press

A 02-13
Relating Ligand Binding to Activation Gating in Human P2X Receptors by Using a Novel Fluorescent ATP Derivative

Xenia Brünings[1], Christian Sattler[1], Ralf Schmauder[1], Frank Schwede[2], Klaus Benndorf[1]

[1] *Physiology II, Jena University Hospital, Friedrich Schiller University Jena, Jena, Germany*
[2] *BIOLOG Life Science Institute GmbH & Co KG, Bremen, Germany*

P2X receptors are trimeric ligand-controlled ion channels that belong to the group of purinergic receptors. They open in response to the binding of ATP at their extracellular side. Seven subunit isoforms have been identified and they can assemble to either homomeric or heteromeric P2X receptors. These receptors are involved in a variety of physiological processes, including modulation of cardiac rhythm and contractility, inflammation, and the generation of pain.

The activity of P2X receptors can be regulated by a variety of signalling events. However, the molecular mechanism and the cooperation of the subunit activity remain elusive. Here, we used fluorescent-ligand assays to rationalize how different ligands modulate gating motions in HEK cells expressing different human P2X receptor subtypes. As an application for the binding assay we investigated the binding of suramine and magnesium on human P2X2 receptors. We confirmed that suramine acts as a competitive antagonist and showed a negative modulating effect of magnesium which might be a due to competitive inhibition.

Our previously synthesized fluorescent ATP derivative, 2-[DY-547P1]-AET-ATP has been used to unravel the gating process in rat P2X2 receptors. In this study we used a novel fluorescent ATP with a hexyl-linker instead of an ethyl-linker coupling the fluorophore DY-547P1 to the 2-position of the adenine ring of ATP, which we term 2-[DY-547P1]-AHT-ATP. This ligand is a full agonist with respect to ATP that reports the degree of binding by bright fluorescence at human P2X receptors. The concentration-activation relationship shows an EC_{50} of 5.34 ± 0.33 µM whereas the concentration-binding relationship requires a fit with a double Hill function to obtain a $BC_{50,1}$ of 6.94 ± 7.54 µM and a $BC_{50,2}$ of 1.70 ± 5.51 µM. We speculate that the double Hill function for binding is the consequence of the overlapping desensitization process

triggered by the binding of the second ligand. We suggest that the second component at higher concentrations is correlated to the degree of desensitization currents.

A 02-14
Modulation of Acid-Sensing Ion Channel 1a by Thyroid Hormones

Lu Qin, Dominik Wiemuth, Stefan Gründer

university hospital rwth aachen, institut for physiologz, Aachen, Germany

Acid-sensing ion channels (ASICs) are receptors for extracellular protons and are expressed mainly in the central and peripheral nervous system. ASICs are involved in different physiological processes, such as synaptic plasticity, learning, pain detection, and fear conditioning. So far, six ASIC isoforms (ASIC1a, ASIC1b, ASIC2a, ASIC2b, ASIC3, and ASIC4) have been identified, with ASIC1a being the most widely expressed in the CNS.
Triiodothyronine (T3) is an important thyroid hormone that plays a key role in the regulation of the metabolism, growth and development of the body. In this study, we used the Two-Electro-Voltage Clamp technique to investigate the effect of T3 hormone on ASIC1a expressed in *X. laevis* oocytes. We found that T3 can strongly modulate ASIC1a activity. ASIC1a currents were potentiated 3-fold by T3 hormone, with an EC_{50} value of 3.3 µM. We also found that T3 did neither change the affinity of ASIC1a for protons nor the reversal potential of ASIC1a, nor did it modify the channel indirectly via changing membrane properties. In addition, qPCR data show that ASIC1a is present in NThy-ori-3-1 cells, a cell line derived from human thyroid follicular epithelial cells.
Since ASIC1a is expressed already early during development of the CNS and thyroid hormones are important for early brain development, we speculate that the modulation of ASIC1a by T3 hormone may play a role in the development of the brain.

A 02-15
The α5 subunit in nAChRs contributes to nicotine induced proliferation and migration in human cancer cells

Irida Papapostolou, Daniela Ross- Kaschitza, Florian Bochen, Christine Peinelt, **Maria C. Maldifassi**

University of Bern, IBMM, Bern, Switzerland

Nicotinic acetylcholine receptors (nAChRs) are ligand gated ion channels that belong to the cys-loop family of receptors. nACHRs are activated by tobacco derived nicotine, leading to tumor promoting effects and chemotherapy resistance. Extensive studies have associated the α5 nicotinic receptor subunit, and a specific polymorphism in this subunit with (i) nicotine administration, (ii) nicotine dependence, and (iii) lung cancer. The mRNA of the α5 subunit, transcribed from the *CHRNA5* gene, is up regulated in several types of cancer including lung, prostate, colorectal, and stomach cancer, and cancer incidence and severity correlate with smoking. Other studies have shown that nicotine induced activation of nAChRs containing the α5 subunit, leads to increased proliferation, migration, invasion and EMT transition in lung cancer cell models. In this study, we describe the role of the α5 subunit in cancer hallmark functions in breast, colon, and prostate cancer cells. Initially, nine human cell lines from different origins were used to determine nAChRs subunit expression levels. From these, we chose three cell lines that highly express the α5 subunit, the MCF7 (breast), SW480 (colon), and DU145 (prostate). We investigated the contribution of the α5 subunit in nicotine-activated nAChRs to proliferation, migration and EMT. With pharmacological and siRNA-based experiments we show that the α5 subunit is essential for these nicotine induced cellular functions. Additionally, in the absence of the α5 subunit, nicotine induced expression of EMT markers and of immune regulatory proteins was impaired. Moreover, the α5 polymorphism D398N, that is linked to nicotine induced reward mechanisms and lung cancer, caused a basal increase ofproliferation and migration in the prostate cancer cell line DU145, and the effect is potentially mediated through G protein-signaling. Taken together, we show that cancer cell proliferation and migration induced by nicotine is mediated via the α5 nicotinic receptor subunit in breast, colon, and prostate cancer cells. Our study characterizes the α5 nicotinic receptor subunit as a putative therapeutical target in the treatment of cancer.

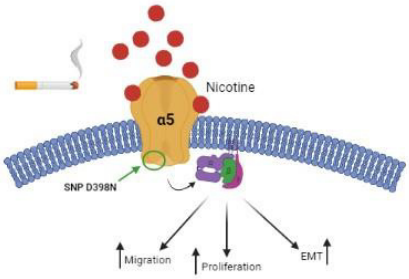

nAChRs and signaling pathway
Nicotine activates α5 containing nAChRs, enhancing proliferation, migration and EMT in breast, prostate, and colon cancer cell lines. Activation of these receptors leads to activation of $G_{a/o}$ proteins, but not of adenylyl cyclase (AC). The presence of the SNP D398N leads to sustained activation of $G_{a/o}$ proteins.

A 02-16
Cyclic Adenosine Monophosphate Enhances Electrophysiological Properties and Gap Junction Neoformation in Human Induced Pluripotent Stem Cell-Derived Cardiomyocytes

Jan-Mischa Sauter[1], Nina D. Ullrich[1,2]

[1] *Heidelberg University, Institute of Physiology and Pathophysiology, Heidelberg, Germany*
[2] *German Center for Cardiovascular Research (DZHK), Partner Site Heidelberg/Mannheim, Heidelberg, Germany*

Question
Human induced pluripotent stem cell-derived cardiomyocytes (hiPSC-CM) bear great potential to solve one major problem of cardiac disease, which is the heart's insufficient capability of regeneration after injury. While there have been major strides in improving the electrophysiological properties of these cells, their cardiogenic phenotype remains mostly immature. To date, these immature features limit the potential of hiPSC-CM to connect with the host cardiac tissue after implantation and form an electromechanical syncytium, which may cause life-threatening arrhythmias in patients.
It has been described previously that the intracellular second messenger cyclic adenosine monophosphate (cAMP) plays a crucial role in the formation of functional gap junctions at the intercalated discs, which are essential for the control of electric signal propagation in the heart. (Somekawa *et al.*, 2005)
In this study we hypothesize that cAMP treatment of hiPSC-CM improves their electrophysiological properties due to enhanced formation of functional gap junctions between adjacent cells.
Methods
We investigated gap junction formation in hiPSC-CM treated with either vehicle or the cAMP analog dibutyryl-cAMP (db-cAMP) for 72 h at the structural level by immunocytochemistry techniques. At the functional level, metabolic and electrical coupling properties were analyzed using Fluorescence Recovery After Photobleaching (FRAP) and Multi Electrode Array (MEA) experiments. Furthermore, calcium transients across multiple cells were evaluated using fluorescence-based confocal imaging.
Results
Our data demonstrate improved gap junction formation in cAMP-treated hiPSC-CMs elucidated by quantification of gap junction plaques at the cell borders. Moreover, FRAP experiments showed significantly faster recovery properties with a half maximum recovery time of 116.13 s in control vs 20.70 s in cAMP treated cells, indicating improved metabolic coupling. Analysis of calcium transients across a cell monolayer showed enhanced transient frequencies in addition to decreased variability of frequency and inter spike intervals. MEA experiments uncovered matching results in field potential frequency and variability as well as accelerated electric signal conduction velocity.

Conclusions

Our data show for the first time the regulatory effect of cAMP on intercellular communication of human stem cell derived cardiomyocytes and point to a possible role in improving their electromechanical integration after implantation in the future.

References

[1] Somekawa, 2005, Enhanced Functional Gap Junction Neoformation by Protein Kinase A–Dependent and Epac-Dependent Signals Downstream of cAMP in Cardiac Myocytes, *Circulation Research,* Volume 97 Issue 7, 655 - 662, Lippincott Williams & Wilkins

A 03 | Hypoxy & HIF

A 03-01
Molecular uncovering of reduced Hypoxia Inducible Factor-1α content in hereditary hemorrhagic telangiectasia

Lars Kleine-Möllhoff, Joachim Fandrey, Anna Wrobeln

University of Duisburg-Essen/University Hospital Essen, Institute of Physiology, Essen, Germany

Hereditary hemorrhagic telangiectasia (HHT) is an inherited autosomal dominant disease with an estimated prevalence between 1 in 5.000 and 1 in 10.000 in the Western population [1]. Affected people suffer from arteriovenous malformations (AVMs) which lead to gastrointestinal bleedings, recurrent epistaxis and telangiectasias. Large AVMs may also affect lungs, liver and brain where bleedings can be life threatening [2]. Besides, the patients have an altered immune response, as depicted in studies that show HHT patients to have a higher risk of infections presumably due to cellular changes, which consequently influence the immune response [3]. Around 96% of HHT patients have mutations in the genes *ENG* and *ACVRL1*, both parts of the TGF-ß/BMP9 pathway. Our group recently showed that HHT patients have a decreased *HIF1A* gene and HIF-1α protein expression [4]. As HIF1α plays an important role in angiogenesis, but also in regulating the immune response our study will investigate how the mutations of the TGF-ß pathway effects the cellular HIF-1α content in more detail. Within our study, we simulate the disease by isolation of non-HHT peripheral blood mononuclear cells (PBMCs) following transfection with siRNA to knockdown *ENG* and *ACVRL1*. Beside HIF-1α gene and protein expression, HIF regulating proteins (PHD, FIH, cofactors) as well as family members of the TGF-β/BMP9 pathway are analyzed via Western blot and quantitative PCR. To enhance clinical translation, human PBMCs are cultured under different oxygen concentrations (21% O_2, 8% O_2 and 1% O_2).

We aim to elucidate the molecular pathway linking HHT to the reduced *HIF1A* gene and protein expression by systematically knocking down proteins in the TGF-ß pathway. The knowledge about these molecular mechanisms may be the key to improve the treatment of HHT-patients.

References

[1] Saparia T, Faughnan ME, Schneider JL, Almers LM, Chow N, Grosse SD, Kim H, Zaroff JG. Assessing the Hereditary Hemorrhagic Telangiectasia Algorithms in a Community-Based Patient Population. Perm J. 2019;23:18-145. doi: 10.7812/TPP/18-145. PMID: 30939282; PMCID: PMC6443364.

[2] McDonald J, Stevenson DA. Hereditary Hemorrhagic Telangiectasia. 2000 Jun 26 [updated 2021 Nov 24]. In: Adam MP, Mirzaa GM, Pagon RA, Wallace SE, Bean LJH, Gripp KW, Amemiya A, editors. GeneReviews® [Internet]. Seattle (WA): University of Washington, Seattle; 1993–2023. PMID: 20301525.

[3] Dupuis-Girod S, Giraud S, Decullier E, Lesca G, Cottin V, Faure F, Merrot O, Saurin JC, Cordier JF, Plauchu H. Hemorrhagic hereditary telangiectasia (Rendu-Osler disease) and infectious diseases: an underestimated association. Clin Infect Dis. 2007 Mar 15;44(6):841-5. doi: 10.1086/511645. Epub 2007 Feb 1. PMID: 17304458.; Cirulli A, Loria MP, Dambra P, Di Serio F, Ventura MT, Amati L, Jirillo E, Sabbà C. Patients with Hereditary Hemorrhagic Telangectasia (HHT) exhibit a deficit of polymorphonuclear cell and monocyte oxidative burst and phagocytosis: a possible correlation with altered adaptive immune responsiveness in HHT. Curr Pharm Des. 2006;12(10):1209-15. doi: 10.2174/138161206776361336. PMID: 16611102.

[4] Wrobeln A, Leu T, Jablonska J, Geisthoff U, Lang S, Fandrey J, Droege F. Altered hypoxia inducible factor regulation in hereditary haemorrhagic telangiectasia. Sci Rep. 2022 Apr 7;12(1):5877. doi: 10.1038/s41598-022-09759-9. PMID: 35393474; PMCID: PMC8988913.

A 03-02
Deciphering the role of hypoxia-inducible factors in ferroptotic cell death in a cell culture model of age-related macular degeneration

Annika Schubert, Ursula S. Blind, Joachim Fandrey, Yoshiyuki Henning

University of Duisburg-Essen, University Hospital Essen, Institute of Physiology, Essen, Germany

Age-related macular degeneration (AMD) is the most common blinding disease in the elderly population. This disease mainly affects the central vision because the photoreceptors in the macula degenerate due to a dysfunction and atrophy of the retinal pigment epithelium (RPE). Advanced AMD is divided into two subtypes, wet and dry AMD. Dry AMD is the most common type, but unlike the wet AMD, there is no promising treatment available against this subtype to date. Major risk factors for AMD are oxidative stress and hypoxia in RPE cells. Both are associated with accumulation of hypoxia-inducible factors (HIFs), dimeric transcription factors with an oxygen-labile α-subunit and a constitutively expressed β-subunit, from which two isoforms, HIF-1 and HIF-2 are most relevant.
In a previous study, we established a cell culture model of dry AMD by combining oxidative stress and HIF stabilization in a human RPE cell line (ARPE-19). Using this model, we demonstrated that HIF stabilization exacerbates oxidative damage in RPE cells leading to cell death by ferroptosis, an iron-dependent cell death mode [1]. Based on these findings, we are investigating the respective roles of HIF-1 and HIF-2 in ferroptotic cell death in our AMD cell culture model. For this purpose, we applied RNA interference by siRNA targeting *HIF1A* and *HIF2A* mRNA, coding for the oxygen-labile α-subunits of HIF-1 and HIF-2. We found cell death induced by sodium iodate under hypoxia (1% O_2) to be aggravated in cells with HIF-2α knockdown, while knockdown of HIF-1α resulted in decreased cell death. Western blot analyses revealed that knockdown of HIF-1α results in a significant upregulation of HIF-2α. To identify the mechanisms underlying the different cell death rates in HIF-1α and HIF-2α knockdown cells, we are focusing on the regulation of the ferroptosis pathway by HIF-1 and HIF-2. Furthermore, we look at the mechanistic target of rapamycin complexes 1 (mTORC1) and 2 (mTORC2) in conjunction with HIF signaling, because dysregulation of mTOR signaling including its downstream effects such as autophagy were already linked to AMD pathophysiology. Thus far, we found that AKT phosphorylation at Ser473, a hallmark of mTORC2 activation, was upregulated by sodium iodate treatment. Furthermore, AKT phosphorylation was downregulated under hypoxia in cells lacking HIF-1α and HIF-2α, suggesting that mTORC2 activation under hypoxia requires HIF-signaling. The functional implications of a possible HIF – mTOR crosstalk with regard to AMD pathophysiology is currently under investigation.

References
[1] Henning Y, Blind US, Larafa S, Matschke J, Fandrey J. Hypoxia aggravates ferroptosis in RPE cells by promoting the Fenton reaction. *Cell Death Dis*. 2022 Jul 29;13(7):662. doi: 10.1038/s41419-022-05121-z.

A 03-03
Expression analysis and functional characterization of an oxygen-binding protein in an unconventional physiological model system

Carina Osterhof[1,2], Thomas Hankeln[2], Simon Sprecher[3], David Hoogewijs[1]

[1] *University of Fribourg, Section of Medicine, Faculty of Science and Medicine, Fribourg, Switzerland*
[2] *University of Mainz, Institute of Organismic and Molecular Evolution, Mainz, Germany*
[3] *University of Fribourg, Departement of Biology, Faculty of Science and Medicine, Fribourg, Switzerland*

Androglobin is the most recent addition to the globin protein family. This strongly conserved protein, from humans to more basal unicellular organisms, consists of a circularly permutated globin domain still capable of binding oxygen, a calmodulin binding domain and a putative calpain protease. Its chimeric nature combines oxygen sensing with calcium signalling and proteolysis, making it an intriguing candidate for signalling cascades under changing oxygen conditions. The cnidarian *Nematostella vectensis* lives in shallow sea water. The sessile adults are frequently subjected to stressors such as varying levels of oxygen or changes in salt concentration and temperature. Up to know, *Nematostella* has been used as a model system for development and regenerative mechanics, but little work has been done on its physiological adaptation to these changing environmental conditions.

We therefore analysed the temporal Adgb expression profile in *Nematostella* of different developmental stages. We detected high levels of Adgb mRNA via RNAScope in epithelial cells and most prominently in cells carrying motile cilia, mirroring Adgb's main expression site in mammals. We are currently generating Adgb-deficient models for multiple functional investigations and will also explore the Adgb-dependent transcriptome under modulated oxygen levels. The abundant Adgb expression levels in cells carrying motile cilia suggest either a supportive role in the energy consuming process of cilia beating or a function as scavenger of reactive oxygen species (ROS) in highly metabolically active cells – consistent with its monomeric relatives from the globin family.

The authors acknowledge funding by the Swiss National Science Foundation (SNSF) grant no. 207460.

A 03-04

Investigation of a crosstalk between hypoxia-inducible factors and mechanistic target of rapamycin in retinal pigment epithelium cells

Gesa Weißenberg, Joachim Fandrey, Yoshiyuki Henning

University Hospital Essen, Institute of Physiology, Essen, Germany

Age-related macular degeneration (AMD) is the most common cause of blindness in elderly people living in industrial countries. In general, AMD is characterized by the degeneration of photoreceptors in the macula, leading to a gradual loss of high acuity vision. Hypoxia and oxidative stress in the retinal pigment epithelium (RPE), a monolayer of cells located adjacent to the photoreceptors, are involved in the pathogenesis of AMD but there are still many uncertainties regarding the pathophysiology at the molecular level. Thus, we are aiming at understanding pathophysiological changes occurring at very early stages of AMD to foster prevention and novel treatment approaches.
Smoking has been shown to be the leading exogenous risk factor promoting AMD in the long-term. Thus, in a previous study, we treated a human RPE cell line (ARPE-19) with cigarette smoke extract (CSE) to analyze effects of cigarette smoking on RPE integrity and metabolism. These studies revealed that CSE treatment disrupts the metabolism of RPE cells by impairing mitochondrial respiration and glycolysis. We also found that the α-subunit of the hypoxia-inducible factor 1 (HIF-1), a dimeric transcription factor that enables the survival of cells under hypoxic conditions, was downregulated at the protein level in CSE-treated cells, contributing to metabolic dysregulation.
In order to assess the mechanisms of HIF-1α downregulation by CSE and its functional implications for early AMD pathophysiology, we focused on a possible HIF – mTOR crosstalk. For this purpose, we investigated CSE effects on the two mTOR complexes mTORC1 and mTORC2 in ARPE-19 cells. Thus far, we could show that CSE had no consistent effect on mTORC1 activity, but autophagy, a cellular recycling process that is negatively regulated by mTORC1, was upregulated in CSE-treated cells. In contrast, mTORC2 activity was significantly increased by CSE treatment in a time-dependent manner. CSE-induced upregulation of mTORC2 was abolished by co-treatment of cells with CSE and Roxadustat, a HIF-stabilizing agent, suggesting that mTORC2 is regulated in a HIF-dependent manner. Currently, we are investigating the effects of pharmacological and genetical inhibition of mTORC1 and mTORC2 on HIF signaling and vice versa.

A 03-05

The Effect of isoleucine preconditioning on neuroprotection via HIF-1α signaling after oxygen-glucose deprivation insult

Xujin Yao, Joachim Fandrey, Tristan Leu

University Duisburg-Essen / University Hospital Essen, Institute of Physiology, Essen, Germany

Introduction

Isoleucine is an essential branched-chain amino acid and key regulator of glucose uptake [1]. Although its role in protein synthesis and nutrition is already known, our knowledge about its role in oxygen on neuronal cells after the onset of ischemic stroke is limited. Most acute ischemic stroke patients show a positive test for hyperglycemia [2]. Hyperglycemia impairs hypoxia-dependent protection of hypoxia-inducible factor-1α (HIF-1α) against proteasomal degradation [3]. Furthermore, previous study reported that isoleucine activates the nutrition sensor, mammalian target of rapamycin (mTOR) complex [4]. Importantly, its main target, P70S6K, is known to regulate HIF-1α. Downstream of HIF-1α, the

relocation of p53 to the nucleus after cellular stress promotes the inhibition of malignant cells growth [5]. In addition, localization of mitochondria is dependent on HIF-1α during long term hypoxia in tumor cells.

In this study, the neuroprotection of isoleucine preconditioning in oxygen-glucose-deprived(OGD) neurons will be validated and be connected to the stabilization of the HIF-1α protein. Besides, the relation between the evidence of increased level of HIF-1α and the promotion of nuclear p53 should be investigated. Moreover, it is important to study whether pretreatment with isoleucine contributes to the amount and distribution of mitochondria.

Research Design

First, different concentrations of isoleucine will be given to cells for different time periods before oxygen-glucose deprivation (OGD) insult. Cell viability will be measured by cell counting kit-8 assay and LDH release assay.

Next, HIF-1α protein and its target genes will be measured after isoleucine preconditioning by western blotting and qPCR. By generating a HIF-1α knockout cell line constructed by a lentivirus- based CRISPR/Cas9 system, nuclear P53 and Somatic mitochondria will be measured by western blotting and immunofluorescence staining.

To evaluate the effect of nuclear P53 and mitochondria on injured cells, MDMM2, P53 nuclear transporter, and CHCHD4, a regulator of mitochondria localization, will be detected by western blotting. As increased somatic mitochondria are accompanied by the accumulation of nuclear reactive oxygen species (ROS), ROS will be detected by immunofluorescence staining.

Discussion and Conclusion

This study aims to investigate the effect of isoleucine pretreatment on cell death after OGD insult and potential regulation of HIF-1α and its downstream, p53. Our current data suggested that a relatively high concentration of isoleucine at an early stage might increase cellular survival after the OGD damage, whereas a later treatment might exert the opposite effect. Isoleucine is likely to affect the mTOR pathway and p53. Therefore, a larger sample size and further research are needed to better understand the relation between isoleucine and neuroprotection and isoleucine-mTOR-HIF-1α-p53 axis.

References
[1] Doi, M., et al., *Isoleucine, a blood glucose-lowering amino acid, increases glucose uptake in rat skeletal muscle in the absence of increases in AMP-activated protein kinase activity.* The Journal of nutrition, 2005. **135**(9): p. 2103-8.
[2] Li, W., et al., *Hyperglycemia in stroke and possible treatments.* Neurological research, 2013. **35**(5): p. 479-91.
[3] Catrina, S., et al., *Hyperglycemia regulates hypoxia-inducible factor-1alpha protein stability and function.* Diabetes, 2004. **53**(12): p. 3226-32.
[4] Appuhamy, J., et al., *Isoleucine and leucine independently regulate mTOR signaling and protein synthesis in MAC-T cells and bovine mammary tissue slices.* The Journal of nutrition, 2012. **142**(3): p. 484-91.
[5] O'Brate, A. and P. Giannakakou, *The importance of p53 location: nuclear or cytoplasmic zip code?* Drug resistance updates : reviews and commentaries in antimicrobial and anticancer chemotherapy, 2003. **6**(6): p. 313-22.

A 03-06

The Functional relationship between the Hypoxia inducible factor 1alpha and primary cilia in neuronal cells

Pascal F. Schneider, Tristan Leu, Joachim Fandrey

University of Duisburg-Essen, Institute of Physiology, Essen, Germany

Primary cilia, also called "the cells antenna", are centriole based sensory cellular organelles, which are present on almost all mammalian cells and became importance during the last decades. They perform a variety of functions, including maintaining neuroplasticity and the adaption to hypoxic conditions via a variety of signalling pathways, including the sonic hedgehog signalling, the Wnt-signalling or the PDGFRa-signalling pathway.[1] Based on these observations, the work pursued the goal to investigate the functional relationship between the hypoxia inducible factor 1alpha and primary cilia in neuronal cells. The establishment of neuronal HIF1alpha-knockout cells, based on the use of a specific tamoxifen induced Cre/LoxP-system,[2] served as the base for this work. Thereby the knockout efficiency was determined by Western-Blotting and especially quantitative PCR analysis. Using these cells, the influence of HIF1alpha on the primary cilia length and diverse signalling pathways was examined. Thereby significant effects on the Notch signalling-pathway could be observed. In addition to the expression of Gata3, this also includes the expression of the Notch receptors Notch3 and Notch4. The relationship between a possible HIF-associated regulation of the Notch signaling pathway and an adaptation to hypoxic conditions must be determined by further experiments.

References
[1] Wheway, G., Nazlamova, L., Hancock, J.T., 'Signaling through the primary cilium', *Frontiers in Cell and Developmental Biology*, 6, Articel 8

[2] Hamidi, A., Wolf, A., Dueva, R., Kaufmann, M., Göpelt, K., Iliakis, G., Metzen, E., '*Depletion of HIF-1alpha by Inducible Cre/loxP Increases the Sensitivity of Cultured Murine Hepatocytes to Ionizing Radiation in Hypoxia.*', *Cells*, 2022. 11(10)

A 03-07
Investigating the Role of HIF-1α in Radiation Sensitivity and Metabolic Changes in Murine Hepatocyte-Derived Cells

Akram Hamidi[1], Alexandra Wolf[1], Rositsa Dueva[1,2], Melanie Kaufmann[1], Kirsten Goepelt[1], George Iliakis[2], Eric Metzen[1]

[1] *University of Duisburg-Essen, Institute of Physiology, Faculty of Medicine, Essen, Germany*
[2] *University of Duisburg-Essen, Institute of Medical Radiation Biology, Faculty of Medicine, Essen, Germany*

Hepatocellular Carcinoma (HCC) is a prevalent cancer affecting a significant number of individuals worldwide. Enhancing the efficacy of radiotherapy, a treatment modality for HCC which is under development, holds great potential for improving patient outcomes. In this study, we aimed to elucidate the impact of Hypoxia-inducible factor 1 alpha (HIF-1α) on DNA damage repair, radiation sensitivity, and cellular metabolism in murine hepatocyte-derived cells (mHDC).

To better understand the role of HIF-1α, we developed an *in vitro* model using murine hepatocyte-derived cells (mHDC) that bear a complete knockout for HIF-1α. We assessed the impact of HIF-1α deficiency on DNA damage repair following ionizing radiation (IR) exposure under hypoxic conditions.

Our findings revealed that HIF-1α-depleted cells exhibited increased accumulation of IR-induced DNA damage, as evidenced by upregulated γH2AX foci. Furthermore, HIF-1α-deficient cells displayed delayed DNA repair after IR treatment in hypoxia, suggesting a potential effect on non-homologous end joining (NHEJ) repair capacity, as observed in neutral comet assays. Notably, there were no significant differences in reactive oxygen species (ROS) levels among the treatment groups, suggesting that the effects caused by HIF-1α deficiency are unlikely to be mediated by ROS.

To further investigate the relationship between HIF-1α and cellular metabolism, we analyzed the respiratory metabolism and mitochondrial morphological changes in HIF-1α knockout cells. Interestingly, HIF-1α-deficient cells exhibited a significant increase in the oxygen consumption rate (OCR) and a reduction in the extracellular acidification rate (ECAR) compared to wildtype cells. Additionally, we observed alterations in mitochondrial morphology, with a decrease in the number of mitochondria following hypoxia, but an increase in knockout cells compared to wildtype cells.Collectively, our results suggest that HIF-1α inactivation enhances radiation sensitivity in mHDC cells, accompanied by an elevation in OCR and reduced glycolysis. These findings contribute to a better understanding of the molecular mechanisms underlying radioresistance and metabolic changes in mHDC.

This study was supported by the Deutsche Forschungsgemeinschaft (DFG) Graduate School 1739.

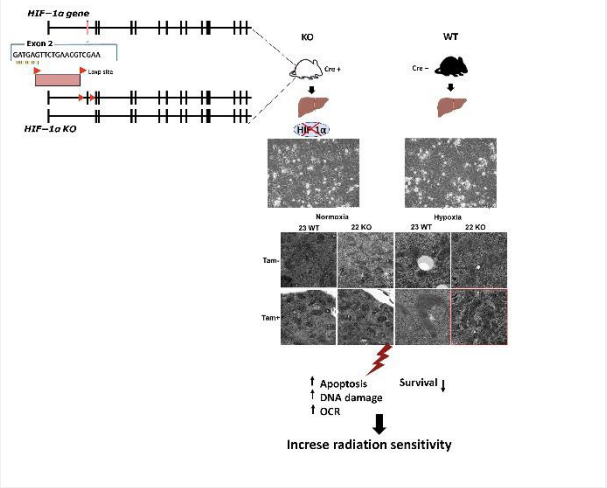

Hepatocyte Isolation and Microscopic Insights into mHDC Mitochondria
Mice were used which carry LoxP sites flanking exon 2 (E2) of HIF-1α. Recombination is accomplished by tamoxifen induced expression of Cre from a ROSA26_CreERT2 locus. Loss of exon 2 results in the inability of HIF-1α to bind to DNA. Isolated mouse hepatocytes maintained their typical cobblestone morphology and a confluent monolayer. The results showed alterations in mitochondrial morphology, with a decrease in the number of mitochondria following hypoxia, but an increase in knockout cells compared to wildtype cells.

A 03-08

Cigarette smoke extract causes a bioenergetic crisis in retinal pigment epithelium cells involving the destabilization of hypoxia-inducible factor-1α

Yoshiyuki Henning[1], Katrin Willbrand[1], Safa Larafa[2], Gesa Weißenberg[1], Veronika Matschke[3], Carsten Theiss[3], Gina-Eva Görtz[4], Johann Matschke[2]

[1] *University Hospital Essen, University of Duisburg-Essen, Institute of Physiology, Essen, Germany*
[2] *University Hospital Essen, University of Duisburg-Essen, Institute of Cell Biology (Cancer Research), Essen, Germany*
[3] *Ruhr University Bochum, Department of Cytology, Institute of Anatomy, Bochum, Germany*
[4] *University Hospital Essen, University of Duisburg-Essen, Molecular Ophthalmology, Department of Ophthalmology, Essen, Germany*

Question

Age-related macular degeneration (AMD) is the leading cause of irreversible vision loss in the elderly population causing progressive degeneration of photoreceptors in the macula. However, there are still many uncertainties regarding the pathophysiology at the molecular level. Dysregulation of mitochondrial function in retinal pigment epithelium (RPE) cells was proposed to drive AMD pathophysiology, because RPE cells and photoreceptors act as a functional unit [1]. Hypoxia-inducible factors (HIFs), dimeric transcription factors with an oxygen-labile α-subunit and a constitutively expressed β-subunit, are important modulators of mitochondrial function [2]. Furthermore, smoking is the most important exogenous risk factor for AMD and is known to impair mitochondrial integrity [3]. Therefore, our aim was to investigate how smoking affects mitochondrial function in conjunction with HIF signaling to identify novel mechanisms underlying AMD pathophysiology.

Methods

We treated a human RPE cell line with cigarette smoke extract (CSE) under normoxia (21% O_2), hypoxia (1% O_2) or by co-treatment with Roxadustat, a clinically approved HIF stabilizer. Treatment effects on mitochondrial function and integrity were analyzed by means of real-time cell metabolic analysis using a Seahorse Bioanalyzer, flow cytometry, immunofluorescence staining, and transmission electron microscopy. HIF protein levels were analyzed by Western Blot.

Results

CSE treatment impaired mitochondrial integrity, involving increased reactive oxygen species, disruption of mitochondrial membrane potential and altered mitochondrial morphology. Mitochondrial respiration and ATP production were impaired in CSE-treated cells under normoxia, possibly by TCA cycle inhibition. Surprisingly, CSE-treated RPE cells also exhibited decreased glycolytic rate under normoxia, causing a bioenergetic crisis, because two major metabolic pathways that provide ATP were impaired by CSE. Downregulation of glycolytic rate was HIF-dependent, because HIF-1α protein levels were downregulated by CSE treatment. Moreover, hypoxia incubation and treatment with Roxadustat restored glycolytic flux.

Conclusions

Impairment of mitochondrial respiration and glycolysis was also observed in RPE cells from human donors with AMD [4], thus our *in vitro* model most likely reflects *in vivo* characteristics of AMD pathophysiology and is a suitable model to investigate metabolic dysregulation in AMD at the molecular level to foster prevention and novel treatment approaches.

References

[1] Pan, WW, Wubben, TJ & Besirli, CG 2021, 'Photoreceptor metabolic reprogramming: current understanding and therapeutic implications', *Commun Biol*, 4(1), 245.
[2] Kaelin, WG & Ratcliffe, PJ 2008, 'Oxygen sensing by metazoans: the central role of the HIF hydroxylase pathway', *Mol Cell*, 30, 393-402.
[3] Velilla, S, García-Medina, JJ, García-Layana, A, Dolz-Marco, R, Pons-Vázquez, S, Pinazo-Durán, MD, Gómez-Ulla, F, Arévalo, JF, Díaz-Llopis, M & Gallego-Pinazo, R 2013, 'Smoking and age-related macular degeneration: review and update', *J Ophthalmol*, 2013, 895147.
[4] Ferrington, DA, Ebeling, MC, Kapphahn, RJ, Terluk, MR, Fisher, CR, Polanco, JR, Roehrich, H, Leary, MM, Geng, Z, Dutton, JR & Montezuma, SR 2017, 'Altered bioenergetics and enhanced resistance to oxidative stress in human retinal pigment epithelial cells from donors with age-related macular degeneration', *Redox Biol*, 13, 255-265.

A 03-09
Hypoxia-Inducible Factor-1 and p53 – friends or foes in the colorectal carcinoma?

Stefanie Saoub, Joachim Fandrey, Anna Wrobeln

University Hospital Essen, Institute of Physiology, Essen, Germany

The colorectal carcinoma (CRC) belongs to the most common cancer-types in western countries [1]. Invasiveness and tumour growth in metastasis strongly depends on hypoxia-inducible factors (HIF) as well as the tumour suppressor p53. P53 plays a key role for cell cycle arrest and apoptosis and is mutated in approximately half of all human cancer-types [2]. CRCs often develop hypoxic regions in which HIF accumulate and mediate the adaptation to hypoxia [3]. The crosstalk of HIF-1α and p53 in CRCs was subject of many studies but remains very controversial. Aim of our study is to investigate the roles of these important transcription factors for survival of CRC cells under hypoxia by elucidating their interaction.

First, we have incubated human CRC cells (HCT116 cells) under normoxia as well as moderate and severe hypoxia (1%, 0.1% O_2) for 4 and 24 hours to analyse the regulation of HIF-1 and p53 under hypoxia. Subsequently, we separately knocked out the transcription factors and examined how this knockout (ko) influences the stability, localisation and activity of the respective other transcription factor (Western Blot, qPCR) as well as metabolism and cell viability under hypoxia.

In wildtype (wt) cells, the P53 protein was stabilized after 24 hours of severe hypoxia with upregulation of the specific proapoptotic p53 target gene *BAX* which could only be observed under this condition and was associated with apoptosis as the main form of cell death. Interestingly, after p53 ko the main cell death mechanism under severe hypoxia remained apoptosis, challenging the role of p53 for hypoxia-induced apoptosis. Ko of p53 did not alter HIF-1α expression, but HIF target genes were significantly downregulated under hypoxia. A HIF-1A ko downregulated *p53* mRNA expression under normoxia and hypoxia. On the other hand, HIF-1A ko cells showed higher P53 protein levels under hypoxia with significantly increased levels of apoptosis compared to wt cells although upregulation of *BAX* was not as high as expected. In addition, the glycolytic shift under hypoxia did not seem to be impaired despite lack of HIF-1α.

In conclusion, we disagree with the hypotheses that p53 loses activity under hypoxia [4] and that a p53 ko leads to survival advantages of CRC cells under hypoxia [5]. We question the importance of p53 function for hypoxia-induced apoptosis. We could show that both transcription factors influence each other concerning stability and transcriptional activity which will be further examined by measuring DNA binding activity. Finally, a HIF-1A knockdown in p53 ko cells will be established to examine whether the cell death of HIF-1A ko cells under hypoxia is dependent on p53 and whether HIF inhibitors could be a treatment option for patients with CRCs with loss of function mutations in the p53 gene.

I thank the Essener Ausbildungsprogramm "Labor und Wissenschaft" für den ärztlichen Nachwuchs (ELAN) and the Stiftung Universitätsmedizin Essen for the financial and scientific support of my work.

References
[1] Mármol I, Sánchez-de-Diego C, Pradilla Dieste A, Cerrada E, Rodriguez Yoldi MJ. Colorectal Carcinoma: A General Overview and Future Perspectives in Colorectal Cancer. International Journal of Molecular Sciences. 2017 Jan 19; 18(1):197.
[2] Levine AJ. p53, the cellular gatekeeper for growth and division. Cell. 1997 Feb 7;88(3):323-31.
[3] Semenza GL. Targeting HIF-1 for cancer therapy. Nature Reviews Cancer. 2003 Oct;3(10):721-32.
[4] Hammond EM, Giaccia AJ. The role of p53 in hypoxia-induced apoptosis. Biochemical and Biophysical Research Communications. 2005 Jun 10;331(3):718-25.
[5] Graeber TG, Osmanian C, Jacks T, Housman DE, Koch CJ, Lowe SW, Giaccia AJ. Hypoxia-mediated selection of cells with diminished apoptotic potential in solid tumours. Nature. 1996 Jan 4;379(6560):88-91.

A 03-10
Hypoxia induced activation of Mineralocorticoid receptor alters metabolism in the hepatocytes that can contribute to the progression of liver cirrhosis.

Mohammad M. Mohib[1], Sindy Rabe[1], Alexander Nolze[1], Quratul Ain[2], Michael Rooney[2], Alexander Zipprich[2], Michael Gekle[1], Barbara Schreier[1]

[1] *Martin Luther University of Halle-Wittenberg, Julius Bernstein Institute of Physiology, Medical School, Halle, Germany*
[2] *Universitätsklinikum Jena, Clinic for Internal Medicine IV, Jena, Germany*

Introduction:

The mineralocorticoid receptor (MR) is a member of the nuclear receptor family being of major importance for regulating water and electrolyte balance in the body. MR activation is known to modulate various physiological processes, including blood pressure, renal function, and electrolyte homeostasis, but also being deletrious by promoting e.g. heart and blood vessel fibrosis. Recent studies have suggested that MR activation may contribute to the progression of liver cirrhosis in animal models. Hypoxia, a common feature in liver cirrhosis, has been found to induce MR activation in various cell types, including hepatocytes. However, the impact of non-physiological MR activation in hepatocytes remains poorly understood.**Methods:**

Next Generation sequencing was performed on rat livers either from control or cirrhotic animals or animals with cirrhosis & eplerenone treatment. With respect to the results of the gene set enrichment analysis (GSEA) we employed HepG2 cells to investigate the impact of MR activation on metabolic processes. To induce non-physiological MR activation, we exposed the cells to hypoxia, using an oxygen concentration of 0.2%. We measured the mRNA and protein levels of key metabolic genes using quantitative PCR and Western blotting. Additionally, we analyzed glucose consumption, lactate production as well as lipid accumulation under normoxic and hypoxic conditions with or without eplerenone treatment.

Results:

GSEA revealed that in a rat model for liver cirrhosis (CCl4 treatment) eplerenone, an MR antagonist, reverses the downregulation of genes annotated to the GOterm “Monocarboxylic acid metabolic process” by cirrhosis. In a former study, we already demonstrated that under hypoxic conditions MR-induced transcriptional activity changes (Schreier, 2018). Therefore, we incubated HepG2 cells with or whithout hypoxia in the presence of eplerenone. We were able to demonstrate that hypoxia reduces the mRNA and protein content of PPARα, PDK4, AMACR, ABCC2 and Lipin1. This effect can be reversed, at least partially, by eplerenone for PPARα, PDK4 and ABCC2, suggesting that the alteration of these genes is MR dependent. As those proteins are key regulators of cell metabolism, we analyzed glucose and lipid metabolism in HepG2 cells. As expected, hypoxia increases glucose consumption and lactate production in HepG2 cells. This could be partially reversed by treatment eplerenone. Furthermore, our results indicate that hypoxia associated lipid accumulation in hepatocytes is at least partially induced by MR activation.

Conclusion:

Taken together, our findings suggest that MR activation may play a role in the dysregulation of glucose and lipid metabolism in hepatocytes thereby contributing to the development of liver cirrhosis. Therefore, MR antagonism may have therapeutic potential in the treatment of liver diseases.

A 03-11
Investigating the Role of Hypoxia-induced CD73 in HIV Persistence and Transcription

Jouly Sbeiti[1,2,4], Hannah Schwarzer-Sperber[2], Carina Elsner[3], Stefan Esser[4], Joachim Fandrey[1], Roland Schwarzer[2], Sandra Winning[1]

[1] *University of Duisburg-Essen, Institute for Physiology, Essen, Germany*
[2] *University of Duisburg-Essen, Institute for Translational HIV Research, Essen, Germany*
[3] *University of Duisburg-Essen, Institute for Virology, Essen, Germany*
[4] *University Hospital Essen, Center for HIV, AIDS, Proctology and STDs, Essen, Germany*

Question

The Acquired Immunodeficiency Syndrome (AIDS) and its etiological agent the human immunodeficiency virus (HIV) remain a major global public health issue. Replication of human immunodeficiency virus (HIV) is suppressed to undetectable levels by effective antiretroviral therapy (ART) but it fails to completely eradicate HIV due to the persistence of latently infected cells. A better understanding of viral persistence and identification of unique features of latently infected cells are needed to develop HIV cure strategies. Recently, the surface protein CD73 has emerged as a key marker of latent infection. CD73 catalyzes the formation of immunosuppressive adenosine and is induced by hypoxia. As viral reservoirs often persist in hypoxic tissues it seems highly plausible that HIV evades antiviral immunity via hypoxic induction of CD73 and adenosine (HCA axis), which ensures long-term persistence of successfully infected cells.

Methods

In the first part of our experiments, the impact of hypoxia on Jurkat cells (human T cell line) on protein and mRNA level was examined with

and without treatment with DMOG (dimethyloxalylglycine) and ROX (roxadustat). In the second part, we tested whether the expression of components of the HCA axis correlated with clinical parameters in the blood of infected individuals, such as the viral load or the size of the HIV reservoir. To that aim, blood was collected from people living with HIV (PLWH) in the clinic and HIV seronegative participants. Isolated peripheral blood mononuclear cells (PBMCs) were analyzed for CD73, CD39 and HIF-1α protein expression via flow cytometry and immunofluorescence staining. In parallel, the size of the HIV reservoir in all individuals was determined using quantitative PCR.

Results

In the first part, in Jurkat cells HIF-1α protein increased after 4 and 24 hours, which was accompanied by an increase of HIF-1 target gene expression (*GLUT1*, *PHD2, PHD3*). In contrast, expression of CD73 and CD39 were unaffected by hypoxia. In the second part: As expected, CD4 T cells are lower in samples of PLWH compared to the samples of healthy donors. Furthermore, CD73 was decreased and CD39 increased on CD4 T cells of HIV infected individuals in comparison to HIV negative participants.

Conclusions

HIV might evade the immune system by hiding in hypoxic areas, favored by the production of immunosuppressive adenosine via CD73. We transferred this model to PLWH, assuming that they might exhibit hypoxia in latently infected tissues. Although CD73 and CD39 expression did not show changes under hypoxia they were altered in PLWH. Furthermore, the general composition of PBMCs was different compared to healthy donors despite ART in PLWH. As the project is still in the beginning phase it is difficult to draw conclusions at this time point. Thus, it needs to be further investigated whether hypoxia influences CD73 and CD39 in HIV patients and whether the latent reservoir can be shaped by hypoxia.

I would like to thank Ms. Buena Delos Reyes, Claudia Padberg, Silke Lauterbach, Tamara Mussfeldt and Barbara Bleekmann for familiarizing myself with the work in the laboratory and for their support by always having an open ear for my countless questions.

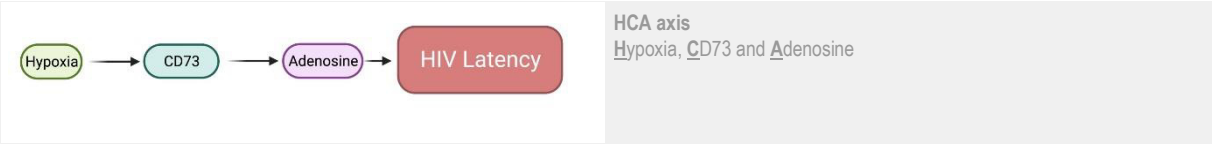

A 04 | Mechanisms of Behavior & Cognition

A 04-01
Effects of Cav1.3-inhibition on DA SN neuron in vivo firing and explore – exploit behavior in mice

Johannes Boehm[1], Pascal Vogel[1], Jörg Striessnig[2], Jochen Roeper[1]

[1] *Goethe University Frankfurt a.M., Institute of Neurophysiology, Frankfurt am Main, Germany*
[2] *University of Innsbruck, Department of Pharmacology and Toxicology, Innsbruck, Austria*

The Dihydropyridine (DHP)-sensitive L-Type calcium channels $Ca_v1.3$ and $Ca_v1.2$ serve various physiological functions e.g. acceleration of pacemaking in the heart or tonus control in arterial vessels. Furthermore, these channels are expressed in substantia nigra (SN) dopamine (DA) neurons. Previous work from our group demonstrated that $Ca_v1.3$ channels function as linear full-range amplifiers of firing rates (FR) selectively in lateral DA SN neurons projecting to the dorsolateral striatum. In addition, this FR amplifier function of $Ca_v1.3$ channels is dampened by clinically relevant concentrations of isradipine (ISR), both in vitro in acute brain slices and in vivo in anesthetized mice (Shin et al., 2022, Science Advances).

We have further demonstrated a similar ISR in vivo effect in awake and freely moving mice in chronic extracellular recordings during open field behavior. Consistently, 15 min after systemic ISR injection (ISR = 3mg/kg BW) in $Ca_v1.2DHP^{-/-}$ mice, where DHPs only act on Cav1.3 channels, we observed a 24% mean firing rate decrease in lateral pharmacologically identified DA SN neurons (> 50% firing rate reduction after Quinpirole i.p. injection) compared to Vehicle injection (n=28, N=3; mean FR baseline = 4,97 Hz compared to mean FR ISR = 3,80 Hz). At the same time the firing rate reduction was positively correlated to the baseline firing rate of the DA lSN neuron (ΔHz-slope = 0.29).

As previous work by Koralek and Costa (Koralek & Costa, 2021, Science Advances) suggested a critical role of electrical activity in DA SN neurons in selectively invigorating exploitative behavior in mice, we hypothesized that an ISR-induced firing rate reduction of lSN neurons might affect exploitative behavior. To test this hypothesis, we trained mice (6 male wildtype and 6 male and female $Ca_v1.2DHP^{-/-}$ mice) to perform a two-poke sequence learning task, where rewarded and thus exploitative action sequences could be differentiated from other explorative actions. After initial pre-training, mice were required to learn a specific two-poke sequence in a three-port operant chamber to receive a sugar-water reward in a central reward-port. Mice learned the task within 10 days of training and reached plateau performance (stable exploitative poking of the target sequence) achieving a mean of 10 rewards/min at the end of this period. At this stage, we injected ISR or VEH i.p. 15min before placing the animal in the operant chamber and also opened an additional exploration port.

A 04-02
Orthogonal coding of food and voluntary exercise by VTA dopamine neurons

Hanna E. van den Munkhof[1,2], Vasyl Mykytiuk[1,2], Tatiana Korotkova[1,2]

[1] *University Of Cologne, Institute of Systems Physiology, Cologne, Germany*
[2] *Max Planck Institute for Metabolism Research, Cologne, Germany*

The author has objected to a publication of the abstract.

A 04-03
Binge eating-induced olfactory cortex suppression promotes feeding

Hung Lo[1], Anke Schönherr[1], Malinda Tantirigama[2], Laura Moreno Velasquez[1], Lukas Faiss[1], Benjamin Rost[1], Matthew E. Larkum[4], Benjamin Judkewitz[1], Katharina Stumpenhorst[3], Marion Rivalan[1], York Winter[3], Dietmar Schmitz[1], **Friedrich Johenning**[1]

[1] *Charité University Medicine Berlin, Neuroscience Research Center, Berlin, Germany*
[2] *NTNU Trondheim, Kavli Institute for Systems Neuroscience, Trondheim, Norway*
[3] *Humboldt Universität zu Berlin, Cognitive Neurobiology, Berlin, Germany*
[4] *Humboldt Universität zu Berlin, Institut für Biologie, Berlin, Germany*

Appropriate feeding behavior is the foundation of maintaining homeostasis. Elevated feeding rate (binge eating) is a common trait of eating disorders, and it is associated with obesity. It is also known that flavor perception regulates feeding. However, the effects of feeding rate on sensory feedback from flavor perception remain unknown. We developed a liquid food delivery system that enables Ensure (artificial energy-dense flavored milk with high incentive salience) consumption at different feeding rates. Using miniscopes for in vivo calcium imaging in freely foraging mice, we identified distinct neuronal responses in the anterior olfactory (piriform) cortex (aPC) upon slow and binge eating; we observed clear excitatory flavor responses during slow eating but unspecific activity suppression upon binge eating. This binge-induced suppression is only observed in aPC, while neuronal responses in gustatory or somatosensory cortices remain similar in both slow and binge eating.

Mechanistically, odor inputs from olfactory bulb mitral cells remain stable upon binge eating, suggesting the suppression is not inherited from upstream elements of the olfactory pathway. Local inhibitory circuits in aPC do not play an active role in suppression, since aPC GABAergic neurons are also suppressed during binge eating. We further excluded inhibitory effects of dopaminergic and serotonergic modulation in aPC since dopamine and serotonin release are decreased upon slow and binge feeding.

We found that the strength of binge-induced suppression in the aPC predicts mice's total Ensure consumptions on different recording sessions and optogenetically suppressing aPC neurons upon binge eating in closed-loop experiments can promote feeding behaviors. Taken together, our results provide clear circuit mechanisms of binge-induced flavor modulation, which may contribute to binge-induced overeating due to reduced sensory feedback of food items.

A 04-04
Parvalbumin expressing excitatory neurons of the subiculum specifically project to areas involved in spatial navigation.

Gilda Baccini[1], Angelica Foggetti[1], Akos Kulik[2], Sören Brandt[1], Peer Wulff[1]

[1] *Christian-Albrechts Universität zu Kiel, Physiologisches institut, Kiel, Germany*
[2] *University of Freiburg, Institute of Physiology II, Freiburg, Germany*

The calcium-binding protein Parvalbumin (PV) is considered one of the most important neuronal markers since it identifies a subset of cortical inhibitory interneurons with specific electrical, morphological and connectivity properties. However, PV is also expressed in specific populations of pyramidal neurons of motor and visual cortex layer V, which have been reported to act as 'drivers' of feed-forward activity in subcortical areas.
The expression of PV may thus also define specific subclasses of excitatory neurons with particular functions within the circuit. In this study, we asked whether PV expression in glutamatergic principal cells of the archicortical hippocampal formation would also delineate a subgroup of neurons with specific connectivity and function. We show that PV-expressing principal cells are found exclusively in the deep layers of the distal dorsal subiculum. These neurons specifically project into regions functionally associated with spatial navigation, making synaptic connections with driver-like properties. In contrast to neighbouring principal cells in the distal subiculum, PV+ principal cells are regular firing. We propose that also in excitatory neurons, PV expression marks confined subgroups of neurons with specific connectivity and functional features.

Our work was supported by the Deutsche Forschungsgemeinschaft (DFG) FOR2143, and SFB 1461 (Project-ID 434434223)

A 04-05
“The role of the prefrontal cortex in the expression of learned safety and fear”

Ceylan-Scarlett Steinecke[1], Markus Fendt[2,3], Judith Kreutzmann[4], This poster is an excerpt from my master's thesis. The experiments and the master's thesis itself were done under the supervision of M. Fendt (and J. Kreutzmann) at the Otto-von-Guericke University Magdeburg.On behalf of CRC1461

[1] *Christian-Albrechts-University, Institute of Physiology, Kiel, Germany*
[2] *Otto-von-Guericke University, Institute of Pharmacology and Toxicology, Magdeburg, Germany*
[3] *Otto-von-Guericke University, Center of Behavioral Brain Sciences, Magdeburg, Germany*
[4] *Karolinska Institutet, C2 Medicinsk biokemi och biofysik, Stockholm, Sweden*

Question
[...] The ability to discriminate between danger and safety is crucial for adaptive behavior and thus for survival across species. While danger signals predict the occurrence of a potentially threatening event, safety signals indicate the absence of an aversive event, thus reducing fear and stress responses. Pavlovian conditioning permits an individual to learn associations between stimuli or events. Pavlovian fear conditioning is used in many species to study the neurobiology of fear learning and the processes that lead to pathological fear, such as in anxiety disorders or post-traumatic stress disorder (PTSD). Studies of learned safety and fear suggest that the prefrontal cortex (PFC) may modulate the expression of these responses.
Methods
[...] In this study it was investigated whether transient chemogenetic silencing of the ventromedial PFC (vmPFC) would block the retention of conditioned safety. To test this, male Sprague-Dawley rats (n = 49) were subjected to different protocols to induce fear and safety learning, both measured by the acoustic startle response.
Results
[...] Fear and safety memory were then tested in a retention test, it was found that none of the protocols used were able to induce a safety memory that could be retrieved under control conditions, however, after silencing the vmPFC, such safety memory could be observed.
Conclusions

[...] These unexpected data indicate that the vmPFC may actually hinder the retrieval or expression of learned safety. These surprising results will have to be studied in more detail in the future to further delineate which role the vmPFC plays in learned safety and fear. It is expected that this research to help in understanding the pathophysiology of disorders such as anxiety, PTSD or depression, and ultimately inform therapeutic approaches to combat some of these debilitating mental illnesses.

I was able to participate in this conference thanks to the Deutsche Forschungsgemeinschaft (DFG, German Research Foundation). SFB 1461.

A 04-06
Silencing of Cholecystokinin-expressing interneurons in the hippocampal CA1 region impairs social recognition memory

Kira Balueva[1], Laura Bollepalli[1,2], Peer Wulff[1]

[1] Christian-Albrechts University of Kiel, Institute of Physiology, Kiel, Germany
[2] Novartis Institutes for BioMedical Research, Novartis Pharma AG, Basel, Switzerland

Question

Social recognition memory is the ability to recognize and memorize familiar conspecifics and is critical for maintaining appropriate social relationships in all animal species. Conversely, impairment in social function is a prominent feature of several neuro-psychiatric disorders, such as autism spectrum disorders and schizophrenia.

In rodents, establishment of social memories relies on multisensory integration of olfactory, auditory and somatosensory cues. Early studies have shown that lesion of the entire hippocampus can impair social memory. In the last decade, several brain regions that form social recognition memory have been identified, including the dorsal CA2 and the ventral CA1 region of the hippocampus, as well as their upstream and downstream circuits: medial and lateral septum, supramammilary nucleus, nucleus accumbens and prefrontal cortex.

Currently, it is assumed that dorsal CA1 does not play an essential role in social behavior. However, this assumption is based on experiments in which either excitatory neurons or inhibitory parvalbumin-expressing neurons in dorsal CA1 had been inactivated.

Methods

We probed the relevance of cholecystokinin (CCK)-expressing interneurons in the dorsal CA1 for social memory by chemogenetic inactivation.

Results

Inactivation of CCK-expressing interneurons impaired discrimination of social, but not non-social, stimuli in mice, without causing any changes in sociability.

Conclusions

Our results suggest that CCK-expressing neurons in dorsal CA1 are required for social recognition memory formation.

A 04-07
Self-paced movement initiation and termination lead to complementary modulations of dopamine neuron firing rates in the medio-lateral axis of the substantia nigra

Daniela Schenkel[1], Marie Kuhn[2], Niklas Hammer[1], Pascal Vogel[1], Sebastian Betz[1], Gaby Schneider[2], Jochen Roeper[1]

[1] Goethe University Frankfurt, Institute of Neurophysiology, Frankfurt am Main, Germany
[2] Goethe University Frankfurt, Institute of Mathematics, Frankfurt am Main, Germany

Dopamine substantia nigra (DA SN) neurons are a major target of Parkinson disease (PD) and their loss is thought to contribute to the motor impairments in PD. Da Silva et al. (2018) demonstrated that subpopulations of DA SN neurons either increased or decreased their firing rates shortly before movement initiations. However, the functional topography of this diversity among DA neurons across the SN has not been fully characterized. We performed chronic multi-electrode recordings of pharmacologically identified DA SN neurons in awake freely-moving male C57Bl/6N mice, aged 8 – 16 weeks, while simultaneously tracking their head and body movements. Overall, our data set of n=59 (N=16) DA SN neurons was in accordance with the results by Da Silva and colleagues (2018) with about 30% of DA SN neurons (n=17/59) transiently

increasing their firing rate (baseline to maximum: +5.3 ± 4.8Hz, mean ± SD) shortly before initiation of self-paced movements and also about 30% of DA SN neurons (n=18/59) transiently decreasing their firing rate (baseline to minimum: -3.6 ± 1.2Hz, mean ± SD) shortly after initiation of self-paced movement in the open field. Additionally, about one third of those DA SN neurons with transient rate increases before movement initiation (n=6/17) also showed a rate reduction with termination of these movements (baseline to minimum: -1.9 ± 1.5Hz, mean ± SD). In contrast, two thirds of DA SN neurons with transient rate reductions before movement initiation (n=13/18) significantly increased their firing rate shortly before movement termination (baseline to maximum: +3.4 ± 1.5Hz, mean ± SD). Furthermore, we observed a frequency-selective increase in local field potential power (3-7 Hz oscillations) shortly before movement onset (baseline to maximum: +1.16 ± 0.71, mean ± SD) as well as after movement termination (baseline to maximum: +1.07 ± 0.67, mean ± SD) in the majority of animals (N=14/16) recorded across the whole SN. A more fine-grained topographical analysis revealed that DA neurons with transient rate reductions before movement initiation were predominantly found in the medial SN (n=11/22) compared to central SN (n=7/30). These responses were absent in the lateral SN (n=0/7). In contrast, the proportion of DA neurons with transient rate increases prior to movement initiation were more prominent in central SN (n=13/30) compared to medial SN (n=3/22) and lateral SN (n=1/7). In light of the functional topography of axonal projections of DA SN neurons (Farassat et al., 2019), our data suggest a differential involvement of distinct nigrostriatal projections in self-paced movement initiation and termination. However, definitive experiments require selective molecular tagging of distinct DA SN projections.

A 04-08
Olfactory memory consolidation in the mushroom body output layer in *Drosophila melanogaster*

Tania Fernandez del Valle Alquicira[1,3], Lisa Scheunemann[1,2], Eric Reynolds[1], Desiree Laber[1], Marine Balcou[1], David Owald[1]

[1] *Charité, Institute of Neurophysiology, Berlin, Germany*
[2] *FU, Berlin, Germany*
[3] *Einstein Center, Berlin, Germany*

Question

The location of olfactory memories in Drosophila melanogaster is well known, and the availability of genetic tools permits the dissection of the circuit underpinnings associated with different stages of memory, e.g. during consolidation, storage and retrieval.

In Drosophila, the mushroom bodies (MBs) are involved in storing different elements of reward and punishment associative memories. Here we aim to investigate the effects of blocking synaptic output of M4/6 MB output neurons and understand its effects on memory consolidation,

Methods

Behavior: Association of an odor with a stimulus was achieved by using a behavioral learning paradigm in the T-maze. After training, the synaptic output of diverse combinations of mushroom body output neurons was blocked via thermogenetic tools and memory performance was later assesed.

Physiology: In-vivo calcium imaging and training under the microscope.

Results

Our work now shows that blocking synaptic output of M4/6 MB output neurons interferes with memory consolidation, reverting aversive to appetitive memories. We show that this memory is distinct from appetitive sugar memories as it is not gated by the animal's hunger state. Moreover, in vivo imaging reveals that aversive training triggers ongoing activity in M4/6 MB output neurons, indicating post training network activity.

Conclusions

Activity after training of single neuron output can reprogram circuit activity and change memory outcome.

A 04-09
Monitoring memory performance after artificial induction of memory in Drosophila

Sridhar Jagannathan, David Owald

Charité – Universitätsmedizin Berlin, Institute of neurophysiology, Berlin, Germany

Question
Recent findings have revealed different forms of memory consolidation, with some dependent on sleep and others independent. Thus elucidating 'not all memory needs sleep'. However the effect of how internal states like thirst, hunger and sleep drive interact and interfere with memory consolidation is largely unknown. Here, we aim to establish a setup to study these unknowns.
Methods
We used Drosophila – 15 flies to artificially induce aversive memories using a closed loop system with aversive memory activiation and further 15 files under the control setup.
Results
We show using a combination of machine learning methods and ball tracking; the memory retrieval performance of drosophila under this system.
Conclusions
The protocol and methods described here will be used to study long-term memory consolidation. Further, we aim at probing the roles of sleep, food and thirst during the monitoring block or prior to the training block to understand the effect of internal states on memory formation and consolidation.

This work was supported by a Walter Benjamin fellowship awarded to S.R.J.

A 04-10
A highly versatile chemotaxis assay for investigating associative learning in undergraduate laboratories using the nematode *Caenorhabditis elegans*

Daniel-Cosmin Marcu[1], Ephraim I. Berthold[1,3], Karl E. Busch[1,2]

[1] *Health and Medical University, IMBB Institute for Mind, Brain and Behavior, Potsdam, Germany*
[2] *University of Edinburgh, Centre for Discovery Brain Sciences, Edinburgh, UK*
[3] *University of Oxford, Department for Physiology, Anatomy and Genetics, Oxford, UK*

Chemotaxis is a behaviour where an animal adjusts its locomotion in relation to the concentration gradient of an external chemical to find food sources, avoid environmental hazards, or locate mates. The nematode *Caenorhabditis elegans* exhibits a broad array of chemotaxis behaviours which, for a given chemical stimulus, can vary substantially depending on age, rearing conditions, environmental factors, and genetic background. Its small size, ease of handling, and ease of generating in large numbers make *C. elegans* an ideal model organism for use in undergraduate teaching towards understanding the physiological underpinnings of behaviour, chemosensation and learning.
Existing chemotaxis experiments in *C. elegans* rely on placing agar 'plugs' containing different concentrations of a chemical compound of interest onto an assay plate for several hours. This allows the chemical to diffuse into the assay plate. The plugs are then removed and animals previously conditioned for this compound are placed at the centre of the resulting chemical gradient and allowed to move freely on the plate. Such experiments rely on stable diffusion rates of the chemical compound from the plug into the experimental agar plate and make replication difficult. We developed a method of performing chemotaxis experiments in nematodes offering superior control of chemical concentrations. Using assay plates divided into quadrants by internal walls, we can pour agar with up to four different concentrations of the chemicals of interest onto a single plate, with contact between all quadrants at the centre of the plate. Animals placed at the centre of the plates are allowed to roam freely for a predetermined time before the number of individuals in each quadrant is assessed.
In this form, the assay becomes highly accessible to undergraduates with no or minimal laboratory experience: by simply washing the worms off a growth plate and into an Eppendorf tube, then pipetting a droplet of worm pellet onto the centre of the assay plate – marked visually by

the intersection of the internal walls - students can quickly and reliably assess the chemotaxis of hundreds of animals at a time in any variety of conditions desired by the educators. A chemotaxis index is then calculated from the worms' distribution on the plate. The experiment requires as little as 1-2 hours of preparation by staff on the day before the class and can be performed within the confines of a 2-3 hour course slot. The assay can be used to test for associative learning and can easily be adapted to test the effects of genotype, different chemicals or environmental contexts.

A 04-11
A virtual-reality based experimental setup for contact-free measurements of behavioural readouts of the lizard *Anolis carolinensis*

Niels Röhrdanz, Anil Menon, Peer Wulff

Christian-Albrechts-Universität zu Kiel, Institute of Physiology, Kiel, Germany

Question

The green anole lizard (*Anolis carolinensis*) is an interesting model organism to study in cognitive neuroscience. It shows a cortical architecture of reduced complexity compared to mammals. Whereas the hippocampus and other allocortical structures are already present, other structures like the neocortex seem to be missing. This raises the question which cognitive tasks the lizard brain can solve.

There are different approaches to study brain function in behavioural experiments: Those that rely on complex active behaviours (e.g. orienting in a maze) and those that rely on observable passive behaviour (e.g. in conditioning experiments). Experiments in reptiles that rely on active behaviour are difficult to implement, because of insufficient motivators due to differences in metabolism and different exploration strategies. Accordingly, passive behavioural readouts are a promising attempt to explore the lizards' cognitive abilities. They permit conclusions on mental processes or states (e.g. arousal, fear and exploration).

Methods

In this study, we aimed to establish a contact-free method to measure different behavioural readouts in the lizard *Anolis carolinensis*: Respiratory rate, head direction, head tilt, movement/ freezing and skin colour change. We used a virtual-reality based experimental testing chamber to present stimuli in a virtual natural context. This setup also allowed recording of the animals' behaviour in 360°. Postural data was extracted with the tracking software DeepLabCut. 21 points on the lizard's body were tracked.

Eight animals were recorded over a total of 15 sessions while different acoustic and visual stimuli were presented (neutral or predator).

Results

The lizards responded differently to the different stimulus-categories. Behaviour changed most strongly in response to acoustic stimuli. In particular calls of the natural predator, the red-tailed hawk, led to behavioural changes in the green anole lizard.

Conclusions

We present a method for reliable contact-free measurements of different behavioural readouts of the green anole lizard from 360° videos. Especially the approach of extracting respiratory rate from video data in reptiles is novel and provides a great advantage against wearable sensors. We anticipate this method to prove useful in the analysis of fear and stress also in other species.

This work was funded by the Deutsche Forschungsgemeinschaft (DFG, German Research Foundation). Project ID 434434223 - SFB 1461.

A 04-12
Time-invariant prefrontal activity patterns during repeated exposure to intense threat

Ole Christian Sylte[1,2], Hannah Muysers[1,2], Hung-Ling Chen[1], Marlene Bartos[1], Jonas-Frederic Sauer[1]

[1] *University of Freiburg, Medical Faculty, Institute of Physiology 1, Freiburg, Germany*
[2] *University of Freiburg, Faculty of Biology, Freiburg, Germany*

Intense threat elicits action in the form of active and passive coping. The medial prefrontal cortex (mPFC) executes top-level control over the selection of threat coping strategies, but the dynamics of mPFC activity upon continuing threat encounters remain unexplored. Here, we used

1-photon calcium imaging in mice to probe the activity of prefrontal pyramidal cells during repeated exposure to intense threat in a tail suspension (TS) paradigm. A subset of prefrontal neurons displayed selective activation during TS, which was stably maintained over days. During threat, neurons showed specific tuning to active or passive coping. These responses were unrelated to general motion tuning and persisted over days. Moreover, the neural manifold traversed by low-dimensional population activity remained stable over subsequent days of TS exposure and was preserved across individuals. These data thus reveal a specific, temporally and inter-individually conserved repertoire of prefrontal tuning to behavioral responses under threat.

This work was supported by the Else Kröner-Fresenius Stiftung (2019_A173 to J.-F.S.) and the German Research Foundation (grant SA3609/1-1 to J.-F.S. and FOR5159 – TP7 to J.-F.S. (grant SA 3609/2-1) and M.B. (grant BA 1582/16-1)).

A 05 | Pathophysiology of Neurons & Networks

A 05-01
Mechanisms of the olfactory dysfunction in the APPswe/PS1$_{G384A}$ mouse model of Alzheimer's disease

Wen-Yu Tzeng, Yury Kovalchuk, Katherine Figarella, Olga Garaschuk

University of Tübingen, Institute of Physiology, Department of Neurophysiology, Tübingen, Germany

Early olfactory dysfunction is a common feature of Alzheimer's disease (AD), with AD patients often showing impairments in odor detection threshold, odor identification and recognition capabilities as well as marked structural and biochemical alterations in the olfactory bulb and the entorhinal cortex, brain regions important for olfaction. The exact cellular/molecular mechanisms underlying the olfactory impairment in AD remain, however, unclear. Here, we investigated the mechanisms of olfactory dysfunction in an APPswe/PS1$_{G384A}$ double transgenic mouse model of AD, overexpressing the human amyloid precursor protein (APP) with the Swedish mutation (KM670/671NL) and a mutant presenilin 1 [Gly384→Ala384 mutation (G384A)] under the control of Thy-1 promoter.

As documented by a buried food pellet test, odor detection was impaired already in 5- to 7-month-old APPswe/PS1$_{G384A}$ mice. A significantly increased time spent searching for buried food compared to wild-type (WT) mice was also observed in 9- to 13- month-old APPswe/PS1$_{G384A}$ mice. Using *in vivo* two-photon Ca^{2+} imaging with the Förster resonance energy transfer-based Ca^{2+} indicator Twitch-2B, we evaluated the ongoing Ca^{2+} signaling and odor-evoked responses in dorsal glomeruli of WT and APPswe/PS1$_{G384A}$ mice. Remarkably, the level of ongoing Ca^{2+} signaling in the dorsal glomeruli was significantly lower in 5- to 7-month-old APPswe/PS1$_{G384A}$ compared to WT mice. The stability of the ongoing Ca^{2+} signaling in dorsal glomeruli was analyzed by comparing glomerular Ca^{2+} levels at days 0, 3, 6 and 21. The glomerular Ca^{2+} levels in 5- to 7-month-old WT and APPswe/PS1$_{G384A}$ mice remained stable from day 0 through 21, indicating that glomerular Ca^{2+} levels in AD mice are consistently lower compared to WT mice. Furthermore, the 5-7 months old group of APPswe/PS1$_{G384A}$ mice exhibited odor-evoked responses with significantly higher $LogEC_{50}$ compared to WT mice.

Taken together, our study demonstrates that APPswe/PS1$_{G384A}$ mice exhibited early dysfunction in olfaction accompanied by a sustained decrease in glomerular Ca^{2+} levels in the dorsal glomeruli, as well as lower sensitivity to odorants. When further analyzed mechanistically, the association between low glomerular Ca^{2+} levels and olfactory dysfunction might pave the way for novel therapeutic strategies for fighting this devastating disorder.

A 05-02
Investigating BACE1's role in mechanosensation and sensory processing

Sarina Höller, Iwona Izydorczyk, Birgit Vogler, Christian Alzheimer, Susanne Sauer, Tobias Huth

Friedrich-Alexander University, Institute for Physiology and Pathophysiology, Erlangen, Germany

Introduction

The β-site APP cleaving enzyme1 (BACE1) accounts for the rate-limiting step in the production of toxic β-amyloid (Aβ) in Alzheimer's disease (AD). Pharmacological intervention targeting BACE1 did not improve cognition in AD patients. Therefore, unraveling physiological functions of the β-secretase is of mandatory interest. Increasing evidence suggests an involvement of BACE1 in peripheral sensory processing, including proprioception, pain and thermosensation. BACE1$^{-/-}$ mice have been reported to exhibit altered thermal thresholds (heat) [1, 2], a decreased number and impaired formation of muscle spindles [3], reduced number of Pacinian corpuscles in the skin [4], as well as deficits in myelination of peripheral nerves [1, 5].

Methods

Further investigating BACE1's role in mechanosensation, we investigated Merkel cells in glabrous skin of BACE1$^{-/-}$ mice and littermates by immunofluorescent stainings. We also recorded action potentials, as well as mechanically evoked currents (poke-method) of dorsal root ganglia (DRG) neurons of BACE1$^{-/-}$ mice to study corresponding sensory afferents. Finally, we examined potential interactions of BACE1 with mechanosensitive Piezo channels in a transiently transfected HEK cell system.

Results

We found significantly reduced numbers of Merkel cells in walking pads of glabrous skin of mice lacking BACE1. Furthermore, BACE1$^{-/-}$ DRG neurons showed a higher frequency of action potential firing. In response to mechanical stimulation, in BACE1$^{-/-}$ DRG neurons with large mechanosensitive currents we observed reduced latencies. Otherwise, Piezo 1 and 2 currents were not significantly altered in the presence of co-expressed BACE1, although minor reduction of current amplitude and increase of decay time occurred.

Conclusions

Our data reinforces the idea that BACE1 contributes to peripheral sensory processing and suggests an involvement of BACE1 in mechanosensation. Diminished number of Merkel cells in glabrous skin of BACE1$^{-/-}$ mice is in line with previous reports of other mechanosensors and might be attributed to BACE1's processing of neuregulin. Furthermore, our data show that BACE1 has an impact on the mechanoelectrical transduction process and our action potential recordings of DRGs indicate that BACE1 alters excitability of sensory afferents. To examine the functional relevance of our data, we will perform comprehensive sensory testing of BACE1$^{-/-}$ mice.

References

[1] Hu X, Hicks CW, He W, Wong P, MacKlin WB, Trapp BD, et al. Bace1 modulates myelination in the central and peripheral nervous system. Nat Neurosci. 2006;9(12):1520–5.

[2] Weber M, Wu T, Meilandt WJ, Dominguez SL, Solanoy HO, Maloney JA, et al. BACE1 across species: A comparison of the in vivo consequences of BACE1 deletion in mice and rats. Sci Rep. 2017;7(February):1–17.

[3] Cheret C, Willem M, Fricker FR, Wende H, Wulf-Goldenberg A, Tahirovic S, et al. Bace1 and Neuregulin-1 cooperate to control formation and maintenance of muscle spindles. EMBO J [Internet]. 2013;32(14):2015–28. Available from: http://dx.doi.org/10.1038/emboj.2013.146

[4] Fleming MS, Li JJ, Ramos D, Li T, Talmage DA, Shin-Ichi Abe, et al. A RET-ER81-NRG1 signaling pathway drives the development of pacinian corpuscles. J Neurosci. 2016;36(40):10337–55.

[5] Willem M, Garratt AN, Novak B, Citron M, Kaufmann S, Rittger A, et al. Control of peripheral nerve myelination by the β-secretase BACE1. Science (80-). 2006;314(5799):664–6.

A 05-03
Effects of pubertal stress on affective behavior and GABAergic inhibition in dentate gyrus of adult mice

Sriity Melley Sadanandan[1], Fang Zheng[1], Liubov S Kalinichenko[2], Christian P. Müller[2], Christian Alzheimer[1]

[1] Friedrich-Alexander-Universität Erlangen-Nürnberg, Institute for Physiology and Pathophysiology, Erlangen, Germany
[2] Department of Psychiatry and Psychotherapy, Universitätsklinikum, Friedrich-Alexander- Universität Erlangen-Nürnberg, Erlangen, Germany

Adolescence is a critical period associated with behavioral and emotional changes. Aversive challenges like chronic stress during this period may increase the likelihood of neuropsychiatric disorders later in life. However, the pathophysiological mechanisms rendering the adult brain susceptible remain largely unknown. Studies have indicated an increase in $GABA_A$ receptors during this late developmental stage. Our previous work showed that activin, a member of the TGF-β family, modulates hippocampal GABAergic inhibition and impacts anxiety-like behavior,

as indicated by a comparison between wild type mice and transgenic mice expressing a dominant-negative mutant of activin receptor IB (dnActRIB). To compare the neuronal circuitry during adolescence (P30-45) and in adulthood (P90-P120), we systemically examined GABAergic inhibition in granule cells of the dentate gyrus (DG), a hippocampal region closely linked to the antidepressant effect of activin

signaling. Whole-cell voltage-clamp recordings from DG granule cells showed a significant decrease in GABAergic inhibitory postsynaptic currents (IPSCs) in granule cells from adolescent mice in dorsal DG, compared to those from adult mice. To elucidate the mechanisms involved in adolescent stress and its effects in adulthood, we established a behavioral model by administering corticosterone during adolescence (P30-P45). A depression-like phenotype in adulthood was manifested in the forced swim test with higher immobility in wild type mice, but not in dnActRIB mice. The stressed mice also displayed higher locomotion in the open field test. These results suggest that adolescent stress produces a hyperlocomotive and depression-like phenotype in adulthood. Preliminary electrophysiological evidence suggests that in the dentate gyrus network, activin signaling modulates the long-term impact of adolescent stress on GABAergic inhibition.

We would like to thank Maria Schulte, Jana Schramm and Iwona Izydorczyk for their technical expertise.

A 05-04
Neurodegenerative tauopathy in biallelic SPRED2 loss-of-function mouse models elicited by autophagosomal dysfunction

Sina Gredy, Denis Hepbasli, Rebecca Holzapfel, Kai Schuh

Julius-Maximilians-University of Wuerzburg, Institute of Physiology, Wuerzburg, Germany

Question

The protein Tau is phosphorylated by MAPKs and then dissociates from microtubules and forms multimeric aggregates, a common marker of neurodegenerative tauopathies. SPRED proteins are potent inhibitors of the ERK-MAPK pathway (2) and play their inhibitory role in a variety of processes, in cardiovascular organ and brain development, hormonal homeostasis, carcinogenesis and metastasis (3). The ERK-MAPK pathway is an important signaling cascade controlling cell homoeostasis but also important steps of autophagy (1). Biallelic SPRED2 KO mice show clear alterations in autophagy related processes (4). We hypothesize that missing inhibition of MAPK by SPRED2 leads to an increase in Tau phosphorylation, dissociation from microtubules, and accumulation within the cell, the pathogenic mechanisms of tauopathies. Furthermore, dissociation of pTau from microtubules destabilizes them and impairs vesicle transport.

Methods

Brain morphology was investigated by MRI and histology. To analyze phosphorylated Tau aggregates in brains of SPRED2 KO mice, we did Western blot analyses and IHC. To check the interaction of SPERD2 with autophagy-related proteins we used pull down assays. Further, we used a Dynein/Kinesin ATPase End-Point Kit, to clarify if lack of SPRED2 influences Kinesin or Dynein ATPase activity.

Results

MRI and histology studies showed enlarged brain ventricles and cortex atrophy in KO brains. Western blots and IHC demonstrated hyperphosphorylated Tau aggregation in hippocampi of SPRED2 KO mice, a common finding in various neurodegenerative diseases. We detected SPRED2 interaction with SQSTM1/p62, an adapter guiding ubiquitinated proteins to LC3-mediated autophagy. GST pull-downs showed that full-length SPRED2 and the SPRED2-EVH1 domain interact with p62 in brain lysates. Western blot analyses revealed a decreased expression of p62 in SPRED2 KO brains, indicating that SPRED2 is required for p62 recruitment and autophagy induction. We detected a reduced autophagic flux (LC3-II/LC3-I ratio) in brains of SPRED2 KO mice. The Dynein/Kinesin ATPase End-Point Kit with vesicle preparations from WT and SPRED2 KO mice revealed that lack of SPRED2 impairs Dynein activity, responsible for retrograde transport in neurons, but not Kinesin activity.

Conclusions

Our data indicate that the autophagosomal dysfunction in SPRED2 KO mice is connected to a tauopathy. Identification of the molecular processes involved will be relevant in many areas of medical research, as a variety of diseases are triggered by disorders of intracellular transport and lack of fusion with lysosomes. In view of the fact that the first people with mutations in the SPRED2 gene have now been identified (5), the knowledge gained from this project is very important for a possible diagnosis or therapy of these surely rare diseases in humans.

This research was funded by Deutsche Forschungsgemeinschaft, project SCHU1600/6-1.

References
[1] Martinez-Lopez, N, Singh, R 2014 'ATGs: Scaffolds for MAPK/ERK signaling', *Autophagy* 10(3) 535-7
[2] Wakioka, T, Sasaki, A, Kato, R, Shouda, T, Matsumoto, A, Miyoshi, K, Tsuneoka, M, Komiya, S, Baron, R, Yoshimura, A 2001 'Spred is a Sprouty-related suppressor of Ras signalling', *Nature* 412(6847) 647-51
[3] Bundschu, K, Walter, U, Schuh, K 2007 'Getting a first clue about SPRED functions', *Bioessays* 29(9) 897-907
[4] Jiang, Km, Liu, M, Lin, G, Mao, B, Cheng, W, Liu, H, Gal, J, Zhu, H, Yuan, Z, Deng, W, Liu, Q, Gong, P, Bi, X, Meng, S 2016 'Tumor suppressor Spred2 interaction with LC3 promotes autophagosome maturation and induces autophagy-dependent cell death', *Oncotarget* 7(18) 25652-67
[5] Motta, M, Fasano, G, Gredy, S, Brinkmann, J, Bonnard, AA, Simsek-Kiper, PO, Gulec, EY, Essaddam, L, Utine, GE, Guarnetti Prandi, I, Venditti, M, Pantaleoni, F, Radio, FC, Ciolfi, A, Petrini, S, Consoli, F, Vignal, C, Hepbasli, D, Ullrich, M, de Boer, E, Vissers, LELM, Gritli, S, Rossi, C, De Luca, A, Ben Becher, S, Gelb, BD, Dallapiccola, B, Lauri, A, Chillemi, G, Schuh, K, Cavé, H, Zenker, M, Tartaglia, M 2021 'SPRED2 loss-of-function causes a recessive Noonan syndrome-like phenotype.' *Am J Hum Genet.* 108(11):2112-2129

A 05-05

Heavy adolescent drinking potentiates neuronal ethanol response later in life: involvement of GIRK current and activin receptor signaling

Fang Zheng, Sophia Stürzenberger, Nicolas Bülow, Christian Alzheimer

Friedrich-Alexander-Universität Erlangen-Nürnberg, Institute of Physiology and Pathophysiology, Erlangen, Germany

Question

Excessive ethanol consumption during adolescence is regarded as a risk factor for the development of alcoholism later in life, but the pathophysiological mechanisms that render the adult brain susceptible to ethanol are largely unknown. G protein-gated inwardly rectifying potassium (GIRK) channels are among the prime targets of ethanol to regulate neural activity in the brain. Previous work from our lab has demonstrated that activin A, a member of the TGF-β family, affects GIRK currents in mouse hippocampus. We asked here, (i) if hippocampal cells from adolescent and adult mice respond differently to alcohol exposure, and how GIRK channels are involved, (ii) how adolescent drinking affects alcohol response upon re-exposure in adulthood, and (iii) if activin plays a role as an adaptive factor.

Methods

Whole-cell patch-clamp recordings were performed from dentate gyrus granule cells (GCs) in dorsal hippocampal slices from adolescent and adult mice.

Results

In voltage-clamped GCs (at -70 mV), ethanol dose-dependently induced outward currents, which were significantly stronger in slices from adolescent compared to adult mice. Ethanol-evoked currents reversed near -90 mV, were largely diminished by the GIRK-inhibitor tertiapin Q, and were fully suppressed by low Ba^{2+}. Unexpectedly, the effects of recombinant activin A on ethanol responses were stage-dependent, being potentiated in adolescence, but inhibited in adulthood. The inverse was true when ethanol responses were re-examined in GCs from adolescent and adult transgenic mice expressing a dominant-negative activin receptor IB mutant, which disrupts activin receptor signaling. These data underscore the essential role of endogenous activin signaling in determining the neural impact of alcohol consumption at different stages of life. Compared to ethanol-naive mice, sustained heavy drinking in the dark (20% ethanol) between postnatal days 32 and 45 produced a long-lasting sensitization so that ethanol-induced currents in adulthood were consistently potentiated, including its tertiapin Q-sensitive component. Consequently, the adolescent drinking paradigm enhanced the silencing of GC firing during ethanol exposure.

Conclusions

Our results show that heavy adolescent drinking exerts a lasting impact on how GIRK channels react upon alcohol re-exposure later in life and that this process might possibly involve activin receptor signaling.

A 05-06
Heterogenous Distribution of cGMP in Neurons and Astrocytes in the awake brain of a mouse model of Alzheimer's disease

Aileen Jehle, Yury Kovalchuk, Olga Garaschuk

University of Tuebingen, Institute of Physiology, Department of Neurophysiology, Tuebingen, Germany

The cyclic guanosine monophosphate (cGMP) molecule acts as a secondary messenger in various signaling cascades in the body and brain, including long-term potentiation and inflammatory modulation. Dysregulation of the intracellular cGMP signaling is seen as an important factor contributing to Alzheimer's disease (AD). Although cGMP upregulation alleviated AD-related cognitive impairments in mouse models of the disease, previous clinical trials have yielded inconsistent results, calling for more insight into underlying cellular and molecular mechanisms.

Methods

Here we use chronic high-resolution *in vivo* two-photon imaging of neurons and astrocytes expressing the cGi500, a ratiometric FRET-based sensor for cGMP, to monitor the changes in the intracellular free cGMP concentration ($[cGMP]_i$) during the early stages of plaque deposition. We hypothesize that the deregulation of cGMP in the AD brain is non-uniform and depends on the cell type and proximity to the plaque. Through repeated measures of individual cells, we tracked the cGMP concentration in neurons and astrocytes during plaque development in the cortex of the APP23*PS45 mouse model.

Results

The data revealed different set points for $[cGMP]_i$ in neurons and astrocytes; a heterogeneous distribution of $[cGMP]_i$ between different cells of the same type and suggested that evoked cGMP production depends on the baseline cGMP concentration. In addition, the study revealed a differential expression of the cGMP-producing enzyme NO-GC.

Conclusions

Overall, our study provides evidence that the regulation of cGMP in the brain is more complex than previously believed, with distinct differences among and within different cell types. These insights highlight the importance of understanding the specific mechanisms involved in the deregulation of $[cGMP]_i$ in the amyloid-depositing brain and may help to guide the development of more effective treatment strategies.

A 05-07
Pronounced histopathology but unaltered and heterogeneous Cortical Spreading Depolarization (CSD) in a mouse model of Alzheimer's disease

Fátima Gimeno-Ferrer[1], Annett Eitner[3], Noor Noora[1], Reinhard Bauer[2], Christoph Schmidt-Hieber[1], Hans-Georg Schaible[1], **Frank Richter**[1]

[1] *University Hospital Jena, Institute of Physiology 1, Jena, Germany*
[2] *University Hospital Jena, Institute of Molecular Cell Biology, CMB-Center for Molecular Biomedicine, Jena, Germany*
[3] *University Hospital Jena, Department of Trauma, Hand and Reconstructive Surgery, Experimental Trauma Surgery, Jena, Germany*

Question

To evaluate the impact of Alzheimer's disease (AD) on cortical excitability and histopathology, we used the TASTPM mouse model of AD. TASTPM mice were bred from sperm provided by Glaxo Smith Kline Co (U.K.). To test whether AD interacts with parameters of cortical homeostasis, we recorded ongoing brain activity and induced cortical spreading depolarization (CSD) both in male and female TASTPM and in wildtype (WT) mice at ages of 3, 6, and 12 months, measured the size of the extracellular space (ECS) fraction, and stained for Amyloid-β (Aβ) deposits.

Methods

In spontaneously breathing anesthetized WT and TASTPM mice (sodium thiopentone, 100 mg/kg, i.p.) the direct current (DC-) electrocorticogram was recorded with arrays of glass microelectrodes in two cortical areas at a depth of 200-250 µm. The size of the ECS volume was assessed with the real time-tetramethylammonium (TMA) method. CSD were induced by microinjection of 1 M KCl. CSD-related

DC potential shifts, and changes in extracellular potassium concentration were monitored over a period of 4 h. After euthanasia, the fixed brains were stained for Aβ deposits, phosphorylated Tau (P-Tau) tangles, astroglia, and activated microglia.

Results

Aβ deposits in cortex were observed with ageing between 3 and 12 months after birth. P-Tau tangles were also detected in some cortical neurons at the age of 12 months. Microglial reaction (CD68, CD39 and Galectin-3) and astrogliosis (GFAP) in cerebral cortex progressively developed with the Aβ-plaques. Accumulation of Aβ in vessels was also observed. The estimation of ECS volume was inversely correlated with these histopathological findings. The TMA method indicated a shrinkage of the cortical ESC with development of AD. Based on our cortical histopathological findings, we recorded CSD in order to study if there was a correspondence between the histological damage in cortex induced by AD and the cortical function and homeostasis. Differences among sexes, ages and genotypes were observed and a large heterogeneity of CSD was found.

Conclusions

The observed changes in brain histology could not explain CSD-heterogeneity. However, a typical hyperexcitability in AD animals was manifested as convulsive behavior after thiopentone anesthesia. Thus, in the TASTPM model of neurodegeneration, replicable pathohistological changes have no well-defined correlation with functional parameters of homeostasis. This deserves future investigations.

This project has received funding from the European Union's Horizon 2020 research and innovation programme under the Marie Skłodowska-Curie grant agreement No 764860.

A 05-08

Shutdown of NHE1 is the primary event at presynapses upon chemically induced ischemia to avoid neurotoxicity

Martin Kahms, Tim Cebulla, Vera Kästingschäfer, Jürgen Klingauf

University Muenster, Institute of Medical Physics and Biophysics, Muenster, Germany

Pre- and postsynaptic mechanisms consume up to 55% of the total ATP used on action potentials. Here, we systematically analyzed the relative ATP demand of action potential generation and presynaptic processes such as exocytosis, release site clearance, Ca^{2+} clearance, endocytosis and SV reformation/refilling in primary hippocampal neurons. We found that chemical interference with ATP production does not affect the excitability of neurons immediately and that with respect to the synaptic vesicle cycle ATP depletion manifests earliest on the process of compensatory endocytosis. However, surprisingly we observed that ATP depletion causes an immediate shutdown of the sodium-proton-antiporter 1 (NHE1-transporter) leading to a block of cytosolic re-alkalinization upon stimulation-induced acidification. Furthermore, the impaired endocytosis phenotype upon ATP depletion can be mimicked by pharmacological block of NHE1 function and can be rescued by optogenetic restoration of the intracellular pH using the light-driven proton pump Arch3. We therefore hypothesize that impaired endocytosis is only a secondary consequence of ATP depletion while block of the NHE1 transporter is the primary effect leading to pronounced and sustained intracellular acidification. In this way, Na^+ toxicity is avoided by block of NHE1 mediated Na^+ influx, but at the expense of intracellular pH and synaptic vesicle recycling.

A 05-09

Conserved potential of the neuropeptide Galanin to inhibit Cortical Spreading Depolarization in rodents

Fatima Gimeno-Ferrer[1], Annett Eitner[2], Reinhard Bauer[3], Alfred Lehmenkühler[4], Hans-Georg Schaible[1], Frank Richter[1]

[1] *University Hospital Jena, Institute of Physiology I, Jena, Germany*
[2] *University Hospital Jena, Dept. of Trauma, Hand and Reconstructive Surgery, Experimental Trauma Surgery, Jena, Germany*
[3] *University Hospital Jena, Institute of Molecular Cell Biology, CMB-Center for Molecular Biomedicine, Jena, Germany*
[4] *Pain Institute & Center for Medical Education, Düsseldorf, Germany*

Question

The neuropeptide Galanin (Gal) has pleiotropic functions ranging from influencing the release of hormones in hypothalamus, control of the release of neurotransmitters in hippocampus, control of food intake, sleep and stress resilience. Here, we investigated its effects on cortical spreading depolarization (CSD) and neuronal excitability represented in parameters of the electroencephalographic activity in rats and mice.

Methods

In spontaneously breathing anesthetized adult rats (sodium thiopentone, 100 mg/kg, i.p.) we recorded the electrocorticogram with arrays of glass microelectrodes in two areas (treated and untreated) at a cortical depth of 400 µm. A wall made from dental acrylic separated both areas. In spontaneously breathing anesthetized 3 to 6 months old C57/BL6 mice (sodium thiopentone, 100 mg/kg, i.p.), we recorded only in one area (control phase: ACSF; treatment phase: Gal) at one cortical depth of 250 µm. CSD were induced by KCl microinjection. CSD-related direct current (DC) potential shifts, changes in extracellular potassium concentration and in regional cerebral blood flow (only in rats) were continuously monitored. We applied Gal at 10^{-7} M for 3 h in rats and for 1 h in mice. Control cortical slices from rats and mice were stained for localization of Gal.

Results

Gal has been identified in all cortical neurons of both rats and mice. After topical application of Gal at 10^{-7} M on the cortex we found a decrease of brain excitability. In rats, we observed responding and non-responding animals (Gal had effect vs. no effect of Gal at all). Here CSD amplitude within 3 h significantly decreased to 67.1 ± 17.2 % of controls (mean value ± standard error, all rats pooled). In mice, CSD amplitude decreased within 1 h to 65.4 ± 19.1 %. CSD propagation velocity in rats decreased to 82.9 ± 6.3 % of controls within 3 h and in mice within 1 h to 67.2 ± 17.1 %. In the same time interval of application (1 h of Gal) only a change in threshold for CSD elicitation in mice was observed, CSD threshold in rats did not change. However, after 3 h of Gal in rat, an increase in CSD threshold similar to mice was seen. In contrast to rats, the effect of Gal in mice was more consistent, all mice responded in a similar manner.

Conclusions

We conclude that Gal has the potential to decrease the generation of CSDs in both rat and mouse cortex. The shorter time interval to induce this inhibition in mice after topical application is probably due to the thinner cortex. Thus, protection against potentially damaging cortical mass depolarization by Gal is conserved in both rodent species.

This project has received funding from the European Union´s Horizon 2020 research and innovation programme under the Marie Skłodowska-Curie grant agreement No 764860.

A 05-10
Hippocampal spiking activity during Local Field Potential events in a Scn2a epilepsy model.

Daniil Kirianov[1,2], Yana Reva[1,2], Katharina Ulrich[1,2], Birgit Engeland[1,2], Stephan Marguet[1,2], Dirk Isbrandt[1,2]

[1] *DZNE e.V. German Center for Neurodegenerative Diseases, Experimental Neurophysiology, Bonn, Germany*
[2] *University of Cologne, Institute for Molecular and Behavioral Neuroscience, Cologne, Germany*

The $Na_v1.2$ sodium channel has been linked to awide range of neurodevelopmental disorders, including epilepsy and autism spectrum disorder. In particular, a p.A263V missense mutation [1] in *SCN2A* has been identified to underlie a form of therapy-resistant neonatal epilepsy in human patients. To further investigate this disease and identify potential treatment strategies, we engineered a mouse line carrying the p.A263V mutation in *Scn2a*. We found that both heterozygous and homozygous mice exhibited hippocampal seizures starting at postnatal day 6-7.

We recorded from hippocampal and cortical regions in awake, restrained head-fixed mouse pups or in awake, head-fixed adult mice moving in a “Mobile HomeCage” setup within an air-floating arena. In addition to quantifying the dynamics of seizure activity, we sought to identify and characterize behavioral and intellectual comorbidities, to relate them to those observed in human patients. Finally, we assessed specific hippocampal Local Field Potential events, known as Sharp Waves in neonatal animals and Sharp Wave Ripples [2] in adults, which are known to be strongly associated with memory consolidation. We analyzed and compared the profiles and dynamics of these events, and neuronal spiking activity during these events, in *Scn2a* mutants and wild-type littermates.

Our analyses revealed changes in the distribution and amplitude of certain types of Sharp Waves in neonatal mutant animals. We also observed differences in hippocampal spiking activity of mutant mice when compared to control animals.

References
[1] Y. Liao et al. SCN2A mutation associated with neonatal epilepsy, late-onset episodic ataxia, myoclonus, and pain, Neurology. 2010.

[2] Gyorgy Buzsaki, Hippocampal Sharp Wave-Ripple: A Cognitive Biomarkerfor Episodic Memory and Planning, HIPPOCAMPUS, 2015

A 05-11
Healthy male first-year students do not experience stress in the new environment as evidenced by mental chronometry

Ketevan Janashia, Ana Chikviladze, Aleksandre Ramishvili, Nikoloz Tvildiani

David Tvildiani Medical University, Central Scientific Research Laboratory, Tbilisi, Georgia

Question

Studies note that some aspects of hard and stressful teaching can negatively affect medical students' mental and emotional health (1, 2). The objective of our study was to test a hypothesis whether first-year medical students due to the new stressful environment have shown worse performance or not compared to second-year students.

Methods

Using mental chronometry as a measurement tool in the acute stress recognition virtual model, healthy male first-year (n=14) and second-year students (n=13) were exposed to two randomized order increased visual complexity tasks, based on the simple and discrimination sensorimotor reaction time (SSMRT; DSMRT), in 25 min. lab experiments.

Results

The means and standard deviations (SD) during SSMRT and DSMRT for both courses were calculated:

Mean SSMRT1=0.3565s; SD SSMRT1=0.1445s; mean DSMRT1=0.6683s; SD DSMRT1=0.1404s;

Mean SSMRT2=0.2752s; SD SSMRT2=0.1233s; mean DSMRT2=0.5759s; SD DSMRT2=0.1022s.

There were no statistically significant differences between the different means and SDs.

Then we calculated the Pearson correlation coefficient to reveal linearity between means and SDs and coefficient of variation (CV=SD/Mean) (3, 4):

r=-0.116; CV SSMRT1=0.388889; CV SSMRT2=0.428571; CV DSMRT1=0.208955; CV DSMRT2=0.172414.

There were no linear correlations between the SDs and means of different groups and no significant differences between the different CVs.

Conclusions

These findings mean a new environment such as acute visual stress in the virtual model does not negatively affect healthy male first-year students mental chronometry compared to second-year students. First-year students have shown well performance, well problem-solving, and less adaptation stress to the new environment, this is explained by no individual differences between students of both courses, their almost equal high mental abilities, and the mobile nervous system of healthy males (5). Our results contribute to a better understanding of the psychophysiology of mental chronometry and help the discovery of the factors that affect processing speed.

References

[1] Dyrbye, LN, Thomas, MR, Shanafelt, TD 2005, 'Medical student distress: causes, consequences, and proposed solutions', *Mayo Clinic Proceedings*, 80(12):1613-22, doi:10.4065/80.12.1613

[2] Guthrie, EA, Black, D, Shaw, CM, Hamilton, J, Creed, FH, Tomenson, B 1997, 'Psychological stress in medical students: a comparison of two very different university courses', *Stress Medicine*, 179–84. doi:10.1002/(SICI)1099-1700(199707)13:3<179::AID-SMI740>3.0.CO;2-E

[3] Wagenmakers, E, Brown, S 2007, 'On the linear relation between the mean and the standard deviation of a response time distribution' *Psychological Review,* (114), 830–841, doi:https://doi.org/10.1037/0033-295X.114.3.830

[4] Puth, MT, Neuhäuser, M, Ruxton, GD 2014, 'Effective use of Pearson's product–moment correlation coefficient', *Animal Behaviour,* 93, 183-189. doi:https://doi.org/10.1016/j.anbehav.2014.05.003

[5] van Ravenzwaaij, D, Donkin, C, Vandekerckhove, J 2011, ' An integrated perspective on the relation between response speed and intelligence', *Cognition*, 381–393, doi:10.1016/j.cognition.2011.02.002.

A 05-12
The oxygen-sensing pathway in neural cells controls intrinsic long-term neuroregeneration after ischemic stroke

Pinar Kilic, Hugo Marti, Reiner Kunze

Heidelberg University, Institute of Physiology and Pathophysiology, Department of Cardiovascular Physiology, Heidelberg, Germany

Question

Cerebral hypoxia, a hallmark of ischemic stroke, initiates adaptive endogenous processes that mitigate acute neuronal cell death and promote long-term neuroregeneration. The latter involves upregulation of genes that drive angiogenesis, neurogenesis, and neuroplasticity through the activation of hypoxia-inducible factors (HIFs), whose activity is regulated by prolyl-4-hydroxylase domain (PHD) proteins in an oxygen-dependent manner. The present project aims to investigate whether the PHD-HIF axis regulates long-term regenerative processes in the stroke-damaged brain, and, thus, might serve as a potential molecular target for a pharmacological neurorestorative stroke therapy.

Methods

The tamoxifen-inducible Cre-loxP system was used to generate transgenic mice deficient for (i) PHD2 (*inPhd2*$^{\Delta/\Delta}$) and (ii) HIF-1α/HIF-2α (*inHif1a/Hif2a*$^{\Delta\Delta/\Delta\Delta}$) in neurons. In a pharmacological approach, C57BL/6 mice were treated with Roxadustat, a low-molecular-weight and blood-brain barrier permeable PHD inhibitor. A low and high dosage of Roxadustat or vehicle solution were systemically applied to mice three times a week from day 4 to 15 post-stroke. Mice were subjected to either transient middle cerebral artery occlusion or sham surgery followed by 42-56 days of reperfusion. The sensorimotor function was determined by evaluation of a modified Neurological Severity Score, Rotarod motor performance test, adhesive removal test, and pole test. Cresyl violet staining was applied to quantify brain tissue atrophy.

Results

In comparison to *Phd2*$^{f/f}$littermates, *inPhd2*$^{\Delta/\Delta}$ mice showed markedly reduced sensorimotor impairment from subacute to chronic stages after stroke. In contrast, *inHif1a/Hif2a*$^{\Delta\Delta/\Delta\Delta}$ mice exhibited more severe sensorimotor impairment as compared to *Hif1a/Hif2a*$^{f/f}$littermates. Delayed pharmacological activation of the HIF pathway in the brain by both low and high dosed Roxadustat substantially improved the sensorimotor performance during subacute and chronic stages after stroke compared to vehicle-treated animals. Interestingly, the extent of brain tissue atrophy due to ischemic stroke was not affected by either activation or inactivation of the HIF pathway, suggesting that HIF-dependent processes improve functional recovery primarily through triggering compensatory neural rewiring in stroke-denervated areas.

Conclusions

Based on these findings, we hypothesize that the HIF pathway in brain-resident cells promotes adaptive neuroplasticity after stroke. In addition, our results may provide the basis for a new therapeutic approach to promote the long-term regeneration of sensorimotor functions upon ischemic stroke with a drug that is already approved for the treatment of chronic diseases in humans. Further experiments including ribosome tagging, anterograde axonal tracing, and histological analysis will be conducted to investigate the plasticity-related gene network and axonal as well as dendritic plasticity.

A 06 | Lung & Right Heart

A 06-01
A role for syntaxin 3 in airway mucus secretion

Hanna Meid, Giorgio Fois, Manfred Frick

University of Ulm, Department of General Physiology, Ulm, Germany

Airway mucus forms an essential barrier that protects the lungs from inhaled particles, pathogens and chemicals. These toxicants are entrapped in mucus, then swept out of the lungs by ciliary action. The main components of airway mucus, mucin 5B (MUC5B) and mucin 5AC (MUC5AC), are secreted via exocytosis from secretory airway epithelial cells. Mucins are secreted at a low baseline rate and a high stimulated rate. Baseline rate supports steady-state mucociliary clearance. Stimulated mucin secretion occurs in response to airway inflammation.

However, excessive mucin hyperproduction and secretion causes pathologic airflow obstruction and infection and results in severe lung diseases, including asthma, COPD and interstitial lung diseases. Baseline and stimulated secretion are mediated by different core exocytic machineries. Delineating the distinct core exocytic machinery offers new avenues for therapeutic manipulation of mucin hypersecretion [1]. Here we set out to delineate the role of syntaxins in mucin secretion.

Primary human airway epithelial cells (hAEpCs) were cultivated for 28 days on air liquid interphase (ALI). We next analyzed expression of syntaxins (STXs) under control and mucous metaplastic conditions (10 ng/ml IL-13 for 21 days) in secretory cells. To this end we established a new FACS-based assay to isolate fully-differentiated secretory airway cells from ALI cultures. Cell identity was confirmed by analyzing the expression of marker genes for specific epithelial cell types (ciliated, club, goblet, basal cells) by RT-PCR. STX expression and cellular localization were confirmed by immunofluorescence labelling (IF). Based on these results we analyzed the role of syntaxin 3 (STX3) on baseline and stimulated mucus secretion. hAEpCs were treated every second day with anti-sense oligonucleotides (1µM ASOs) to knock down (KD) *STX3*. KD efficiency was analyzed by IF and Western blot (WB) confirming specific and significant KD of *STX3*. Next, we analyzed the effect of *STX3* KD on baseline and stimulated secretion of MUC5AC using a recently described, WB based assay [1].

Together, our data confirm expression of *STX3* in secretory airway cells and a likely role thereof in mucin secretion.

References
[1] Lai Y., Fois G., Flores J.R., Tuvim M.J., Zhou Q., Yang K., Leitz J., Peters J., Zhang Y., Pfuetzner R.A., Esquivies L., Jones P., Frick M.*, Dickey B.F.*, Brunger A.T.* (2022). Inhibition of Ca^{2+}-triggered secretion by hydrocarbon-stapled peptides. *Nature*, 603(7903):949-956

A 06-02
Role of beta arrestin 1 in respiratory pathophysiology

Annika Simon[1], Stefanie Darnauer[1], Anja Vöge[1], Daniela Wenzel[1,2]

[1] *Ruhr-University Bochum, Department of Systems Physiology, Medical Faculty, Bochum, Germany*
[2] *University of Bonn, Institute of Physiology I, Medical Faculty, Bonn, Germany*

Question

Obstructive lung diseases characterized by elevated airway resistance are a major public health problem and represent a leading cause of morbidity and mortality in children and adults worldwide. Current treatment regimens mainly target G protein-coupled receptors (GPCRs) to lower airway tone. Beta arrestins are ubiquitously expressed cytosolic proteins that can modulate GPCR signaling or act as scaffolding proteins Thereby, beta arrestins are also involved in the pathophysiology of numerous diseases. Interestingly, the absence of beta arrestin2 has been shown to prevent the development of allergic asthma by defective macrophage-derived chemokine–mediated CD4+ T cell migration to the lung. However, the role of betaarrestin1 in the development of obstructive pulmonary disease is still unclear.

Methods

In our first experiments we analyzed the impact of beta arrestin1 (beta arr1) on airway tone and inflammation in the ovalbumin (OVA)-induced asthma models. Therefore, C57BL/6 WT and beta arr1$^{-/-}$ mice were sensitized on days 0 and 14 by i.p. injection of 20 µg OVA in 2 mg Alum followed by challenge with 1% OVA inhalation on d21-23, analysis was performed on d24 and d25. Successful asthma induction was confirmed by elevated cell counts in the bronchoalveolar lavage fluid (BALF) and a prominent cell invasion around the airways as determined by H&E stainings of lung sections. For analysis, we first determined airway resistance using flexiVent measurements and quantified inflammatory cells in BALF after DiffQuick staining.

Results

Flexivent measurements revealed airway hyperresponsiveness (AHR) in WT animals with OVA asthma (Rrs at 50 mg/ml MCh (Rrs 50): 6.5±0.7 cmH2O.s/ml, n=4) compared to NaCl control group (Rrs 50: 3.6±1.3 cmH2O.s/ml, n=5, **p*=0.04). In asthmatic beta arr1$^{-/-}$ mice AHR was much stronger (Rrs 50: 10.6±0.6 cmH2O.s/ml, n=4, **p*=0.01 compared to asthmatic WT. Also in BALF we found a distinct increase in total cell counts (TC; OVA: 7.1±1.4 x 10^4 1/ml, n=4; NaCl: 2.9±0.9 x 10^4 1/ml, n=5, **p*=0.04) and eosinophils (Eos) (OVA: Eos 26000± 6000 x 10^1 1/ml, 36.7±4.1% Eos of TC, n=4; NaCl: Eos 5.2±5.2 x 10^1 1/ml, 0.3±0.3% Eos of TC, n=5, ***p*=0.0018) in OVA WT vs NaCl WT mice.

Again, these changes were much more pronounced in asthmatic beta arr1$^{-/-}$ compared to OVA WT mice for TC (OVA: 39.3±10.5 x 10^4 1/ml, n=8) as well as Eos (334000±102000 x 10^1 1/ml, 82.7±4.0% Eos of TC, n=8).

Conclusions

Our results highlight that arrestin 1 may play an important role in the pathophysiology of obstructive lung diseases. Further analyses will have to reveal the underlying mechanism.

A 06-03
The Impact of SARS-CoV-2 M Protein on Tight Junctions in Lung Epithelial Cells

Lara A. Gutjahr[1], Lennart Koepke[2], Konstantin M. Sparrer[2], Frank Kirchhoff[2], Paul Dietl[1], Oliver H. Wittekindt[1]

[1] *Universität Ulm, Allgemeine Physiologie, Ulm, Germany*
[2] *Universität Ulm, Molecular Virology, Ulm, Germany*

Question

SARS-CoV-2, the causative agent of COVID19, infects and damages lung epithelia. The SARS-CoV-2 Membrane protein (M), one of the four structural proteins of SARS-CoV-2, has been shown to interfere with intracellular transport of trans-membrane proteins (Boson et al., 2021). Transmembrane spanning proteins like claudins establish tight junctions (TJ) that seal epithelia. TJ are mainly formed by claudins, an individual protein superfamily. They determine the functional properties of TJ. Thus, we hypothesized that M is involved in epithelial damaging processes via perturbing intracellular transport. To test this hypothesis, we assessed the impact of SARS-CoV-2 M on epithelial integrity and protein assembly at tight junctions (TJ).

Methods

To express the M protein individually, we transduced NCI-H441 cells with lentiviral expression vectors and differentiated them at air-liquid interface conditions to obtain functional epithelia. TJ protein expression was analyzed by semi-quantitative real time PCR. TJ protein assembly was tested in immunofluorescence experiments. Epithelial permeability and integrity were measured using impedance spectrometry.

Results

M protein expression was confirmed in 30% of transduced cells. This is in the range of the infection rate after 48 hours of infection with SARS-CoV-2, as we observed in human primary lung epithelial cells. The most abundantly expressed claudins in lung epithelia cells were cldn1, cldn10, cldn12 and cldn4, with highest expression of cldn4. Z-score analysis revealed significant downregulation of cldn8 upon M protein expression by 1.6-fold compared to transduced control cells that express GFP. Although cldn8 levels were reduced, we were not able to detect any changes in ion permeability by TEER measurements in M transduced lung epithelia.

Conclusions

We have previously shown that cldn8 has an influence on TJ protein assembly. Probably, SARS-CoV-2 M plays an essential role in lung damage through tight junction dysregulation by downregulating cldn8 expression.

Supported by Deutsche Forschungsgemeinschaft (DFG) grant 458685876

References

[1] Boson, B., Legros, V., Zhou, B., Siret, E., Mathieu, C., Cosset, F.-L., Lavillette, D., & Denolly, S. (2021). The SARS-CoV-2 envelope and membrane proteins modulate maturation and retention of the spike protein, allowing assembly of virus-like particles. *Journal of Biological Chemistry*, *296*, 100111. https://doi.org/10.1074/jbc.RA120.016175

A 06-04

The relationship between air pollution and fractional exhaled nitric oxide in primary school children after walking roadside and park routes at school pick-up time.

Scarlett Moloney, Gavin Devereux

University of Suffolk, School of Health and Sports Sciences, Ipswich, UK

Question

Participating in active travel to and from school is encouraged as daily exercise for children[1]. However, air pollution is the largest environmental risk factor for premature death[2], exacerbates respiratory diseases and is associated with deficits in children's lung function[3]. It is also a contemporary public policy issue that considers car idling rules and policies around schools.

There is a lack of intervention studies that investigate the combined effects of physical activity and the environment on respiratory physiology, especially in children. The study aims to investigate the relationship between air pollution and airway inflammation in primary school children at school pick-up time, and to report on the feasibility of implementing the research methods around the school day.

Methods

18 children (9.6 ± 1.0 years) completed a crossover design study, involving six 30-minute outdoor walks immediately after a school day starting at 15:10 GMT. Three walks followed a roadside route, and three were in a park located beside the school, the order of which were counterbalanced. Each walk was separated by 7-days. Fractional exhaled nitric oxide (FeNO) was measured before and after each walk. Intraclass Corelation Coefficient (ICC) with 95% confidence interval was used for all pre-walk absolute FeNO (ppb) measurements to determine reliability of pre-walk values. A paired sample *t*-test was used to assess for a difference between the average pre- and post-walk FeNO values for the three roadside and three park walks. Repeated measures ANOVA was used to assess for differences in both FeNO change scores, and measured air pollutants of fine particulate matter ($PM_{2.5}$), coarse particulate matter (PM_{10}), and volatile organic compounds (VOCs), for both conditions. Significance was set at $P < 0.05$.

Results

The ICC for all pre-walk FeNO was 0.882, classified as good[4] (0.792 – 0.947; Figure 1). There was a difference (reduction) in pre- *vs.* post FeNO values for both roadside (20.87 ± 17.14 *vs.* 18.96 ± 15.63 ppb, $P = 0.006$) and park walks (19.13 ± 2.22 *vs.*16.60 ± 2.74 ppb, $P < 0.001$). However, there were no differences in FeNO change scores between any of the roadside and park walk sessions (Figure 2). $PM_{2.5}$, (5.9 ± 2.2 vs. 6.5 ± 2.6 $mg.m^3$) PM_{10} (14.9 ± 11.9 vs. 14.8 ± 8.1 $mg.m^3$) and VOCs (132 ± 91 vs. 80 ± 50 ppb) were not different between roadside and park conditions respectively.

Conclusions

Consistent FeNO values were measured at baseline on six separate occasions, suggesting that FeNO can be reliably measured at the end of a school day, with little control over participant behaviour in the hours prior to taking FeNO measurements. The modest reductions in FeNO after walking are consistent with previous research involving light to moderate exercise[5]. Despite this, there were no differences in airway inflammation between roadside and park routes (Figure 2), which is not surprising given the similar levels of particulate matter in both conditions.

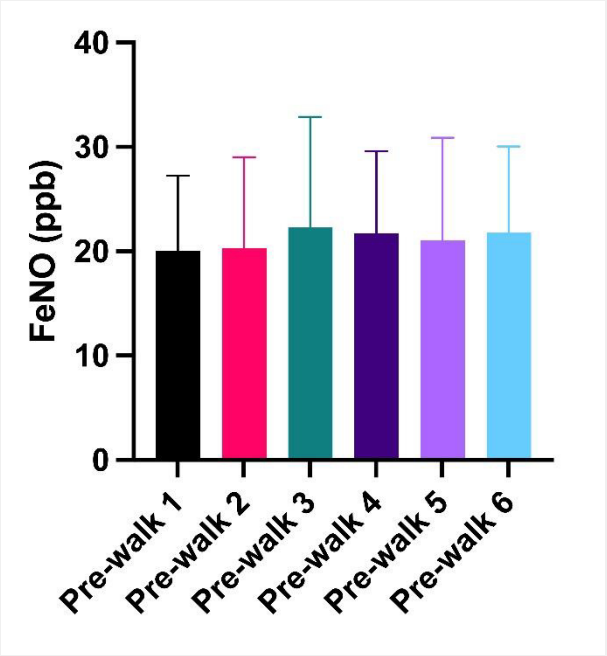

Figure 1.
Group mean (and 95% CI's) for baseline fractional exhaled nitric oxide (FeNO) measured in parts per billion (ppb) before walking, at the end of the school day.

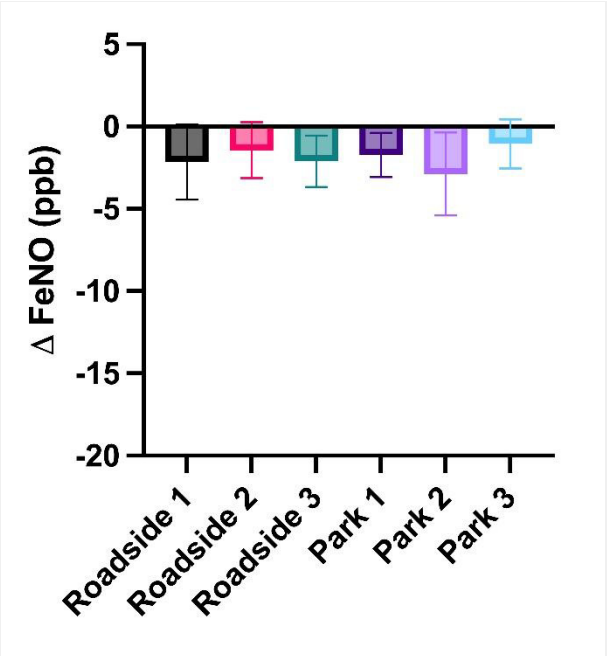

Figure 2.
Group mean (and 95% CI's) for change (Δ) in fractional exhaled nitric oxide (FeNO) measured in parts per billion (ppb) following three roadside and park walking routes.

References

[1] Pang B, Kubacki K, Rundle-Thiele S 2017, 'Promoting active travel to school: a systematic review (2010–2016)', *BMC public health,* 17, 1, 1-5.

[2] Fuller R, Landrigan PJ, Balakrishnan K, Bathan G, Bose-O'Reilly S, Brauer M, Caravanos J, Chiles T, Cohen A, Corra L, Cropper M 2022, 'Pollution and health: a progress update' *The Lancet Planetary Health,* 6, e535-e547

[3] Gauderman, WJ, Vora, H, McConnell, R, Berhane, K, Gilliland, F, Thomas, D, Lurmann, F, Avol, E, Kunzli, N, Jerrett, M, Peters, J 2007, 'Effect of exposure to traffic on lung development from 10 to 18 years of age: a cohort study', *The Lancet,* 369(9561), 571-7

[4] Koo, TK, Li, MY 2016, 'A guideline of selecting and reporting intraclass correlation coefficients for reliability research', *Journal of chiropractic medicine,* 15(2), 155-163

[5] Gabriele, C, Pijnenburg, MW, Monti, F, Hop, W, Bakker, ME, De Jongste, JC 2005, 'The effect of spirometry and exercise on exhaled nitric oxide in asthmatic children', *Pediatric Allergy and Immunology*, 16(3), 243-7

A 06-05

Caspase-6 is necessary and specific for morphological adaptation specifically to shear stresses in pulmonary artery endothelial cells *in vitro*

Corey Wittig[1,2], Laura Michalick[2,4], Wolfgang Kuebler[2,4,5], Robert Szulcek[1,2,3]

[1] *Charité - Universitätsmedizin Berlin, Laboratory of In Vitro Modeling Systems of Pulmonary and Thrombotic Diseases, Institute of Physiology, Berlin, Germany*
[2] *Charité - Universitätsmedizin Berlin, Institute of Physiology, Berlin, Germany*
[3] *Deutsches Herzzentrum der Charité - Medical Heart Center of Charité and German Heart Institute Berlin, Department of Cardiac Anesthesiology and Intensive Care Medicine, Berlin, Germany*
[4] *DZHK (German Centre for Cardiovascular Research), partner site Berlin, Berlin, Germany*
[5] *DZL (German Centre for Lung Research), partner site Berlin, Berlin, Germany*
[6] *St. Michael's Hospital, Keenan Research Centre for Biomedical Science, Toronto, Canada*
[7] *University of Toronto, Departments of Surgery and Physiology, Toronto, Canada*

Question

Caspases are proteases classically thought to be regulators and effectors of cell death and inflammation. However, an emerging body of new research reveals they may have further unidentified non-apoptotic functions. The goal of this study was to identify potential roles of caspases in morphological adaptability of human pulmonary artery endothelial cells (hPAEC) when subjected to known morphology-modulating stresses *in vitro*.

Methods

First, we subjected hPAEC (n=3 pooled) to a constant, unidirectional shear stress of 15 dyn/cm^2 in an *in vitro* fluid flow system for 72h. All known caspases were examined for modulation of endothelial morphological elongation parallel to flow through the addition of 2 µM cell-permeable fluoromethyl ketone-derivatized peptides acting as irreversible, selective, and non-cytotoxic caspase inhibitors. Finding an effect only with caspase-6 inhibition, we then looked to determine if caspase-6 necessity for shear-induced elongation was shear-specific, generally mechano-specific, or non-specific. We therefore utilized a number of elongation-driving stimuli with hPAEC under caspase-6 inhibition (n=2-3): *in vitro* uniaxial cyclic strain at 5% elongation and 1 Hz for 72h, micropatterned arrays with 10 µm-wide RGD binding motif lines as a growth patterning stimulus, 10 ng/mL TNF-α for 24h as a chemical inducer of elongation, and a mechanical wound or real-time impedance-based cell migration monitoring with an electrically-induced wound.

Results

Using 72h fluid flow at 15 dyn/cm^2, hPAEC morphological adaptation to flow in terms of cell elongation in the direction of flow was fully functional in all caspase-inhibited cases except with caspase-6 inhibition, in which the hPAEC showed no trend towards adaptation whatsoever (74.8% cells adapted vs. 20.5% cells adapted, p=0.02). When hPAEC were subjected to other elongation-driving stimuli with or without caspase-6 inhibition, there was no impairment in morphological adaptation whatsoever, indicating no role of caspase-6 in morphological adaptation, migratory, or adhesive capabilities.

Conclusions

Our findings suggest caspase-6 plays a vital role in allowing hPAEC to adapt to fluid shear stress specifically. This finding may have important implications for developing new targeted therapeutic approaches for cardiovascular diseases characterized by endothelial damage due to increased mechanical shear stress (e.g. reperfusion injury), and provides novel insight into our growing understanding of the non-apoptotic functions of caspases.

A 06-06
Modelling ER stress in Alveolar Type 2 epithelial cells to study early-stage events in Idiopathic pulmonary fibrosis

Louisa Vinkovic, Annika Schundner, Manfred Frick

University of Ulm, Department of General Physiology, Ulm, Germany

Idiopathic pulmonary fibrosis (IPF) is a progressive, irreversible, and usually fatal respiratory disease with limited therapeutic options. The current model for the pathogenesis of IPF postulates that recurrent micro-injuries to the bronchoalveolar epithelium, triggers abnormal repair and wound healing responses in the lung. Activated cells of the bronchoalveolar epithelium, in particular alveolar type 2 (AT2) epithelial cells, secrete mediators that result in activation of (myo)fibroblasts, which deposit excessive amounts of extracellular matrix (ECM), resulting in overall remodelling of the alveolar structure. ER stress in AT2 cells has been identified as a main cause of AT2 cell activation. To identify pro-fibrotic mediators that are released from activated AT2 cells, we established a model of ER stress in primary AT2 cells.
Primary AT2 cells were isolated from rat lungs. To initiate ER stress, isolated AT2 cells were treated with ither 10 µM navitoclax, a Bcl-2 inhibitor, or 2,5 µg/ml tunicamycin, an inhibitor of N-linked glycosylation, for up to 48 h. The induction of ER stress and the UPR were monitored by analysing the expression of downstream targets of the three main UPR stress sensors inositol-requiring protein 1 (IRE1), protein kinase RNA-like ER kinase (PERK) and activating transcription factor 6 (ATF6). Quantitative RT-PCR analysis of C/EBP homologous protein (*CHOP*), binding immunoglobulin protein (*BiP*) and spliced X-box binding protein 1 (*XBP1s*) expression revealed that only tunicamycin, but not navitoclax induced ER stress and the UPR in primary AT2 cells. Expression of *CHOP*, *BiP* and *XBP1s*, increased significantly within 3-6 h after start of tunicamycin treatment and persisted for up to 24 h after removal of tunicamycin. This was effect was also confirmed on the protein level by Western Blot. Expression of all markers (CHOP, Activating Transcription Factor 4 (ATF4), Activating Transcription Factor 6 (ATF6)) increased following treatment with tunicamycin. Indicating successful activation of the UPR in AT2 cells. Supernatants from untreated and tunicamycin treated AT2 cells were collected 24 h after tunicamycin removal and transferred on to a recently established fibrosis-sensitive, fibroblast cell line (10-4A) [1]. Fibroblast activation was confirmed by analysis of the expression of pro-fibrotic markers *Acta2* and *Ctgf* in 10-4A cells.
In a next step, we will use this model to identify specific pro-fibrotic mediators released from tunicamycin treated AT2 cells by mass spectrometry to identify novel pathways in the onset of IPF that may provide targets for the development of new therapeutics.

References
[1] Nemeth, J., Schundner, A., Quast, K., Winkelmann, V. E. & Frick, M. (2020). A Novel Fibroblast Reporter Cell Line for in vitro Studies of Pulmonary Fibrosis. *Front. Physiol.* 11, 567675

A 06-07
Knockout of the complex III subunit *Uqcrh* causes respiratory impairment and cardiac contractile dysfunction

Nadine Spielmann[1], Christina Schenkl[2], Tímea Komlódi[3,4], Patricia da Silva-Buttkus[1], Estelle Heyne[2], Jana Rohde[1], Oana V. Amarie[1], Birgit Rathkolb[1,5,6], Erich Gnaiger[3], Torsten Doenst[2], Helmut Fuchs[1], Valérie Gailus-Durner[1], Martin Hrabě de Angelis[1,6,7], **Marten Szibor**[2,8]

[1] *Helmholtz Center Munich, Institute of Experimental Genetics, German Mouse Clinic, Neuherberg, Germany*
[2] *Jena University Hospital, Department of Cardiothoracic Surgery, Center for Sepsis Control and Care (CSCC), Jena, Germany*
[3] *Oroboros Instruments, Innsbruck, Austria*
[4] *Semmelweis University, Department of Biochemistry and Molecular Biology, Budapest, Hungary*
[5] *Ludwig-Maximilians-Universität München, Institute of Molecular Animal Breeding and Biotechnology, Munich, Germany*
[6] *Member of German Center for Diabetes Research (DZD), Neuherberg, Germany*
[7] *Technische Universität München, Chair of Experimental Genetics Experimental Genetics, Freising, Germany*
[8] *Tampere University, Faculty of Medicine and Health Technology, Tampere, Finland*

Ubiquinol cytochrome *c* reductase hinge protein (UQCRH) is required for the electron transfer between cytochrome c_1 and *c* of the mitochondrial cytochrome bc_1 complex (CIII). A two-exon deletion in the human *UQCRH* gene has recently been identified as the cause for a rare familial mitochondrial disorder. Deletion of the corresponding gene in the mouse (*Uqcrh*-KO) resulted in similar biochemical and clinical

defects in particular showing a decrease in CIII activity. Here, we set out to test how global ablation of the murine *Uqcrh* affects cardiac morphology and contractile function. Hearts from *Uqcrh*-KO mutant mice were macroscopically smaller compared to wildtype controls despite similar geometries as assessed by transthoracic echocardiography. Calculating the heart to body mass ratio revealed the development of a subtle cardiac enlargement, but histopathological analysis showed no excess collagen deposition. Nonetheless, *Uqcrh*-KO hearts developed a marked contractile dysfunction by 9 weeks of age. To assess mitochondrial functions, we used a newly developed high-resolution respirometer, NextGen-O2k, to monitor mitochondrial respiratory capacity simultaneously with ETS-reactive CoQ-redox state or production of reactive oxygen species (ROS). Compared to wildtype littermate controls, the mitochondrial respiratory capacity was decreased and the CoQ pool more reduced in *Uqcrh*-KO, indicative of an impaired respiratory electron transfer system (ETS). Yet, mitochondrial ROS production was not increased. Our data suggest that *Uqcrh*-KO impairs mitochondrial respiratory capacity, leading to cardiac contractile dysfunction, but this is not related to increased ROS production as seen in ischemia-reperfusion injury.

A 06-08

Does cell-type specific silencing of MAO-B interfere with the development of right ventricle (RV) hypertrophy or RV failure in pulmonary hypertension?

Paulin Brosinsky[1], Jacqueline Heger[1], Akylbek Sydykov[2], Rainer Schulz[1]

[1] *Justus Liebig Univesity Giessen, Institute for Physiology, Giessen, Germany*
[2] *Justus Liebig Univesity Giessen, EXCELLENCE CLUSTER CARDIO-PULMONARY SYSTEM, Giessen, Germany*

Increased mitochondrial reactive oxygen species (ROS) formation and a metabolic switch directing heart metabolism from fatty acid to carbohydrate consumption are important for the development of right ventricular (RV) hypertrophy (RVH) and failure (RVF) during pulmonary hypertension (PH). Thereby differences in the expression of proteins that contribute to either mitochondrial ROS formation or metabolism exists between species, organs and on the level of the heart, between ventricles.

ROS molecules are produced in different compartments of the cell, with mitochondria known to produce the strongest ROS signal. Mitochondrial outer membrane compounds known as monoamine oxidases (MAOs) are capable of degrading neurotransmitters that can be released in various situations in the body, thereby increasing ROS generation. Inhibition of monoamine oxidase B (MAO-B) has been shown to reduce ROS production. Therefore, we analysed the effect of decreased mitochondrial ROS generation using heart-specific inducible MAO-B knockout mice. To induce pulmonary arterial hypertension (PAH), pulmonary artery banding (PAB) surgery was performed. Dimensions and function of RV was measured by echocardiography, isolated cardiomyocytes function was analysed *in vitro*, and ROS production and systemic hemodynamics were quantified.

Our data showed a significant decrease of ROS molecules in MAO-B KO mice during treatment with PEA (phenethylamine, a common substrate of MAO-B), suggesting that MAO-B had been successfully deleted. There were no differences in isolated cardiomyocyte function with or without MAO-B. In all animals that underwent PAB surgery, pressure overload was similarly induced. In contrast to wildtype mice and littermates, RV dimensions and function of MAO-B KO mice were unaffected in response to PAB.

Genotype	RVID [mm]	RVWT [mm]	TAPSE [mm]
WT PAB	1.81 ± 0.15	0.47 ± 0.04	0.8 ± 0.13
MAO-B $^{fl/fl}$ PAB	1.77 ± 0.16	0.52 ± 0.08	0.83 ± 0.13
MAO-B KO PAB	1.24 ± 0.1***	0.3 ± 0.04***	1.17 ± 0.08***

Data are shown as means ± SD. ***: $p<0.05$. RVID (right ventricular internal diameter), RVWT (right ventricular wall thickness), TAPSE (tricuspid annular systolic excursion).

In conclusion, MAO-B KO mice appear to be protected against RV hypertrophy and dysfunction compared to controls. These results support the hypothesis that MAO-B is a key player in causing RV hypertrophy and failure.

A 06-09

The ubiquitin E3 ligase SIAH2 contributes to right ventricular hypertrophy through direct interaction with the apelin receptor

Nicole S. Molenda[1], Ling Li[1], Simone Kraut[4], Bernd Niemann[2], Norbert Weißmann[4], Akylbek Sydykov[4], Lienhard Schmitz[3], Susanne Rohrbach[1]

[1] *Justus Liebig University Giessen, Institute of Physiology, Giessen, Germany*
[2] *Justus Liebig University Giessen, Department of Cardiovascular Surgery Giessen, Giessen, Germany*
[3] *Justus Liebig University Giessen, Institute of Biochemistry, Giessen, Germany*
[4] *Justus Liebig University Giessen, Department of Internal Medicine, Giessen, Germany*

Background: An increased afterload of the right ventricle (RV) can be experimentally induced by mechanic obstruction of the RV outflow via pulmonary artery banding, resulting in RV remodeling. Hypoxia has been reported to be involved in the development of right ventricular failure (RVF). One of the proteins regulating the hypoxic response is the ubiquitin E3 ligase SIAH2 (seven in absentia 2), but its impact on RV remodeling is unknown.
Objectives: The role of SIAH2 was investigated in *Siah2*$^{-/-}$ mice in a model of RV hypertrophy (RVH) induced by pulmonary artery banding (PAB).
Methods: Cardiac remodeling was characterized by echocardiography, hemodynamic measurements and histology. Isolated cardiac fibroblasts were utilized in functional studies. The interaction of SIAH2 with potential targets was characterized by immunoprecipitation (IP) and loss of function studies in fibroblast and HEK293 cells.
Results: *Siah2*$^{-/-}$mice were largely protected from RV hypertrophy and RV fibrosis induced by PAB. No such changes were observed in the LV. Reduced fibrosis in Siah2-deficient PAB animals was due to a strongly increased anti-fibrotic Apelin signaling. We report the novel observation, that the apelin receptor (APJ) is directly targeted by SIAH2, resulting in its ubiquitination and proteasomal degradation. In Siah2-deficient fibroblasts APJ is stabilized, associated with decreased proliferation, migration and lower expression of pro-fibrotic genes.
Conclusions: SIAH2 promotes cardiac fibrosis in response to RV overload induced by PAB. Understanding the precise role of SIAH2 may provide novel therapeutic targets to interfere with the development of cor pulmonale.

A 06-10

Bacterial toxins as selective modulators of excessive monocyte recruitment and differentiation in lung repair

Robin J. Schönegg[1], Joscha Borho[2], Michael Fauler[1], Holger Barth[2], Manfred Frick[1]

[1] *Ulm University, Institute of General Physiology, Ulm, Germany*
[2] *Ulm University, Institute of Experimental and Clinical Pharmacology, Toxicology and Pharmacology of Natural Products, Ulm, Germany*

The acute respiratory distress syndrome (ARDS) is a common cause of respiratory failure in critically ill patients. ARDS is caused by disruption of the alveolar-capillary barrier separating air and blood in the lung. The resolution of ARDS requires repair of the damaged alveolar tissue to restore lung function. Monocytes recruited to the injured lung, play a crucial role in the resolution of lung injury. However, excessive recruitment of monocytes and polarization into M2 macrophages has also been linked to fibrotic remodelling and development of pulmonary fibrosis. It has therefore been proposed that selective inhibition of monocyte recruitment to the injured lung and differentiation into M2 macrophages may relieve fibrosis severity. In this study we investigate the use of various (monocyte-selective) bacterial toxins to selectively modulate the migration and differentiation of monocytes and macrophages.
In initial experiments, we established a protocol for isolation of highly pure and viable human monocytes from buffy coats. Monocyte to macrophage differentiation was induced by factors M-CSF and GM-CSF. Macrophage polarization was primed towards an M1- or M2-phenotype by LPS and IFN-γ or IL-4 and IL-13, respectively. Differentiation and polarization were confirmed by immunofluorescence labelling against CD206, CD163, HLA-DR, CCR7, CD68, and CD14. We then analyzed the effects of bacterial toxins from *C. botulinum*(C2IIa and C2I) and monocyte-selective derivatives of these toxins (C3bot1) on monocyte (macrophage) migration and differentiation. Cell migration towards chemoattractants (MCP-1) was monitored in live cell imaging experiments using µ-Slide chemotaxis chambers. From these experiments we

derived the potency and efficacy of toxins for modulating chemokinetic and chemotactic behavior of monocytes (and macrophages) at different states of differentiation and polarization.

Our results indicate that cell-secelctive bacterial toxins are promising candidates for targeted inhibition of excessive monocytes recruitment and differentiation. Next, we will elaborate these findings in a disease relevant *in vitro* model of the alveolar endothelial barrier [1]. These experiments will help to further elucidate whether targeted pharmacological inhibition of monocyte immigration and modulation of macrophage differentiation can ameliorate fibrotic remodelling of the alveolus after ARDS.

References
[1] Eisele, J, et al. 2022, 'The Pore-Forming Subunit C2IIa of the Binary Clostridium botulinum C2 Toxin Reduces the Chemotactic Translocation of Human Polymorphonuclear Leukocytes', Frontiers in pharmacology, 13, 810611–810611

A 06-11
Altered pressure-induced right ventricular cardiac remodeling in a heterozygous titin deletion model

Kimberley Stein[1], Andreas Unger[3], Wolfgang A. Linke[3], Daniela Wenzel[1,2]

[1] *Ruhr-Universität-Bochum, Systems Physiology, Bochum, Germany*
[2] *University of Bonn, Institute of Physiology I, Bonn, Germany*
[3] *University of Münster, Institute of Physiology II, Münster, Germany*

In humans, heterozygous titin truncating variants are among the most important genetic causes of dilated cardiomyopathy. However, many patients with titin variants do not develop heart disease. This incomplete penetrance suggests that additional factors, so-called "second hits", are required for disease development. To date, the contribution of titin mutations to heart disease has been studied primarily for left ventricular (LV) dysfunction. However, alterations in titin phosphorylation and stiffness have also been found in the right ventricle (RV) of patients with pulmonary arterial hypertension. Therefore, we wondered whether a heterozygous titin knockout affects RV structure and function under basal conditions and if the induction of pulmonary hypertension (PH) as a "second hit" induces altered RV morphology and performance.

We used a heterozygous titin knockout ($Ttn^{tm1a/+}$) mouse model characterized by terminated translation of the titin protein after exon 3 (Swist, 2020). $Ttn^{tm1a/+}$ mice appeared phenotypically normal. To induce PH, WT and $Ttn^{tm1a/+}$ animals were exposed to hypoxic conditions (10% O_2, weekly Sugen5416 s.c. injections (20 mg/kg)) for 3 weeks; controls were kept under normoxia. Cardiac function was assessed by pressure-volume catheter measurements. For morphological analysis, transversal heart sections were generated, sirius red and wheat germ agglutinin stainings were performed, immunohistochemistry (IHC) and electron microscopy (EM) were applied to study cardiomyocyte substructure.

In normoxic animals, IHC of LV and RV cardiomyocytes using a-actinin and titin antibodies demonstrated wavy Z-discs and a disturbed organization of the contractile apparatus. EM analysis showed areas with degradation of sarcomeres. When PH was induced by Sugen+hypoxia, hemodynamic analysis demonstrated the expected increase in right ventricular systolic pressure in WT and $Ttn^{tm1a/+}$ mice when compared to normoxia ($Ttn^{tm1a/+}$: 24.3±0.8 mmHg, n=6 (NX) vs 34.4±1.2 mmHg, n=9 (HX), p=0.0002). There was no difference in ejection fraction or enddiastolic/endsystolic volumes of the right ventricle in NX vs HX or WT vs $Ttn^{tm1a/+}$ animals. End systolic elastance (Ees) was increased in HX in both genotypes, whereas stiffness was only elevated in WT HX. Morphometry revealed that elevated afterload in HX-induced PH resulted in RV hypertrophy in WT animals as we found enhanced RV thickness (421.5±12.7 µm (NX), n=12 vs 533.1±20.4 µm, n=12, (HX), p<0.0001) and increased cardiomyocyte areas ((219.1±5.7 µm^2 (NX), n=12 vs 300.0±12.1 µm^2, n=12, (HX), p<0.0001). In contrast, in $Ttn^{tm1a/+}$ animals, RV thickness was unaltered (400.0±11.6 µm (NX), n=11 vs 453.0±14.9 µm, n=12, (HX), p>0.05) and there was no change in cardiomyocyte areas (216.4±5.1 µm^2 (NX), n=11 vs 249.9±8.7 µm^2, n=12, (HX), p>0.05) after PH induction. These data suggest that impaired cardiomyocyte integrity alters pressure-induced right ventricular remodeling in $Ttn^{tm1a/+}$ mice.

A 06-12

Reversibility of vascular remodeling and right ventricular hypertrophy in pulmonary hypertension with left heart disease in a rat model of aortic banding/debanding

Donghai Tian[1,2,3], Mariya Kucherenko[1,2,3], Pengchao Sang[1,2,3], Christoph Knosalla[1,3], Wolfgang Kuebler[2,3]

[1] German Heart Center of the Charité (DHZC), Department of Cardiothoracic and Vascular Surgery, Berlin, Germany
[2] Charité - Universitätsmedizin Berlin, Institute of Physiology, Berlin, Germany
[3] DZHK (German Centre for Cardiovascular Research), Partner Site Berlin, Berlin, Germany

Background: Pulmonary hypertension due to left heart disease (PH-LHD) is the most common form of pulmonary hypertension. Previous work shows that PH-LHD causes pulmonary artery (PA) remodeling that correlates with right ventricular (RV) hypertrophy, thereby contributing relevantly to morbidity and mortality in PH-LHD. The pathophysiologic mechanisms of pulmonary vascular remodeling remain unclear, and no therapies can effectively reverse this process at present. In clinical PH-LHD, however, implantation of left ventricular assist devices (LVAD) or heart transplantation can normalize pulmonary vascular resistance over months, indicating that unloading of the pulmonary circulation triggers regenerative programs that may be harnessed for the development of novel therapeutic strategies for reverse remodeling. To better understand these processes, we extended our established rat model of aortic banding (AoB) by an additional surgical debanding (Deb) step to induce reverse remodeling.
Objective: To characterize reverse vascular remodeling and RV hypertrophy in a rat model of aortic banding/debanding.

Methods: Congestive heart failure was induced by surgical placement of a clip (0.8 mm inner diameter) on the ascending aorta (aortic banding, AoB). At week 3 after AoB (AoB 3w), debanding (Deb) surgery was performed by removing the clip from the aorta. After additional 2 weeks, right ventricular (RV) hemodynamics were assessed by right heart catheterization and echocardiography, and RV hypertrophy was assessed as Fulton´s index, by cardiomyocyte histology, and by Western blot analysis. Pulmonary vascular wall thickness and muscularization were assessed from H&E and α-smooth muscle actin-stained lung histological sections. Proliferation and apoptosis of smooth muscle cells (SMC) or endothelial cells (EC) were evaluated by ki67/PCNA and cleaved caspase 3 immunostaining, respectively.
Results: Hemodynamic assessment and histological analyses identified normalization of pulmonary and RV hemodynamics and reverse pulmonary vascular and RV wall remodeling in Deb 5w vs. AoB 3w rats. Immunostaining revealed reduced SMC and EC proliferation rates in pulmonary arteries of Deb 5w vs. AoB 3w rats. Width, area of cardiomyocytes, and RV expression of MYH6 (myosin heavy chain 6) were decreased in Deb 5w vs. AoB 3w rats.
Conclusions: Our results demonstrate that surgical aortic debanding can reverse pulmonary vascular remodeling and RV hypertrophy in a preclinical model of PH-LHD. Ongoing multiscale–omics and mechanistic analyses in this model may provide a better understanding and therapeutic exploitation of physiological mechanisms of lung vascular regeneration and homeostasis.

This study was supported by grants from the German Center for Cardiovascular Research (DZHK), the German Research Foundation (DFG), and the Berlin Institute of Health (BIH).

References
[1] Sang P, Kucherenko MM, Yao J, Li Q, Simmons S, Kuebler WM, Knosalla C. A Model of Reverse Vascular Remodeling in Pulmonary Hypertension Due to Left Heart Disease by Aortic Debanding in Rats. J Vis Exp. 2022 Mar 1;(181). doi: 10.3791/63502. PMID: 35311828.

A 06-13
Comparison of the stage-dependent mitochondrial changes in response to pressure overload between the diseased right and left ventricle in the rat

Ling Li[1], Fabienne Knapp[1], Bernd Niemann[2], Christian Mühlfeld[4], Jan P. Schneider[4], Liane M. Jurida[3], Michael Kracht[3], Susanne Rohrbach[1]

[1] *Justus Liebig University Giessen, Institute of Physiology, Giessen, Germany*
[2] *Justus Liebig University Giessen, Department of Cardiovascular Surgery Giessen, Giessen, Germany*
[3] *Justus Liebig University Giessen, Rudolf Buchheim Institute of Pharmacology, Giessen, Germany*
[4] *Medizinische Hochschule Hannover, Institut für Funktionelle und Angewandte Anatomie, Hannover, Germany*

Background: The right ventricle (RV) differs developmentally, anatomically and functionally from the left ventricle (LV). Therefore, adaptation characteristics of the LV response to chronic pressure overload cannot be simply extrapolated to the RV. Mitochondrial abnormalities are considered a crucial contributor in heart failure (HF). However, changes in mitochondrial function, gene expression and morphology have never been compared directly in RV and LV tissue and cardiomyocytes.

Methods: To identify RV-specific mitochondrial signatures, we established rat models, which show two slowly developing disease stages (compensated and decompensated) in response to pulmonary artery banding (PAB) or ascending aortic banding (AOB). We investigated mitochondrial functional (respiration; respiratory chain enzyme activities) or morphological (electron microscopy) changes and compared mitochondrial biogenesis in the RV and LV tissue at both disease stages. RNA sequencing was utilized to identify differentially expressed mitochondrial genes, which were then confirmed by RT-qPCR. Isolated cardiomyocytes were employed to identify the cellular source of altered gene expression by RT-qPCR and Western Blotting.

Results: Two clearly distinguishable disease stages, which culminated in a comparable systolic impairment of the respective ventricle at decompensation, were observed in both models. Mitochondrial respiration was similarly impaired at the decompensated stage in both failing ventricles, while respiratory chain activity or mitochondrial biogenesis was more severely deteriorated in the failing LV. Bioinformatic analyses of the RNA-seq data sets identified specific pathways involving known or predicted mitochondrial genes. Among the confirmed differentially regulated genes were respiratory chain subunits and genes involved in respiratory chain complex assembly or electron transfer to the respiratory chain, suggesting that these might have contributed to the altered mitochondrial function. Changes in tissue as well as cardiomyocyte mRNA and protein expression were more pronounced in the diseased LV in the AOB model. Only few mitochondrial genes showed opposite changes in gene expression in the failing RV and LV cardiomyocytes.

Conclusions: Mitochondrial dysfunction contributes to disease progression in right and left heart failure. There are profound stage-specific differences in mitochondrial gene expression and function in both ventricles. However, ventricle-specific differences were mostly related to the extent of the observed changes, suggesting that despite developmental, anatomical and functional differences the mitochondrial adaptation to chronic pressure overload is similar in the LV and RV.

A 07 | Renal /Gastrointestinal

A 07-01
Renal acetylcholinesterase as a regulator of kidney function

Sabrina Habel[1], Philipp Tauber[1], Anna Federlein[1], Katharina Krieger[1], Rosmarie Heydn[1], Frank Schweda[1]

[1] *Universität Regensburg, Physiologie II, Regensburg, Germany*
[2] *Universität Regensburg, Physiologie II, Regensburg, Germany*

Question

Proper kidney function requires communication between cells of different renal compartments such as tubules and interstitial cells. The underlying intrarenal signaling cascades are only partially understood. Therefore, this study aimed at identifying yet unrecognized communication signals of renal tubules.

Methods

Adjusting urine volume to drinking volume is one of the essential challenges of the kidney and the adjustment processes involve all compartments of the kidney. Water deprivation (wd) was used as a model to study intrarenal communication. Accordingly, mice received either water ad libitum or were subjected to wd for 24 hours, renal tubules were isolated by microdissection and gene expression was determined using mRNA microarrays (Affymetrix). Results were confirmed using real time PCR (qPCR), in situ hybridization (ISH), immunofluorescence staining (IF) and western blot (WB). Renal perfusion and urine flow were determined in the isolated perfused mouse kidney model (IPMK). Tubular cells were stimulated *in vitro* with different stimuli occurring during wd such as vasopressin and high osmolality.

Results

Besides other mRNAs coding for signaling molecules or relevant enzymes, collecting ducts (CD), which play the main role in urine concentration, expressed acetylcholinesterase (AChE) at high abundance already under control conditions (c) and AChE was markedly upregulated by water deprivation (wd). ISH showed clear and selective AChE mRNA expression in CDs and glomeruli and confirmed upregulation of AChE in CDs of wd mice. In contrast to wd, CDs of mice with high urinary flow (loop diuretics) had low AChE mRNA expression levels. In cell culture experiments (mouse collecting duct cell line), increasing extracellular osmolarity by NaCl and mannitol, but not urea, resulted in increases in mRNA expression of AChE and NFAT5, a transcription factor that regulates genes involved in osmotic stress. AChE protein was located around CDs in the renal interstitium of c and wd mice. Renal tissue of control mice showed clear AChE activity, which was further stimulated by wd. Since AChE inactivates acetylcholine (ACh) it might be involved in the regulation of ACh signaling in the kidney. In fact, ACh concentration-dependently stimulated renal perfusion and urine flow in isolated perfused mouse kidneys and this effect was markedly augmented by concomitant pharmacological inhibition of AChE (donepezil hydrochloride).

Conclusions

AChE mRNA expression increases in CDs in response to wd. This increase results from high interstitial osmolarity most likely via the NFAT-5 pathway. AChE protein is secreted from CDs and is distributed in the interstitium, where it degrades acetylcholine. Since acetylcholine stimulates renal perfusion and urine flow and these effects are augmented by pharmacological inhibition of AChE, AChE might play a functional role in urine concentration and the adaptation of kidney function to wd.

A 07-02
Cyclosporin A-associated constriction of renal vasculature is associated with microvascular remodeling

Cem Erdogan[1], Xingyu Qiu[2], Hasan Demirci[3], Minze Xu[1], Liang Zhao[4], Pratik Khedkar[1], Enyin Lai[1,2], Pontus Persson[1], Kerim Mutig[1], Sebastian Bachmann[3]

[1] *Charité Universitätsmedizin Berlin, Institute for translational Physiology, Berlin, Germany*
[2] *Zhejiang University School of Medicine, Department of Physiology, Hangzhou, China*
[3] *Charité Universitätsmedizin Berlin, Department of Cell and Neurobiology, Berlin, Germany*
[4] *Zhejiang University School of Medicine, Department of Nephrology, Hangzhou, China*

Calcineurin inhibitor cyclosporine A (CsA) is instrumental for immunosuppression in transplant recipients, but nephrotoxicity limits its therapeutic benefit. Renal vasoconstriction increases the risk of allograft loss at short term and aggravates functional and morphological renal damage at long term. Underlying mechanisms may involve increased sympathetic tone and hyperactivity of the renin-angiotensin system. This study analyzes acute and chronic vasotoxic effects of CsA.

Isolated perfused mouse afferent arterioles and isolated perfused mouse kidneys were used to assess acute effects of CsA. Chronic vascular effects were characterized in rats treated with CsA for 3 weeks. CsA produced strong vasoconstriction in afferent arterioles which was not increased by consecutive application of angiotensin II, suggesting a direct, potent effect of CsA. In line with this, CsA increased total vascular resistance in isolated perfused mouse kidneys. Chronic vascular CsA toxicity was reflected by significantly reduced creatinine clearance and morphological changes of renal arterioles and microvasculature. Interlobular and afferent arterioles revealed expansion of the tunica media layer along with augmented contractile apparatus. Terminal afferent arterioles showed hypergranularity reflecting enhanced renin biosynthesis. Glomerular capillaries showed defects in endothelial fenestration.

The present results suggest that acute CsA-induced vasoconstriction is caused by calcineurin inhibition of the vascular wall. Chronic vascular alterations by CsA include significant arterial and microvascular endothelial remodeling likely contributing to nephrotoxic alterations.

A 07-03
Piezo1 inhibition blunts glomerular hyperfiltration in response to acute hyperglycemia in mice

Lingyan Fei[1,2], Minze Xu[1], Honghong Wang[3], Cheng Zhong[1], Shan Jiang[2], Falk-Bach Lichtenberger[1], Cem Erdoğan[1], Han Wang[1], Julia S. Bonk[1], Enyin Lai[3], Pontus B. Persson[1], Richard Kovács[4], Zhihua Zheng[2], Andreas Patzak[1], **Pratik H. Khedkar**[1]

[1] *Charité – Universitätsmedizin Berlin, Institute of Translational Physiology, Berlin, Germany*
[2] *Sun Yat-sen University, Department of Nephrology, Center of Kidney and Urology, the Seventh Affiliated Hospital, Shenzhen, China*
[3] *Zhejiang University School of Medicine, Department of Physiology, School of Basic Medical Sciences, Hangzhou, China*
[4] *Charité – Universitätsmedizin Berlin, Institute of Neurophysiology, Berlin, Germany*

Acute hyperglycemia (HG) increases the risk of acute kidney injury in critically ill patients and leads to poor renal outcomes. However, the role of renal vasculature in this context remains unclear. We hypothesize that HG-induced hyperosmolarity causes vasodilation by activating eNOS via the mechanosensitive calcium channel Piezo1. We analyzed vasoreactivity in isolated mouse mesenteric (MA) and renal interlobar (ILA) arteries using wire myography and using microvascular perfusion in renal afferent (AA) and efferent arterioles (EA), and vasa recta (VR). Immunofluorescence and western blot were used for molecular analyses of isolated vessels and HUVECs. ILA and MA showed increased acetylcholine (ACh)-induced relaxation in ILA and MA, which could be prevented by blocking NOS using L-NAME. Replacing excess glucose with mannitol had a similar effect on vasoreactivity. AA, EA and VR, pre-constricted with angiotensin II, showed immediate dilation in response to HG. This effect could likewise be inhibited using L-NAME. HG-induced dilation was stronger in AA than in EA, which corresponded with the increased GFR that we observed *in vivo.* In HUVECs, HG as well as the Piezo1 agonist Yoda1 increased the expression of Piezo1 protein and phosphorylation of CaMKII, Akt and eNOS (S1177). Piezo1 inhibitor GsMTx4 and CaMKII inhibitor KN93 could abrogate this effect. GsMTx4 also abrogated the HG-effect in microvessels and arteries. Moreover, in arteries and microvessels, Yoda1 induced relaxation and dilation, respectively under normoglycemic conditions. Taken together, our results reveal that HG-induced renal vasodilation is caused by hyperomsolarity and mediated by Piezo1.

A 07-04
Inhibition of renoprotective angiotensin I-converting enzyme 2 axis diminishes protection against aristolochic acid nephropathy in mice with reduced renal angiotensin I-converting enzyme

Hermann Somschor, Jeannine Witte, Antje C. Steinbach, Carsten Scholz, **Annett Juretzko**

University Medicine, Institute of Physiology, Greifswald, Germany

Question

We previously demonstrated that mice (C57BL/6J-*tm*$^{(ACE3/3)}$ = ACE$^{-/-}$) with reduced renal angiotensin I-converting enzyme (ACE) are protected against aristolochic acid nephropathy (AAN) compared to wildtype. In ACE$^{-/-}$ mice, aristolochic acid may activate the renoprotective ACE2/angiotensin (1-7)/Mas receptor (Mas) axis. To elucidate the specific role of ACE2 and Mas in this protective phenotype, we treated ACE$^{-/-}$ mice with ACE2 inhibitor and Mas antagonist, respectively and investigated whether the downstream pAkt/Akt signaling pathway is modulated.

Methods

AAN was induced using aristolochic acid I (AAI, 3 mg/kg body weight, i.p., every three days for six weeks followed by six weeks without treatment). During the six weeks of treatment with AAI, ACE$^{-/-}$ mice got MLN-4760 (ACE2 inhibitor, 10 mg/kg/d) via drinking water and A779 (Mas antagonist, 31 µg/kg/h) via osmotic mini pump, respectively. At the end of the protocol, the glomerular filtration rate (GFR) was determined using inulin clearance und the kidneys were removed. Renal protein abundances of Akt and pAkt (Ser473) were determined by immunoblot analyses and subsequently quantified.

Results

GFR was similar in vehicle-treated and AAI-treated ACE$^{-/-}$ mice, underlining the protective effect of renal ACE deficiency in AAN. ACE2 inhibition decreased GFR in AAI-treated ACE$^{-/-}$ mice significantly, whereas Mas blockade showed a trend towards a decreased GFR. In AAI-treated ACE$^{-/-}$ mice, the pAkt/Akt ratio was significantly increased compared to vehicle-treated ACE$^{-/-}$ mice. Even though ACE2 inhibition and Mas blockade increased pAkt/Akt ratio significantly compared to vehicle-treated ACE$^{-/-}$ mice, the increase was not as high as in AAI-treated ACE$^{-/-}$ mice.

Conclusions

Overall, our data demonstrate that ACE2 inhibitor or Mas antagonist treatment reverses the protective effect of renal ACE deficiency in AAN. Thus, ACE2 and Mas may play an important role in the development of AAN, due to modulation of downstream signal transduction pathways and may represent novel therapeutic targets for the development of a treatment for AAN. To get further information about the underlying mechanisms that may be involved in the protection of ACE deficient mice against AAN, other signaling pathways need to be examined.

A 07-05
Autoregulation of renal blood flow in wildtype and P2X1-purinoreceptor-deficient mice

Marcel Dautzenberg, **Armin Just**

Albert-Ludwigs-Universität Freiburg, Physiologisches Institut, Freiburg, Germany

Background

Autoregulation of renal blood flow (RBF) is mediated by myogenic response (MR), tubuloglomerular feedback (TGF), and an unknown third mechanism (3rdM). P2X1 purinoreceptors (P2X1R) are expressed on afferent arterioles and induce vasoconstriction upon activation by ATP. However, their contribution to RBF autoregulation remains unclear. Micropuncture studies in superficial nephrons indicate no essential role of P2X1R for TGF, but studies on total RBF and juxtamedullary afferent arterioles suggest an important contribution to RBF autoregulation. However, the role of P2X1R in the integrative function of all nephrons is unknown. Also unclear is, whether P2X1R contributes to or mediates the 3rdM. To investigate the role of P2X1R in total RBF autoregulation and in the autoregulatory mechanisms, we studied RBF autoregulation in wildtype (WT) and P2X1R-knockout (KO) mice at baseline, after furosemide to eliminate TGF, and during angiotensin II (AngII) or NO-synthase (NOS) inhibitor LNAME to challenge the autoregulatory effort by hypertension, vasoconstriction, and modulation of the autoregulatory mechanisms.

Methods

Under pentobarbital anesthesia (80 mg/kg ip, additional doses ip or sc as needed to abolish motor and pressor responses to toe and tail pinch) catheters were inserted into the femoral artery and jugular vein, an adjustable clamp on the suprarenal aorta, and a flowprobe on the left renal artery. RBF autoregulation was tested by a small rapid step increase in renal arterial pressure, induced by swift opening of the occluder following a pressure reduction by 20 mmHg below baseline for a duration of ~70s. MR was estimated from the rise in renal vascular resistance (RVR) during the first 5s, TGF from 5 to 30s, and 3rdM from 30 to 120s after the pressure step.

Results

At baseline, overall autoregulatory efficiency and the contributions of MR, TGF, and 3rdM were virtually identical in WT and KO mice. Furosemide augmented MR, modified the TGF-pattern, diminished 3rdM, and reduced total autoregulation, but did not reveal any difference between WT and KO. AngII augmented MR and TGF at the cost of 3rdM and LNAME augmented MR at the cost of TGF and 3rdM, but without difference between WT and KO.

Conclusions

No discernable contribution of P2X1R to RBF autoregulation, nor to any of its underlying mechanims could be detected, neither at baseline, nor with inhibited TGF, nor during hypertension and autoregulatory modulation by AngII or NO-deficiency. We conclude that P2X1R do not play a dominant role in overall TGF or 3rdM in the kidney nor in autoregulation.

This work was supported by FRIAS Freiburg

A 07-06
Androglobin knockout leads to endocrine imbalance and hyperkalemia under high-potassium diet

Miguel Correia[1], Angèle Clerc[1], Darko Maric[1], Denise Winter[2], Alex Odermatt[2], David Hoogewijs[1], Anna Keppner[1]

[1] *University of Fribourg, Department of Medicine/Phisiology, Fribourg, Switzerland*
[2] *University of Basel, Department of Pharmaceutical Sciences, Basel, Switzerland*

The author has objected to a publication of the abstract.

A 07-07
Inflammatory diarrhea in inflammatory bowel disease (IBD) patients may be due to defective terminal differentiation of absorptive enterocytes in the inflamed colon

Evaldas Tytmonas[1], **Katerina Nikolovska**[1], Anna Elisabeth Seidler[1,2], Gabriella di Stefano[1], Timo Hellms[1], Ursula Seidler[1]

[1] *Hannover Medical School, Department of Gastroenterology, Hannover, Germany*
[2] *Leibniz University of Hannover, Institute of Quantum Optics, Hannover, Germany*

Crohn's disease and ulcerative colitis are chronic inflammatory bowel diseases (IBD) characterized by disturbed homeostasis of the immune system, the intestinal mucosa and the microbiome. A hallmark of these diseases is chronic or recurrent inflammatory diarrhea, whose pathophysiology is controversially discussed, but a reduced epithelial Na^+ and fluid absorption is a prominent feature. Fluid absorption in the ileocolonic region is predominantly mediated by the Na^+/H^+ exchanger SLC9A3 (NHE3) in conjunction with the H^+-SCFA cotransporter MCT1, the Cl^-/HCO_3^- exchanger SLC26A3 (DRA), and the epithelial Na^+ channel (ENaC). The objective of the current study was to evaluate whether the downregulation of specific absorptive ion transporters or a general defect in enterocyte differentiation correlates with the degree of diarrhea and inflammation.

For this reason, we analyzed the mRNA expression and/or protein abundance of DRA, NHE3, MCT1, ENaC, CFTR, as well as stem cell and proliferative markers, and a panel of genes that determine or correlate with the differentiation state of the colonic epithelium, in different segments of the ileocolon of healthy individuals and IBD patients with mildly, moderate-severely or noninflamed colonic mucosa. Endoscopy and histopathologic scoring and TNFα mRNA levels were used to grade inflammation, clinical scores for disease activity and diarrhea frequency and consistency.

mRNA expression and immunohistochemical staining of DRA and NHE3 in healthy colonic tissue revealed differences in the expression pattern of DRA and NHE3 along the human colon, with DRA being most abundant in the transverse and descending colon and NHE3 in the ascending colon (n=10). The reduction of MCT1, DRA and NHE3 mRNA expression/abundance in the membrane correlated with the degree of inflammation as well as the diarrhea score (n=42), while in inactive disease the expression and abundance of MCT1, DRA and NHE3 did not differ from healthy controls (n=13). Since the addressed ion transporters are expressed on differentiated intestinal epithelial cells, we further investigated if their altered expression is linked to a possible defect of the epithelial differentiation program. It was found that the mRNA expression of the absorptive enterocyte differentiation markers intestinal alkaline phosphatase (iALP), villin, Elf3, and HES1 was significantly decreased in inflamed colon, while the expression of the proliferative marker Ki67, HOPX, BM1 and Claudin2 was significantly increased. However, the expression of the stem cell marker LGR5 was not altered (n=30).

The results showed a disrupted transcriptional regulation of the epithelial ion transporters DRA, NHE3 and ENaCγ in the inflamed epithelium of IBD patients, which will lead to their reduced function and cause luminal electrolyte/water accumulation leading to diarrhea.

A 07-08
Organoids as a long-term approach for ruminal epithelial cell culture

Saeed Khomeijani Farahani[1], Franziska Liebe[2], Ilka Slosarek[2], Johanna Plendl[2], Friederike Stumpff[3,2], Dorothee Günzel[1]

[1] *Charité - Universitätsmedizin Berlin, Clinical Physiology/Nutritional Medicine, Division of Gastroenterology, Berlin, Germany*
[2] *Freie Universität Berlin, Institute of Veterinary Anatomy, Department of Veterinary Medicine, Berlin, Germany*
[3] *Health and Medical University, Institute of Physiology, Potsdam, Germany*

Question

In ruminants, the largest compartment of the gastrointestinal tract is the rumen. Its cornified stratified epithelium forms an effective barrier against pathogens. Simultaneously, short chain fatty acids can be absorbed for energy, while cations such as NH_4^+ (for hepatic amino acid synthesis) or Mg^{2+} and Ca^{2+} are taken up, most likely via TRP channels as recently proposed [1].

To reduce animal testing by working with native epithelia, our main objective is to establish a high-yield biobank for rumen keratinocyte stem cells by generating rumen organoids. These can then be seeded onto cell culture inserts, differentiate, and form a multilayered epithelium like in-vivo tissue. We hypothesize that this will enhance the capacity to perform a significant number of reproducible cell culture insert experiments.

Organoids are a powerful 3D in-vitro technique that mimics real tissues by maintaining many stem cells, by carefully controlling the cytokines and growth factors, even after multiple cell culture passages. Culturing organoids enables the long-term expansion of adult stem cells in a genetically stable manner. It is possible to transform organoids in every stage into fully differentiated tissues by removing the key factors such as Wnt and R-spondin proteins from the culture medium e.g., in [2].

Methods

Isolation of keratinocyte stem cells, which are located in the basal layer of rumen tissue, was performed as described previously [3]. Following [3], ruminal papillae were cut from the rumen and trypsinized. Deviating from protocol, we introduced the isolated keratinocyte stem cells into Cultrex Basement Membrane Extract (BME; R&D Systems) in order to generate organoids. Isolated cells from rumen or proliferated cells from organoids were seeded onto cell culture inserts, and were investigated using transepithelial resistance (TER) measurements, immunohistochemical staining (IHC), and Electrical Impedance Spectroscopy (EIS), which has proven to be a valuable tool for investigating the epithelial architecture, electrical properties, and ionic transport processes [4,5].

Results

Cells grew to confluence, reaching TER values ranging from 600 to 800 $\Omega \cdot cm^2$. We observed the expression of rumen-specific tight junction proteins, namely Claudins 1 and 4 [3] via IHC. We utilized EIS to gather detailed information about the physiological characteristics of the model ruminal epithelium. We recorded comparative EIS curves between inserts from keratinocyte stem cells and organoids upon applying TRP channel activators (such as 2-APB).

Conclusions

To the best of our knowledge, we are the first group generating organoids from ruminal keratinocyte stem cells as a source for the generation of model epithelia. Our next objective is RNA sequencing data among: 1) inserts produced from the organoids, 2) inserts derived from primary cells, and 3) the native rumen tissue, which will help to characterize and validate this new 3D-model.

Funded by DFG GRK2318, Project ID 318905415

References

[1] Liebe F, Liebe H, Sponder G, Mergler S, Stumpff F, 2022. Effects of butyrate− on ruminal Ca2+ transport: evidence for the involvement of apically expressed TRPV3 and TRPV4 channels. Pflugers Arch - Eur J Physiol 474, 315–342.

[2] Smith D, Price DRG, Burrells ., Faber MN, Hildersley KA, Chintoan-Uta C, Chapuis AF, Stevens M, Stevenson K, Burgess STG, Innes EA, Nisbet AJ, McNeilly TN, 2021. The Development of Ovine Gastric and Intestinal Organoids for Studying Ruminant Host-Pathogen Interactions. Front Cell Infect Microbiol. 8;11:733811.

[3] Stumpff F, Georgi MI, Mundhenk L, Rabbani I, Fromm M, Martens H, Günzel D, 2011. Sheep rumen and omasum primary cultures and source epithelia: barrier function aligns with expression of tight junction proteins. J Exp Biol. 1; 214(Pt 17):2871-82.

[4] Gerasimenko T, Nikulin S, Zakharova G, Poloznikov A, Petrov V, Baranova A, Tonevitsky A, 2020. Impedance Spectroscopy as a Tool for Monitoring Performance in 3D Models of Epithelial Tissues. Frontiers in Bioengineering and Biotechnology, vol. 7.

[5] Beier LS*, Waldow A* (*shared first authorship), Khomeijani Farahani S, Mannweiler R, Vidal-Y-Sy S, Brandner JM, Piontek J°, Günzel D° (°shared last authorship), 2022. Claudin targeting as an effective tool for directed barrier modulation of the viable epidermis. Ann. NY Acad. Sci. 1517(1): 251-265.

A 07-09
Effect of secretin stimulation on pendrin (*Slc26a4*) in murine *ex vivo* kidney slices

Kimberley Dreger, Desiree Loreth, Leya Eckermann, Catherine Meyer-Schwesinger, Heimo Ehmke, Helga Vitzthum

University Medical Centre Hamburg-Eppendorf, Institute of Cellular and Integrative Physiology, Hamburg, Germany

Question

The kidneys play a crucial role in acid base homeostasis. In the distal nephron, the α-intercalated cells contribute to urinary acid (H^+) secretion and the β-intercalated cells accomplish urinary base (HCO_3^-) secretion. Mechanistically, in the β-intercalated cells the apical located HCO_3^-/Cl^- exchanger pendrin (*Slc26a4*) is activated upon alkalosis, which leads to increased urinary HCO_3^- excretion and to normalization of the acid base balance. Recent studies have shown that the hormone secretin stimulates HCO_3^- secretion into the urine via a CFTR-dependent increase of pendrin activity (1). So far, the effect of secretin on the abundance and the subcellular localization of pendrin has not been studied in detail.

Methods

The effects of secretin on pendrin were studied in precision-cut kidney slices (PCKS). Kidneys of C57BL/6J mice were harvested and bisected along the longitudinal axis. Each half was cut with a tissue chopper (McIlwain) into 300 µm slices. The PCKS were cultured in Williams' Medium E (supplemented with 2.7 g/L glucose) at 37 °C in an 80 % O_2 and 5 % CO_2 atmosphere. After 1.5 h of acclimation, the slices were treated with secretin (10, 55, 100, and 550 nM) or PBS (control) for 6 h. Pendrin mRNA level and protein abundance were determined by qRT-PCR and Western blot, respectively. Subcellular localization of pendrin was analysed by immunofluorescence microscopy.

Results

At a high concentration (550 nM) secretin induced an upregulation of pendrin mRNA and protein levels, whereas stimulation of PCKS with moderate concentrations (10 - 100 nM) of secretin had no effect on either pendrin mRNA or protein levels. Redistribution of pendrin from the subapical cytosolic region to the apical membrane was not detected on immunofluorescence staining of PCKS at any concentration.

Conclusions

Our data demonstrate pendrin upregulation can be induced in *ex vivo* kidney slices culture, however, only at a very high, unphysiological concentration. Whether the cellular regulation of pendrin can also be altered by more physiological concentrations of secretin in *ex vivo* kidney slices under modified experimental conditions remains to be determined.

References
[1] Berg, P. et al. 2021 `The molecular mechanism of CFTR- and secretin-dependent renal bicarbonate excretion´, *J Physiol, 599,* 3003-3011.

A 07-10
Cannabidiol effects on gastrointestinal tight junction proteins

Elisa Boehm, Marie L. Vollstaedt, Laura Stein, Linda Droessler, Salah Amasheh

Freie Universität Berlin, Department of Veterinary Medicine, Institute of Veterinary Physiology, Berlin, Germany

Question

Recent studies focusing on effects of pro-inflammatory cytokines and secondary plant compounds on gastrointestinal epithelial barrier function revealed adverse effects on function and integrity of tight junction protein complexes [Cornelius et al., 2022; Droessler et al., 2022]. Moreover, studies were extended to direct tight junction protein interaction studies focusing on *Xenopus laevis* oocytes as a heterologous expression system [Stein et al., 2022]. In our current study, we aimed to investigate whether cannabidiol (CBD), extracted from Cannabis sativa might positively affect gastrointestinal tight junction proteins.

Methods

Intestinal porcine epithelial cells (IPEC-J2) were seeded on permeable supports, and transepithelial electrical resistance (TEER) was measured using an epithelial volt/ohm meter. Once the cells reached confluency, CBD was applied apically to the cell culture inserts at µM concentrations, and TEER measurements were performed with and without co-incubation with TNF. Cells were then fixed for

immunohistochemistry, and protein extraction was performed for immunoblots. Statistical analysis was conducted using one-way ANOVA, and statistical significance was determined using Dunnett's post hoc test ($p < 0.05$).

Results

After 8 hours of incubation, 40 µM CBD exhibited significantly higher TEER values compared to controls (**$p < 0.01$, $n = 8$). This functional enhancement correlated with an increase in the expression of claudin-4, as observed in immunoblots and immunohistochemical images. Moreover, CBD attenuated a TNF-induced decrease of tight junction proteins. A direct interaction assay employing *Xenopus* oocytes heterologously expressing gastrointestinal tight junction proteins did not reveal a significant effect (n = 16-20).

Conclusions

In our study CBD showed a beneficial effect on tight junctions in IPEC-J2 cells, whereas a direct effect on protein-protein interaction of oocytes expressing tight junction proteins could not be observed. The findings demonstrate that CBD enhances the epithelial barrier function of intestinal epithelial cells on a regulatory level. Further experiments may provide insights into selectivity, signaling, and potential therapeutic benefits in intestinal health and disease, especially under inflammatory conditions.

This study was supported by a grant of the German Research Foundation, AM141/11-2.

References
[1] Cornelius, V, Droessler, L, Boehm, E, Amasheh, S, 2022. Concerted action of berberine in the porcine intestinal epithelial model IPEC-J2: Effects on tight junctions and apoptosis. *Physiol Rep.* 10(7):e15237.
[2] Droessler, L, Cornelius, V, Boehm, E, Stein, L, Brunner, N, Amasheh, S, 2022. Barrier perturbation in porcine Peyer's patches by Tumor Necrosis Factor is associated with a dysregulation of claudins. *Front Physiol.* 13:889552.
[3] Stein, L, Brunner, N, Amasheh, S, 2022. Functional analysis of gastric tight junction proteins in *Xenopus laevis* Oocytes. *Membranes (Basel)* 12(8):731.

A 07-11

Characterization of a ruminal 3D epithelial cell model

Franziska Liebe[2], Saeed Khomeijani-Farahani[3], Ilka Slosarek[2], Johanna Plendl[2], Dorothee Günzel[3], Friederike Stumpff[1]

[1] *Health and Medical University Potsdam, Physiology, Potsdam, Germany*
[2] *Freie Universität Berlin, Institute of Veterinary Anatomy, Berlin, Germany*
[3] *Charité - Universitätsmedizin Berlin, Clinical Physiology/Nutritional Medicine, Berlin, Germany*

Question

Publications utilizing cell culture models have risen exponentially within the last two decades, driven in part by the desire to reduce animal testing but also by the possibility of understanding more about the formation of tissues and organs. The problems involved in obtaining viable tissues for studies of epithelial transport are pronounced. In particular when studying the rumen of cattle and sheep, problems arise in obtaining the animals and extracting viable tissues. There is thus a need for establishing and characterizing a ruminal epithelial model. However, the generation of such a model may suffer from the difficulty of separating epithelial cells from the underlying structures, i.e. the ruminal lamina propria mucosae with blood and lymphatic vessels and particularly active fibroblasts. It is therefore an additional aim of the present study to asses to what extent such cultures are contaminated by fibroblasts.

Methods

Performed essentially as previously described [1, 2], papillae of the ventral sac of sheep rumen were removed and keratinocytes isolated via stepwise trypsinization, discarding the first two fractions and then cultivating the subsequent five fractions. The cells were characterized immunohistochemically using antibodies against fibronectin, cytokeratin AE1 and AE3, and MNF. Fibroblasts from a previous isolation from the bovine claw were stained in parallel. After ~3 passages for expansion, keratinocytes were seeded on filters (polycarbonate membrane, pore size 0.4 µm). The model epithelia were investigated via measurement of the transepithelial electrical resistance and transmission electron microscopy.

Results

Approximately 6 days after isolation of cells from ruminal papillae, two types of cells could be visually identified: round and spindle shaped cells. Both types of cells showed staining for the cytokeratin markers and for fibronectin. Conversely, control fibroblasts only stained for fibronectin, but not for the cytokeratin markers. Cells grown 12 days on filters developed resistances of 400 to 900 $\Omega \cdot cm^2$. Transmission

electron microscopy showed a multilayered structure with cell-cell contacts similar to the tight junctions seen in native ruminal epithelium of sheep.

Conclusions

We confirm that it is possible to generate multi-layered model epithelia with barrier properties that indicate functional cellular tight junctions from cells isolated from the ruminal epithelium. While contamination by fibroblasts seemed to be minor, development of further methods is required for the reliable differentiation of fibroblasts from keratinocytes.

References
[1] Stumpff F, Georgi MI, Mundhenk L, Rabbani I, Fromm M, Martens H, Günzel D 2011, YYYY, ' Sheep rumen and omasum primary cultures and source epithelia: barrier function aligns with expression of tight junction proteins ', *J Exp Biol*, 214(Pt 17), 2871
[2] Liebe F, Liebe H, Sponder G, Mergler S, Stumpff F 2022, 'Effects of butyrate$^-$ on ruminal Ca^{2+} transport: evidence for the involvement of apically expressed TRPV3 and TRPV4 channels', *Pflugers Arch*, 474(3), 315

A 08 | Cell Biology & Signal Transduction

A 08-01
The role secreted modular calcium binding protein (SMOC1) on resolution of inflammation and atherosclerosis development

Urün Ukan[1], Mahmoud Amer[1], Fredy Delgado Lagos[1], Ingrid Fleming[1,2]

[1] *Goethe Universität, Institute for Vascular Signalling, Frankfurt am Main, Germany*
[2] *DZHK (German Centre for Cardiovascular Research), Partner site Frankfurt Rhein-Main, Frankfurt am Main, Germany*

Question

TGF-β plays an important role in numerous diseases and drives macrophage polarization to a pro-resolving phenotype and the reprogramming of endothelial cells to cells with mesenchymal characteristics (endothelial cell to mesenchymal transition or EndMT). Indeed, chronic inflammation such as that associated with atherosclerosis are partly due to the failure of mechanisms that drive the resolution of inflammation. Here we assessed the role of secreted modular calcium binding protein (SMOC) 1, which was previously reported to be a TGF-β receptor I (ALK5) antagonist in endothelial cells as well as an activator of thrombin that affects macrophage polarization, on the development of atherosclerosis.

Methods and results

Bone marrow derived macrophages from SMOC1-deficient ($SMOC1^{+/-}$) mice treated with oxLDL particles for 20 minutes accumulated more particles than cells from their wild-type littermates. This effect was attributed to the inability to form functional lysozomes. To assess the impact of endothelial cells and myeloid cell SMOC1 on vascular pathology, mice that lacked SMOC1 selectively in either myeloid cells ($SMOC1^{\Delta LysM}$) or endothelial cells ($SMOC1^{\Delta EC}$) were generated. Atherogenesis was initiated by the intraperitoneal administration of AAV-PCSK9 followed by partial carotid ligation and high fat diet and the atherosclerotic burden assessed after twenty one days. First results revealed that the deletion of SMOC1 from either endothelial cells or myeloid cells accelerated the development of atherosclerosis. Moreover, in $SMOC1^{\Delta EC}$ mice some endothelial cells from aortae expressed mesenchymal markers (e.g. SM22α) indicating the occurrence of EndMT.**Conclusions**

Taken together, the expression of SMOC1 by endothelial cells seems to protect against the development of EndMT while in macrophages it is required for the TGF-b-induced formation of functional lysosomes. The deletion of the protein from either cell type results in negative effect that accelerates the development of atherosclerosis.

A 08-02
Interaction of Connexin 43 with SHP-2 augments paxillin de-phosphorylation and controls focal adhesion turnover during migration

Hanna Mannell[1,2], Petra Kameritsch[2,3], **Kristin Pogoda**[1,2]

[1] *Universität Augsburg, Institute for Theoretical Medicine, Physiology, Augsburg, Germany*
[2] *Ludwig-Maximilians-Universität München, Institute of Cardiovascular Physiology and Pathophysiology, Planegg, Germany*
[3] *Ludwig-Maximilians-Universität München, Walter Brendel Center of Experimental Medicine, University Hospital, München, Germany*

Question

We have previously demonstrated that Connexin 43 (Cx43) promotes endothelial cell migration and that the interaction with the tyrosine phosphatase SHP-2 is essential for this process. During cell migration a fast focal adhesion turnover is characterized by the formation of small focal complexes and the disassembly of large focal adhesions (FA), which is required for the forward progression of migrating cells. In this study we analysed the effect of Cx43 and SHP-2 on the regulation of actin dynamics and focal adhesions.

Methods

Cell shape and FA dynamics were analysed in Cx43-expressing or Cx-deficient HeLa cells as controls (CTL). To visualize FA, cells were stained for tyrosine phosphorylated paxillin with subsequent staining of the actin cytoskeleton using Alexa Fluor labelled phalloidin. Downregulation of SHP-2 was achieved by SHP-2 siRNA transfection. Interaction between SHP-2 and Cx43 was assessed by immunoprecipitation.

Results

The staining of the actin cytoskeleton revealed less stress fibres in Cx43 cells (fluorescence units, mean ± SEM, CTL: 85.4 ± 6.2; Cx43: 57.1 ± 3.2, n=3, $p<0.05$). Phospho-paxillin containing FA of control cells were larger and located both centrally and at the membrane, whereas Cx43 expressing cells formed focal complexes with smaller FA mainly located at the membrane. Western blot analyses demonstrated an increased dephosphorylation of paxillin in Cx43 expressing cells compared to CTL (n=4, $p<0.05$). Interestingly, the interaction of Cx43 and SHP-2 was observed to increase SHP-2 activity (n=4, $p<0.05$). Finally, preliminary data using SHP-2 siRNA suggests increased phosphorylation of paxillin, FA distribution and stress fibres formation in Cx43-expressing cells (n=2).

Conclusions

Our results demonstrate that the interaction of Cx43 with SHP-2 seems to be crucial for an enhanced dephosphorylation of the SHP-2 target FA protein paxillin which is required for a fast focal adhesion turnover associated with less stress fibres formation. This may be an underlying mechanism for the increased migration of Cx43 expressing cells (as shown previously).

A 08-03
PKC regulates αKlotho gene expression in MDCK and NRK-52E cells

Julia Vogt, Lisa Wolf, Jana Alber, Martina Feger, Michael Föller

University Hohenheim, Physiologie, Stuttgart, Germany

Question

Particularly expressed in the kidney, αKlotho is a transmembrane protein that acts together with bone hormone fibroblast growth factor 23 (FGF23) to regulate renal phosphate and vitamin D homeostasis. Soluble Klotho (sKL) is released from the transmembrane protein and controls various cellular functions as a paracrine and endocrine factor. αKlotho deficiency accelerates aging, whereas its overexpression favors longevity. αKlotho confers a better prognosis in cardiovascular and renal disease owing to anti-inflammatory, -fibrosis, or -oxidant effects and is a tumor suppressor. Serine/threonine protein kinase C (PKC) is ubiquitously expressed, affects several cellular responses and is also implicated in heart or kidney disease as well as cancer. We explored whether PKC is a regulator of αKlotho.**Methods**

Experiments were performed in renal MDCK or NRK-52E cells, and PKC isoform and αKlotho transcripts determined by qRT-PCR and Western Blotting.

Results

MDCK cells expressed PKCα, PKCγ, PKCδ, PKCε, PKCζ, PKCη, PKCθ and PKCι. In both cell lines, PKC activation with phorbol ester phorbol-12-myristate-13-acetate (PMA) down-regulated, while PKC inhibitor staurosporine enhanced αKlotho mRNA abundance. Further experiments with PKC inhibitors sotrastaurine or Gö6976 and RNAi suggested that PKCγ is the major isoform for the regulation of αKlotho gene expression in the two cell lines.

Conclusions

PKC is a negative regulator of αKlotho gene expression, an effect which may be relevant for the unfavorable effect of PKC on heart or kidney disease and tumorigenesis.

A 08-04

Direct interaction of endothelial progenitor cells (EPC) and endothelial cells (EC) induces the formation of angiogenic networks

Christina Steininger[1], Petra Kameritsch[2,3], Hanna Mannell[1,2], Kristin Pogoda[1,2]

[1] *University of Augsburg, Physiology, Institute of Theoretical Medicine, Augsburg, Germany*
[2] *LMU Munich, Institute of Cardiovascular Physiology and Pathophysiology, Biomedical Center, Planegg, Germany*
[3] *LMU Munich, Walter Brendel Center of Experimental Medicine, University Hospital, Munich, Germany*

Question: EPC are considered to support neovascularization and to participate in endothelial repair. EPC specifically express Cx43 in contrast to EC, which express Cx37, Cx40 and Cx43. Here, we investigated the role of the gap junctional communication (GJC) between EPC and EC in the formation of angiogenic networks in co-cultures *in vitro*.

Methods: Mouse embryonic EPC (E7.5) were co-cultured with EC (HUVEC, HMEC or PAEC) for 3-6 days. The GJC between EC and EPC was functionally assessed by fluorescent dye spreading of Alexa Fluor 488. EPC and EC were labelled with different fluorescent dyes (EC with PKH67; EPC with PKH26) prior to co-cultivation or by fluorescence *in situ* hybridization after fixation to identify the contribution of both cell types. Cx43 localisation in co-cultures was assessed by immunofluorescence staining.

Results: Capillary-like network structures were formed spontaneously in co-cultures of EC with EPC (CTL) after 3-5 days on uncoated plastic dishes (HUVEC n=7, HMEC n=6, PAEC n=6) but not in monocultures. This effect could not be mimicked by the incubation of EC with supernatants of EPC or vice versa (n=5). In contrast, pharmacological inhibition of GJC by heptanol and meclofenamic acid (hep/mec) or carbenoxolone (CBX) significantly abolished the angiogenic network formation (mean±SEM; length of branches: HMEC: CTL: 428±9 µm, hep/mec: 285±7 µm, n=6, $p<0.01$, PAEC: CTL: 451±18 µm, hep/mec: 281±28 µm, n=6, $p<0.01$; branching points/frame: HMEC: CTL: 3.2±0.4, hep/mec: 1.8±0.4 µm, n=6, $p<0.01$, PAEC: CTL: 4.2±0.6 µm, hep/mec: 1.5±0.5 µm, n=6, $p<0.01$). Dye injection studies confirmed GJC between both cell types (n=3). Immunofluorescence stainings in co-cultures of EPC with EC demonstrated a strong membrane localisation of Cx43 at contact sites of adjacent cells.

Conclusions: Our results suggest that the spontaneous formation of angiogenic networks in co-cultures of EC with EPC is dependent on a gap junctional communication of both cell types. Further analyses are necessary to clarify whether Cx43 might additionally contribute to the formation of capillary-like networks in a channel-independent manner via regulating endothelial cell migration.

A 08-05

Visualization and quantification of spatial inhomogeneities in confluent endothelial cell migration

Anselm Hohlstamm, Andreas Deussen, Stephan Speier, Peter Dieterich

TU Dresden, Institut für Physiologie, Dresden, Germany

Question

Cell migration is an ongoing and fundamental process in nearly all tissues, whereby cell division and apoptosis are central to maintain the organ's function. During the cells' turnover, the structure is locally disturbed, causing temporary or even permanent changes in the cell

arrangement. As this heterogeneity might play a crucial part in the tissue's responsiveness and function, we aim to investigate the occurrence and influence of spatial inhomogeneities on cell migration in confluent cultures.

Methods

We used human umbilical vein endothelial cells (HUVECs) and seeded them in a nearly confluent manner. After one day and prior to 48-hours live-cell imaging the dye Hoechst 33342 was added to mark the positions of the cell nuclei. Using self-developed automated image segmentation, tracking and analysis, we studied the movements of up to 50.000 cells in a cell layer of size 6x7 millimeters.

Results

The observed cell layers from 10 different experiments showed heterogeneous patterns of cell density, which were changing over time. Hereby, we quantified the effects on cell velocity, which showed a constant deceleration between certain density thresholds. Nevertheless, cell division itself transiently increased mean cell velocities causing disturbed movement patterns. We could explain the coupling of mean velocities and cell densities by a mathematical model of the temporal development of cell division activities. In addition, we analyzed and visualized the local velocity, direction and persistence of the moving cells within the confluent culture. We found a local emergence of collective movements where groups of cells migrated in forms of spirals, streets or in a convective manner. Using the mean squared displacement and velocity correlation functions, we measured and quantified these cluster movements with respect to duration, size and influencing factors like the interaction with other large clusters. It is noteworthy, that we could observe intermittent long-range spatial velocity correlations extending over distances of up to several millimeters.

Conclusions

In summary, we found distinct areas with specific cell arrangements and dynamics leading to locally different cell migration. In future, we will be able to investigate the correlation of this heterogeneity with the individual tissue function and resilience to pathological changes.

A 08-06

The tyrosine phosphatase SHP-2 is important for endothelial barrier function by promoting expression of endothelial tight junctional proteins

Georg Hupel[2], Yvonn Heun[2], Kristin Pogoda[1,2], **Hanna Mannell**[1,2]

[1] *Universität Augsburg, Physiology, Augsburg, Germany*
[2] *LMU, Institute of Cardiovascular Physiology and Pathophysiology, Munich, Germany*

Question

Inflammatory conditions impair endothelial barrier integrity and increase vascular permeability. Tight junction (TJ) and adherens junction (AJ) proteins join adjacent EC and thus play a pivotal role in controlling endothelial barrier function. Inactivation of the tyrosine phosphatase SHP-2 has been shown to increase vascular leakage. Moreover, in a previous study, we observed an inactivation of SHP-2 by inflammatory conditions. Here, we thus investigated if SHP-2 inactivation influences endothelial tight-junctions and IL-1β mediated permeability *in vitro*.

Methods

Wild type (WT), dominant negative (CS) or constitutively active SHP-2 (E76A) were over-expressed in human umbilical vein endothelial cells (HUVEC) by lentiviral transduction. Endothelial permeability *in vitro* was assessed by transendothelial electrical resistance (TEER) as well as immunofluorescent staining of VE-Cadherin upon stimulation with 10 ng/ml IL-1β over 24 h and 30 min., respectively. Expression of the TJ proteins claudin-5, occludin as well as the TJ adaptor protein ZO-1 were performed by western blot and qRT-PCR.

Results

IL1β induced endothelial permeability in SHP-2 WT cells compared to non-stimulated cells ($p<0.05$, n=5) and expression of SHP-2 CS further increased IL-1β mediated permeability ($p<0.05$, n=5). Interestingly, barrier integrity was significantly impaired already under basal conditions in SHP-2 CS cells compared to non-stimulated WT cells ($p<0.05$, n=5). This effect was confirmed by VE-Cadherin staining (n=5). While IL-1β stimulation did not affect the expression of the TJ proteins claudin-5, occludin or the TJ adaptor protein ZO-1 (all n=3), SHP-2 CS cells showed reduced expression of all investigated TJ proteins under basal conditions compared to SHP-2 WT (all $p<0.05$; n=8-10). Inhibition of proteasomal degradation by MG132 or lysosomal degradation by chloroquine did not reverse this. Accordingly, expression of the constitutively active SHP-2 EA enhanced the TJ protein expression (n=8-10). Likewise, the mRNA expression of claudin-5 (n=4), occludin (n=9) and ZO-1

(n=8) was impaired in SHP-2 CS cells compared to SHP-2 WT (all $p<0.05$). No effect on the expression of the AJ protein VE-Cadherin was observed (n=10-14).

Conclusions

SHP-2 seems to be important for maintaining the endothelial barrier by positively influencing the expression of tight junctional proteins. A loss of its activity induces endothelial permeability under basal as well as inflammatory conditions. Taken together with our previous findings showing inactivation of SHP-2 under inflammation, SHP-2 inactivation may be a fundamental step in the progression of diseases involving vascular leakage.

A 08-07

Patient age-related changes of redox parameters in female subdermal human adipose-derived stem cells (hASCs)

Anne Bernhardt[1,2], Alan Jamil[1], Tanvir Morshed[1], Maria Wartenberg[2], Heinrich Sauer[1]

[1] *Justus Liebig University Gießen, Physiology, Gießen, Germany*
[2] *Friedrich Schiller University Jena, Cardiology, Jena, Germany*

Question

With increasing period of life, mesenchymal stem cells including human adipose stem cells (hASCs) undergo aging processes. The aim of this study was to investigate possible changes of oxidative and nitrosative stress, NOX enzymes, inducible nitric oxide synthase (iNOS), stem cell genes, sirtuins (Sirt) as well as mitochondrial membrane potential, reactive oxygen species (ROS) and ATP in hASCs, which correlate with increasing patient age.

Methods

Subdermal hASCs were harvested by enzymatic dissociation of female subdermal patient-derived fat tissue. Protein expression of the NADPH oxidases (NOX1, NOX2, NOX4, DUOX1, DUOX2), the nuclear lamina proteins (Lamin B1+B2) and Sirt were assessed by western blot. For the analysis of gene expression of stem cell genes (Oct3/4, Sox2, Nanog, Rex1) qPCR was applied. Confocal laser scanning fluorescence microscopy (cLSM) was used to measure ROS (H_2DCF-DA), nitric oxide (NO) (DAF-FM), mitochondrial ATP (ATP-Red), mitochondrial superoxide (MitoSOX Red) and the membrane potential of mitochondria (JC-1).

Results

Female patients were categorized in four different age groups (20-34 yr, 35-49 yr, 50-64 yr, 65-80 yr). Our data demonstrated that cytoplasmic ROS concentration increased with patient age. To assess the source of ROS generation, protein expression of various NADPH oxidases was analysed. NOX2 was undetectable, the expression of NOX1 and NOX4 decreased with patient age, DUOX1 and DUOX2 remained stable. Mitochondrial superoxide increased with patient age, suggesting mitochondria as potential source for age-related upregulation of ROS generation. This was paralleled by increased ATP production in mitochondria, but no change in mitochondrial membrane potential. In contrast to ROS generation, NO concentration decreased with increasing patient age, presumably caused by downregulation of iNOS. All investigated patient age classes expressed the stem cell genes Oct3/4, Nanog, Sox2 and Rex1. The protein expression of the nuclear lamina protein Lamin B1+B2 increased with age. A significant age-dependent decrease of the longevity-associated protein Sirt1 was detected. Sirt2, Sirt3 and Sirt5 did not show significant age dependency.

Conclusions

With increasing patient age, mitochondrial ROS generation increases, while NO generation is downregulated. Nuclear lamina proteins and Sirt 1 change with increasing patient age, suggesting potential regulation by redox processes.

This work was supported by the German Research Foundation (DFG) grant no. WA 1087/8-1

A 08-08

Cadmium triggers reactive oxygen species, autophagy and the lysosomal ion channel TRPML1 in human renal cells.

Kaya Elisa Witte, **Wing-Kee Lee**

Bielefeld University, Medical School OWL, Physiology & Pathophysiology of Cells and Membranes, Bielefeld, Germany

Human cadmium (Cd) exposure is increasingly deteriorating global health status because of sustained growth in industrial activities and consumption of Cd-containing foodstuffs, leading to persistent Cd accumulation in the body. In cells, Cd leads to mimicry of calcium-related processes and elevated reactive oxygen species (ROS). Linked to ROS is autophagy, which balances cellular energy homoeostasis and is initiated by cargo-encapsulating autophagosomes. Lysosomal fusion results in autolysosomes with subsequent cargo degradation. We have previously reported deregulation of autophagy by lysosomal instability during Cd stress (Lee, W.-K. *et al., Arch. Toxicol.* 2017). Lysosomes coordinate various stress-sensing mechanisms, in part through the transient receptor potential cation channel, mucolipin subfamily, member 1 (TRPML1). Oxidative stress directly activates TRPML1, inducing calcium release and concomitant triggering of autophagy. Hence, the aim of our study was to analyze potential interactions between Cd-induced ROS, autophagy and TRPML1 as well as the potential Cd uptake in lysosomes via TRPML1.

In cultured human proximal convoluted tubule (HPCT) cells, Cd (1-2.5µM, 1-24h) increased TRPML1 expression by 1.5-fold (1h) up to 2.8-fold (24h) in parallel to disruption of autophagic flux by monitoring autophagy markers LC3-II (autophagosome marker) and p62 (autophagy cargo), which were upregulated 2.7-fold after 24h by immunoblotting. The promoter region of TRPML1 contains antioxidant response elements (ARE). To ascertain involvement of ROS, HPCTs were treated with the antioxidants α-tocopherol or TEMPOL. TEMPOL reduced LC3-II, p62 and TRPML1 protein after combined Cd exposure whereas α-tocopherol was ineffective. Co-treatment with brusatol, which inhibits NF-E2-related factor 2 (Nrf2, ARE binding-transcription factor), abolished increased Nrf2 target gene *HO1* by Cd. The lysosomal biogenesis marker, transcription factor EB, uncovered a switch from initial 1h Cd (2.5µM)-associated increase (1.9-fold) to downregulation at 24h Cd (0.3-fold) via immunoblotting. Acidic organelles were elevated in Cd-exposed (1-2.5µM, 1-3h) compared to control cells using LysoTracker and live cell imaging.

We therefore conclude Cd activates a ROS-Nrf2-TRPML1 axis to alter autophagic flux. Thus, we hypothesize crucial interaction of lysosomes with calcium-mimicking Cd via TRPML1, which potentially disrupts autophagic flux in human renal cells.

A 08-09

Nuclear eNOS interacts with and S-nitrosates RNA-binding proteins to modulate endothelial gene expression.

Xiaozhu Zhou[1,2], Carsten Künne[3], Stefan Günther[3], Ilka Wittig[4], Mauro Siragusa[1,2], Ingrid Fleming[1,2]

[1] *Institute for Vascular Signalling, Frankfurt am Main, Germany*

[2] *German Centre for Cardiovascular Research (DZHK), Partner site Rhein-Main, Frankfurt am Main, Germany*

[3] *Bioinformatics and Deep Sequencing Platform, Max Planck Institute for Heart and Lung Research, Bad Nauheim, Germany*

[4] *Functional Proteomics, Institute for Cardiovascular Physiology, Goethe University, Frankfurt am Main, Germany*

Introduction. Nitric oxide (NO) generated by the endothelial NO synthase (eNOS) regulates vascular tone and endothelial homeostasis to counteract vascular inflammation. The effects of NO are attributable to its interaction with heme-containing proteins e.g., soluble guanylyl cyclase, or to the post-translational modification of proteins i.e., S-nitrosation. It is well known that eNOS is localized to the cell membrane and the Golgi apparatus. However, the protein has also been detected in the endothelial cell nucleus. In this study we assessed the potential role of nuclear eNOS in endothelial cells.

Methods and Results. Confocal microscopy studies confirmed the presence of eNOS in the nucleus of unstimulated human and murine endothelial cells and stimulation with vascular endothelial growth factor (VEGF – 50 ng/ml, 10 minutes) elicited eNOS nuclear translocation. Co-immunoprecipitation studies coupled with proteomics revealed the VEGF-dependent association of nuclear eNOS with 81 proteins involved in RNA binding and processing in human endothelial cells. Among these, nuclear eNOS associated with splicing factor proline- and glutamine-

rich (SFPQ) and non-POU domain-containing octamer-binding protein (NONO), which are core components of paraspeckles, specialized nuclear membrane-less organelles involved in the regulation of gene expression. Interestingly, VEGF stimulation (50 ng/ml, 10 minutes) induced the S-nitrosation of SFPQ and eNOS knockdown in human endothelial cells altered the expression of >4000 genes. Nuclear eNOS also bound double-stranded RNA-specific adenosine deaminase 1 (ADAR1), an enzyme involved in RNA editing via the deamination of adenosine to inosine in double-stranded RNA (dsRNA). VEGF stimulation induced the S-nitrosation of ADAR1 in human endothelial cells and the knockdown of eNOS was associated with an increase in the amount of dsRNA (immunofluorescence) and altered the expression of interferon-stimulated genes. In HEK cells, dsRNA content was decreased by introducing wild-type eNOS, while a loss-of-function mutant (eNOS-Y657D) had no effect. ADAR1-mediated A-I editing (RNA sequencing) was significantly altered in the absence of eNOS, underscoring the importance of the eNOS-ADAR1 interaction and ADAR1 S-nitrosation for ADAR1 function.

Conclusion. These results demonstrate that eNOS/NO signalling modulates nuclear processes that are essential for the regulation of endothelial cell gene expression.

A 08-10
NoxO1 and Erbin- a cooperation to control EGF-signaling

Dana Maureen Hebchen[1], Tim Schader[1], Niklas Mueller[1], Manuela Spaeth[1], Johannes Graumann[2], Katrin Schroeder[1]

[1] *Institute for Cardiovascular Physiology / Vascular Research Centre, Goethe University Frankfurt, Frankfurt, Germany*
[2] *Biomolecular Mass Spectrometry, Max Planck Institute for Heart and Lung Research, Bad Nauheim, Germany*

Question

NADPH oxidase organizer 1 (NoxO1), a subunit of the reactive oxygen species (ROS)-producing Nox1 complex, plays a role in various cellular processes like proliferation and differentiation of colon epithelia[1-3]. We recently identified and validated ErBB2-Interacting Protein (Erbin) as novel interaction partner of NoxO1. So far, nothing is known about importance or consequences of this newly discovered interaction. Erbin however, has been described as a negative regulator of Epidermal Growth Factor receptor (EGFR) signaling [4,5]. We hypothesize that NoxO1 *via* interaction with Erbin modifies EGF signal transduction. Thus, we aim to explore the impact of NoxO1 on EGF-mediated signaling and EGFR trafficking .

Methods and Results

Both Erbin and NoxO1 overexpression in HEK293 cells delay EGF-related MAPK / AKT phosphorylation in Western Blot analysis upon short time course of stimulation. Upon NoxO1 overexpression, Erbin and EGFR are in closer proximity, while EGFR protein level is reduced in a cycloheximide-based stability assay. NoxO1 overexpression induces an elevated expression of markers for early / late endosomes and lysosomes. We examined the dependency of these marker proteins on NoxO1 and Erbin pointing onto a cooperative mechanism of action. Moreover, EGF-induced ROS formation is lowered by Erbin overexpression confirming Erbin's function as negative regulator of NoxO1 mediated ROS formation.

Conclusion

Analysis of NoxO1 and Erbin expression in human cancer cell lines support the hypothesis that NoxO1 negatively affects EGFR internalization and signaling. We conclude that NoxO1 and Erbin cooperatively regulate EGFR signal transduction and turnover.

References

[1] Buchmann, Giulia K.; Schürmann, Christoph; Warwick, Tim; Schulz, Marcel H.; Spaeth, Manuela; Müller, Oliver J. et al. (2020): Deletion of NoxO1 limits atherosclerosis development in female mice. In: *Redox Biology* 37 DOI: 10.1016/j.redox.2020.101713

[2] Moll, Franziska; Walter, Maria; Rezende, Flávia; Helfinger, Valeska; Vasconez, Estefania; Oliveira, Tiago de et al. (2018): NoxO1 Controls Proliferation of Colon Epithelial Cells. In: *Frontiers in Immunology* 9 DOI: 10.3389/fimmu.2018.00973.

[3] Schader, Tim; Reschke, Christina; Spaeth, Manuela; Wienstroer, Susanne; Wong, Szeka; Schröder, Katrin (2020): NoxO1 Knockout Promotes Longevity in Mice. In: *Antioxidants* 9 (3) DOI: 10.3390/antiox9030226.

[4] Borg, J. P.; Marchetto, S.; Le Bivic, A.; Ollendorff, V.; Jaulin-Bastard, F.; Saito, H. et al. (2000): ERBIN: a basolateral PDZ protein that interacts with the mammalian ERBB2/HER2 receptor. In: *Nature cell biology* 2 (7) DOI: 10.1038/35017038.

[5] Santoni, Marie-Josée; Kashyap, Rudra; Camoin, Luc; Borg, Jean-Paul (2020): The Scribble family in cancer: twentieth anniversary. In: *Oncogene* 39 (47) DOI: 10.1038/s41388-020-01478-7.

A 08-11

The pro-inflammatory response of embryoid bodies differentiated from mouse embryonic stem cells towards lipopolysaccharide from gram-negative bacteria

Jennifer Scharmacher[1], Maria Wartenberg[2], Heinrich Sauer[1]

[1] *Justus Liebig University Gießen, Physiology, Gießen, Germany*
[2] *Friedrich Schiller University Jena, Cardiology, Jena, Germany*

Question

Embryonic stem (ES) cells differentiate towards all three germ layers, including cardiac cells and leukocytes, and may be therefore suitable to model inflammatory reactions in vitro. In the present study, embryoid bodies differentiated from mouse ES cells were treated with increasing doses of lipopolysaccharide (LPS) to mimic infection with gram-negative bacteria.

Methods

Cardiac cells differentiated from ES cells were characterized by immunohistochemistry. CD68 and CD69 expression was analyzed by immunohistochemistry and western blot. Intracellular calcium, nitric oxide (NO), and reactive oxygen species (ROS) generation were assessed by fluo-4, H_2DCF, and DAF microfluorometry and confocal microscopy.

Results

LPS treatment dose-dependent increased contraction frequency of cardiac cell areas and calcium spikes and increased protein expression of α-actinin. LPS treatment increased the expression of the macrophage marker CD68 and CD69, which is upregulated after activation on T cells, B cells and NK cells. LPS dose-dependent increased protein expression of toll-like receptor 4 (TLR4). Moreover, upregulation of NLR family pyrin domain containing 3 (NLRP3), IL-1ß and cleaved caspase 1 was observed, indicating activation of inflammasome. In parallel, generation of reactive oxygen species (ROS), nitric oxide (NO), and expression of NOX1, NOX2, NOX4 and eNOS occurred. ROS generation, NOX2 expression and NO generation were downregulated by the TLR4 receptor antagonist TAK-242 which abolished the LPS-induced positive chronotropic effect of LPS.

Conclusions

Our data demonstrate that LPS induced a pro-inflammatory cellular immune response in tissues derived from ES cells, recommending the in vitro model of embryoid bodies for inflammation research.

This work was supported by the Alan and Helene Goldberg Foundation, Johns Hopkins University, Baltimore

References
[1] Finkensieper A, Bekhite MM, Fischer H, Nitza S, Figulla HR, Müller JP, Sauer H, Wartenberg M. Antibacterial capacity of differentiated murine embryonic stem cells during defined in vitro inflammatory conditions. Stem Cells Dev. 2013 Jul 15;22(14):1977-90. doi: 10.1089/scd.2012.0528.

A 08-12

The high proinflammatory secretome is a unique hallmark of Interferon-γ- and Tumor Necrosis Factor-induced senescence in melanoma cells

Lorenzo Homann[1], Maximilian Rentschler[1,2], Ellen Brenner[1], Susanne Weidemann[1], Martin Röcken[1], Thomas Wieder[2]

[1] *University of Tübingen, Department of Dermatology, Tübingen, Germany*
[2] *University of Tübingen, Department of Physiology, Tübingen, Germany*

Question

Immune checkpoint blockade (ICB) does not directly target melanoma cells but instead disinhibits immune effector cells, i. e. CD4- and CD8-positive T cells (for review see [1]). ICB may also induce tumor cell senescence [2], which is characterized by a permanent growth arrest of the tumors [3]. Along this line, different therapeutic regimen, e. g. chemotherapeutics, cell cycle inhibitors and the cytokines interferon-γ (IFN-γ) and tumor necrosis factor (TNF) [4] are established triggers of cellular senescence. As senescent cells are metabolically active and secrete

proinflammatory factors [5], we hypothesized that IFN-γ- and TNF-treated melanoma cells adopt a unique senescence-associated secretory phenotype (SASP) which may affect tumor growth thereby stabilizing permanent growth arrest.

Methods

To compare the state of senescence and the SASP in the setting of cytokine-induced senescence (CIS) and therapy-induced senescence (TIS), human melanoma cell lines SK-MEL-28 and WM115 were treated for 96 h with IFN-γ and TNF, the chemotherapeutic agent doxorubicin, or the cell cycle inhibitor palbociclib. Then, the senescence inducers were removed, cells were washed thoroughly with PBS and subsequently replenished with fresh medium and cultured in the absence of the substances for additional 48 h. Senescence was analyzed by SA-ß-gal staining, growth assays to demonstrate stable inhibition of cell proliferation, western blot to show different senescence marker proteins (p16Ink4a or p21), and flow cytometry to demonstrate cell cycle arrest. The SASP was analyzed on a transcriptional level by quantitative polymerase chain reaction (PCR) arrays, and the secretome of the senescent cells by Proteome Profiler arrays and ELISA.

Results

All three therapeutic regimen induced senescence in both cell lines, i. e. they enhanced SA-ß-gal activity, induced a senescent morphology, and a stable growth arrest with strong reduction of the S-phase of the cell cycle. Interestingly, the transcriptional activity of SASP genes in CIS melanoma cells was permanently enhanced as compared with SASP genes in TIS melanoma cells. Accordingly, the SASP generated by CIS melanoma cells showed a higher proinflammatory profile as compared with the SASP generated by TIS cells, and the conditioned medium of CIS cells was able to induce senescence features, e. g. SA-ß-gal activity and senscent morphology, in naïve melanoma cells.

Conclusions

The conditioned medium produced by senescent melanoma cells following treatment with cytokines contains high amounts of proinflammatory factors which in turn induce senescence in neighbouring melanoma cells. Thus, senescence induction via cytokines may lead to self-sustaining senescence surveillance of melanoma (Fig. 1).

This research was funded by the IZKF Promotionskolleg of the University of Tübingen (grant number 2020-1-03), the Wilhelm Sander-Stiftung (grant number 2020.100.1), and the Deutsche Forschungsgemeinschaft (grant numbers RO 764/15-2 and WI 1279/4-1).

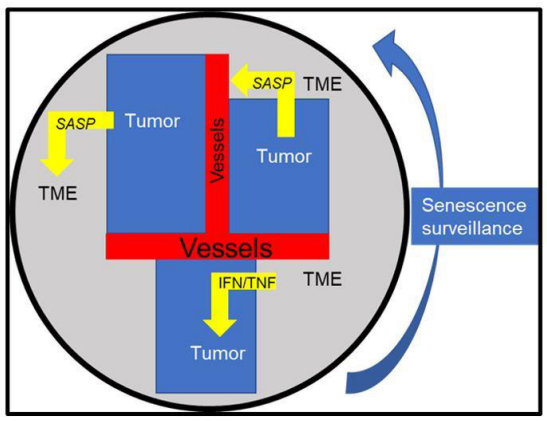

Fig. 1: Senescence surveillance of tumors.
IFN, interferon; SASP, senescence-associated secretory phenotype; TME, tumor microenvironment; TNF, tumor necrosis factor.

References
[1] Kelly, PN 2018, 'The Cancer Immunotherapy Revolution', *Science*, 359, 1344–1345.
[2] Brenner, E et al. 2020, 'Cancer immune control needs senescence induction by interferon-dependent cell cycle regulator pathways in tumours', *Nat. Commun.*, 11, 1335.
[3] Campisi, J 2013, 'Aging, cellular senescence, and cancer', *Annu. Rev. Physiol.*, 75, 685–705.
[4] Braumüller, H et al. 2013, 'T-helper-1-cell cytokines drive cancer into senescence', *Nature*, 494, 361–365.
[5] Birch, J, Gil, J 2020, 'Senescence and the SASP: Many therapeutic avenues', Genes Dev., 34, 1565–1576.

A 09 | Blood & Immune Cells

A 09-01
Effects of propofol on the Hypoxia-inducible factor pathway in human leukocytes under physiological oxygen conditions

Jessica Hüssen, Joachim Fandrey, Anna Wrobeln, Tina Schönberger

University of Duisburg-Essen, University Hospital Essen, Institute of Physiology, Essen, Germany

Propofol (2,6-diisopropylphenol) is a GABA-receptor agonist, formulated as an lipid-based emulsion and the most frequently used intravenous anesthetic in the clinic. It is used for induction and maintenance of general anesthesia and to enhance sedation in mechanically ventilated patients. The common pathophysiological functions of propofol mainly include reduction of blood pressure and inhibition of respiration, followed by immune system and nervous system abnormalities.[1] It can also lead to the propofol infusion syndrome (PRIS), which often results in death. Although the pathophysiology and risk factors of PRIS remain unknown, propofol treatment has been linked to changes in the activation of the Hypoxia-inducible factor (HIF) pathway in some immune cells.[2] Precise regulation of the HIF pathway is important to ensure adequate immune response and metabolic adaption of leukocytes in environments with insufficient oxygen supply (hypoxia) or inflammation. However, it is not clear how propofol influences the HIF pathway and human leukocyte function in detail. A more in-depth understanding of potential immunological side effects of propofol on human leukocytes is needed to improve patients' outcome under long-time anesthesia. Therefore, we studied the *in vitro* effects of different oxygen concentrations (21 %, 8 %, 1 %) on human peripheral blood mononuclear cells (PBMCs) regarding its potency to activate the HIF pathway by protein analysis via immunoblotting and gene expression analysis through quantitative real-time PCR. First results show a strong HIF pathway activation of leukocytes under hypoxic conditions but no differences between normoxic conditions of 21% and 8% oxygen. Further, we investigate the influence of propofol treatment and its solvent (soybean oil mix) on the HIF pathway on human PBMCs with the same methods. For this purpose, we are using physiological oxygen concentrations of 8 % and 1 % over a 24 hour period with clinically relevant propofol concentration of 10, 25 and 50 µM in comparison to the same amount of a soybean oil mix. Additionally, we are using a soybean oil mix to investigate, if effects are due to the drug itself or its soy bean emulsion. We further plan to analyse immune cell function under propofol treatment by measuring oxygen consumption rate and extracellular acidification rate of living cells in a time-dependent manner (Seahorse Extracellular Flux Analysis).

[1] Yi S, Tao X, Wang Y, Cao Q, Zhou Z, Wang S. Effects of propofol on macrophage activation and function in diseases. Front Pharmacol. 2022 Aug 17;13:964771. doi: 10.3389/fphar.2022.964771. PMID: 36059940; PMCID: PMC9428246.

[2] Ichikawa T, Okuyama K, Kamata K, Masui K, Ozaki M. Suspected propofol infusion syndrome during normal targeted propofol concentration. J Anesth. 2020 Aug;34(4):619-623. doi: 10.1007/s00540-020-02773-z. Epub 2020 Mar 28. PMID: 32222909.

We thank the team of the Institute for Transfusion Medicine, University Hospital Essen for buffy coats for PBMC isolation.

References

[1] Yi S, Tao X, Wang Y, Cao Q, Zhou Z, Wang S. Effects of propofol on macrophage activation and function in diseases. Front Pharmacol. 2022 Aug 17;13:964771. doi: 10.3389/fphar.2022.964771. PMID: 36059940; PMCID: PMC9428246.

[2] Ichikawa T, Okuyama K, Kamata K, Masui K, Ozaki M. Suspected propofol infusion syndrome during normal targeted propofol concentration. J Anesth. 2020 Aug;34(4):619-623. doi: 10.1007/s00540-020-02773-z. Epub 2020 Mar 28. PMID: 32222909.

A 09-02
TGF-β leads to HIF-1α degradation by increasing PHD2 in human leukocytes

Isabel Ruf, Joachim Fandrey, Anna Wrobeln

University of Duisburg-Essen/University Hospital Essen, Institute of Physiology, Essen, Germany

Transforming growth factor beta (TGF-β) is a regulatory cytokine involved in angiogenesis and the immune response. Beside TGF-β, hypoxia inducible factors (HIFs) play a critical role in the regulation of the immune response. Studies have shown that immune cells lacking HIF-1α are dysfunctional. Several publications indicate an interaction of TGF-β with HIFs.

Patients who suffer from mutations affecting genes of the TGF-β pathway (Hereditary Hemorrhagic Telangiectasia (HHT)) have dilated abnormal vessel structures and an impaired immune response. Our group recently showed that HHT leukocytes have a decreased *HIF1A* gene and HIF-1α protein expression. Detailed information how TGF-β influences HIF-1α expression in human leukocytes is still missing.
We isolated human peripheral blood mononuclear cells (PBMCs) from buffy coats and treated them with TGF-β (5, 25, 50, 100 ng/ml) for 4 and 24 hours under normoxic and hypoxic conditions (1% O_2). Our results indicate that under normoxic conditions, TGF-β leads to HIF-1α protein degradation by increasing the protein level of the HIF-1α degrading prolyl hydroxylase 2 (PHD2) in human PBMCs. In addition, TGF-β induces *HIF1A*, *HIF2A* and *PHD2* gene expression. Preliminary results show that under hypoxic conditions TGF-β leads to enhanced HIF-1α accumulation compared to hypoxia alone.
Our findings could help to understand the general effect of TGF-β on HIF-1α in leukocytes and thus the impaired immune response in HHT, revealing new therapeutic options.

A 09-03
Hypoxia inducible factor in a commonly used mouse model of Hereditary Hemorrhagic Telangiectasia and affected human leukocytes

Anna Wrobeln[1], Freya Droege[2], Joachim Fandrey[1]

[1] *University of Duisburg-Essen / University Hospital Essen, Institute of Physiologie, Essen, Germany*
[2] *University of Duisburg-Essen / University Hospital Essen, Department of Otorhinolaryngology, Head and Neck Surgery, Essen, Germany*

About 85,000 people in Europe suffer from hereditary hemorrhagic telangiectasia (HHT or Morbus Osler). Various mutations, particularly of the endoglin and ALK-1 gene, both members of the transforming growth factor-β (TGF-β) signaling pathway lead to pathological widening of blood vessels (telangiectasia). As a result, HHT patients suffer from recurrent hemorrhages. Telangiectasias in liver, lungs, intestines and brain can cause life-threatening bleedings. Beside the regulation of angiogenesis, TGF-β influences, as regulatory cytokine, the immune response. Therefore, HHT patients suffer from an impaired immune response. Little is known about this impairment, but it has been reported that 35% of HHT patients die from sepsis, which is the most common cause of death in this patient population.[1]The interplay between TGF-β and the hypoxia inducible factors (HIF) in inflammatory and angiogenic processes is well characterized.[2] Even though HIFs play a key role in both, angiogenesis and immune response, no one has yet addressed the consequences of mutations in HHT-patients. Our group recently reported reduced HIF-1α gene and protein expression in whole blood of HHT patients.[3]
In our study, we investigated gene expression and protein content of HIFs and their target genes in human leukocytes from HHT patients as well as in organs from an established HHT mouse model of tamoxifen induced endothelial ALK-1 knockout mice. HHT leukocytes showed decreased gene expression of *HIF1A*and its target genes. In contrast, *Hif1α* gene expression in nearly all organs harvested from ALK-1 knockout mice was increased. Both, human leukocytes and organs from ALK-1 knockout mice showed decreased *HIF2A* gene expression. Analysis of HIF-1α protein revealed a reduction in human HHT leukocytes as well as in the murine model of HHT.
To conclude, our results indicate that the murine HHT model reflects HIF protein levels of HHT-patients, but not HIF-1α gene expression. Tamoxifen induction of homozygous ALK-1 knockout may rather reflect an acute response to changes in the TGF-β signaling, whereas in patients we observe the manifestation of the long-term impact and its adaption to it. Further studies will show to what extent HIF may function as a therapeutic target.

References
[1] Droege, F. *et al.* Life expectancy and comorbidities in patients with hereditary hemorrhagic telangiectasia. *Vascular Medicine***23**, 377-383 (2018).
[2] Frede, S. *et al.* Regulation of hypoxia-inducible factors during inflammation. *Methods in enzymology***435**, 403-419 (2007).
[3] Wrobeln, A. *et al.* Altered hypoxia inducible factor regulation in hereditary haemorrhagic telangiectasia. *Scientific Reports***12**, 1-9 (2022).

A 09-04
The role of the hypoxia inducible factor 1 alpha in myeloid derived immune cells in urinary bladder infection and cancer

Clara Roggendorf, Joachim Fandrey, Nora M. Koll

Universitätsklinikum Essen, Institut für Physiologie, Essen, Germany

The hypoxia inducible factor (HIF) is a dimeric transcription factor, which is responsible for the adaption of cells to low oxygen concentrations (hypoxia). Under hypoxia the HIF1α subunit accumulates in the cell. It then migrates into the nucleus were it dimerizes with the β subunit to form a functional transcription factor. Not only hypoxia, but also inflammation can lead to the accumulation of HIF1α. It is known that HIF play an important role in hypoxic regions in tumors and in the function of the immune system.[1] Therefore HIF is likely to have an influence in tumor growth and inflammation. To better understand the role of the hypoxia inducible factor 1 (HIF1) in myeloid derived immune cells (monocytes, macrophages, dendritic cells) in the context of bladder infection and bladder cancer a murine experimental model was set up. A new combination of two mouse models was established to get hints for the discussed influence of previous bladder infection on bladder cancer pathogenesis.

Mice with and without functional HIF1α in myeloid derived immune cells were bred ($Hif1\alpha^{flox/flox}$LysM(Cre)-knockout). Urinary bladder infection was induced by instillation of a solution of 10^8 CFU uropatogenic E. coli (UPEC) in culture medium with a catheter directly into the bladder of anesthetized mice. This was performed three times with a time distance of one week to simulate a reoccurring urinary bladder infection. In mice with and without previous UPEC infection bladder cancer was induced. A treatment with the cancerogenic substance N-Butyl-N-(4-hydroxybutyl)nitrosamine (BBN) via drinking water for 20 weeks led to tumor growth in primarily the urinary bladder. Also corresponding control mice (regarding genotype, UPEC infection and BBN treatment) were used.

Urine samples were collected weekly and additionally one day after UPEC instillation to confirm and monitor infection and carcinogenic processes. Colony forming units of UPECs were counted after cultivating the urine over night on selective agar plates. Urine cytology could show signs of infection and tumor cells. Cancer induction was additionally confirmed by outer appearance, weight, lenght and histological hematoxylin and eosin staining of the bladders.

RNA, protein and immunohistochemical analyses will show the role of HIF in immune cells in the context of bladder infection and cancer and the influence of urinary bladder infections themselves on cancerogenesis.

References

[1] Palazon A, Goldrath AW, Nizet V, Johnson RS 2014, 'HIF transcription factors, inflammation, and immunity.', *Immunity*, 41.4, 518-528

A 09-05
Oxygen tension plays a major role in TH1 cell generation

Inga Vorwick, Joachim Fandrey, Anna Wrobeln

University Duisburg-Essen / University Hospital Essen, Institute of Physiology, Essen, Germany

T cells are immune cells that migrate from blood and lymphoid organs into the tissue to protect against pathogen infiltration. During this migration they experience rapid change in oxygen tension. Current standard condition for preclinical studies is the incubation under atmospheric oxygen concentrations (21% O_2) and not the physiological concentration in the blood of 8% O_2, or in the lymph node and tissue (1% O_2). There is evidence that Hypoxia inducible factor (HIF-1α) stabilization at low oxygen concentrations affects CD4+ T cell function.

Only few studies address the relevance of the oxygen tension for the differentiation and regulation of human T cells. In our study, we investigate the influence of oxygen tension on the differentiation of human CD4+ T cells to Th1 cells. T cells are treated for one week under atmospheric oxygen (21% O_2), physioxia (8% O_2) and hypoxia (1% O_2) simulating the period of differentiation. At day seven, the cells are characterized using flow cytometry for Th1 cell differentiation markers.

We expect the differentiation and expansion to be altered. Preliminary results show reduced proliferation of cells under hypoxic conditions compared to the cells under physioxic and atmospheric conditions. In addition, the expression of INF-γ seems to be reduced in 1 % O_2 and 8 % O_2.
Our findings highlight the necessity of mimicking physiological oxygen tensions during immunological studies for the enhancement of clinical translation.

A 09-06
Effects of the ciliary proteasome on the function of hypoxia-inducible factors at primary cilia

Stephan Schieren, Joachim Fandrey, Tristan Leu

University of Duisburg-Essen / University Hospital Essen, Institute of Physiology, Essen, Germany

The primary cilia is a non-motile antenna-like organelle on the surface of most cell types in the human body. It plays an essential role in processes such as proliferation, apoptosis, migration and differentiation. Primary cilia are involved in many signalling pathways including Hedgehog, WNT and TGF-β. Consequently, ciliary dysfunctions leads to severe diseases known as ciliopathies.
The formation and function of the primary cilia is closely associated to oxygen supply of the cell. Sufficient oxygen levels are key for proper cell function; therefore, cells must quickly react to any deviation from the norm. Key factors in the hypoxic response are hypoxia-inducible factors (HIFs).
Recent studies indicate that HIF accumulates in the cilia under hypoxia influencing different target genes. It was shown that HIF-2α affects the MEK/ERK signalling pathway via the primary cilia [1]. Under hypoxia, primary cilia are elongated while HIF-2α translocates into the cilia through the ciliary gate.
Within our studies, we focus on the effect of hypoxia on the activity of the ciliary proteasome by analysing the localisation and intensity of β-catenin and ubiquitin in primary cilia by immunofluorescence microscopy. The ciliary proteasome is a special proteasome of the cell that is exclusively regulated by ciliary proteins [2]. Previous studies discovered that Gli3, a protein of the Hedgehog signalling pathway is proteasomally cleaved in primary cilia [3]. Functions of this proteasome in relation to HIF and hypoxia are not known and part of this study. We are also looking at different HIF target genes to see if there are different levels of gene expressions under hypoxia.

References
[1] Leu T, Denda J, Wrobeln A, Fandrey J. Hypoxia-Inducible Factor-2alpha Affects the MEK/ERK Signaling Pathway via Primary Cilia in Connection with the Intraflagellar Transport Protein 88 Homolog. Mol Cell Biol. 2023;43(4):174-183. doi: 10.1080/10985549.2023.2198931. Epub 2023 Apr 19. PMID: 37074220; PMCID: PMC10153011.
[2] Gerhardt C, Lier JM, Burmühl S, Struchtrup A, Deutschmann K, Vetter M, Leu T, Reeg S, Grune T, Rüther U. The transition zone protein Rpgrip1l regulates proteasomal activity at the primary cilium. J Cell Biol. 2015 Jul 6;210(1):115-33. doi: 10.1083/jcb.201408060. PMID: 26150391; PMCID: PMC4494006.
[3] Wang B, Fallon JF, Beachy PA. Hedgehog-regulated processing of Gli3 produces an anterior/posterior repressor gradient in the developing vertebrate limb. Cell. 2000 Feb 18;100(4):423-34. doi: 10.1016/s0092-8674(00)80678-9. PMID: 10693759.

A 09-07
Modulation of myeloid cell efferocytosis regulates pathological retinal angiogenesis in the mouse oxygen-induced retinopathy model

Anne Klotzsche - von Ameln[1], Irina Korovina[2], Canelif Yilmaz[1], Andreas Deussen[1], Stephan Speier[1]

[1] *TU-Dresden, Faculty of Medicine, Institute of Physiology, Dresden, Germany*
[2] *TU-Dresden, National Center for Radiation Research in Oncology, Dresden, Germany*

Proliferative retinopathies, such as retinopathy of prematurity or proliferative diabetic retinopathy are major vision threatening diseases. They account for a significant loss of life quality and productivity of affected individuals, and are currently the leading causes of blindness in the industrialized countries. Interestingly, the pathogenesis of proliferative retinopathies is complex and several neuronal, vascular and inflammatory mechanisms are involved [1].

Using a murine model for proliferative retinopathy, the oxygen induced retinopathy (OIR)-model [2], we have addressed the role of inflammatory cells in proliferative retinopathies.

In previous studies we could show that the pathological vessels in the OIR-model comprise of many apoptotic endothelial cells, and the apoptosis can partially be mediated by retinal myeloid cells [3]. These damaged/dying endothelial cells must be efficiently cleared to prevent the exposure of the surrounding tissue to uncontrolled enzyme activity, such as proteases leaking from the dying cells, and/or other intracellular components. This efferocytosis process is well described in many inflammatory conditions, however, to our knowledge a regulatory role of this pathway in pathological retinal angiogenesis has not been addressed yet. Based on these facts, we addressed the question, whether retinal inflammatory cells could affect the degree of retinal neovascularization, by elimination (efferocytosis) of the “abnormal” endothelial cells in the pathological tufts.

In order to study this, we utilized mice with a myeloid specific deletion of the suppressor of cytokine signaling protein 3 (SOCS3; LysM-cre x SOCS3$^{fl/fl}$).

As compared to SOCS3-sufficient counterparts, we found that SOCS3-deficient microglia and macrophages displayed an increased phagocytic activity towards apoptotic endothelial cells, which was associated with an enhanced expression of the opsonin growth arrest-specific 6 (GAS6), a major pro-phagocytic molecule [4]. Furthermore, we found that myeloid SOCS3-deficiency significantly reduced angiogenesis in an *ex-vivo* mouse aortic ring assay, as well as in the mouse *in vivo* OIR-model, which could be reversed by the inhibition of the GAS6 receptor Mer. In addition, we could reduce pathological neovascularization in the OIR-model by an intravitreal injection of the opsonin GAS6 (recombinant mouse GAS6 at P14).

Together our findings provide novel insights regarding the complex interplay between immune cells and endothelial cells and may have implications for novel therapeutic approaches in proliferative retinopathies.

This work was funded by a grant of Anne Klotzsche-von Ameln from the Deutsche Forschungsgemeinschaft (DFG: KL 3351/1–1).

References

[1] Klotzsche-von Ameln, A. and D. Sprott, *Harnessing retinal phagocytes to combat pathological neovascularization in ischemic retinopathies?* Pflugers Arch, 2022. **474**(6): p. 575-590.
[2] Smith, L.E., et al., *Oxygen-induced retinopathy in the mouse.* Invest Ophthalmol Vis Sci, 1994. **35**(1): p. 101-11.
[3] Korovina, I., et al., *Hematopoietic hypoxia-inducible factor 2alpha deficiency ameliorates pathological retinal neovascularization via modulation of endothelial cell apoptosis.* FASEB J, 2018: p. fj201800430R.
[4] Korovina, I., et al., *Myeloid SOCS3 Deficiency Regulates Angiogenesis via Enhanced Apoptotic Endothelial Cell Engulfment.* J Innate Immun, 2019: p. 1-9.

A 09-08
Comprehensive in silico and functional studies of genetic variants identified in patients with erythrocytosis

Valéna Karaghiannis[3,4], **Darko Maric**[1,2], Céline Garrec[5], Nada Maaziz[6], Alexandre Buffet[7,8], Loïc Schmit[4], Vincent Antunes[1,2], Fabrice Airaud[5], Bernard Aral[6], Amandine Le Roy[4], Sébastien Corbineau[4], Lamisse Mansour-Hendili[9,10], Valentine Lesieur[4], Antoine Rimbert[4], Fabien Laporte[4], Marine Delamare[4], Minke Rab[11,12], Stéphane Bézieau[4,5], Bruno Cassinat[13], Frédéric Galacteros[10,14], Anne-Paule Gimenez-Roqueplo[7,8], Nelly Burnichon[7,8], Holger Cario[15], Richard van Wijk[11], Celeste Bento[16], ECYT-4 consortium ECYT-4 consortium[19], François Girodon[6,17,18], David Hoogewijs[1,2], Betty Gardie[3,4,18]

[1] University of Fribourg, Department of Endocrinology, Metabolism and Cardiovascular System (EMC), Fribourg, Switzerland
[2] National Center of Competence in Research "Kidney.CH", National Center of Competence in Research "Kidney.CH", Zurich, Switzerland
[3] Université PSL, Ecole Pratique des Hautes Etudes, EPHE, Paris, France
[4] Nantes Université, CNRS, INSERM, l'institut du thorax, Nantes, France
[5] CHU de Nantes, Service de Génétique Médicale, Nantes, France
[6] CHU de Dijon, Service d'Hématologie Biologique, Pôle Biologie, Dijon, France
[7] Université Paris Cité, Inserm, PARCC, Paris, France
[8] Hôpital européen Georges Pompidou, Département de Médecine Génomique des Tumeurs et des Cancers, AP-HP, Paris, France
[9] Hôpitaux Universitaires Henri Mondor, Département de Biochimie-Biologie Moléculaire, Pharmacologie, Génétique Médicale, AP-HP, Créteil, France
[10] Université Paris-Est Créteil, IMRB Equipe Pirenne, Laboratoire d'excellence LABEX GRex, Créteil, France
[11] University Medical Center, Central Diagnostic Laboratory - Research, Utrecht, Netherlands
[12] University Medical Center Utrecht, Department of Hematology, Utrecht, Netherlands
[13] Université Paris Cité, APHP, Hôpital Saint-Louis, Laboratoire de Biologie Cellulaire, Paris, France
[14] Hôpitaux Universitaires Henri Mondor, Red Cell Disease Referral Center-UMGGR, AP-HP, Créteil, France
[15] University Medical Center Ulm, Department of Pediatrics and Adolescent Medicine, Ulm, Germany
[16] Centro Hospitalar e Universitário de Coimbra, Hematology Department, Coimbra, Portugal
[17] Université de Bourgogne, Inserm U1231, Dijon, France
[18] Laboratoire d'Excellence GR-Ex, Paris, Germany
[19] ECYT-4 consortium, Paris, France

Erythropoietin (Epo) is the key hormone promoting red blood cell production and is induced by the activation of the hypoxia-inducible factors (HIFs) pathway in response to hypoxia and anemia, contributing to restore the normal plasmatic oxygen levels. However, under pathological conditions, such as erythrocytosis, Epo plasma levels are high, leading to a dramatic increase of the red blood cell mass and resulting in blood hyperviscosity and thrombosis. A number of mutations in genes involved in the oxygen-sensing pathway have been identified, however for the majority of congenital secondary erythrocytosis patients the cause remains unknown.

In the present gain-of-function mutations in the *EPAS1/HIF2A* gene study, we identified patients with hereditary erythrocytosis, which can be associated with the development of paraganglioma, pheochromocytoma and somatostatinoma. We describe a unique European collection of 41 patients and 28 relatives diagnosed with erythrocytosis associated with a germline genetic variant in *EPAS1*. Clinical blood measures displayed significantly higher Epo, Haematocrit (Hct) and Haemoglobin (Hb) levels in these patients as compared to healthy individuals. Moreover, to assess the impact of 13 different HIF-2α variants we used different *in silico* and functional approaches. Notably, to identify the potential functional impact of these mutations, we employed reporter gene assay screening procedures and a novel edited vector containing an expanded region of the erythropoietin promoter combined with distal regulatory elements, which substantially enhanced the observed responses and conferred higher HIF-2α-dependent inductions.

Our results, allowed the classification of 11 mutations as pathogenic in 17 patients and 23 relatives. F374Y that was initially described as causal in patients with erythrocytosis and paraganglioma was not associated to any gain of function according to our results. Furthermore, we identified four new mutations (D525G, L526F, G527K, A530S) close to the key proline P531 and two germline mutations previously identified at somatic state in tumours (A530S and Y532C), which broadens the spectrum of mutations involved in erythrocytosis. Altogether, our study will contribute to the accurate clinical follow-up of patients, detection of previously not associated variants and will open the possibility for these patients to benefit from a newly developed HIF-2α inhibitor treatment.

All experiments were performed according to institutional guidelines, and conform to the principles of the Declaration of Helsinki. All subjects were duly informed and gave written consent.

References

[1] Karaghiannis, V., Maric, D., et al., *Comprehensive in silico and functional studies for classification of EPAS1/HIF2A genetic variants identified in patients with erythrocytosis.* Haematologica, 2023.

A 09-09
Interactions between SARS-CoV protein 6 and importins – effect on the STAT pathway

Johanna-Theres Borutta, Reinhard Depping

University of Luebeck, Institute of Physiology, Luebeck, Germany

For almost 3 years, the coronavirus affected all of our lives. Every day, both print and digital media report about the coronavirus. Approximately 7 million people have lost their lives in connection with the coronavirus. In addition, several viral mutations are spreading that accelerate person-to-person transmission, are associated with more severe disease progression, or are less effective against previously approved vaccines. SARS-CoV is a single-stranded virus. Approximately two-thirds of the viral genome is used for regulated replication. The last third encodes structural proteins and accessory proteins. One of the accessory proteins is Orf6 (Open Reading Frame 6, also referred to as protein 6). Different studies have shown that protein 6 is localized to the rough ER membrane, as well as to the Golgi membrane, autophagosome membrane, and lysosome membrane. The immobilized protein 6, which binds karyopherin α2, competes with the complex of STAT1:STAT2:IRF9 and karyopherin α1 for karyopherin β1. Thus, the STAT1:STAT2:IRF9:karyopherin α1 complex cannot bind karyopherin β1 and consequently cannot translocate to the nucleus. As a result, no antiviral response occurs. Thus, protein 6 antagonizes the STAT1 signaling pathway. Further research has shown that protein 6 interacts with importin α1 to interfere with STAT1 signaling as described above and subsequently prevents an antiviral response by the immune system. The importin α adapter proteins play an important role in nuclear transport. They mediate the import of proteins holding a specific signal sequence, the nuclear localization signal (NLS). Importin α binds both cargo protein and importin β, which interacts with nucleoporins to facilitate nuclear import. Studies report that the action of the broad-spectrum antiparasitic ivermectin is due to its attack on importin α and importin β. Since importin plays a significant role in nuclear transport and protein 6, which is localized to the ER membrane among other sites, binds importin α1 and thus interferes with the STAT1 signaling pathway, the goal of our research is to investigate interactions between protein 6 and other importins. These studies will provide the basis for future therapeutic and preventive measures.

A 09-10
Functional analysis of the LncRNA *N342419* in human monocytes

Lisa M. Weiss[1,2], Simonida Zehr[1,2], Timothy Warwick[1,2], James A. Oo[1,2], Ilka Wittig[1,2], Sebastian Wolf[3], Thomas Oellerich[3], Matthias S. Leisegang[1,2], Ralf P. Brandes[1,2]

[1] *Goethe Universität, Frankfurt, Germany, Institute for Cardiovascular Physiology, Frankfurt, Germany*
[2] *Partner site RheinMain, Frankfurt, Germany, German Center o fCardiovascular Research (DZHK), Frankfurt, Germany*
[3] *University hospital Frankfurt, Germany, Department of Medicine II, Hematology/Oncology, Frankfurt, Germany*

Motivation: The majority of the human transcriptome is non-coding, leading to questions about the importance of non-translated transcripts. Long non-coding RNAs (lncRNA) are a crucial class of non-coding RNAs that play a fundamental role in physiological and cellular processes. Expression profiling of lncRNA *N342419* showed high expression levels in peripheral blood mononuclear cells (PBMCs). Interestingly, lncRNA *N342419* was upregulated in monocytes differentiated from inducible pluripotent stem cells. Therefore, we aim to analyse the functional and molecular relevance of *N342419* in blood cells.

Methods/Results: During the differentiation of inducible pluripotent stem cells to monocytes, *N342419* expression strongly appeared with the formation of monocytes and was lost once monocytes differentiated into macrophages. RNA-Seq of a (>100) patient cohort with acute myeloid leukemia (AML) displayed a reduction of *N342419* with the degree of AML differentiation. CRISPR/Cas9-mediated deletion of *N342419* in THP-1 monocytes followed by RNA-Seq showed a significant upregulation of genes involved in cell differentiation, mineralization, and ossification. Given the fact, that monocytes are an important part of the innate immune system initiating an inflammatory response, cells were stimulated with lipopolysaccharide (LPS). Upon stimulation, inflammatory genes such as *CCL5* and *IL-33* were significantly downregulated after *N342419* deletion. To address the inflammatory signaling pathways *N342419* possibly interferes with, luciferase reporter gene assays were applied. NF-κB, but not AP-1 and STAT1, promoter activities were suppressed. RNA-FISH showed that the cellular localization of

N342419 was predominantly in the nucleus of THP-1 monocytes. Interestingly, RNA antisense-pulldown with oligonucleotides targeting *N342419* revealed the transcription factor RUNX1, a frequent mutational target in AML, as *N342419* interaction partner. CUT&RUN sequencing on RUNX1 revealed 381 significant differential peaks with *N342419* deletion including peaks close to genes such as *RELB* and *TNF*-superfamily. These data indicate a diverse function of the lncRNA in promoting the inflammatory response in monocytes.

Conclusion: These data indicate a diverse function of lncRNA *N342419* in inflammatory response of monocytes. *N342419* interaction with RUNX1 is especially interesting for AML, hematopoietic- and osteoclastogenesis differentiation and might imply an attractive target for anti-inflammatory therapy.

References
[1] Leisegang et al. (2017). Long Noncoding RNA MANTIS Faciliates Endothelial Angiogenic Function. Circulation. 136(1):65-79
[2] Leisegang et al. (2019). Pleiotropic effects of laminar flow and statins depend on the Krüppel-like factor induced lncRNA MANTIS. European heart Jounal. 40(30):2523-2533
[3] Oo et al. (2021). Long non-coding RNAs: novel regulator of celular physiology and function. Pflugers Archiv: European Journal of Physiology. 474(2):191-204

A 09-11
Hereditary hemorrhagic telangiectasia and its consequences for the immune response - a ciliary view

Sebastian Kromat, Joachim Fandrey, Tristan Leu

University of Duisburg-Essen/University Hospital Essen, Institute of Physiology, Essen, Germany

Hereditary hemorrhagic telangiectasia (HHT, also known as Morbus Osler) is a genetic disorder with a prevalence of 1 in 5,000-10,000 people worldwide [1]. Heterozygous mutations in several proteins associated with the TGF- β/BMP9/10-signaling pathway lead to vascular malformations in skin and inner organs like lung, liver and brain [2]. Additionally, these patients show an increased rate of sinusitis, pneumonia and urinary tract infections that suggests an altered immune response.
Although we know that TGF-beta signaling plays an important role in the development and differentiation of immune cells [3], hardly any molecular biological studies examine this part of the disease.
As another aspect, recent studies closely link the TGF-beta pathway to the primary cilium [4]. This antenna-like structure of cells functions as a hub for many signaling pathways like hedgehog, Wnt or Notch. Disturbance of the cilium causes various diseases (e.g. Bardet–Biedl syndrome) named ciliopathies [5].
Since both issues have not yet been addressed in combination, we assume that a dysfunction of the signaling pathway combined with possible changes of the primary cilium may cause the altered immune response.
To find out, we isolate peripheral blood mononuclear cells (PBMCs) from HHT and non-HHT patients.Of particular interest are the morphology and length of the primary cilium as well as TGF-beta and HHT associated proteins like Endoglin, ALK1 and various SMADs.Their expression and target gene regulation is analysed by Western-Blot and qPCR. The primary cilium and TGF-beta-associated proteins are visualized by immunofluorescence staining.

References
[1] Saparia T, Faughnan ME, Schneider JL, Almers LM, Chow N, Grosse SD, Kim H, Zaroff JG. Assessing the Hereditary Hemorrhagic Telangiectasia Algorithms in a Community-Based Patient Population. Perm J. 2019;23:18-145. doi: 10.7812/TPP/18-145. PMID: 30939282; PMCID: PMC6443364.
[2] Robert F, Desroches-Castan A, Bailly S, Dupuis-Girod S, Feige JJ. Future treatments for hereditary hemorrhagic telangiectasia. Orphanet J Rare Dis. 2020 Jan 7;15(1):4. doi: 10.1186/s13023-019-1281-4. PMID: 31910860; PMCID: PMC6945546.
[3] Batlle E, Massagué J. Transforming Growth Factor-β Signaling in Immunity and Cancer. Immunity. 2019 Apr 16;50(4):924-940. doi: 10.1016/j.immuni.2019.03.024. PMID: 30995507; PMCID: PMC7507121.
[4] Anvarian Z, Mykytyn K, Mukhopadhyay S, Pedersen LB, Christensen ST. Cellular signalling by primary cilia in development, organ function and disease. Nat Rev Nephrol. 2019 Apr;15(4):199-219. doi: 10.1038/s41581-019-0116-9. PMID: 30733609; PMCID: PMC6426138.
[5] Reiter JF, Leroux MR. Genes and molecular pathways underpinning ciliopathies. Nat Rev Mol Cell Biol. 2017 Sep;18(9):533-547. doi: 10.1038/nrm.2017.60. Epub 2017 Jul 12. PMID: 28698599; PMCID: PMC5851292.

A 09-12
Red blood cell substitutes: From structure to function

Katja B. Ferenz[1,3], Fabian Nocke[1,2], Jan-Eric Sydow[1,2], Jacqueline Hausherr[1,4], Ozan Karaman[1,2], Miriam Cantore[1], Martin A. Schroer[5]

[1] *University Duisburg-Essen, University Hospital Essen, Institute of Physiology, Essen, Germany*
[2] *University Duisburg-Essen, University Hospital Essen, Institute of Physiological Chemistry, Essen, Germany*
[3] *University of Duisburg-Essen, CeNIDE (Center for Nanointegration Duisburg-Essen), Duisburg, Germany*
[4] *University Hospital Essen, Department of Thoracic and Cardiovascular Surgery, Division of Thoracic Transplantation, Essen, Germany*
[5] *University of Duisburg-Essen, Nanoparticle Process Technology, Faculty of Engineering, Duisburg, Germany*

Question

Red blood cell substitutes, such as our perfluorodecalin-based albumin-derived artificial oxygen carriers (A-AOCs)[1], grow further in importance as availability of red blood cells is more and more limited. Intravenous application presumes hemocompatibility and the use of organ preservation solutions requires stability in plasma-like media. In this study, we refined our previously developed A-AOCs in order to improve their stability in aqueous plasma-like media.

Methods

Changes of the ultrastructure and size of A-AOC nanoemulsions, consisting of a perfluorodecalin core and an albumin shell, for different temperatures (5-65°C) and salt concentrations (up to ~300 mOsm/L) were monitored with small angle X-ray scattering (SAXS) and dynamic light scattering (DLS) measurements. Hemocompatibility was checked by mixing A-AOCs with human whole blood (local ethics approval no. 21-10314-BO) at a clinically relevant ratio for up to 24 h at body temperature (37 °C) and static conditions. Free hemoglobin, glucose and lactate levels were detected photometrically. To check the function as an oxygen carrier in a physiologically relevant set-up we developed a two-chamber cell culture model simulating ischemia/reperfusion injury (IRI) by using HL-1 cardiomyocytes, where the inner phase mimicks the tissue and the outer phase the blood vessel (Figure: Work-flow to simulate IRI *in vitro*). Western Blot was used to monitor O_2 supply (accumulation of hypoxia inducible factor-1α, HIF-1α) and cell viability (cleaved caspase-3, clCasp-3). Measurements of O_2 kinetics were performed with PreSens© (O_2 phosphorescence quenching). Reactive O_2 species (2',7'-dichlorofluorescein diacetate, DCF-DA) and release of lactate dehydrogenase (LDH) were monitored by fluorescence microscopy and spectrophotometry, respectively.

Results

A-AOCs with a particle size of 20-1950 nm showed no hemolysis when mixed 4:1 with whole blood. SAXS revealed aggregation with increasing temperature and salt concentration. The 2-chamber model successfully imitated strong IRI as shown by high levels of clCasp-3, LDH, DCF-DA and HIF-1a. A-AOCs successfully supplied oxygen to the cells reflected by increased oxygen partial pressure and decreased HIF-1a, LDH and clCasp-3.

Conclusions

Stability in plasma-like media of A-AOCs still needs to be improved; however, the refined A-AOCs showed promising results in our IRI model as they successfully reduced IRI damage.

We thank Prof. Hengen-Cotta, Cardioscience Lab, University Hospital Essen Clinic for Angiology and Kardiology, for donating HL-1 cardiomyocytes.

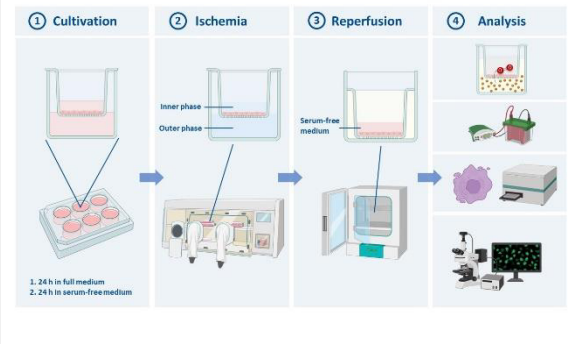

Work-flow to simulate IRI in vitro
Work-flow to simulate IRI *in vitro*: HL-1 cells were cultivated in inserts (full medium for 24 h followed by 24 h serum-free medium). Ischemia was induced by transfer into the hypoxic chamber (0.1 % O_2). The inner phase of the insert was exchanged for hypoxic medium, whereas the outer phase consisted of modified Krebs-Henseleit-buffer +/- pre-oxygenated A-AOCs. After 3 h of ischemia, cells were submitted to 1 h reperfusion in serum-free medium under normoxic conditions.

References
[1] Wrobeln, A, Ladien, J, Groß-Heitfeld, C, Linders, J, Mayer, C, Wilde, B, Knoll, T, Naglav, D, Kirsch, M, Ferenz, KB, 2017, 'Article', *Eur J Pharm Biopharm*, 115, 52-64, Amsterdam, The Netherlands: Elsevier

POSTER SESSION B

B 01 | Sodium or Proton Channels & Sodium-dependent Transporters

B 01-01
Identification of a binding site for the small molecule activator S3969 in the β-subunit of the human epithelial sodium channel (ENaC)

Florian Sure, Christoph Korbmacher, **Alexandr Ilyaskin**

Friedrich-Alexander-Universität Erlangen-Nürnberg, Institute of Cellular and Molecular Physiology, Erlangen, Germany

The epithelial sodium channel (ENaC) is essential for mediating sodium absorption in the distal nephron, lung epithelia, distal colon, salivary and sweat glands. Impaired ENaC function leads to severe disorders, e.g. pseudohypoaldosteronism type 1 and respiratory distress due to reduced alveolar fluid clearance. Patients suffering from diseases associated with reduced ENaC activity may benefit from treatment with ENaC activators. A small molecule ENaC activator (S3969) has been developed and can stimulate human but not mouse ENaC in its αβγ-subunit configuration [1]. The aim of this study was to identify an S3969 binding site in human ENaC by using structure-based computer simulations in combination with molecular biology approaches and two-electrode voltage clamp recordings. ENaC was heterologously expressed in *Xenopus laevis* oocytes. Channel function was assessed by measuring amiloride-sensitive whole-cell currents. Previously it was demonstrated that replacing the extracellular loop of mouse βENaC with that of human βENaC converted mouse ENaC into an S3969-sensitive ion channel [1]. This suggests that the binding site for S3969 is localised in the extracellular loop of the channel's β-subunit. To investigate this further, we generated a series of mouse-human chimeric channels by transplanting different portions of the extracellular loop of human βENaC into the corresponding regions of mouse βENaC. By testing which of these chimeric channels could be activated by S3969, we narrowed down the channel region responsible for the stimulatory effect of S3969. Importantly, we found that the β-thumb domain was critically involved in ENaC stimulation by S3969. Using molecular docking based on a recently published cryo-electron microscopy structure of ENaC (PDB ID 6WTH, [2]), we predicted a putative S3969 binding site in the channel's β-subunit which was partially formed by the β-thumb domain and localised at the β-γ-subunit-interface. The docked ENaC-S3969 complex was analysed in atomistic molecular dynamics (MD) simulations. As a result, key amino acid residues for coordinating S3969 in βENaC were identified (R388, Y406 and F391). Importantly, mutating each of these positions strongly reduced (R388H; R388A) or nearly abolished (Y406A; F391G) the S3969-mediated ENaC activation. MD simulations also predicted that S3969 binding to ENaC increases the distance between β-thumb and γ-palm domains. Consistent with this, introduction of two cysteine residues (βR437C – γS298C) to form a disulfide bridge connecting these two domains prevented ENaC stimulation by S3969, unless the disulfide bond was reduced by DTT. Thus, the predicted conformational change seems to be necessary for S3969-mediated ENaC stimulation. In conclusion, we have characterised the functional interaction of S3969 with ENaC at the molecular level. These findings may help to identify novel endogenous or pharmacological ENaC activators with potential physiological and therapeutic implications.

Funded by the Deutsche Forschungsgemeinschaft (DFG, German Research Foundation), project number 509149993, TRR 374 (subproject A4 to A.I. and C.K.).

References
[1] Lu, M., Echeverri, F., Kalabat, D., Laita, B., Dahan, D.S., Smith, R.D., Xu, H., Staszewski, L., Yamamoto, J., Ling, J., Hwang, N., Kimmich, R., Li, P., Patron, E., Keung, W., Patron, A., Moyer, B.D. 2008. Small molecule activator of the human epithelial sodium channel. *J Biol Chem*, 283(18):11981-94.
[2] Noreng, S., Posert, R., Bharadwaj, A., Houser, A., Baconguis, I. 2020. Molecular principles of assembly, activation, and inhibition in epithelial sodium channel. *Elife,* 9:e59038.

B 01-02
Mg-Protoporphyrin IX is a potent and specific inhibitor of human cardiac voltage-gated sodium channels

Mahdi Jamili[1], Johann Roessler[1], Guido Gessner[1], Roland Schoenherr[1], Toshinori Hoshi[2], **Stefan H. Heinemann**[1]

[1] Friedrich Schiller University Jena and Jena University Hospital, Center for Molecular Biomedicine, Department of Biophysics, Jena, Germany
[2] University of Pennsylvania, Department of Physiology, Philadelphia, USA

We have previously demonstrated that hemin (Fe(III)-protoporphyrin IX) inhibits cardiac voltage-gated Na^+ channels ($Na_V1.5$ channels) with an effective half-maximal concentration of about 80 nM by interfering with the channel's voltage sensor in domain II (1). This interaction results in a reverse use-dependence phenotype, where depolarization-induced channel activity antagonizes channels inhibition. Here we explored other metal protoporphyrins (MePPIX) to discover biocompatible molecules that could function as specific $Na_V1.5$ antagonists.
Various types of Na_V channels were transiently expressed in HEK293T cells and the resulting currents were measured with the whole-cell patch-clamp method. The impact of various types of extracellularly applied MePPIX was measured using pulse protocols designed to examine the reverse use-dependence. Single-site mutations in $hNa_V1.5$ were introduced by PCR-based methods.
We measured the inhibitory effect of 1 µM MePPIXs on cardiac Na_V after 5-min application, resulting in the following potency rank order: Mg >> Ga ≈ Zn > Fe (III) > Mn > Co >> Cu, Sn, Ni. MgPPIX was the most potent, with an IC_{50} of 1.05 ± 0.10 nM. Cu-, Sn-, and Ni-PPIX showed no effect. 100 µM MgPPIX was used to characterize the reverse use-dependence. Half-maximal current recovery after 500-ms prepulse of varying voltage yielded half-maximal voltages of -21.8 ± 1.1 mV for MgPPIX compared to -70.9 ± 1.4 mV for hemin (Fe(III)PPIX). Time constants of block removal at 50 mV were 52.7 ± 1.6 ms and 8.7 ± 1.1 ms, respectively. The time constants of re-block after partial voltage-dependent reversal were 0.14 s for MgPPIX and 1.2 s for hemin. Thus, MgPPIX exerts a much stronger impact on $hNa_V1.5$ channels compared to hemin because of faster on-rate and slower off-rate. The impact of MgPPIX was highly specific for cardiac ($Na_V1.5$) channels; at 1 µM none of the following channel types were inhibited by MgPPIX: $Na_V1.2$, $Na_V1.4$, $Na_V1.7$, and $Na_V1.8$. Mutation N803G in the S3/S4 linker of domain II strongly diminished the sensitivity of $hNa_V1.5$ channels for MgPPIX, thus identifying this site as a major determinant for the subtype specificity. The high potency of MgPPIX in inhibiting cardiac Na_V channels is specific to the human isoform because mouse $Na_V1.5$ is inhibited by MgPPIX with an about 35-fold greater IC_{50} value. Mutation $hNa_V1.5$-S802G, which converts the S3/S4 sequence in domain II into a sequence found in $mNa_V1.5$, shifts the IC_{50} value to that found for the mouse isoform.
Our study identified MgPPIX, a naturally occurring compound and precursor in chlorophyll synthesis, as a potent and specific inhibitor of human cardiac voltage-gated Na^+ channels. Metal protoporphyrins such as MgPPIX may thus represent a new class of $Na_V1.5$-specific voltage-sensor modifiers with potential application in basic research or as lead structures for drug development.

References
[1] Gessner G, Jamili M, Tomczyk P, Menche D, Schönherr R, Hoshi T, Heinemann SH. Extracellular hemin is a reverse use-dependent gating modifier of cardiac voltage-gated Na^+ channels. Biological Chemistry. 2022;403(11-12):1067-81.

B 01-03
Light-sensitive cardiac sodium channels for action potential studies in *Xenopus laevis* oocytes and HEK293 cells

Xhevat Berisha, Eugena Sylaj, Christian V. Dahl, Christoph E. Müller, Thomas Zimmer

Friedrich Schiller University Jena, Institute of Physiology II, Jena, Germany

Voltage-gated sodium channels play a critical role in the generation and propagation of action potentials in excitable cells, including neurons and cardiac muscle cells. These channels allow the flow of sodium ions across the cell membrane in response to depolarization, leading to the rapid upstroke of the action potential. In human atrial and ventricular cardiomyocytes, this initial depolarization is mediated by $hNa_v1.5$. Mutations in *SCN5A*, the gene encoding $hNa_v1.5$, were related to various life-threatening arrhythmias, like Brugada syndrome, Cardiac conduction disease, and Long QT syndrome type 3 (LQT3).

To gain a better understanding of the effects of LQT3 mutations on the action potential shape, we first coupled $hNa_v1.5$ to channelrhodopsin-2 (ChR2), a light-sensitive ion channel of the green algae *Chlamydomonas reinhardtii*. ChR2 responds to blue-light illumination with pore opening, allowing a small influx of protons and mono- and divalent cations. The $hNa_v1.5$-ChR2 fusion channel was expressed in both *Xenopus laevis* oocytes and HEK293 cells. Two-microelectrode and patch-clamp experiments confirmed that $hNa_v1.5$ properties remained unchanged in the $hNa_v1.5$-ChR2 fusion. In the current-clamp mode, we were able to generate action potentials by short blue-light pulses in both expression systems. In a second step, we genetically introduced several LQT3 mutations in the $hNa_v1.5$-ChR2 coding region (A1330T, F1473C, deltaKPQ, T1620K, R1623Q). Action potential parameters, like threshold potential, upstroke velocity, and action potential duration were (1) compared to those obtained after expressing wild-type $hNa_v1.5$-ChR2, and (2) correlated to the distinct alterations in mutant channel kinetics. As the main result, we found significantly longer action potentials in mutant channels generating a non-inactivating (persistent) current fraction (F1473C, deltaKPQ). The size of this current fraction positively correlated with the action potential duration. Moreover, we noticed more positive threshold potentials in mutant channels characterized by a depolarizing shift of steady-state activation. Surprisingly, some of the mutant channels did not result in a change of the action potential shape, despite prolonged QTc values in patients and altered channel kinetics (A1330T, T1620K). In conclusion, coupling ChR2 to voltage-gated sodium channels generates novel optical switches for action potential studies. Our optogentic model allows for structure-function relation studies of various wild-type and mutant channels and bears the potential for high-throughput drug testing. Ongoing research is aimed at coupling other sodium channel isoforms to ChR2 and at transferring our optogenetic tool to mammalian cell lines, stems cells and cardiomyocytes.

B 01-04
Biophysical properties of sodium channels in dopaminergic midbrain neurons defined by axonal projections.

Marle Jahnke, Jochen Roeper

Goethe University Frankfurt, Institut of Neurophysiology, Frankfurt Am Main, Germany

A diverse dopamine (DA) midbrain system is critical for key brain functions, like working memory, movement control, motivation, and reward-based learning. Dysfunction of distinct DA subpopulations respectively contribute to major disorders such as Parkinson disease, schizophrenia, and drug addiction. DA release in each striatal territory depends on action potential discharge patters in projecting DA neurons as well as local striatal control mechanisms. To better define the axonal projection-specific electrical output of DA subpopulations the biophysical properties of their respective voltage-gated sodium (Na^+)channels need to be studied.

Previous studies investigated the differences between the functional characteristics of voltage-gated Na^+currents in midbrain GABAergic and DA neurons using nucleated outside-out patch (Seutin and Engel., 2010) as well as Na_v channel subunit expression in rat DA neurons (Ding et al., 2011). Another study compared the Na^+ current's properties between DA neurons of the ventral tegmental area (VTA) and substantia nigra (SN) (Yang et al., 2019). However, sodium current properties of projection-defined DA subpopulations have yet to be defined. Therefore, we combined axonal retrograde tracing with nucleated outside-out patch clamp recordings of labelled DA neurons in adult male C57Bl6N mice. As a first step, we recorded voltage-gated Na^+currents of the nucleus accumbens (NAc)core and NAc-medial shell-projecting DA subpopulations. These two subpopulations in the VTA both belong to a fast-firing DA phenotype (Lammel et al., 2008, Knowlton, Ziouziou et al. 2021). Indeed, we observed no significant differences in the functional properties of their Na^+currents (activation 10-90% rise time (at - 20 mV): NAc core: 263.2 ± 43.5 µs, n = 11, N = 4; NAc medial shell: 251.1 ± 36.6 µs, n = 22, N = 5; p = 0.84; inactivation 10-90% rise time (at -20 mV): NAc core: 2.12 ± 0.71 ms, n = 11, N = 4; NAc medial shell: 4.16 ± 0.8 ms, n = 21, N = 5; p = 0.1; Na^+ current density (at - 20 mV): NAc core: 22.6 ± 8.1 pA/pF, n = 10, N = 4; NAc medial shell: 27.5 ± 4.4 pA/pF, n = 21, N = 5; p = 0.57). Next, we will explore Na^+current properties in nucleated outside-out patches of a VTA subpopulation with a slow firing electrophysiological phenotype such as NAc-lateral shell-projecting DA neurons.

B 01-05

Sodium/hydrogen exchanger 8 affects proliferation and migration of HT29 human colon epithelial cells via modulation of intracellular pH

Ju Wang, Merle Gatz, Christian Stock, **Katerina Nikolovska**, Ursula Seidler

Hannover Medical School, Gastroenterologie, Hepatologie, Infektiologie und Endokrinologie, Hannover, Germany

Question

NHE8 is a Na^+/H^+ exchange transporter expressed in the gastrointestinal tract. Loss of NHE8 expression in the mouse intestine results in reduced mucus production, altered gut bacterial composition, and enhanced expression of inflammatory cytokines. Reduced NHE8 expression was reported in both human ulcerative colitis and colitis animal models. Ulcerative colitis as chronic inflammatory condition is characterized by repeated injury of the colonic surface and requires constant repair via epithelial restitution. Therefore, we addressed the impact of NHE8 deficiency on intestinal epithelial restitution by accessing cell proliferation and migration.

Methods

HT29MTX cells, a human colon epithelial cell line, characterized by high NHE8 expression was used as an experimental model. NHE8 expression was knocked-down using shRNA lentivirus particles. The knockdown efficiency was verified by qPCR, Western blot and immunofluorescence. The role of NHE8 in pH_i regulation, cell proliferation, adhesion and migration was addressed in knock-down and control cells.

Results

Two clonal cell lines with ~40 % (HT29/shRNA[1]) and 80 % (HT29/shRNA[2]) reduction of NHE8 mRNA expression were selected for further experiments. The altered NHE expression resulted in more acidic intracellular pH_i compared to the control cells. Cell migration was addressed by wound scratch assay that showed significantly decreased migration rate in both shNHE8 cell lines when compared to the control cells or the mock transduced cells. The difference in the migration rate became evident 3 h post-wounding. At this time point the mock transduced cells started to flatten and form actin elongations at the leading edge. However, in the NHE8 knock-down cells tight actin accumulations at the leading edge were detected, that remained unchanged even 24 h post wounding. Actin cytoskeleton remodeling and cell migration can be regulated by transient pH_i increases. In the control cell line, the front leading cells had a more alkaline pH_i compared to their neighboring cells in the back rows, while in the NHE8 knock-down cells this difference was smaller. Also at single cell level, NHE8 knock-down cells displayed decreased directional migration and velocity. In contrast to cell migration, both selected shNHE8 cell lines showed a significant increase in both cell proliferation rate and adhesion to collagen 1 coated surfaces.

Conclusions

Restitution is the initial phase of mucosal repair, characterized by rapid migration and proliferation of the cells to re-establish surface epithelium. Conceivably NHE8 localized at the apical membrane of intestinal epithelial cells facilitates their migration via regulating the pH_i. Lack of NHE8 in HT29 cells creates more acidic pH_i beneficial for epithelial cell proliferation but impairing their migratory capacity due to deceased cytoskeletal actin dynamics.

B 01-06

Evaluation of Mg-protoporphyrin IX as a specific inhibitor for $Na_V1.5$ channels in non-excitable human cells

Mahdi Jamili[1], Marwa Ahmed[1], Toshinori Hoshi[2], Roland Schoenherr[1], **Stefan H. Heinemann**[1]

[1] *Friedrich Schiller University Jena and Jena University Hospital, Center for Molecular Biomedicine, Department of Biophysics, Jena, Germany*

[2] *University of Pennsylvania, Department of Physiology, Philadelphia, USA*

Fe^{3+}-protoporphyrin IX (hemin) is a potent and specific inhibitor of cardiac voltage-gated sodium channels ($Na_V1.5$) [1]. Further investigations revealed that Mg-protoporphyrin IX (MgPpIX) exhibits even greater potency against $Na_V1.5$ (IC_{50} about 1 nM). Here we assessed the usefulness of MgPpIX as a specific inhibitor of $Na_V1.5$ channels endogenous to non-excitable cells including cancer cells.

Using the whole-cell mode of the patch-clamp technique, endogenous Na_V currents were measured in the human embryonic kidney cell line HEK293T and in the triple-negative human breast cancer cell line MDA-MB-231, derived from an aggressive metastatic mammary carcinoma. MDA-MB-231 cells express the neonatal splice variant of $Na_V1.5$, and specific interference with $Na_V1.5$ in these cells alters their growth properties [2,3]. As a control, variants of recombinant $hNa_V1.5$ and $Na_V\beta$ subunits were transiently overexpressed in HEK293T. MgPpIX, diluted from stock solution in DMSO, was extracellularly applied, and Na_V currents were measured during repetitive pulses to -10 mV at an interval of 4 s. Solutions were chosen to largely suppress K^+ and Ca^{2+} currents.

Human $Na_V1.5$ overexpressed in HEK293T cells was nearly completely inhibited by 100 nM MgPpIX with a fractional current block of 96.5 ± 0.9% (n=6) within 10 min. Without transfection, a Na_V current density of 23 ± 5 pA/pF was measured in HEK293T cells. This endogenous current was also blocked by 100 nM MgPpIX by 87.2 ± 2.9% (n=5). Endogenous Na_V current in MDA-MB-231, measuring at 42 ± 13 pA/pF, was blocked by 89.6 ± 0.9% (n=5) following application of 100 nM MgPpIX. For both cell lines, the endogenous Na_V currents also showed a reverse use-dependence typical for $Na_V1.5$ inhibition by metal protoporphyrins. The amount of block by MgPpIX strongly argues that by far the largest fraction of endogenous Na_V current in HEK293T and MDA-MB-231 originates from $Na_V1.5$ channels.

While blocking effects were qualitatively similar between recombinant and endogenous Na_V channels, a small but consistent quantitative difference was observed. We thus examined the impact of exogenous $Na_V\beta1$ and $Na_V\beta2$ in HEK293T cells. In both cases, the blocked fraction with MgPpIX application was diminished with respect to the α subunit only: 92.0 ± 0.9% (n=5) and 92.2 ± 1.1% (n=6), respectively. The findings indicate that the $Na_V\beta$ subunits may have a modulatory impact on the MgPpIX-channel interaction.

This study demonstrates that MgPpIX is a potent and specific inhibitor of $Na_V1.5$ channels endogenously expressed in HEK293T cells. Since HEK293T cells are commonly used as host system for the expression of various Na_V isoforms, the inevitable background current carried by endogenous $Na_V1.5$ can be specifically inhibited without interference with other Na_V types. Given the inhibitory potency on Na_V currents native to MDA-MB-231 cells, MgPpIX may become a promising tool to modulate the function of this and other breast cancer cell types.

German Reseach Foundation (GRK 2155).

References
[1] Gessner G, Jamili M, Tomczyk P, Menche D, Schönherr R, Hoshi T, Heinemann SH. Extracellular hemin is a reverse use-dependent gating modifier of cardiac voltage-gated Na^+ channels. Biological Chemistry. 2022;403:1067-81.
[2] Brackenbury WJ, Chioni AM, Diss JK, Djamgoz MB. The neonatal splice variant of Nav1.5 potentiates in vitro invasive behaviour of MDA-MB-231 human breast cancer cells. Breast cancer research and treatment. 2007;101:149-60.
[3] Erdogan MA, Yuca E, Ashour A, Gurbuz N, Sencan S, Ozpolat B. SCN5A promotes the growth and lung metastasis of triple-negative breast cancer through EF2-kinase signaling. Life Sciences. 2023;313:121282.

B 01-07

Expression of the Na^+/H^+ exchanger NHE8 affects single cell behaviour of human mucus-forming colorectal carcinoma cells (HT29-MTX)

Merle Gatz, Ju Wang, Ursula Seidler, Katerina Nikolovska, Christian Stock

Hanover Medical School, Department of Gastroenterology, Hepatology, Infectious Diseases and Endocrinology, Hannover, Germany

Introduction: The Na^+/H^+ exchanger isoform 8 (NHE8) contributes to colonic mucosal protection by stimulating mucin production particularly in goblet and Paneth cells. NHE8 deficiency has been reported to promote inflammatory bowel disease in both mice and humans. In addition, NHE8 expression is strongly inhibited in human colorectal cancer and loss of function results in increased tumour growth in mice. However, the contribution of NHE8 to the metastatic behaviour of colorectal cancer cells remains unknown. We therefore studied the NHE8-dependent motility of human colorectal cancer cells at single cell level.

Methods and Results: The human colorectal cancer cell line HT29-MTX was used to analyse cell migration and invasion. Time-lapse video microscopy of undifferentiated HT29-MTX cells migrating on a collagen I matrix revealed that an 80% NHE8 knock-down significantly reduced migration velocity and distance covered. Upon short-term serum deprivation, addition of 50 ng ml^{-1} of epidermal growth factor (EGF) partially rescued migration of the NHE8 knock-down cells. In 24-hour invasion experiments, NHE8 deficient HT29-MTX cells started to invade a confluent hepatocyte layer (Huh7) with a marked delay and the number of invasive cells was reduced. Furthermore, NHE8 deficiency led to an enhanced adhesion of fluorescently labelled HT29-MTX cells to the Huh7 cell layer, measured after 3 hours of incubation, and also the cell

proliferation was increased. Ratiometric pH measurements using BCECF and the NH_4Cl/acid prepulse technique in the absence of CO_2 showed a higher cytosolic pH in the NHE8-deficient cells, before and after acidification. Starting from this higher pH after acidification, the Na^+-dependent pH recovery, and therefore the total number of protons transported, was lower in the NHE8-deficient cells. This was not caused by an actively altered alternative transport mechanism.

Conclusion: Although the absence of NHE8 has been discussed as a precursor to colorectal cancer in ulcerative colitis and has been shown to lead to increased tumour growth, it is in fact the presence of NHE8 that promotes migration and accelerates invasion. However, the difference in motility between NHE8-deficient HT29-MTX cells and their mock control is not caused by the modification of an actively controlled Na^+-dependent, HCO_3^-- independent pH regulation mechanism. Thus, our observations at the single-cell level, even though confirming an increased cell proliferation rate, point to a decrease in malignancy of NHE8-deficient cells regarding their motility parameters adhesion, migration and invasion.

B 01-08
Response of glioblastoma cells to acidic stress: aberrant regulation of ion dynamics and its impact on intracellular pH

Jakob Vanek, Klaus-Daniel Cortés Franco, María Schilling, Stefan Gründer

Institute of Physiology, RWTH Aachen University, Aachen, Germany

The microenvironment of highly aggressive tumours such as the brain tumour glioblastoma multiforme (GBM) is often acidic due to an accumulation of metabolic waste products. Regardless of the acidic extracellular pH, GBM cells can maintain their intracellular pH within a physiological range. However, the mechanisms regulating the intracellular pH, which enable GBM cells to thrive under those conditions, are poorly understood.

In this study, we investigated the expression and function of the main acid extruding mechanisms in R54 GBM stem cells (GSCs) as well as the impact of acidic stress on their sphere formation rate (SFR).

R54 GSCs were incubated for 14 days at pH 7.4 or pH 6.6 to mimic isolated acidic stress. Subsequently, their transcriptome was determined by RNA-sequencing. A comparison of the expression of genes involved in acid extrusion revealed that especially Na+/HCO3- cotransporters (NBCs) were upregulated by chronic acidic stress.

To functionally study the relevance of these proteins for acid extrusion, and to describe the consequences of chronic acidic stress on pH balance, we imaged the intracellular pH by fluorescence microscopy.

Analysis of the intracellular pH recovery rate following an NH4Cl-prepulse revealed that inhibiting NHE1 or NBCs decreased the acid extrusion capacity.

Following chronic acidic stress, the cells not only had a higher steady-state intracellular pH at pH 7.4, but also an increased intracellular pH recovery rate. However, this increase in recovery rate was almost completely abolished after inhibiting NBCs.

It was already known that the SFR of individual R54 GSCs is decreased by an acidic environment. Here we used a sphere formation assay to demonstrate that adapting R54 cells to acidic stress for 2 weeks prior to the experiment diminished the decrease in SFR. Furthermore, when returned to physiological pH, the cells displayed an increase in SFR.

These results indicate that NHE1 and NBCs are involved in acid extrusion in GSCs and that NBCs are upregulated during acidic stress and contribute to an increased intracellular pH. Additionally, these findings imply that adapting cells to chronic acidic stress increases their sphere formation ability, suggesting that an acidic microenvironment may act as a driver of cancer cell aggressiveness and that interfering with pH-regulating mechanisms might provide a new therapeutic opportunity.

References

[1] Clusmann, J., et al. (2022). "Acidosis induces RIPK1-dependent death of glioblastoma stem cells via acid-sensing ion channel 1a." Cell Death Dis **13**(8): 702, London (GBR)

[2] Gerweck, L. E. and K. Seetharaman (1996). "Cellular pH gradient in tumor versus normal tissue: potential exploitation for the treatment of cancer." Cancer Res **56**(6): 1194-1198, Philadelphia (USA)

[3] Webb, B. A., et al. (2011). "Dysregulated pH: a perfect storm for cancer progression." Nat Rev Cancer **11**(9): 671-677, Berlin (GER)

B 01-09
Structural and functional diversity of novel voltage-gated proton channels

Gustavo Chaves, Christophe Jardin, Christian Derst, Boris Musset

Paracelsus Medical University - Klinikum Nürnberg Medical School, Physiology, Pathophysiology and Biophysics, Nuremberg, Germany

Voltage-gated proton channels (H_V) are present in a wide range of organisms, from unicellular organisms to humans. They play crucial roles in various physiological processes, including pH homeostasis, sperm maturation, B-cell receptor signalling, the respiratory burst of phagocytes, and are highly expressed in some malignant cancer. The H_V family is small compared to other voltage-activated ion channels like Na_V or K_V, with species having only a single H_V1 encoding gene. However, our recent studies have broken this paradigm by discovering paralogs of the typical H_V1 channel within a single species, revealing previously unrecognized diversity. These novel H_V channels exhibit typical biophysical characteristics, including perfect proton selectivity, pH- and voltage-regulated proton conductance, and inhibition by divalent cations. Nevertheless, subtle differences in their functioning have been observed, potentially attributed to small but significant structural components. One notable example is the structural similarity of some paralogs to the regular proton extruder H_V1, e.g., H_V type-2 channels. H_V2 exhibits the common voltage-sensor motif (VSM) of H_V1 channels, RxWRxxR, but with the curious property of activating negatively to the Nernst potential for protons. This enables proton influx into the cell, depolarizing the membrane and potentially leading to the generation of action potentials. Other paralogs, such as H_V3 and H_V4, exhibit distinct structural features compared to H_V1 or H_V2. H_V4 channels, the smallest H_V channels found in nature, possess a natural variation in the third gating charge carrier (K3) of their VSM, substituting the archetypal Arg (R3). On the other hand, H_V3 channels are the largest proton channels discovered thus far. These H_V3 channels harbor an atypical LPWRxxR VSM, resulting in a disrupted channel that leaks protons even in the closed state and demonstrates weak voltage-dependence of gating. Interestingly, similar effects were observed when altering the physicochemical properties of the hydrophobic gasket of human H_V1.
Our findings, combined with electrophysiological characterization, provide valuable insights into the structural determinants that underlie the functional diversity of H_V molecules. By uncovering the existence of paralogs and their unique properties, we expand our understanding of H_V channels and their roles in diverse physiological processes.

Kerscher'sche Stiftung to GC

B 01-10
Generation und electrophysiological analysis of a gain-of-function polycystin-1/polycystin-2 heteromeric ion channel

Tobias Staudner, Juthamas Khamseekaew, Linda Geiges, Christoph Korbmacher, Alexandr Ilyaskin

Friedrich-Alexander-Universität Erlangen-Nürnberg, Institute of Cellular and Molecular Physiology, Erlangen, Germany

Autosomal-dominant polycystic kidney disease (ADPKD) is caused by mutations in the PKD1 or PKD2 gene coding for polycystin-1 (PC1) or polycystin-2 (PC2), respectively. Mutations affect PC1 in ~85% and PC2 in ~15% of ADPKD patients. Conflicting results have been published regarding the functional interaction of PC1 and PC2. Intriguingly, recently published structural data indicate that PC1 and PC2 can form a heterotetrameric ion channel with a 1:3 stoichiometry, in which PC1 directly contributes to the channel pore. Structure-based analysis suggests that three amino acid residues of PC1 (R4100, R4107, and H4111) and two amino acid residues of each PC2 subunit (L677, N681) block the ion permeation pathway [1]. We hypothesized that substituting these putative pore blocking residues by alanines has a gain-of-function effect on the PC1/PC2 heteromeric ion channel. Alanine substitutions were introduced to wild-type (WT) PC2 and a C-terminal fragment of PC1 (PC1-CTF, amino acid residues 3049-4303) using site-directed mutagenesis. WT or mutant PC2 was heterologously expressed in *Xenopus laevis* oocytes with or without co-expression of WT or mutant PC1-CTF for functional analysis using the two-electrode voltage clamp technique. Sodium inward currents were measured in the absence of divalent cations in the bath solution. Monovalent cation selectivity was assessed by replacing bath sodium by lithium or potassium. As reported previously, alanine substitutions in PC2 (L677A N681A) resulted in a gain-of-function (GOF) construct, which produced significantly larger sodium inward currents compared to those mediated by WT PC2 [2]. Co-expression of WT PC1-CTF with WT PC2 or GOF PC2 significantly decreased sodium inward currents, probably due to the formation of heteromeric PC1/PC2 channel complexes with reduced ion permeability. In oocytes expressing a PC1-CTF mutant (R4100A R4107A H4111A)

alone or in combination with WT PC2 no detectable sodium inward currents were observed. In contrast, co-expression of PC1-CTF (R4100A R4107A H4111A)with GOF PC2 led to a fourfold increase of sodium inward currents compared to those observed in oocytes expressing GOF PC2alone. Thus, to achieve a GOF effect on the heteromeric PC1/PC2 channel it was necessary to mutate the pore regions of both PC1 and PC2. Interestingly, monovalent cation selectivity of this GOF PC1/PC2-complex was significantly different from that of GOF PC2. Indeed, heteromeric PC1/PC2 ion channels conducted sodium, potassium and lithium equally well, whereas the homomeric PC2 channels exhibited a clear preference for potassium oversodium or lithium. These results support the hypothesis that PC1 and PC2 form a heteromeric ion channel complex and both contribute to its pore. Moreover, they suggest a regulatory role of PC1 due to its ability to block the channel pore. The generated GOF PC1/PC2-construct may serve as a useful model to explore the ion channel function of the PC1/PC2 complex in future studies.

This study was supported by a grant from the IZKF Erlangen (subproject F8 to C.K.).

References
[1] Su, Q., Hu, F., Ge, X., Lei, J., Yu, S., Wang, T., Zhou, Q., Mei, C., & Shi, Y. (2018). Structure of the human PKD1-PKD2 complex. *Science*, *361*(6406).
[2] Wang, Z., Ng, C., Liu, X., Wang, Y., Li, B., Kashyap, P., Chaudhry, H. A., Castro, A., Kalontar, E. M., Ilyayev, L., Walker, R., Alexander, R. T., Qian, F., Chen, X. Z., & Yu, Y. (2019). The ion channel function of polycystin-1 in the polycystin-1/polycystin-2 complex. *EMBO Rep*, *20*(11), e48336.

B 01-11

The sodium-coupled neutral amino acid transporter SNAT2 promotes alveolar fluid clearance and regulates alveolar epithelial cell homeostasis in acute lung injury/ARDS.

Juliana Falivene, Sarah Weidenfeld, Wolfgang Kuebler

Charité – Universitätsmedizin Berlin, corporate member of Freie Universität Berlin and Humboldt-Universität zu Berlin, Institute of Physiology, Berlin, Germany

Inhibition of alveolar fluid clearance (AFC) and increased alveolar epithelial cell (AEC) apoptosis are hallmarks of ARDS/acute lung injury. AFC inhibition results from dysregulation of epithelial Na^+ transport and promotes fluid accumulation in the distal airspaces resulting in impaired gas exchange and respiratory failure. Despite the central role of the epithelial sodium channel (ENaC), 40% of AFC is amiloride-insensitive and activation of ENaC failed to attenuate pulmonary edema in clinical trials, suggesting that other Na^+ transporters may provide novel therapeutic targets. One such transporter is the Na^+-coupled neutral amino acid (AA) transporter SNAT2: a System A transporter of the SLC38 gene family, which transports one neutral AA along with one Na^+. We hypothesized that SNAT2 may contribute to AFC through its Na^+ transport function, while promoting AEC homeostasis and prevent excessive autophagy and apoptosis through its AA transport function.
In vitro, qPCR identified SNAT2 as the highest expressed System A transporter in AECs. In line with a potential role of SNAT dysregulation in AEC injury, we found SNAT2 to be downregulated in AEC stimulated with soluble mediators mimicking the inflammatory and infectious milieu of ARDS. Inhibition of SNATs by α-methylaminoisobutiric acid (MeAIB) or SNAT2 siRNA-mediated knockdown reduced transport of L-alanine across AEC and increased AEC apoptosis. Analogously, MeAIB stimulation of precision-cut lung slices (PCLS) from LC3-GFP mice increased the number of GFP^+ cells as compared to untreated PCLS, indicating induction of autophagy by SNAT2 inhibition. Similarly, SNAT2 inhibition induced markers of autophagy and apoptosis in primary AEC. In isolated perfused mouse and rat lungs (IPL), pharmacological inhibition of SNATs impaired AFC, and IPL of *Slc38a2*$^{+/-}$ (partial SNAT2 deficient) mice developed higher wet-to-dry weight ratios (W/D) as compared to wild type (WT) mice in response to hydrostatic stress. *In vivo*, 24h after LPS-induced ALI, *Slc38a2*$^{+/-}$ mice had increased BALF protein content and increased pro-apoptotic CHOP expression in lung tissue compared to WT mice.

Our findings suggest a dual protective role for SNAT2 as a functional transporter for Na^+ and neutral AA in pulmonary epithelial cells with a critical role in AFC and alveolar epithelial cell homeostasis.

Supported by the German Research Foundation, operating grant KU1218/11-1.

B 01-12
Zymosan activates the toll like receptors TLR2 and TLR5

Stefanie Reuter[1,2], Kristina Herold[1], Jana Domrös[1], Ralf Mrowka[1,2]

[1] *Universitätsklinikum Jena, Exp. Nephrologie, KIM III, Jena, Germany*
[2] *Thüringer Innovationszentrum für Medizintechnik Lösungen, Thimedop, Jena, Germany*

Question

Zymosan is a cell wall preparation of the yeast *Saccharomyces cerevisiae* consisting of glucan, mannan, protein and lipoprotein components. Zymosan is recognized by receptors of the innate immune system, like Dectin1A and Toll-like receptors (TLRs). TLRs are key elements for the recognition of microbial pathogens and belong to the group of pattern recognition receptors (PRRs) which play a crucial role in activating the innate immune system. Microbial pathogens like bacteria, viruses and fungi carry a huge number of microbial structures named pathogen-associated molecular patterns (PAMPs). By binding these PAMPs TLRs initiate a signaling pathway which results in the activation of different transcription factors. It is not fully clear in detail which TLR is involved in the recognition of the fungal component zymosan.

Methods

To investigate the activation of TLRs by the fungal cell wall component zymosan and other ligands we generated HEK293 luciferase reporter cells. These cells stably express a NF-κB sensitive promotor to control firefly luciferase reporter gene transcription. Furthermore HEK293 luciferase reporter cells were stably transfected with single TLRs. TLR activation and signaling induces the activation and translocation of the transcription factor NF-κB. NF-κB binds to a designed sensitive promoter element consisting of three different consensus sequences for the NF-κB subunits p65 and p50 and activates the firefly luciferase generation. This results in the generation of bioluminescence in living cell. To investigate the activation of TLR2 and TLR5 by different microbial ligands HEK293 reporter cells were treated with the TLR ligands FSL-1, flagellin and zymosan.

Results

We show a concentration dependent activation of HEK293-TLR2-CD14 reporter cells and HEK293-TLR5 reporter cells after the treatment with zymosan. Zymosan-induced luciferase activity in HEK293-TLR5 reporter cells was inhibited by TLR5 antagonists.

Conclusions

The fungal cell wall component zymosan is an activator of TLR5 signaling in a dose-dependent manner in addition to flagellin. TLR5 may is involved in the activation of the innate immune system after recognition of fungal compartments

We thank Silke Noßmann, Christiane Pilz and Konrad Fischer for technical assistance cell culture.

B 01-13
The organic cation transporter 3 (OCT3) as a histamine transporter in granulocytes

Moritz Pernecker, Miriam Dibos, Sophie Götz, Rita Schröter, Giuliano Ciarimboli

University Hospital Münster, Medical Clinic D, Experimental Nephrology, Münster, Germany

The organic cation transporter 3 (OCT3) is a polyspecific transporter responsible for the movement of organic cations across the plasma membrane. One endogenous OCT3 substrate is the monoamine histamine, whose production by granulocytes such as basophils and mast cells is an important step in the development of type I hypersensitivity. A specific histamine transporter has not yet been identified. For this reason, we investigated whether OCT3 is involved in histamine release by basophils, and whether it plays a role in allergic reactions. To do this, bone marrow cells (BMC) were isolated from wild type mice (WT) and from mice with an ubiquitous genetic deletion of OCT3 ($OCT3^{-/-}$). BMC were differentiated to basophils by incubation with IL-3, the most important growth and activating factor for basophils. Histamine release in supernatant of BMC was measured by an ELISA with/without IgE/anti-IgE incubation. Furthermore, the ear swelling in a contact-dermatitis model induced by 2,4-dinitrofluorobenzene (DNFB) was compared in WT and $OCT3^{-/-}$ mice. Finally, histamine release by the human basophilic KU812 cell line incubated or not with IgE/anti-IgE in the presence or not of the OCT3 substrate or inhibitor 1-methyl-4-phenylpyridinium (MPP^+) or corticosterone, respectively was measured. Stimulation of BMC isolated from WT and $OCT3^{-/-}$ mice by IgE/anti-IgE incubation provoked a

significant release of histamine, which was significantly lower in BMC from OCT3$^{-/-}$ mice than that from WT mice (mean±SEM: 31.1±2.6 n=12 vs 76.7±3.5 ng histamine/mg protein, n=12, respectively). Furthermore, application of DNFB induced a stronger ear swelling in WT than in OCT3$^{-/-}$ mice (10.46±0.72 mm, n = 13 vs 3.2±0.54 mm, n = 13, respectively). Histamine release in the KU812 cell line was significantly stimulated by IgE/anti-IgE incubation (159.4±6.9% , n = 13, compared to controls, which were set to 100%). Addition of MPP$^+$ strongly increased histamine release to 283.2±9.2% (n=9), while addition of corticosterone suppressed its stimulation (106.7±8.6 %, n = 4). These results suggest that MPP$^+$ as an OCT3 substrate trans-stimulates the transporter, in this way increasing OCT3-mediated histamine release, while corticosterone inhibits this part of histamine efflux from the basophils. Taken together, these results suggest that OCT3 mediates at least a part of histamine release by basophils and may be the long-sought histamine transporter in granulocytes.

Supported by the DFG (CI107/14-1).

B 01-14
The voltage-gated proton channel discovers its family

Boris Musset

Paracelsus Medical University, Center of Physiology, Pathophysiology and Biophysics, Nürnberg, Germany

Question

A little over four decades ago, the first voltage-clamp recording of the voltage-gated proton channel sparked a new research field. Almost two and a half decades later, the discovery of the channel's gene paved the way for further advancements in understanding its biophysical properties, structure, function, and physiology. Nevertheless, the field of proton channels continues to expand, with several unanswered questions remaining.

Methods

We showcase our progress in understanding the structure and function of the proton channel. By integrating molecular dynamics simulations with patch-clamp recordings, we focus specifically on investigating the gating mechanism of the proton channel. Our findings shed light on the intricate relationship between the channel's structure and its functional properties.

ResultsOne significant characteristic of the voltage-gated proton channel was the observation that each species examined thus far possesses only one gene responsible for coding the proton channel. In this study, we present the discovery and characterization of three distinct and independent genes coding for proton channels within a single species, Aplysia californica. Aplysia californica is a well-established model organism for studying neural plasticity.

Conclusions

Lastly, we propose a potential evolutionary path for the proton channel, drawing upon the accumulated knowledge in the field.

B 02 | Calcium Dependet Signaling & Methods

B 02-01
Vasopressin modulates calcium oscillations in adrenal cortex via V1a receptor

Hoang A. Dinh[1,2], Kerim Mutig[2], Ute Scholl[1], Pontus B. Persson[2], Gabriel Stölting[1]

[1] *Berlin Institute of Health at Charité – Universitätsmedizin Berlin, Center of Functional Genomics, Berlin, Germany*
[2] *Charité – Universitätsmedizin Berlin, Institut für Translationale Physiologie, Berlin, Germany*

Aldosterone is critical for renal sodium and potassium handling thereby participating in the arterial pressure regulation and maintenance of intact extracellular potassium concentration. Angiotensin II (Ang II) and increased plasma K^+ levels belong to classical stimuli for aldosterone production and release in ZG cells of the adrenal gland. The stimulation is mediated by calcium influx via T-type and L-type voltage-gated calcium channels (VGCC) resulting in transient calcium oscillations, whereby the $Ca_V3.2$ T-Type calcium channel is postulated to play a major role. Vasopressin (VP), often referred to as the antidiuretic hormone, has been shown to modulate the aldosterone plasma levels as well, but

the underlying mechanisms remain poorly characterized. The present study addresses the hypothesis that VP exerts direct effects in cells of ZG.

We combined localization studies with RNA sequencing and calcium imaging recordings in murine adrenal glands to characterize the calcium response to VP and identify the relevant VP receptor type. Using selective blockers of T-type or L-type VGCCs and $Ca_V3.2$-deficient mice ($Ca_V3.2^{-/-}$) we assessed the balance between T-type and L-type calcium channels in mediating the VP action.

Immunofluorescence labeling using an antibody to vasopressin V1a receptor (V1aR) produced signals in all three zones of the murine adrenal cortex, whereas application of antibodies to V1b- or V2 receptor types yielded no detectable signals. RNA sequencing revealed only expression of *Avpr1a* mRNA (encodes V1aR) in adrenal cortical cells. In line with the localization data, acute application of VP on freshly prepared murine adrenal slices elicited calcium oscillations in ZG in a dose-dependent fashion. The character of observed calcium response to VP reflected the pattern of well-established stimulation by Ang II. Selective inhibition of L- or T-type VGCCs suggested involvement of both calcium channel types in the VP signaling. Moreover, evaluation of $Ca_V3.2^{-/-}$ mice revealed no deviations in plasma aldosterone levels suggesting a certain evolutionary redundancy for the two channel types.

Our data thus far demonstrate VP-induced stimulation of ZG activity mediated by V1aR activation and calcium influx via both T-type and L-type VGCCs. These events are expected to result in enhanced aldosterone secretion and release thus deserving further characterization *in vivo*.

B 02-02
Calcium oscillations regulate endocytotic albumin uptake in subdermal adipose stem cells derived from human patients of different age.

Tanvir Morshed[1], Anne Bernhardt[1], Maria Wartenberg[2], Heinrich Sauer[1]

[1] *Justus Liebig University Gießen, Physiology, Gießen, Germany*
[2] *Friedrich Schiller University Jena, Cardiology, Jena, Germany*

Question
Intracellular calcium oscillations of unknown function occur in human adipose tissue stem cells (hASCs). The current study was undertaken to relate intracellular calcium oscillations to albumin import processes in hASCs

Methods
Intracellular calcium was evaluated by fluo-4 microfluometry and confocal laser scanning microscopy (cLSM). Uptake of albumin was recorded using fluorescence labelled Albumin-Alexa 594 and cLSM.

Results
In the present study, calcium oscillations were recorded in hASCs from subcutaneous fat tissue derived from patients of increasing age (20-34yr, 35-49yr, 65-80yr). Cell doubling times of hASCs increased with patient age. Spontaneous calcium oscillations occurred in all age groups, oscillation frequency decreased and spike duration increased with patient age. In serum-free incubation medium calcium oscillations were absent, but could be induced by addition of either fetal calf serum, albumin, IgG or an antibody against the neonatal Fc-receptor (FcRn) which is involved in the recycling of albumin and IgG. Consequently, FcRn expression was demonstrated in ASCs of all age classes by western blot analysis. The uptake of fluorescence labelled albumin was abolished by the calcium chelating agent BAPTA, the store-operated Ca^{2+} entry (SOCE) inhibitor SKF96365, the calcium sensing receptor (CaSR) inhibitor NPS-2143, the macropinocytosis inhibitors cytochalasin D and wortmannin, and the caveolae-dependent endocytosis inhibitor genistein.

Conclusions
In summary our data suggest that calcium oscillations in human ASCs regulate albumin uptake and presumably IgG recycling.

This work was supported by the German Research Foundation (DFG) (grant no. WA 1087/8-1).

References
[1] Sauer H, Sharifpanah F, Hatry M, Steffen P, Bartsch C, Heller R, Padmasekar M, Howaldt HP, Bein G, Wartenberg M. 2011. NOS inhibition synchronizes calcium oscillations in human adipose tissue-derived mesenchymal stem cells by increasing gap-junctional coupling. *J Cell Physiol*. 226(6):1642-50.doi: 10.1002/jcp.22495

B 02-03
Pacemaker currents of R5 neurons and their role in sensory filtering in *Drosophila melanogaster*

Anatoli Ender, Raquel Suárez-Grimalt, Davide Raccuglia, David Owald

Charité-Universitätsmedizin, Institute of Neurophysiology, Berlin, Germany

Over the day we are bombarded with external stimuli, most of which gets filtered out in our brain in order to extract behaviorally relevant information. Sensory filtering is active even during sleep and only salient stimuli can wake us up. Although, some of the brain regions and circuits involved in sensory filtering are known, the underlying neuronal mechanism remains poorly understood.
Sleep is highly conserved and can be observed in vertebrates as well as in invertebrates. Recently, we discovered slow wave oscillations in the R5 network of the ellipsoid body, which encodes sleep drive in *Drosophila melanogaster* [1,2]. We found that at a single cell level R5 neurons discharge slow rhythmic bursts of action potentials at frequencies at around 1 Hz. Periodic activity patterns of cells are often generated by intrinsic membrane currents which have been shown to be able to establish neuronal signal filters. Therefore, we hypothesized that periodic activity patterns generated by intrinsic membrane currents in R5 neurons are important for sensory filtering. In the present study we first aim to identify putative pacemaker currents in the R5 system. We use *in vivo* patch clamp recordings to characterize the neuronal intrinsic properties and the mechanisms underlying the rhythmic firing pattern of R5 neurons.
First recordings identified network independent activity in R5 neurons which correlates to the animal's sleep need. Furthermore, our results indicate that the *Drosophila* T-type Ca_v3 channel is involved in the cell intrinsic pacemaking mechanism of R5 neurons. Eventually, we aim to understand the role of the identified ion channels and their pacemaking function in sensory filtering and the behavior of the animals.

References
[1] Raccuglia, D. et al., Network-Specific Synchronization of Electrical Slow-Wave Oscillations Regulates Sleep Drive in Drosophila, Current Biology, Volume 29, Issue 21, 3611 - 3621.e3
[2] Raccuglia, Suarez-Grimalt et al.,Coherent multi-level network oscillations create neural filters to favor quiescence over navigation in *Drosophila*, *bioRxiv*, 2022.03.11.483976; doi: https://doi.org/10.1101/2022.03.11.483976

B 02-04
South american rattlesnake toxin blocks high-voltage-activated calcium channels

Markus Eicheldinger, Francisco J. Castilla Porras, Patricia Hidalgo

Forschungszentrum Juelich, Institute of Biological Information Processing (IBI-1), Jülich, Germany

The author has objected to a publication of the abstract.

B 02-05
A novel state-dependent inhibitor of N-type channel (DP-2) Orally Available to Relieve Neuropathic Pain

Gustavo A. Guzman[1], Janine Kutzsche[1], Dieter Willbold[1,2]

[1] *Forschungszentrum Jülich, Institute of Biological Information Processing, IBI-7: Structural Biochemistry, Jülich, Germany*
[2] *Heinrich-Heine-Universität Düsseldorf, Institut für Physikalische Biologie, Düsseldorf, Germany*

Background: The first line of drugs for managing neuropathic pain (NP) are antidepressants, anticonvulsants followed by topical agents, and potent opioids. However, patients frequently do not respond to the classic treatment mentioned above. The N-type ($Ca_v2.2$) voltage-gated calcium channel (VGCC) is a validated target for managing chronic and neuropathic pain. Thus, another alternative drug to relieve NP is the

$Ca_v2.2$ channel-blocking peptide, Prialt (SNX-111, ziconotide). However, Prialt must be delivered intrathecally and constantly monitored due to its narrow therapeutic index[1-2]. Thus, the aim of our investigation is to develop highly potent and selective N-type blockers administered orally to manage NP without side effects.

Methods: The whole-cell patch-clamp technique was used to demonstrate the effect of a new drug candidate named DP-2 (all-D-enantiomeric peptide) on various VGCCs. We used HEK293 cells, stably expressing the human α_{1A-2} ($Ca_v2.1$), α_{1B-1} ($Ca_v2.2$), and α_{1E-1} ($Ca_v2.3$) splice variants. $Ca_v3.2$ was transiently transfected with Lipofectamine 2000 expressed in tsA201 cells.

Results: Our data demonstrated that DP-2 potently inhibited channel ionic currents mediated by the $Ca_v2.2$ in a dose-dependent and reversible manner with submicromolar potency (IC_{50} of 0.66 µM ± 0.13 µM). Applying 1 µM, DP-2 led to 54 % inhibition of the current and did not reveal a significant change in the voltage dependence of activation properties. Furthermore, the blocking characteristic of DP-2 was evaluated at different holding potentials (HP) and frequencies. Our data demonstrated that DP-2 had a more potent blocking effect towards more positive potentials, i.e., at –60 mV, approximately 77 % of the current was reduced, and 56 % recovered. In contrast, DP-2 applied at more negative potentials (-100 mV) inhibited $Ca_v2.2$ currents by about 48 %. Thus, these data suggest a state-dependent blocking mechanism for DP-2. The time constant to achieve a similar inhibition during 1 µM application showed a linear frequency-dependent inhibition at the stimulus of 0.05 Hz (14. 6 s), 0.1 Hz (10.01 s), and 0.5 Hz (7.2 s). Further analysis revealed that DP-2 did not affect the channel in the resting state. DP-2 did not remarkably affect the transiently expressed $Ca_v3.2$ channel at 1 µM and 10 µM. A minor inhibition of 20 % and 6.5 % of the current was observed when 1 µM was applied to the $Ca_v2.1$, and $Ca_v2.3$ channels, respectively. A ten-fold higher concentration of DP-2 significantly reduced the $Ca_v2.1$, and $Ca_v2.3$ -mediated ionic currents by about 70 %, and 25 %, respectively.

Conclusion: DP-2 is a novel therapeutic agent that can be expected to have a broader therapeutic window than the calcium channel blocker ziconotide. DP-2 is a state and use-dependent $Ca_v2.2$ calcium channel blocker that shows higher selectivity for $Ca_v2.2$ than the $Ca_v2.1$, $Ca_v2.3$, and $Ca_v3.2$ channels at submicromolar concentrations.

We are grateful to David Adams, who kindly provided the stable cell lines $Ca_v2.1$, $Ca_v2.2$, and $Ca_v2.3$.

References
[1] Patel R, Montagut-Bordas C, Dickenson AH (2018) Calcium channel modulation as a target in chronic pain control. Br J Pharmacol
[2] Jain KK (2000) An evaluation of intrathecal ziconotide for the treatment of chronic pain. Expert Opin Investig Drugs

B 02-06
Cacna1d$^{Ile772Met/+}$ mice with PASNA syndrome

Gabriel Stölting[1], Hoang An Dinh[1], Marina Volkert[1], Nicole Hellmig[1], Julia Schewe[1], Luise Hennicke[1], Eric Seidel[1], Herbert Oberacher[2], Junhui Zhang[3], Richard P. Lifton[3,4], Iris Urban[5], Melissa Long[6], Marion Rivalan[6], Timothy Nottoli[7], Ute I. Scholl[1]

[1] *Berlin Institute of Health @ Charité - Universitätsmedizin Berlin, Center of Functional Genomics - AG Hypertension and Molecular Biology of Endocrine Tumors, Berlin, Germany*
[2] *Medical University of Innsbruck, Institute of Legal Medicine and Core Facility Metabolomics, Innsbruck, Austria*
[3] *Yale University School of Medicine, Department of Genetics and Howard Hughes Medical Institute, New Haven, USA*
[4] *The Rockefeller University, Laboratory of Human Genetics and Genomics, New York, USA*
[5] *Charité – Universitätsmedizin Berlin, Transgenic Technologies, Berlin, Germany*
[6] *Charité – Universitätsmedizin Berlin, Animal Behavior Phenotyping Facility, Berlin, Germany*
[7] *Yale University School of Medicine, Section of Comparative Medicine, Yale Genome Editing Center, New Haven, USA*

Somatic gain-of-function mutations in the L-type calcium channel $Ca_V1.3$ can cause primary aldosteronism (PA) due to the occurrence of adrenal aldosterone-producing adenomas (APA) and micronodules. Germline mutations are also result in PA as well as in the more complex disorders such as PASNA syndrome (**PA**, **s**eizures and **n**eurologic **a**bnormalities). We generated mice carrying the heterozygous Ile772Met mutation (Het) which, in humans, is found in APA as well as in PASNA syndrome. Het mice were unable to reproduce naturally, requiring in vitro fertilization. Newborns showed higher mortality than wild type controls and were smaller and lighter when reaching adult age. Intracellular calcium signaling in the adrenal zona glomerulosa was enhanced and the aldosterone:renin ratio in the serum was increased. Incomplete aldosterone suppression by a high salt diet confirmed the diagnosis of primary aldosteronism. Seizures could be elicited following anesthesia

using ketamine and xylazine. Het mice showed hyperlocomotion, impaired coordination on the rotarod and deficits in nest construction. Oral administration of the L-type calcium channel inhibitor isradipine decreased intracellular calcium concentrations in the ZG – in particular of the baseline - as well as reduced serum aldosterone levels and improved the rotarod performance of Het mice relative to untreated controls. Treatment with dihydropyridines may thus represent a therapeutic strategy for the treatment of PA but also PASNA syndrome due to mutations in $Ca_V1.3$.

B 02-07
Orai1 modulates vitamin C-dependent collagen release from pancreatic stellate cells

Rieke Schleinhege, Albrecht Schwab, Zoltan Pethö

University of Münster, Institute of Physiology II, Münster, Germany

Question

The collagen-rich fibrotic stroma is a hallmark of the pancreatic ductal adenocarcinoma (PDAC). In PDAC, fibrosis promotes tumor cell invasion, and it hampers therapeutical drug delivery. The main drivers for pancreatic fibrosis are pancreatic stellate cells (PSCs). When activated, PSCs produce excessive amounts of a collagen-rich extracellular matrix (ECM). It is known that vitamin C promotes collagen synthesis. However, little is known about the fine-tuned regulation of ECM release from PSCs. We hypothesize that collagen exocytosis is Ca^{2+}-dependent, and that vitamin C is involved in this Ca^{2+}-dependent regulation. In a first step, we established a model to obtain stellate cell-derived matrices *in vitro*. Based on that, we modulated the culturing of pancreatic stellate cells to assess the role of vitamin C and of the Ca^{2+} channel Orai1 in the regulation of collagen release.

Methods

We induced matrix formation *in vitro* with the human PSC cell line PS-1. The composition of the PSC-derived ECM was analyzed with mass spectroscopy. Cell-derived ECM was visualized and quantified with CNA35-tdTomato, a fluorescently labeled bacteria-derived collagen adhesion protein. The same staining was applied to visualize the distribution of intracellular collagen in PS-1 cells. To address the mechanistic role of vitamin C in collagen release we performed Ca^{2+} imaging in PSCs. The role of Orai1 in collagen release was assessed by analyzing the impact of channel inhibition on the PSC-derived ECM and by performing vitamin C-dependent Ca^{2+}-imaging under Orai1 inhibition.

Results

We found that PS-1 cells produce large amounts of ECM composed of glycoproteins and multiple collagens which build up a complex, three-dimensional matrix network. Stimulating PS-1 cells with vitamin C greatly increases matrix quantity. Single-cell imaging of CNA35-tdTomato-stained PS-1 cells revealed that vitamin C promotes a shift of collagen-containing vesicles towards the cell membrane resulting in collagen release. To analyze whether vitamin C modulates collagen exocytosis in a Ca^{2+}-dependent manner we performed Ca^{2+} imaging and showed that vitamin C induces Ca^{2+} influx into PSCs. Next, we investigated whether Ca^{2+} channels known to be functionally expressed in PSCs might contribute to the vitamin C-dependent regulation of collagen exocytosis. We screened for different channels and found that the inhibition of Orai1 reduces collagen deposition. Mechanistically, we revealed that the vitamin C-induced Ca^{2+} influx into PSCs is attenuated when Orai1 is inhibited.

Conclusions

In conclusion, we established a powerful *in vitro* model to mimic ECM synthesis and showed that Orai1 modulates the vitamin C-dependent collagen release from PSCs.

RS was supported by a scholarship from the Medizinerkolleg (MedK) Münster.

B 02-08

Automatic detection, localization, and classification of Ca^{2+} release events in cardiomyocytes with a deep learning-based approach

Prisca Dotti[1], Miguel Fernandez-Tenorio[1,3], Radoslav Janicek[1], Pablo Márquez-Neila[2], Marcel Wullschleger[1], Raphael Sznitman[2], Marcel Egger[1]

[1] *University of Bern, Department of Physiology, Bern, Switzerland*
[2] *University of Bern, ARTORG, Bern, Switzerland*
[3] *Instituto de Biomedicina de Sevilla (IBiS), Hospital Universitario Virgen del Rocío/CSIC/Universidad de Sevilla, Departamento de Fisiología Médica y Biofísica, Seville, Spain*

Question

The release of Ca^{2+} from intracellular stores, which manifests as localized Ca^{2+} release events, plays a crucial role in regulating cardiac muscle contraction. Dysregulation of Ca^{2+} signaling can lead to various health issues, including arrhythmias and cardiac hypertrophy. Therefore, distinguishing between distinct types of spontaneous Ca^{2+} release events occurring during diastole, such as Ca^{2+} sparks [1] and Ca^{2+} puffs [2], is essential for understanding their impact on disease development. However, localizing and classifying Ca^{2+} release events can be time-consuming, especially with full-frame confocal imaging [3]. We propose an efficient automated model based on deep learning (DL) techniques to address this challenge.

Methods

We analyzed fast xyt confocal imaging data of cardiomyocytes loaded with a calcium-sensitive fluorescent dye. We semi-automatically annotated subcellular Ca^{2+} events in 43 recordings. Initially, we obtained a binary events segmentation through processing and denoising. Then, we manually corrected the segmented movies and classified the events as Ca^{2+} sparks, Ca^{2+} puffs, and Ca^{2+} waves.

We trained a DL model based on the UNet architecture [4] to localize and classify Ca^{2+} release events automatically. The model's output was further processed to eliminate artifacts and obtain individual event instances. Figure 1 illustrates our pipeline.

Matching the model's detected events with annotated instances, we computed precision, recall, percentage of event detection, and alignment of detected event classes with annotations. However, validating the segmentation of Ca^{2+} release events presented challenges due to factors like Ca^{2+} diffusion influencing border delineation and a low signal-to-noise ratio in several samples. To address this, we asked six experts to annotate ten frames, enabling us to assess inter-observer variability. We measured agreement between observers (human or model) and the majority vote of the other observers using Cohen's kappa, which accounts for chance agreement.

Results

Across all types of Ca^{2+} release events, the average precision was 0.59, and recall was 0.57. Regardless of correct classification, the percentage of detected events was 75.1%. Additionally, 75.1% of the detected events belonged to the correct class. Figure 2 shows examples of the model's output.

Our analysis revealed no statistically significant difference between the results obtained with our model and the human experts, with a p-value of 0.775 obtained from the Kruskal-Wallis test on the agreement between all observers and the majority vote.

Conclusions

Our results demonstrate that our DL-based model is a valuable tool for detecting and classifying Ca^{2+} release events in cardiomyocytes, achieving comparable performance to human experts. It offers a fully automated approach that significantly reduces the time and effort required compared to manual annotation methods.

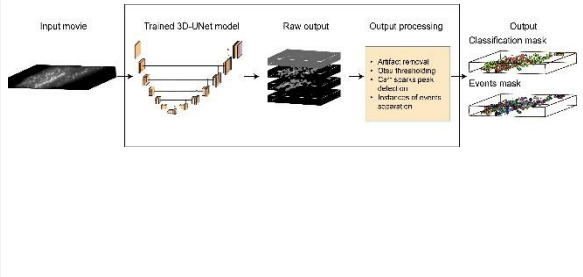

Figure 1
Pipeline illustrating the proposed model for analyzing full-frame confocal Ca^{2+} fluorescence recordings. The analysis generates two output movies: one for localizing and classifying Ca^{2+} release events, and another displaying numbered event instances. The input movie is initially processed by the DL model, which produces as outputs probability distributions for each class (background, Ca^{2+} sparks, Ca^{2+} puffs, and Ca^{2+} waves). Subsequently, the outputs undergo further processing to separate different event instances and classify them accordingly.

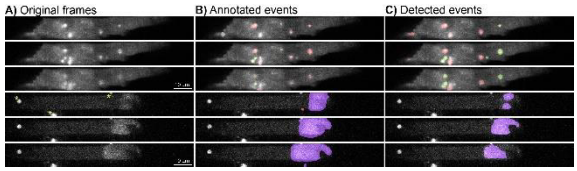

Figure 2
Qualitative performance of the proposed model on selected slices from two test recordings. A) Original frames from the movies at different ordered time steps, with asterisks denoting dye loading artifacts. B) Annotated frames showing different types of Ca^{2+} release events (green: Ca^{2+} sparks, red: Ca^{2+} puffs, purple: Ca^{2+} waves). C) Predicted frames with the same color coding. It is possible to observe variations in event sizes between annotated and predicted frames, even for correctly predicted events (e.g. the Ca^{2+} wave in the bottom three frames).

References
[1] Cheng, H, Lederer, WJ, Cannell, MB 1993, 'Calcium sparks: elementary events underlying excitation-contraction coupling in heart muscle', *Science*, vol. 262(5134), 740–744
[2] Parker, I, Yao, Y 1991, 'Regenerative Release of Calcium from Functionally Discrete Subcellular Stores by Inositol Trisphosphate', *Proceedings: Biological Sciences*, vol. 246(1317), 269–274
[3] Wullschleger, W, Blanch, J, Egger, M 2017, 'Functional local crosstalk of inositol 1,4,5-trisphosphate receptor- and ryanodine receptor-dependent Ca^{2+} release in atrial cardiomyocytes', *Cardiovascular Research*, vol. 113(5), 542–552
[4] Ronneberger, O, Fischer, P, Brox, T 2015, 'U-Net: Convolutional Networks for Biomedical Image Segmentation', *Medical Image Computing and Computer-Assisted Intervention – MICCAI 2015*, Lecture Notes in Computer Science, 234–241, Cham: Springer

B 02-09
A polymer partitioning probe of aerolysin's astonishing asymmetry

Ishan Ghai, Hannah Altenbach, Jan C. Behrends

Department of Physiology, Faculty of Medicine, University of Freiburg, Freiburg, Germany

The pore formed by the bacterial toxin aerolysin has been shown to be of outstanding sensitivity when used as a single molecule sensor, in particular, due to a strong interaction with both neutral and charged polymer analytes (molecular trap) [1]. Early on, size-dependent block by disperse poly (ethylene glycol) (PEG) of M_w=1500 g/ml with monomer (M_m=44 g/ml) resolution [2] was shown to have superior resolution with this pore [3], leading to subsequent applications for the sizing of short polynucleotides and polyarginine (M_m=251 and 174 g/ml, respectively) [4]. In all of these studies, it was noted that, in contrast to the alpha-hemolysin pore the aerolysin pore was unaffected by any of the analytes, no matter the polarity and amplitude of the potential bias, when they were present in the *trans*-compartment, suggesting that for unknown reasons these polymers were able to enter the beta-barrel structure only by way of the *cis*-side opening through the "rivet head", not directly into the *trans*-side beta-barrel. This is particularly surprising because some of these analytes have been clearly shown to be transported through the pore in the *cis*-*trans* direction at suitable driving voltages (e.g. Ref. 1 in [4]).

Here, we begin to investigate this problem using a classical approach [5] with dispersed solutions of PEG of various M_w at high concentrations (10% w/v) under conditions (0.5 M KCl), where polymer-pore-interaction is minimized, as evidenced by the absence of resistive pulses. Aerolysin was added to one (*cis*) compartment of a classical vertical bilayer chamber and insertions were followed over time with a (50 mV bias, *trans*+) and current step sizes converted into conductance. Using this protocol, it is highly unlikely that aerolysin pores would insert with the "rivet head" in the *trans*-compartment.

The average single aerolysin pore conductance was 251 ± 23 pS (S.D.), in agreement with the literature. With PEG present *cis*-side, pore conductance was significantly reduced for M_w=600, 1000, and 1500 g/mol but remained at control level for M_w= 2000, 3400, and 6000. In contrast, with PEG present *cis*-side, reduced pore conductance was only found for M_w=600 and 1000 while PEG 1500 had no significant effect. These preliminary results suggest a significant difference in the steric/entropic barrier for PEG partitioning between the *cis* and *trans*-ward entry of analytes into aerolysin's beta-barrel. Further investigation is underway to determine whether this difference can account for the complete lack of interaction with *trans*-side analytes in the earlier experiments.

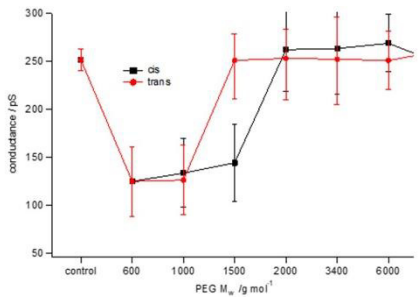

Conductance vs PEG Plot

References
1. Ouldali, H.et al. 2020 Nature Biotechnology. 38:176–181.
2. Ensslen, T. et al. 2022 J. Am. Chem. Soc. 144:16060–16068.
3. Krasilnikov, O.V. et al. 2006 Phys. Rev. Lett. 97:018301.
4. Robertson, J.W.F et al. 2007 Proc. Natl. Acad. Sci. U S A. 104:8207-8211.
5. Rodrigues, C.G. et al. 2008 Biophys. J. 95:5186–5192.
6. Baaken, G. et al. 2011 ACS Nano. 5:8080–8088.
7. Baaken, G. et al. 2015 ACS Nano. 9:6443–6449.
8. Cao, C. et al, 2016 Nature Nanotechnology. 11:713–718.
9. Piguet et al. 2017 Nat Comms. 9:169–13.
10.Krasilnikov et al. 1992. FEMS Microbiol Immunol. 105:93–100.
11. Merzlyak et al. 1999 Biophys. J. 77:3023–303.

B 02-10
Evaluating whole cell and single channel data from Patch Clamp experiments with Igor Pro

Friederike Stumpff[1], David Manneck[1]

[1] *Health and Medical University Potsdam, Physiology, Potsdam, Germany*
[2] *Freie Universität Berlin, Veterinary Anatomy, Berlin, Germany*

Question

Evaluating patch clamp data tends to be very time-consuming. The tools provided by commercial software are helpful, but not sufficient. In particular, intuitive macros are lacking that allow a rapid representation and statistical evaluation of whole cell and single channel patch clamp data with a step-by-step introduction for use by beginners in scientific data evaluation (e.g. medical doctoral students). Furthermore, fitting routines for evaluation of single channel conductances in asymmetrical solutions are not generally available.

Methods

The commercially available program Igor Pro was used to program macros for evaluation of whole cell and single channel data obtained with HEKA Patchmaster software. In measurements, a low frequency voltage protocol was used to monitor solution changes, automatically followed by a high resolution protocol for analysis of current kinetics (whole cell) or single channel activity.

Results

To allow an overview of the data, routines were programmed to allow automatic labelling of data with the solutions used. All images of a series could then be adjusted to a common scaling, as desired, and appended to a pdf with a routine. For whole cell data, individual data files could be automatically merged and labelled with solution changes to give an overview of current changes during the entire experiment. Routines were developed to allow automatic data collection in tables for subsequent statistical evaluation [1]. For the analysis of single channel data, further macros were developed to allow selection of individual traces and automatic generation of amplitude histograms. From these histograms, peaks were automatically fitted for analysis of peak amplitudes. The user was prompted to enter comments after which the macro automatically entered the peak data obtained into an Igor Pro table with the corresponding pipette potential and solution used. Further automatic fitting routines allow calculation of single channel conductances in asymmetrical solutions assuming independence of ionic currents according to the Goldman-Hodgkin-Katz equation [2]. Finally, macros were developed to allow entry of data from different experiments into tables for statistical analysis.

Conclusions

Analysis of whole cell and single channel patch clamp data with the macros developed can be performed by doctoral students and greatly reduces the time required and the errors made.

DFG-STU 258/7-1, Akademie für Tiergesundheit

References
[1] Manneck, D, Manz, G, Braun, HS, Rosendahl, J, Stumpff, F. 2021, ' The TRPA1 Agonist Cinnamaldehyde Induces the Secretion of HCO3− by the Porcine Colon ', *International Journal of Molecular Sciences*, 22(10): 5198
[2] Liebe, F, Liebe, H, Sponder, G, Mergler S, Stumpff F. 2022, 'Effects of butyrate(-) on ruminal Ca(2+) transport: evidence for the involvement of apically expressed TRPV3 and TRPV4 channels`, *Pflugers Archiv,* 474(3): 315

B 02-11
Brightness optimization of an ultrasensitive genetically encoded voltage indicator

Anagha G. Nair, Philipp Rühl, Saasrika C.N.W. Dehiwalage, Roland Schönherr, Stefan H. Heinemann

Center for Molecular Biomedicine, Friedrich Schiller University Jena and Jena University Hospital, Department of Biophysics, Jena, Germany

The cellular membrane potential (Vm) is a critical physiological parameter in neuronal signaling, membrane transport, and even cell differentiation. Because the electrical measurement of Vm is invasive and laborious, there is a strong demand for bright and sensitive Genetically Encoded Voltage Indicators (GEVIs) suited for Vm measurements in a high-content approach.
Our optimization started from the GEVI ASAP3 (Accelerated Sensor for Action Potentials), which consists of a voltage-sensing domain (VSD, S1-S4) and a circularly permuted GFP (cpGFP) inserted in the extracellular linker between S3 and S4 of the VSD.1 An N-terminally fused red fluorescent protein (mKate2, mK2) provided a constant signal for determining the molecular brightness of voltage-dependent cpGFP-originating green fluorescence.2 Systematic mutagenesis in S3 and S4 optimized the brightness and shifted the half-maximal voltage (Vhalf), i.e., the voltage of the sensor's maximal resolution into the range of typical resting membrane potentials to yield mK2-ASAP3:GTR.3
To further enhance the molecular brightness of mK2-ASAP3:GTR, we introduced mutation S318A to yield mK2-rEstus. An equivalent was reported to increase fluorescence intensity in GFP.4 We characterized 318S and 318A by dual-color fluorescence imaging under whole-cell voltage-clamp control after expression in HEK293T cells. At pHextra 7.4, the S318A mutation increased the maximum molecular brightness of the sensor by ≈ 75% (arrow in Fig. 1A). The voltage dependence of the cpGFP fluorescence was described by the following parameters (before/after mutation): maximum brightness Bmax 77.5 / 54.3%EGFP; maximal change in brightness ΔB 57.0 / 39.7%EGFP; Vhalf -32.0 / -42.2 mV, inverse voltage dependence 26.0 / 25.7 mV.
To get further insight to the origin of the molecular brightness increase, both constructs were functionally evaluated with respect to their pHextra dependence. Before imaging, the cell culture medium was replaced with an external solution where the pH was adjusted from 5.9 to 8.9. The pH of the pipette solution was kept constant at 7.4. From the pH titration curve of Bmax we derived an apparent pKa value of 6.9 for 318A and 7.7 for 318S (Fig. 1A). Therefore, the observed increase in brightness at pH 7.4 mainly originates from the shift in pH dependence. Interestingly, the pH did not only influence the brightness of the sensor as Vhalf was a linear function of pH for both sensors, with a slope of 11.1 mV per pH unit (Fig. 1B). Furthermore, mK2-rEstus outperformed ASAP3 in single-spike (2 ms, -80 to 40 mV) detection by 3.2-fold.
The optimized GEVI has great potential as a tool for electrophysiological research due to its improved brightness and single-spike detection capabilities, and it may provide access to quantitative high-content Vm measurements. Moreover, owing to the improved sensitivity it may even serve as optical voltage control in electrophysiological voltage-clamp experiments.

Simons Foundation Autism Research Initiative (SFARI) (S.H.H, 705944SH)

German Academic Exchange Service (A.G.N., 91819480)

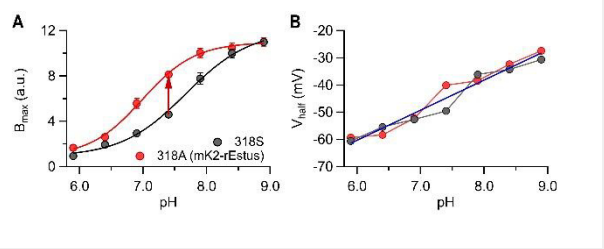

Figure 1: Bmax and Vhalf as a function of pH

References
[1] Villette, V. et al. Ultrafast two-photon imaging of a high-gain voltage indicator in awake behaving mice. Cell 179, 1590-1608.e23 (2019).
[2] Rühl, P. et al. Monitoring of compound resting membrane potentials of cell cultures with ratiometric genetically encoded voltage indicators. Communications Biology 4, 1–11 (2021).
[3] Rühl, P. et al. Genetically encoded voltage indicators optimized for measuring the cellular resting membrane potential. ACTA PHYSIOLOGICA 236, 157-157 (2022).
[4] Teerawanichpan, P. et al. Investigations of combinations of mutations in the jellyfish green fluorescent protein (GFP) that afford brighter fluorescence, and use of a version (VisGreen) in plant, bacterial, and animal cells. Biochimica et Biophysica Acta (BBA) - General Subjects 1770, 1360–1368 (2007).

B 03 | Endocrinol Metabolism

B 03-01
Use of Pancreas Tissue Slices for the in Situ Study of the Endocrine Pancreas in Health and Disease

Christian M. Cohrs[1,2,3], Ana K. Mojica Avila[1,2,3], Mariama Guirgus[1,2,3], Stephan Speier[1,2,3]

[1] Technische Universität Dresden, Institute of Physiology, Faculty of Medicine Carl Gustav Carus, Dresden, Germany
[2] Technische Universität Dresden, Paul Langerhans Institute Dresden (PLID) of the Helmholtz Zentrum München at University Clinic Carl Gustav Carus, Dresden, Germany
[3] German Center for Diabetes Research (DZD), München-Neuherberg, Germany

The endocrine pancreas and its functional units, the islets of Langerhans, constitutes about 2% of the organ and is spread throughout the entire parenchyma. Due to their spatial separation, assessment of endocrine cell function is primarily performed on isolated islets. Being the gold standard for the study of islet function and physiology for decades, the isolation process entails a cell recovery phase in vitro and is known to alter morphology, gene expression and cell biology thereby limiting the comparability to the in vivo situation. Furthermore, enzymatic digestion and mechanical separation may induce a selection bias for a subset of islets that may lead to a loss of structurally compromised islets found in pathological settings like type 1 diabetes. In order to overcome several methodological limitations of the existing technologies and to bridge the gap between isolated islets and systemic metabolism we established the pancreas tissue slice technique for multiple species that allows the acute study of islets in their preserved native environment, facilitating the investigation of a close reflection of in vivo pancreas cell physiology and pathogenesis. Obtained tissue slices of 120-150µm thickness allow functional studies at different levels from individual cells within islets to several islets simultaneously and also allow the study of intra-organ crosstalk within the islet surrounding. Functional assays are complemented with the possibility to perform high quality 3D morphometric imaging of whole tissue slices in order to correlate functional and morphological parameters for a better understanding of cell physiology and disease related mechanisms.
Here we present our established multi-species pancreas tissue slice platform with their different experimental approaches including live-cell imaging, hormone secretion and 3D morphometry using mouse and human tissue. In combination with assessed in vivo parameters prior to our comprehensive in situ analyses, we are able to evaluate the contribution of islet mass and function to both type 1 and type 2 diabetes pathogenesis at multiple steps in disease development. Specifically, we could show that in human type 1 diabetes development a functional decline is preceding significant beta cell mass loss at the time of clinical disease onset, an observation that is different to the NOD mouse model. Such a functional decline is also observed for the pre-diabetic states in human type 2 diabetes pathogenesis without obvious islet mass changes. Investigating similar conditions in a murine high-fat diet model revealed that functional decline is most probably counteracted by a higher plasticity of beta cells in mice.
Collectively, the in situ tissue slice approach enabled us to shed light onto the distinct contribution of endocrine mass and function during the natural history of diabetes in both humans and mice and will allow to develop novel strategies for therapeutic approaches.

This work was supported with funds from the DFG-SFB/Transregio 127, the German Ministry for Education and Research (BMBF) and the German Centre for Diabetes Research (DZD).

References
[1] Marciniak A, **Cohrs CM**, Tsata V, Chouinard JA, Selck C, Stertmann J, Reichelt S, Rose T, Ehehalt F, Weitz J, Solimena M, Slak Rupnik M, **Speier S**. 2014, Using pancreas tissue slices for in situ studies of islet of Langerhans and acinar cell biology, Nat Protoc, Dec;9(12):2809-22
[2] **Cohrs CM**, Panzer JK, Drotar DM, Enos SJ, Kipke N, Chen C, Bozsak R, Schöniger E, Ehehalt F, Distler M, Brennand A, Bornstein SR, Weitz J, Solimena M, **Speier S**., 2020, Dysfunction of Persisting β Cells Is a Key Feature of Early Type 2 Diabetes Pathogenesis, Cell Rep., Apr 7;31(1):107469
[3] Panzer JK, Hiller H, **Cohrs CM**, Almaça J, Enos SJ, Beery M, Cechin S, Drotar DM, Weitz JR, Santini J, Huber MK, Muhammad Fahd Qadir M, Pastori RL, Domínguez-Bendala J, Phelps EA, Atkinson MA, Pugliese A, Caicedo A, Kusmartseva I, **Speier S**., Pancreas tissue slices from organ donors enable in situ analysis of type 1 diabetes pathogenesis, 2020, JCI Insight, Apr 23;5(8):e134525

B 03-02
Does Regular Physical Activity generally reduce Basal Energy Expenditure? Arguments against an Alleged Paradigm Change

Dieter Böning[1], Jürgen Steinacker[2]

[1] *Charité-Universitätsmedizin Berlin, Institut für Physiologie, Berlin, Germany*
[2] *Universität Ulm, Abt. Sport- und Rehabilitationsmedizin, Ulm, Germany*

Question

A reduction of basal energy expenditure (BEE) has been occasionally observed after weeks of intense physical training in previously untrained subjects (so-called energy compensation). According to some scientists (e. g. Careau et al. (Curr Biol 31 (20): 4659-4666) this is a general phenomenon also in daily live. They have evaluated measurements of total energy expenditure (TEE), BEE and activity energy expenditure (AEE). Based on a negative correlation between single measurements of BEE and AEE in subjects varying in sex, age and body mass they suggest that physical activity generally reduces BEE. Is this conclusion really correct?

Methods

Analysis of data in this paper and related articles.

Results

The conclusions raise various questions: 1. The authors compare measurements of TEE over several days with one measurement of BEE. But BEE varies during 24 hours at least because of body temperature oscillation. 2. Many smaller (and leaner) subjects with low BEE are more active than larger and/or more fatty people. 3. Careau et al. present energy expenditure values per subject “adjusting for weight (and body composition) by a regression model“. But BEE and AEE have to be calculated also for kg body mass to avoid a confusing influence on the data, when subjects are compared. This is also done by other investigators (e. g. Westerterp KR Front. Physiol. 2013;4.90). The calculation for kg is not possible with Carreau`s data, but from mean values in a similar article by Pontzer (Pontzer H. Sci Am. 2017; 316: 26-31). Body mass and TEE in frequently moving small subjects in African and South American villages were compared to heavy North American citizens. TEE per kg was clearly higher in the rural physically active population than in the more sedentary North Americans, while total TEE was slightly higher in the latter. 4. Energy compensation is usually not observed in physically training subjects.

Conclusions

The hypothesis of a general reduction of BEE following intense exercise is not proven by this article. A loss of body mass during physical training mainly depends on 2 factors: energy consumption by exercise and energy uptake by eating. For hard training athletes necessary regeneration and filling of energy stores do not allow energy compensation.

References
[1] 1. Böning D. Fat in spite of exercise? An alleged paradigm change results from calculation mistakes. Dtsch Z Sportmed. 2018; 69: 3-4.
2. Careau V, et al. Energy compensation and adiposity in humans. Curr Biol. 2021; 31: 4659-4666.
3. Pontzer H, Raichlen DA, Wood BM, Mabulla AZ, Racette SB, Marlowe FW. Hunter-gatherer energetics and human obesity. PLoS One. 2012; 7: e40503
4. Speakman JR, Selman C. Physical activity and resting metabolic rate. Proc Nutr Soc. 2003; 62: 621-634.
5. Westerterp KR. Physical activity and physical activity induced energy expenditure in humans: measurement, determinants, and effects. Front Physiol. 2013; 4: 90.

B 03-03
Impact of extracellular glucose and glutamine concentrations on tumor cell metabolism

Christina M. Baumbach, Alexander Lasch, Sarah Reime, Anne Riemann, Oliver Thews

Martin Luther University Halle-Wittenberg, Medical Faculty, Julius Bernstein Institute of Physiology, Halle/Saale, Germany

Question Many tumors rely on anaerobic or aerobic glycolysis to fuel their elevated demands for biosynthesis and energy production. However, this massive glucose consumption often leads to its deprivation in the tumor tissue. To still maintain energy supply and biosynthetic processes, obviously other nutrients have to be utilized, e.g. glutamine, and the metabolic pathways need to be adapted. This work aims to explore the impact of a combined, reduced glucose and glutamine supply upon cancer cell metabolism and signaling.
Methods Rat prostate carcinoma cells were incubated for 3 and 24 h in media supplemented with different glucose (5.5 mM, 11 mM) and glutamine (0 mM, 2 mM) concentrations. Glucose and glutamine consumption and lactate production as well as the cellular ATP level were measured. In addition, the expression and phosphorylation of different proteins relevant for modulating the cellular metabolic pathways were analyzed by qPCR and Western Blot.
Results After 3 h, glucose and glutamine consumption as well as ATP levels were nor altered by any of the different conditions. After 24 h, the combined deprivation of glucose and glutamine led to a significantly decreased protein synthesis and ATP production. For all other conditions, ATP production was kept at the control level. Reduced extracellular glucose levels were compensated by an increased glutamine consumption. Glutamine deprivation did not significantly alter glucose consumption or lactate production. However, glutamine restriction decreased mTOR signaling throughout the experiments. Glucose restriction induced Akt phosphorylation but only after 3 h; towards the end of culture, the combined glucose and glutamine deprivation reduced Akt phosphorylation. cMYK expression was upregulated in all conditions at both time points.
Conclusions In the cell line analyzed in this study the available energy sources, i. e. glutamine and/or glucose, were metabolized to always maintain the ATP levels. As long as glucose is present, the high lactate production indicates the ongoing glycolytic metabolism. When glutamine is the only available energy source, this amino acid is metabolized to ATP without a significant lactate production. Further experiments will be conducted to elucidate the interplay of mTOR and cMYK and the influence they might exert on the underlying metabolic pathway.

B 03-04
Local and systemic sex differences of islet of Langerhans physiology in glucose homeostasis

Celina Funke[1,2], Christine Herrmann[1,2], Stephan Speier[1,2]

[1] *TU Dresden, Institute of Physiology, Dresden, Germany*
[2] *University Hospital and Faculty of Medicine Carl Gustav Carus, Paul Langerhans Institute Dresden (PLID) of Helmholtz Center Munich, Dresden, Germany*

Question
It has been shown that sex differences exist in glucose homeostasis and diabetes prevalence and progression whereby female subjects are diagnosed later and with higher BMI compared to male subjects. In basic research, mouse studies often ignore one sex and consider mostly male mice, which show a better response to diabetes inducers such as high fat diet. Therefore, we included both sexes in this study to carefully analyze *in vivo* glucose homeostasis as well as *in situ* islet function, to gain further insight into sex dependent differences in the function of islets of Langerhans and the role of systemic factors driving these differences.
Materials and methods
To investigate this question, we performed body composition analysis and *in vivo* glucose and insulin tolerance tests with male and female C57Bl/6N mice with an age of 20 weeks. Additionally, we assessed insulin secretion kinetics *in situ* using acute and cultured pancreatic tissue slices and *in vitro* using isolated islets from male and female mice.
Results
In vivo analysis of glucose homeostasis showed an improved glucose tolerance with lower fasted and stimulated c-peptide levels in female mice compared to male mice. HOMA-IR and insulin tolerance tests confirm higher insulin sensitivity of female mice, although relative fat and

lean mass was not different in both sexes. Analyzing insulin secretion of islets acutely from pancreatic tissue slices showed similar results to *in vivo* data with higher insulin secretion in male islets. After culturing pancreatic slices or isolation of islets these sex specific differences in insulin secretion seem to disappear or even reverse with a higher secretion in female islets.

Conclusions

So far, our data show that the secretion patterns of islets of Langerhans in healthy C57Bl/6N mice are controlled by sex-related systemic factors. Impaired glucose homeostasis and higher *in vivo* c-peptide secretion in male mice compared to female mice seems to be driven by lower insulin sensitivity in combination with other systemic factors that are currently being analyzed. Insulin secretion of cultured tissue slices as well as isolated and rested islets leads to adjustment of their function to the new conditions. Consequently, we will study systemic sex specific factors driving islet function more in detail und furthermore focus on functional sex differences in islets under physiological and pathological conditions.

B 03-05

Thyroid Hormone-Induced Expression of Na^+/K^+-ATPase in Neural Cells Depends on Na^+ Influx

Heiko M. Lesslich[1], Sivaraj Mohana Sundaram[2], Marius Strachowitz[1], Irmgard D. Dietzel[1]

[1] *Ruhr-Universität Bochum, RUBION, Bochum, Germany*
[2] *SRM Institute of Science & Technology, Division of Medical Research, Faculty of Medical Health & Science, Kattankulathur, India*

Thyroid hormones –mainly the active form triiodothyronine (T3)– are known to accelerate many brain functions, such as EEG rhythms, reflexes and evoked potentials. Concomitant with these electroencephalographic changes, hyperthyroidism causes nervousness, restlessness, irritability and can even evoke epileptic seizures, while absence of thyroid hormones leads to retardation and slowed reflexes. In previous investigations, we observed an increase in Na^+ current density in neurons as a dominant underlying mechanism of the action of T3 [1]. Furthermore, we have obtained evidence that the modulation of neuronal excitability is induced by factors, most prominently fibroblast growth factor 2 (FGF-2, formerly known as bFGF), secreted from surrounding glial cells, especially astrocytes. The effect of thyroid hormone in mixed neuron / glia cultures was abolished by antibodies against FGF-2, suggesting that FGF-2 is a prominent factor in the regulation of neuronal excitability by T3 [2, 3].

On the other hand, thyroid hormone T3 is mainly known for its regulation of metabolism. Several investigations have shown that T3 regulates the membrane expression of Na^+/K^+-ATPases which account for about 40 % of resting metabolic rate. A selective increase in Na^+/K^+-ATPase activity alone, would, however, stabilize the resting membrane potential and hyperpolarize cells, rendering them less excitable. To resolve this apparent contradiction, we hypothesized that the regulation of the Na^+/K^+-ATPase is not directly induced by T3 but by the increased Na^+-load of the excitable cells resulting from an upregulation of voltage-activated Na+ channels and potentially also Na^+-coupled transporters. Here, we present evidence, that in mixed neural cultures from postnatal rat brains, alpha1 and alpha2 subunits of the Na^+/K^+-ATPase are up-regulated by T3. Additionally, the number of [^{3}H]-ouabain binding sites is upregulated by treatment of mixed cultures for 4 days with T3 or of neuron enriched cultures by FGF-2. We also found that these effects are partially reversible by blocking voltage-activated Na^+ currents with tetrodotoxin, suggesting that enhancement of the basal metabolic rate induced by T3 is to some extent a consequence of increased cellular excitability.

References

[1] Hoffmann, G, Dietzel, ID 2004, Tyhroid hormone regulates excitability in central neurons from postnatal rats, *Neuroscience*, 125, 369-379, doi: 10.1016/j.neuroscience.2004.01.047

[2] Niederkinkhaus, V, Marx, R, Hoffmann G, Dietzel ID 2009, Thyroid Hormone (T3)-Induced Up-Regulation of Voltage-Gated Sodium Current in Cultured Postnatal Hippocampal Neurons Requires Secretion of Soluble Factors from Glial Cells, *Molecular Endocrinology*, 23, 1494-1504, doi: 10.1210/me.2009-0132

[3] Igelhorst, BA, Niederkinkhaus, V, Karus, C, Lange, MD, Dietzel, ID 2015, Regulation of neuronal excitability by release of proteins from glial cells, *Philos Trans R Soc Lond B Biol Sci*, 370, 20140194, doi: 10.1098/rstb.2014.0194

B 03-06

Nutritional regulation by leptin receptor-expressing neurons in the lateral hypothalamus under healthy and anorectic conditions

Rebecca Figge-Schlensok[1,2], Anne Petzold[1,2], Nele Hugger[1], Tatiana Korotkova[1,2,3]

[1] University of Cologne, Institute for Systems Physiology, Cologne, Germany
[2] Max Planck Institute for Metabolism Research, Neuronal Circuits and Behavior, Cologne, Germany
[3] University of Cologne, Excellence Cluster on Cellular Stress Responses in Aging Associated Diseases and Center of Molecular Medicine Cologne, Cologne, Germany

The author has objected to a publication of the abstract.

B 03-07

Longitudinal In Vivo Imaging of Islet Physiology and Pathophysiology in the Anterior Chamber of the Mouse Eye

Farid Abdallah[1,2,3], Christian Cohrs[1,2,3], Chunguang Chen[1,2,3], Stephan Speier[1,2,3]

[1] Technische Universität Dresden, Institue of Physiology, Faculty of Medicine Carl Gustav Carus, Dresden, Germany
[2] Technische Universität Dresden, Paul Langerhans Institute Dresden (PLID) of the Helmholtz Zentrum München at University Clinic Carl Gustav Carus, Dresden, Germany
[3] German Center for Diabetes Research (DZD), München-Neuherberg, Germany

Type 2 diabetes (T2D) is a complex multifactorial disease primarily caused by a combination of peripheral insulin resistance and the progressive loss of β-cell function, within the pancreatic islet of Langerhans. In fact, impaired insulin secretion in response to changes in blood glucose levels, constitutes one of the major hallmarks of the disease. Despite growing evidence of compromised mitochondrial function and cellular metabolism in in-vitro studies of isolated islets from T2D patients and rodent diabetes models, little information is known about the underlying cause and kinetics leading to the aforementioned observations during different disease stages (early, pre-diabetic and late disease) in vivo. This is largely due to lack of available longitudinal in vivo imaging techniques with cellular resolution, allowing for proper functional assessment of islets of Langerhans in their natural milieu, the pancreas. Furthermore, studies involving isolated islets lack the longitudinal potential to assess islets in different diseases stages, as well as the signaling complexity found in-vivo (e.g. hormonal, neural and metabolic signaling). We therefore propose to study β-cell metabolism and mitochondrial function in-vivo in islets transplanted into the anterior chamber of the eye of immune deficient mice. Here we present that post-engraftment; longitudinal in-vivo imaging of transplanted islets can be performed via confocal and multiphoton microscopy on the anaesthetized mouse. This in vivo imaging platform allows for the necessary temporal resolution crucial for longitudinal studies, and gives access to the islet for functional assessment during different disease stages. We are currently adapting an array of genetically encoded fluorescent reporters of interest necessary for qualitative and quantitative assessment of multiple physiological parameters in vivo. In the future, we aim to employ this in vivo imaging platform to study the effects of inflammation, hyperglycemia and/or dyslipidemia on islet mass, mitochondrial turnover, cell metabolism and bioenergetics and hormonal function (i.e. insulin secretion in response to metabolic challenge) post islet engraftment.

This work was supported with funds from the DFG-SFB/Transregio 127, the German Ministry for Education and Research (BMBF) and the German Centre for Diabetes Research (DZD).

References
[1] Cohrs CM, Chen C, **Speier S.** Transplantation of Islets of Langerhans into the Anterior Chamber of the Eye for Longitudinal In Vivo Imaging. Methods Mol Biol. 2020;2128:149-157. doi: 10.1007/978-1-0716-0385-7_11

B 03-08
Dysregulation of hypothalamic-pituitary-thyroid hormone secretion in SPRED3- deficient mice

Luisa Haas, Denis Hepbasli, Rebecca Holzapfel, Sina Gredy, Kai Schuh

JMU Wuerzburg, Institute of Physiology, Wuerzburg, Germany

Question

SPRED (Sprouty-related EVH-1 domain) proteins are inhibitors of the mitogen-activated protein kinase (MAPK) signalling pathway controlling cell proliferation and differentiation. To investigate the physiological impact of SPRED3 in vivo, we generated SPRED3 knockout mice by gene targeting.

Methods and Results

Because SPRED3 KO mice showed lowered body (WT vs. KO, 36.06 vs. 25.29 g; ***p< 0.0001) and organ weights (WT vs. KO, heart 0.1471 vs. 0.1279 g; * p=0.0247. brain 0.468 vs. 0.4395 g; **p=0.0038, spleen 0.1385 vs. 0.07316 g; ***p<0.0005) as well as a shortened tibia (19.83 vs. 19.47 mm; *p<0.05) plasma levels of the growth associated hormones thyroxin (T4) and growth hormone (GH) were measured. T4 was significantly reduced in SPRED3 deficient mice (289.2 vs. 226.4 ng/ml; **p<0.01), whereas GH levels were unaltered in mice younger than 120 days and significantly reduced in SPRED3 deficient mice older than 120 days (1664 vs. 555.3 pg/ml; *p<0.05). To investigate the HPT axis further, thyroid stimulating hormone (TSH) plasma levels were investigated. SPRED3 KO mice showed elevated TSH levels (458.8 vs. 865.8 pg/ml; **p<0.01) which combined with the lowered T4 levels indicate a primary hypothyroidism. To find out, whether SPRED3 could possibly influence thyroid hormone production by being expressed in the thyroid or other organs of the HPT axis, X-Gal staining of thyroids, brain, and pituitary gland from WT and SPRED3 KO mice were performed. This staining method uses an enzyme, whose gene is placed behind the SPRED3 promoter in the gene targeting construct and thus displays whether SPRED3 is expressed in a certain tissue or not. X-Gal staining revealed expression of SPRED3 in the thyroid, hypothalamus, and pituitary gland. Evaluation of thyroid morphology in WT and KO mice using HE stained thyroid sections showed a significantly higher portion of follicle (equals colloid) area per thyroid area (36.32 vs. 45.21%; **p<0.01) but unaltered numbers of thyrocytes and mean follicle area.

Conclusions

We conclude that SPRED3 deficiency causes a primary hypothyroidism in mice, which possibly leads to impaired development and growth. The mechanisms through which SPRED3 impacts thyroid health have yet to be characterized but there are indicators that, like SPRED1 and 2, SPRED3 also influences the MAPK signalling cascade. Furthermore, the elevated percentage of follicle area per thyroid area could point towards an impaired uptake of thyroglobulin into the thyrocytes due to SPRED3 deficiency.

This research was funded by Deutsche Forschungsgemeinschaft, project SCHU1600/6-1 and supported by the Graduate School of Life Sciences Wuerzburg.

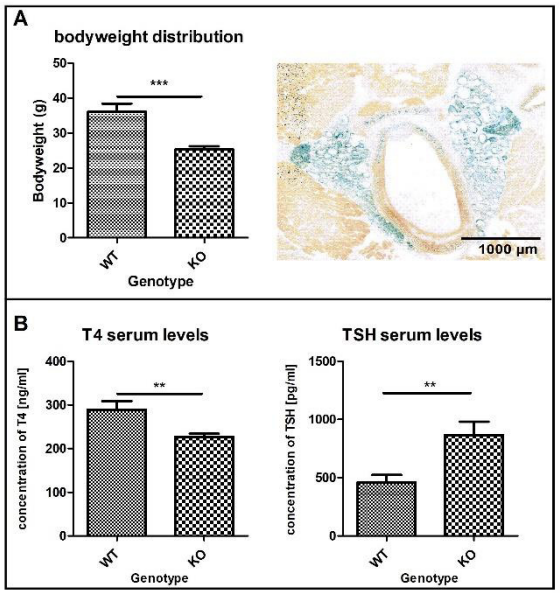

Primary hypothyroidism in SPRED3 deficient mice
A. SPRED3 deficient mice show significantly decreased body weights compared to WT mice (***p<0.001). On the right, the X-Gal-stained thyroid of a SPRED3 KO mouse is shown. Distinct blue coloration of thyroid tissue is visible. **B**. SPRED3 KO mice have significantly lower T4 serum levels as well as significantly elevated TSH serum levels in comparison with the WT mice (**p<0.01).

B 04 | Cell Biology & Signal Transduction

B 04-01
Detection of citrulline modification in histone peptides using biological nanopore

Priyanka Jain, Tobias Ensslen, Jan C. Behrends

University of Freiburg, Institute of Physiology II, Freiburg im Breisgau, Germany

Citrullination, a particularly subtle (-1 Da) post-translational modification (PTM), has recently gained significant interest in the field of biomedicine because of its suspected involvement in human diseases like rheumatoid arthritis, multiple sclerosis and tumours. In spite of minimal change in residue size introduction of citrulline in histone proteins is known to drastically change the structure and function of proteins. Hence, sensitive techniques are in demand for the detection of citrullination.

Currently, advanced MS techniques and chemical derivatization strategies are employed for detecting citrullination. However, no single molecule technique is available to identify such subtle translational modification. Single molecule nanopore techniques might, therefore, be of potential use in this problem. In the light of recent demonstrations of the high sensitivity of the aerolysin pore to peptide volume (Piguet et al. 2018 *Nat.Comm*., Ouldali et al. 2020 *Nat.Biotechn.,* Piguet et al. 2021 *Meth.Enz.*) and, most recently, shape (Ensslen et al. 2022 *JACS*), we were interested in ascertaining whether citrullination can also be detected as well. Here, we demonstrate the use of a mutant of the protein nanopore Aerolysin (AeL) namely R220S-AeL to not only detect but also discriminate different sites of citrulline modification on a peptide derived from human histone H3 protein(H3f), (A1-K9), containing 2 citrullination sites at position 2(H3f.R2-cit) and 8(H3f.R8-cit). These pores were reconstituted in synthetic membranes (Di-phytanoyl-phosphocholine, 5 mg/ml), formed by painting (air bubble method) over cavities (50 µm diameter) on MECA16 chips (Ionera). Experiments were conducted in aqueous 4M KCl solution buffered with 25 mM TRIS and set to pH 7.5 (HCl). The cis side was kept grounded while a negative voltage was applied on the trans side of the bilayer and the peptides were characterized using relative residual current (I/Io) and mean residence time (τ /ms) of resistive pulses resulting from analyte-pore interactions. We found small but clearly detectable differences in I/Io values for all 4 peptides: H3f(uncitrullinated), H3f.R2-cit, H3f.R8-cit and H3f.R2,8-cit in the order of increasing I/Io which could be accounted for by change of arginine's guanidium group (Topological Polar Surface Area: 77.6 Å²) to urea (69.1 Å²) as well as the increase in hydrophobicity. This is further evidence that single molecule nanopore techniques are a valuable solution for rapid and easy detection of PTMs.

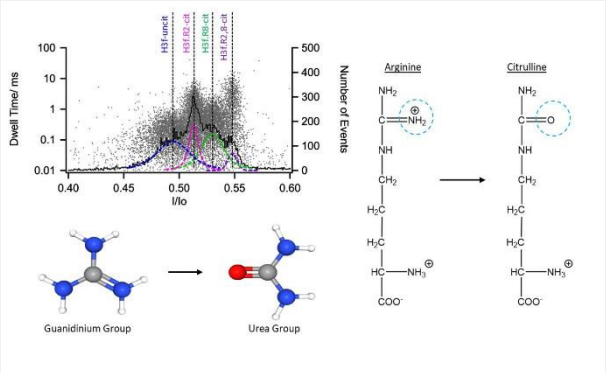

Detection of Citrulline modification using nanopore

References

[1] Ouldali, Hadjer, et al. "Electrical recognition of the twenty proteinogenic amino acids using an aerolysin nanopore." *Nature biotechnology* 38.2 (2020): 176-181.

[2] Ensslen, Tobias, et al. "Resolving Isomeric Posttranslational Modifications Using a Biological Nanopore as a Sensor of Molecular Shape." *Journal of the American Chemical Society* 144.35 (2022): 16060-16068.

[3] Piguet, Fabien, et al. "Pore-forming toxins as tools for polymer analytics: From sizing to sequencing." *Methods in Enzymology*. Vol. 649. Academic Press, 2021. 587-634.

[4] György, Bence, et al. "Citrullination: a posttranslational modification in health and disease." The international journal of biochemistry & cell biology 38.10 (2006): 1662-1677.

[5] Gill, Adam D., et al. "Sensing of citrulline modifications in histone peptides by deep cavitand hosts." Chemical Communications 55.88 (2019): 13259-13262.

B 04-02
Mapping the signaling network of macrophage chemotactic navigation using knockout mouse models

Markus Horsthemke[1,2], **Peter J. Hanley**[1,2]

[1] *HMU Health and Medical University Potsdam, Potsdam, Germany*
[2] *HMU Research, Development und Innovation gGmbH (HMU RDI), Potsdam, Germany*

Macrophages play a crucial role in inflammatory diseases, yet the mechanisms underlying their recruitment to inflamed sites by chemoattractants like complement C5a remain incompletely understood. Here, we present a comprehensive model (Fig. 1) of complement C5a-mediated macrophage chemotaxis. To investigate cell shape control, motility, and chemotaxis, we studied macrophages from knockout mouse models (highlighted in green, Fig. 1)[1,2] and incorporated pertinent findings from previous studies. Our model underscores the importance of regulators involved in cytoskeletal dynamics, including Rho GTPases, RhoGEFs (guanine nucleotide exchange factors), RhoGAPs (GTPase-activating proteins), myosins, actin NPFs (nucleation promoting factors), and actin nucleators and elongation factors. Currently, in collaboration with Ulla G. Knaus (Dublin, Ireland), we are examining the roles of kinases Pak1, Pak2, Limk1, and Limk2 (highlighted in red, Fig. 1), previously proposed to mediate step 12 of the modified dendritic nucleation model of membrane protrusion by Pollard and Borisy[3], in macrophage motility and chemotaxis, utilizing loss-of-function mouse models.

This work was supported by Deutsche Forschungsgemeinschaft (DFG) grant HA 3271/3-2 (to P. J. H.).

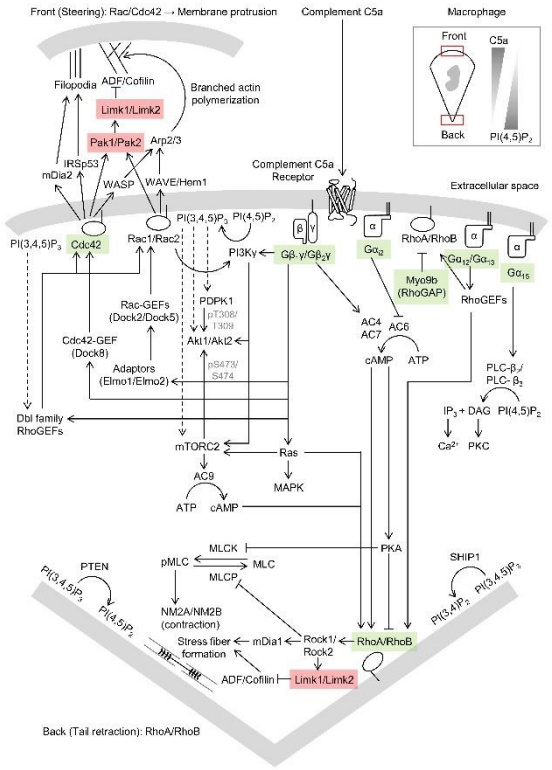

Figure 1
Schematic representation of the signaling pathways connecting complement C5a receptors to membrane protrusions at the leading edge and retractions at the trailing end of a macrophage migrating in a complement C5a gradient.

References

[1] van den Bos, E, Ambrosy, B, Horsthemke, M, Walbaum, S, Bachg, AC, Wettschureck, N, Innamorati, G, Wilkie, TM, Hanley, PJ. 2020, Knockout mouse models reveal the contributions of G protein subunits to complement C5a receptor-mediated chemotaxis, *Journal of Biological Chemistry*, 295(22):7726-7742.

[2] van den Bos, E, Walbaum, S, Horsthemke, M, Bachg, AC, Hanley PJ. 2020, Time-lapse Imaging of mouse macrophage chemotaxis, *Journal of Visualized Experiments*, (158), doi: 10.3791/60750.

[3] Pollard, TD, Borisy, GG. 2003, Cellular motility driven by assembly and disassembly of actin filaments, *Cell*, 112(4):453-65.

B 04-03
High throughput screening strategies for identifying novel PI(3,4)P_2-sensitive PH domains

Julia Jeschke[1], Marc Geissler[1,2], Imran G. Shaikh[1], Dominik Oliver[1], Vijay Renigunta[1]

[1] *Philipps University of Marburg, Neurophysiology, Institute for Physiology and Pathophysiology, Marburg, Germany*
[2] *Technische Universität Dresden, Center for Regenerative Therapies, Dresden, Germany*

Phosphoinositides are a group of seven different phospholipids found in biological membranes. They play an important role in a variety of cell signaling pathways, such as the PI3K-Akt signal transduction pathway, by recruiting pleckstrin homology domain (PH domain) or phox homology (PX domain) containing proteins to the plasma membrane. Since PI(4,5)P_2 and PI(3,4,5)P_3 are the major phosphoinositides in the plasma membrane of eukaryotic cells, their interactions with PH or PX domains have been well studied. However, their binding behavior with respect to PI(3,4)P_2 remains understudied - mostly due to the lack of appropriate cellular assays.

Here we have established a method to screen a library of PH and PX domains for their sensitivity towards PI(3,4)P_2. Firstly, we coexpressed each of these domains from the library with LepB, a prokaryotic kinase, allowing us to generate PI(3,4)P_2 by non-canonical phosphorylation of PI(3)P at the endosomal membrane. Live-cell confocal imaging confirmed the translocation of the PI(3,4)P_2-sensitive PH probes to endosomes. To further validate PI(3,4)P_2 binding also at the plasma membrane, each positive PH or PX domain from the LepB screening was further examined in a knock-in HEK 293 cell line stably expressing both the potassium channel ROMK2 and the voltage-sensing phosphatase Ci-VSP. In this assay, the activation of Ci-VSP via depolarization induced by high K^+ concentration, lead to the generation of PI(3,4)P_2 from its

precursor $PI(3,4,5)P_3$, and lipid binding was revealed as the subsequent translocation of the candidate protein domain to the plasma membrane monitored by TIRF microscopy.
This combination of methods allowed us to ascertain binding to $PI(3,4)P_2$ in living cells of 6 PH domains and one PX domain, thereby identifying potential new tools for surveillance of $PI(3,4)P_2$ concentrations in living cells.

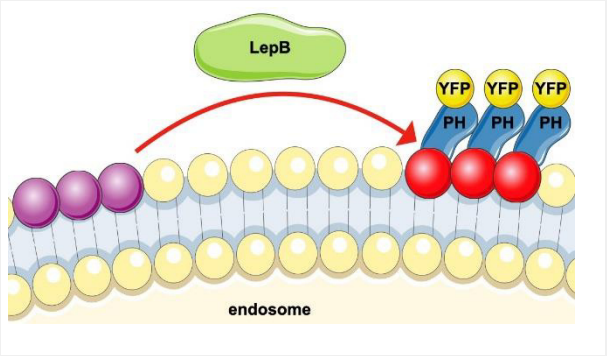

Schematic representation of the function of LepB used for the first phase of the screening
purple: $PI(3)P$, red: $PI(3,4)P_2$

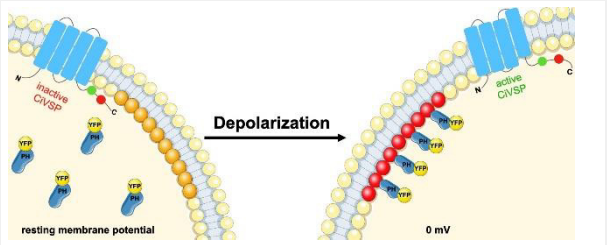

Schematic representation of the VSP based assay
[if !supportLineBreakNewLine]orange: $PI(3,4,5)P_3$, red: $PI(3,4)P_2$
[endif]

B 04-04
Determinants of plasma membrane targeting of mammalian voltage-sensing phosphatase (VSP)

Wencai Zhao, Vijay Renigunta, Imran G. Shaikh, Dominik Oliver

Philipps University of Marburg, Institute of Physiology and Pathophysiology, Marburg, Germany

The author has objected to a publication of the abstract.

B 04-05
Using Bayesian inference to integrate biological data and mathematical modeling to assess cell cycle dynamics: How does the soluble adenylate cyclase ADCY10 control the cell cycle of endothelial cells?

Mats L. Moskopp[1,2], Warunya Woranush[1], Thomas Noll[1], Peter Dieterich[1]

[1] *Technische Universität Dresden, Institut für Physiologie, Dresden, Germany*
[2] *Klinikum im Friedrichshain, Klinik für Neurochirurgie, Berlin, Germany*

Question

While bicarbonate blood levels are considered physiologically stable in mammals, intracellular bicarbonate levels in different cellular sub-compartments are assumed to be highly dynamic. Under varying metabolic load the soluble adenylate cyclase ADCY10 acts as an endogenous HCO_3^- sensor. Adenosine-3', 5'-cyclic monophosphate (cAMP) produced by ADCY10 is known as an essential second messenger. Depending on different cell types, cAMP can either inhibit or activate cell proliferation. However, the influence of ADCY10 on cell cycle control in endothelial cells remains unclear. It is the central aim of this study to identify how ADCY10 influences the timing of the individual phases of the cell cycle in human umbilical vein endothelial cells (HUVECs) using a combined approach of biological experiments and mathematical modeling.

Methods

HUVECs were synchronized in G0/G1 phases by starvation. Subsequently, cells were either exposed to different concentrations of HCO_3^- or to the ADCY10 inhibitor KH7. Cell number and cell cycle stages were assessed at different time points using flow cytometry resulting in a time series of cells per cell cycle stage. Based on these numbers, cell cycle dynamics were analyzed using a mathematical model. The mathematical model approach allows to assess information contained within the biological data that is not directly apparent. The suggested mathematical model represents a description of cells per cell cycle stage, formally described by a coupled set of nonlinear first-order differential equations. The model parameters allow a quantitative description such as the mean duration of individual cell cycle stages. Bayesian inference was used to integrate biological data and the mathematical model of the cell cycle.

Results

We were able to show that Bayesian inference retrieve information of synthetic test data generated by model simulations with added noise as artificial measurement errors. This allowed for educated experimental planning balancing the work load for the experimenter and precision of parameter estimation. With regards to biological data Bayesian inference enables to evaluate different mathematical models based on the amount of information contained by the data. Inactivation of ADCY10 by CO_2 withdrawal resulted in prolongation of the mean duration of one cell cycle. Pharmacological inhibition with KH7 resulted in functional arrest of the cell cycle. In summary, all cell cycle stages progressed slower due to ADCY10 inactivation. However, the G1-S transition was quantitatively the most influenced by ADCY10.

Conclusions

For broader accessibility, we designed a web-application that allows for model simulations of the cell cycle, experimental planning as well as parameter estimation. This tool requires no additional software or hardware and is free of charge. The main biological result is that in HUVECs ADCY10 activation affects all cell cycle phases and controls the duration of G1 phase in particular.

B 04-06

Gene-COCOA: comparative co-expression analysis focussed on a gene of interest

Simonida Zehr[1,2], Timothy Warwick[1,2], Lisa M. Weiss[1,2], Sebastian Wolf[3,4], Thomas Oellerich[3,4], Marcel H. Schulz[2,5], Matthias S. Leisegang[1,2], Ralf P. Brandes[1,2]

[1] *Goethe University, Institute for Cardiovascular Physiology, Frankfurt, Germany*
[2] *German Center for Cardiovascular Research (DZHK), Partner site Frankfurt Rhein-Main, Frankfurt, Germany*
[3] *Goethe University, Hematology/Oncology, University Hospital Frankfurt, Frankfurt, Germany*
[4] *Goethe University, Frankfurt Cancer Institute, Frankfurt, Germany*
[5] *Goethe University, Institute for Cardiovascular Regeneration, Frankfurt, Germany*

Motivation

Functional enrichment analyses are important for deriving meaningful biological insights. Standard enrichment tools help characterise a feature of interest (e.g., disease-relevant cell type) in contrast to a background distribution (e.g., wildtype). As of now, they focus on the comparison of two conditions and thus do not allow for inferences about certain genes of interest (GOIs).

Development

Here we present an approach to the **co**mparative **co**-expression **a**nalysis focussed on a specific **gene** of interest (Gene-COCOA). Gene-COCOA takes a list of curated gene sets as an input and ranks them according to their strength of association with the gene of interest (GOI). From each gene set, n genes are sampled as predictor variables in a linear regression modelling the expression of the GOI as the outcome variable. For bootstrapping, this procedure is repeated 1k times. The resulting model errors are compared in a t-test. Gene sets with adjusted *P*-values of <0.05 model the GOI expression better than random. This method provides insights on the functional association networks of a GOI whilst avoiding common artefacts arising from gene expression data.

Proof of principle

In an exemplary use case, the co-expression patterns of *SOD1* with the 50 MSigDB hallmark gene sets were studied in peripheral blood lymphocytes of 11 patients with amyotrophic lateral sclerosis (ALS). Compared to expression in peripheral blood lymphocytes of 11 healthy controls, *SOD1* shows an overall decrease in association with nearly all hallmark gene sets in ALS, notably those related to immune function

and cell cycle. Notably, stronger associations of *SOD1* with gene sets indicating oxidative phosphorylation, reactive oxygen species and unfolded protein response are reported in the disease samples.

Conclusion

Standard enrichment analyses focus on the identification of gene sets overrepresented in a feature of interest. Here we present a different approach to comparative co-expression studies, focussing on a GOI. In our Gene-COCOA analysis of *SOD1* in ALS, we could replicate well-described mechanisms of a monogenic disease, such as the association of *SOD1* mutations with ROS and protein misfolding.

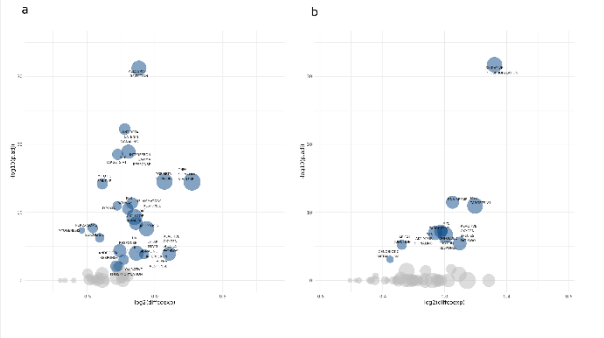

Fig 1.
In healthy lymphocytes (**a**), Gene-COCOA reports *SOD1* co-expression with gene sets indicating cell cycle and immune function. In ALS (**b**), overall association with gene sets is reduced; instead, *SOD1* is co-expressed with pathways associated with reactive oxygen species and protein misfolding.

B 04-07
Simultaneous Single Photon Counting and Ion Current Readout from Free-Standing Lipid Bilayers - Membranes under Investigation

Tobias Ensslen, Jan Behrends

University of Freiburg, Physiology II, Freiburg i.Br., Germany

Fluorescence microscopy and, in particular, single molecule optical spectroscopy is of great potential value in characterizing the structural dynamics of membranes and membrane proteins. A particular challenge is to combine such high-resolution optical measurements with high-resolution voltage clamp electrical recordings that can provide direct information on single ion channel gating, or a block by drugs and analytes. Here, we report on the use of a novel chip-based, 2 x 2 arrangement of microelectrode cavities with borosilicate glass windows, which facilitates optical access on an inverted microscope with water-, or oil-immersion objectives of high numerical aperture to horizontal free-standing lipid membranes, while controlling membrane voltage and recording currents using individual micropatterned, ring-shaped Ag/AgCl-electrodes to perform time-resolved single photon counting on free-standing membranes spanning sub-nanoliter cavities [1]. This device allows for rapid formation of four membranes that are simultaneously monitored electrically using a four-channel amplifier and can be sequentially optically addressed, greatly reducing the time needed for successful experimentation. Single channel activity induced by the pore forming peptide Ceratotoxin-A was simultaneously acquired to FLIM. Further, we demonstrate transport of fluorescently labeled polyarginine peptides through channels of the poreforming toxin Aerolysin, by confocal optical readout correlated to electrophysiological measurements. In summary, the novel device increases the likelihood of realizing the long standing ambition to correlate structural and functional dynamics of single membrane proteins on the single molecule level.

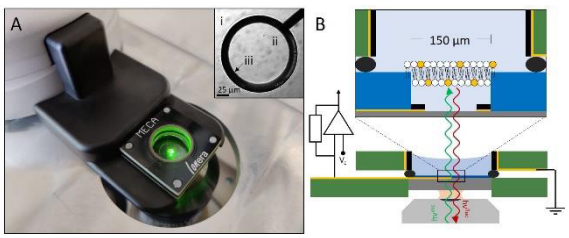

Micro-Electrode -Cavity-Array (MECA) for Simultaneous Optical an Electric Readout
A: photography of the MECAopto device connected to a commercial voltage clamp amplifier (ORBITmini, Nanion GmbH) placed on a standard inverted fluorescence microscope. The inset represents the 150 µm aperture microstructured by photoresist i on a glass chip ii, equipped with a Ag/AgCl ring-electrode iii; B: cartoon of the experimental setup with increased assembly of a micro-cavity

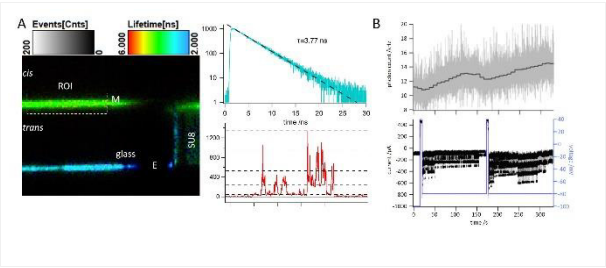

Experimental Results
A: confocal z/x-scan through a single cavity on the MECAopto. The apperture spanning DPhPC membrane was overlayed with fluorescently labeled CtxA. Lifetimes of 3.8 ns have been measured by FLIM while channel activity was recorded; B: confocally measured increase in fluorescence due to transport of fluorescently labeled peptides through 5 parallel AeL channels, reconstituted in one membrane. Voltage induced, reversible channel closing could be correlated to the rate of photon count

References

[1] Ensslen, T.S., Behrends, J.C., 2022, 'A chip-based array for high-resolution fluorescence characterization of free-standing horizontal lipid membranes under voltage clamp', *Lab Chip*, **22**, 2902

B 04-08
FRET measurements of claudins in fixed cells – an inappropriate approach

Catrin Przibylla-Diop, Susanne Milatz

Christian-Albrechts-Universität zu Kiel, Institute of Physiology, Kiel, Germany

Förster resonance energy transfer (FRET) provides a well-established and reliable tool to study protein interaction on the molecular scale. The proximity of two fluorescent molecules (i. e. fluorophore-tagged proteins) enables the non-radiative energy transfer process between a donor and acceptor (FRET-pair). The FRET efficiency is determined by the spatial distance between FRET donor and acceptor. This parameter not only depends on the distance between the FRET pair, it is also depending on the relative orientation of their respective transition dipole moments. FRET measurements are performed in both, living and fixed cells. But so far, there is only little information about the comparability of the method in these two different conditions. Additionally, no data is available for FRET measurements of the protein family of claudins in fixed cells. The claudin family members are expressed in various tissues and determine the properties of tight junctions. They differ not only in their expression, but also in their particular functions. Some of them act as paracellular cleft sealing barriers, whereas others like claudin-10 and -2 function as channel forming proteins with size-, charge- and water-selective properties. FRET measurements of claudin-transfected living-cells are widely used to examine structural and functional features of these proteins. However, for several proteins, the FRET technique is also performed in fixed cells. To investigate the suitability of paraformaldehyde fixation for analysis of claudin claudin interactions, we compared the respective energy transfer efficiency of fluorophore-tagged claudins in both fixed and live cell conditions. The obtained experimental results show that the energy transfer efficiency of claudin-transfected HEK-293 cells is affected by the fixation. Thus, we demonstrate that FRET measurements of claudins in paraformaldehyde-fixed cells represent an inappropriate approach. It also emphasizes the important role of testing controls before studying a new family of proteins with this tool.

B 04-09
Modern open-source data analysis platform specialized for beta cells.

Johannes U. Pfabe, Srdjan Sarikas, Marjan Slak Rupnik

Medical University of Vienna, Institute of Physiology, Vienna, Austria

Objective

Analysis of calcium imaging data is time-consuming and often lacks objectivity. Moreover, analysis software is mostly specialized for neuroscience or simply not publicly available. We want to overcome those issues by providing a modern, open-source analysis software specialized for pancreatic beta cells. As researchers are usually not advanced in programming, we provide an easy-to-use environment including templates and interactive web-apps. This shall speed up analysis of experiments and raise comparability.

Methods

We use Python and common data science packages. Nearly every imaging data format can be loaded. Before image processing, we correct the movie for motion and phase, and calculate a mean image. Segmentation works by applying two Gaussian blur filters with different kernel size on the mean-image and subtracting the results. Regions of interest are then created by searching for local maxima. Sequential filtering at different timescales and checking whether the z-score is above 3 (equal to $p < 0.002$), distinguishes events from noise. Derivation of an event graph detects temporal summated events. Event half-width, time points, and area-under-curve are some calculated parameters. For statistics, we use linear mixed effect models and standard statistical tests in pooled or individual samples.

Result

We provide a software solution [1], which is easy to use, and publications [2-4] show its relevance for research in the field. Deployment as a docker container is easy, and the "JupyterLab" environment supports further customization. Results are stored in open formats like HDF5 or CSV. Integrated apps make it easy to analyze and visualize islets, cells, traces, and events with high temporal resolution. Additionally, we provide an experiment database system and possibilities to analyze electrophysiology data. We will enhance and add features in the future and seek for acceptance by researchers and contributions by data scientists.

References
[1] Sarikas, S., Pfabe, J., 'Physio_Ca', https://github.com/szarma/Physio_Ca
[2] Postić, S., Sarikas, S., Pfabe, J., Pohorec, V., Križančić Bombek, L., Sluga, N., Skelin Klemen, M., Dolenšek, J., Korošak, D., Stožer, A., Evans-Molina, C., Johnson, J. D., & Slak Rupnik, M. (2023). High-resolution analysis of the cytosolic Ca^{2+} events in β cell collectives in situ. *American journal of physiology. Endocrinology and metabolism*, *324*(1), E42–E55. https://doi.org/10.1152/ajpendo.00165.2022
[3] Sluga N, Križančić Bombek L, Kerčmar J, Sarikas S, Postić S, Pfabe J, Skelin Klemen M, Korošak D, Stožer A, Slak Rupnik M. Physiological levels of adrenaline fail to stop pancreatic beta cell activity at unphysiologically high glucose levels. Front Endocrinol (Lausanne). 2022 Oct 25;13:1013697. doi: 10.3389/fendo.2022.1013697. PMID: 36387857; PMCID: PMC9640998.
[4] Postić, S., Gosak, M., Tsai, W. H., Pfabe, J., Sarikas, S., Stožer, A., Korošak, D., Yang, S. B., & Slak Rupnik, M. (2022). pH-Dependence of Glucose-Dependent Activity of Beta Cell Networks in Acute Mouse Pancreatic Tissue Slice. *Frontiers in endocrinology*, *13*, 916688. https://doi.org/10.3389/fendo.2022.916688

B 04-10
The SUMO isopeptidase SENP2-regulated muscle function is disrupted in chemotherapy-induced cachexia

Bushra Khan[1], Luis V. Gand[1], Dongchao Lu[2], Christian Bär[2], Andreas Pich[3], Theresia Kraft[1], Mamta Amrute-Nayak[1], **Arnab Nayak**[1]

[1] *MHH, Institute for Molecular and Cell Physiology, Hannover, Germany*
[2] *MHH, Institute of Molecular and Translational Therapeutic Strategies, Hannover, Germany*
[3] *MHH, Institute of Toxicology, Hannover, Germany*

Question: The precise organization of the sarcomere coupled with proper calcium transient is critical for force generation and is indispensable for muscle contraction. Sarcomere disorganization is a hallmark of muscle dysfunction associated with cachexia, a severe muscle-wasting disorder prevalent in 80% of cancer patients with 30% mortality rate. Cells employ SUMO (Small Ubiquitin-like Modifier) machinery to fine-tune cellular functions. In this study, we tested a possible link between SUMO isopeptidase SENP2 with striated muscle function.
Methods: We performed siRNA-mediated depletion of endogenous SENP2 in mouse skeletal muscle cells and neonatal rat cardiomyocytes. To investigate the effect of SENP2 depletion on muscle cell architecture and function, we checked sarcomere organization, changes in cytoplasmic Ca^{2+}, and muscle cell contraction. We mapped and quantified endogenous SENP2 interactome by SENP2 proteomics and confocal microscopy to establish detailed molecular mechanism of SENP2-regulated sarcomere organization. To determine SENP2-goverened gene expression program in striated muscle cells, we performed RNAseq assays.
Results: The expression and subcellular distribution ofSENP2 was temporally regulated during myogenic differentiation. SENP2-depleted progenitor myoblasts failed to generate mature muscle cells (myotubes). In differentiated muscle cells, SENP2 deficiency led to a significant loss of muscle cell contractile ability due to sarcomere disorganization and perturbed calcium transients. Transcriptomic analysis revealed 3109 genes were deregulated upon SENP2 depletion. The genes govern sarcomerogenesis, sarcomere assembly (*Mef2c, Myh1, Myh2*), and key components of sarcoplasmic reticulum (*Ryr1, Atp2a1, Casq1*) were most significantly downregulated, corroborating the possible mechanism behind contractile dysfunction upon SENP2 deficiency. Proteomic studies identified diverse protein groups as novel SENP2 interactors, potentially required for functional coordination by SENP2 in muscle cells. Interestingly, specific classes of chemotherapeutic drugs

(tyrosine kinase inhibitor, Sorafenib) affected SENP2 protein stability, leading to deregulated transcriptional signaling and thereby expression of SENP2 target genes. This was ultimately impinged on sarcomere organization and defective muscle cell contractile function.

Conclusions: These unpublished data established an unprecedented role of SENP2 in myogenesis, sarcomere organization, and calcium transient, thus affecting muscle cell function. Our preliminary data suggests that transcriptional remodeling of muscle-specific genes is among one of the underlying mechanisms that is regulated by SENP2 in muscle cells. Importantly, specific chemotherapeutic drug targets SENP2 function in striated muscle cells, resulting in cachectic phenotype. Our ongoing investigation is testing possibilities to alleviate chemotherapy-induced muscle wasting by interfering with SENP2 function.

We are thankful to the Deutsche Forschungsgemeinschaft (DFG) for funding. This research was partly supported by a grant from DFG to Arnab Nayak (NA 1565/2-1).

B 05 | Cardiac Function 1

B 05-01
Endo- to epicardial gradient of the transverse tubular system in failing and non-failing human hearts

Zafar Iqbal[1], Dominik Fiegle[1], Ghazali Minabari[2], Christian Heim[2], Hendrik Milting[4], Eric Rytkin[3], Igor Efimov[3], Tilmann Volk[1], Thomas Seidel[1]

[1] FAU Erlangen, Institut für Zelluläre und Molekulare Physiologie, Erlangen, Germany
[2] Universitätsklinikum Erlangen Herzchirurgische Klinik, Allgemeine Chirurgie, Erlangen, Germany
[3] Northwestern University, Chicago IL, Department of Biomedical Engineering, Chicago, USA
[4] Ruhr-Universität Bochum, Bad Oeynhausen, Erich und Hanna Klessmann-Institut, Bad Oeynhausen, Germany

Introduction

Human hearts and hearts of larger mammals, such as dogs, show significant transmural gradients in action potential (AP) duration, K^+ currents and intracellular Ca^{2+} signals, reflecting physiological differences between subendocardial and subepicardial ventricular cardiomyocytes. For instance, I_{to} density near the epicardium is multiple times higher than near the endocardium. In heart failure (HF), these gradients are disturbed or lost, promoting arrhythmia and contractile dysfunction. Another feature of HF is a reduced density of the transverse tubular system (t-system), which contains particularly high densities of I_{to}, I_{K1} and $I_{Ca,L}$ channels and is important for efficient Ca^{2+} cycling. Therefore, we investigated whether non-failing human ventricles exhibit transmural differences in t-system density and how this may change in heart failure. Furthermore, we investigated the t-system in different regions of the human heart (apex, free wall, base).

Methods

Transmural specimens from human failing hearts were obtained either during left-ventricular assist device implantation or procured from the explanted heart during transplantation from a total of 16 patients. Specimens from 8 non-failing hearts were obtained from donors without known cardiac disease. The myocardium was cut in parallel to the epicardium to create slices with known distance from the endo- and epicardium. We stained the extracellular matrix, t-system, ryanodine receptors or troponin T as a myocyte marker, and the nuclei. Confocal microscopy was applied to record 3D and large 2D images, which were subjected to automated image analysis to quantify cell size, fibrosis, t-system density and mean intracellular t-tubule distance (ΔTT).

Results

In the LV free wall of donor hearts, linear regression revealed a significant increase in t-system density from endo- to epicardial regions as indicated by a decreasing ΔTT (from 1.16±0.07 to 0.91±0.04 µm, $p<0.01$) and increasing myocyte volume fraction of the t-tubule skeleton (from 0.13±0.01 to 0.18±0.01 %, $p<0.01$). When comparing midmyocardial regions from failing hearts, we found increased fibrosis (failing vs donor: 28±3% vs 21±1%, $p<0.001$, n=8/8), larger cell width (39±6 vs 24±2 µm, $p<0.001$) and ΔTT (1.22±0.1 vs 1.0±0.06 µm, $p<0.001$). Moreover, we found that in failing hearts the transmural difference of t-system density and ΔTT were cancelled and reduced, respectively. No differences were found between the apex, free wall and base of failing hearts.

Conclusion

The presented results reveal that the non-failing human ventricle exhibits an endo- to epicardial gradient in the density of the t-system, which is in accordance with previous findings showing gradients of the I_{to} and other important ionic currents and of Ca^{2+} signals. The t-system gradient is blunted in HF, suggesting that the t-system contributes to the transmural functional heterogeneity found in healthy hearts and its pathological suppression in HF.

We are grateful for the technical support from Celine Grüninger.

B 05-02

Metabolic reprogramming of cardiac cells differentiated from mouse embryonic stem cells and rat cardiac myoblasts exposed to diabetic cell culture media

Leopold Stabbauer[2], Maria Wartenberg[3], Sybille Mazurek[2], Fatemeh Sharifpanah[1], Heinrich Sauer[1]

[1] *Justus Liebig University Gießen, Physiology, Gießen, Germany*
[2] *Justus Liebig University Gießen, Veterinary Medicine, Gießen, Germany*
[3] *Friedrich Schiller University Jena, Cardiology, Jena, Germany*

Question

Heart failure is often related to insulin resistance and type 2 diabetes mellitus, namely diabetic cardiomyopathy (DCM). Driving force behind this is insulin resistance resulting in a disproportionate amount of energy (ATP) being produced by fatty acid oxidation (FAO), while glycolysis is inhibited. One of the most important proteins for uptake and utilization of glucose is AMP-activated protein kinase (AMPK), which stimulates expression of GLUT4 and mitochondrial biogenesis. In this study the effects of the direct AMPK-activator Metformin in combination with the beta-oxidation-inhibitor Trimetazidine as well as the indirect AMPK-activator Exendin-4 in combination with the L-Carnitine inhibitor Mildronate on glucose metabolism, energy homeostasis, oxidative stress, alpha-actinin structure, lipid droplets, mitochondrial health and calcium homeostasis were investigated utilizing rat cardiomyoblasts (H9C2) and cardiomyocytes (CMs) differentiated from mouse embryonic stem cells (mESC).

Methods

H9C2 cells and mouse CMs were exposed to normoglycemic (5mM glucose) medium, and hyperglycemic medium (30mM glucose) supplemented with Cortisol and Endothelin-1 (ET-1) to make diabetic medium (DM). DM exposed cells were treated with either Metformin and Trimetazidine (MT) or Mildronate and Exendin-4 (ME). Intracellular ROS and NO were measured by H_2DCFDA and DAF-DM respectively, mitochondrial ROS by MitoSOXRed. Alpha-actinin structure was evaluated by immunohistochemical staining. Lipid droplet amount was detected with either BioTracker 488 Green Lipid Droplet Dye or Oil Red O staining. Mitochondrial health was evaluated with the membrane potential sensitive dye JC-1, and calcium homeostasis with Ca^{2+}-sensitive dye Fluo-4 AM. Glucose metabolism was assessed by visualization of glucose transporters 1 and 4 as well as uptake of the glucose analogon 2-NBDG. Energy levels were measured with ATPRed dye. To assess protein levels of NOS and NOX, as well as inflammatory proteins western blot (WB) was utilized

Results

Intracellular elevated ROS levels, as well as decreased NO levels under diabetic conditions were ameliorated by treatment with MT and ME. Alpha-actinin amount increased and fewer lipid droplets were present in relation to DM treated cells. Compared to treated cells, diabetic cells had a lower uptake of glucose. These results suggest that CM-structure and lipid accumulation normalizes under ME and MT treatment, oxidative stress decreases and GLUT1 and 4 expression, glucose uptake, as well as ATP generation increases in treated versus untreated cells. Mitochondria show a decreased membrane potential under diabetic conditions which could be alleviated by MT and ME treatment. No differences in expression of ROS and NO generating proteins were evident by WB.

Conclusions

The derailed diabetic metabolism in diabetic cardiac cells and cardiomyoblasts can be reprogrammed by AMPK activation in combination with inhibition of β-oxidation.

This work was supported by the von Behring-Röntgen Foundation, Marburg

B 05-03

Endothelial deletion of Secreted Modular Calcium Binding protein 1 (SMOC1) increased damage in response to myocardial infarction in mice.

Bardia Amirmiran[1], Fredy D. Lagos[2], Giulia Buchmann[1], Florian Sicklinger[3], Ingrid Fleming[2], Ralf R. Brandes[1]

[1] Goethe Universität Frankfurt am Main, Institute for Cardiovascular Physiology, Frankfurt am Main, Germany
[2] Goethe Universität Frankfurt am Main, Institute for cardiovascular signaling, Frankfurt am Main, Germany
[3] University of Heidelberg, 3 Department of Internal Medicine III, Heidelberg, Germany

Question

The damage response after myocardial infarction (MI) determines healing and scar formation.[1] Transforming growth factor β (TGF-β) is a central signalling molecule controlled on multiple levels to orchestrate aspects of the healing response.[2] The secreted modular calcium binding protein 1 (SMOC1) modulates TGF-β signalling by acting as an antagonist on the TGFβ receptor ALK5, but the physiological relevance of this interaction particular in endothelial cells is unclear.[3]

Methods

Endothelial-specific tamoxifen-inducible SMOC1 knockout mice ($SMOC1^{\Delta EC}$) were generated by crossing cdh5-$CreERT2^{+/0}$ into a $SMOC1^{flox/flox}$ line. Control mice (CTL, cdh5-$CreERT2^{0/0}$ - $SMOC1^{flox/flox}$) and $SMOC1^{\Delta EC}$ both received tamoxifen to activate the cre-recombinase at least 2 weeks prior to experiments. Animals were subjected to minimal invasive myocardial infarction (MI).[4] 14 after MI, cardiac function was assessed by measuring left ventricular ejection fraction (LVEF%) using echo cardiography and sirius red histo staining. Inflammatory activation was determined by fluorescence associated cell sorting (FACS) from cardiac samples.

Results

After MI, $SMOC1^{\Delta EC}$ mice exhibited reduced LVEF as compared to CTL littermates. Histological analysis using Sirius red staining revealed an increased infarct area in $SMOC1^{\Delta EC}$ mice compared to WT animals at 14 days post-MI. FACS three days after MI revealed increased infiltration of pro-inflammatory Ly6C+ monocytes as well as CD4+ lymphocytes in $SMOC1^{\Delta EC}$ mice compared to $SMOC1^{flox/flox}$ mice.

Conclusions

Endothelial SMOC1 promotes healing and has an anti-inflammatory function after MI.

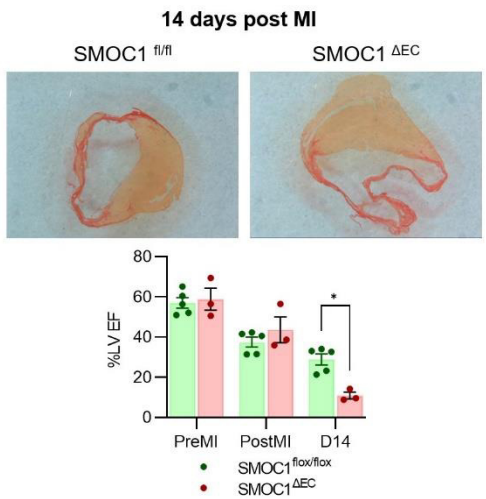

14 days post MI Histo-staining (SA) + 14 days post MI LV EF (%)
Sirius red staining of murine hearts at 14 days after MI induction (above). Left ventricular ejection fraction (LVEF) and left ventricular end-diastolic volume (LVEDV) were measured by echocardiography (down)

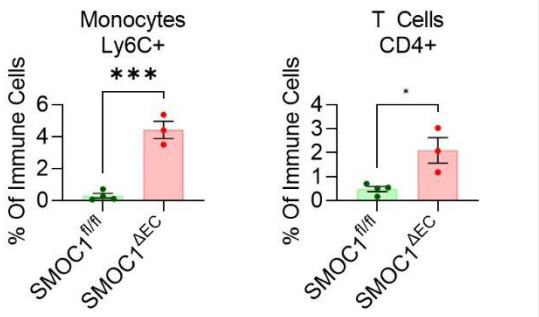

Immune panel 3 days after myocardial infarction evaluated by FACS
Immune panel obtained from SMOC1fl/fl and SMOC1ΔEC hearts 3 days after myocardial infarction and evaluated by FACS.

References
[1] Palasubramaniam J, Wang X, Peter K. Myocardial Infarction-From Atherosclerosis to Thrombosis. *Arterioscler Thromb Vasc Biol*. 2019;39(8):176-185. doi:10.1161/ATVBAHA.119.312578
[2] Bujak M, Frangogiannis NG. The role of TGF-beta signaling in myocardial infarction and cardiac remodeling. *Cardiovasc Res*. 2007;74(2):184-195. doi:10.1016/j.cardiores.2006.10.002
[3] Awwad K, Hu J, Shi L, et al. Role of secreted modular calcium-binding protein 1 (SMOC1) in transforming growth factor β signalling and angiogenesis. *Cardiovasc Res*. 2015;106(2):284-294. doi:10.1093/cvr/cvv098
[4] Sicklinger F, Zhang Y, Lavine KJ, et al. A Minimal-Invasive Approach for Standardized Induction of Myocardial Infarction in Mice. *Circ Res*. 2020;127(9):1214-1216. doi:10.1161/CIRCRESAHA.120.317794.

B 05-04
Mild uncoupling in mitochondria by UCP2 does not generally affect functional recovery of rodent hearts at the early reperfusion

Laureen Czech, Nadja Itani, Hanna Kutsche, Rolf Schreckenberg, Rainer Schulz, Klaus-Dieter Schlüter

Justus Liebig University, Institute of Physiology, Giessen, Germany

Reperfusion of cardiac tissue after an ischemic period is a challenging situation for cardiac tissue, because immediate restoration of energy supply by the electron transport chain of the mitochondria is mandatory for functional recovery but also risky as it may add oxidative stress. Recovery of mitochondria function is therefore a strictly controlled mechanism allowing the mitochondria to supply the cell with energy and control oxidative stress evoked by mitochondria.

For this control, the uncoupling properties of uncoupling protein 2 (UCP2) in the heart seems of specific relevance. Hearts from mice and rats differ in the cellular distribution of UCP2. In mice UCP2 is predominantly seen in non-myocytes but in rat myocytes the expression is rather high. Therefore, one would expect species differences between mice and rats if UCP2 plays an important role in this process. In the current study we used ex vivo perfused hearts from WT and UCP2 deficient mice and rats to clarify the role of UCP2 for reperfusion injury.

We compared the functional recovery of male WT mice and male UCP2 KO mice. No-flow perfusion was used as an index ischemia of 45 min and subsequently the hearts were reperfused for two hours. WT and KO mice did not differ in left ventricular developed pressure (LVDP), dp/dt max, and dp/dt min prior to ischemia. During ischemia rigor contraction increased the pressure in WT and KO mice similarly. Two hours after reperfusion, LVDP was recovered to 59.5% und 61.7%, in WT and KO mice respectively. 90% of WT and 100% of KO mice had difficulties to perform regular beating during the first 15 min of reperfusion. Similarly to the mouse model, no significant difference occurred in WT and KO rats prior to ischemia. Again, ischemia increased rigor contraction, in WT and KO rats, respectively. Functional recovery was 65.0% in WT rats and 68.1% in KO rats. 10% of WT rats and 40% of KO rats had difficulties to perform regular beating. Interestingly, a subgroup analysis revealed detrimental effects of UCP2 deficiency in rats with strong ischemic damage. In these rats LVDP recovery was 57.3% in WT rats but only 46.0% in KO rats. 10% of these WT rats and 60% of these KO rats had difficulties to perform regular beating during the first 15 min of reperfusion. ROS production from rat hearts revealed no differences between the groups.

The data show that mild uncoupling of mitochondria has a minor effect on functional recovery after an ischemia period. The conclusion is based on our similar finding in mice and rats with different cellular distribution of UCP2 expression. Uncoupling by UCP2 may contribute to protection against arrhythmia and functional recovery after severe infarcts.

B 05-05

Protective effects of a cytosolic mitochondrial variant of renin (renin-b) in doxorubicin-induced cell damage in cardiac cells.

Miriam Hartmann, Florian Bauer, Doreen Staar, Heike Wanka, Jörg Peters

Universtity Medicine Greifswald, Institute of Physiology, Greifswald, Germany

Question

Doxorubicin (Dox) is an anthracycline with potent antineoplastic properties. Unfortunately, Dox-induced cardiotoxicity (DIC) has so far been a dose-limiting side effect. The mechanism of DIC is supposed to be multifactorial, including DNA damage, dysregulation of the mitochondrial electron transport chain, disturbances in autophagic flux and formation of reactive oxygen species (ROS). DIC is often associated with increased phosphorylation of AMP-activated kinase (AMPK) and reduced phosphorylation of Akt and mechanistic target of rapamycin (mTOR). Activation of Akt/mTOR signalling seems to alleviate Dox-induced cardiac damages. We recently demonstrated that overexpression of a cytosolic mitochondrial variant of renin (renin-b) resulted in increased phosphorylation of Akt in H9c2 cells. Under ischaemia-related conditions overexpression exerted protection against necrosis, apoptosis, and ROS formation. We therefore analysed the effects of Dox on renin-b overexpressing cells compared to control cells.

Methods

H9c2 rat cardiomyoblast control cells (empty pIRES vector-transfected) and cells overexpressing cytosolic renin-b were cultured under control conditions as well as under Dox-treatment (0.5, 1, 3 µM) for 24 h or 48 h. Transcript levels of secretory renin-a and cytosolic renin-b were quantified by real-time qPCR. Functionally, we examined necrotic [LDH ratio (release/content)] and apoptotic cell death (Annexin V and CaspACE labelling).

Results

Treatment with 3 µM of Dox of control cells led to an increase of renin-b transcripts after 24 h (17.78-fold) and 48 h (9.82-fold). Transcript levels in overexpressing cells were only enhanced 4.39- (24 h) and 4.45-fold (48 h), but still higher than in the control cells. Dox-treatment for 24 h slightly increased renin-a transcript levels in both cell lines (1.89- and 1.65-fold). Control cells showed similar effects after 48 h, while transcript levels remained unchanged in overexpressing cells.

The number of CaspACE-positive cells was significantly enhanced after 24 h and 48 h treatment with 3 µM Dox in control cells, while it remained unchanged in renin-b overexpressing cells.

Furthermore, renin-b overexpression reduced the amount of Annexin V-positive cells after 3 µM Dox-treatment for 48 h. The LDH ratio was enhanced in renin-b overexpressing cells under control conditions, but did not further increase due to 24 h of Dox-treatment in contrast to control cells.

Conclusions

Cardiac H9c2 control cells showed an increased renin-b expression after Dox-treatment, suggesting that upregulation of renin transcripts could counteract cell death. In fact, overexpression of renin-b prior to treatment seems to attenuate a doxorubicin-induced increase in apoptosis and necrosis rates.

B 05-06

Treatment with hyperbaric oxygen reveals spatiotemporal plasticity of activity and composition of OXPHOS complexes in the porcine heart

Juliana Heidler[1,2], Ilka Wittig[1], Alfredo Cabrera-Orefice[1], Estelle Heyne[3], Jan-Niklas Tomczak[1], Björn Petersen[4], Dirk Henze[5], Jaakko L.O. Pohjoismäki[6], **Marten Szibor**[3,7]

[1] *Goethe University Frankfurt, Functional Proteomics, Institute of Cardiovascular Physiology, Frankfurt a. Main, Germany*
[2] *Innsbruck Medical University, Experimental Vascular Surgery, Innsbruck, Austria*
[3] *Jena University Hospital, Department of Cardiothoracic Surgery, Center for Sepsis Control and Care (CSCC), Jena, Germany*
[4] *Friedrich-Loeffler-Institute (FLI), Institute of Farm Animal Genetics, Mariensee, Germany*
[5] *Dr. Henze & Partner GbR, Praxis für Anästhesiologie, Halle, Germany*
[6] *University of Eastern Finland, Department of Environmental and Biological Sciences, Joensuu, Finland*
[7] *Tampere University, Faculty of Medicine and Health Technology, Tampere, Finland*

The heart meets its high ATP demand almost exclusively by oxidative phosphorylation (OXPHOS), thereby showing remarkable metabolic stability. This is surprising because cardiomyocyte size and sarcomere structures should inevitably limit oxygen availability, particularly in the center of the cells, during high demand or hypertrophy. Sophisticated mechanisms must exist to adjust OXPHOS complex activities in a spatiotemporal manner. Here, we studied OXPHOS complex activities in piglet hearts in two anatomically differently located and presumably differently oxygenated mitochondrial subpopulations, *i.e.*, subsarcolemmal (SSM) and interfibrillar (IFM). We found significantly lower OXPHOS enzyme and F_1F_O-ATP synthase activities specifically in IFM. To test whether this phenomenon was due to lower oxygen availability, we ventilated piglets for 240 minutes under hyperbaric oxygen (HBO) conditions, a treatment known to improve tissue oxygenation. HBO treatment induced the expression of genes involved in mitochondrial biogenesis and raised enzyme activities and matrix pH of IFM to the level of SSM. Most importantly, HBO induced the activity of F_1F_O-ATP synthase, which reassembled from F_O subcomplexes and protein subunits of disintegrated catalytic F_1 subcomplexes preserved in the inner membrane. The observed oxygen-dependent increase of enzyme activities in IFM was unexpected because it implies that oxygen deficits may exist in cardiomyocytes of the unstressed heart. The extent to which this mechanism may be responsible for the development of contractile dysfunction is currently unknown. However, we suggest that HBO may be used to aid convalescence, especially in patients with ischemic heart disease or after prolonged immobilization.

B 05-07

Regulation of mitochondrial calcium transient decay in atrial and ventricular cardiomyocytes

Victoria Hammer, Jelena Plackic, Ahmad N. Nasri, Carsten Culmsee, Jens Kockskämper

University of Marburg, Institute of Pharmacology and Clinical Pharmacy, Marburg, Germany

Question

In cardiomyocytes, mitochondrial calcium (mitoCa) is regulated by influx and efflux of Ca from the cytosol and this is thought to occur mainly via the mitoCa uniporter (MCU) and the mitochondrial Na/Ca/Li exchanger (NCLX), respectively. How mitoCa transient decay is regulated in cardiomyocytes and whether these mechanisms differ between atrial and ventricular myocytes is largely unknown.

Methods

Atrial and ventricular myocytes were isolated from adult rat hearts. MitoCa was measured by confocal linescan imaging in cells loaded with X-Rhod-1-AM (5 µM, 30 min). Expression of mitochondrial proteins was determined by means of Western blotting of protein extracts obtained from atrial and ventricular tissue.

Results

Following initial loading, X-Rhod-1 exhibited rather uniform fluorescence in the cytoplasm of atrial and ventricular myocytes. After $CoCl_2$ quenching, however, atrial and ventricular myocytes showed a striated pattern of X-Rhod-1 fluorescence. Co-staining with MitoTracker Green suggested that the striated X-Rhod-1 pattern originated from mitochondria. Comparison of electrically stimulated Ca transients (CaTs) before and after $CoCl_2$ quenching revealed that the mitoCaTs (measured after quenching) displayed lower amplitudes but faster kinetics than the cytoplasmic CaTs (measured before quenching). In atrial myocytes (n=15), the time constant of CaT decay (tau) amounted to 103±16 ms

before vs 75±10 ms after $CoCl_2$ quenching (P<0.05). In ventricular myocytes (n=10), the respective tau values were 237±39 ms before vs 135±24 ms after $CoCl_2$ quenching (P<0.01). MitoCaTs exhibited frequency-dependent regulation with increases of diastolic mitoCa and acceleration of mitoCaT decay at higher stimulation frequencies in both atrial (0.5–1–2 Hz) and ventricular (1–2–4 Hz) myocytes. Comparison of mitoCaTs between atrial and ventricular myocytes at 1 Hz stimulation revealed faster tau of decay in atrial (n=96) vs ventricular (n=31) myocytes (73±5 ms vs 142±14 ms; P<0.01). Expression of NCLX was increased about two-fold in atrial vs ventricular tissue (N=8 hearts) when normalized to either GAPDH or Tim23 (in both cases P<0.01).

Conclusion

X-Rhod-1 loads into mitochondria and allows for determination of mitoCaTs in both atrial and ventricular myocytes. MitoCaTs exhibit faster decay kinetics than cytoplasmic CaTs. MitoCaT decay is accelerated with increasing stimulation frequencies. Atrial myocytes show faster mitoCaT decay than ventricular myocytes and this may be explained by higher expression of NCLX.

B 05-08
Growth differentiation factor 6 promotes pulmonary arterial remodeling in pulmonary hypertension due to left heart disease

Qiuhua Li

Charite, Berlin, Germany

Question

Pulmonary hypertension due to left heart disease (PH-LHD) is the most common type of pulmonary hypertension (PH) and contributes considerably to morbidity and mortality in left heart disease. While PH-LHD is initially a result of passive lung congestion, it later progresses into a reactive process with extensive pulmonary arterial (PA) remodeling. Previous studies identified an imbalance between bone morphogenetic protein (BMP) and transforming growth factor-β (TGFβ) signaling that contributes to PA remodeling in pulmonary artery hypertension (PAH) by promoting proliferation of PA smooth muscle cells, endothelial cells and fibrosis. Growth differentiation factor (GDF) ligands act through shared BMP and TGFβ receptors. Here, we demonstrate upregulation of growth differentiation factor 6 (GDF6) in PH-LHD and test for its potential involvement in PA remodeling in PH-LHD.

Methods and Results

To understand the regulation of PA remodeling in PH-LHD, we performed bulk RNA sequencing of PA samples isolated during heart transplantation from PH-LHD patients (n=15) and corresponding healthy heart-heart donors (n=8), as well as in an experimental PH-LHD rat model (induced by surgical aortic-banding, AoB) and sham operated controls (n=4 and 5, respectively). Analysis of differentially expressed BMP-signaling pathway genes, identified by gene ontology (GO:0030509), revealed upregulation of GDF6 in both PH-LHD patient and AoB rat PA samples as compared to corresponding healthy donors or sham controls. Western blotting confirmed upregulated levels of GDF6 protein expression in PAs of PH-LHD patients and lungs of AoB rats. PA immunohistology revealed that GDF6 colocalizes with smooth muscle actin (α-SMA) and CD31, markers of smooth muscle cells (SMC) and endothelial cells (ECs), respectively. Consistently, primary PA SMCs and ECs isolated from PH-LHD PAs showed a 2-fold and 1.5-fold increase in GDF6 protein levels relative to corresponding control cell types by Western blotting. Treatment of healthy PA SMCs and ECs with 300 ng/mL of recombinant GDF6 protein increased cell migration and proliferation as assessed by wound-healing assay and immunofluorescent detection of the cell cycle marker Ki67.

Conclusions

GDF6 expression is increased in PA SMCs and ECs of PH-LHD patients and AoB rats. GDF6 may contribute to PA remodeling by increasing proliferation and migration of both SMCs and ECs, highlighting the need for further in-depth study of GDF6´s functional role in vivo.

Supported by the DZHK (German Centre for Cardiovascular Research), the DFG (German Research Foundation), the BMBF (German Ministry of Education and Research), and the CSC (China Scholarship Council).

B 05-09
A kinase anchoring protein 7 γ/δ knockout mice have a normal cardiac function

Karoline Morhenn[1,3], Hariharan Subramanian[2,3], Helga Vitzthum[1,3], Heimo Ehmke[1,3], Viacheslav Nikolaev[2,3]

[1] *University Medical Center Hamburg-Eppendorf, Institute of Cellular and Integrative Physiology, Hamburg, Germany*
[2] *University Medical Center Hamburg-Eppendorf, Institute of Experimental Cardiovascular Research, Hamburg, Germany*
[3] *German Center of Cardiovascular Research (DZHK), Partner site Hamburg/Kiel/Lübeck, Hamburg, Germany*

Question

In heart failure, myocardial Ca^{2+} homeostasis is impaired resulting in changes in contraction and relaxation. Underlying cellular mechanisms leading to these alterations in cardiac function include modifications in the SERCA/phospholamban (PLN) complex, which result in a reduced Ca^{2+} filling of the sarcoplasmic reticulum (SR), as well as a diminished Ca^{2+} release by ryanodine receptors (RyR). A kinase anchoring protein 7 γ/δ isoforms (AKAP7γ/δ) have been shown to increase SERCA activity through phosphorylation by anchoring PKA as well as calmodulin-dependent protein kinase II (CaMKII) to the SERCA/PLN complex and RyR [1,2]. We therefore investigated *in vivo* effects on heart function of a cardiomyocyte specific *Akap7γ/δ* deletion in two models of heart failure in mice. We expected superinhibition of SERCA in *Akap7γ/δ*-deficient mice, resulting in the development of cardiac insufficiency and an accelerated development of experimentally induced heart failure.

Methods

Heart failure was induced in cardiomyocyte specific *Akap7γ/δ*-deficient mice (KO) and wildtype littermates (WT) by transverse aortic constriction (TAC) or ligation of the left anterior descending artery (LAD). Sham operated animals served as controls. Echocardiographic analysis was conducted in anaesthetized mice before and 2, 6 and 10 weeks after operation. Blood samples and organs were taken 12 weeks post operation. AKT, ERK and PLN phosphorylation were assessed by immunoblot. Neurohumoral responses were assessed by quantification of plasma renin activity (PRA), plasma aldosterone concentrations and plasma ANP concentrations.

ResultsUnexpectedly, echocardiographic analysis showed no difference in basal heart function and morphology between KO and WT (n=10). The induction of heart failure by TAC led in both genotypes to similar increases in heart weight compared to Sham (n=4-11), as well as a similar decrease in ejection fraction and fractional shortening (n=4-10). PLN phosphorylation was not altered, and prohypertrophic AKT and ERK phosphorylation remained unchanged in hearts from KO compared to WT. Induction of heart failure by LAD ligation led to no difference in cardiac function between KO and WT; ejection fraction and fractional shortening were similarly decreased compared to Sham (n=8-12). PRA as well as plasma aldosterone and ANP concentrations were unaffected by *Akap7γ/δ* deletion in both models of heart failure (n=6-13). Survival after TAC and LAD ligation was unchanged.

Conclusions

Despite of the well-known *in vitro* effects of AKAP7γ/δ anchoring PKA on the SERCA/PLN complex and RyR, we could not detect any physiological or pathophysiological consequences of a cardiomyocyte-specific deletion of *Akap7γ/δ* in mice *in vivo*.

References
[1] Lygren, B, Carlson, CR, Santamaria, K, Lissandron, V, McSorley, T, Litzenberg, J, Lorenz, D, Wiesner, B, Rosenthal, W, Zaccolo, M, Taskén, K, Klussmann, E 2007, 'AKAP complex regulates Ca2+ re-uptake into heart sarcoplasmic reticulum', *EMBO Rep*, Nov;8(11):1061-7
[2] Carlson, CR, Aronsen, JM, Bergan-Dahl, A, Moutty, MC, Lunde, M, Lunde, PK, Jarstadmarken, H, Wanichawan, P, Pereira, L, Kolstad, TRS, Dalhus, B, Subramanian, H, Hille, S, Christensen, G, Müller, OJ, Nikolaev, V, Bers, DM, Sjaastad, I, Shen, X, Louch, WE, Klussmann, E, Sejersted, OM 2022 'AKAP18δ Anchors and Regulates CaMKII Activity at Phospholamban-SERCA2 and RYR', *Circ Res*, Jan 7;130(1):27-44

B 05-10
Remote ischemic conditioning and electrical auricular tragus stimulation in humans – vagal projection to the heart?

Umut Paket, Andreas Skyschally, Helmut R. Lieder, Petra Kleinbongard, Gerd Heusch

University Hospital of Essen, West German Heart and Vascular Center, Institute for Pathophysiology, Essen, Germany

Question

Both, remote ischemic conditioning (RIC) by brief cycles of ischemia/reperfusion (I/R) in tissues distant from the heart [1] and electrical auricular tragus stimulation (ATS) [2] attenuate myocardial injury in patients with acute myocardial infarction. RIC´s signal transfer involves activation of vagal nerves with subsequent release of circulating cardioprotective factors from the spleen, as shown in animal models [3]. In functional magnetic resonance imaging studies in humans, ATS activates vagal nuclei in the brainstem [4]. However, whether or not the RIC- or ATS-mediated activation of efferent vagal nerves projects to the heart is unclear.

Thus, we used the analysis of heart rate variability (HRV) as a marker of cardiac autonomic balance [5] to investigate cardiac vagal activity in humans during RIC or ATS, respectively.

Methods

Ten healthy volunteers were randomly subjected to RIC at the left or right arm and ATS at the left or right tragus, respectively. Sham RIC/ATS procedures served as control. A continuous 1-lead ECG was recorded. RIC was performed on the upper arm by three 5 min cycles of arm ischemia, induced by cuff inflation to 200 mmHg and followed by 5 min reperfusion after rapid cuff deflation. ATS was performed by a transcutaneous electrical nerve stimulator through a bipolar clamp using biphasic pulses at 30 Hz, 200 µs pulse width, and an additional microprocessor-controlled circuit periodically interrupted the stimulation signal at a 5/5s on/off scheme. The individual stimulus strength was set at a level which the participant did not perceive as intolerable or painful over the total stimulation period of 30 min (pulsed current: ATS left 5.5±0.8 mA; ATS right 5.3±1.3 mA). HRV was analyzed by using Kubios HRV standard 3.4.2 (Kubios Oy, Kuopio, Finland). We focused on heart rate (HR) and spectral power in the low (LF) and high (HF) frequency band. LF is supposed to reflect sympathetic activity and HF vagal activity at the heart, and the LF/HF-ratio may reflect the sympathetic/parasympathetic balance.

Results

HR did not change with left/right RIC or left/right ATS vs. sham RIC/ATS (Figure A). There was also no apparent response of LF, HF and LF-HF-ratio during left/right RIC or left/right ATS vs. sham RIC/ATS (Figure B-D).

Conclusion

Neither HR nor HRV, as a marker of cardiac autonomic balance, indicated an impact of RIC or ATS on cardiac vagal nerve activity in healthy volunteers.

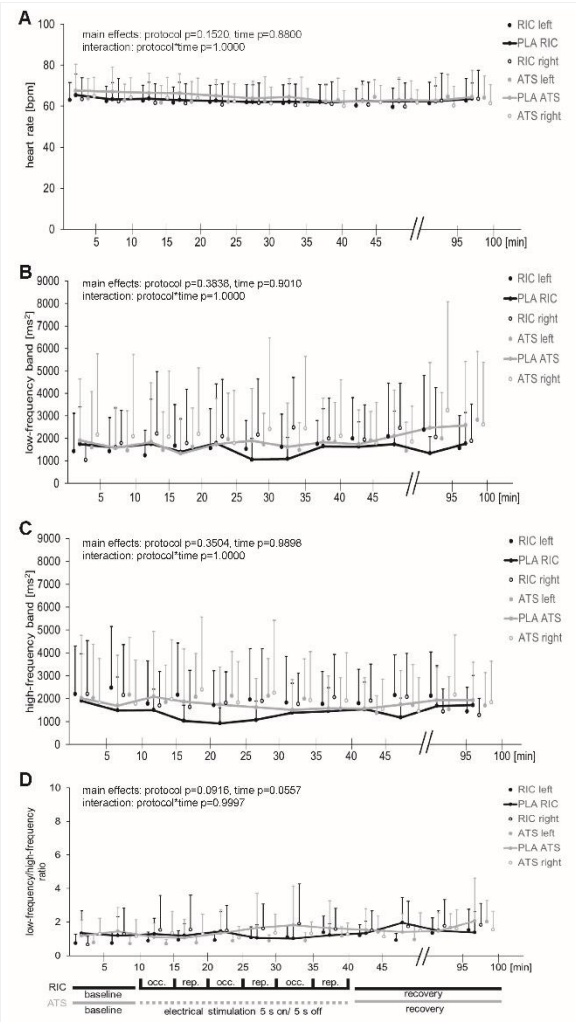

No impact of RIC or ATS on HR and HRV in humans
Figure: Heart rate **(A)**, low-frequency band **(B)**, high-frequency band **(C)**, low-frequency band/ high-frequency band ratio **(D)** of healthy volunteers subjected to remote ischemic conditoning **(RIC)**, electrical auricular tragus stimulation **(ATS)** or placebo protocols **(PLA)**.

Values are means ± standard deviations; two-way analysis of variance for repeated measures; occ.: occlusion, inflation of the blood pressure cuff; rep.: reperfusion, deflation of the blood pressure cuff.

References
[1] Heusch G. (2020). Myocardial ischaemia-reperfusion injury and cardioprotection in perspective. *Nature reviews. Cardiology*, *17*(12), 773–789.
[2] Yu, L., Huang, B., Po, S. S., Tan, T., Wang, M., Zhou, L., Meng, G., Yuan, S., Zhou, X., Li, X., Wang, Z., Wang, S., & Jiang, H. (2017). Low-Level Tragus Stimulation for the Treatment of Ischemia and Reperfusion Injury in Patients With ST-Segment Elevation Myocardial Infarction: A Proof-of-Concept Study. *JACC. Cardiovascular interventions*, *10*(15), 1511–1520.
[3] Lieder, H. R., Kleinbongard, P., Skyschally, A., Hagelschuer, H., Chilian, W. M., & Heusch, G. (2018). Vago-Splenic Axis in Signal Transduction of Remote Ischemic Preconditioning in Pigs and Rats. *Circulation research*, *123*(10), 1152–1163.
[4] Badran, B. W., Dowdle, L. T., Mithoefer, O. J., LaBate, N. T., Coatsworth, J., Brown, J. C., DeVries, W. H., Austelle, C. W., McTeague, L. M., & George, M. S. (2018). Neurophysiologic effects of transcutaneous auricular vagus nerve stimulation (taVNS) via electrical stimulation of the tragus: A concurrent taVNS/fMRI study and review. *Brain stimulation*, *11*(3), 492–500.
[5] Sztajzel J. (2004). Heart rate variability: a noninvasive electrocardiographic method to measure the autonomic nervous system. *Swiss medical weekly*, *134*(35-36), 514–522.

B 05-11

Progressive attenuation of ST-segment elevation with ischemic preconditioning cycles does not reflect cardioprotection in Ossabaw minipigs.

Virginie Adam, Helmut Lieder, Andreas Skyschally, Petra Kleinbongard, Gerd Heusch

Universität Duisburg-Essen, Institut für Pathophysiologie, Essen, Germany

Question

Ischemic preconditioning (IPC; brief cycles of coronary occlusion/ reperfusion) reduces myocardial infarct size. We have recently demonstrated that IPC failed to reduce infarct size in minipigs of a particular strain (Ossabaw), which have a genetic predisposition to develop, but not yet established a metabolic syndrome. Progressive attenuation of ST-segment elevation during IPC coronary occlusions results from sarcolemmal K_{ATP} channel activation and is considered to reflect cardioprotection, thus possibly serving as an online marker of infarct size reduction. We now wanted to investigate whether IPC's lack of infarct size reduction in the Ossabaw minipig goes along with lack of attenuated ST-segment elevation.

Methods

Maximum ST-segment elevations during IPC by three cycles of 5 min/ 10 min coronary occlusion/ reperfusion were analyzed from surface chest electrocardiographic traces (ECG, V2 Wilson lead using a single channel, calibrated amplifier) of anesthetized, open-chest Ossabaw minipigs and compared to those in contemporary Göttingen minipigs. Minipigs of both strains without and with IPC were then subjected to 60 min/ 120 min coronary occlusion/ reperfusion and infarct size quantified. ST-segment elevation was defined as the voltage amplitude difference between a point 30 ms before the P-wave and 20 ms after the J-point. Thirty consecutive cardiac cycles were averaged. Data are presented as means ± standard deviations. ST-segment elevation was analyzed by 2-way ANOVA for repeated measures.

Results

In both, Ossabaw minipigs and Göttingen minipigs, ST-segment elevation was progressively attenuated during the IPC cycles (figure). Infarct size was 25±13 % of the area at risk in Göttingen minipigs with IPC versus 45±10 % without IPC. In Ossabaw minipigs, infarct size was 50±11 % with IPC and 54±11 % without IPC.

Conclusions

The progressiveattenuation of ST-segment elevation by IPC is dissociated from infarct size reduction in Ossabaw minipigs. IPC's block in the cardioprotective signaling of Ossabaw minipigs is located distal to the sarcolemmal K_{ATP} channels.

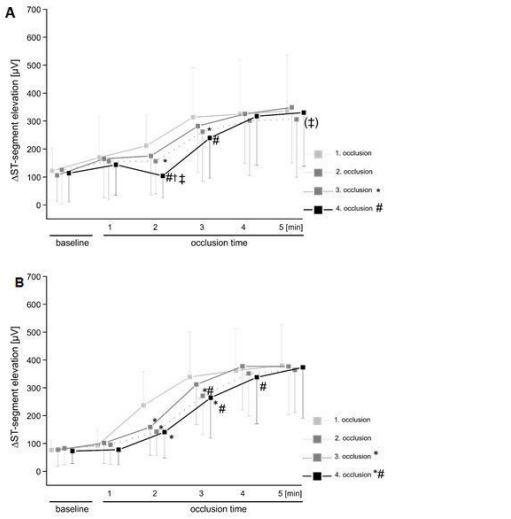

Figure: A: Attenuation of ST-segment elevation during repetitive cycles of coronary occlusion with IPC in Ossabaw minipigs. * The 4. occlusion represents the first 5 min of the 60 min index ischemia. p<0.05 vs. 1. occlusion; #p<0.01 versus 1. occlusion; ‡p<0.01 versus 2. occlusion; (‡)p=0.058 versus 2. occlusion; †p<0.05 versus 3. occlusion; two-way analysis of variance for repeated measurements with Fisher's least-significant differences post-hoc tests. **B: Attenuation of ST-segment elevation during repetitive cycles of coronary occlusion with IPC in Göttingen minipigs**. The 4. occlusion represents the first 5 min of the 60 min index ischemia. *p<0.01 versus 1. occlusion; #p<0.05 versus 2. occlusion; two-way analysis of variance for repeated measurements with Fisher's least-significant differences post-hoc tests.

Attenuation of ST-segment elevation during repetitive cycles of coronary occlusion with IPC

References

[1] Kleinbongard P, Lieder H, Skyschally A, Heusch G. No sex-related differences in infarct size, no-reflow, and protection by ischaemic pre-conditioning in Göttingen minipigs. Cardiovasc Res. 2023 Mar 31;119(2):561-570. doi: 10.1093/cvr/cvac062.

[2] Kleinbongard P, Lieder HR, Skyschally A, Alloosh M, Gödecke A, Rahmann S, Sturek M, Heusch G. Non-responsiveness to cardioprotection by ischaemic preconditioning in Ossabaw minipigs with genetic predisposition to, but without the phenotype of the metabolic syndrome. Basic Res Cardiol. 2022 Nov 11;117(1):58. doi: 10.1007/s00395-022-00965-0.

[3] Kleinbongard P, Amanakis G, Skyschally A, Heusch G. Reflection of Cardioprotection by Remote Ischemic Perconditioning in Attenuated ST-Segment Elevation During Ongoing Coronary Occlusion in Pigs: Evidence for Cardioprotection From Ischemic Injury. Circ Res. 2018 Apr 13;122(8):1102-1108. doi: 10.1161/CIRCRESAHA.118.312784.

[4] Birincioglu M, Yang XM, Critz SD, Cohen MV, Downey JM. S-T segment voltage during sequential coronary occlusions is an unreliable marker of preconditioning. Am J Physiol. 1999 Dec;277(6):H2435-41. doi: 10.1152/ajpheart.1999.277.6.H2435.

[5] Schulz R, Rose J, Heusch G. Involvement of activation of ATP-dependent potassium channels in ischemic preconditioning in swine. Am J Physiol. 1994 Oct;267(4 Pt 2):H1341-52. doi: 10.1152/ajpheart.1994.267.4.H1341.

B 05-12
Teaching medical students the QT interval and its autonomous regulation in a practical ECG course in physiology

Tobias Heinrich[1], Marc Lemoine[2], Susanne Sehner[3], Karl Wegscheider[3], Heimo Ehmke[1], **Alexander P. Schwoerer**[1]

[1] University Medical Centre Hamburg-Eppendorf, Institute of Cellular and Integrative Physiology, Hamburg, Germany
[2] University Medical Centre Hamburg-Eppendorf, Clinic and Policlinic of Cardiology, UHZ, Hamburg, Germany
[3] University Medical Centre Hamburg-Eppendorf, Department of Medical Biometry and Epidemiology, Hamburg, Germany

Question

The QT interval is a well established marker for ventricular repolarization. As the QT interval is inversely regulated with the heart rate (HR), several correction formula are established to calculate corrected QT intervals (QT_c). In practical courses of physiology, medical students learn the correct measurement of the QT interval and its autonomous regulation. For this, students record and analyse ECGs under resting conditions and during/following a workout. However, little is known about teaching QT/QT_c skills in students. In particular, it is not established whether untrained medical students can determine the length of the QT interval in rest and following an exercise with sufficient accuracy to allow discussion of its physiological regulation.

Methods

3rd year medical students (n=380) participated in a practical ECG course. In each course (20 students), ECGs of volunteers were recorded in small groups (2-4 students) under resting conditions and immediately following standardised physical exercise. Students calculated HR, QT intervals and QT_c intervals using Bazett's exponential correction. Automatically calculated QT intervals were retrieved from the ECG devices. Following the course, QT intervals of the same ECG passages were measured by experienced physiology teachers and expert clinical electrophysiologists. QT_c was also calculated for all retrieved intervals using Framingham, Fridericia and Hodges.

Results

On cohort level (n=117), students reported resting HRs of ~70 bpm and corresponding QT intervals of ~360 ms. Moreover, they found an average increase of the HR by ~70% and a decrease of QT by ~20% following exercise. QT was inversely correlated with the HR, and QT_c (Bazett) was independent of the HR. On the level of individual experiments, however, students reported an adequate decrease of QT only in ~70% of the experiments. Moreover, QT_c (Bazett) remained stable only in ~55%. Students HR data were highly concordant with the data generated by the automated ECG routines, the experienced physiologists and the clinical electrophysiologists. While average QT and QT_c intervals were also comparable between the groups, the variance was substantially higher in students data than in the other groups, especially in the exercise ECGs. In the HR ranges generated in the course, QT_c correction by Fridericia and Framingham was less efficient than by Bazett and Hodges.

Conclusions

Untrained students can determine QT intervals from ECGs recorded under resting conditions and following a workout with sufficient accuracy to demonstrate the general concept of autonomous regulation of this important (bio)marker. Variance of individual data sets affects the interpretation on the level of individual students. To overcome this didactic limitation, we recommend prior training and/or pooled data when discussing the regulation of ventricular repolarization. The frequency correction using standard QT_c formulas is well suitable in this teaching context.

B 05-13

Practical course in Physiology in midwifery science master´s curricula - more than just a practical course for medical students?

Peter Dreischer, Harald Abele, Claudia Plappert

University Hospital Tübingen, Midwifery science, Tübingen, Germany

There is no doubt that teaching in Physiology is essential for students of midwifery science.
As the midwifery science master´s course has been introduced last year, it is worth to discuss how and to which extent the physiological contents should be presented.
In the master´s course the Department of midwifery science from the medical faculty of the University Tübingen decided to offer a practical course in Physiology for the master students on the basis of the preclinical practical course for medical students.
According to this the contents were defined as:

1. Respiratory system / Breathing
2. Blood / Blood parameters
3. Energy expenditure and exercise
4. Cardiovascular system / Circulation
5. Heart and ECG
6. Muscle and EMG
7. Nervous system / Nerve function
8. Urinary system
9. Pain / Pain reception
10. Sensory Physiology

The different lessons are presented in a hybrid format meaning a mixture of theory and practice, with a total duration for each lesson of 5 h including 3 breaks. These lessons start with a theoretical introduction followed by the practical part, then again theory and practice. We work with a browser-based software called Lt from ADInstruments (Dunedin, New Zealand) to perform the experiments. Lt also serves as a platform to present the theoretical background and instructions and to check the progress of the students.
The contents were preferentially changed to fit the requirements of midwifery science master students. For example an extra lesson “pain and pain reception” was implemented in the practical course. Here we physically demonstrate what is pain by measuring the pain threshold and how it can be influenced.
Our main focus is to discuss and understand the context of physiological principles without going too far into details, e. g. the nomenclature of ion channels, transporters and detailed signaling pathways.
The advantage of the introduction part at the beginning of each lesson is that the students are better prepared and therefore better able to follow the practical instructions and understand the procedures.Furthermore, the lecturer has direct contact to the students, and the experimental results can be discussed directly at the bench. We consider this a sustainable teaching method providing a strengthening and consolidation of the learning process.

At the end of each lesson, we included an internal evaluation in the Lt-Software presentation to better fit the contents of the course with the needs of the students.

References
[1] https://www.adinstruments.com/lt/human-physiology

B 06 | Renal

B 06-01

Blood pressure increase upon high dietary potassium supplementation is not associated with renal sodium retention or plasma volume expansion

Helga Vitzthum, Philine Steffen, Christian Marx, Jan Ewald, Karoline Morhenn, Anika Seniuk, Heimo Ehmke

University Medical Center Hamburg-Eppendorf, Institute of Cellular and Integrative Physiology, Hamburg, Germany

Question

Moderate dietary potassium (K^+) supplementation lowers arterial blood pressure by decreasing renal sodium (Na^+) retention. As the relationship between K^+ and blood pressure is nonlinear, an excessive K^+ intake causes blood pressure to rise again. The mechanisms underlying the high K^+ induced pressure increase are still controversial. In contrast to our findings, Little et al. (2023) reported a prominent role of the epithelial sodium channel (ENaC) and renal Na^+ retention for the blood pressure increase upon high KCl intake. Since our observations were made with a high KCitrate diet, we tested whether the accompanying anion modifies the effects of a high K^+ intake on renal Na^+ retention, plasma volume, and the responsiveness of blood pressure to amiloride.

Methods

Na^+-replete C57BL/6J mice were subjected to either a normal (0.93%) or a high (5%) KCl or KCitrate diet for up to 14 days. Blood pressure was determined using telemetry. We measured renal gene expression by RT-qPCR, plasma aldosterone concentrations, and urinary Na^+ excretion. To detect plasma volume expansion, we used a dilution method (Evans blue), determined blood hematocrit, and estimated end diastolic left ventricular volume (EDV) by echocardiography after 10 days of diet. In addition, the effect of the ENaC blocker amiloride on blood pressure was analyzed.

Results

No increase of blood pressure was observed in Na^+-replete mice subjected to normal K^+ diets. Even though the gene expression of renal Na^+ transporters and channels differed considerably between the two high K^+ diets, blood pressure increased by an identical extent. Despite high aldosterone levels, neither renal Na^+ retention nor plasma volume increase was detected upon the two high K^+ diets. The ENaC blocker amiloride failed to normalize blood pressure in Na^+-replete mice receiving high KCl or high KCitrate diet.

Conclusions

Our findings strongly argue against a contribution of volume retention to the blood pressure increase associated with excessive K^+ intake in Na^+-replete mice.

References

[1] Little, R, *et al.*, Dissociation of sodium-chloride cotransporter expression and blood pressure during chronic high dietary potassium supplementation. *JCI Insight***8** (2023).

B 06-02

Mineralocorticoid receptor-dependent and -independent renal outer medullary K^+ channel activity in mouse distal nephron

Viatcheslav Nesterov, Marko Bertog, **Christoph Korbmacher**

Institut für Zelluläre und Molekulare Physiologie, Erlangen, Germany

IntroductionThe renal outer medullary K^+ channel (ROMK) is the rate limiting step for K^+ secretion in the distal nephron and critical for maintaining K^+ homeostasis. ROMK is colocalized with the epithelial Na^+ channel (ENaC) in the late distal convoluted tubule (DCT2), connecting tubule (CNT), and cortical collecting duct (CCD). ENaC-mediated Na^+ absorption generates the electrical driving force for ROMK-mediated K^+ secretion. In response to a rise in plasma K^+ concentration, plasma aldosterone increases and stimulates ENaC through the mineralocorticoid receptor (MR) promoting ROMK-mediated K^+ secretion. In the transition zone of CNT/CCD ENaC activity entirely depends on aldosterone and the presence of MR [1, 2]. In contrast, in the transition zone of DCT2/CNT ENaC activity is constitutively high and independent of aldosterone [1], albeit largely reduced by MR deficiency [2]. Recently, we found that baseline ROMK activity is higher in DCT2/CNT than in CNT/CCD [3]. Whether aldosterone also stimulates ROMK is still a matter of controversy. Moreover, a potential site-specific

role of MR in regulating ROMK activity remains to be established. The aim of the present study was to investigate the effects of MR deficiency on ROMK activity in DCT2/CNT and CNT/CCD.

MethodsIn isolated CNT/CCD or DCT2/CNT fragments from control mice and from mice with doxycycline-inducible nephron-specific MR knockout (MR KO mice) whole-cell amiloride-sensitive ENaC currents (ΔI_{ami}) and tertiapin-sensitive ROMK currents (ΔI_{TPNQ}) were measured as previously described [3].

ResultsWe confirmed that in MR KO mice ΔI_{ami} is essentially absent in CNT/CCD (1.98 ± 0.61 pA in MR KO mice vs 148 ± 24 pA in controls; n=15 vs 21; $p = 4\times10^{-6}$) and is strongly reduced in DCT2/CNT (98.5 ± 28.8 pA in MR KO mice vs 461 ± 72 pA in controls; n=16 vs 23; p = 0.00001). In CNT/CCD from MR KO mice ΔI_{TPNQ} was reduced, but not completely abolished (235 ± 56 pA in MR KO mice vs 630 ± 61 pA in controls; n=15 vs 18; p = 0.0002). In DCT2/CNT from MR KO mice ROMK currents were similar to those in DCT2/CNT from controls averaging 1248 ± 134 pA (n=16) and 1134 ± 140 pA (n=23), respectively.

ConclusionThe prominent ROMK activity in DCT2/CNT in combination with a high and aldosterone-independent ENaC activity supports the concept that this nephron segment is particularly important for mediating baseline K^+ secretion. Interestingly, we demonstrated that in DCT2/CNT ROMK activity is completely MR-independent, whereas ENaC activity is largely MR-dependent. Thus, in DCT2/CNT MR signaling is likely to modulate K^+ secretion by affecting ENaC rather than ROMK activity. In CNT/CCD ENaC activity is completely MR-dependent, but ROMK activity is also reduced by MR deficiency. Thus, MR inhibition may compromise renal K^+ secretion not only by inhibiting ENaC but also by inhibiting ROMK activity.

Funded by the Deutsche Forschungsgemeinschaft (DFG, German Research Foundation), project number 391676485 (KO 1057/10-1 to CK).

References
[1] Nesterov V, Dahlmann A, Krueger B, Bertog M, Loffing J, Korbmacher C. 2012, Aldosterone dependent and -independent regulation of the epithelial sodium channel (ENaC) in mouse distal nephron. *Am J Physiol Renal Physiol* 303: F1289–F1299
[2] Nesterov V, Bertog M, Canonica J, Hummler E, Coleman R, Welling P, Korbmacher C. 2021, Critical role of the mineralocorticoid receptor in aldosterone-dependent and aldosterone independent regulation of ENaC in the distal nephron. *Am J Physiol - Ren Physiol* 321: F257–F268 StartFragmentEndFragment
[3] Nesterov V, Bertog M, Korbmacher C. 2022, High baseline ROMK activity in the mouse late distal convoluted and early connecting tubule probably contributes to aldosterone-independent K^+ secretion. *Am J Physiol - Ren Physiol* 322: F42–F54EndFragmentEndFragment

B 06-03
AQP1 expression in the thick ascending limb of Henle is reduced in the absence of claudin-10

Markus Bleich, Chiara Maset, Jendrik Kühne, Nina Himmerkus, Catarina Quintanova

Christian-Albrechts-Universität zu Kiel, Physiologisches Institut, Kiel, Germany

Question

The thick ascending limb (TAL) of the loop of Henle is effectively separating salt and water (water tight) while re-absorbing around 30% of the filtered NaCl. However, basolateral ion fluxes along the basolateral cleft and within the space of deep membrane invaginations (basolateral infoldings) have to be osmotically balanced. Claudin-10b is the main component of TAL tight junctions and facilitates paracellular Na^+ transport. Absence of Claudin-10b leads to a re-arrangement of the TJ architecture and to the take-over by other claudins (mainly -16, -19), increasing divalent cation- and decreasing Na^+ permeability. In addition, claudin-10b is also highly expressed in the basolateral infoldings where it stabilizes and regulates diffusional accessibility of these unique extracellular space. We propose that the water channel AQP1 is involved in cellular water circulation and basolateral solute flux in TAL.

Methods

Nephron segments of kidney specific (Ksp-Cre) Claudin-10 knockout mice (C10 cKO) and their respective littermates (control) have been investigated by Western blot analysis of AQP1 expression and qPCR analysis for AQP1, AQP2, AQP3 and AQP12 expression. In addition,

AQP1 wild-type (AQP1 WT) and knock-out animals (AQP1 KO) have been used for Western blot analysis. Urin and plasma osmolality was measured as a correlate for water homeostasis.

Results

Besides the prominent expression of AQP1 in proximal tubules we could show a consistent expression of AQP1 protein in TAL, glycosylated and unglycosylated, absent in AQP1 KO tissue. There was no AQP1 expression in distal convoluted tubules and collecting ducts. In C10 cKO TAL, the amount of AQP1 protein was reduced to approx. 30% of the amount in WT. This was confirmed by qPCR showing a 7-fold reduction in AQP1 mRNA expression comparing cKO TAL with control TAL. As C10 cKO mice suffer from water loss and hydronephrosis (urine osmolality 566 +/- 34 mosm/kg^{-1} vs. 1308 +/- 207 mosm/kg^{-1} in control) we also investigated AQP expression in other nephron segments. In contrast to the findings in TAL, we found an increase in AQP expression in proximal tubules (AQP12) and collecting ducts (AQP2 and AQP3).

Conclusions

AQP1 expression in the TAL and its reduction in claudin-10b indicates an involvement of AQP1 in the alignment of basolateral water- and solute fluxes.

B 06-04

Expression of TMEM16J modulates release of interleukin-2 and controls intracellular calcium signaling in Jurkat T- lymphocytes

Rainer Schreiber, Jiraporn Ousingsawat, Khaoula Talbi, Katharina Broecker, Michaela Fuchs, Karl Kunzelmann

Universität Regensburg, Institut für Physiologie, Regensburg, Germany

TMEM16J (T16J), a putative calcium-activated ion channel or phospholipid scramblase together with SIGIRR (single immunoglobulin IL-1 related receptor) and PKP3 (plakophilin 3) controls immune response, and the extend of inflammation. Variants of SIGIRR/PKP3/T16J leaded to severe inflammatory diseases such as pneumonia, enterocolitis and kidney graft rejection. Meta-analysis of genome-wide association studies identified a T16J variant as a strong promotor for chronic kidney disease (CDK), but the disease mechanism and function of T16J remain open.

T16J is expressed intracellularly and in the apical membrane of tubular epithelial cells of murine and human kidneys. In an adenine induced model for CKD (adenine treatment for 3 weeks) epithelial T16J expression was significantly reduced in mouse tubular epithelial cells. Expression of T16J was detected in interstitial immune cells, while co-staining of T16J with CD45 in human CKD kidneys suggested that expression in leukocytes. We therefore examined a possible role of T16J for the immunological function of T- lymphocytes. Jurkat T-cells (Clone E6-1) were activated with phytohaemagglutinin (PHA, 1 µg/ml) and phorbol 12-myristate 13-acetate (PMA, 50 ng/ml), which induced expression of IL-2 mRNA and IL-2 release after 24 hours. Downregulation of T16J with siRNA (siT16J) enhanced expression of IL-2, suggesting an inhibitory effect of T16J on the immune response of Jurkat T-cells.

Our previous study showed a role of T16J for ATP-induced intracellular Ca^{2+} signaling in renal epithelial cells. Similarly, Jurkat T-cells also express purinergic P2Y1 and P2Y2 receptors. We therefore investigated in single cells the effect of downregulation of T16J on the basal intracellular calcium concentration ($[Ca^{2+}]_i$) and on ATP- or ADP- induced changes in $[Ca^{2+}]_i$. Jurkat T-cells embedded in Matrigel™ were activated by PHA/PMA and loaded with Fura-2, which enhanced basal $[Ca^{2+}]_i$ and increase of $[Ca^{2+}]_i$ elicited by ATP/ADP. In contrast, both basal $[Ca^{2+}]_i$ and ATP/ADP-induced $[Ca^{2+}]_i$ was attenuated by siT16J.

In summary, T16J controls IL-2 release in Jurkat T-cells by modulation of basal $[Ca^{2+}]_i$ or intracellular calcium signaling. Modulation of T16J-activity by small molecules may therefore provide a novel toolbox to control T-cell response and inflammation.

Funded by the Deutsche Forschungsgemeinschaft (DFG, German Research Foundation) – Project-ID 509149993, TRR 374 Project A3

B 06-05
Protein analysis and activity-based protein profiling in human extracellular vesicles

Sarah Frömbling[1], Karen Lahme[1], Johannes Brand[1], Oliver Kretz[2], Desiree Loreth[1], Stephanie Zielinski[1], Catherine Meyer-Schwesinger[1]

[1] *University Medical Center Hamburg-Eppendorf, Institute of Cellular and Integrative Physiology, Hamburg, Germany*
[2] *University Medical Center Hamburg-Eppendorf, III. Medical clinic, Nephrology, Hamburg, Germany*
[3] *Universitätsklinikum Hamburg-Eppendorf, Hamburg, Germany*

Question

Proteostatic and enyzmatic disturbances of the ubiquitin proteasomal system (UPS) are a hallmark for progressive kidney cell injury. An upregulation of the UPS and an accumulation of aggrieved proteins in the cytosol of podocytes are a feature of podocyte injury, especially in membranous nephropathy (MN). Podocytes are specialized cells of the kidney blood filter, which are challenged during autoimmune diseases such as MN resulting in breakdown of the renal filter. In MN the UPS is impaired in podocytes. The assessment of UPS enzyme activities is not feasible in archived kidney biopsies from patients. Extracellular vesicles (EVs) provide opportunities in biomarker discovery for diagnosis, prognosis as well as therapy monitoring. Here we focus on the potential of EVs from human podocytes as a source for protein-biochemical assessment of proteostasis disbalances.

Methods

Human cultured podocytes exposed to autoantibodies and isolated podocyte-derived urinary EVs from patients with MN or other kidney diseases were analyzed. From cultured podocytes, EVs were collected in exosome depleted medium and isolated by differential ultracentrifugation. Total EVs were isolated from healthy control and patient urine with kidney diseases using a combination of liquid size exclusion chromatography and differential ultracentrifugation. The amount of EVs was measured by image stream. The pulldown of human podocyte-derived EVs was established via immunoprecipitation with podocyte-specific antibodies and analyzed by electron microscopy. Next to total protein abundance, the activity of DUBs and of proteolytic subunits of the proteasome were examined by activity-based protein profiling.

Results

Upon autoimmune injury the amount of podocyte-derived EVs from cultured podocytes and from patient urine increased. Protein biochemical analysis unraveled the presence of mainly inactive enzymes of the UPS within released EVs from cultured podocytes after exposure to autoantibodies. Content of inactive enzymes of the UPS was highly abundant in urinary EVs from patients with MN compared to other kidney diseases.

Conclusions

Podocyte-derived EVs are a suitable source for protein biochemical analyses of the functional state of the UPS and have the potential to give insight in the proteostatic status of podocyte, possibly reflecting prognosis.

B 06-06
Stimulation of NO-sGC-cGMP signaling prevents vasoconstriction in ex vivo acute kidney injury model

Minze Xu[1], Falk B. Lichtenberger[1], Cem Erdoğan[1], Enyin Lai[2], Kerim Mutig[1], Pontus B. Persson[1], Andreas Patzak[1], Pratik H. Khedkar[1]

[1] *Charité – Universitätsmedizin Berlin, Institute of translational physiology, Berlin, Germany*
[2] *Zhejiang University, Department of Physiology, Hangzhou, China*

Ischemic acute kidney injury (AKI) is a common clinical event associated with high morbidity due to the high risk of ensuing chronic kidney disease (CKD) and end-stage renal disease. Prolonged ischemia of the renal tissue leads to irreversible nephron loss thus setting up a relatively short time frame for therapeutic interventions. Rapid and efficient vasodilation of renal arteries is obviously the best option to restore the adequate perfusion and oxygen supply of kidney tissue. Though, glomerular filtration and perfusion of the renal cortex depend on a fine balance between the afferent (AA) and efferent (EA) arteriolar tone arising from paracrine factors, such as adenosine or eicosanoids, and endocrine modulation by the angiotensin II (Ang II) and other vasoactive hormones. The renal medulla functions upon physiologic hypoxia and

critically relies on vasa recta (VR). The present study addresses the hypothesis that pharmacologic stimulation of cGMP-signaling exerts renoprotective potential in AKI via the relaxation of renal microvessels.

To this end, hypoxia/re-oxygenation (achieved by a hypoxia chamber) and oxidative stress (induced by ODQ) were performed on isolated perfused rodent AA, EA, and descending VR (DVR). Activation or inhibition of NO-sGC-cGMP-pathway at the levels of NO biosynthesis (L-NAME for inhibition), soluble guanylate cyclase (sGC) activity (cinaciguat, runcaciguat or BAY 60-2770 for activation or ODQ for inhibition), or cGMP degradation by the phosphodiesterase 5 (PDE5, sildenafil for inhibition) were assessed in the context of AKI microenvironment.

The supraphysiologic concentration of Ang II (10^{-6} mol/L) was applied for pre-constriction, as it may occur upon AKI. At normal oxygenation, pretreatment with L-NAME or ODQ exerted moderate albeit significant vasoconstriction in AA, EA, and DVR. Hypoxia/re-oxygenation produced vasoconstriction in AA, EA, and DVR, whereas sGC activation partially abolished this effect. Similar to sGC activators, inhibition of PDE5 caused vasodilating effects in all three microvessel types.

The present data suggest that stimulation of the NO-sGC-cGMP signaling may exert renoprotective effects via maintaining adequate microperfusion thus supporting the glomerular filtration and oxygen supply of kidney zones at risk for hypoxic damage.

The research was supported through funding by the German Research Foundation (DFG): CRC1365 "Renoprotection"

B 06-07

Cadmium-induced mitochondrial membrane fluidity changes cause respiratory supercomplex disruption and peroxide production in the kidney.

Nadiya Romanova[1], Kevin Sule[2], Daniel Hebrok[1], Travis Issler[2], Frank Thévenod[1,3], Elmar J. Prenner[2], **Wing-Kee Lee**[1]

[1] Bielefeld University, Medical School OWL, Physiology & Pathophysiology of Cells and Membranes, Bielefeld, Germany
[2] University of Calgary, Department of Biological Sciences, Calgary, Canada
[3] Witten/Herdecke University, Institute for Physiology, Pathophysiology & Toxicology, Witten/Herdecke, Germany

Divalent cadmium ion (Cd) is a redox-active transition metal that is toxic to eukaryotes. In the kidney, Cd is taken up by essential metal ions transporters by molecular mimicry. Moreover, Cd alters membrane fluidity by interacting with negatively charged phospholipids, which may disrupt lipid packing and their stabilizing effects on protein structure [1]. We have previously shown that Cd permeates the inner mitochondrial membrane (IMM) via the calcium uniporter to disrupt mitochondrial function [2] in addition to lysosome membrane stability [3], culminating in apoptosis. We hypothesized that Cd binding to mitochondrial cardiolipin, essential for electron transport chain (ETC) function, underlines its detrimental effects.

Methods and results: Fluorescent indicators laurdan and 1,6-diphenyl-1,3,5-hexatriene (DPH) report membrane phase properties at the polar region and hydrophobic core, respectively. In mitochondria isolated by differential centrifugation from cultured human renal proximal tubule cells (HPCT) exposed to 2.5µM Cdfor 6h, laurdan generalized polarization (GP) decreased from 0.48±0.02 to 0.46±0.01 ($p<0.01$, n=7), indicating membrane fluidization. Addition of 2.5µM Cd for 1h to isolated rat kidney mitoplasts increased surface membrane fluidity (GP 0.17±0.09 to 0.11±0.04, $p>0.05$, n=4) yet hydrophobic core rigidification (GP 0.185±0.01 to 0.192±0.01, $p>0.05$, n=4). In liposomes prepared from cardiolipin only or an IMM lipid mixture, phase transition temperatures reported by laurdan were increased by Cd, indicating stabilized gel phase and delayed melting to the liquid-crystalline phase. Similarly, GP 0.32±0.09 decreased to -0.07±0.02 ($p<0.01$, n=10-13 images) in laurdan-loaded HPCT cells after 1µM Cd for 1h using multiphoton microscopy. The assembly of respiratory chain supercomplexes was assessed by blue native gel electrophoresis and immunoblotting. Supercomplexes decreased by 38.71±9.26% in HPCT cells after 5µM Cd for 6h, without affecting total cellular ATP, and confirmed in rat kidney cortex mitochondria (rKC_m) treated post-isolation with 2.5µM Cd for 1h. Amplex Ultrared, corresponding to peroxide generation, increased by ~30% in rKC_m treated post-isolation with 5µM Cd for 1h.

Conclusions: Cd exposure inhibits respiratory efficiency via supercomplex disruption, oxidative stress and IMM rigidification, which may be rooted in direct or indirect Cd interaction with charged phospholipids, essential for ETC complex assembly, stability and function.

References
[1] Kerek, EM, Prenner, EJ 2016, 'Inorganic cadmium affects the fluidity and size of phospholipid based liposomes', *Biochim Biophys Acta,* 1858(12), 3169-3181
[2] Thévenod, F, Lee, WK, Garrick, MD 2020, 'Iron and Cadmium Entry Into Renal Mitochondria: Physiological and Toxicological Implications', *Front Cell Dev Biol,* 8:848
[3] Lee, WK, Probst, S, Santoyo-Sánchez, MP, Al-Hamdani, W, Diebels, I, von Sivers, JK, Kerek, E, Prenner, EJ, Thévenod, F 2017, 'Initial autophagic protection switches to disruption of autophagic flux by lysosomal instability during cadmium stress accrual in renal NRK-52E cells', *Arch Toxicol,* 91(10), 3225-3245.

B 06-08
Spatial resolution of gene expression by single cell sequencing analysis in a mouse model of kidney transplantation and immunosuppression

Robert Labes[1], Vera A. Kulow[1,2], Muhammad I. Ashraf[3], Susanne Mathia[1], Janna Leiz[2], Christian Hinze[4,2], Pontus Persson[1], Christian Rosenberger[2], Michael Fähling[1]

[1] *Charité - Universitätsmedizin Berlin, Institut für Translationale Physiologie, Berlin, Germany*
[2] *Charité - Universitätsmedizin Berlin, Medizinische Klinik m.S. Nephrologie und Internistische Intensivmedizin, Berlin, Germany*
[3] *Charité - Universitätsmedizin Berlin, Chirurgische Klinik, Charité, Berlin, Germany*
[4] *Medizinische Hochschule Hannover, Klinik für Nieren- und Hochdruckerkrankungen, Hannover, Germany*

Question

The calcineurine inhibitor Cyclosporine-A (CsA) is widely used in organ transplantation and various autoimmune diseases for its immunosuppressive effects. Despite its beneficial effects, nephrotoxicity and anemia are major problems. Although the pathophysiology remains unclear, we recently showed that hypoxia and capillary loss play a crucial role. Here we used single cell RNA sequencing (scRNAseq) in a setting of kidney transplantation (KTx) to systematically analyze the cell type specific effects of CsA in the transplanted kidney.

Methods

Mice undergo kidney transplantation (KTx) or sham operation. Daily treatment with CsA or vehicle for 8 weeks was started after a recovery phase of one week. Kidneys were removed, homogenized and analyzed by scRNAseq. Cells were clustered as following: podocytes, proximal tubules (PT), thin limb (tL), thick ascending limb (TAL), distal convoluted tubule (DCT), connecting tubule and collecting duct principal cells (CNT/CD-PC), intercalated cell type A (CD-IC-A), intercalated cell type B (CD-IC-B), endothelial cells (EC), interstitial cell and immune cell. In addition, gene set enrichment analysis (GSEA) was performed.

Results

After daily CsA treatment, scRNAseq revealed 370 differentially regulated genes. Compared to the sham group 659 genes were regulated after KTx. The combination of CsA and KTx resulted in the highest number of regulated genes (1077). Strikingly, the most differentially expressed genes under KTx conditions were found in the cluster CNT/CD-PC (415). CsA treatment on top of KTx showed the most alterations in gene expression in the PT (280), CNT/CD-PC (231), TAL (194) and DCT (167) clusters. Pathway analysis by GSEA revealed regulation of proliferation, survival, differentiation and inflammatory pathways after CsA treatment, preferentially in the CNT/CD-PC cluster. Hypoxia and apoptosis related pathways were regulated by KTx. CsA treatment on top of KTx mainly affected pathways involved in energy metabolism .

Conclusions

Spatial investigation of gene expression signatures by scRNAseq for KTx with and without CsA treatment revealed an unexpected strong alteration under KTx and CsA in the CNT/CD-PC cell cluster. Pathways that are activated by KTx were severely influenced by CsA treatment. Although the PT and TAL are well-known areas of risk in several conditions of kidney injury, our data indicate that cells of the distal nephron might play a underestimated role in the pathophysiology of kidney transplantation and immune suppression.

B 06-09
Medullary *Nfat5* deregulation results in substantial kidney fibrosis

Vera A. Kulow[2,4], Michael Fähling[2], Dmitry Chernyakov[1], Kristina Engel[1], **Bayram Edemir**[1,3]

[1] *Universität Witten/Herdecke, Lehrstuhl für Physiologie, Pathophysiologie und Toxikologie, Witten, Germany*
[2] *Charité - Universitätsmedizin Berlin, corporate member of Freie Universität Berlin and Humboldt-Universität zu Berlin, Medizinische Klinik m.S. Nephrologie und Internistische Intensivmedizin, Charitéplatz 1, D-10117 Berlin, Germany, Berlin, Germany*
[3] *Martin-Luther-Universität Halle-Wittenberg, Klinik für Innere Medizin IV, Halle, Germany*
[4] *Charité - Universitätsmedizin Berlin, corporate member of Freie Universität Berlin and Humboldt-Universität zu Berlin, Institut für Translationale Physiologie, Charitéplatz 1, D-10117 Berlin, Germany, Berlin, Germany*

Question

Acute kidney injury can be induced by different factors. It is often associated with disturbed kidney function and changes in the gene expression pattern. However, in many cases it is still unknown how these changes in gene expression are induced. Here we show that medullary loss of the transcription factor NFAF5 leads to an acute kidney injury like phenotype resulting in massive renal fibrosis.

Methods

We generated a collecting duct principal cell specific *Nfat5*-KO mice by breeding *Nfat5*-floxed with a *Aqp2*-Cre delete mice. After 12-20 weeks, kidneys of *Nfat5*-KO and wild type (WT) mice were dissected in renal cortex and inner medulla, followed by gene expression profiling using next generation sequencing. For histological analysis, we also used kidneys from 44 weeks old mice. Staining of WT and *Nfat5*-KO kidneys served to detect kidney injury markers kidney injury molecule-1 (KIM-1) and lipocalin-2 (NGAL). Furthermore, Sirius red staining was performed to quantify renal fibrosis.

Results

The *Nfat5*-KO mice developed a diabetes insipidus like phenotype due to massive reduction of AQP2 expression in the collecting duct. Gene set enrichment analysis indicated that loss of NFAT5 is associated with an inflammatory and kidney injury like phenotype. In addition, in the *Nfat5*-KO kidneys we observed massive expression of NGAL and KIM-1 proteins, further supporting the findings obtained by gene expression profiling. Sirius red staining revealed substantial fibrosis as a result of *Nfat5*-KO.

Conclusions

Using large-scale gene expression data combined with histological staining, we show that the transcription factor NFAT5 is required for maintaining kidney function. A loss of medullary *Nfat5* is associated with specific changes in gene expression throughout the nephron that finally leads to severe renal fibrosis.

B 06-10
Can podocytic extracellular vesicles affect the metabolism of tubular epithelial cells?

Johannes Jägers

University Hospital Essen, Children's Clinic II, Essen, Germany

Extracellular vesicles (EVs) are phospholipid double-membrane coated nanoparticles that nearly all cells of the human body secrete under physiological conditions. EVs transport proteins, DNA and RNA to other cells for cell-to-cell communication. Under pathological conditions, not only the amount of EVs-release changes, but also the composition of the transported cargo. The resulting altered cell-cell communication may influence the course of a disease.[1]

The nephron consists of approximately 20 different cell types with different physiological functions and unique metabolic requirements. The epithelial cells of the proximal tubule deserve special mention, as their energy requirements are tremendously high and are strictly glucose - free. In progressive kidney disease, the metabolism of these cells switches to glycolytic sugar utilization.[2]

The majority of kidney diseases are diseases of the kidney filter (glomerulus), which contains highly specialized cells like podocytes. Podocytes are unable to regenerate and loss of the cell is irreversible. In the case of glomerular diseases, podocytes can die, resulting in the loss of the entire nephron as the disease progresses.[3]

It remains unclear whether podocytes have an influence on the metabolism of the downstream tubular cells via EVs and thus on the progression of the kidney disease.

To answer this question we isolate EVs originating in podocytes and incubate tubular epithelial cells with these EVs. We test whether podocyte derived EVs can influence the expression pattern of metabolic genes and proteins in tubular epithelial cells. In a second step, we will test if the expression pattern in tubular epithelial cells changes after EV incubation with EVs isolated after stressing the podocytes through e.g. cold-stress, hypoxia, inflammation and puromycin.

In addition, we plan to investigate the impact of these conditions on tubular respiration using the Agilent Seahorse FTX system.

In summary, we want to understand the physiological effects of EVs in the nephron and their impact on progressive kidney disease in order to identify specific targets for possible therapeutic intervention.

References

[1] Grange, Cristina, and Benedetta Bussolati. "Extracellular vesicles in kidney disease." *Nature Reviews Nephrology* 18.8 (2022): 499-513.

[2] Balzer, M. S., Rohacs, T., & Susztak, K. (2022). How many cell types are in the kidney and what do they do?. *Annual review of physiology*, *84*, 507-531.

[3] Li, Y., Fan, J., Zhu, W., Niu, Y., Wu, M., & Zhang, A. (2023). Therapeutic potential targeting podocyte mitochondrial dysfunction in focal segmental glomerulosclerosis. *Kidney Diseases*, 1-1.

B 06-11
Renal expression of natriuretic peptide receptors and their protective effects in proximal tubular cells

Elena-Sofia Heinl, Antonia Heinl, Frank Schweda

University of Regensburg, Institute of Physiology, Regensburg, Germany

Question

Natiuretic peptides (NP) are commonly known for their blood pressure lowering and natriuretic effects. The cardiac peptides atrial natriuretic peptide (ANP) and B-type natriuretic peptide (BNP) mediate their physiological functions by activating the membrane-bound guanylate cyclase-A (GC-A = Natriuretic Peptide Receptor-A, NPR-A). The C-type natriuretic peptide (CNP) is mainly released from the endothelium and acts via guanylate cyclase-B (GC-B = NPR-B) in a more paracrine manner. In contrast to ANP and BNP, CNP has no significant natriuretic effect at physiological concentrations. Besides their relevance in maintaining blood pressure all three NPs possess cardio- and renoprotective properties, as, for instance, we previously found strong protection of renal podocytes by GC-A signaling. Despite of the major importance of NPs in controlling renal function, their renal target cells have not been investigated in detail.

Methods

To identify renal target cells of natriuretic peptides we performed systematical expression analysis of NP receptors in mouse kidneys using mRNA in-situ hybridization, immunofluorescence staining and realtime PCR. Further, we investigated the renoprotective potential of CNP in cisplatin-induced cell injury of proximal tubular cells (LLC-PK1 cells) via annexin V apoptosis assay (FACS) and expression analysis of genes which are associated with cisplatin nephrotoxicity.

Results

mRNA of both NP receptors was detectable in mouse kidneys. While podocytes and intrarenal blood vessels expressed GC-A at high abundance, no expression of GC-A was detectable in the tubular system. In contrast, the CNP-receptor GC-B was highly expressed in the proximal tubule but CNP did not regulate electrolyte excretion or diuresis in isolated-perfused mouse kidneys. Instead, CNP had protective effects in proximal tubular cells (LLC-PK1) since it significantly ameliorated apoptosis of cells that had been treated with cisplatin, a well-known cytotoxic agent.

Conclusion

The NP receptors GC-A and -B are expressed in the kidney, however they have different distribution patterns. GC-B is highly expressed in the proximal tubule and exerts the nephroprotective effects of CNP since CNP treatment of proximal tubular cells reduces cisplatin-induced nephrotoxicity and thereby improves cell viability.

References

[1] Heinl ES, Broeker KA, Lehrmann C, Heydn R, Krieger K, Ortmaier K, Tauber P, Schweda F. Localization of natriuretic peptide receptors A, B, and C in healthy and diseased mouse kidneys. Pflugers Arch. 2023 Mar;475(3):343-360. doi: 10.1007/s00424-022-02774-9

B 07 | Vascular Function

B 07-01
Modulation of the endothelial SWI/SNF chromatin remodelling complex by long non coding RNAs

James A. Oo[1,2,5], Katalin Pálfi[1,2,5], Timothy Warwick[1,2,5], Frederike Boos[1,2,5], Ilka Wittig[1,2,3], Stefan Günther[4], Francois McNicoll[6], Michaela Müller-McNicoll[6], Ralf P. Brandes[1,2,5], Matthias S. Leisegang[1,2,5]

[1] Institute for Cardiovascular Physiology, Goethe University, Frankfurt, Germany
[2] German Center of Cardiovascular Research (DZHK), Partner site RheinMain, Frankfurt, Germany
[3] Functional Proteomics, Goethe University, Frankfurt, Germany
[4] Max Planck Institute for Heart and Lung Research, ECCPS Bioinformatics and Sequencing Facility, Bad Nauheim, Germany
[5] Cardio Pulmonary Institute, Frankfurt, Germany
[6] Institute for Molecular Biosciences, Goethe University, Frankfurt, Germany

Background: Long non-coding RNAs modulate the activity and targeting of chromatin remodelling complexes and thereby gene expression. The mechanisms governing the recruitment of these complexes to specific gene promoters are largely unknown. It has been shown, however, that lncRNAs are required for the function of various complexes that modify or remodel chromatin, such as the Polycomb Repressive Complex 2 (PRC2) and the SWItch/Sucrose Non-Fermentable (SWI/SNF) complex. We previously identified the lncRNA MANTIS as a crucial component of the endothelial SWI/SNF complex. MANTIS stabilised the complex and enabled its gene-targeting. On this basis we hypothesise that a broader network of lncRNAs modulates chromatin remodelling through a cell-specific and context-dependent recruitment of the SWI/SNF chromatin remodelling complex to ultimately mediate endothelial cell and vascular function.

Methods and Results: The core ATPase of the SWI/SNF complex, BRG1, is required for normal endothelial cell function. Knockdown of BRG1 in human umbilical vein endothelial cells (HUVEC) reduced proliferative capacity as well as migration and angiogenic sprouting potential. BRG1 siRNA and RNA-sequencing alongside BRG1 CUT&RUN revealed multiple enriched genes and pathways crucial to endothelial cell function that were significantly differentially expressed after BRG1 knockdown. BRG1 RNA-IP-sequencing and iCLIP identified novel RNA interaction partners of BRG1. This technique recovered (among others) the lncRNAs EPHA1-AS1, CACNA1G-AS1, MALAT1 and NEAT1, which have been implicated in endothelial function. Subsequent screens with a customised siRNA library against 20 BRG1-bound lncRNAs revealed that many of these alter endothelial functional capacity and, importantly, BRG1 genomic binding. Furthermore, protein interaction partners of the endothelial SWI/SNF complex were identified by mass spectrometry and found to be dependent on the presence of RNA to interact with SWI/SNF.

Conclusions: Endothelial cells contain a considerable number of functionally important lncRNAs that interact with the SWI/SNF chromatin remodelling complex. BRG1 CUT&RUN and RNA-seq following BRG1-bound lncRNA knockdown will reveal further specific gene targetting mechanisms and programs that depend upon lncRNAs. RedChIP will also be performed to confirm that these lncRNAs directly recruit BRG1 to its genomic targets to mediate endothelial and vascular function.

B 07-02
Role of RhoA-kinase and ribosomal S6-kinase II pathways in the regulation of vascular contractility of senescent human renal and mesenteric arteries

Lubomir T. Lubomirov[1,2], Doris Metzler[2], Tatjana Korotkova[2], Jürgen Hescheler[3], Gabriele Pfitzer[2], René Mantke[4,5], Thomas Enzmann[6], Olaf Grisk[1]

[1] Brandenburg Medical School, Physiology, Neuruppin, Germany
[2] University of Cologne, Vegetative Physiology, Center of Physiology, Cologne, Germany
[3] University of Cologne, Neurophysiology, Center of Physiology, Cologne, Germany
[4] Brandenburg Medical School, General and Visceral Surgery Clinic, Brandenburg, Germany
[5] Brandenburg Medical School, Faculty of Health, Brandenburg, Germany
[6] Brandenburg Medical School, Urology and Children Urology Clinic, Brandenburg, Germany

Question

Mechanisms regulating vasoconstriction vary in the small arteries from different organs. In the present study, we investigated the role of RhoA-kinase (ROK) and ribosomal S6-kinase II (RSK2) pathways in the regulation of vascular contractility in senescent human renal and mesenteric arteries.

Methods

Contractility of human intrarenal (h-RA) and mesenteric (h-MA) arteries obtained from patients undergoing elective surgery was explored by

wire myography. Furthermore, contractility of interlobar (m-IAs) and mesenteric (m-MA) arteries from young and aged mice was studied by the same method. Phosphorylation of the regulatory subunit of myosin light chain (MLC_{20}), myosin light-chain-phosphatase (MLCP), MYPT1 at phosphosite T853 (ROK-site) and RSK2 at phosphosite S227, responsible for kinase activation (RSK2-S227) were determined by Western blot.

Results

h-RA showed higher stretch-induced tone and higher reactivity to α1 adrenergic receptor stimulation than h-MA (-log EC50= 6.1±0.2 in h-RA vs. 5.1±0.3 in h-MA; $p<0.05$). Maximal force (F_{max}) calculated as percent of force achieved by depolarization with 60 mmol/l K^+ was also weaker in h-MA (118.8±5.2% vs. 56.2±10.4%; $p<0.001$). Similarly, concentration dependency of the thromboxaneA2 agonist, U46619 was rightward shifted in h-MA (-log EC50= 7.9±0.1 in h-RA vs. 6.8±0.3 in h-MA; $p<0.0001$), but no change in F_{max} was observed (130.7±5.3 in h-RA vs. 124.2±4.9 in h-MA; $p>0.05$). Rho-kinase (ROK) inhibition resulted in a greater decrease in Ca^{2+} and depolarization-induced tone in h-RA than in h-MA ($p<0.001$). Basal and α1 adrenergic receptor stimulation-induced phosphorylation of MLC_{20} was higher in h-RA than in h-MA. This was associated with higher ROK-dependent phosphorylation of MYPT1-T853. In h-RA phosphorylation of RSK2-S227 was significantly higher than in h-MA. Similarly, MYPT1-T853 and RSK2 phosphorylation were also higher in m-IAs from aged mice than in respective vessels from young mice and in m-MA from both age groups. Moreover, only aged m-IAs generated a stretch-induced tone.

Conclusions

Vasoconstriction in human intrarenal arteries shows a greater ROK-dependence than in mesenteric arteries. Our study also suggests that activation of RSK2 may contribute to intrarenal artery tone dysregulation associated with aging. Compared with h-RA, h-MA undergo age-related remodeling leading to a reduction of the contractile response to α1 adrenergic stimulation.

B 07-03
Piezo1 is a mediator of endothelial nanomechanics and vascular inflammation

Johanna-Theres Borutta[1], Erik Hertel[1], Kristina Kusche-Vihrog[1,2], Benedikt Fels[1,2]

[1] *University of Luebeck, Institute of Physiology, Luebeck, Germany*
[2] *DZHK (German Research Centre for Cardiovascular Research), Partner Site Hamburg/Luebeck/Kiel, Luebeck, Germany*

Vascular tone must be constantly regulated to ensure proper blood flow to the organs. Thus, endothelial cells (ECs) lining blood vessels are exerted to mechanical and biochemical forces. The top layer of endothelial cells, the so-called glycocalyx (eGC), and the underlying cortex form a nanobarrier between blood vessels and tissue. The mechanical properties of EC surface, is highly flexible, alternating between "soft" and "stiff" conditions and essential for proper endothelial function. Changes in the nanomechanics of ECs are associated with endothelial dysfunction and vascular inflammation. In addition, structures like the eGC and mechanosensitive ion channels are important endothelial mechanosensors. One candidate is the mechanosensitive nonspecific cation channel Piezo1. In this project, we aim to understand the role of Piezo1 in endothelial nanomechanics and vascular inflammation.

We treated ECs with TNF-α to induce vascular inflammation. In co-treatments with or without the Piezo1 agonist Yoda1 the effect of Piezo1 on the nanomechanics of eGC were quantified by using the Atomic Force Microscope (AFM). Furthermore, in single cell force spectroscopy measurements we analyzed the adhesion forces between isolated human monocytes and ECs. Effects of the absence of Piezo1 on nanomechanical properties by CRISPR-Cas9 induced Piezo1 knockout in ECs were quantified.

TNFα-induced inflammation and activation of ECs leads to eGC damage and consequently to a decrease in eGC height. The Piezo1 agonist Yoda1 prevented these negative effects when treated concomitantly with TNF-α. Using wheat germ agglutinin (WGA) staining, we were able to confirm these results. At the functional level, cell-cell adhesion analyses have shown that Yoda1 prevents the TNF-α-mediated increase in adhesion forces. In monocyte wash away assays, we demonstrated that TNF-α increased the number of monocytes adherent to ECs, corroborating our previous results. Of note, a CRISPR-Cas9 mediated Piezo1 knockout resulted in a reduction in eGC height.

Based on our results, we postulate that Piezo1 is an important regulator of endothelial nanomechanics and its activity has beneficial effects

on eGC and enhances the vasoprotective function of the EC surface. We hypothesize that Piezo1 may serve as a pharmaceutical target to prevent the development of cardiovascular pathologies.

B 07-04
Mathematical model for diffusion and enzymatic degradation of AMP in rat aorta predicts concentration gradients of nucleotides/nucleosides in vessel wall

Arvid Pietsch, Andreas Deussen, Stephan Speier, Peter Dieterich, Melanie Martin

TU Dresden, Institut für Physiologie, Dresden, Germany

Question

Disturbances of extracellular nucleotide degradation and release are known to effect intramural nucleotide concentrations and may cause medial calcification in human vessels. Diffusion processes of nucleotides between the bloodstream and vessel layers may play a role for medial calcification by affecting intramural nucleotide concentrations. Aims of this study are to analyze CD73 and alkaline phosphatase activities in human and rat cell cultures and rat aortic ring and further, to evaluate the effect of the competing processes of diffusion and enzymatic AMP degradation on the nucleotide/nucleoside distribution within the aortic ring.

Methods

Time courses of degradation of etheno-AMP (εAMP) to etheno-Adenosine (εAdo) were quantified in cell cultures of endothelial and smooth muscle cells and in ex vivo aortic rings of rats by HPLC. The role of endothelium was studied by mechanical removal of the endothelial cell layer. Endothelial cell lines studied included: Human Umbilical Vein Endothelial Cells (HUVEC), Human Umbilical Artery Endothelial Cells (HUAEC) and Rat Aortic Endothelial Cells (RAEC). Additionally, one smooth muscle cell line (Rat Aortic Smooth Muscle Cells, RASMC) was used. Michaelis-Menten parameters were estimated using mathematical modelling and Bayesian data analysis. The analysis was extended to a model representing 20 cell layers of rat aorta, each with combined diffusion-reaction processes for AMP and Ado.

Results

Michaelis-Menten parameters estimated for HUVEC, HUAEC, RAEC, RASMC and rat aortic ring are given in table 1. Compared to the other cell cultures, RAEC have lower enzymatic activity, whereas RASMC showed average enzymatic activity. Parameter estimation for HUVECs and HUAECs showed high degradation of εAMP with especially increased V_{max} values. Compared to the parameters in cell experiments rat aortic rings showed medium enzymatic activity. Removal of endothelium did not change K_m significantly, but slightly increased V_{max}, suggesting a diffusion associated effect of intact endothelium on nucleotide degradation. Combining diffusion and enzymatic parameters of the cell measurements, the model reproduced measured εAMP and εAdo concentrations in the medium surrounding the aorta ring. In addition, modeling predicted a quasi-steady-state nucleotide/nucleoside distribution in the vessel wall, with the lowest concentrations occurring in the middle of the simulated vessel wall.

Conclusions

Our studies show clear differences in the ecto-nucleotidase activities of different cell types of the vessel wall as well as considerable species differences. Further, this study indicates that both, diffusion and enzymatic reaction, contribute to the local intramural nucleotide concentration. In-vivo, the presence of other nucleotidase activities will further complicate the scenario. Further experiments in conjunction with quantitative model analysis are needed to explore vessel wall nucleotide concentrations in a realistic manner.

	K_m µmol/l	V_{max} nmol/min in well plate	average εAMP degradation % after 3 h
HUVEC	12 ± 7	1.47 ± 0.1	98 ± 1
HUAEC	43 ± 2	5.04 ± 0.1	99 ± 0.4
RAEC	70 ± 10	0.02 ± 0.005	1 ± 0.2
RASMC	31 ± 17	0.5 ± 0.2	62 ± 11
rat aortic ring with endothelium	70 ± 10	0.4 ± 0.1	25 ± 3
rat aortic ring without endothelium	76 ± 13	0.6 ± 0.1	30 ± 5

Table 1: Enzymatic parameters of different cell types and rat aortic ring

B 07-05
The nuclear Corepressor NCoR1 limits endothelial angiogenic function

Tom Teichmann[1], Pedro Malacarne[1], Tim Warwick[1], Simonida Zehr[1], Stefan Günther[2], Beatrice Pflüger-Müller[1], Ralf P. Brandes[1]

[1] *University Frankfurt, Cardiovascular Physiology, Frankfurt, Germany*
[2] *Max-Planck-Institute for Heart- and Lung Research, Bad Nauheim, Germany*

Corepressors negatively regulate gene expression by chromatin compaction. Alteration of the gene expression profile could be used as strategy to switch the phenotype of endothelial cells, key players during the process of new blood vessel formation, from a quiescent to a pro-angiogenic state. Here we hypothesized that by specifically targeting corepressor proteins, the endothelial angiogenic function could be improved. To study this, we characterized the function of nuclear repressor complexes in human umbilical vein endothelial cells (HUVECs) as well as in organ culture of mouse aortic tissue.
Single cell data sets revealed that the corepressors NCoR1, SMRT and REST are particularly high expressed in vasculature, especially endothelial cells. Importantly, targeted knockdown of these corepressors in HUVECs demonstrated that exclusively NCoR1 depletion increased the angiogenic capacity as determined by spheroid- and mouse aortic outgrowth assays. The underlying mechanism was explored by RNA- and ATAC-Seq. NCoR1 depletion significantly upregulated the expression of angiogenesis-associated genes, especially tip cell genes, including ESM1, DLL4 and NOTCH4. Confrontation assays comparing cells with and without NCoR1-deficiency revealed that loss of NCoR1 promoted a tip-cell position during spheroid sprouting. Interestingly, a proximity ligation assay identified NCoR1 as a direct binding partner of the transcription factor RBPJk, regulating NOTCH signaling during tip and stalk cell selection. Loss of this interaction, after NCoR1 depletion, increased NOTCH activity as determined by luciferase activity measurements. Finally, targeted NOTCH4 depletion in NCoR1 deficient cells abolished the previously described effects on angiogenic capacity.
NCoR1 is an interesting target allowing the positive modulation of pathophysiological angiogenesis via its direct interaction with the NOTCH specific transcription factor RBPJk. Targeted depletion of NCoR1 promotes a tip cell position and thus increased angiogenic capacity in endothelial cells.

B 07-06
Magnesium-Oxygen-Therapy – a physiological effective treatment of patients with Long Covid and Post Vac

Elfriede Leniger-Follert

Medical Practice, Hagen, Germany

In 1983 we already discovered that extracellular K^+ activity ($[K^+]_0$) exerts a dual effect on smooth muscle cell membrane voltage and therefore on microflow. In the range of 3 to 20 mM hyperpolarization occurs with concomitant increase in microflow. Above the ceiling level of 20 mM the further increase in $[K^+]_0$ leads to depolarization and to constriction of arterioles with decreasing microflow.
In 1995 and 2004 we reported that Magnesium ions are suited to change the depolarization of smooth muscle cell membrane into repolarization and therefore, ameliorates perfusion in ischemic regions in patients.
Now we report about the results of intravenous injection of 6 mM Magnesium ions within 15 to 20 seconds in patients with severe symptoms of Long Covid and Post Vac. As a negative charged anion, we used sulfate. We measured the time in seconds from the beginning of injection until heat was registered by the patients in the different regions of the body. These special circulation times of the patients were compared to the corresponding circulation times of the healthy individuals. They are directly related to the microflow in different organs. The injections were performed until the circulation times became normal. Additionally, all patients inhaled oxygen (5 liter per minute) to increase capillary $pO_2$and therefore increase the oxygen pressure gradient in tissue.
Until now we have successfully treated more than 80 Long/Post Covid patients and about 40 Post Vac patients. The duration of treatment depended on the extent of neurological, cardiological, muscular and fatigue symptoms as well as on the degree of constriction of the small vessels and tissue hypoxia.

B 07-07
Red blood cells mediate endothelial glycocalyx and actin adaptation in response to flow speed variation

Max Dietrich[1], Kristina Kusche-Vihrog[1,2], Benedikt Fels[1,2]

[1] *Universität zu Lübeck, Institut für Physiologie, Lübeck, Germany*
[2] *DZHK (German Research Centre for Cardiovascular Research), Hamburg/Luebeck/Kiel, Germany*

Question

Endothelial cells (EC) as well as red blood cells (RBC) are both covered with surface glycocalyx to monitor blood flow. In response to shear stress variations, EC release nitric oxide (NO) to induce the flow-mediated vasodilation. Also RBC-derived NO directly impacts the blood flow. However, the interaction of EC and RBC (and RBC-derived NO) with the endothelial surface (e.g. eGC) is unknown.

Methods

In this study, human umbilical vein endothelial cells (HUVEC) were cultured in an *in-vitro* setup using Y-shaped µ-Slides (ibidi GmbH) and then kept under flow conditions using an ibidi pump, with or without free-flowing human RBC. The µ-Slides allow simulation of bifurcated blood vessels, generating laminar flow with varying shear stress, with 6 dyn/cm² at the singular parts, dropping at the bifurcation to 3 dyn/cm² in the split channel section. EC were co-stained for eGC and actin using WGA and Phalloidin respectively. Fluorescence images were taken at zones of low (3 dyn/cm$^{2)}$ and high (6 dyn/cm^2) shear stress and the mean fluorescence intensity of the combined area above the nuclei was measured. Supernatant was stored for quantification of NO release. Fluorescence values were normalised to intensities of the first channel segment (control: laminar flow, 6 dyn/cm^2, w/o RBC).

Results

In the presence of RBC the eGC of HUVEC was increased by 39.0% in regions of the Y-shaped µ-Slide with 3 dyn/cm² (N=4, $p<0.0001$) compared to control conditions w/o RBC. Downstream, at again 6 dyn/cm², intensities were increased by 22.3% ($p = 0.018$) vs. the control region. This indicates an increase of the eGC layer in the presence of RBC following variation in flow speed. This effect persists even downstream after flow speed returns to previous levels (6 dyn/cm^2).

At 3 dyn/cm^2 the actin cortex showed increased fluorescence intensities by 35.6% (N=3, $p<0.01$) in presence of RBC compared to cells at 6 dyn/cm^2. Also after returning to 6 dyn/cm^2, actin fluorescence intensities remained increased by +33.9% (N=3, $p>0.01$) compared to control regions w/o RBC. This indicates a polymerization of cortical F-actin in the presence of RBC after a drop in shear stress. Measurements of Erythrocyte-derived nitric oxide as a possible mediator of the RBC-endothelium interaction are ongoing.

Conclusions

The results demonstrate the impact of RBC on the endothelial cell surface is dependent on shear stress rates, leading to alternation of eGC structure and associated cortical actin compared to cells that had no interaction with RBC. This could possibly be mediated by mechanosensitive structures of the RBC, resulting in NOS activation and NO release.

B 07-08
Role of lipid mediator in lymphangiogenesis and lymphatic maturation

Zumer Naeem

Goethe University, Institute for vascular signaling, Frankfurt, Germany

Lymphatic vessels are essential for tissue homeostasis in physiological conditions as we all as in diverse pathologies, including cancer metastasis, lymphedema, and organ graft rejection. In the present study, we aimed to investigate the role of cytochrome P450-derived epoxides and their soluble epoxide hydrolase-derived respective diols in lymphangiogenesis and lymphatic maturation during development.

In a spheroid-based assay using embryonic stem cells (mESC) and tumour cells, we observed that PUFA epoxide/diol pairs elicited differential effects on mESC differentiation into either blood endothelial cells (BECs) or lymphatic endothelial cells (LECs). Indeed, while the linoleic acid epoxide (12,13-EpOME) increased the expression of genes implicated in angiogenesis e.g. *Vegfr1* and *Ephb4*, the corresponding diol; 12,13-DiHOME promoted the expression of *Vegfr3*, *Coup-tf*, *Sox18* and *Prox1* i.e., genes linked to lymphangiogenesis. Based on this information, we studied lymphangiogenesis in the ears of young Cyp2c44$^{-/-}$ and sEH$^{-/-}$ pups (P21) and discovered profound effects. Deletion of Cyp2c44$^{-/-}$

(to decrease epoxide and diol formation) attenuated lymphatic vessel maturation and severely affected valve formation, without having any major effect on lymphatic vessel density or branching. On the other hand, the deletion of sEH (to increase epoxide and decrease diol formation) resulted in a less dense lymphatic network with fewer branching points. Although valve morphology seemed normal in these mice, the lymphatic collecting vessels showed a higher coverage of smooth muscle cells.
In conclusion, we could show that Cyp, sEH and their derived lipid mediators plays important role in endothelial cell specification, lymphatic development, lymphatic vessels maturation, and valve formation.

B 07-09
Deletion of the Soluble Epoxide Hydrolase Impairs Intestinal Angiogenesis and Lacteal development

Yanis Afir, Zumer Naeem, Timo Frömel, Rüdiger Popp, Ingrid Fleming

Goethe University, Institute for Vascular Signalling, Frankfurt am Main, Germany

Question
Blood and lymphatic capillaries of the small intestine are characterized by their key role in nutrient absorption as well as their unique dynamic regenerative state. Despite their importance, the molecular mechanisms governing their generation and homeostasis are insufficiently understood. Epoxides of polyunsaturated fatty acids (PUFAs), generated by cytochrome P450 enzymes, and the diols generated by the subsequent activity of the soluble epoxide hydrolase (sEH), have been shown to play an important role in angiogenesis and lymphangiogenesis in the retina and in cancer. Here, we assessed the impact of the sEH-related lipid mediators on intestinal angiogenesis and lymphangiogenesis.
Results
Mapping of the expression of the sEH (immunohistochemistry) revealed its high abundance in enterocytes, predominantly in the proximal small intestine. Expression of the protein was also higher at the top of the villi. Developing lacteals also expressed the sEH (P7 and P21), as did the nascent capillaries but sEH expression was not detectable in lacteals and blood capillaries from adult mice. Deletion of the sEH had a clear impact on blood vessel and lymphatic development at P7 and P21, with both a significant decrease in the lacteal/villi ratio and length but with a higher number of lacteal sprouts and a higher expression of Prox1. In $sEH^{-/-}$ mice we also observed a decrease in blood capillary density within the villi.
Moreover, we found evidence suggesting that sEH inhibition modulates lipid uptake in the gut, with a bigger size of lipid droplets inside the enterocytes of the top villi.
Conclusions
Overall, our findings suggest an important role for sEH-related lipid mediators in the intestinal angiogenesis and lymphangiogenesis in a developmental model, as well as regulatory effect of lipid absorption. Experiments are ongoing to determine the mechanisms by which PUFA epoxides and diols act on angiogenesis and lymphangiogenesis.

B 07-10
Activation of free fatty acid receptors modulates pulmonary vascular tone *ex vivo*

Alexander Seidinger[1], Claudia Groll[1], Daniela Wenzel[1,2]

[1] *Ruhr-University Bochum, Department of Systems Physiology, Bochum, Germany*
[2] *University of Bonn, Institute of Physiology I, Bonn, Germany*

The free fatty acid receptor (FFAR) family comprises four members, FFAR2 and FFAR3, that can be activated by short chain fatty acids (SCFA) as well as FFAR1 and FFAR4, that respond to long chain fatty acids (LCFA). All FFARs are G-Protein coupled receptors and are expressed in numerous organs. SCFA and LCFA have been demonstrated to relax systemic vessels and reduce systemic blood pressure. Therefore, we wondered if activation of FFARs could also directly modulate the tone of pulmonary arteries (PAs) and be a therapeutic target in pulmonary hypertension (PH).

Vascular tone of PAs was determined in isometric force measurements in a wire-myograph. The impact of FFARs on small intrapulmonary arteries was assessed in functional lung slices. To measure pulmonary arterial pressure (PAP) *ex vivo* we used the isolated perfused lung system (IPL) of mouse. For the activation of FFAR2/3 propionate or butyrate were applied while compound A (compA) and TUG 891 (TUG) were applied for FFAR1/FFAR4 stimulation. In all experiments female and male C57BL/6 mice were used.

In isometric force measurements of mouse PAs first results indicate that single dose application of the SCFA butyrate (50 mM) induces a vasoconstriction of 0.8 ± 0.1 mN (n=3). Furthermore, the constriction by butyrate was dose-dependent from 1 mM to 50 mM. Because the FFAR1/FFAR4 agonists (compA or TUG (10 µM)) did not increase baseline force a potential vasorelaxant effect of FFAR1/FFAR4 agonists was investigated by single dose application of the respective agonists (10 µM) and subsequent dose-response curves of the vasoconstrictor serotonin (5-HT). FFAR4 activation induced a pronounced right shift of 5-HT dose response curves (log EC_{50}: -5.72 ± 0,05 (n=6, compA) vs. -6,28 ± 0.05 (n=6, solvent), p<0.001) that was prevented by the FFAR4 antagonist AH7614 (10 µM) but remained unaffected by the FFAR1 antagonist GW1100 (10 µM). In addition, a single dose of compA induced a strong vasorelaxation after 5-HT pre-constriction in isometric force measurements (55.5 ± 2.4 % (n=6, compA) vs. 5.5 ± 3.4 % (n=6, solvent), p<0.001) and also in functional lung slices (66.0 ± 4.5 % (n=8, compA) vs. 11.4 ± 3.4 % (n=6, solvent), p<0.001). Consistently, in the IPL model our preliminary results show an increase of PAP after application of the SCFA propionate on baseline levels (30 mM, 2.2 ± 0.6 cmH_2O (n=3)) and a decrease of PAP when compA was applied after 5-HT pre-constriction (35.8 ± 3.1 % (n=6, compA) vs. 6.7 ± 2.6 % (n=6, solvent), p<0.001). This effect could again be attenuated by the FFAR4 antagonist AH7614.

In conclusion, our data indicate that FFAR2/3 and FFAR4 modulate pulmonary tone differentially. While FFAR2/3 activation by SCFA induces constriction, FFAR4 activation evokes a pronounced pulmonary vasorelaxation in mouse *ex vivo*. Future experiments will focus on the downstream signaling mechanisms of FFARs in the pulmonary vasculature.

B 07-11
Role of A2B receptor activation in tone regulation of the pulmonary vasculature

Jana Lewandowski[1], Daniela Wenzel[1,2]

[1] *Ruhr-Universität Bochum, Systemsphysiology, Bochum, Germany*
[2] *Universität Bonn, Institute of Physiology I, Bonn, Germany*

Question

The adenosine A2B receptor (A2BR) is a G protein-coupled receptor that couples to G_s, $G_{q/11}$, G_i and $G_{12/13}$ and is upregulated in humans suffering from pulmonary hypertension (PH). Adenosine, the endogenous ligand of this receptor, is known to be involved in the regulation of vascular tone and smooth muscle cell growth that are both pathophysiological characteristics of PH. Furthermore, adenosine levels are elevated under hypoxic conditions that can promote PH. Therefore, we were interested in the role of A2BR signaling in pulmonary arteries (PAs).

Methods

PCR, Western Blotting and immunohistochemistry were used to analyze A2BR expression in different organs and tissues on mRNA and protein level. The effect of adenosine, receptor agonist and antagonists on pulmonary arterial tone regulation was examined using wire-myography, functional lung slices and the isolated perfused lung (IPL). To investigate the role of A2BR activation in the modulation of smooth muscle cell growth, we performed growth assays in human pulmonary arterial smooth muscle cells (hPASMCs).

Results

Using PCR, Western Blotting and immunohistochemistry, we were able to demonstrate A2BR expression in lung and main PAs, in particular in the smooth muscle layer of PAs and in alveolar epithelial cells. In isometric force measurements, preincubation of mouse PAs with adenosine (10^{-4}M) or the A2BR specific agonist BAY 60-6583 (BAY, 10^{-4}M) induced a right shift of 5-HT dose-response curves (EC_{50} BAY: -6.5 ± 0.11 (n=9) vs EC_{50} DMSO: -6.9 ± 0.06 (n=9), p<0.0001 (Two-way ANOVA)). This could be attenuated by additional preincubation with the A2BR specific antagonist PSB-603 (10^{-5}M) (EC_{50} PSB+BAY: -6.5 ± 0.05 (n=6) vs EC_{50} DMSO: -6.7 ± 0.04 (n=6), p>0.05 (Two-way ANOVA)), while the A2A receptor antagonist ZM241385 (10^{-6}M) had no effect. In addition, single dose application of BAY (10^{-4}M) after 5-HT-induced contraction caused a pronounced vasorelaxation in PAs (BAY: 16.6 ± 3.2% (n=16) vs DMSO: 1.4 ± 2.7% (n=16), p<0.01 (One-way ANOVA)). Similar to the results in large PAs, adenosine (10^{-4}M) and BAY (10^{-5}M) evoked a strong vasorelaxation in small intrapulmonary arteries of

functional lung slices and the effect of BAY proved to be dose-dependent (10^{-7}M: 0.8 ± 2.8%, p>0.05; 10^{-6}M: 12.1 ± 2.5%, p<0.01; 10^{-5}M: 33.5 ± 3.5%, p<0.001; 10^{-4}M: 49.6 ± 2.6%, p<0.001 compared to solvent control (Two-way ANOVA)). In addition, BAY (10^{-5}M) also reduced pulmonary arterial pressure in the IPL (BAY: 16.5 ± 2.3% (n=7) vs DMSO: -1.36 ± 2.47% (n=6), p<0.001 unpaired students t-test). Finally, in vitro experiments in hPASMCs revealed that BAY (10^{-5}M) was able to strongly diminish cell growth (PDGF vs native: 2.29 ± 0.2 (n=6); PDGF+BAY vs native: 0.87 ± 0.1 (n=6) p<0.001, one way ANOVA).

Conclusions

Activation of A2BR results in prominent pulmonary vasorelaxation and limits PASMC growth. Further investigation is needed to determine the underlying signaling pathway and a potential role of A2BR in PH.

B 07-12
Modulation of purinergic contractions of murine vas deferens by carbachol

Pei Yee Wong, Mark Hollywood, Keith Thornbury, Gerard Sergeant

Dundalk Institute of Technology, Smooth Muscle Research Centre, Dundalk, Ireland

Classically, electrical stimulation of sympathetic nerves in the vas deferens yields a biphasic contraction comprised of an initial fast component, mediated by release of ATP, followed by a slower developing sustained component brought about by release of noradrenaline [1-2]. It is also recognized that sympathetic nerve-mediated contractions of the vas deferens can be modulated by acetylcholine [3-5], however there is considerable disagreement regarding the precise contribution of cholinergic nerves to contraction of the vas deferens. The aim of the present study was to examine the effects of the cholinergic agonist carbachol on purinergic contractions of the murine vas deferens.

C57BL/6 wild-type (WT, 10-16 weeks) and B6N.129S4(Cg)-Chrm2^{tm1Jwe}/J (M_2R KO) male mice (15-22 weeks) were killed by i.p. injection of sodium pentobarbital (100mg/kg). Isometric tension recordings were made on segments of murine VD (10-15mm in length). Contractions were evoked by: 1) electric field stimulation (EFS, 4Hz, 1s duration, 100s interval), in the presence of the α_1-adrenoceptor antagonist prazosin (100 nM) to isolate the purinergic component of the response, or 2) exogenous application of ATP (1μM). Prazosin (100nM) reduced the amplitude of EFS responses in WT mice by ~70% and the remaining contractions were sensitive to the $P2X_1$R desensitising agonist, α,β-meATP (10μM) indicating that these responses were purinergic in nature. CCh (1μM), enhanced the amplitude of EFS-evoked purinergic responses by ~283% (n=30, p<0.0001) and this effect was also abolished by α,β-meATP (n=12, p<0.0001). Similarly, CCh enhanced the amplitude of ATP-evoked contractions by 288% (n=12, p<0.001). Experiments were performed to examine if the potentiating effects of CCh were mediated by activation of M_2 or M_3 muscarinic receptors. The M_3R antagonist 4-DAMP (3 nM) reduced the effects of CCh on EFS responses by 95% (n=12, p<0.01) and those induced by ATP by 76% (n=12, p<0.01). The M_2R antagonist methoctramine (100 nM), reduced the potentiating effects of CCh on EFS responses by 74% (n=12, p<0.001), but only reduced CCh-induced enhancement of ATP responses by 25% (n=12, p=ns). To further determine the role of M_2Rs and M_3Rs in the potentiating effects of CCh, experiments were performed on tissues taken from M_2R knock-out mice. Application of CCh enhanced EFS-induced contractions of the VD (in the presence of prazosin) by 267% (n=10, p<0.05), whereas ATP-contractions were enhanced by 208% (n=6, p=ns). 4-DAMP abolished the potentiating effects of CCh on EFS responses (n=10, p<0.05) and reduced the effects on ATP-evoked contractions by 89%, respectively (n=6, p=ns).

In summary, purinergic contractions of the vas deferens were potentiated by the cholinergic agonist carbachol, and these effects are mediated by activation of M_3Rs and, to a lesser extent, M_2Rs.

The authors are grateful for Landscape and Covid19 Relief funding to PYW from the Higher Education Authority via the DKIT Research Office.

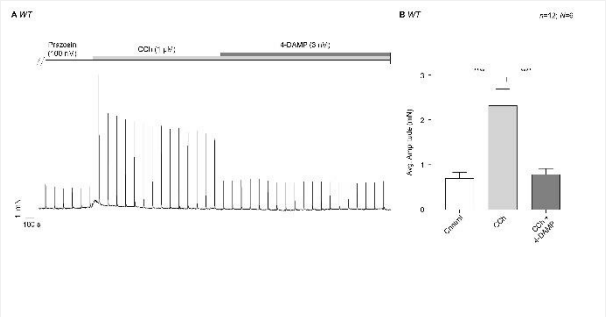

Effects of the M3R antagonist, 4-DAMP, on EFS-evoked purinergic contractions of murine vas deferens
A) Representative tension recording showing that EFS-evoked contractions of the vas deferens that remained in the presence of prazosin were potentiated by application of the cholinergic agonist carbachol (CCh, 1 µM). This effect was reversed by the M_3R antagonist 4-DAMP. EFS was applied for 1 second, at 100 second intervals, at frequency of 4 Hz. *B*) Summary bar chart showing the mean amplitude of EFS-induced contractions in control, CCh and CCh + 4-DAMP. Error bars represent SEM and data were analysed using one-way ANOVA (****p<0.0001; *n*=12, *N*=6).

References
[1] Allcorn, R. J., Cunnane, T. C., and Kirkpatrick, K. 1986. 'Actions of α, B-methylene ATP and 6-hydroxydopamine on Sympathetic Neurotransmission in the Vas Deferens of the Guinea-pig, Rat and Mouse: Support for Co-transmission'. *British Journal of Pharmacology*, 89(4), 647–59. doi: 10.1111/j.1476-5381.1986.tb11169.x.
[2] Koslov, D. S., and Andersson, K. 2013. 'Physiological and Pharmacological Aspects of the Vas Deferens—an Update'. *Frontiers in Pharmacology*, 4,1–11. doi: 10.3389/fphar.2013.00101.
[3] Cuprian, A. M., Solanki, P., Jackson, M. V. and Cunnane, T.C. 2005. 'Cholinergic Innervation of the Mouse Isolated Vas Deferens'. *British Journal of Pharmacology*, 146(7), 927–34. doi: 10.1038/sj.bjp.0706357.
[4] Kaschube, M., and Zetler, G. 1989. 'Noradrenergic, Purinergic, and Cholinergic Transmission in the Mouse Vas Deferens: Influence of Field-Stimulation Parameters, Reserpinization, 6-Hydroxydopamine and 4-Aminopyridine'. *Journal of Neural Transmission*, 76(1),39–53. doi: 10.1007/BF01244990.
[5] Solanki, P., Cuprian-Beltechi, A. M., and Cunnane, T. C. 2007. 'Cholinergic Innervation of the Guinea-Pig Isolated Vas Deferens'. *Naunyn-Schmiedeberg's Archives of Pharmacology*, 376(4), 265–74. doi: 10.1007/s00210-007-0198-y.

B 07-13
Non-coding genetic variation contributes to human physiology and pathology via disrupted RNA:DNA:DNA triple helix formation

Timothy Warwick[1,4], Sandra Seredinski[1,4], Nina M. Krause[2], Jasleen K. Bains[2], Harald Schwalbe[2], James A. Oo[1,4], Matthias S. Leisegang[1,4], Marcel H. Schulz[3,4], Ralf P. Brandes[1,4]

[1] *Goethe University Frankfurt, Institute for Cardiovascular Physiology, Frankfurt am Main, Germany*
[2] *Goethe University Frankfurt, Institute for Organic Chemistry and Chemical Biology, Frankfurt am Main, Germany*
[3] *Goethe University Frankfurt, Institute of Cardiovascular Regeneration, Frankfurt am Main, Germany*
[4] *Deutsches Zentrum für Herz-Kreislaufforschung (DZHK), Partner site Frankfurt Rhein-Main, Frankfurt am Main, Germany*

Question:
Formation of RNA:DNA:DNA triple helices (triplex) is a novel mechanism by which the epigenetic landscape of the cell can be modulated. It remains unclear, however, whether triplex formation directly contributes to human physiology and disease. We hypothesise that genetic variation in non-coding transcripts has the potential to disrupt triplex formation, and therefore contribute to individual traits and diseases detectable in genome-wide association studies.

Methods:
Large-scale prediction of triplex interactions between human RNAs and gene regulatory elements, using our published method TriplexAligner, identified triplex-forming regions of transcripts as well as their target genes. Disease- and trait-relevant single nucleotide polymorphisms (SNPs) from the NHGRI GWAS Catalogue were mapped onto triplex-forming regions. Disease-relevance of triplex SNPs and predicted target genes were compared to stratify triplex interactions with potential relevance to disease.

Results:
TriplexAligner was used to predict triplex targets of 962 SNP-harbouring human lncRNAs. For each lncRNA, the number of predicted target genes ranged from 1 to more than 10 000. Those RNAs with SNPs located in predicted triplex-forming regions were subjected to further analysis. Disease and trait associations of the SNP were compared to ontologies of predicted triplex target genes, identifying potential triplex networks. One example of this was a SNP associated with red blood cell count in the triplex-forming region of the transcript *RP11.936I5.1*, which was predicted to bind at the promoter of *ARID1B* - a key regulator of erythropoiesis.

Conclusions:

SNPs in triplex-forming regions of human RNAs may lead to aberrant target gene expression, and therefore represent a novel mechanism by which non-coding genetic variation contributes to human traits or diseases.

B 07-14
Uremic toxin-induced damage of the endothelial surface is mediated by the Aryl hydrocarbon receptor (AhR) in CKD

Nadina Kompalla[1], Johannes Holle[3], Hendrik Bartolomaeus[4], Kristina Kusche-Vihrog[1,2], Benedikt Fels[1,2]

[1] *University of Luebeck, Institute of Physiology, Lübeck, Germany*
[2] *DZHK (German Research Centre for Cardiovascular Research), Hamburg/Lübeck/Kiel, Germany*
[3] *Charité - Universitätsmedizin, Department of Pediatrics, Division Gastroenterology, Nephrology and Metabolic Medicine, Berlin, Germany*
[4] *Experimental and Clinical Research Center, a joint cooperation of Max Delbruck Center for Molecular Medicine and Charité - Universitätsmedizin, Berlin, Germany*

Question

Cardiovascular disease has been shown to be the leading cause of death in patients with chronic kidney disease (CKD) [1]. It is known that the nanomechanical properties and function of the endothelial cell (EC) surface are involved in the proposed pathomechanism. We could demonstrate a damage of the endothelial glycocalyx (eGC) and stiffening of the underlying actin-rich cortex after EC *in vitro* treatment with sera from CKD patients [2]. As these changes of the endothelial surface structure correlated with a reduced release of nitric oxide [3], they can be seen as hallmark for endothelial dysfunction.

Since the uremic toxins indoxyl sulfate (IS) and p-cresyl-sulfate (PCS) are elevated in the sera of CKD patients, the aim of this study was to reveal their specific impact on the endothelial nanomechanics and endothelial surface damage. Furthermore, the effects of the aryl hydrocarbon receptor (AhR) antagonist CH223191 (CH) on the endothelium were studied, as IS was already shown to be one of its activators [4].

Methods

Primary Human Umbilical Vein Endothelial Cells (HUVEC) were cultured with different concentrations of IS (250µM, 500µM, 750µM) and PCS (100µM, 250µM, 500µM). Measurements of the cortex and glycocalyx stiffness were performed using atomic force microscopy (AFM). Effects on nanomechanics were validated by fluorescence staining with wheat germ agglutinin (WGA) and Phalloidin-TRITC. In a second series, HUVEC were treated with IS in combination with CH.

Results

After *in vitro* treatment of HUVEC with IS (500µM), the cortical stiffness was increased by approx. 16% (IS: 0.94±0.18pN/nm, control: 0.82±0.14pN/nm). Under the same conditions, the height of the eGC was reduced by approx. 11% (IS: 177.8±77.6nm, control: 198.9±82.6nm) and the stiffness of the eGC was increased by approx. 19% (IS: 0.41±0.17pN/nm, control: 0.34±0.13pN/nm).

Specific inhibition of AhR with CH prevented the IS effect on the cortex (control: 0.82±0.14pN/nm, IS: 0.95±0.18pN/nm, IS+CH: 0.89±0.16pN/nm). However, CH treatment did not decrease the EC stiffness to control level. In addition, AhR-inhibition mitigated the IS-effects on the eGC height (control: 140.1±43.8nm, IS: 118.1±36.0nm, IS+CH: 136.1±44.6nm) and eGC stiffness (control: 0.34±0.09pN/nm, IS: 0.37±0.09pN/nm, IS+CH: 0.33±0.09pN/nm).

Conclusions

These results indicate structural damage of the endothelial surface *in vitro* after treatment with the uremic toxin IS which can be partially prevented by CH treatment of the cells.

These data let assume that the AhR is a major modulator of the IS-induced damage of the endothelial surface.

References
[1] Jaradat MI, Molitoris BA. Cardiovascular disease in patients with chronic kidney disease. Semin Nephrol. 2002 Nov;22(6):459-73. doi: 10.1053/snep.2002.35964. PMID: 12430090.
[2] Fels B, Beyer A, Cazaña-Pérez V, Giraldez T, Navarro-González JF, Alvarez de la Rosa D, Schaefer F, Bayazit AK, Obrycki Ł, Ranchin B, Holle J, Querfeld U, Kusche-Vihrog K. Effects of Chronic Kidney Disease on Nanomechanics of the Endothelial Glycocalyx Are Mediated by the Mineralocorticoid Receptor. Int J Mol Sci. 2022 Sep 13;23(18):10659. doi: 10.3390/ijms231810659. PMID: 36142571; PMCID: PMC9503126.

[3] Fels J, Kusche-Vihrog K. Endothelial Nanomechanics in the Context of Endothelial (Dys)function and Inflammation. Antioxid Redox Signal. 2019 Mar 1;30(7):945-959. doi: 10.1089/ars.2017.7327. Epub 2018 Mar 22. PMID: 29433330; PMCID: PMC6354603.
[4] Lano G, Burtey S, Sallée M. Indoxyl Sulfate, a Uremic Endotheliotoxin. Toxins (Basel). 2020 Apr 5;12(4):229. doi: 10.3390/toxins12040229. PMID: 32260489; PMCID: PMC7232210.

B 07-15
Endothelial cytochrome P450 reductase-derived cholesterol limits angiogenesis

Pedro Malacarne[1], Niklas Müller[1], Melina Lopez[1], Stefan Günther[2], Dieter Lütjohann[3], Timothy Warwick[1], Ralf Brandes[1], Flávia Rezende[1]

[1] Goethe Universität, Institute for Cardiovascular Physiology, Frankfurt, Germany
[2] Max Planck Institute for Heart and Lung Research, Bad Nauheim, Germany
[3] University of Bonn, Institute of clinical Chemistry and clinical Pharmacology, Bonn, Germany
[4] Institute für Kardiovaskuläre Physiologie, Frankfurt, Germany

Objective: Cholesterol is an important membrane constituent and is involved in cell signaling. Cellular cholesterol is determined by uptake and de novo synthesis. Endothelial cells are capable of cholesterol metabolism through a pathway that requires the cytochrome P450 reductase (POR) as well as cyp51 monoxygenase. High circulating cholesterol is linked to cardiovascular diseases. The role of endogenous cholesterol synthesis for endothelial function, in contrast, is unknown and was studied here.
Methods & Results: To induce a loss of cholesterol synthesis in endothelial cells, POR and Cyp51 knockout was performed in human umbilical vein endothelial cells (HUVECs) and an endothelial-specific tamoxifen-inducible POR knockout mouse (ecPOR-/-) was generated.
Knockout of POR in HUVEC led to an accumulation of the Cyp51 substrate lanosterol, whereas its product, desmosterol was reduced. Functionally, this was associated with increased basal and VEGF-stimulated angiogenic sprouting. Similarly, endothelial sprouting from aortic segments was increased in ecPOR-/- mice as compared to control mice. Importantly, this effect was also observed in vivo as retina angiogenesis was increased after endothelial-specific deletion of POR.
Cellular cholesterol levels are sensed by the SREBP2 (sterol regulatory element-binding proteins) system, and indeed, SREBP2 signalling was increased after deletion of POR in cultured cells as well as in vivo. Analysis of publicly available SREBP2 CHIP-seq data from statin treated mice show a high correlation between cholesterol metabolism and NOTCH signaling. RNAseq of CRISPR POR knockout HUVEC showed significant changes in cholesterol genes (ABCG1, DHCR24, and CYP26B1). Meanwhile, RNAseq of whole aorta as well as isolated aortic endothelial cells revealed a significant decrease in Notch signaling genes (Notch2, Ep300, Rbpj and Psenen). Functionally, this should lead to increased proliferation and a tip cell phenotype in ecPOR-/-, as we indeed observed.
Conclusion: Inhibition of the endothelial POR/CYP-axis improves endothelial cell angiogenic function through an activation of the SREBP2 system and subsequent tip cell specification.

B 08 | Synapses, Neurons & Glia

B 08-01
10x Cryo-Expansion Microscopy of Primary Oligodendrocyte Progenitor Cell Growth Cones

Annika Haak[1], Max Halupczok[1], Irmgard D. Dietzel[2]

[1] Ruhr-Universität Bochum, RUBION - AG Nanoskopie, Bochum, Germany
[2] Ruhr-Universität Bochum, Department of Biochemistry II - Electrobiochemistry of Neural Cells, Bochum, Germany

Unlike neural growth cones, the growth cones of oligodendrocyte progenitor cells (OPCs) have not yet been extensively investigated. Although various proteins, which regulate process dynamics have been identified, the cell physiological mechanisms leading to membrane propulsion and retraction are not fully understood. Especially, smaller structures of sizes below 200 nm such as filopodia and lamellipodia cannot be resolved with diffraction-limited light microscopy. On the other hand, the relative localization of more than one type of protein cannot be

detected using electron microscopy. During the last years, the invention of expansion microscopy (ExM) has enabled super-resolution fluorescence microscopy on conventional diffraction-limited microscopes. Furthermore, this method can be combined with most established labeling methods. One of the disadvantages of ExM is that it can only image fixed samples, which may suffer from fixation artifacts and only represent a single point in time. Here we applied a novel 10x cryofixation ExM protocol, which minimizes fixation artifacts. Using this method we imaged the cytoskeleton within the growth cones of OPCs. Before applying our ExM protocol we also acquired time lapse images to be able to distinguish between extending and retracting processes. In this manner, we were able to image filopodia, lamellipodia, microtubules and actin filaments of retracting and proceeding growth cones with resolutions of about 50 nm.

B 08-02
Proteomic and Metabolomic Assessment of Lipopolysaccharide-induced Inflammation in Cellular Metabolism of Brain Microglia

Canelif Yilmaz[1,2], Evangelia Thanou[3], Eleftheria Karadima[2], Mirko Peitzsch[2], Ka Wan Li[3], Vasileia Ismini Alexaki[2]

[1] Technische Universität Dresden, Institut für Physiologie, Dresden, Germany
[2] Universitätsklinikum Carl Gustav Carus Dresden, Institut für Klinische Chemie und Laboratoriumsmedizin, Dresden, Germany
[3] Vrije Universiteit Amsterdam, Center for Neurogenomics and Cognitive Research, Department of Molecular and Cellular Neurobiology, Amsterdam, Netherlands

Innate immune cells function as a fast acting, nonspecific defense against invading pathogens. Upon detection of pathogenic stimuli, they respond by secreting cytokines to drive inflammation and recruit the adaptive immune cells, secrete bacteriotoxic reactive oxygen species (ROS) and nitric oxide (NO), and phagocytose the pathogens to eliminate the threat. All of these processes greatly increase the energy expenditure of the cell, and therefore are coupled with changes in the cellular metabolic processes. In activated macrophages, numerous changes have been reported, such as the switch from Oxidative Phosphorylation (OxPhos) to glycolysis, which enables the cells to produce ATP at a higher rate, and also the disruption of the TCA cycle after induction of ACOD1 (Aconitate Decarboxylase 1) expression. Furthermore, activated macrophages express NOS2 (Nitric Oxide Synthase 2), whose activity drives changes in the aspartate-argininosuccinate shunt, pentose phosphate pathway and arginine metabolism[1-3].
Although the cellular metabolic changes in peripheral immune cells have been widely researched, the cellular metabolic changes observed in activated brain microglia, the tissue resident macrophages of the central nervous system have not been well studied. While there is some research on cellular metabolism of microglia, it is mostly performed *in vitro*, on cell lines or primary microglia cultures, which often poorly reflect the true conditions observed *in vivo*. Several phenomena observed in macrophages, such as the metabolic switch to glycolysis, and NO production related changes were also observed in microglial cells *in vitro[4]*.
Here we wanted to address whether cellular metabolic changes occurred in activated brain microglia *in vivo*. To this end, we have used the LPS-induced neuroinflammation model, and we have sorted activated brain microglia using FACS or MACS. 6 or 24h after intraperitoneal LPS injection, we have FACS sorted microglia and performed proteomics. We have observed some small changes 6h after injection, namely a dysregulation of amino sugar metabolism, and an upregulation of mRNA transcription and interleukin production. At 24h after injection, we have observed further changes, characterized by an upregulation of mitochondrial processes, mainly an increase in OxPhos proteins, and further increases in TCA cycle, Amino Acid Metabolism and Fatty Acid Metabolism proteins were observed. We have then performed untargeted metabolomics and Seahorse XF assays on MACS-sorted microglia at 24 hours after LPS injection. With untargeted metabolomics, we have observed most importantly an increase in carnitines, supporting the changes observed in Fatty Acid Metabolism proteins, and differential regulation of several additional pathways. Finally, Seahorse XF assay, revealed that LPS activation increased the basal respiration, ATP production and maximal respiration capacity of microglia, again confirming our findings in proteomic analyses.

This project has received funding from the European Union's Horizon 2020 research and innovation programme under the Marie Skłodowska-Curie grant agreement No 765704.

References
[1] Gaber, T., C. Strehl, and F. Buttgereit, *Metabolic regulation of inflammation.* Nat Rev Rheumatol, 2017. **13**(5): p. 267-279.

[2] O'Neill, L.A.J. and M.N. Artyomov, *Itaconate: the poster child of metabolic reprogramming in macrophage function.* Nature Reviews Immunology, 2019. **19**(5): p. 273-281.
[3] Gauthier, T. and W. Chen, *Modulation of Macrophage Immunometabolism: A New Approach to Fight Infections.* Frontiers in Immunology, 2022. **13**.
[4] Lauro, C. and C. Limatola, *Metabolic Reprograming of Microglia in the Regulation of the Innate Inflammatory Response.* Frontiers in Immunology, 2020. **11**.

B 08-03
THIK-1 controls microglial interleukin-1ß release in the human brain

Ali Rifat[1], Bernardino Ossola[2], Kevin Doyle[2], Mark B. Carlton[2], Nicola L. Brice[2], Roland W. Bürli[2], Lee A. Dawson[2], Jörg R.P. Geiger[1], Christian Madry[1]

[1] *Charité - Universitätsmedizin Berlin, Institute of Neurophysiology, Berlin, Germany*
[2] *Cerevance Ltd, Cambridge, UK*

The TWIK-related Halothane-Inhibited K^+ channel 1 (THIK-1) regulates ATP-evoked release of pro-inflammatory interleukin-1ß (IL-1ß) from rodent microglia. IL-1ß is involved in many neuroinflammatory brain pathologies, hence pharmacological inhibition of THIK-1 is considered to have high therapeutic potential. Release of IL-1ß depends on the activation of the NLRP3 inflammasome. As a key signaling event, this requires a sharp drop in intracellular potassium concentration via K^+ efflux, in which THIK-1 is presumably involved, but the mechanism of which is still unknown. Current mechanistic concepts of NLRP3 activation have so far mainly relied on artificial cell lines or cultured macrophages or microglia from rodent models. Therefore, to derive therapeutic options for humans, these processes need to be studied in microglia embedded in their natural environment in the human brain. Here, using a novel, selective inhibitor of THIK-1, we investigate the involvement of THIK-1 for NLRP3-dependent release of IL-1ß in human brain slices of acutely resected temporal lobe. Using whole-cell patch-clamp electrophysiology, we characterize the electrical membrane properties of microglia in human brain slices and examine the role of THIK-1 as a K^+ efflux mechanism underlying the ATP-triggered activation of NRLP3 in human microglia.

B 08-04
Microglia contribute to full maturation of glutamatergic networks but are dispensable for pruning of synapses during hippocampal development

Michael Surala[1], Luna S. Zdravkovic[1], Ali Rifat[1], Koliane Ouk[2], Claire Pridans[3], Imre Vida[4], Josef Priller[2,5], Christian Madry[1]

[1] *Charité – Universitätsmedizin Berlin, Corporate member of Freie Universität Berlin and Humboldt Universität zu Berlin, Institute of Neurophysiology, Berlin, Germany*
[2] *Charité – Universitätsmedizin Berlin, Corporate member of Freie Universität Berlin and Humboldt Universität zu Berlin, Neuropsychiatry and Laboratory of Molecular Psychiatry, Berlin, Germany*
[3] *University of Edinburgh Centre for Inflammation Research, The Queen's Medical Research Institute, Edinburgh, UK*
[4] *Charité – Universitätsmedizin Berlin, Corporate member of Freie Universität Berlin and Humboldt Universität zu Berlin, Institute for Integrative Neuroanatomy, Berlin, Germany*
[5] *UK Dementia Research Institute at University of Edinburgh, Edinburgh, UK*

Microglia, the tissue-resident macrophages of the brain, are believed to sculpt developing neural circuits by eliminating excessive synapses in a process called synaptic pruning, removing apoptotic neurons, and promoting neuronal survival. To elucidate the role of microglia during embryonic and postnatal brain development, we used a mouse model deficient in microglia throughout life as a consequence of deletion of the fms-intronic regulatory element (FIRE) in the *Csf1r* locus. Surprisingly, young adult $Csf1r^{\Delta FIRE/\Delta FIRE}$ mice displayed no changes in excitatory synapse number and spine density and length of CA1 hippocampal pyramidal neurons compared to $Csf1r^{+/+}$ littermates. However, hippocampal neurons were less excitable and received less excitatory input from the CA3 region, indicating weakened excitatory neurotransmission in $Csf1r^{\Delta FIRE/\Delta FIRE}$ mice. This is corroborated by a lack of synaptic multiplicity and postsynaptic NMDA receptor hypofunction, suggesting immaturity of glutamatergic synapses. These changes mirror the electrophysiological profile that results from acute microglial depletion in adult mice that had undergone normal development. Thus, our findings challenge the prevailing view that microglia are indispensable for the establishment of neural networks during development.

B 08-05
A molecular definition of the readily-retrievable pool at presynaptic terminals

Lakshmi Penothil Sunil[1,2,3], Sai Krishnan[1,3], Julia Lehrich[1,3], Yaroslav Tsytsyura[1,3], Nataliya Glyvuk[1,3], Jürgen Klingauf[1,2,3]

[1] *Institute of Medical Physics and Biophysics, Muenster, Germany*
[2] *CiM-IMPRS Graduate Program, Muenster, Germany*
[3] *Universitätsklinikum Münster, Muenster, Germany*

Synaptic vesicles (SVs) are released at active zones (AZ), and SV constituents are retrieved by compensatory endocytosis at distinct sites called peri-active zones (periAZ). Although various modes of SV recycling have been put forward, clathrin-mediated endocytosis (CME) appears predominant under physiological stimulation paradigms. De novo generation of release-competent SVs is too slow to balance SV fusion rates. Therefore, neurons expedite this process by sorting previously exocytosed SV components in a process called release site clearance (RSC) and further organizing them into preformed patches called the readily-retrievable pool (RRetP), which waits for a trigger to proceed. Whilst the modest speed advantage is beneficial, the main advantage of a tightly controlled system is the sorting fidelity achieved at steady-state. Previously, SV cargo was shown to be part of the RRetP but their molecular state remains speculative. The small size of vertebrate synaptic boutons has hampered direct observation of the spatio-temporal dynamics of exo-endocytosis. To overcome this, we developed 'xenapses', purely presynaptic boutons formed on micropatterned coverslips, that provide an advantage owing to their size, TIRF amenability, and the absence of apposed post-synapses. Ultrastructural studies in xenapses show stably decorated clathrin structures, a preliminary indication of clathrin being associated with the RRetP.

The presence of distinct AZ and periAZ in xenapses was exploited to study the sorting of one of the SV components, Synaptobrevin2 (Syb2) by its cargo-specific adaptor, AP180. Combining super-resolution and TIRF microscopy, we revealed a population of AP180 stably enriched at the periAZ at rest. Upon stimulation, free AP180 from the cytosol translocates first to the AZ, and later along with exocytosed Syb2 to the periAZ. This is hampered in AP180 mutants with reduced affinity for Syb2, confirming previous biochemical data and **corroborating the notion of AP180 as an important RSC factor**.

To pinpoint the stage of RRetP arrest, we dissected the spatio-temporal recruitment signatures of various molecular players involved in constitutive CME and compared them to our studies of compensatory endocytosis. This included investigating adaptor protein 2 (AP2), Fer/Cip4 homology domain-only proteins (FCHO), epidermal growth factor pathway substrate 15 (EPS15), Intersectins, Sorting nexin 9 (SNX9), Epsin1, Amphiphysin1, Dynamin1, and F-actin. We conclude that **in addition to SV components, the RRetP is composed of clathrin, generic and cargo-specific adaptor proteins, and proteins supporting domed clathrin-coated structures (CCS)**. N-Bar proteins, dynamin, and actin are recruited to endocytic spots following the trigger. Incidentally, this favors the ability of preformed low curvature CCS to transition into highly curved pits before scission. Our xenaptic system thus provides a platform for visualizing molecular events during RSC and exo-endocytosis.

B 08-06
Microglia modulate gamma oscillatory network activity by P2Y12 receptor-mediated purinergic signaling

Ecem Tütüncü, Zoltan Gerevich, Christian Madry

Charite Universitätsmedizin Berlin, Institute of Neurophysiology, Berlin, Germany

Microglia continuously survey the brain parenchyma with their highly dynamic cellular processes. Due to their ability to sense neuronal activity, this enables them to rapidly establish functional interactions with neural structures, which is thought to contribute to brain homeostasis. By monitoring the functional state of synapses, microglia can induce changes in synaptic transmission, excitability and plasticity of neurons. However, the mechanisms by which microglia detect and respond to changes in neuronal activity, and how this affects network function are still poorly understood. Here we investigate the morphological and functional interactions between microglia and hippocampal neurons elicited by gamma oscillatory network activity, a hallmark of the hippocampal network implicated in higher cognitive functions such as memory formation and sensory processing. We show that kainate-induced gamma oscillations in acute brain slices are sensed by microglia by increasing their spatial interactions with parvalbumin positive interneurons, a key determinant in the generation of gamma activity, compared

to non-oscillatory control conditions. We further identify that this interaction is regulated by microglial P2Y12 receptors, which act as a purinergic sensor of increases in neuronal activity. Blockade of P2Y12 receptors causes an increase in the power of gamma oscillations, which is mechanistically related to changes in adenosine levels and signaling via adenosine receptors. Our findings suggest a bidirectional communication between neuronal structures and activity-recruited microglia to modulate network function in the gamma frequency range, which may have implications on hippocampus-dependent spatial memory formation.

Supported by a research stipend of the Sonnenfeld Foundation to E.T.

B 08-07
Human synapses on artificial substrate

Alexander Ivanenko[1,2,3], Julia Lehrich[1,2], Nataliya Glyvuk[1,2], Jaroslav Tsytsyura[1,2], Jürgen Klingauf[1,2,3]

[1] University of Münster, Institute of Medical Physics and Biophysics, Münster, Germany
[2] Universitätsklinikum Münster, Institute of Medical Physics and Biophysics, Münster, Germany
[3] CiM-IMPRS Graduate Program, Münster, Germany

Presynaptic boutons induced on artificial substrate (Xenapses), allow detailed investigation of synaptic transmission using TIRF (Total Internal Reflection Fluorescence) microscopy. Originally the technique of Xenapse induction was developed for mouse primary neurons. However, using only primary neuron cultures imposes a limitation on neuronal phenotypes being used: many neuronal phenotypes highly demanded in translational biomedical research (e.g. dopaminergic and serotonergic neurons) are notoriously difficult to isolate due to their low abundance in the brain.

We extended the Xenapse induction technique to human neurons derived from induced pluripotent stem cells (IPSCs). Stem cell reprogramming methods allowderivation of many neuronal phenotypes thus removing the limitation imposed by the usage of primary neuronal cultures. Moreover, applying Xenapse induction to patient-specific neurons enables translational research of human neurological diseases related to synaptic dysfunction (e.g. Parkinson's disease). Stem cell lines designed to constitutively express Cas9/dCas9 proteins allow to do multiple disease-related presynaptic genes knockout/knockdown in acute manner. Additionally, for the neurons releasing oxidizible neurotransmitter (e.g. dopamine) TIRF imaging can be combined with amperometric detection of exocytic events.

IPSCs are converted to neurons by the transduction of neurogenic factors and then transferred to glass coverslips, functionalized with synaptogenic proteins. By means of immunocytochemistry and electron microscopy we show that induced neurons can form functional Glutamatergic and GABAergic Xenapses on the functionalized substrate. As a proof of concept, using dCas9-expressing stem cell line, we generated human Xenapses with conditional α-synuclein knockdown allowing investigation of the normal physiological function of the protein and its role in neurological disorders.

B 08-08
Distinct GABAergic Modulation of Spike Timing-Dependent Plasticity in Mouse CA1 Pyramidal cells across the Longitudinal Axis of the Hippocampus

Babak Khodaie[1,3], Elke Edelmann[1,2], **Volkmar Lessmann**[1]

[1] Otto-von-Guericke University, Institute of Physiology, Magdeburg, Germany
[2] Christian-Albrechts-Universität, Institute of Physiology, Kiel, Germany
[3] Ruprecht-Karls-Universität, Institute of Physiology, Heidelberg, Germany

The hippocampus, along with its associated medial temporal lobe structures, develops as a complex micro-network of excitatory and inhibitory synapses to facilitate the processing of learning and the formation of memories. The longitudinal axis of the hippocampus extends from the dorsal to the ventral pole, each showing distinct involvement in spatial and emotional learning processes. Throughout this axis, various

receptors such as GABA, glutamate, and neuromodulatory transmitter receptors are expressed in different patterns, offering diverse mechanisms for regulating synaptic activity. GABAergic inhibition plays a crucial role in balancing the excitatory responses and the release of neuromodulatory transmitters. The expression of $GABA_A$ and $GABA_B$ receptors varies along the longitudinal axis, potentially resulting in differential modulation of synaptic plasticity through this diverse GABAergic inhibition.
STDP is a paradigm based on precise ms delays of action potentials (APs) in pre- and postsynaptic neurons. Patch clamp recorded CA1 neurons were subjected to canonical (1 presynaptic: 1 postsynaptic AP) or burst t-LTP protocols (1:4), repeated 6 times at 0.5 Hz in acute mouse hippocampal slices taken from dorsal (DH), intermediate (IH), or ventral (VH) hippocampus to test timing-dependent LTP (t-LTP) induction under diverse settings for GABAergic inhibition. We used either intact GABAergic inhibition, fully blocked inhibition using co-applied $GABA_AR$ (100µM picrotoxin) and $GABA_BR$ antagonists (10µM CGP55845), or recorded in the presence of only picrotoxin.
In our study, we observed an intricate relationship between excitatory and inhibitory responses that varied depending on the type of stimulation protocols (canonical or burst) and the specific regions under investigation (DH or VH). Interestingly, when using the 6x 1:1 protocol, we observed that the dependency on GABAergic signaling was diminished in inducing strong t-LTP from DH to VH pole. However, with our 6x 1:4 protocol, we found that active $GABA_BR$ signaling played a significant role during the induction of t-LTP.

Funding for this study was provided by: Federal State Saxony-Anhalt and the European Structural and Investment Funds (ESF, 2014-2020) (ZS/2016/08/80645) (ABINEP); DFG (ED 280/1-1, SFB779/B06, CRC1436/A06); Federal State of Saxony-Anhalt and the European Regional Developmental Fund (ERDF 2014-2020), Project: Center for Behavioral Brain Sciences (CBBS) (FKS: ZS/2016/04/78113).

B 08-09
Dynamin disruption acutely alters synaptic morphology

Robert Jacobi[1], Sven Dannhäuser[1], Achmed Mrestani[1,2], Manfred Heckmann[1]

[1] *University of Wuerzburg Institute of Physiology, Neurophysiology, Würzburg, Germany*
[2] *University of Leipzig Medical Center, Neurology, Leipzig, Germany*

Synaptic transmission represents the basis of information processing in animal nervous systems. Chemical synapses operate by exocytosis of neurotransmitters which then bind to postsynaptic receptors and elicit downstream reactions with subsequent presynaptic endocytosis being critical for the recovery of vesicle pools and enabling sustained transmission.
The Drosophila mutant shi^{ts1} [1] shows a temperature dependent block of endocytosis through inhibition of Dynamin GTPase function [2] and allows for analysis of synaptic transmission and morphology at the neuromuscular junction of third instar larvae during this disrupted state. Using Structured Illumination Microscopy (SIM) of PFA fixed larval filets we found a significant increase in distal synaptic Ib bouton area and presynaptic active zone (AZ) number per Ib bouton while still maintaining the previously described size differentiation along the bouton chain [3]. An observed decrease in bouton number per synaptic branch with unchanged total number of branches and active zones per branch implies fusion of boutons. “In vivo” Imaging of unfixed preparations of shi^{ts1} larvae expressing CD8::GFP in release promoting high [K+] HL3 also showed an increase in bouton area and signs of fusion, though not to the extent of fixed filets. We will use High-Pressure-Freezing as an alternative to formaldehyde fixation to more accurately describe the shi^{ts1} phenotype.
In order to elucidate AZ structure, we employed *d*STORM (direct stochastic optical reconstruction microscopy) imaging revealing an accumulation of the ELKS/CAST homolog Bruchpilot [4] and Unc13A outside of AZs in turn indicating a dysregulation of AZ cohesion during endocytic arrest. These results enable us to investigate potential dynamin dependent regulators of AZ integrity such as actin remodeling, either through direct [5] or indirect interaction with dynamin, membrane dynamics or vesicle pools.

We thank S. Sigrist for the Unc13A antibody and M. Oppmann and F. Köhler for their technical assistance.

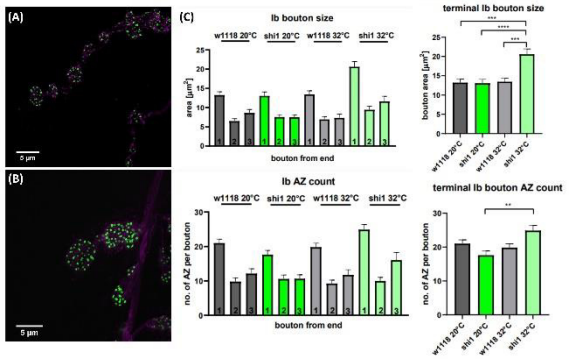

Bouton area and active zone (AZ) number increase at non permissive temperatures
(A) shi^{ts1} at 20°C and (B) shi^{ts1} with 10min of incubation at 32°C; Structured Illumination Microscopy (SIM) of third instar larval NMJs (α-hrp: magenta, Brp^{Nc82}: green)
(C) SIM of w1118 and shi^{ts1} shows terminal Ib bouton area and AZ number increase significantly at 32°C; the previously described size differentiation from distal to proximal Ib boutons (Paul et al. 2015) is maintained (p<0.01: **, p<0.001:***, p<0.0001:****)

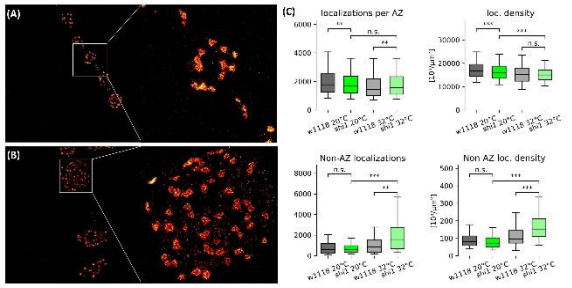

Brp accumulates outside of AZs at non permissive temperatures
(A) w1118 with 10 min of incubation at 32°C and (B) shi^{ts1} with 10 min of incubation at 32°C; direct stochastic optical reconstruction microscopy (*d*STORM) images of third instar larval NMJs show a visible accumulation of brp localizations outside of AZs (Brp^{Nc82}: red)
(C) further analysis of *d*STORM data using HDBSCAN implies decrease in both AZ localizations and density and shows significant increase in Non-AZ localizations and Non-AZ localization density

References
[1] Grigliati TA, Hall L, Rosenbluth R, Suzuki DT 1973, 'Temperature-sensitive mutations in Drosophila melanogaster. XIV. A selection of immobile adults', *Molecular Genetics and Genomics*, 120, 107-114
[2] van der Bliek AM, Meyerowitz EM 1991, 'Dynamin-like protein encoded by the Drosophila shibire gene associated with vesicular traffic', *Nature*, 351(6325), 411-414
[3] Paul MM, Pauli M, Ehmann N, Hallermann S, Sauer M, Kittel RJ, Heckmann M 2015, 'Bruchpilot and Synaptotagmin collaborate to drive rapid glutamate release and active zone differentiationf', *Frontiers in Cellular Neuroscience*, 9, 29
[4] Kittel RJ, Wichmann C, Rasse TM, Fouquet W, Schmidt M, Schmid A, Wagh DA, Pawlu C, Kellner RR, Willig KI, Hell SW, Buchner E, Heckmann M, Sigrist SJ 2006, 'Bruchpilot promotes active zone assembly, Ca2+ channel clustering, and vesicle release', *Science*, 312, 1051-1054
[5] Zhang R, Lee DM, Jimah JR, Gerassimov N, Yang C, Kim S, Luvsanjav D, Winkelman J, Mettlen M, Abrams ME, Kalia R, Keene P, Pandey P, Ravaux B, Kim JH, Ditlev JA, Zhang G, Rosen MK, Frost A, Alto NM, Gardel M, Schmid SL, Svitkina TM, Hinshaw JE, Chen EH 2020, 'Dynamin regulates the dynamics and mechanical strength of the actin cytoskeleton as a multifilament actin-bundling protein', *Nature Cell Biology*, 22(6), 674-688

B 08-10
Identification and functional characterization of distinct phenotypes in complexin N-terminus domain

Estelle Toulme, Christian Rosenmund, Thorsten Trimbuch

Charite Universitatsmedizine, Neurophysiologie, Berlin, Germany

The release of neurotransmitters at central synapses involves a cascade of proteins that ultimately enable the fusion of synaptic vesicles with the presynaptic plasma membrane. A key step in synaptic vesicle fusion is the formation of a tripartite interface corresponding to the assembly of the SNARE (Soluble N-ethylmaleimide sensitive factor Attachment protein REceptor) protein complex with the calcium sensor Synaptotagmin and the activator/regulator complexin[1]. Complexins (Cpx) are small (18 kDa) cytosolic proteins that can bind to the SNARE complex. Complexin consists of 4 domains: the NTD (N-Terminal Domain), the accessory domain, the central domain and the CTD (C-Terminal domain)[2]. Despite extensive studies, the role played by complexins as a synaptic transmission regulator remains incompletely defined. In the present study, we used site directed mutagenesis of the NTD, in the context of molecular replacement in Cpx knock-out neurons, to show that not only this domain is important for the activation of the calcium-triggered release but also for synaptic vesicle fusogenicity. Through a combination of electrophysiological recordings in hippocampal autaptic neurons, immunocytochemistry and biochemistry, we identified several relevant release phenotypes at independent sites in the first 26 amino acids that constitute the NTD of Cpx. More specifically, we focused on position D15, confirming that is critical for spontaneous release of neurotransmitter and more surprisingly that this site affects the size of the

readily-releasable pool. Overall, our results further demonstrate the wide regulation of synaptic vesicle fusion and therefore synaptic transmission by complexin.

References
[1] *Zhou et al, Nature 2017*
Trimbuch and Rosenmund, Nat Rev Neurosci. 2016

B 08-11
Fast synaptic vesicle docking and re-arrangement of the vesicle cluster after short stimuli

Junxiu Duan[1,2,3], Julia Lehrich[1,3], Yaroslav Tsytsyura[1,3], Nataliya Glyvuk[1,3], Jürgen Klingauf[1,2,3]

[1] *Institute of Medical Physics and Biophysics, Münster, Germany*
[2] *CiM-IMPRS Graduate Program, Münster, Germany*
[3] *Universitätsklinikum Münster, Münster, Germany*

In synapses replenishment of the readily releasable pool by physical movement and docking of synaptic vesicles (SVs) to the plasma membrane (PM) is essential for maintaining synaptic transmission. While the kinetics of fusion and repriming can be measured electrophysiologically, the kinetics of re-docking can be inferred only very indirectly. The inferred repriming rate constants, however, could reflect both priming from an already docked state or docking and subsequent priming. In the Calyx of Held repriming can be as fast as 50 ms, raising the question, whether such fast rates could involve SVs that are not yet docked.
Here we used cultured hippocampal 'xenapses', purely presynaptic boutons formed by neurons on micropatterned coverslips, functionalized with synaptogenic cell adhesion proteins. Xenapses expressing synaptophysin-EGFP (syp1-EGFP) as well as pH-sensitive syp1-mScarlet (as exocytosis reporter) were subjected to stimulated total internal reflection fluorescence recovery after photobleaching (TIR-FRAP): after bleaching a large fraction of syp1-EGFP in docked and primed vesicles with a short high intensity laser pulse xenapses were stimulated with 5 action potentials (100 Hz) at various intervals. This elicited a marked step-like increase in fluorescence at sites of exocytosis, detected by mScarlet, within 30 – 40 ms. When omitting the bleaching pulse, a stimulated rise in EGFP fluorescence should reflect both, flattening of the fusing SV membrane resulting in a 20 nm net movement towards the PM, as well as re-docking. Such control experiments revealed the same rapid increase, indicating that SV flattening and re-docking have similar kinetics. A stimulation-induced increase could still be observed as late as 4 min after photobleaching. However, this increase was more transient in nature, indicating that most of the intensity increase was caused by SV flattening and not re-docking. Our results indicate that SVs are swiftly replaced after fusion, supporting the view of a fixed number of available slots or release sites. The measured re-docking time of about 30 ms thus provides a lower bound for the refractoriness of a given release site. In electron micrographs SVs appear to be interconnected by short tethers. Thus, our results are in line with the notion that fusing SVs simply pull SVs of the second row to the PM while collapsing.

B 09 | Neuronal Networks

B 09-01
Development of prefrontal afferents in health and disease

Malte F. Stelzer, Anne Günther, Jastyn Pöpplau, Ileana Hanganu-Opatz

Institute of Developmental Neurophysiology, Center for Molecular Neurobiology Hamburg, Hamburg, Germany

The medial prefrontal cortex (mPFC) is one of the most interconnected brain regions, receiving direct axonal projections from most cortical and subcortical areas. By these means, the mPFC receives information on the environmental context and internal state, enabling it to orchestrate various cognitive behaviors at adult age. However, recent data suggest that afferent projections to the mPFC also play a crucial role for the development of cognitive abilities. Moreover, rodent models for neuropsychiatric disorders, such as schizophrenia and autism, show an early disruption of prefrontal afferent projection patterns (e.g. fewer projecting cells) and impaired myelination that lead to long-lasting

functional and behavioral impairments throughout life. As the developmental trajectory of prefrontal afferents as well as their interhemispheric connectivity and myelination have not been systematically investigated, we aim to provide a comprehensive timeline of multiple regional projections to the mPFC in rodents (e.g. hippocampus, thalamus, amygdala). We injected a retrograde viral fluorescent tracer for excitatory neurons into the mPFC at postnatal (P0), prejuvenile (P10), juvenile (P20), or early adult (P50) age, to label prefrontal projection neurons for confocal microscopy. Images underwent automatic cell quantification with Cellpose2 as to measure projection strength. Moreover, we combined viral labeling with myelin staining of corpus callosum to quantify the degree of myelination and interhemispheric connection strength at different ages. Experiments were carried out in C57bl6 wildtype and dual-hit genetic (G, DISC-1 (+/-)) / environmental (E, injection of Poly I:C during pregnancy) mice as a model for mental diseases. We showed that the spatial and temporal organization of prefrontal afferents is altered in dual-hit GE mice. These results will provide a comprehensive view on the dynamic formation of direct inputs to the mPFC that is the substrate for the maturation of cognitive functions in health and disease.

B 09-02
Network synchrony creates neural filters that switch brain state from navigation to sleep in *Drosophila*

Davide Raccuglia[1], **Raquel Suárez-Grimalt**[1,2], Laura Krumm[3,2], Cedric B. Brodersen[1], Anatoli Ender[1], Sridhar Jagannathan[1], Martin Krück[3], York Winter[6,2], Genevieve Yvon-Durocher[1], Richard Kempter[3,2,5], Jörg R. Geiger[1,2], David Owald[1,2,4]

[1] *Charité – Universitätsmedizin Berlin, Institute of Neurophysiology, Berlin, Germany*
[2] *Einstein Center for Neurosciences Berlin, Charité – Universitätsmedizin Berlin, Berlin, Germany*
[3] *Humboldt-Universität zu Berlin, Institute for Theoretical Biology, Berlin, Germany*
[4] *NeuroCure, Charité – Universitätsmedizin Berlin, Berlin, Germany*
[5] *Bernstein Center for Computational Neuroscience Berlin, Berlin, Germany*
[6] *Humboldt-Universität zu Berlin, Department of Biology, Berlin, Germany*

All animals require undisturbed periods of rest in which they undergo recuperative processes. However, it is currently unclear how quiescent brain states arise that are able to dissociate an animal from its external world, while retaining vigilance to salient sensory cues. Here, we describe a neural mechanism in *Drosophila* that creates neural filters that engender a quiescent brain state by generating coherent slow-wave activity (SWA) between R5 sleep-need and locomotion-promoting neural networks. Emergence of coherent activity is under circadian control and arises through interactions with the *Drosophila* sleep homeostat. Optogenetic mimicry of coherent activity reveals that temporally fine-tuned R5 oscillations reduce responsiveness to visual stimuli by rhythmically associating neural activity of locomotion-promoting cells, effectively overruling their output. On a circuit level, we find that these two networks bidirectionally regulate behavioral responsiveness by providing antagonistic inputs to downstream head direction cells. Thus, coherent oscillations provide the mechanistic basis for neural filters by temporally associating opposing signals resulting in reduced functional connectivity between locomotion-gating and navigational networks. We propose that the temporal pattern of SWA provides the structure to create a 'breakable' filter, allowing strong or salient stimuli to 'break' the neural interaction and, in contrast to comatose states, allow the animal to wake up, while maintaining body posture.

B 09-03
Behavioural classes and assembly of lateral hypothalamic neurons during synchronous and non-rhythmic states.

Mahsa Altafi[1], Changwan Chen[2,3], Kristin Weineck[4], Franziska Bender[4], Marta Carus-Cadavieco[4], Tatiana Korotkova[2,3], Alexey Ponomarenko[1,4]

[1] *Friedrich-Alexander-Universität Erlangen-Nürnberg, Institute of Physiology and Pathophysiology, Erlangen, Germany*
[2] *Max Planck Institute for Metabolism Research, Cologne, Germany*
[3] *University of Cologne, Institute for Vegetative Physiology, Faculty of Medicine, Cologne, Germany*
[4] *Leibniz Institute for Molecular Pharmacology (FMP)/ NeuroCure Cluster of Excellence, Behavioural Neurodynamics Group, Berlin, Germany*

The author has objected to a publication of the abstract.

B 09-04
Dopamine's role as a modulator of dopaminergic neuron response in *Drosophila*

Michael-Marcel Heim, David Owald

Charité Universitätsmedizin Berlin, Neurophysiologie, Berlin, Germany

Activity of dopaminergic neurons in higher animals, invertebrates and vertebrates alike, is critical for associative learning and motivation. In the fruit fly *Drosophila melanogaster*, dopaminergic neurons strongly innervate the mushroom bodies. This higher order brain center is essential for associative learning and memory. Modulation of the mushroom bodies' circuitry has been intensely studied in the context of learning. However, it is still unclear whether interactions between dopaminergic neurons are also involved in learning. To address this, we performed focal dopamine injections onto dopaminergic neurons of the mushroom bodies. Using the genetically encoded voltage indicator ArcLight, we demonstrate that applying dopamine dendritically, hyperpolarizes dopaminergic neurons. Moreover, we provide evidence that this signaling cascade is mediated by the receptor Dop2R, which likely interacts with a G protein coupled inwardly rectifying potassium channel. Our results are reminiscent of mammalian Dop2R auto-receptor signaling, indicating an evolutionarily conserved role for Dop2R signaling in learning and reward driven behavior.

B 09-05
Neuromodulatory mechanisms of rebound timing and gain control in dorsolateral striatum-projecting dopamine substantia nigra neurons

Strahinja Stojanovic, Jochen Roeper

Goethe University Frankfurt, Intitute for Neurophysiology, Frankfurt am Main, Germany

Rebound properties of dopaminergic (DA) midbrain neurons vary significantly between distinct subpopulations [1]. We identified DA neurons in the substantia nigra (SN) projecting to the dorsolateral striatum (DLS) to be unique among these DA subpopulations in vitro in displaying a spontaneous bimodal distribution of rebound timing. Rebound timing was quantified as the latency to spike after terminating a hyperpolarizing current injection (CTRL median rebound delay: 329.1 ms, n= 24, N= 7). Rebound gain was characterized by the transient post-inhibitory firing response ranging from single spike to high-frequency bursts (CTRL median rebound FR: 3.7 Hz, n= 24, N= 7). Using selective ion channel blockers, we defined the biophysical rebound control mechanisms in DLS-projecting DA SN neurons. While inhibition of Kv4, GIRK2, SK3 or K-ATP channels uniformly accelerated rebound timing in comparison to control (AmmTX3: median rebound delay: 32.3 ms, p= 0.0002, n= 14, N= 3; Tertiapin-Q: median rebound delay: 98.1 ms, p= 0.0017, n= 17, N= 3; Apamin: median rebound delay: 114.9 ms, p= 0.0015, n= 19, N= 3; Glibenclamide: median rebound delay: 105.0 ms, p= 0.001, n= 20, N= 3, respectively), inhibition of SK3 channels was most effective in increasing rebound gain (Apamin: median rebound FR: 38.04 Hz, p< 0.0001, n= 19, N= 3). In contrast, inhibition of T-type, but not L-type calcium channels removed the bimodality of rebound timing and reduced rebound gain. Furthermore, we found that various GPCRs strongly influenced the rebound properties of DLS-projecting DA SN neurons. When the endogenous activation of D2R- and GABAb-receptors was inhibited, the intrinsic bimodality of rebound timing was removed. The same outcome was seen when noradrenergic, muscarinergic and glutamatergic GPCRs were activated. In contrast to mitochondrial calcium uniporter inhibition (Ru360: median rebound delay: 408.4 ms; median rebound FR: 3.2 Hz, n= 18, N= 3) the GCPS results were phenocopied by either enhancing intrinsic calcium buffering (1 mM BAPTA: median rebound delay: 170.4 ms, p= 0.0267; median rebound FR: 12.9 Hz, p< 0.0001, n= 17, N= 4) or inhibiting the ER calcium pumps (CPA: median rebound delay: 133.7 ms, p= 0.0321; median rebound FR: 19.1 Hz, p< 0.0001, n= 16, N= 2). Therefore, we are currently exploring a projection-specific, AAV9-based approach to overexpress calbindin-D28k, a calcium-buffering protein that will allow us to decouple the T-to-SK-channel crosstalk. Our approach aims to induce rapid rebound spiking unique to DLS-projecting DA SN neurons for further in vivo investigations.

References

[1] Lammel, Stephan, et al. "Unique properties of mesoprefrontal neurons within a dual mesocorticolimbic dopamine system." *Neuron* 57.5 (2008): 760-773. APA

B 09-06
Environmental Enrichment increases GABAergic dendritic inhibition in dentate gyrus of mouse hippocampus

Stylianos Kouvaros, Ekaterina Verdiyan, Josef Bischofberger

University of Basel, Department of Biomedicine, Basel, Switzerland

Activation of inhibitory pathways in the dentate gyrus (DG) is essential for maintaining the balance between excitation and inhibition during hippocampal information processing. Somatostatin (SOM) and Parvalbumin (PV) positive GABAergic neurons are two major classes of interneurons in the DG providing strong dendritic and peri-somatic inhibition to granule cells (GCs), respectively.
It is well known that exposure of mice to an enriched environment (EE) reliably increases performance on hippocampus-dependent learning and memory tasks. However, the mechanisms underlying the behavioral improvements and the effects of EE on synaptic transmission and cellular excitability remain still largely unclear. Therefore, we sought to study the effect of two weeks of EE on inhibition mediated by SOM and PV interneurons onto GCs of the mouse dentate gyrus.
By using in vitro whole-cell recordings in acute hippocampal brain slices, we discovered that EE leads to a substantial increase of the SOM- but not the PV-mediated inhibitory postsynaptic currents (IPSCs) onto GCs. The maximal amplitude of dendritic inhibitory currents at 0 mV was 2.25 nA ± 0.18 nA in EE versus 1.45nA ± 0.14 nA in control cages ($p=0.0014$, $n = 22$ and 23 GCs, respectively). Furthermore, EE reduced the paired-pulse ratio (PPR) and increased the quantal content ($1/CV^2$) of the SOM-mediated IPSCs to GCs, indicating a contribution of presynaptic mechanisms in EE-enhancement of IPSCs. To assess the activity of DG granule cells *in vivo*, we performed cFos-labelling in adult mice, after exploration of a novel environment. Interestingly, cFos-expression in DG granule cells was decreased in animals living in cages with environmental enrichment. These findings suggest that EE promotes GABAergic dendritic inhibition of DG granule cells, to maintain E/I-balance in DG during periods of enhanced hippocampal activity.

B 09-07
Neuronal Basis of interindividual Differences in Microcircuits

Henrike Planert[1], Franz X. Mittermaier[1], Sabine Grosser[2], Ulf C. Schneider[5,7], Helena Radbruch[6], Pawel Fidzinski[3], Julia Onken[7], Martin Holtkamp[4], Dietmar Schmitz[3], Henrik Alle[1], Imre Vida[2], Jörg R.P. Geiger[1], Yangfan Peng[1]

[1] *Charité Universitätsmedizin Berlin, Corporate member of Freie Universität Berlin and Humboldt Universität zu Berlin, Institute of Neurophysiology, Berlin, Germany*
[2] *Charité Universitätsmedizin Berlin, Corporate member of Freie Universität Berlin and Humboldt Universität zu Berlin, Institute for integrative Neuroanatomy, Berlin, Germany*
[3] *Charité Universitätsmedizin Berlin, Corporate member of Freie Universität Berlin and Humboldt Universität zu Berlin, Neuroscience Clinical Research Center, Berlin, Germany*
[4] *Charité Universitätsmedizin Berlin, Corporate member of Freie Universität Berlin and Humboldt Universität zu Berlin, Department of Neurology, Berlin, Germany*
[5] *Luzerner Kantonsspital, Luzern, Switzerland*
[6] *Charité Universitätsmedizin Berlin, Corporate member of Freie Universität Berlin and Humboldt Universität zu Berlin, Department of Neuropathology, Berlin, Germany*
[7] *Charité Universitätsmedizin Berlin, Corporate member of Freie Universität Berlin and Humboldt Universität zu Berlin, Department of Neurosurgery, Berlin, Germany*

Diversity of cells and synapses in the brain is a foundation of all intelligent behaviors. Heterogeneity is suggested to improve network stability and learning, and it may thus reflect shared principles of network functionality within each brain as well as microcircuit differences between individuals. To disentangle within and between individual sources of heterogeneity, we recorded up to 100 pyramidal neurons and 150 monosynaptic connections per single subject through advanced multineuron patch-clamp recordings in slices from human temporal cortex. We characterized principles of cellular and synaptic diversity that are shared across human individuals, including different functional types (e-types), depth-dependence of cellular but not synaptic properties, and log normal synaptic amplitude distributions. Quantifying the respective amounts of interindividual versus intraindividual diversity reveals large intraindividual contributions as opposed to contributions attributable to

between individual difference such as age or sex. This multilevel analysis highlights general principles of microcircuit organization and advances the understanding of human neuron diversity from an individual, phenotypic, and synaptic perspective.

B 09-08
Hippocampal neurons driven by sleep spindles are uniquely regulated during sleep

Diego M. Pagano[1], Yury Kovalchuk[1], Niels Niethard[2], Nima Mojtahedi[1], Jan Born[2,3], Olga Garaschuk[1,3]

[1] *University Tuebingen, Neurophysiology, Tübingen, Germany*
[2] *University of Tübingen, Institute of Medical Psychology and Behavioral Neurobiology, Tübingen, Germany*
[3] *University of Tübingen, Center for Integrative Neuroscience, 3Center for Integrative Neuroscience, Germany*

Question

Slow oscillations (SO) and sleep spindles play a central role for the consolidation of hippocampus-dependent memories during sleep, but the underlying cellular mechanisms remain unclear.

Methods

We addressed this issue in trained head-fixed mice by measuring the ongoing Ca^{2+} signaling of the CA1 pyramidal neurons. Simultaneous EEG and EMG recordings allowed us to monitor this activity across naturally occurring cycles of wakefulness, slow wave (SWS) or rapid eye movement (REM) sleep.

Results

In vivo two-photon imaging at single-cell resolution revealed that only 28% of the neuronal population was active during wake, the fraction of active cells progressively increased during sleep, with 42% of cells active during SWS and 48% active during REM sleep. The frequency of ongoing Ca^{2+} transients was highest during SWS and lowest during REM sleep. The opposite trend was found when comparing the median amplitudes of the detected Ca^{2+} transients. Next, we focused on cells that were particularly active during solitary SOs, solitary spindles as well as during spindles that occurred during the SO up-states. Across the SWS epochs, SO-active and SO+spindle-active cells showed a higher mean frequency of ongoing Ca^{2+} transients compared to spindle-active cells ($F = 11.59$, $p < 0.001$). Whereas SO-active cells did not change the mean frequency of ongoing Ca^{2+} transients throughout the brain states, spindle-active and SO+spindle-active cells showed significantly higher frequencies of Ca^{2+} transients during SWS compared to wake or REM sleep (spindle-active: $F = 4.6$, $p < 0.05$; SO+spindle-active: $F = 3.5$, $p < 0.05$). This pattern was unique to the above cells because SO-, spindle- and SO+spindle-inactive cell populations had similar frequencies of Ca^{2+} transients during wake, SWS and REM sleep. Finally, we examined the activity of different cell populations across SWS-REM-SWS triplets and found that only SO+spindle-active cells significantly downregulated their activity across REM sleep.

Conclusions

These results support the idea that the cells that are activated during spindles occurring during the SO up-state upregulate their activity during sleep, potentially explaining beneficial effects of these oscillatory patterns on memory consolidation. Furthermore, our data reveal the ability of REM sleep to downscale neural network involved in memory-related activity patterns, with the strongest impact on the SO+spindle-active neurons.

B 09-09
Cross-species analysis of ex vivo high-frequency oscillations using multi-electrode arrays

Michael D. Hadler, Jörg R.P. Geiger

Charité - Universitätsmedizin Berlin, Institute for Neurophysiology, Berlin, Germany

Question

Extracellularly recorded neural oscillations are observed across mammalian species with a highly conserved form-and-function relationship. In the human temporal cortex, high-frequency oscillations (100 - 250 Hz) are tightly associated with verbal memory tasks, their task-specific spatiotemporal profiles being re-instated during successful recall [1 - 2]. In states of disease, the successful detection and analysis of ripples

is however obscured by the presence of unphysiological oscillation patterns also spanning higher frequencies (100 – 600 Hz) [3]. This prompts the questions how such phenomena a) are similar or differ mechanistically and b) can be successfully identified in extracellular recordings.

Methods

Acute brain slices were obtained from the medial temporal gyrus (MTG) of human epilepsy patients undergoing therapeutic surgery and compared with brain slices obtained from mice or rats containing the hippocampal-temporal formation. Recordings were performed as either single local field potential recordings, perforated multi-electrode array recordings (200 µm inter-electrode distance) or high-density MEA recordings (17 µm inter-electrode distance).

Results

In human MTG slices, we pharmacologically induced recurrent episodes of high-frequency oscillations (HFOs, 150 – 500 Hz). HFOs were evoked by bath-application of either NMDA, dopamine (DA) or the D1R-agonist SKF-38393. HFOs originated in the deep cortical layers and spread across these layers with a velocity of approx. 3 cm/s, but multi-site recordings revealed a steep decline of coherence over distance. Maintenance of HFOs required calcium-permeable AMPA receptors (CP-AMPARs) and protein kinase C and was sensitive to the gap junction blocker carbenoxolone. This mechanistic profile was mirrored in mouse and rat slices containing the temporal association cortex (TeA), suggesting a common mechanism of action across species.

We further found mechanistic commonalities between HFOs and a physiological reference model of ripple oscillations, spontaneous sharp-wave ripple complexes (SPW-Rs, 150 - 250 Hz) in the mouse hippocampus [4]: SPW-Rs are dependent on both CP-AMPARs and D1Rs and originate from a preferred site of origin. However, the velocity of SPW-R propagation surpassed that of HFOs and ripple oscillations remained coherent over a longer distance, demonstrating a spatio-temporal demarkation between SPW-R and human MTG HFOs.

Conclusions

Using a multi-level platform for the investigation of high-frequency events, we extract mechanistic and spectral commonalities between putatively physiological SPW-R and pathological HFO complexes. Multi-site recordings are required to reveal profound differences in their propagation patterns and spatio-temporal profiles. Further investigations into the cause of such divergencies may highlight how pathological oscillations occur in diseased tissues and shed light on how physiological oscillations may be re-instated.

MDH and JRPG are supported by the Deutsche Forschungsgemeinschaft (DFG, German Research Foundation, TRR 295 Project ID 424778381 and FOR 2143 Project ID 245861656).

References
[1] Vaz et al., 2019. Science. "Coupled Ripple Oscillations between the Medial Temporal Lobe and Neocortex Retrieve Human Memory".
[2] Vaz et al., 2020. Science. "Coupled Ripple Oscillations between the Medial Temporal Lobe and Neocortex Retrieve Human Memory".
[3] Liu et al., 2022. Nat. Neurosci. "A consensus statement on detection of hippocampal sharp wave ripples and differentiation from other fast oscillations".
[4] Maier et al., 2011. Neuron. "Coherent Phasic Excitation during Hippocampal Ripples".

B 09-10
Morphological correlates of electrophysiological changes in prefrontal network activity along adolescent development

Timo Schwarze, Jastyn A. Pöpplau, Ileana Hanganu-Opatz

Center for Molecular Neurobiology, Hamburg Center of Neuroscience, University Medical Center Hamburg-Eppendorf, Institute of Developmental Neurophysiology, Hamburg, Germany

Higher cognitive abilities of mammalian species rely on prefrontal function. In line with the late emergence of these abilities, the prefrontal circuits have been shown to develop over an extended period throughout adolescence. We recently monitored the activity patterns in the prefrontal cortex (PFC) of mice and showed that they have specific dynamic features that relate to the emergence of cognitive abilities. The morphological substrate of these age-dependent changes of prefrontal activity remains largely unknown. Here, we fill this knowledge gap and provide an in-depth analysis of neuronal morphology and function in relationship to the activity of microglia. First, we quantified the morphological features of layer (L) 2/3 pyramidal neurons (PYRs) targeted by in utero electroporation. We show that the complexity of dendritic

arborizations as well as the dendritic length of L2/3 PYRs peaks during early adolescence. Furthermore, mice in the same age presented higher synaptic density than younger or older mice, regardless of the dendritic type. Second, we used in utero electroporation to target the post synaptic density protein of L2/3 PYRs with a fluorophore. In combination with a lysosomal and microglia cell marker we quantified the microglial morphology as well as the phagocytic activity specifically for L2/3 PYRs. While microglial density decreased from pre-juvenile age until late adolescence, adolescent microglia displayed the most rounded and least ramified morphology. Moreover, microglial phagocytic activity on spines of L2/3 PYRs peaked during early adolescence. Thus, increased prefrontal activity is associated with major microglia-controlled dendritic and synaptic maturation of L2/3 PYRs in the PFC.

B 10 | Cardiac Function 2

B 10-01
sEH derived PUFAs affect pericyte-endothelial cell integrity and the function of the diabetic heart

Sebastian Kempf[1], Xiaoming Li[1], Fredy Delgado-Lagos[1], Rüdiger Popp[1], Timo Frömel[1], Stephan Klatt[1], Baktybek Kojonazarov[2], Jiong Hu[1], Ingrid Fleming[1]

[1] Goethe University Frankfurt am Main, Institute for vascular signaling, 60590, Germany
[2] University of Giessen and Marburg, Lung Center, 35392, Germany

Question
Polyunsaturated fatty acid (PUFA) metabolites generated by the sequential action of cytochrome P450 (CYP) and soluble epoxide hydrolase (sEH) enzymes are important modulators of vascular function and integrity. Given the reported role of the sEH in regulating vascular stability in the retina, this study aimed to explore the effects of the PUFA metabolites generated by CYP/sEH on pericyte-endothelial cell junctions and to characterize the effects of sEH related PUFAs on vessel in the diabetic heart.

Methods
LC-MS, snRNA, WB, IHC

Results
A comparison of wild-type mice and animals with type1 diabetes (Ins2Akita mice), revealed significantly elevated sEH expression in cardiomyocytes in the diabetic group. Diabetic mice also displayed characteristics of heart failure with preserved ejection fraction (HFpEF) at the age of 6 months, and developed heart failure with reduced ejection fraction (HFrEF) by 12 months. Attenuated cardiac function in the oldest group of diabetic animals was accompanied by in left ventricular capillary density versus their non-diabetic littermates; however, pericyte coverage was markedly reduced. Consistent with the change in sEH expression, fatty acid profiling of the left ventricle reveled increased levels of sEH-derived PUFA diols, e.g. 12,13-dihydroxy-octadecenoic acid (12,13-DiHOME) and 14,15-dihydroxyeicosatrienoic acid (14,15-DHET) in mice with diabetes. Next we generated mice lacking the sEH specifically in cardiomyocytes (sEH^{DMhy6}) and crossed them onto the Ins2Akita background. After 10-12 months we observed a clear improvement in cardiac function (EF 58% in non diabetic, 45 % in diabetic, and 55 % in diabetic sEHDMhy6 mice), as well as pericyte coverage. In vitro studies with 12,13-DiHOME revealed that it induced pericyte migration.

Conclusions
Taken together our data indicate that increased in sEH expression in cardiomyocytes affects cardiac function and the development of heart failure. At least one product of the sEH i.e. 12,13-DiHOME, whose concentration was elevated in cardiac tissue, was found to promote pericyte migration and may contribute to vascular destabilization and the development of microvascular dysfunction.

Deutsche Forschungsgemeinschaft SFB1531/B03

B 10-02
Elevated expression of acetylcholine receptor and collagen in hearts of db/db mice

Tobias Hofebauer[1], Sebastian Kötter[1], Katharina Bottermann[2], Katharina Voigt[1], Daniela Müller[1], Joachim P. Schmitt[2], Martina Krüger[1]

[1] *Heinrich-Heine University Duesseldorf, Institute of Cardiovascular Physiology, Duesseldorf, Germany*
[2] *Heinrich-Heine University Duesseldorf, Institute of Pharmacology, Duesseldorf, Germany*

Background: After myocardial infarction (MI), mortality of diabetic patients is higher than in non-diabetic patients. We previously showed that after MI in diabetic (db/db) mice, functional adaptation of the remote myocardium (RM) by increased titin-based passive tension (PT) fails. This dysfunction is likely due to already increased PKCα-dependent phosphorylation of S11878 in the PEVK domain of titin, which leads to chronically increased cardiomyocyte PT, preventing further acute changes. The pathomechanism for increased PKCα-induced titin modification in diabetic hearts is still not fully resolved. Here, we test the hypothesis that mRNA expression of muscarin-2- (M2R), muscarin-3- (M3R) and α7-nicotinic-receptor (α7nR) is increased in diabetic mice, which may result in PKCα activation and the described hyper-phosphorylation of PEVK titin. Myocardial PT is further determined by collagen expression and crosslinking. Therefore, we analyzed mRNA expression of collagen3-a (col3a) and its cross-linking enzyme lysyl oxidase-like-1 (loxl1).
Methods: 10-12-week-old leptin-receptor deficient homozygous diabetic db/db mice (n=6) and non-diabetic db/+ littermates (n=6) were killed by cervical dislocation. Cardiac tissue was frozen in liquid nitrogen and stored at -80°C. qPCR experiments were performed in atrial and left ventricular tissue for M2R, M3R, α7nR, col3a and loxl1.
Results: In left ventricle, receptor mRNA expression was unchanged. In contrast, receptor mRNA expression levels were significantly increased in atrial tissue (M2R: +68,7% ± 13,5%, p=0,0006; M3R: +118,6% ± 26,1%, p=0,0014; α7nR: +72,2% ± 26,6%, p=0,024). Col3a mRNA expression was significantly reduced in the left ventricle (col3a: -31,4% ± 8,6%, p=0,007) and a mild trend towards loxl1 reduction was detected (loxl1: -30,5% ± 14,6%, p=0,07). In atrial tissue col3a and loxl1 expression level were significantly reduced (col3a: -34,9% ± 8,1%, p=0,002; loxl1: -20,1% ± 7,5%, p=0,021).
Conclusion: Increased receptor mRNA expression may provide an explanation for increased PKC-mediated titin phosphorylation in atria of db/db mice. Complementary analyses of protein expression and receptor distribution in tissues will resolve whether these changes are restricted to the atria or involve also the ventricles. Reduced mRNA expression of col3a and loxl1 in atrial and ventricular tissues of db/db mice suggests that increased titin PT could be an adaptive response to reduced matrix-induced stiffness.

Many thanks to Sabine Bongard for the excellent technical support and to Anne Hemmers and Dr Andre Spychala for the introduction to qPCR measurements and its troubleshooting.

B 10-03
Chemogenetic generation of hydrogene peroxide in cardiac endothelial cells induces cardiac remodeling

Melina Lopez[1,2], Niklas Müller[1,2], Pedro F. Malacarne[1,2], Ralf Gilsbach[1,2,3], Flávia Rezende[1,2], Ralf Brandes[1,2]

[1] *Goethe University, Institute for Cardiovascular Physiologie, Frankfurt am Main, Germany*
[2] *German Center of Cardiovascular Research, DZHK, Frankfurt, Germany*
[3] *Heidelberg University, Institute of Experimental Cardiology, Heidelberg, Germany*

The author has objected to a publication of the abstract.

B 10-04
Altered sarcomere properties in adult murine cardiomyocytes in response to lipid droplet accumulation

Katharina Voigt, Maurice Brucker, Martina Krüger

Heinrich-Heine University Düsseldorf, Institute of Cardiovascular Physiology, Düsseldorf, Germany

Question

Accumulation of lipids in myocardial lipid droplets (LDs) is associated with heart failure in obesity and diabetes mellitus. LDs can create a lipotoxic microenvironment and impair cardiomyocyte function. Here, we investigate whether LD accumulation affects the sarcomere protein titin and may contribute to increased cardiomyocyte passive tension in diabetes mellitus.

Methods

We established a cell culture protocol for accumulation of lipid droplets in isolated cardiomyocytes from adult C57BL/6N wildtype mice. Cells were incubated with oleic and palmitic acid (each 200µM) for 6h followed by microscopic and biochemical analysis. Lipid droplets were counted in three 400µm² regions of interest/cell using ImageJ software. Titin expression and phosphorylation was analyzed using agarose-stabilized SDS-PAGE and Western blotting using phosphosite-directed antibodies.

Results

LD numbers were significantly higher in cardiomyocytes treated with oleic and palmitic acid, with an average of 63.7 ±7.3 LDs per ROI, compared to 3.0 ±3.5 LDs per ROI in control cells. Importantly, LD accumulation did not change cardiomyocyte area or cellular dimensions, cell size was 234.8 ± 38.6µm² in controls and 149.6 ± 60.5µm² in fatty acid treated cells. Average sarcomere length was 1.86 ± 0.15µm in control cardiomyocytes and was significantly reduced to 1.66 ±0.16µm in cardiomyocytes treated with oleic and palmitic acid. First results indicate that LD accumulation increases relative phosphorylation of titin PEVK domain at serine 12022 by approx. 20% compared to controls. We hypothesize that LD accumulation mechanically compresses the sarcomere structure, leading to rapid stiffening of the titin filament and increased cardiomyocyte passive tension.

Conclusions

We hypothesize that LD accumulation mechanically compresses the sarcomere structure, leading to rapid stiffening of the titin filament and increased cardiomyocyte passive tension.

B 10-05
Course of immune cell infiltration and the onset of cardiac fibrosis in pressure overload induced heart failure

Anne Hemmers, Rianne Nederlof, Lisa Kalfhues, Axel Gödecke

Heinrich-Heine University, Institute of Cardiovascular Physiology, Düsseldorf, Germany

Question

Cardiac metabolic remodeling is one of the early changes that drive the progression of heart failure and predates apparent cardiac dysfunction. In mice with cardiomyocyte (CM) specific deletion of p38 MAPKa (KO), we observed strongly deteriorated heart function, accompanied by pronounced left ventricular (LV) dilation after 48h of pressure overload, induced by angiotensin II (AngII). This functional depression was reversible and heart function returned to baseline level. Hence we asked to what extent prolonged AngII treatment (7d) led to irreversible heart failure, development of fibrosis and altered immune cell infiltration.

Methods/Results

7d AngII treatment resulted in persistent LV dilation in KO mice (EDV [µl] Ctrl: 80/KO: 124). Interestingly, heart function of Ctrl mice did not change even during AngII administration and an expected LV hypertrophy did not occur. Of note, cardiac dysfunction persisted in KO mice even 14d after end of AngII treatment (EF [%] Ctrl: 56/KO: 30), demonstrating that 7d AngII treatment led to irreversible cardiac remodeling in KO mice. We further discovered substantial differences in immune cell accumulation in heart tissue, by FACS analysis. An increase of leukocytes, mainly neutrophils, within the first 48h occurred in KO and Ctrl mice. Afterwards, the number of leukocytes decreased significantly at 7d AngII and stayed low after 14d recovery phase in both groups. Neutrophils accumulated particularly in KO hearts after 48h of AngII (250-

fold), while a minor increase (47-fold) was detected in Ctrl mice. After 7d AngII, neutrophils vanished entirely in both groups. Macrophages peaked later (3-fold increase) after 7d of AngII, and decreased again after recovery time in both groups. Further analysis showed, that these were mainly CD206$^+$ macrophages and therefore have anti-inflammatory properties. Interestingly, cytotoxic CD8$^+$ T-cells were elevated (12-fold) in KO hearts due to AngII treatment, and remained elevated even after 14d recovery, while their number in Ctrl mice returned almost to baseline level. Moreover, αSMA$^+$ fibroblasts increased 37-fold in KO hearts after 7d AngII revealed the onset of fibrosis. As expected, they were depleted after recovery time. WGA staining on hearts showed elevated fibrosis particularly in KO hearts. Furthermore, KO hearts showed high expression of fibrosis-related genes compared to Ctrl and thus confirming previous findings.

Conclusions

Long-term pressure overload caused persistent impairment of cardiac function in KO mice. The infiltration of immune cells, especially neutrophils and cytotoxic T-cells, appear to play a decisive role in the development of this heart failure. In addition, loss of p38 MAPKa extensive cardiac fibrosis. Thus, CM-specific p38 attenuates the development of heart failure caused by pressure overload, most likely by reduced accumulation of immune cells in heart tissue and by inhibiting cardiac fibrosis.

Funded by IRTG1902

B 10-06
cAMP microdomain signaling at RyR2 in cardiomyocytes using subcellular targeted optogenetics

Berivan Mansuroglu[1,2], Philipp Sasse[1]

[1] *University of Bonn, Medical Faculty/ Institute of Physiology 1, Bonn, Germany*
[2] *University of Bonn, Research Training Group 1873, Bonn, Germany*

Cardiac arrhythmia can be triggered by pathologic cAMP-dependent (hyper-)phosphorylation of the Ryanodine Receptor type 2 (RyR2) leading to Ca^{2+} release in the diastole. Using cAMP imaging with targeted sensors, it has been suggested that RyR2 has its own cAMP microdomain. Here we present a complementary approach to investigate the functional impact of RyR2 microdomains in cardiomyocytes by localized cAMP generation using targeted optogenetics.

To increase cAMP levels with light locally at the RyR2, the photo-activated adenylate cyclase from *Turneriella parva* (TpPAC)[1] and mCitrine was targeted to the RyR2 by fusion with the high-affinity protein FKBP12.6[2]. Cytosolic TpPAC-EYFP expression served as a control for global cAMP generation. Functionality of fusion proteins was proven in HEK293 cells co-expressing the cAMP-sensitive GloSensor in which blue light elevated cAMP levels in a light dose-dependent manner.

After expression in neonatal mouse cardiomyocytes with nucleofection, cytosolic TpPAC-EYFP showed homogeneous distribution whereas TpPAC-mCitrine-FKBP12.6 localized near z-discs indicating RyR2 targeting. Functionality was tested by analyzing spontaneous beating frequency, which highly dependents on RyR2 Ca^{2+} release and oscillation (Ca^{2+} clock mechanism) in neonatal cardiomyocytes. Brief blue light flashes of various durations resulted in transient acceleration of spontaneous beating frequency in a light dose-dependent manner. The peak frequency was similar but cAMP production locally at the RyR2 led to a significant shorter lasting (~ 120s) effect than global cytosolic cAMP generation (~290 s) indicating higher local PDE activity.

To investigate the effect on Ca^{2+} handling, Ca^{2+} imaging of electrically (0.75-1 Hz) paced cardiomyocytes with the red-shifted dye Cal630 was performed, which showed a light dose-dependent increase of Ca^{2+} transient heights. Interestingly the maximum peak height was reached earlier by cAMP generated locally at the RyR2 (~6 s) compared to cytosolic cAMP (~11 s). Importantly, cAMP at the RyR2 but not in the cytosol resulted in an increase of diastolic Ca^{2+} levels suggesting increased spontaneous Ca^{2+} leak. Phosphorylation was analyzed using a PKA-substrate (RRXS*/T*) specific antibody after illumination of cardiomyocytes with different light doses. Importantly low light stimulation led to already ~80% of the maximum effect by RyR2 targeted cAMP generation whereas cytosolic cAMP generated by same light intensity only reached ~30% of the maximum effect.

In conclusion, in comparison to global cytosolic cAMP generation, local generation of cAMP at the RyR2 microdomain leads to faster and shorter lasting effects with higher sensitivity on pacemaking and systolic Ca^{2+} release and promotes diastolic Ca^{2+} leak. The novel approach

of generation cAMP microdomains by targeting fusion proteins will allow the direct investigation of players involved in microdomain signaling and cardiac arrhythmia mechanisms.

Funded by Deutsche Forschungsgemeinschaft (DFG, German Research Foundation, 214362475 / GRK1873/3)

Prof. Peter Hegemann, Dr. Yinth Andrea Bernal Sierra (Humboldt Universität zu Berlin) for providing Plasmids

References
[1] Penzkofer et al., 2015, doi: 10.1016/j.jphotobiol.2015.08.027
[2] Despa, S et al., 2014, doi: 10.1161/CIRCRESAHA.115.303582

B 10-07
Programming of human induced pluripotent stem cells to cardiac pacemaker-like cells and characterization of action potentials

Jonathan Kindermann[1], Christian Rimmbach[2,3], Julia J. Jung[2,3], Robert David[2,3], **Heinrich Brinkmeier**[1]

[1] *University Medicine Greifswald, Institute of Pathophysiology, Greifswald, Germany*
[2] *University Medicine Rostock, Clinic and Polyclinic for Cardiac Surgery, Department Life, Light & Matter, Rostock, Germany*
[3] *University Medicine Rostock, Research Building BMFZ, Rostock, Germany*

Question

Cardiomyocytes derived from human induced pluripotent stem cells (iPSC) can be useful in vitro models of disease and may serve as tools for drug testing and cardiac safety pharmacology. The aim of the current study was the programming and differentiation of iPSC to cardiac pacemaker-like cells.

Methods

To this end a plasmid-based vector system was used to ensure the stable expression of the transcription factor TBX3 in an iPSC line (SC950A-1) derived from human dermal fibroblasts. To improve cell purity of the cardiac phenotype, an additional selection system under control of the α-cardiac myosin heavy chain promoter was established (Klug et al. 1998, J Clin Invest, 98, 216-224). The re-programmed cells differentiated and formed beating aggregates of cardiomyocyte-like cells. For electrophysiological recordings, the aggregates were dissociated and seeded in standard culture dishes. Electrodes were filled with an intracellular solution containing K^+, gluconate$^-$ and Cl^- as the major electrolytes to record action potentials (APs); alternatively intracellular CsCl was used for the precise recording of Na^+ inward currents.

Results

Contraction frequencies of single cells and small aggregates ranged between 0.3 Hz and 2 Hz. The aggregates were obviously electrically coupled since their contractile activity was synchronized. In some of the cultures contractile activity remained stable for up to six weeks. Electrophysiological recordings in the current clamp mode allowed the recoding of action potentials. We observed two types of AP morphology, the ventricular type and the nodal type. Most of the tested cells (n>80) showed spontaneous electrical activity. Ventricular APs were characterized by a fast rise (<10 ms), a stable or slowly declining plateau of between 200 ms and 1000 ms duration followed by a repolarisation phase. In the voltage-clamp mode large Na^+ currents could be recorded from the same cells. APs of pacemaker-like cells were characterized by a slow diastolic depolarization phase, followed by a faster depolarization and a repolarisation phase (both > 100 ms). Injection of hyperpolarizing currents of -10 to -20 pA frequently stopped spontaneous electrical activity. In cells that did not show any spontaneous electrical activity APs could be induced by 100-ms lasting small depolarizing currents. Besides Na^+ inward currents, K^+ outward currents could be recorded sometimes, while HCN currents were hardly detectable.

Conclusions

In conclusion, the applied method of forward programming of iPSC to pacemaker-like cells was successful and reproducible. However, action potentials were variable in shape and sometimes driven by Na^+ inward currents. Further experiments will be required to test whether, besides TBX3, additional transcription factors have to be expressed, whether growth factors should be supplemented or whether the results are a matter of cellular differentiation and maturation.

This work was supported by the European Social Fund, grant No. ESF/14-BM-A55-0025/18

B 10-08
Cardiopulmonary effects of prolonged normobaric hypoxia and norepinephrine in rats

Charly Bambor[1], Sarah Daunheimer[1], Annekathrin Hoschke[1], Aida Salameh[2], Beate Raßler[1]

[1] *University of Leipzig, Carl-Ludwig-Insitute for Physiology, Leipzig, Germany*
[2] *University of Leipzig, Dept. of Pediatric Cardiology, Heart Centre, Leipzig, Germany*

Background: Normobaric hypoxia (10% O_2 in N_2) depresses left ventricular (LV) inotropic function in rats. Previous studies showed that acute hypoxia (6 h) decreased LV systolic pressure (LVSP) and LV contractility (LV dP/dtmax) to 68% and 55% of normoxic values, respectively. In the lung, first signs of pulmonary edema occurred. We speculated that prolonged hypoxia (72 h) would induce acclimatization and hence, recovery of LV function and resolution of pulmonary edema. As sympathetic blockade further deteriorated LV function and pulmonary edema, we additionally investigated the effects of norepinephrine administration on the cardiopulmonary function in hypoxia.
Methods: Rats (n = 63) were exposed over 72 h either to normal room air (N) or to normobaric hypoxia in a chamber with 10% O_2 in nitrogen (H). The animals received infusion (0.1 ml h^{-1}) with 0.9% NaCl (control groups) or norepinephrine (NE, 0.1 mg kg^{-1} h^{-1}). After 72 h of hypoxia, a subgroup from each the H-NaCl and H-NE groups was transferred to a normoxic environment with NaCl infusion for further 72 h (recovery groups). At the end of the experiment, heart catheterization was performed in all animals for examination of hemodynamic function. Finally, lung tissue was obtained for histological analysis.
Results: After 72h of hypoxia, hypoxic rats presented a significantly elevated hematocrit compared to normoxic control animals (49% vs 44%). At that time, LVSP and LV dP/dtmax were with about 80% of normoxic values still significantly diminished. Interestingly, NE infusion reduced both parameters in normoxia and even more in hypoxia compared to the respective controls. Three days of recovery fully restored LVSP and LV dP/dtmax. Pulmonary edema developed during exposure to hypoxia and showed only partial resolution after 3 d of recovery. NE infusion induced formation of pulmonary edema even in normoxia but aggravated it only slightly under hypoxic conditions.
Conclusions: After 72 h of hypoxia, LV depression is mitigated, but not fully restored compared to the first hours of hypoxic exposure. NE did neither prevent hypoxic depression of LV inotropic function nor alleviate hypoxic pulmonary edema. LV function completely recovered after three further days under normoxic control conditions, but pulmonary edema was still present. It is well known that NE may induce pulmonary edema. Regionally differential effects on adrenoceptors of NE and hypoxia, among others, may account for the failure of NE administration to restore LVSP and LV dP/dt max under hypoxic conditions.

B 10-09
Cold storage of hearts for 24 hours preserves cardiomyocyte structure and function: an approach to reduce costs and the number of experimental animals

Benedikt Pfeilschifter[1], Prapassorn Potue[2,1], Dominik Fiegle[1], Tilmann Volk[1], Thomas Seidel[1]

[1] *Friedrich Alexander Universität Erlangen, Institut für Physiologie 2, Erlangen, Germany*
[2] *Khon Kaen Universtiy, Department of Physiology, Khon Kaen, Thailand*

Question
Isolation of cardiomyocytes from animals remains an important technique in basic cardiovascular research as it is essential to obtain answers to many research questions. However, when removing the heart, the donor animal is sacrificed. Furthermore, animal models, in particular gene-modification and disease models in mice, are frequently and possibly unnecessarily replicated because it is believed that cardiomyocytes must be immediately isolated and investigated after heart removal to avoid unacceptable qualitative losses in structure, function and gene expression. Here, we investigated if mouse hearts can be preserved for at least 24h prior to myocyte isolation without affecting subsequent experiments.
Methods

After analgesia and cervical dislocation, mouse hearts were excised and used for enzymatic cardiomyocyte isolation either immediately (CTRL) of after 24h of conservation at 4°C (CONS). Isolated cells were stained with Di-8-ANEPPS to characterize the t-tubular system. Action potentials and membrane currents were measured using the whole-cell patch-clamp technique. Intracellular Ca^{2+}-transients and contractility were characterized after loading cells with Fura-2. The transcription pattern was analyzed by RNAseq from total RNA of cardiac myocytes from both groups.

Results

Action potentials did not show any significant differences in resting potential, upstroke velocity, overshoot and duration (n = 23/22 in CTRL/CONS). Densities of the transient outward potassium current (I_{to}) were similar in both groups (40.3±2.7 vs 41.8±4.1 $pApF^{-1}$ at V_{Pip} = 60 mV; n = 29/20). Kinetics of I_{to} showed no difference as well. Moreover, the density of the inwardly rectifying K^+ current (I_{K1}) was comparable in cardiomyocytes form both groups (5.2±0.5 vs 6.3±0.3 $pApF^{-1}$ at V_{Pip} = -120 mV, n = 16/7). The L-type Ca^{2+} current was not significantly changed (-5.9±0.5 vs -7.1±0.3 $pApF^{-1}$ at V_{Pip} = 0 mV, n = 9/7). T-tubular system showed nearly identical t-tubular distance (0.41±0.01 vs 0.44±0.02 µm, n=28/30) and regularity (spectral density = 0.07±0.004 vs 0.09±0.004 %, n=28/30).

Sarcomere shortening during contraction was almost equal in both groups at several different pacing frequencies (0.11±0.01 vs 0.11±0.01 µm at 0.5 Hz and 0.09±0.01 vs 0.1±0.01 µm at 2 Hz, n=30/40). Ca^{2+} imaging indicated unchanged kinetics and magnitudes of intracellular of Ca^{2+} release. The 90% duration of the transient was 258.5±15.1 and 229.5±8.6 ms at 0.5Hz and 252.4±8.7 and 255±8.8 ms at 2 Hz; n =30/40). RNAseq showed only a small number of differentially expressed genes.

Conclusions

We suggest that the described method offers a 24 h time window after heart removal without affecting the results from isolated myocytes qualitatively. This allows high experimental flexibility, the exchange of hearts between institutions, and, therefore, a reduction in the number of laboratory animals used for cardiac research.

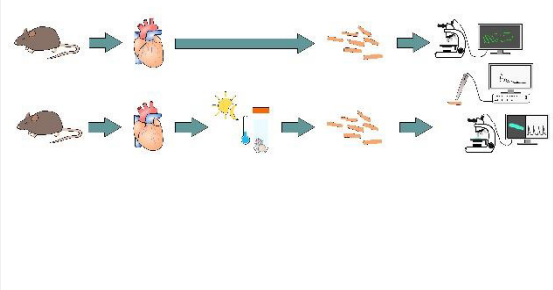

Graphicalabstract
After analgesia and cervical dislocation, mouse hearts were excised and used for enzymatic cardiomyocyte isolation either immediately (CTRL) of after 24h of conservation at 4°C (CONS). Isolated cells were stained with Di-8-ANEPPS to characterize the t-tubular system. Action potentials and membrane currents were measured using the whole-cell patch-clamp technique. Intracellular Ca^{2+}-transients and contractility were characterized after loading cells with Fura-2. The transcription pattern was analyzed by RNAseq from total RNA of cardiac myocytes from both groups.

B 10-10
Characterization of a recently identified myosin, Myo18Ay, in the A-band of cardiac sarcomeres

Markus Horsthemke[1,2], Peter J. Hanley[1,2]

[1] *HMU Health and Medical University Potsdam, Potsdam, Germany*
[2] *HMU Research, Development and Innovation gGmbH (HMU RDI), Potsdam, Germany*

Myosins represent a diverse superfamily of motor proteins, with 13 classes in humans and mice. Class II myosins form bipolar filaments in cardiac and skeletal muscle cells, serving as the force-generating components of thick filaments within the A-bands of sarcomeres. Recent research has shown that another class of myosins, class XVIII myosins, also localize to the A-bands of sarcomeres. Class XVIII myosins consist of two members, Myo18A and Myo18B. We found that a striated muscle-specific isoform of Myo18A, Myo18Aγ, is predominantly expressed in the heart during embryo development, similar to Myo18B[1,2]. Furthermore, we found that deletion of Myo18A, similar to deletion of Myo18B, in mouse causes early embryonic lethality (around E12.5) and hearts lacking either Myo18A or Myo18B exhibit highly disorganized sarcomeres[1,2]. In further work, we plan to use Myo18A isoform-specific knockout mouse models, epitope mapping, interaction screens and functional assays to elucidate the role of Myo18Aγ in cardiac sarcomeres.

This work is supported by Deutsche Forschungsgemeinschaft (DFG) grant HA 3271/12-1 (to P. J. H.).

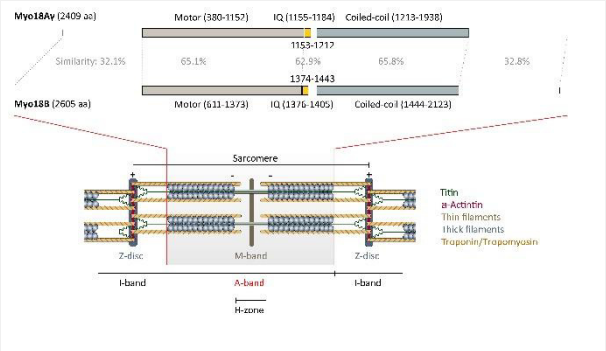

Figure 1
Schematic representation of the domain structure and localization of Myo18Ay and Myo18B in the cardiac sarcomere.

References
[1] Ajima, R., Akazawa, H., Kodama, M., Takeshita, F., Otsuka, A., Kohno, T., et al. (2008). Deficiency of Myo18B in mice results in embryonic lethality with cardiac myofibrillar aberrations. Genes Cells 13, 987–999.
[2] Horsthemke, M., Nutter, L. M. J., Bachg, A. C., Skryabin, B. V., Honnert, U., Zobel, T., et al. (2019). A novel isoform of myosin 18A (Myo18Agamma) is an essential sarcomeric protein in mouse heart. J. Biol. Chem. 294, 7202– 7218.

B 10-11
Electrophysiological characterization of heart function in the incubated chicken egg

Judith Rees[1,2,3], Niklas Hegemann[1,2,3], Michael Höpfner[2], Wolfgang M. Kuebler[2,3], Bianca Nitzsche[2,3], Jana Grune[1,2,3]

[1] Charité - Universitätsmedizin Berlin, Department of Cardiothoracic and Vascular Surgery, Deutsches Herzzentrum der Charité (DHZC), Berlin, Germany
[2] Charité - Universitätsmedizin Berlin, Institute of Physiology, Berlin, Germany
[3] German Center for Cardiovascular Research (DZHK), partner site Berlin, Berlin, Germany

Introduction: Echocardiography and electrocardiograms are the mainstay for clinical and preclinical assessment of cardiac electrophysiology and hemodynamic function. Here we investigated if the *in-ovo* incubated chicken egg may provide a feasible alternative to conventional animal models for cardiovascular research by these techniques. The heart of the chick embryo is fully developed after just eight days of incubation and the cardiovascular system is easily accessible for monitoring as well as interventions via the chorioallantoic membrane. We recently realized *in-ovo* echocardiographywith pre-existing infrastructure for small animal echocardiography. In parallel, placement of electrodes in the electrically conductive egg white of chick embryos allows for *in-ovo* recording of electrocardiograms. As experiments in the incubated chicken egg are not classified as animal experiments until day 13 of embryonic development (ED), the realization of combined echo- and electrocardiography *in-ovo* could help to significantly reduce experimental animal numbers in cardiovascular research, and facilitate rapid screening for therapeutic as well as adverse drug effects on the beating heart.

Methods: Fertilized white leghorn chicken eggs (VALO BioMedia GmbH) were incubated at 37.8 °C and >58% humidity. In 8 to 13- day old chicken eggs cardiac electrophysiology and hemodynamic function was assessed using an Animal Bio Amp device coupled with Labchart (ADInstruments) and a commercially available high resolution ultrasound system for small animals (Vevo 3100, Fujifilm Visualsonics Inc.) equipped with a high frequency probe (MX700; centre transmit: 50 MHz), respectively. Incubated chicken eggs were treated with the non-selective β-blocker isoproterenol or the β_1-selective blocker metoprolol to demonstrate the sensitivity of *in-ovo* echocardiography and electrocardiography.

Results: For *in-ovo* echocardiography, we provide standard operating procedures for egg preparation, image acquisition, data analysis, reference values for left and right ventricular function and dimensions, and inter-observer variabilities. We were able to produce B- and M-Mode cine loops as well as Color Doppler guided flow profiles of the developing heart at several time points from day 8 till day 13 ED. Subjecting incubated chicken eggs to hypoxia for a period of time alters the cardio-pulmonary flow profiles in a way that mimics features of pulmonary hypertension. Treating the incubated chicken eggs with metoprolol led to a proto-typic response that can be detected via echocardiography. Additionally, we demonstrate the feasibility of *in-ovo* electrocardiography and demonstrate induction of ventricular tachycardias by isoproterenol in incubated chicken eggs.

Conclusions: Our *in-ovo* model provides a versatile platform for echocardiographic and electrocardiographic studies in the beating heart while refining, and reducing animal experiments according to the 3R principle.

Funded by Charité 3R

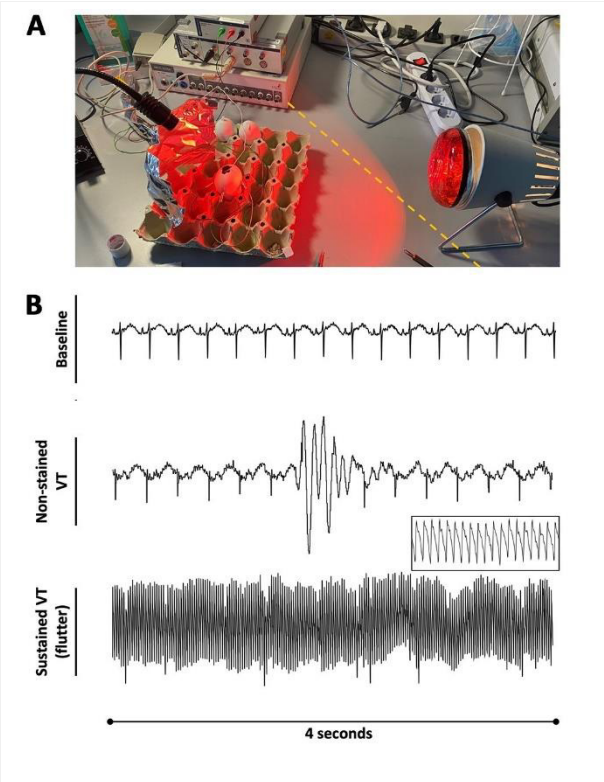

Chick embryo electrocardiogram
A) Current experimental setup
B) Preliminary ECG curves of chick embryos showing arrhythmia inducibility with non-sustained and sustained ventricular tachycardia (VT)

INDEX

Author Index

C

D

E

F

G

H

I

L

M

N

O

P

Q

R

S

T